

N O T I C E

THIS DOCUMENT HAS BEEN REPRODUCED FROM
MICROFICHE. ALTHOUGH IT IS RECOGNIZED THAT
CERTAIN PORTIONS ARE ILLEGIBLE, IT IS BEING RELEASED
IN THE INTEREST OF MAKING AVAILABLE AS MUCH
INFORMATION AS POSSIBLE

CONF-771131 - -

Dr. 442

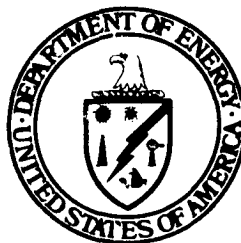
Sponsored by
U.S. Department of Energy
Assistant Secretary for Energy Technology
Division of Energy Storage Systems
Washington, D.C. 20545

August 1978

**Proceedings of the DOE
Chemical/Hydrogen Energy
Systems Contractor Review**

MASTER

Held November 16-17, 1977
Hunt Valley, Maryland



DISTRIBUTION OF THIS DOCUMENT IS UNLIMITED

BLANK PAGE

Sponsored by
U.S. Department of Energy
Assistant Secretary for Energy Technology
Division of Energy Storage Systems
Washington, D.C. 20545

CONF-771131
UC-94d

Proceedings of the DOE Chemical/Hydrogen Energy Contractor Review Systems

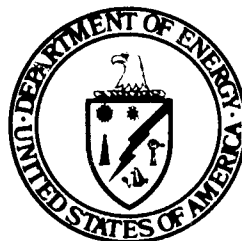
Held November 16-17, 1977
Hunt Valley, Maryland

August 1978

NOTICE

This report was prepared as an account of work sponsored by the United States Government. Neither the United States nor the United States Department of Energy, nor any of their employees, nor any of their contractors, sub-contractors, or their employees, makes any warranty, express or implied, or assumes any legal liability or responsibility for the accuracy, completeness or usefulness of any information, apparatus, product or process disclosed, or represents that its use would not infringe privately owned rights.

Proceedings prepared by
Jet Propulsion Laboratory
California Institute of Technology
Pasadena, California 91109



file

FOREWORD

A Contractor Review meeting is scheduled annually by the DOE Division of Energy Storage Systems (STOR) to provide an opportunity for all participants in the Chemical and Hydrogen Energy Storage Systems Program to become familiar with the scope of the program and to appraise the progress of the technical effort. The FY 1977 Contractor Review meeting was called by Dr. James H. Swisher, Assistant Director for Physical Storage Systems, and was held at Hunt Valley, Maryland, on November 16-17, 1977.

All government and contractor personnel who were involved in the STOR-sponsored effort were requested to submit presentations which would (1) give all participants an insight into the background and the objectives of the hydrogen-related task, (2) show the status of the study or technical effort, (3) relate any problems which had impeded progress, and (4) state projected solutions for eliminating or working around the identified problems. The meeting was structured to allow ample time for all participants to directly discuss their specific program interests with the other people who were performing similar or related tasks. On November 18, 1977, a program review panel met with STOR staff to provide observations on the hydrogen program content and objectives; and on future program direction.

The Contractor Review meeting was planned and organized by personnel from the Jet Propulsion Laboratory in accordance with one task of a project management role for that portion of the DOE Hydrogen Energy Storage Program which the National Aeronautics and Space Administration has assumed responsibility under an Interagency agreement (EC-77-A-31-1035). As the chairman for this meeting, I especially thank the persons who made the presentations and contributed to the success of this review. I wish to express my appreciation to Dr. Beverly J. Berger, Program Manager, and to Dr. James H. Swisher, Mr. John Gahimer, Mr. Frank J. Salzano, and Mr. Gerald Strickland for their guidance and assistance in the formulation of plans for this meeting.

James H. Kelley, Manager
Hydrogen Systems and Technology
Project
Jet Propulsion Laboratory
Pasadena, CA

ABSTRACT

The Chemical/ Hydrogen Energy Systems Contractor Review was held at the Hunt Valley Inn, Hunt Valley, Maryland, on November 16-17, 1977. This Review meeting, scheduled annually by the DOE Division of Energy Storage Systems (STOR), was coordinated for DOE by the Jet Propulsion Laboratory in accordance with a task defined in the inter-agency agreement (EC-77-A-31-1035) between DOE and the NASA Office of Energy Programs. The meeting served as an effective means to (1) give all participants an insight into the background and objectives of thirty-nine hydrogen-related tasks, (2) show the status of the studies or technical effort, (3) relate any problems that had impeded the progress, and (4) state projected solutions for resolving the identified problems. Approximately 100 representatives from government and the private sector participated in the Contractor Review.

CONTENTS

SESSION I. PROGRAM OVERVIEWS

ELECTROLYSIS-BASED HYDROGEN STORAGE SYSTEMS: OVERVIEW AND RATIONALE OF THE BROOKHAVEN NATIONAL LABORATORY MANAGED PROGRAM	3
F. J. Salzano Brookhaven National Laboratory	
NASA'S SUPPORT OF DOE'S HYDROGEN ENERGY STORAGE PROGRAM	5
J. H. Kelley Jet Propulsion Laboratory	

SESSION II. HYDROGEN PRODUCTION

A. Electrolysis

DEVELOPMENT STATUS OF SOLID POLYMER ELECTROLYTE WATER ELECTROLYSIS FOR LARGE SCALE HYDROGEN GENERATION	17
J. H. Russell and L. J. Nuttall General Electric Company	
DEVELOPMENT OF A REGENERATIVE SOLID POLYMER ELECTROLYTE HYDROGEN/HALOGEN FUEL CELL FOR HIGH EFFICIENCY ENERGY STORAGE	27
J. F. McElroy General Electric Company	
INVESTIGATIONS ON MATERIALS FOR ADVANCED WATER ELECTROLYZERS	34
S. Srinivasan, P. W. T. Lu, G. Kissel, F. Kulesa, C. R. Davidson, H. Huang, S. Gottesfeld, and J. Orehotsky Brookhaven National Laboratory	
ADVANCED ALKALINE ELECTROLYSIS CELL DEVELOPMENT	42
J. N. Murray and M. R. Yaffe Teledyne Energy Systems	
SELECTION AND CHARACTERIZATION OF MATERIALS FOR ADVANCED WATER ELECTROLYZERS: ASBESTOS DIAPHRAGM FAILURE AND CATHODE KINETICS	47
P. J. Moran, G. L. Cahen, Jr., and G. E. Stoner University of Virginia	
OPTICAL INVESTIGATION OF THE OXIDES OF RUTHENIUM AND IRIIDIUM IN RELATION TO THEIR ELECTROCATALYTIC ACTIVITY	50
F. H. Pollak Belfer Graduate School of Science	

THE HYDROGEN-CHLORINE ENERGY STORAGE SYSTEM	54
J. McBreen, R. S. Yeo, A. Beaufriere, D-T. Chin, and S. Srinivasan Brookhaven National Laboratory	

B. Thermochemical Cycles

THE SULFUR CYCLE WATER DECOMPOSITION SYSTEM	63
G. H. Farbman Westinghouse Electric Corporation	

CURRENT STATUS OF THE THERMOCHEMICAL WATER-SPLITTING PROGRAM AT GENERAL ATOMIC	71
J. D. de Graaf, J. L. Russell, J. H. Norman, T. Ohno, P. W. Trester, and K. M. McCorkle General Atomic Company	

ASSESSMENT OF THERMOCHEMICAL HYDROGEN PRODUCTION	79
J. R. Dafler, S. E. Foh, and J. D. Schreiber Institute of Gas Technology	

THERMOCHEMICAL HYDROGEN PRODUCTION REVIEW PANEL	83
J. E. Funk University of Kentucky	

THE LASL THERMOCHEMICAL HYDROGEN PROGRAM STATUS ON OCTOBER 31, 1977 . . .	87
K. E. Cox and M. G. Bowman University of California Los Alamos Scientific Laboratory	

REVISED FLOWSHEET AND PROCESS DESIGN FOR THE ZnSe THERMOCHEMICAL CYCLE	93
O. H. Krikorian and H. H. Otsuki Lawrence Livermore Laboratory	

STATUS OF EUROPEAN THERMOCHEMICAL HYDROGEN PROGRAMS	102
M. G. Bowman University of California Los Alamos Scientific Laboratory	

C. Advanced Concepts

APPLICATIONS OF SOLUBILITY PARAMETERS - PART I	109
D. D. Lawson Jet Propulsion Laboratory	

HYDROGEN PRODUCTION BY PHOTOELECTROLYTIC DECOMPOSITION OF WATER USING SOLAR ENERGY	115
R. D. Rauh, T. F. Reise, and S. Alkaitis EIC Corporation	

DEVELOPMENT OF A PRACTICAL PHOTOCHEMICAL ENERGY STORAGE SYSTEM	122
C. Kutal, R. R. Hautala, and R. B. King University of Georgia	

SESSION III. TRANSPORT AND CONTAINMENT MATERIALS

NASA EXPERIENCE WITH GASEOUS HYDROGEN	129
R. Hagler, Jr. Jet Propulsion Laboratory	
STUDY OF THE BEHAVIOR OF GAS DISTRIBUTION EQUIPMENT IN HYDROGEN SERVICE: UPDATE - 1977	135
J. B. Pangborn, D. G. Johnson, and W. J. Jasionowski Institute of Gas Technology	
HYDROGEN-METAL INTERACTIONS	141
H. G. Nelson NASA-Ames Research Center	
HYDROGEN COMPATIBILITY OF STRUCTURAL MATERIALS FOR ENERGY STORAGE AND TRANSMISSION APPLICATIONS	146
S. L. Robinson Sandia Laboratories	
EFFECT OF STRESS STATE ON HYDROGEN EMBRITTLEMENT PROCESSES	158
M. R. Louthan, Jr., and R. P. McNitt Virginia Polytechnic Institute	
EVALUATION OF LASER WELDING TECHNIQUES FOR HYDROGEN TRANSMISSION	164
J. A. Harris, Jr., and J. Mucci Pratt & Whitney Aircraft Group	

SESSION IV. HYDROGEN STORAGE - HYDRIDES

THE METAL HYDRIDE DEVELOPMENT PROGRAM AT BROOKHAVEN NATIONAL LABORATORY	171
J. R. Johnson and J. J. Reilly Brookhaven National Laboratory	
HYDROGEN-TECHNOLOGY EQUIPMENT TEST PROGRAM AT BNL	177
G. Strickland, A. H. Beaufriere, and M. J. Rosso Brookhaven National Laboratory	
HYCSOS: A CHEMICAL HEAT PUMP AND ENERGY CONVERSION SYSTEM BASED ON METAL HYDRIDES	181
D. M. Gruen, I. Sheft, G. Lamich, and M. H. Mendelsohn Argonne National Laboratory	
DRI RESEARCH PROGRAM ON IMPROVED HYDRIDES	191
C. E. Lundin, F. E. Lynch, and C. B. Magee Denver Research Institute	

A THERMODYNAMIC AND ECONOMIC STUDY OF VARIOUS TECHNIQUES FOR THE
LARGE SCALE PRODUCTION OF HYDRIDING GRADE FeTi 196
C. J. Trozzi and G. D. Sandrock
The International Nickel Company, Inc.

STATIONARY HYDRIDE VESSEL OF LARGE DIAMETER - PROGRAM PLAN 206
R. E. Billings, R. L. Woolley, and J. H. Ruckman
Billings Energy Corporation

SESSION V. SYSTEM STUDIES

HYDROGEN AS A CHEMICAL FEEDSTOCK (STUDY AND WORKSHOP) 213
C. J. Huang
University of Houston
K. K. Tang
Jet Propulsion Laboratory

USE OF HYDROGEN ENERGY SYSTEMS TO IMPLEMENT SOLAR ENERGY 218
T. Fujita, C. Miller, K. H. Chen, G. Voecks, and W. Mueller
Jet Propulsion Laboratory

SOLAR-CHEMICAL ENERGY CONVERSION AND STORAGE: CYCLOHEXANE
DEHYDROGENATION 234
A. B. Ritter, G. B. DeLancey, J. Schneider, and H. Silla
Stevens Institute of Technology

SYSTEM EVALUATION OF SUPPLEMENTING NATURAL GAS SUPPLY WITH HYDROGEN 246
W. S. Ku
Public Service Electric and Gas Company

HYDROGEN FROM FALLING WATER: ASSESSMENT OF THE RESOURCE AND
CONCEPTUAL DESIGN PHASE 253
W. J. D. Escher
Institute of Gas Technology
J. P. Palumbo
Pennsylvania Gas & Water Company

HYDROGEN ENGINE/STORAGE SYSTEM -- APPLICATION STUDIES 256
A. M. Karaba and T. J. Pearsall
Teledyne Continental Motors

SESSION VI. NATURAL GAS SUPPLEMENTATION

NATURAL GAS SUPPLEMENTATION WITH HYDROGEN	267
C. R. Guerra, J. E. Griffith, K. Kelton, and D. C. Nielsen	
Public Service Electric and Gas Company	
HYDROGEN AS A MID-TERM GASEOUS FUEL SUPPLEMENT BY BLENDING WITH NATURAL GAS	273
G. F. Steinmetz	
Baltimore Gas and Electric Company	

SESSION I
PROGRAM OVERVIEWS

**ELECTROLYSIS-BASED HYDROGEN STORAGE SYSTEMS:
OVERVIEW AND RATIONALE OF THE BROOKHAVEN
NATIONAL LABORATORY MANAGED PROGRAM**
F. J. Salzano
Brookhaven National Laboratory

**NASA'S SUPPORT OF DOE'S HYDROGEN ENERGY STORAGE
PROGRAM**
J. H. Kelley
Jet Propulsion Laboratory

ELECTROLYSIS-BASED HYDROGEN STORAGE SYSTEMS
OVERVIEW AND RATIONALE OF THE
BROOKHAVEN NATIONAL LABORATORY MANAGED PROGRAM

F.J. Salzano
Brookhaven National Laboratory
Upton, New York

The rationale for determining program direction, emphasis, and allocation of resources is presented in this brief summary. The rationale has been developed through interaction with the "Hydrogen" R&D Community and in light of information available on competing energy systems and on-going systems studies. It is reviewed periodically based on technical progress in the program and DOE policy guidance, and is the basis of our recommendations for changes in program direction.

A number of key problems must be solved before hydrogen can serve as a common energy carrier derivable from coal or nonfossil resources such as nuclear and solar energy. These problems generally involve the technologies of production, storage, transmission, distribution, and application in a variety of end-use devices. A number of systems studies pertaining to hydrogen technology have identified promising applications and the key research and development needs. These studies have indicated the need for a program focused on the electrolytic production of hydrogen, and safe, efficient storage of hydrogen for stationary and transportation applications. Since Brookhaven National Laboratory has exhibited significant experience in these areas, it has been chosen to develop and manage the program for DOE's Division of Energy Storage Systems. It is recognized that a program focused on these needs must involve ties with industry in order to achieve commercialization of those applications judged to be economically viable.

At the present time, hydrogen is generally not competitive with current fuel sources such as petroleum and natural gas. In time, it is expected that coal will be the major source of hydrogen for large-scale industrial applications and use of hydrogen as a chemical commodity. In general, it is believed that very large-scale uses of hydrogen as an energy carrier will exist in the long term, but enough potential applications exist in the near term involving the use of hydrogen as a chemical commodity to warrant a vigorous program at this time. These smaller industrial applications of hydrogen, e.g., as a natural gas substitute, etc., can be served by electrolytic hydrogen generated in relatively small plants at dispersed sites supplied by electric energy.

At the present time, electrolytic production plants exist in sizes ranging from 100 megawatts down to the kilowatt range. The larger plant sizes in the megawatt range are available from European manufacturers. A primary purpose of the existing program is to stimulate the development of an electrolytic equipment industry in the United States. A key objective is to achieve costs below \$150 per kW(t) and efficiencies in the range of 90%. Current costs are three times this value and efficiencies are typically in the range of 60% to 70%.

Work in the areas of electrolytic hydrogen production and storage is dedicated to the production of advanced technology prototype hardware, proof testing of components and related systems, and associated engineering systems studies. In the area of water electrolysis, both the alkaline technology currently available and the advanced solid polymer electrolytic (SPE) systems are being pursued with the emphasis on the latter SPE systems.

In conjunction with the work on hydrogen production, compatible large-scale storage systems are being developed involving metal hydrides to establish reference designs, reliable comparative cost data, and to address full-scale engineering problems.

Hydrogen has a variety of other potential applications aside from the industrial uses as a chemical commodity. These applications include the generation of electric energy in fuel cells, storage of electrical energy, and use as a transportation fuel.

The internal combustion engine can be converted to use hydrogen; however, the automotive fuel cell is potentially a more efficient (hydrogen fueled) device for vehicle propulsion. Irrespective of the propulsion source in vehicle applications, the key problem in utilization as a transportation fuel is the storage of hydrogen. The current program is focused on chemical storage methods. This primarily involves the use of metal hydride materials, but work is in progress to identify other hydrogen occluder materials. At the present stage of development the major program emphasis is on demonstration of hydrogen storage in FeTi alloys in small engineering scale prototype systems. Work is being sponsored to develop higher capacity hydrogen storage materials using lighter weight alloys more suitable for automotive applications.

In considering a number of hydrogen sources such as seasonally available electric generating capacity, there is value in methods for storage of large bulk quantities of hydrogen for seasonal periods. At the present time, helium, natural gas, and, in some places, producer gas (H_2 - CO) are stored underground. The potential for large-scale engineered storage is yet unexplored, e.g., deep undersea storage at high pressures. The present program is also aimed at development of such large-scale bulk storage methods for hydrogen produced seasonally.

An important related effort is work on the development of an electric energy system based on the storage of hydrogen in a metal hydride. This system involves the electrolysis of hydrochloric acid (HCl) to produce hydrogen and chlorine which are stored and subsequently recombined in the electrolysis cell to produce electric energy. The electrolysis technology for this scheme is closely related to the SPE technology required for electrolytic hydrogen production. SPE water electrolysis and HCl cell development are parallel efforts involving similar hardware systems.

Because of the need to involve the commercial sector, a very large fraction of the DOE funding is directed at industrial contracts and a smaller fraction at related university research efforts.

The management of these contracts within Brookhaven is done by full time representatives from the Conservation Program Management Group (CPMG) who are also concerned with overall program planning and continuous liaison with DOE Headquarters.

A Program/Budget Chart is presented in Figure 1 showing the program aggregation by technical area, funding level and emphasis, and individual contracts or projects.

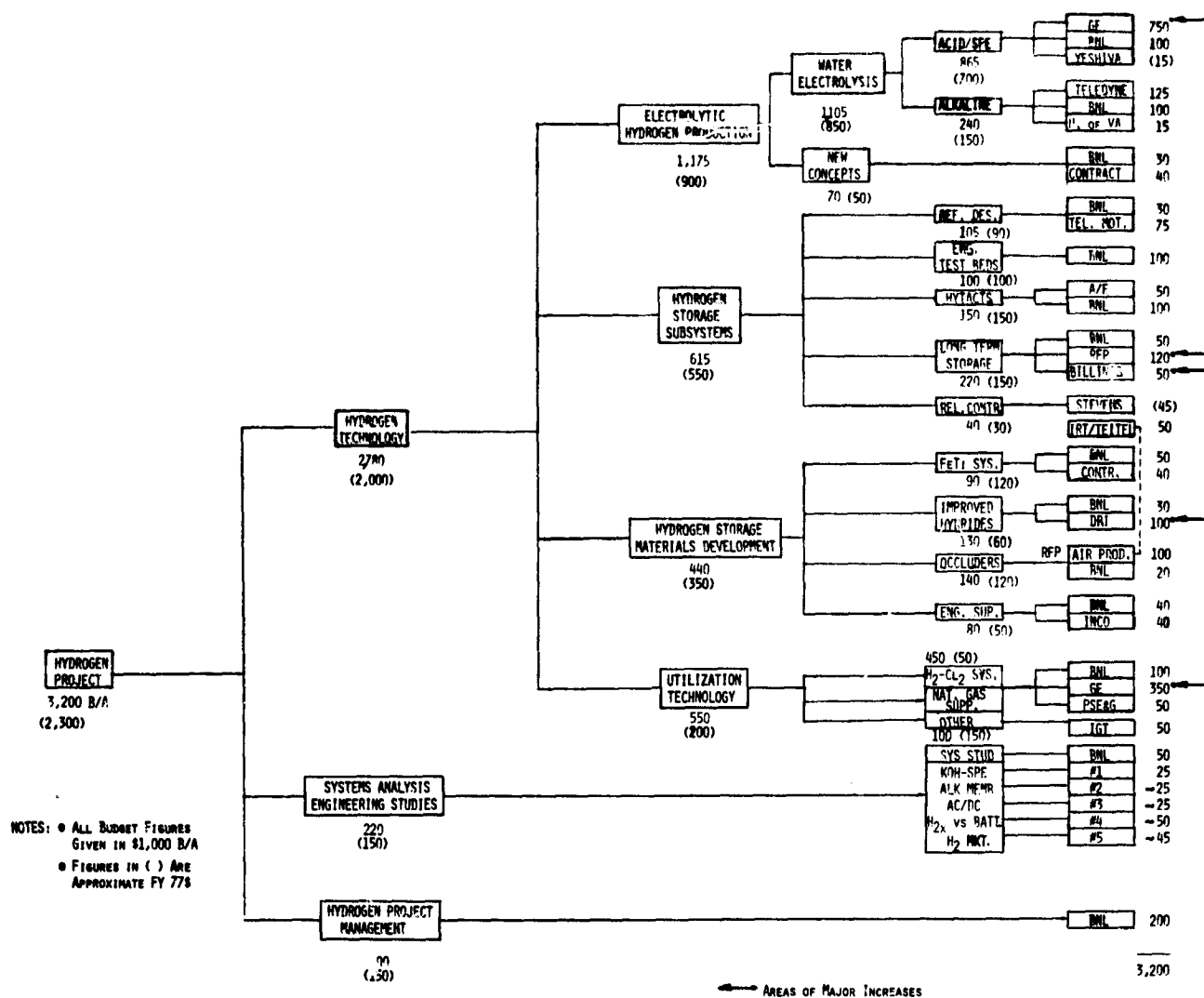


Fig. 1. Hydrogen Project Budgetary Breakdown for FY 78

NASA's SUPPORT OF DOE's HYDROGEN ENERGY STORAGE PROGRAM

J. H. Kelley

Jet Propulsion Laboratory
California Institute of Technology
Pasadena, California

ABSTRACT

Early in 1977, ERDA and NASA established Interagency Agreement EC-77-A-31-1035 through which NASA is providing assistance to ERDA in their Hydrogen Energy Storage Program. The total supporting effort has been brought together as a NASA project. It is composed of a number of elements which will be conducted at several NASA centers. The project is being coordinated and managed at the Jet Propulsion Laboratory with the Ames Research Center and the Lewis Research Center participating in the conduct and management of several elements.

In FY77, the project is largely concerned with monitoring ongoing ERDA contracts and planning for FY78 technical work. A number of specific technical tasks are planned for FY78.

INTRODUCTION

The Energy Research and Development Administration (ERDA), now Department of Energy (DOE), Division of Energy Storage Systems (STOR), in implementing a Hydrogen Energy Storage Program in 1977, requested NASA to assume project management responsibility for a portion of the program. The project encompasses thermochemical and other advanced hydrogen production techniques and containment and transport technologies. NASA brings to the project resources of existing experience and demonstrated capabilities in hydrogen technology.

BACKGROUND

The Hydrogen Energy Systems Technology (HEST) study, conducted in 1975 by NASA, was undertaken to augment an understanding of the hydrogen energy field and ensure that all potentially fruitful opportunities for energy systems via hydrogen technology were examined. Considerable scattered work in hydrogen technology and hydrogen systems had previously been undertaken by various institutions, and some consideration had been given to hydrogen in other broad studies. The HEST study was specifically an effort to identify national needs for research and technology in hydrogen production, handling and use.

In 1976, with the concurrence of ERDA/STOR, NASA undertook the development of a plan for conducting hydrogen energy storage R, D & D. In developing this plan, NASA reviewed recent studies and assessments to identify viable hydrogen energy storage system applications and to define the technology advancements needed to implement viable hydrogen energy storage options. The findings of that assessment continue to provide the basis for the development of the second-year plan presented in this document.

Assignments within the project are made with the intention of maximizing the potential benefits from previous experience. Applicable NASA experience covers a broad spectrum which includes systems analysis and studies, organic chemistry, hydrogen fuel technology, and the storage and handling of a variety of liquids and gases. Recent NASA experience, which required interfacing with several private sectors of the economy, is also of value. The personnel from the participating centers come from professional staffs having familiarity with applicable areas of hydrogen technology.

The Hydrogen Energy Storage Technology Project is a set of work elements from the DOE Hydrogen Energy Storage Program which will be conducted by NASA in FY78. Early in 1977, ERDA and NASA established an Interagency Agreement through which NASA would provide assistance to DOE by applying appropriate technical and management talents during FY77 to precursor tasks of these elements.

PROJECT ORGANIZATION

During FY78 the responsibility for implementing the elements under NASA cognizance is assigned to the Jet Propulsion Laboratory (JPL) with support from the Ames Research Center (ARC). These organizations have the required concentrations of technical expertise for implementing the NASA assignments which include hydrogen combustion

and handling, materials compatibility, and thermochemistry. JPL has provided a project manager for the activities assigned to NASA. Figure 1 presents the organization of the project for FY78 and beyond. The following assignments under the NASA project have been made.

- Ames Research Center. The Containment Materials Element is the responsibility of the ARC Materials and Physical Sciences Branch.
- Jet Propulsion Laboratory. JPL will manage the System Studies and Assessments Element, the Advanced Concepts Element, the Thermochemical Cycles Element, and the Transmission, Distribution, and Storage Container Element. (During FY77 the NASA Lewis Research Center managed the Thermochemical Cycles activities.)

ELEMENTS

PROJECT MANAGEMENT AND SUPPORT ELEMENT

The Project Management and Support Element provides the direction and principal cohesive force for the NASA project. This element brings together interfacing NASA organizations and provides a central focus for the DOE program manager. The responsibility for overall project review, analysis and planning resides within the project manager under this element. Project-level progress reporting is also accomplished within this element.

SYSTEM STUDIES AND ASSESSMENTS ELEMENT

System studies and assessments are analytical activities specifically focused on key issues regarding candidate hydrogen energy storage systems. The results from these activities will contribute to a coherent basis for programmatic decisions by identifying promising applications, expected time-frames for implementation and required technology thrusts. Comparisons among hydrogen system options as well as comparisons with non-hydrogen alternatives must be conducted in order to identify developmental areas where solutions to technical problems would make particular hydrogen systems more practicable.

Assessment of Solar/Hydrogen Systems Task

This task will identify, characterize, and analyze the potential role of hydrogen energy storage systems in facilitating the implementation of solar energy systems. Hydrogen energy storage systems add a new dimension to solar energy implementation by introducing the possibility of gaseous pipeline transmission coupled with gaseous storage, as well as the possibility of direct conversion of solar thermal energy to hydrogen. This ongoing study will focus on achieving an understanding of the role that solar/hydrogen systems can play in the context of scenarios for development and implementation of solar energy systems. Particular emphasis will be given to the analysis of unique operational modes for energy transmission and storage that are peculiar to hydrogen systems. Based on these potentially attractive operational modes, descriptions of the solar/hydrogen systems will be formulated. These systems will then be the subject of preliminary design and costing activities so that systems analyses, which

encompass practical aspects of implementation, can be performed. An integral part of the scenarios/systems analyses will be comparisons with non-hydrogen alternatives. One of the studies is:

Chemical Markets/Supply Options for Hydrogen Task

This task will determine steps which can, and should, be taken (particularly by the government) to enable and encourage chemical industries to shift hydrogen feedstocks from natural gas and naphtha to other sources. The steps may include technology enhancement in the areas of hydrogen production, delivery or storage, additional analyses or assessments, and recommendations for modifications to regulatory policies.

Current hydrogen usage in the United States is dominated by applications within the chemical and petroleum industries. During the next 25 years, the projected annual growth (between 6 and 12 percent) in hydrogen usage will cause the prices of the traditional captive-hydrogen feedstocks, natural gas and naphtha, to increase. This increase will tend to expedite the market penetration of merchant hydrogen produced from other feedstocks and by techniques less affected by increasing scarcity and rising cost. In the near future, new government energy policies could accelerate this trend toward non-traditional sources; however, the market for merchant hydrogen may be adversely affected by several basic issues, such as technology, economics, water availability, environmental impact, and regulatory policies. This task will interface closely with a University of Houston workshop and use the workshop as a data source. It will concentrate on usage by the chemical and petrochemical industries but will consider other captive users of hydrogen as appropriate. Alternative hydrogen production from coal gasification, electrolysis, and heavy oil will be considered. For each industry, the needed mixtures of gases with hydrogen and the value of hydrogen purity will be determined. The prospects of byproduct utilization will be ascertained.

ADVANCED PRODUCTION, CONVERSION, AND STORAGE CONCEPTS ELEMENT

The Advanced Production, Conversion, and Storage Concepts Element will support innovative and unusual technological findings that may lead to new approaches in hydrogen energy storage systems. Advanced technical concepts such as photolytic and biological hydrogen-production processes and the storage of hydrogen in organic compounds will be investigated and evaluated for promise of significant technological advancement. The results from this applied research will identify new methods of hydrogen production, conversion, and storage that may have advantages over present technologies in the areas of high gain, new opportunities, or the ability to take advantage of under-utilized energy sources.

Specific tasks, which bring the requirements and technology of the advanced concepts element into sharper focus and identify new technological opportunities and/or problem areas, will be selected and conducted.

Hydrogen Production by Photoelectrolytic Solar Energy Conversion Task

This task will investigate and determine the practicability of a semiconductor-electrolytic device that uses solar energy to decompose water into hydrogen and oxygen in a single-step process. The conceptual basis for this semiconductor photo-electrolyzer is that an interface between a semiconductor and an electrolyte behaves like a Schottky barrier; thus, irradiation of the semiconductor surface results in the production of pairs of electrons and holes which are separated in the field of the space-charge layer. Carriers of appropriate sign, when supplied to the electrode surface, can effect oxidation or reduction of electrolyte species. For example, O_2 is evolved from an illuminated n-type TiO_2 electrode at or below the H_2 evolution potential. When n-type TiO_2 is coupled with a metal electrode, O_2 and H_2 will be spontaneously generated by irradiation.

Photocatalytic Decomposition of Water Task

This task will prepare organic rhodium complexes and determine the feasibility of the use of these complexes for the photodecomposition of water. These complexes are often metal-cluster complexes coordinated to ligands with low-lying electronic orbitals. Some materials involving the nitrilo group with rhodium complexes have been reported in the literature. They produce hydrogen gas on excitation at 500 nm wavelength. These materials also will cause the decomposition of hydrogen bromide and hydrogen iodide. A number of rhodium complexes will be evaluated for capability during water photodecomposition through the proposed novel route.

Application of Solution Theory to Hydrogen Energy Storage Task

This task will investigate physical and chemical interactions of hydrogen with metals and determine the applicability of the solution theory of Hildebrand and Scott to the selection of materials for hydrogen production, containment, and storage devices. The results of this investigation could provide a method for quantitatively determining the optimum composition for alloys used as:

- a) Electrocatalysts for electrolysis of water and other compounds
- b) Shift catalysts for hydrogen reactions
- c) Hydrogen containment materials (low solubility)
- d) Hydrogen storage materials (hydrides)

Organic Storage of Hydrogen Task

This task will investigate reversible organic chemical reactions to determine practicability as a workable system for hydrogen storage. The bulk of the research in hydrogen storage has been in the inorganic or metallic systems. Practical metal hydrides will absorb about 2 to 4 percent hydrogen by weight. The benzenecyclohexane system can store

about 6.6 percent by weight of hydrogen. One of the problem areas with this system is that the vapor pressure of the material is high (about 100 mm at 25°C). This task will investigate more suitable organic reactions and/or compounds that can be used for hydrogen storage. The following are the ground rules.

- a) The hydrogenation-dehydrogenation reactions should have low energy requirements. Temperatures need to be under 250°C.
- b) System pressures should be less than 600 psig.
- c) Required catalytic agents must withstand a large number of cycles.
- d) The materials should not degrade under normal usage conditions.
- e) Organic-metallic compounds can be considered in this task area.

THERMOCHEMICAL CYCLES ELEMENT

A pure thermochemical cycle for hydrogen production is a system of linked, regenerative, chemical reactions which accept only water and heat and produce hydrogen. Hybrids of these cycles may also include electrolytic or photochemical reactions. These cycles can be thought of as either a source of hydrogen (for industrial use) or as a means of storing energy (by utilities, for example). Both high-temperature nuclear reactors and solar concentrators are potential sources for the high-temperature process heat required by such cycles.

The overall element objective is to find and develop cycles which use heat to thermochemically decompose water for hydrogen production. Element objectives and activities are grouped according to the task categories of the thermochemical cycles element. The element approach will be to investigate the key reactions and any problem areas of specific cycles. When all the reactions of a cycle have been demonstrated individually in the laboratory (at least on a batch-scale basis) and an engineering flowsheet for the overall process has been prepared, a preliminary assessment of cycle performance will be obtained from an objective group. Using this information, two cycles will be selected for assembly into closed bench-scale demonstrations by FY80. Bench-scale demonstration is defined as the continuous operation of a complete thermochemical cycle in a closed, integrated mode for several hundred hours. The scale for such a demonstration is somewhat greater than laboratory scale but much less than pilot-plant scale. In parallel with this effort, a supporting research and technology program emphasizing generic technologies will be conducted.

Specific Cycle Development

The objective of this task is to provide some of the laboratory data necessary for the subsequent evaluation of existing cycles prior to the selection of the three cycles for concentrated effort. Operation of a single step of a thermochemical cycle in a bench-scale, continuous mode provides valuable data (contaminant build-up, work of separation, pumping work, heat transfer, etc.) which cannot

be obtained from batch-reaction studies. These data will make it possible to develop more realistic engineering flowsheets which are required for each cycle before the cycle can be reviewed by the Evaluation Panel which is coordinated by the University of Kentucky.

- a) Complete testing of the operation of the first step of the sulfur-iodine (General Atomic) cycle in a continuous bench-scale mode.
- b) Design a pressurized electrolysis cell for H_2SO_3 electrolysis.
- c) Design and start construction of a laboratory model of the hybrid sulfur cycle.
- d) Complete updated engineering flowsheets for the sulfur-iodine cycle.

Thermochemical Water-Splitting Cycle (General Atomic) Task

The objectives of this effort are to perform process engineering on the sulfur-iodine cycle and bench-scale testing of the individual steps of the cycle. Additional engineering is required to refine and improve the process design which already shows promise. Bench-scale testing of the individual process steps will provide the data necessary for the preparation of a realistic engineering flowsheet, which is prerequisite to conducting a bench-scale demonstration of an entire cycle. The FY78 task will include the following activities:

- a) Complete the bench-scale testing of the initial reaction of the sulfur-iodine cycle.
- b) Design, construct, and start testing of a bench-scale model for iodine and water recovery from the $HI-H_2O-I_2$ lower phase produced in the initial reaction of the cycle.
- c) Complete the computer code designed to aid process optimization and flowsheet preparation and update the flowsheet for the GA cycle. This computer code should significantly reduce the time required for incorporating new laboratory developments into an engineering flowsheet.

Hydrogen Production Process Equipment (Westinghouse) Task

The objective of this effort is to assess the technical and economic feasibility of a hybrid (electrolytic/thermochemical) hydrogen-generation process based on the electrolysis of sulfurous acid. Because the theoretical cell voltage (0.17 volt) for sulfurous acid electrolysis is only 14 percent of the corresponding voltage (1.23 volts) for pure water, this hybrid process could produce hydrogen from water more economically than direct electrolysis. For this potential to be realized, cell over-voltage must be minimized, and an efficient and economic method for concentrating and decomposing the sulfuric acid which is produced by the electrolysis must be developed. A meaningful assessment of the potential for this cycle will require experimental determination of

the operating characteristics of the key process steps. These data can then be used in the engineering and economic analyses of the total system. For FY78, DOE (STOR) funds will be concentrated on the electrolyzer portion of the system. Funds for sulfur trioxide reduction are expected from DOE (Solar) under a separate contract. During FY78, this task will concentrate on the following activities:

- a) Conduct experiments aimed at choosing the electrocatalyst and electrode configurations for eventual scale-up of the electrolyzer.
- b) Design a pressurized, heated electrolyzer capable of operating at pressures up to 20 atmospheres and temperatures up to 400°K. Operation at higher pressure should improve performance by increasing the solubility of SO₂ in the anolyte at the elevated operating temperature desired for the electrolysis step.
- c) Conduct a 200-hour endurance test of a single-cell electrolyzer which embodies the best technology (anode and cathode materials and configurations) available at this time.
- d) Design and start construction of a working laboratory model of the hybrid sulfur cycle. This model will prove the scientific feasibility of water-splitting via thermochemical cycles and will serve as a test bed for subsequent testing of electrolyzer catalysts, electrodes, etc. This task will be co-funded by Westinghouse.

Supporting Research and Technology

The objective of this effort is to provide some of the data necessary for developing technologies that are common to several thermochemical cycles or for identifying new technologies that may offer alternatives to existing approaches. Activities include:

- a) Identify suitable electrode material for HBr electrolysis and determine the operating parameters for the resulting cell.
- b) Assess the feasibility of using a solar heat source, either alone or in combination with a nuclear heat source, for thermochemical cycles.
- c) Assess the trade-off between decomposing HBr and concentrating H₂SO₄ solutions.
- d) Determine the operating parameters of a selected catalyst for SO₃ reduction.
- e) Develop containment materials for thermochemical cycles.

Advanced HBr Electrolysis Studies and Solar Heat Source Feasibility Study (Inst. of Gas Technology) Task:

Advanced HBr Electrolysis Study

Hybrid electrochemical cycles may operate more efficiently and produce hydrogen at less cost than

either a pure thermochemical or a pure electrolytic process. The purpose of this electrolysis effort is to study the decomposition of HBr which is recognized as the key problem area for the sulfur-bromine cycle. If an efficient process for decomposing HBr could be found, the sulfur-bromine cycle would represent an alternative to the hybrid sulfur cycle, which utilizes electrolysis of sulfurous acid. Since the H₂SO₄ produced in the electrolysis of sulfurous acid is relatively dilute, it must be concentrated prior to decomposition. In contrast, the sulfur-bromine cycle avoids the costly concentration process because the H₂SO₄ produced in the first step of this cycle is already concentrated. The work planned for HBr electrolysis in FY78 will be a follow-on to preliminary studies started in FY77 and will involve the following activities:

- a) Experimentally determine the required voltage at a selected current density and acid concentration for a minimum of five electrode materials and five electrode catalysts. This testing will identify low-cost, corrosion-resistant materials for the electrode and the electrode catalyst.
- b) Experimentally evaluate the cell voltage over a range of current densities (50-500 mA/cm²) and acid concentrations for the best electrode material/catalyst combination determined by the initial testing.
- c) Construct an electrolysis cell capable of producing hydrogen at pressures in the range of at least 2 to 5 atmospheres over a temperature range of at least 300-400°K.

Solar Heat Source Feasibility Study

The primary objective of this effort is to analytically evaluate the technical feasibility of supplying heat to hydrogen-producing chemical cycles from solar energy alone or from solar energy in combination with nuclear energy. If the use of solar energy as the high-temperature (1150°K) heat source for thermochemical cycles is feasible, then solar energy would represent an alternative to the high-temperature nuclear reactor usually considered as the potential heat source. A secondary objective is to evaluate the feasibility of supplying heat to thermochemical cycles via a combination of high-temperature and low-temperature sources rather than from a single high-temperature source. This feasibility study will concentrate on two activities during FY78.

- a) Catalog costs for the solar and nuclear heat in the high-temperature range (1000-1150°K for nuclear sources; 1000-1500°K for solar sources) that will be required for thermochemical cycles. These costs will be obtained from the DOE Solar Electric Division and from nuclear reactor manufacturers.
- b) For two specific thermochemical cycles and two specific hybrid (electrochemical) cycles, the net heat and work will be calculated via the IGT maximum attainable efficiency methodology. The overall cycle efficiency and the estimated cost for the produced hydrogen will be calculated for each cycle assuming the

various solar and nuclear heat source combinations.

Thermochemical Processes for Hydrogen Production (DOE-Los Alamos) Task

The primary role of the Los Alamos Scientific Laboratory (LASL) in the overall thermochemical-hydrogen program (as conceived at this time) is to provide supporting research and technology in problem areas common to a number of thermochemical cycles. New techniques for solution concentration and thermochemical decomposition of HBr are examples of such activities. Technology developed in these studies will be transferred to industry. With respect to the DOE National Laboratories such as LASL, the NASA role is to provide DOE with guidelines for activities within the element plan.

Experimental Investigation of H₂SO₄ Dissociation Task

The objective of this study is to establish a base of experimentally-determined, reaction-rate and heat-transfer data for the catalytic dissociation of H₂SO₄. This decomposition is one of the key reactions occurring in several of the current contending, thermochemical water-splitting cycles. In addition, dry SO₃ dissociation, which is of interest for thermochemical cycles and as a possible means of thermal energy storage, will be investigated. The planned activities for FY78 are:

- a) Design, construct, and test the experimental apparatus.
- b) Complete experiments on dry SO₃ dissociation using a short reactor (no heat-transfer effects) and publish the results.

Materials Development for Thermochemical Cycles (DOE-Lawrence Livermore)

The objective of this study as presently perceived is to test and evaluate materials for the sulfuric acid vaporizer which will be used in the sulfur-iodine (General Atomic) and hybrid-sulfur (Westinghouse) cycles. These studies will be closely coordinated with materials studies at Westinghouse and GA to avoid unnecessary duplication. In addition to determining the amounts of corrosion occurring for a given set of conditions, the nature of the attack will also be studied for a better understanding of the corrosion mechanisms.

Cycle Evaluation

The evaluation of promising cycles for requisite data to designate the reference cycle will be continued in FY78. The review and evaluation of two thermochemical cycles designated by DOE/NASA will be completed during FY78.

Evaluation of Thermochemical Hydrogen Production Processes (University of Kentucky) Task

This task provides an independent, unbiased, standardized review and evaluation of promising thermochemical cycles, designated by NASA and approved by DOE. To carry out these reviews, the University of Kentucky established an Evaluation Panel in FY77. Representatives of the academic

community, the DOE National Laboratories, and private industry have been included on this panel. To enhance the credibility of the economic analysis of these cycles, members of chemical engineering design organizations (such as Combustion Engineering-Lummus) will be included on the panel. In order for a cycle to be a candidate for evaluation by the panel, all the individual chemical reactions in the cycle must have been demonstrated in the laboratory (at least on a batch-reaction basis) and an engineering flowsheet for the process must be available. Using a standardized format, the panel will prepare a report for each reviewed cycle which constitutes their best appraisal of the current status of the cycle.

TRANSMISSION, DISTRIBUTION, AND STORAGE CONTAINER ELEMENT

This element addresses the transport of hydrogen, particularly as a compressed gas, and the technically-related storage of gaseous hydrogen. These subjects are combined into the same grouping because of related technical disciplines, such as containment and compression. Widespread distribution of gaseous hydrogen in residential and commercial applications appears to be a far-term possibility; however, storage and relatively short-distance transmission are integral parts of all gaseous hydrogen systems. Planned activities will promote a better understanding of the longer-range needs of large-scale hydrogen transmission and distribution and provide the data base for the development of low-cost, facility-scale transmission and distribution methods and inexpensive bulk storage techniques for near-term applications.

The fundamental objective of this element is to develop minimum-cost technology for transmission, distribution, and storage of gaseous hydrogen. One 5-year goal is to determine the techno-economic characteristics of bulk storage techniques which have potential for low-cost bulk storage. Another 5-year goal is to understand the technical necessity for and the economic trade-offs associated with new pipeline and storage materials for conformance with pressure vessel safety requirements. Designs of innovative pipeline/storage systems using conventional and new materials will be closely coordinated with containment materials research studies. Initial efforts will be directed toward the identification and exploitation of systems which appear to be promising near-term candidates for gaseous hydrogen containment. Systems which have only longer range possibilities will be evaluated for practicability and future study efforts will be recommended.

Hydrogen Service Equipment Testing Task

This task is conducting performance and degradation tests on commercially-available natural gas service equipment while simulating operation in a hydrogen grid. The nation has a large investment in existing natural gas transmission and distribution equipment. Should it become desirable in the future to make widespread distribution of hydrogen, either pure or as a diluent, clearer decisions will be possible if the performance of existing equipment is understood. In FY77, a small-scale test grid was set up to flow hydrogen or mixtures of natural gas and hydrogen through standard natural gas equipment in a controlled

manner for assessment of equipment performance and identification of compatibility problems. Phase II of this task plans to use that facility to continue the testing of standard equipment as follows:

- a) Materials testing and operational testing of selected components from Phase I.
- b) Evaluation of technical problems associated with distribution of various mixtures of natural gas and hydrogen.
- c) Additional loop testing of selected components with hydrogen.
- d) Permeability studies on plastic and composite piping.

Storage Containers for Gaseous Hydrogen Task

This task will identify factors in the current design criteria for gaseous hydrogen storage containers which are conducive to excess weight or cost and will evaluate novel designs or construction techniques for improved storage container capability. The commercially-utilized storage containers ("K" bottles and "tube" tanks) for small quantities of gaseous hydrogen represent the "brute-force" approach to pressure vessel design. Facility tanks for storage of larger quantities of hydrogen do not significantly improve the ratio of the stored volume of hydrogen to container weight. Recent advances in the determination of the precise physical properties for containment materials and in the verification of container construction techniques have resulted in safe, lightweight tanks for containment of hostile media (pressurants and propellants) in aerospace applications. Improvements in the fabrication of parts from composite materials are continually being demonstrated in successful aircraft applications. This task will consolidate the existing design requirements for gaseous hydrogen storage containers and identify the criteria which represent overdesign. Recommendations for appropriate reductions in design safety factors will be made. Suggestions for studies and investigations which would enlarge the existing data base and extend the optimization process for storage containers will be made. Novel construction materials and techniques will be evaluated for capability and suitability for the fabrication of storage containers for gaseous hydrogen. A design approach for further evaluation and possible demonstration will be recommended.

CONTAINMENT MATERIALS ELEMENT

The Containment Materials Element is a supporting technology which is inherently associated with potential successes in the production, storage, transport, and energy conversion of hydrogen. All technological elements of the Hydrogen Energy Storage Program require the containment of chemical environments; therefore, a full knowledge of potential interactions between the specific environments which must be contained and the containment materials is required for prediction of the lifetimes of components and systems and the determination of potential extensions of capability. For the Transmission, Distribution, and Storage Vessels Element, containment materials are integral to the optimum design and economic trade-offs associated

with systems studies. Hydrogen safety, where safety is the result of good design and correct materials selection, requires a complete knowledge of hydrogen material interactions.

Present materials technology permits the selection of containment materials which will remain reasonably free from environmental degradation in most aggressive environments of concern to the various technological elements; however, the operating conditions of the systems are either constrained or the materials are expensive. For example, hydrogen containment materials are either ferrous alloys containing high concentrations of alloying additions, such as austenitic stainless steels, or are based on some nonferrous alloy system. Such materials are expensive and their required use could seriously hinder the future development of large-scale hydrogen energy storage, transport, and conversion systems. If future systems must be based upon our present materials technology, a serious depletion of our supply of rarer metals will result. Therefore, in order to permit the implementation of large-scale hydrogen energy systems, methods must be found for the effective use of existing low-cost materials or new materials which will retain their compatibility for long and predictable periods of environmental exposure must be developed. The presently envisioned objectives for this element are based upon the extension of knowledge concerning H₂/ferrous alloy behavior as related to the presently identifiable needs of the technological elements of the Hydrogen Energy Storage Program.

Thermal Processing Task

This task will:

- a) Develop an understanding of the influences of microstructure on the susceptibility of mild steels to hydrogen degradation.
- b) Identify the least susceptible microstructure which can be easily obtained in commercially-available, mild steels through normal thermal processing procedures.

Insufficient knowledge is presently available regarding the potential degrading influence of hydrogen on the mechanical properties of mild steels. If, as indicated, susceptibility to embrittlement is strongly sensitive to microstructural variations, material microstructures, obtainable by normal thermal processing techniques, may yield inexpensive, commercially-available alloys which are reasonably free from the degrading effects of environmental hydrogen. This task will be carried out in an in-house program at the Ames Research Center-NASA using commercially available alloys and normal thermal processing techniques.

State of Stress Task

The task will determine the importance of the state of stress effect on the ease of crack initiation and propagation in structural steels exposed to and/or containing hydrogen. An extended knowledge of the state of stress influence could provide important information which would increase the flexibility and the reliability of materials selection for hydrogen service. This task will be

accomplished by contract and will be a continuation of current effort in this area. Data will be taken on well-characterized materials using unique specimen configurations which provide uniaxial, biaxial, and triaxial states of stress.

Stable Crack Growth Task

This task will establish the role of hydrogen in the stable crack growth behavior of mild steel at stress levels approaching those required for unstable fracture.

Stable crack growth will occur in ductile materials at stress levels approaching those required for unstable fracture. Because this could be a primary mode of failure in a statically-stressed, hydrogen pipeline, the influence of a gaseous hydrogen environment on stable crack behavior should be established. Hydrogen-enhanced crack growth will be investigated at stress levels near the unstable fracture domain using such experimental techniques as J-integral or COD measurement.

Manufacturing and Fabrication Defects Task

As presently perceived this task will:

- a) Determine if structural defects, resulting from the manufacturing and fabricating techniques utilized in pipeline construction, accentuate the susceptibility of mild steel to environmental hydrogen degradation.
- b) Establish the influence of mechanical flaws (external and internal to the pipeline wall) on the mechanical integrity of pipeline material during simulated pipeline operation.
- c) Determine the mechanical integrity of welded pipe sections fabricated under well-characterized procedures when tested under simulated conditions of pipeline operation.

A data base on the suitability of well-characterized manufacturing and fabrication procedures is required to reliably and accurately

predict the integrity of an operational hydrogen pipeline system. Well-characterized processes and procedures will be studied under simulated operational conditions using the unique hydrogen pipeline-loop located at Sandia Laboratory, Livermore.

This task will be carried out at the Sandia Laboratory, Livermore, using their extensive expertise in manufacturing and process techniques and their unique hydrogen pipeline-loop test facility.

Hydrogen/Methane Blends and Metal Hydrides Task

This task will determine if potential compatibility problems exist when mild steels under stress are exposed to environments of molecular hydrogen in hydrogen/methane blends or when protonic hydrogen, created by the dissociation of metal hydrides, is in intimate contact with the metal. Hydrogen in the form of hydrogen/methane blends is being considered as a possible supplement to our natural gas supply. It is important to establish whether or not such blends will degrade the mechanical integrity of pipeline steels. Metal hydrides are being developed as one method of hydrogen storage. It is important to establish whether or not the intimate contact of the protonic hydrogen, which is created by the dissociation of such hydrides, will have a degrading effect on mild steel. This task is a continuation of an in-house effort at the Ames Research Center-NASA.

Laser Welding Task

This task will determine if laser welding is a feasible method for joining hydrogen transmission systems. The feasibility of laser welding as a technique for the construction of hydrogen pipelines will be determined by comparing the mechanical and metallurgical properties of parent materials and weldments produced by arc and electron-beam welding with similar properties of laser weldments. This task is a continuation of a contract with the Pratt and Whitney Aircraft Group.

ACKNOWLEDGEMENT

This overview is primarily a condensation of our draft Annual Operating Plan for FY78. Major contributions were made to it by Dr. Charles Baker of LeRC, Dr. Howard Nelson of ARC and Messrs Ray Hagler and Gene Laumann of JPL.

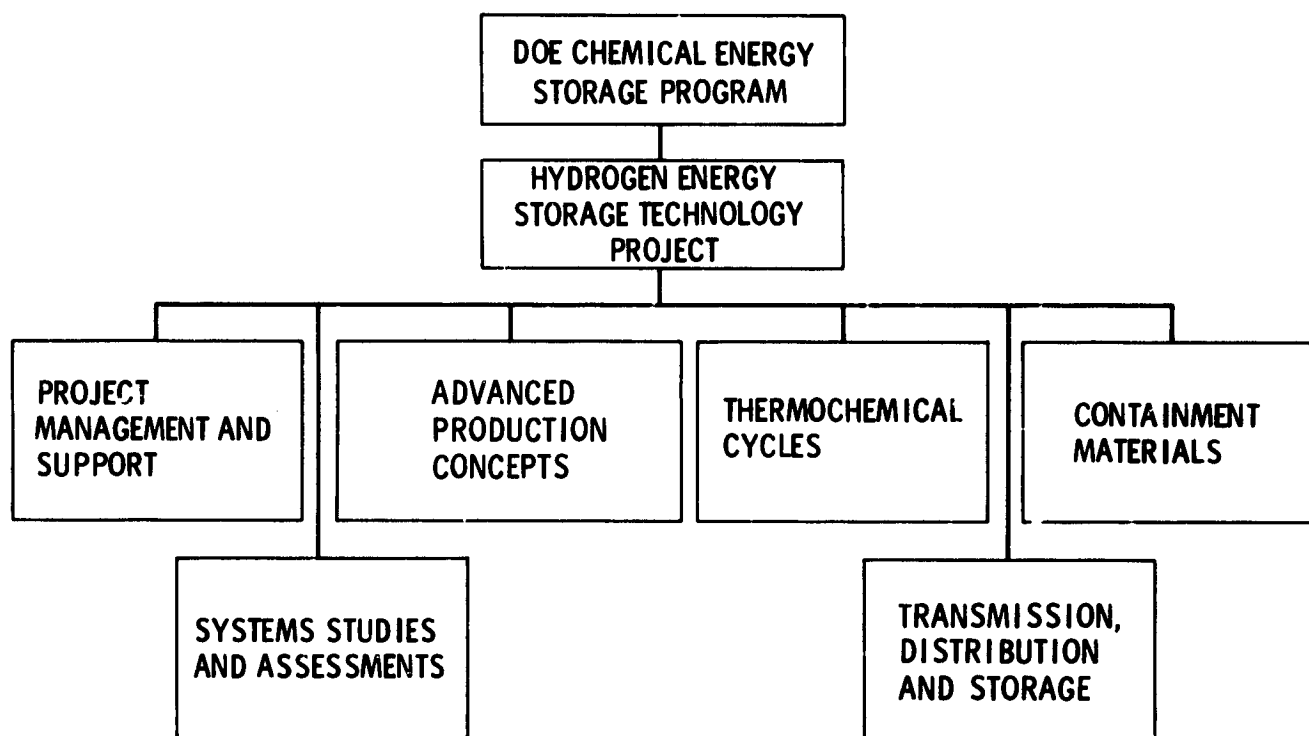


Fig. 1. Project Structure

SESSION II
HYDROGEN PRODUCTION

A. ELECTROLYSIS

**DEVELOPMENT STATUS OF SOLID POLYMER ELECTROLYTE WATER
ELECTROLYSIS FOR LARGE SCALE HYDROGEN GENERATION**

J. H. Russell and L. J. Nuttall
General Electric Company

**DEVELOPMENT OF A REGENERATIVE SOLID POLYMER ELECTROLYTE
HYDROGEN/HALOGEN FUEL CELL FOR HIGH EFFICIENCY ENERGY STORAGE**

J. G. McElroy
General Electric Company

INVESTIGATIONS ON MATERIALS FOR ADVANCED WATER ELECTROLYZERS

**S. Srinivasan, P. W. T. Lu, G. Kissel, F. Kulesa, C. R. Davidson,
H. Huang, S. Gottesfeld, and J. Orehtsky**
Brookhaven National Laboratory

ADVANCED ALKALINE ELECTROLYSIS CELL DEVELOPMENT

J. N. Murray and M. R. Yaffe
Teledyne Energy Systems

**SELECTION AND CHARACTERIZATION OF MATERIALS FOR ADVANCED
WATER ELECTROLYZERS: ASBESTOS DIAPHRAGM FAILURE AND
CATHODE KINETICS**

P. G. Moran, G. L. Cahen, Jr., and G. E. Stoner
University of Virginia

**OPTICAL INVESTIGATION OF THE OXIDES OF RUTHENIUM AND IRIIDIUM
IN RELATION TO THEIR ELECTROCATALYTIC ACTIVITY**

F. H. Pollak
Belfer Graduate School of Science

THE HYDROGEN-CHLORINE ENERGY STORAGE SYSTEM

J. McBreen, R. S. Yeo, A. Beaufre, D-T. Chin, and S. Srinivasan
Brookhaven National Laboratory

Page intentionally left blank

DEVELOPMENT STATUS OF SOLID POLYMER ELECTROLYTE WATER ELECTROLYSIS FOR LARGE SCALE HYDROGEN GENERATION

J. H. Russell and L. J. Nuttall

General Electric Company
Wilmington, Mass.

Abstract

In a joint U. S. Department of Energy, Utility and Company sponsored program, General Electric is developing the solid polymer electrolyte (SPE) water electrolysis technology for large scale hydrogen generation applications. The goals for this program were established on the basis of a design study for a 58 MW plant that was conducted in 1975.¹ Subsequent parallel technology development and hardware scale-up efforts have resulted in significant progress toward the accomplishment of these goals.

Developments to date under this program include a cell design capable of operation at much higher temperatures (up to 150°C) and having a much lower manufacturing cost than the baseline design used in previous aerospace electrolysis applications. An improved oxygen evolution electrocatalyst has also been found which is both less expensive and more efficient than the baseline cell.

As a first step in scaling up to large size cells, the design of a 2-1/2 ft² active area cell has been completed and fabrication is in progress. A 50 KW module, consisting of 12 cells of this design is expected to be on test by mid-1978. Photographs of the cell hardware are shown and preliminary test results presented.

Background

In last year's meeting, General Electric reported on the program which we are engaged in to develop an efficient, economic, large scale water electrolysis system using the solid polymer electrolyte cell technology. The goal of this program is to develop an improved technology which can make water electrolysis a viable alternative in the overall energy field as a means of conserving and supplementing increasingly scarce supplies of natural gas. This effort is presently being sponsored by the U.S. Energy Research and Development Administration, the Niagara Mohawk Power Company, the Empire State Electric Energy Research Corporation and the General Electric Company.

The solid polymer electrolyte technology was selected for this program on the basis of outstanding performance and operating characteristics which have been demonstrated in systems developed for aerospace and military applications. These characteristics include the following:

1. Significantly higher cell efficiency than conventional electrolyzers, resulting in lower power consumption per unit of gas generated¹.
2. Higher current density capability resulting in lower capital cost, size and weight for the electrolysis modules.
3. The electrolyte is chemically bound in the polymer chain, resulting in a system with no free corrosive liquids to be concerned with during design, assembly, operation or maintenance of the system.
4. A solid electrolyte makes possible greater simplicity in the system design as well as improved reliability and safety.

At the outset of the program in 1975, a design study was conducted for a 58 MW_t system (625,000 SCFH OF H₂), an artists concept of which is shown in Figure 1. On the basis of the study

results, the goals for the development program were established as follows:

Overall System Efficiency	85 - 90%
System Capital Cost	≤\$100/KW
Life	Cell - 40,000 hours System - ≥20 years
Scale up	5MW Demo. Syst.

The goals relating to the system efficiency and capital costs are shown more specifically in Table 1. Using the values for the high pressure system, the cost for electrolytic hydrogen produced by such a system is shown on Figure 2 as a function of electric power costs and duty cycle. Under the ground rules established for the study it was assumed that off-peak electric power would be available at 10 mils/KWH for a 40% duty cycle. Under these conditions the resulting hydrogen would cost approximately \$5/MBTU without taking any credit for the by-product oxygen.

In a separate study which relates to the possible large scale use of electrolytic hydrogen to supplement natural gas supplies, the Institute of Gas Technology estimated the possible economics of using this type of advanced electrolysis in conjunction with a dedicated nuclear plant to generate the electrical power. The results are shown on Table 2, indicating a possible cost for the hydrogen of \$5.36/MBTU with no credit for the by-product oxygen, and \$4.22/MBTU including a \$10/ton oxygen credit.

Development Program

In order to achieve the above cost and efficiency goals, the development program is directed primarily at the following areas:

For lower cost -

1. Low cost materials for separators and current collectors.
2. Elimination of gasket seals.
3. Use of lower cost catalyst.
4. Reduced catalyst loadings.
5. Lower cost electrolyte.

¹L. J. Nuttall, "Conceptual Design of a Large Scale Water Electrolysis System Using Solid Polymer Electrolyte Technology," presented at 1st World Hydrogen Energy Conference, March, 1976.

For higher efficiency --

1. Operation at higher temperature (up to 150°C).
2. Improved catalytic electrodes.
3. Optimization of the electrolyte and cell design.

In parallel with these technology development efforts, a cell scale-up effort is underway to design, fabricate and test: first, a 200KW (2160 SCFH) module which will continue to be used for in-house development testing as the various improved technology items reach a point where they are ready for incorporation into the scaled-up cell design; second, a 500 KW (5400 SCFH) prototype system which will be delivered to the Brookhaven National Laboratory (or some other site to be designated) where it will be tested under typical operational conditions, possibly in conjunction with a metal hydride hydrogen storage system; and, finally a 5MW full scale demonstration system which is planned to be installed in the Niagara Mohawk Power Company network where it will generate hydrogen using off-peak electrical power. The hydrogen produced at this installation will be injected into the natural gas pipeline where it would supplement the natural gas to meet peak energy demands at other locations in their system.

Current Status

Development progress in all of the above areas has been very encouraging and continues to support the feasibility of achieving, or very nearly achieving, the original program goals (recognizing that the cost goals were based on 1975 dollars).

Reduced Cost

In the area of reduced costs, the progress made to date is presented in Table 3 which compares the 1977 baseline (which forms the basis for the initial scaled-up cell design) with the 1975 baseline, representing the technology at the beginning of the program. Also shown is an estimate of the 1978 baseline which represents additional improvements that have been identified and are in the process of laboratory cell evaluation and which are expected to be ready to begin incorporating in the large scale cells in 1978.

A graphic representation of this information is shown on Figure 3.

The greatest part of the cost reduction realized to date has resulted from the development of a molded carbon and phenolic separator/current collector to replace the transition metal screens and separator sheet which was used in the 1975 configuration. This development also includes a gasketless sealing configuration which not only eliminates the need for expensive silicone rubber gaskets as used in the earlier design, but also provides a more reliable seal that will permit leak-tight operation up to 500-600 psi gas pressures.

This cell configuration has demonstrated good performance (comparable to that of the previous metal current collectors) out to current densities in excess of 5000 amps/Ft², as shown on Figure 4. Life testing of this configuration now exceeds 5000 hours at 1000 ASF, more than 700 hours at 2000 ASF and 400 hours at 3000 ASF, all at 300°F.

The other area contributing to the reduction is the use of a lower cost catalyst on the anode (which also provides a significant increase in performance as described below) and a slightly lower catalyst loading on the cathode (2 gm/Ft² vs. 4 gm/Ft²).

During the next year major emphasis will be placed on further reductions in catalyst loadings and on the continued development

of a lower cost SPE material. Catalyst loadings as low as 0.2 gm/Ft² on the cathode and 1 gm/Ft² on the anode have been tested, and methods for practical application of even lighter loadings are being investigated.

Radiation grafted poly trifluorostyrene (TFS) still appears promising as a lower cost SPE material. Two probable causes for the performance decay with time have now been identified and corrective measures have been established. Operational evaluation of the improved material is just getting underway.

Improved Efficiency

The performance goal of this development program is represented by the estimated 1980 polarization curve shown in Figure 5. Most of the improvement from the 1975 baseline performance, also shown on this curve, results from increasing the operating temperature from 180°F to 300°F. As mentioned above, more than 5000 hours of life testing has been accumulated to date without any serious problems. The results of this testing tends to confirm the potential for achieving more than 40,000 hours of life for the cell operating under these conditions.

Most of the additional ~ 70 mv improvement needed at 1000 ASF to achieve the program goal is expected to result from improved anode catalyst development, with some further improvement possible in the electrolyte performance. More than 20 candidate catalysts have been screened to date and the three most promising have been subjected to longer term life testing. The results shown on Figure 6 indicate that the catalyst WE-3 is very stable, comparable with the baseline WE-4 catalyst, and is demonstrating a sustained 40 - 50 mv superior performance. In addition, this catalyst is considerably less expensive, having a cost of approximately 55% of that for the WE-4.

Cell Scale-up

An initial scale-up from the laboratory cell size of 7.2 in² to 1 Ft² with a carbon separator/current collector configuration was made under a privately funded HCl electrolysis program. A 2-cell module of this size is shown in Figure 7. The performance and operating characteristics have been virtually identical with the smaller laboratory cells.

Under the water electrolysis program, a 2 1/2 Ft² cell design has been completed and fabrication of the components for a 12-cell (~50 KW) module is in progress. Figure 8 shows one of the early membrane/electrode assemblies (M&E's) which has been fabricated. Although the hardware is not yet available to test the complete cell, smaller cut outs from the first four M&E's made have been tested, and show performance comparable to, or better than, the baseline laboratory cells as shown on Figure 9.

Figure 10 shows a mock-up of the 50 KW module which will be on test by the middle of next year. A cut away of this module is shown in Figure 11 which illustrates the cell design details.

Program Milestones

A reduction in the amount of funding available from ERDA in 1977 and 1978 has resulted in a slippage in the schedule for this program as reported last year. A revised program plan was therefore submitted earlier this year which indicated the possible timing and milestones as shown on Table 4.

TABLE 1

PROGRAM GOALS
BULK HYDROGEN GENERATION - WATER ELECTROLYSIS

SYSTEM COST:

INSTALLED ELECTROLYSIS SYSTEM		\$82/KW _e
● ELECTROLYSIS MODULE	\$13/KW _e	
● POWER CONDITIONER	\$39/KW _e	
● ANCILLARY COMPONENTS	\$15/KW _e	
● INSTALLATION	\$ 8/KW _e	

SYSTEM PERFORMANCE:

SYSTEM ENERGY EFFICIENCY	90%	85%
ELECTROLYSIS MODULE EFFICIENCY	93%	88%
- CELL VOLTAGE AT 1000 ASF	1.58	1.63
- OPERATING TEMPERATURE -°F	300	300
- HYDROGEN PRESSURE	100 psia	600 psia
ACTIVE CELL AREA 10FT ²		

TABLE 2

NUCLEAR-ELECTROLYTIC HYDROGEN PRODUCTION FACILITY
ESTIMATED ANNUAL COSTS*

ITEM	ANNUAL COST, \$10 ⁶	\$ / 10 ⁶ Btu OF H ₂ PRODUCED
NUCLEAR-TO-ELECTRICITY SUBSYSTEM		
FUEL	27.5	0.79
OPERATING AND MAINTENANCE	6.1	0.17
FIXED CAPITAL CHARGES (\$ 737 X 10 ⁶ AT 17.6%)	129.7	3.72
SUBTOTAL	163.3	4.68
ELECTRICITY-TO-HYDROGEN SUBSYSTEM		
PRODUCTION MATERIALS	0.2	0.01
WATER	0.8	0.02
DIRECT LABOR	1.3	0.04
MAINTENANCE LABOR	1.4	0.04
MAINTENANCE SUPPLIES	1.4	0.04
SUPERVISION	0.4	0.01
ADMINISTRATION AND OVERHEAD	5.8	0.17
FIXED CAPITAL CHARGES (\$ 69 X 10 ⁶ AT 17.6%)	12.1	0.35
SUBTOTAL	23.4	0.68
TOTAL COST	186.7	5.36
POSSIBLE OXYGEN BY-PRODUCT CREDIT (\$10/SHORT TON)		.64
NET COST		4.72

* FROM "EFFICIENCY AND COST ADVANTAGES OF AN ADVANCED TECHNOLOGY
NUCLEAR-ELECTROLYTIC HYDROGEN-ENERGY PRODUCTION FACILITY"
-T.D. DONAKOWSKI & W.J.D. ESCHER. ACS CENTENNIAL MEETING, APR 4-9, 1976.

TABLE 3

ESTIMATED MODULE PRODUCTION COSTS

KEY COMPONENT	1975 BASE	1977 BASE	1978 EST	GOAL
CURRENT COLLECTOR	\$160/FT ²	\$30/FT ²	23	\$7/FT ²
CATALYTIC ELECTRODES	\$69/FT ²	\$27/FT ²	8	\$2/FT ²
SOLID POLYMER ELECTROLYTE	\$25/FT ²	\$25/FT ²	12	\$3/FT ²
STACK HARDWARE	\$6/FT ²	\$6/FT ²	6	\$6/FT ²
	\$260/FT ²	\$88/FT ²	50	\$18/FT ²
	(\$188/KW)	(\$84/KW)	(\$36/KW)	(\$13/KW)

TABLE 4

PROGRAM GOALS
SCALED-UP HARDWARE PERFORMANCE

	TECHNOLOGY			
	50 KW _e	200 KW _e	500 KW _e	5 MW _e
PROPOSED TIME PERIOD	MID '77	MID '79	END '81	EARLY '83
PROJ. MODULE COST (IN PRODUCTION HARDWARE)	\$88/FT ²	\$70/FT ²	\$50/FT ²	\$18/FT ²
ELECTROLYSIS MODULE EFFICIENCY (100 psia)	80%	85%	90%	93%
- CELL VOLTAGE AT 1000 ASF (100 psia)	1.85	1.75	1.65	1.58
- OPERATING TEMP.	180	180/300	300	300°F
- OPERATING PRESSURE	300	300/600	600	600
- CELL ACTIVE AREA	2½ FT ²	2½ FT ²	10 FT ²	10-30 FT ²

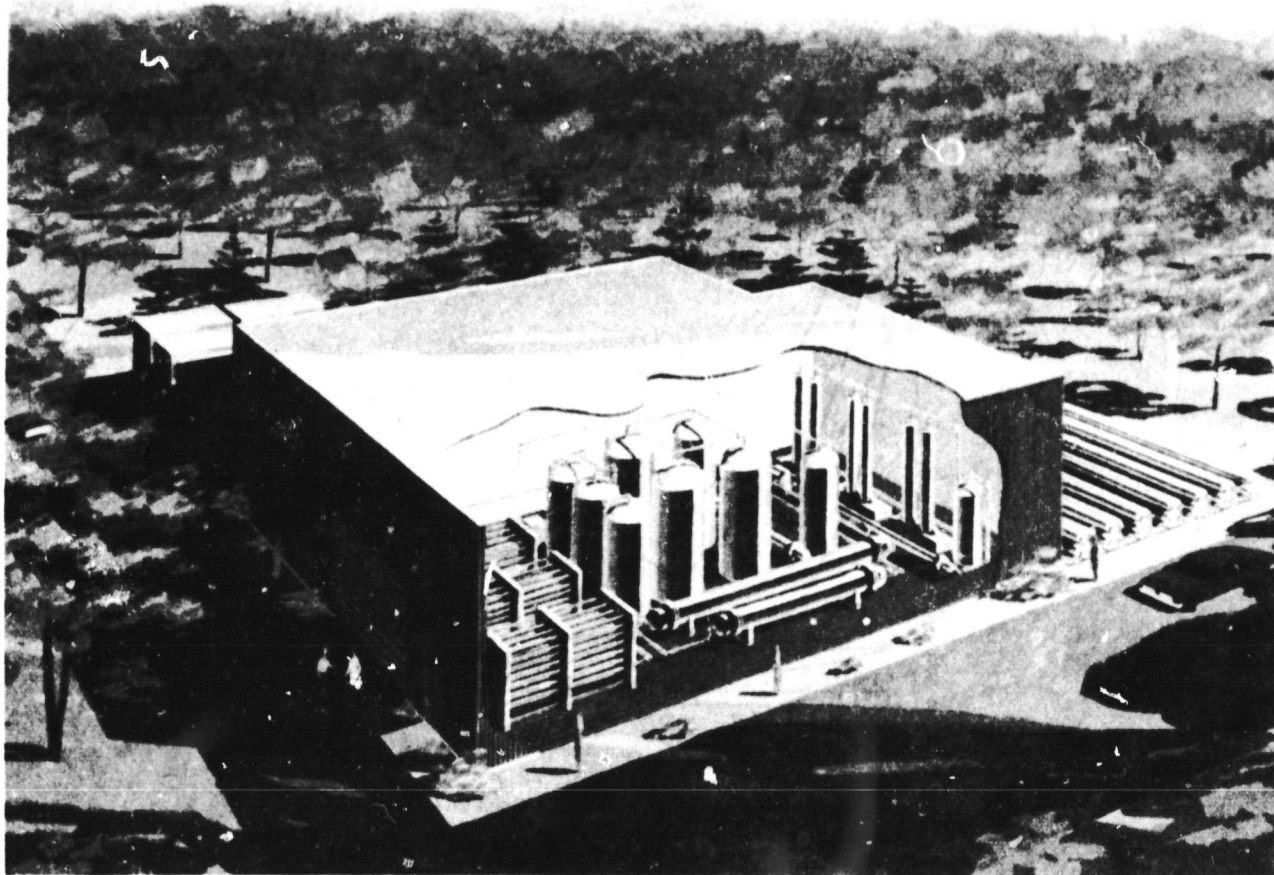


Figure 1. 58 MW SPE Water Electrolysis Plant

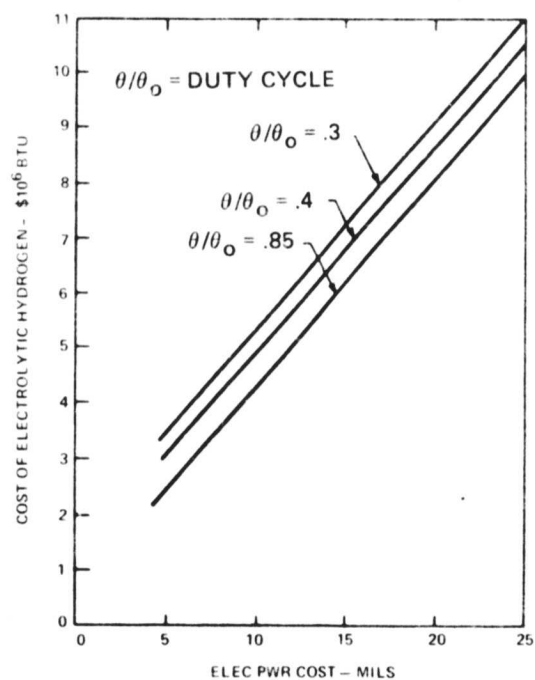


Figure 2. Cost of Electrolytic Hydrogen

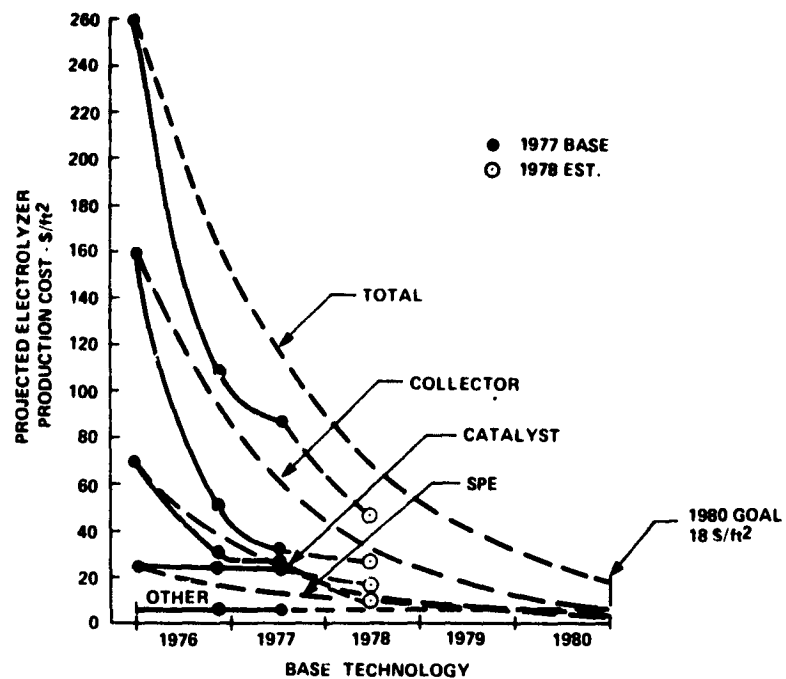


Figure 3. Projected Production Cost - SPE Electrolyzer Module



Figure 4. Performance High Current Density

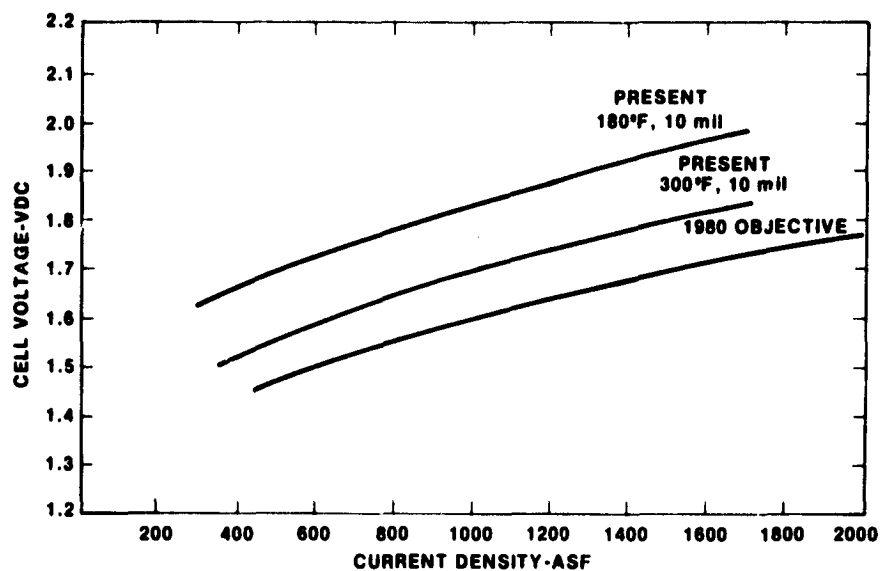


Figure 5. SPE Electrolysis Performance

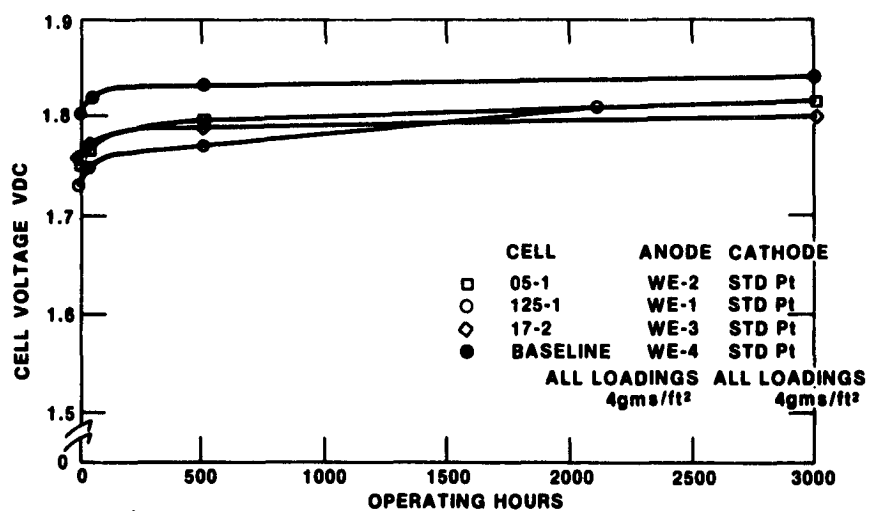


Figure 6. 3000 Hour Anode Alloy Evaluation

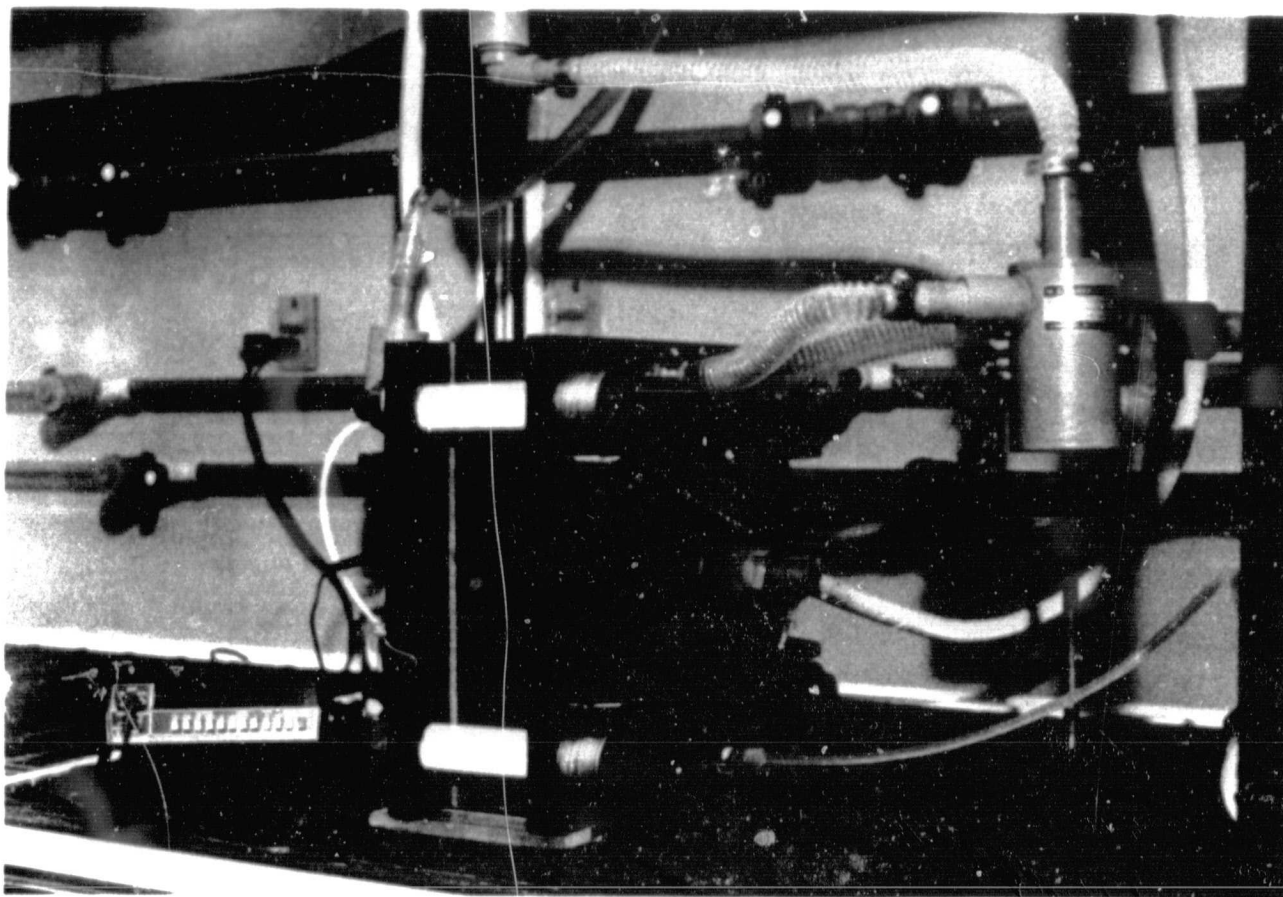


Figure 7. HCl Electrolysis 2-Cell Module – (1 Foot² Cell Area)



Figure 8. 2½ Foot SPE Membrane/Electrode Assembly

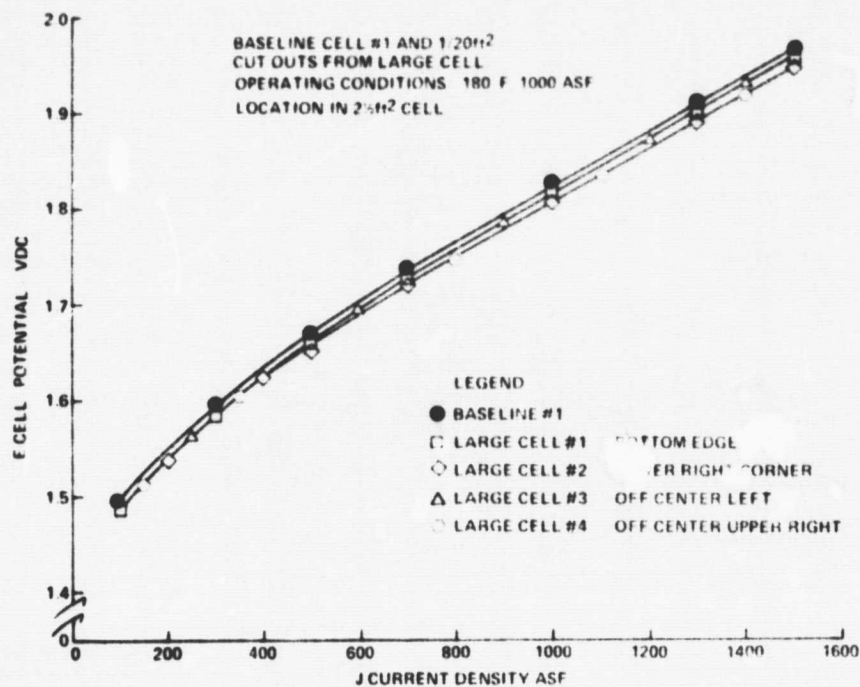


Figure 9. Water Electrolysis
48 Hour Performance Comparison

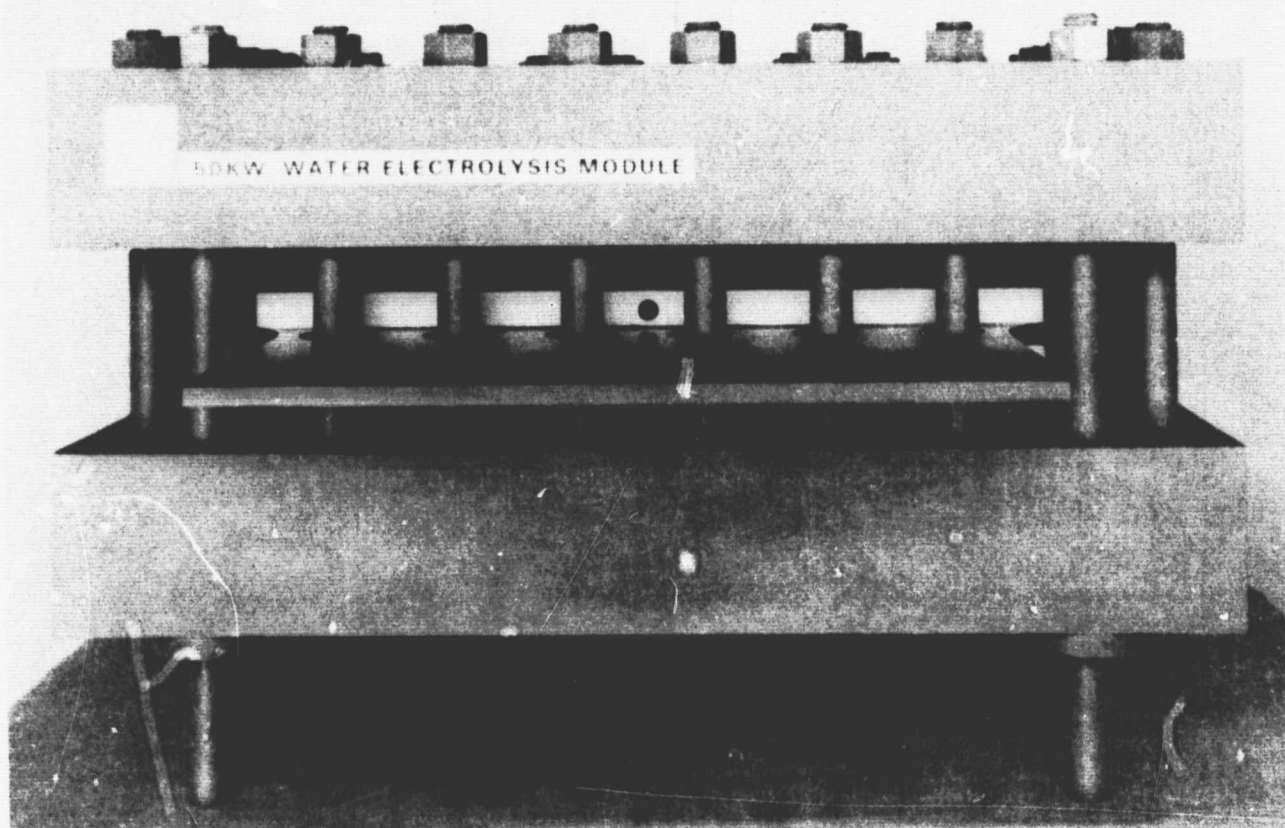


Figure 10. Mockup - 50 KW Electrolysis Module

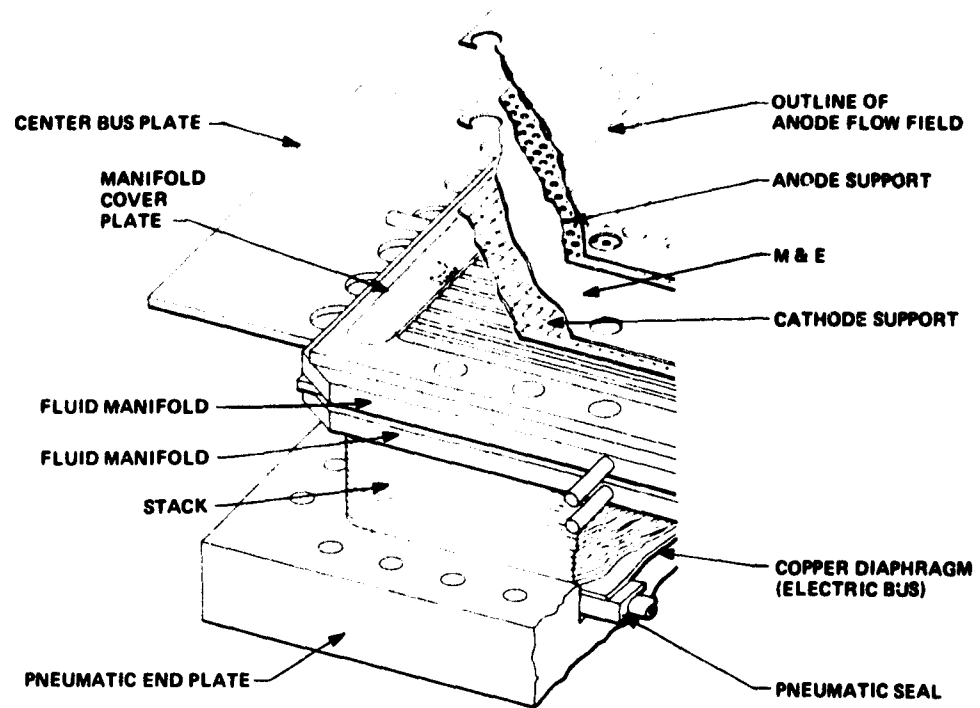


Figure 11. Single Cell Detail

DEVELOPMENT OF A REGENERATIVE SOLID POLYMER ELECTROLYTE HYDROGEN/HALOGEN FUEL CELL FOR HIGH EFFICIENCY ENERGY STORAGE

James F. McElroy
General Electric Co.
Wilmington, Mass.

Abstract

An economic and efficient means of energy storage has long been desired by electric utilities and others. Pumped hydro requires large land use whereas storage batteries can be of higher costs and lower reliability. The use of the solid polymer electrolyte with its proven long life (>45,000 demonstrated) provides the basis for a high reliability hydrogen/halogen regenerative fuel cell for energy storage. With current densities in excess of 300 ASF the system economics becomes attractive.

A preliminary system description is provided for the hydrogen-chlorine cycle. The results of feasibility tests, initial cell development and preliminary cost analyses are also discussed.

System Description

A preliminary system design concept is shown in Figure 1. In this concept the solid polymer electrolyte electrochemical unit will produce gaseous hydrogen and chlorine during the electrolysis charge mode and consume gaseous hydrogen and chlorine dissolved in aqueous HCl during the discharge mode with an overall electric to electric efficiency in excess of 70%. The gaseous chlorine produced during the HCl electrolysis is liquified utilizing 40°C cooling water and separately stored. This technique sets the chlorine storage system pressure considerably below that which would be obtained by producing liquid chlorine in the cell at 90°C with a significant storage system cost reduction. During discharge, the liquid chlorine is metered into the circulating aqueous HCl solution at a rate determined by the electrical load demand.

The hydrogen gas produced during the electrolysis charge mode is purified and stored in an iron titanium hydride storage bed. This hydrogen is then released to the cell during discharge utilizing waste heat from the electrochemical cell to liberate the hydrogen from the hydride.

The Hydrogen/chlorine energy storage system concept utilizing the solid polymer electrolyte electrochemical cell has many unique advantages. Some of the more significant advantages are:

- The system can be separately sized for power and energy storage.
- Enhanced safety with only a minute fraction of the stored reactants within the electrochemical cell stack.
- High current density capabilities of the cell (i.e., > 300 ASF).

- Minimized materials problems due to the low operating temperature (i.e., < 100°C).
- System pressurization via the electrochemical cell with reactant differential pressure capabilities in excess of 500 psi.

Feasibility Test Results

Preliminary laboratory tests of the solid polymer electrolyte cell have indicated that system electric to electric (E.T.E.) storage efficiencies of > 70% can be obtained at current densities > 300 ASF. Through the use of a specially configured chlorine electrode, almost complete reversibility has been achieved when producing chlorine gas during charge and consuming chlorine dissolved in aqueous HCl during discharge. Figure 2 displays the demonstrated cell characteristics at ambient conditions with almost all of the performance slope being IR related. This figure shows the reversibility of the cell and a demonstrated 61% E.T.E. voltage efficiency at 300 ASF and ambient conditions. The performance goals and the means of obtaining these goals are also displayed. An 80% E.T.E. voltage efficiency goal has been established to allow up to 10% losses in parasitic system characteristics such as pumping power, current inefficiencies, and power conditioning inefficiencies.

Cell Development

To demonstrate the performance goals the hydrogen/chlorine cells must be operated at the operational conditions reflected on Figure 2. A system to accomplish this task has been designed and two systems are presently undergoing final assembly and checkout. Figure 3 displays the system layout.

This high temperature/high pressure system has been well over-designed such that larger units and higher pressures can be evaluated. Major system characteristics include:

- 1000 PSI working pressure for both hydrogen and chlorine subsystems
- 205° F working temperature
- 1500 cc's electrolyte reactant
- 0 to 4 GPM electrolyte reactant flow

It is anticipated that these systems will provide valuable operational parametric data in the weeks and months ahead.

During the design and fabrication of the two high temperature/high pressure systems, work has continued in cell development utilizing room temperature/room pressure hydrogen/bromine facilities. The bromine halogen was selected for the ambient condition tests due to its similarity to the chlorine at operational conditions (i.e., liquid flow).

Initial tests on the hydrogen bromine cell, shown on Figure 4, showed that the bromine electrode configuration was quite reversible. The hydrogen/bromine cell performance and the hydrogen/chlorine cell performances were in fact quite similar with the exception that the open circuit voltage of the bromine cell was approximately 0.3 volt lower than the chlorine cell at approximately equivalent acid concentrations. This cell configuration with its special halogen electrode was operating through three 160 hour cycles at up to 300 ASF on hydrogen/bromine. This rather stable performance of the cell is displayed on Figure 5.

Several materials were tested for corrosion compatibility at approximately 200°F and several were selected as good candidates for cell component parts. A cell was fabricated which utilized only the materials that had displayed thousands of hours of corrosion compatibility at 200°F with insignificant weight, appearance, and mechanical characteristics changes. The hydrogen-bromine performance of this cell, which utilized a non noble metal halogen electrode is shown on Figure 6. An ambient temperature life test of this cell actually displayed performance improvement with operational time. Figure 7 shows performance characteristics at various points in the 600 hour test.

The effect of high acid concentration on performance is an important consideration due to its impact on the size and cost of the halogen storage subsystem. Testing of a cell up to 48 WT% hydrobromic acid was performed with the test results shown on Figure 8. This figure displays the cell performances at various points in the charge discharge cycle. The change in open circuit with acid concentrations appeared as predicted but the encouraging aspect was that little change in the fuel cell slope resulted from the high acid concentrations.

Preliminary Cost Analyses

The demonstration of compatible materials, non noble metal halogen electrodes, and performance over a large range of acid concentrations have enabled the preliminary costing of the hydrogen/chlorine electrochemical module. Table I reflects the production costs of a 2 MW (electric output) module with six hundred 10 ft² cells. Also included in this table are the costs of the hydrogen purification and control subsystem. All costs have been determined utilizing the EPRI costing approach.

Utilizing the Table I cost figures and suitable cost projections for the hydrogen and chlorine storage systems, a production capital cost projection for the desired uninstalled system can be generated. Figure 9 [1] shows the dollars per KW projection versus the system discharge hours.

TABLE I

HCl REGENERATIVE FUEL CELL COST BREAKDOWN (October 1977) Average Performance (15% HCl)

(20 MW Output System - 10 Modules
(@ 2 MW each with 10 Ft² Cells)

Cost/Ft ² (Module)	15.072 \$/Ft ²
(@ 1.13 Volts @ 300 ASF) 2.95 Ft ² = 1 KW	
FC/Elect. Module \$15.072 (2.95) =	44.46 \$/KW
FC/Elect. Module & H ₂ Subsystem Controls	\$54.06 \$/KW
TOTAL Manufacturing Cost	\$59.46 \$/KW

Cost Based on: 10% G and A, \$7./Hour Labor and 150% Labor Overhead

The low capital cost of the system is achieved primarily by operation of the electrochemical cell at high current density and producing chlorine gas in the charge mode which results in a low pressure chlorine subsystem.

Summary

The solid polymer electrolyte technology offers some unique advantages as a hydrogen/halogen energy storage device. Some of the major characteristics are displayed on Table II.

Work is continuing on the development of the hydrogen/chlorine energy storage system under the auspices of the U.S. Energy Research and Development Administration. Operation of a laboratory scale system is planned for later this year and continuous materials and configurations development and system analysis is planned for GFY 1978. (Figure 10)

References

1. Beaufre, A et al., "A Hydrogen Halogen Energy Storage System for Electric Utility Applications". Paper presented at the 12th IECEC Meeting, August 28 - September 2, 1977, Washington, D.C.

TABLE II

SUMMARY OF ADVANTAGES OF GE'S SPE HYDROGEN-HALOGEN BATTERY FOR ENERGY STORAGE

- INDEPENDENT SIZING FOR POWER AND ENERGY
- HIGH CURRENT DENSITIES @ HIGH EFFICIENCY (>300 ASF @ >70%) (>6 TIMES ZN/CL BATTERY CURRENT DENSITY)
- ABLE TO WITHSTAND LARGE DIFFERENTIAL PRESSURES (5000 PSI DEMONSTRATED)
- ELIMINATES NEED OF COMPRESSOR FOR HYDROGEN STORAGE
- OPERATIONAL PARAMETERS COMPATIBLE WITH INTERFACE CONDITIONS OF ENERGY STORAGE SYSTEMS
- HIGHLY REVERSIBLE ELECTRODES CAPABLE OF OPERATION IN REGENERATIVE MODE (BOTH CHLORINE AND BROMINE DEMONSTRATED)
- CELL ASSEMBLY MATERIAL COMPATIBLE WITH HALOGENS (THOUSANDS OF HOURS OF CORROSION TESTS AT 200°F)
- LONG STABLE LIFE DEMONSTRATED ON POLYMER IN ELECTROLYSIS AND FUEL CELL MODES (+45,000 HOURS)
- COMMONALITY BETWEEN HYDROGEN-HALOGEN AND WATER ELECTROLYSIS, CHLORINE ELECTROLYSIS AND HYDROGEN OXYGEN FUEL CELL TECHNOLOGIES (ALLOWS TECHNOLOGY SPIN OFF)

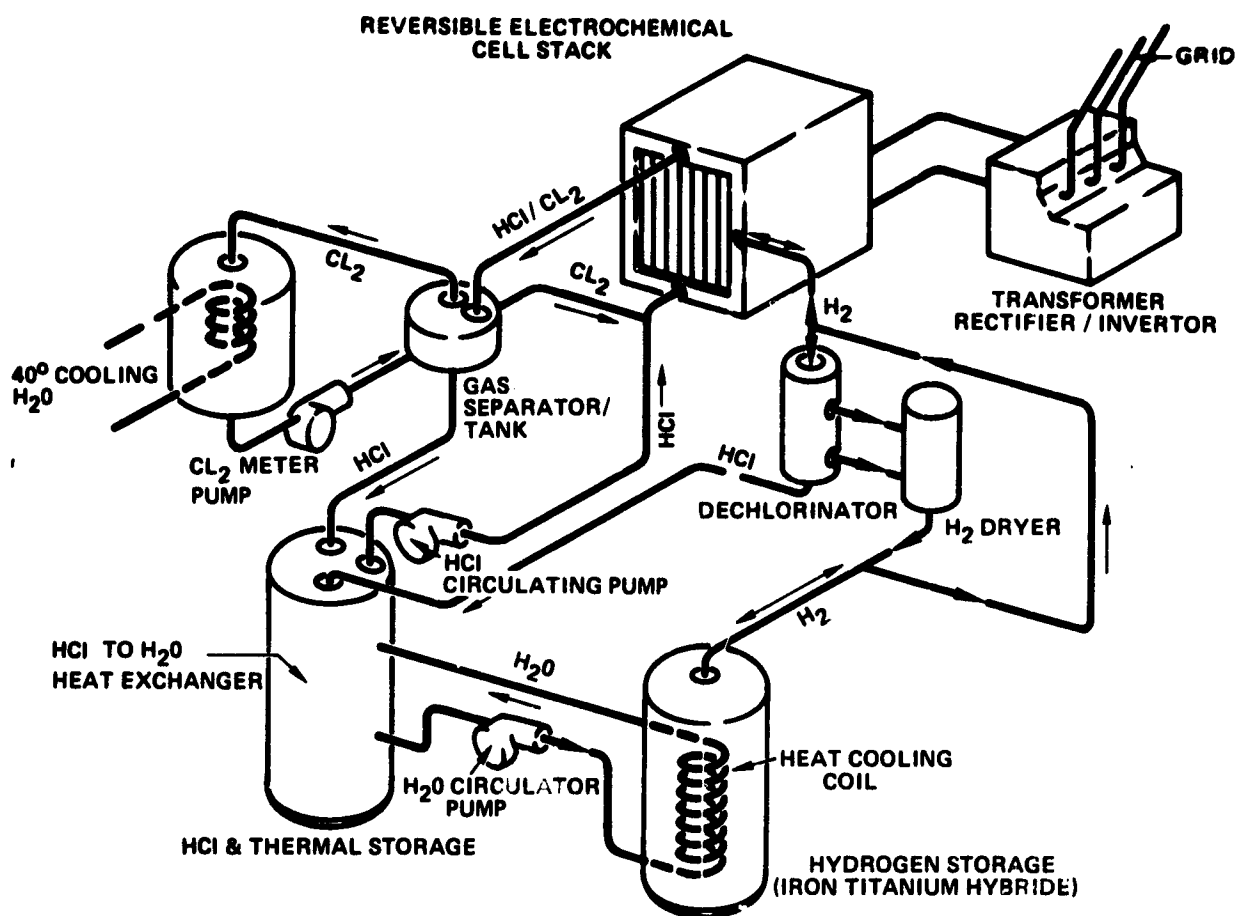


Figure 1. Schematic of Proposed Hydrogen-Chlorine Energy Storage System

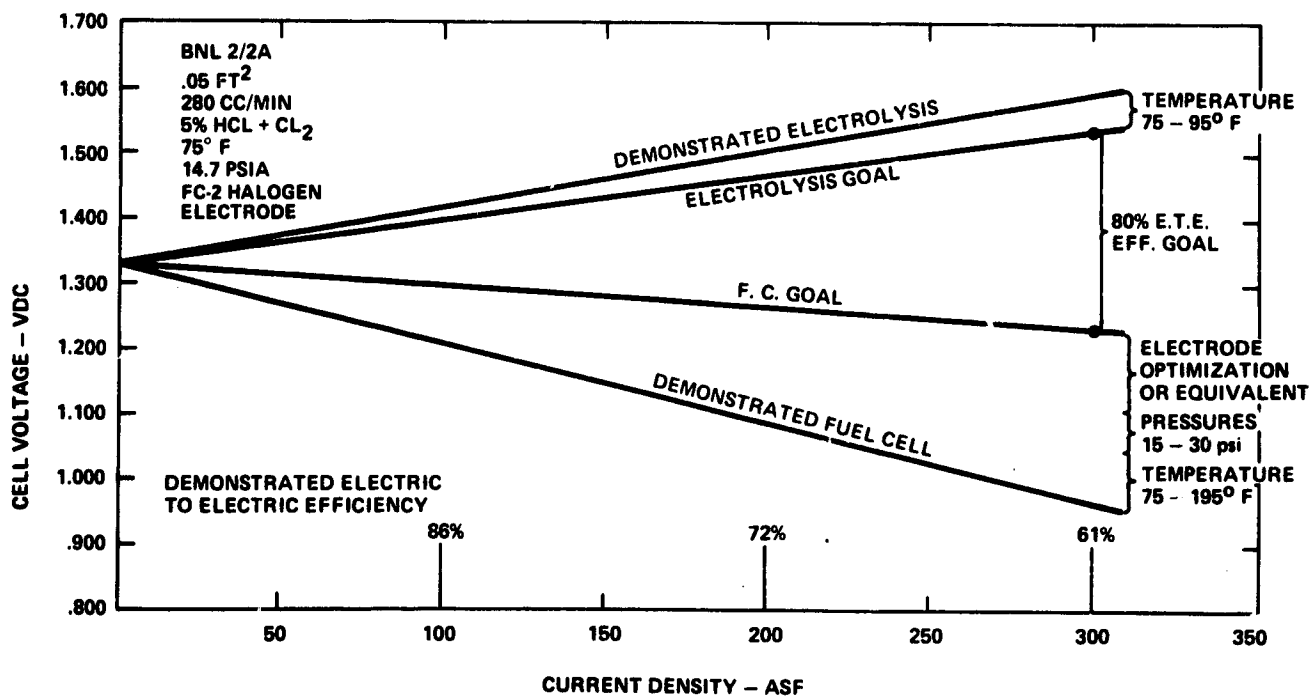


Figure 2. Hydrogen-Chlorine Regenerative Fuel Cell

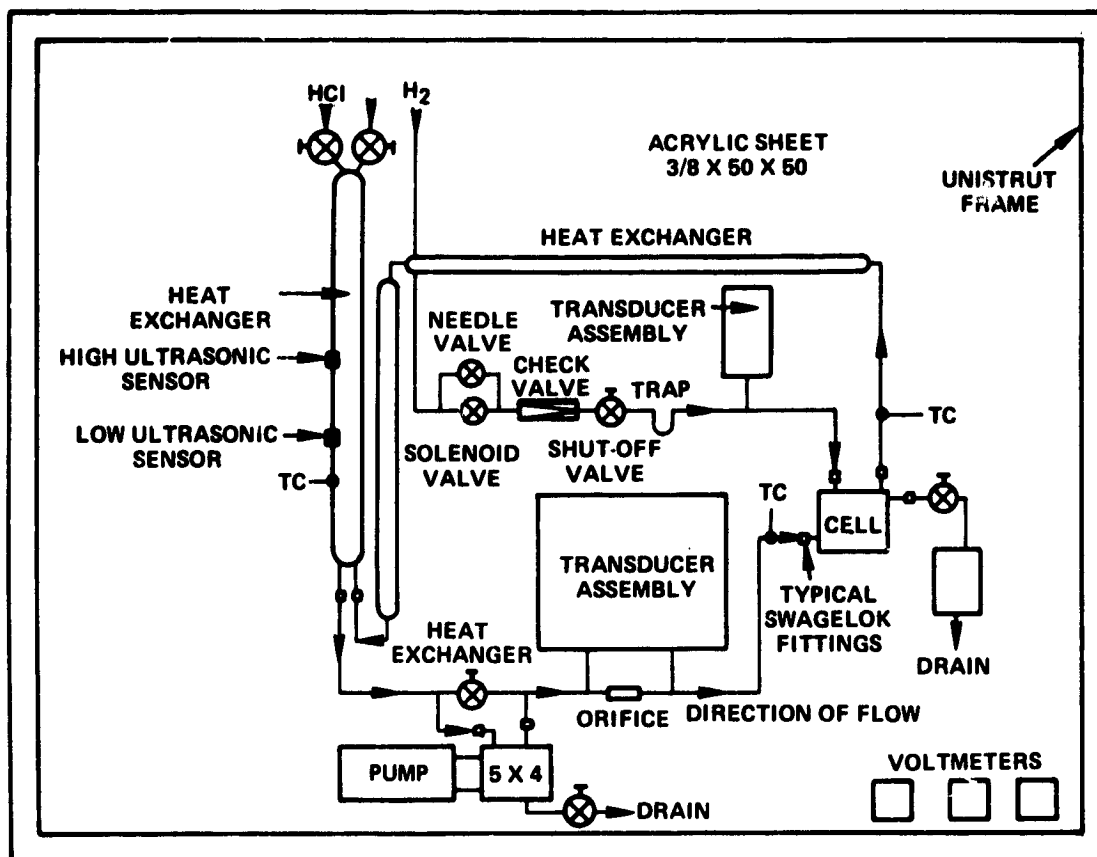


Figure 3. Layout of Hydrogen/Halogen Single Cell Energy Storage System

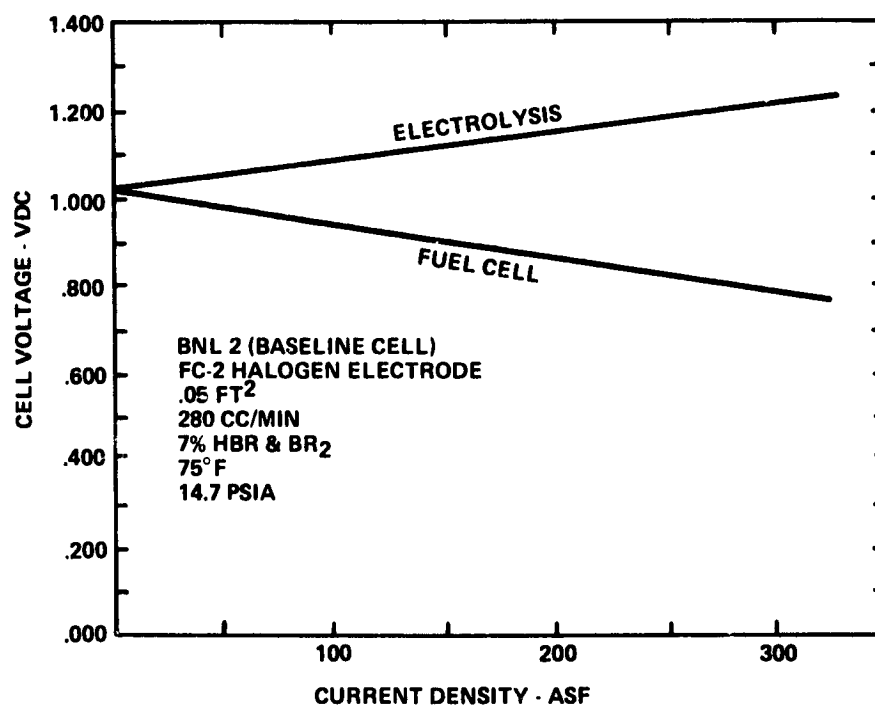


Figure 4. Baseline Hydrogen Bromine Regenerative Fuel Cell

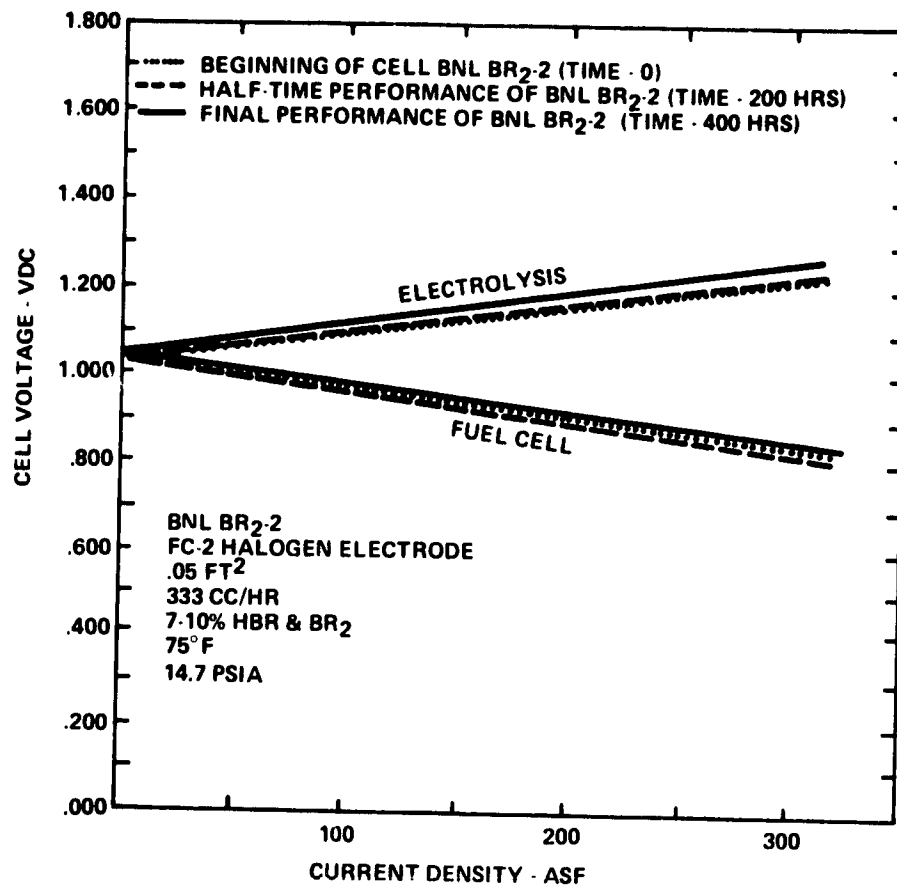


Figure 5. Baseline Endurance Hydrogen Bromine Regenerative Fuel Cell

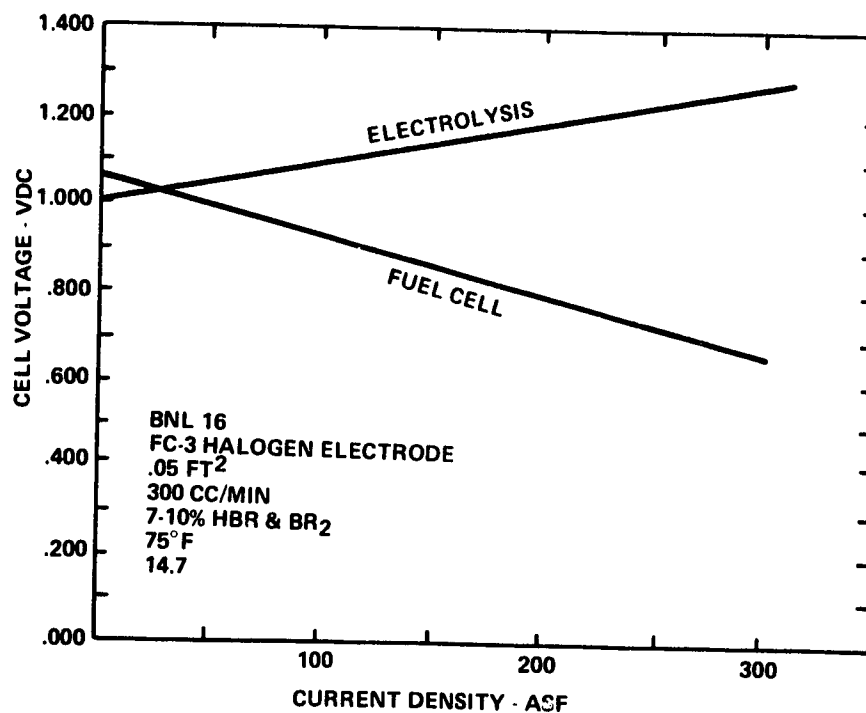


Figure 6. Low Cost Halogen Electrode Hydrogen Bromine Regenerative Fuel Cell

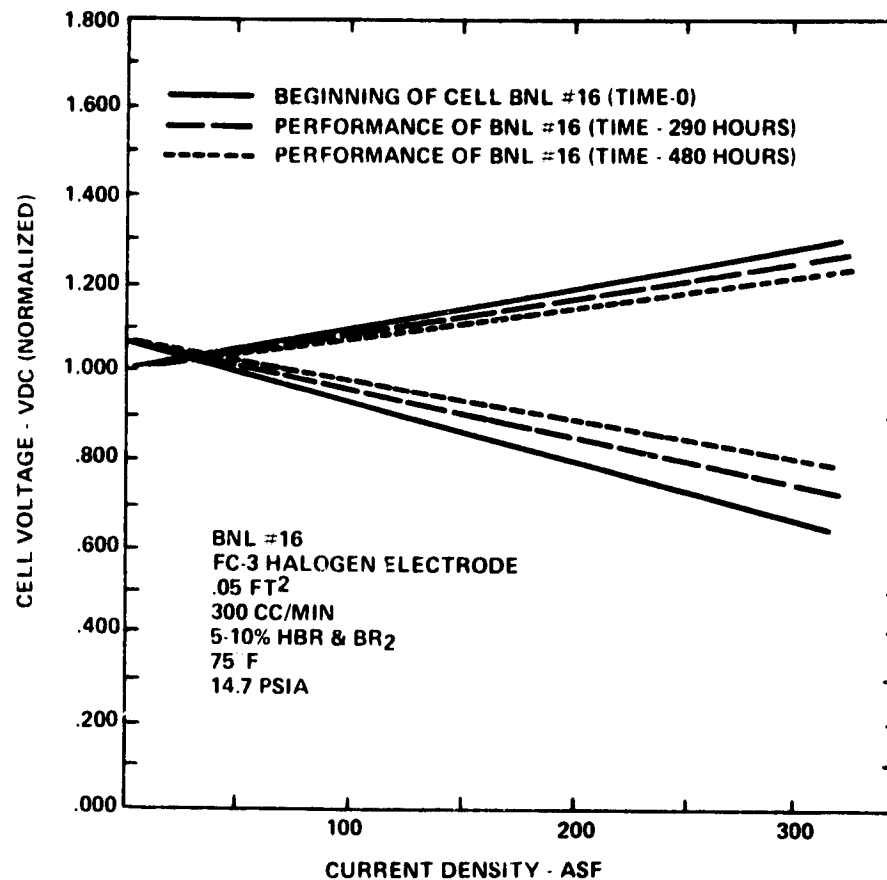


Figure 7. Low Cost Halogen Electrode Endurance Hydrogen Bromine Regenerative Fuel Cell

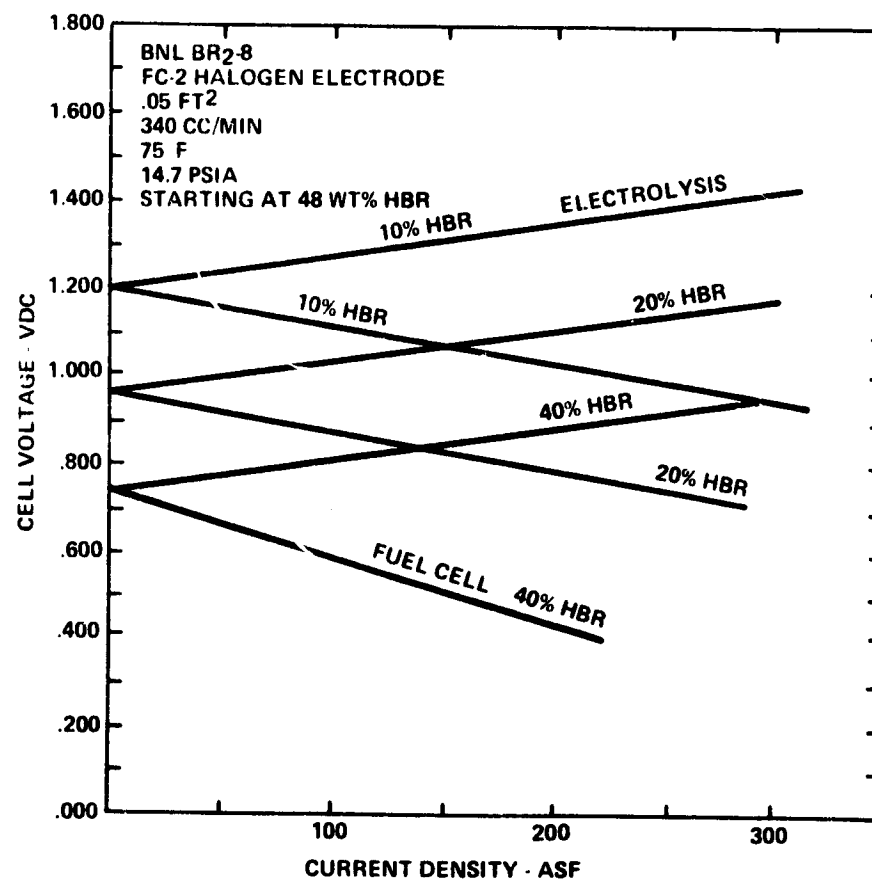


Figure 8. Acid Concentration Effects Hydrogen Bromine Regenerative Fuel Cell

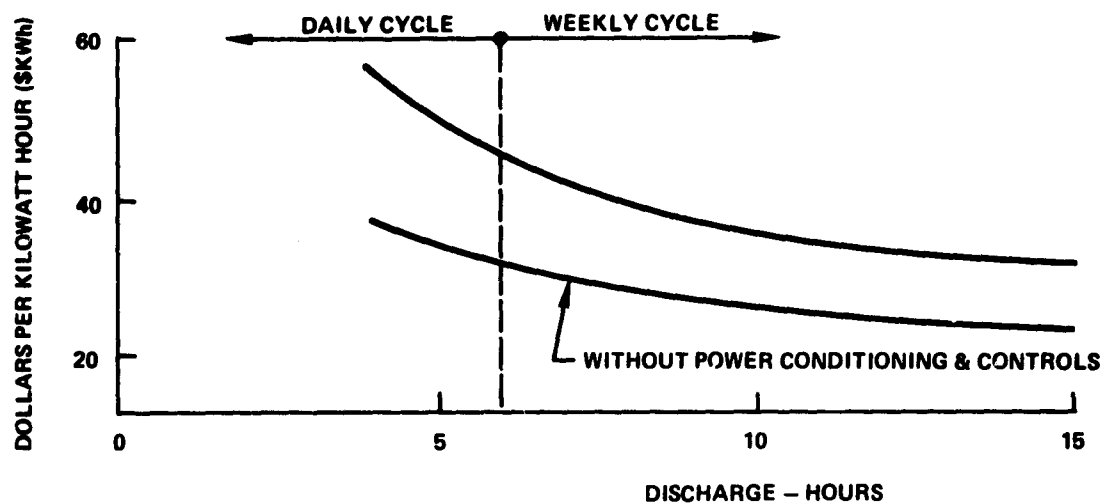


Figure 9. 20 MWe Hydrogen - Chlorine Energy Storage Plant
Capital Cost (\$/kWh vs Discharge Hours)

PROGRAM MILESTONES

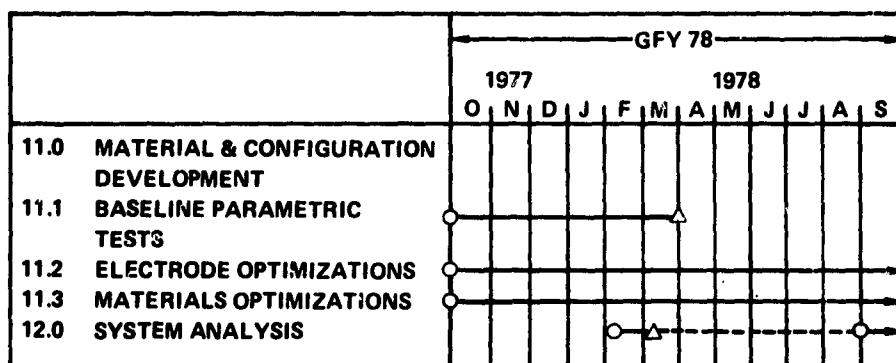


Figure 10. Halogen Acid Regenerative Fuel Cell Energy Storage

INVESTIGATIONS ON MATERIALS FOR ADVANCED WATER ELECTROLYZERS†

S. Srinivasan, P. W. T. Lu, G. Kissel, F. Kulesa,
C. R. Davidson¹, H. Huang², S. Gottesfeld³,
and J. Orehtsky⁴

Department of Energy and Environment
Brookhaven National Laboratory
Upton, N. Y. 11973

Abstract

The development of advanced water electrolyzers is currently aimed at the further increased energy efficiency, reduced capital costs and prolonged life time. Efforts have been made to find stable materials for cell construction and to search for better electrocatalysts for the hydrogen and oxygen electrodes. Optical techniques were used to determine the correlations between optical properties of oxide films formed on Ir and Ru and their electrocatalytic activities for the OER. Ellipsometric studies revealed that the variation of oxygen overpotential with time on Ni is essentially due to the gradual conversion of Ni^{3+} to Ni^{4+} in the oxide film on the electrode surface. The electrocatalytic activities of aged electrodes are rejuvenated using electrochemical methods. Oxide catalysts of spinel or perovskite structure such as $NiCo_2O_4$ and Ba_2MnReO_6 were investigated as oxygen electrodes. Effects of magnetic properties on the electrocatalysis for the OER were studied on lithiated nickel oxide and on Ni-Cu alloys. Nickel boride and $NiCo_2O_4$ show higher catalytic activities than Ni for hydrogen and oxygen evolution, respectively, particularly for long term operations. Materials for separators, gaskets, seals and cell frame have been evaluated in single cells, operating at temperatures up to 150°C. The preliminary results indicate that there is a loss of 2% in coulombic efficiency for the electrolytic hydrogen production at 120°C as compared with 25°C.

1. Introduction

There are three promising approaches to improve water electrolysis technology: (i) development of solid polymer electrolyte (SPE) water electrolysis cells, in which there is a maximization of surface of the electrodes and minimization of inter-electrode spacing; (ii) increasing the operating temperature of alkaline electrolyzers from 80°C to a temperature in the range of 120-150°C; and

†This work was performed under the auspices of the U.S. Department of Energy

¹Present address: Dept. of Materials Science, Univ. of Virginia, Charlottesville, Va.

²Present address: Dept. of Chemistry & Physics, Middle Tennessee State Univ., Murfreesboro, Tenn.

³Permanent address: Dept. of Chemistry, Tel Aviv Univ., Tel Aviv, Israel

⁴Permanent address: Engineering Dept., Wilkes College, Wilkes-Barre, Pa.

(iii) development of advanced concepts, e.g., finding more reversible electrodes, use of anode depolarizers, water vapor electrolysis in molten or solid electrolytes, thermochemical-electrochemical hybrid cycles, hydroxyl ion transporting membranes and photoelectrolysis of water. The needed areas of investigation for the development of the first two technologies are (i) finding stable materials for cell construction (electrodes, current collectors, gaskets, seals, etc.); (ii) searching for better electrocatalysts for the hydrogen and oxygen electrodes; (iii) determining reasons for time variation of performance of water electrolysis cells and methods to inhibit it; and (iv) determining the coulombic efficiencies of cells operating at relatively high temperatures and pressures. The activities at BNL carried out in these areas using electrochemical, ellipsometric and other techniques in short and/or long term experiments are described briefly in the following sections.

2. Optical and Electrochemical Properties of Oxide Films Formed on Metals in the Oxygen Evolution Reaction

2.1 Rationale for Approach

The oxygen evolution reaction (OER) always occurs on oxide covered metallic surfaces or on oxides. The properties of the surface oxides determine the kinetics of this reaction. The problem of performance deterioration in commercial as well as in advanced (e.g., the General Electric Solid Polymer Electrolyte Cell) water electrolyzers is partly due to the increase of oxygen overpotential with time. The latter phenomenon is probably due to changes in physical (e.g., thickness, electronic conductivity) and chemical (e.g., oxidation state, nonstoichiometric oxides) properties of the oxide film. During the previous year, the influence of the electronic conductivity of the film on the electrocatalytic activity was illustrated, by using a combined ellipsometric-electrochemical technique, with platinum or nickel as test electrodes. This work(1) was presented at the last Hydrogen Contractors' Meeting. The same techniques were used in the current year to determine the correlations between the optical properties of oxide films formed on iridium and ruthenium and their electrocatalytic activities for the OER. In addition, this approach was also used to elucidate the mechanism of time variation of oxygen overpotential on nickel electrodes.

2.2 Studies on Iridium

The optical and electrochemical analysis(2) of oxide layers, formed on iridium, performed by combined ellipsometric and reflectometric measurements shows that a hydroxide layer with a refractive index $n_f = 1.44 - 0.01i$ and a thickness which may exceed 2000 Å remains even at cathodic potentials on the Ir electrode, as a result of multicycling. Applications of anodic potentials, close to that for oxygen evolution, results in an increase of the extinction coefficient to a level typical for semiconductors ($n_f = 1.43 - 0.10i$ at 1.50 V). This thick semiconducting phase oxide on iridium in the OER region seems to have a high level of bulk defects and a high concentration of active sites, the generation of both being related to the gradual variation of the oxidation state of Ir in the

oxide, prior to and simultaneously with the oxygen evolution of oxygen. The oxygen evolution rates on Ir between 1.5 and 1.6 V are shown to increase significantly in the presence of such oxides; a lower Tafel slope of $0.8RT/F$ is also observed on these thick oxides.

2.3 Studies on Ruthenium

For the OER from acidic media, Ru exhibits even higher electrocatalytic activity than Ir. As a first approach to understanding the kinetics of anodic reaction in SPE water electrolyzers, the electrochemical behavior of Ru for this reaction was investigated in 1N H_2SO_4 at 20°C, coupled with ellipsometric and reflectometric measurements. As illustrated in Figure 1, the overpotential for oxygen evolution at 1 mA/cm² on Ru is only ~210 mV, while at the same current density, Pt and Ir show oxygen overpotentials of 640 and 360 mV, respectively. Ellipsometric investigations revealed that the oxide film, formed on Ru during oxygen evolution, is highly light-absorbing and thus is an excellent electronic conductor. At constant potentials below 1.43 V vs RHE, the current densities for oxygen evolution, either on freshly prepared or preanodized Ru electrodes, are practically stable, exhibiting a Tafel slope of $\sqrt{RT}/2F$. However, ruthenium oxide (RuO_x) dissolves at higher potentials. The onset potential of the anodic dissolution of RuO_x in 1N H_2SO_4 is in the range of 1.44-1.46 V (see Figure 1). After polarization of a ruthenium electrode of geometric area 0.25 cm² at 1.5 V for 20 hours, the subsequent chemical analysis of the electrolyte using an atomic absorption spectroscopic technique, showed that it contains 30 µg of Ru ions/ml. This significant dissolution of RuO_x also resulted in an enhancement of current density at the constant potential of 1.5 V from 44 to 70 mA/cm² (geometric area), which is essentially due to the gradual increase of real surface area of the electrode. The stabilization of RuO_x by alloying Ru with several transition elements is underway.

2.4 Mechanism of Time Variation of Oxygen Overpotential on Nickel Anodes

One of the significant factors, contributing to the performance degradation with time in commercial water electrolyzers, is due to the gradual increase of overpotential for oxygen evolution, at a constant current density, which occurs over a period of two years or even more. More recently, the performance decay on oxygen evolving electrodes has been observed on platinum in the potential range of 1.6-2.0 V vs RHE(3), on iridium(4) and on nickel(5). The mechanism of the performance degradation on nickel anodes was investigated in 1N KOH solution by using ellipsometry to analyze the nature of anodic films(6). Effects of electrochemical pretreatment of the films on the kinetics of the oxygen evolution reaction were also investigated.

Figure 2 shows that nickel oxide films, formed potentiostatically at 1.5 V, are more active than the untreated (i.e., freshly prepared) nickel for oxygen evolution at a constant potential of 1.8 V. The *in situ* ellipsometric analysis revealed that the oxide film formed on Ni at 1.5 V is mainly composed of β -NiOOH, which is presumably "the right type of nickel oxide" for the OER. Further anodization of β -NiOOH films results in the

chemical transformation of Ni^{3+} to Ni^{4+} ions, which are inactive for the OER. The ratio of Ni^{3+} to Ni^{4+} ions in the nonstoichiometric oxide film is strongly dependent on the anodization potential(7) and the polarization time(8). Therefore, the time variation of current density, for oxygen evolution at constant potentials (above 1.56 V), as demonstrated in Figure 2, is interpreted as being due to the gradual conversion of Ni^{3+} to Ni^{4+} ions in the oxide film on the surface of nickel electrodes.

In general, higher oxides such as NiO_2 are less stable at elevated temperature. The rate of the conversion of Ni^{3+} to Ni^{4+} ions in oxide films also increases with increasing temperature. Thus, as seen from Figure 3, the higher the electrolyte temperature, the shorter the period of time for approaching a stable current density. The electrocatalytic activities of aged electrodes are regained by "rejuvenating" the electrodes at 1.5 V. Ellipsometric investigations revealed that the "rejuvenation" of aged oxide films is essentially attributed to the recovery of active sites (i.e., Ni^{3+} ions) on the very top layers of the films, rather than the diminution of the film thickness. Figure 3 also shows that, with increasing temperature, there is a more significant improvement of the electrocatalytic activity by "rejuvenation" on aged electrodes.

Effects of electrochemical pretreatment of oxide films on nickel electrodes on the kinetics of the OER are shown in Figure 4. Tafel plots, for this reaction on nickel preanodized or "rejuvenated" at 1.5 V, exhibit only one linear region with $b \approx 40$ mV, while dual Tafel regions are observed on nickel prepolarized at 1.8 or 2.0 V: $b \approx 40$ mV at low η and $b \approx 170$ mV at high η . As demonstrated in Table 1, the thickness of oxide film on nickel electrodes plays a less important role than its chemical identity in determining the kinetics of the OER. From the practical point of view, the performance degradation of nickel anodes can be retarded by (i) increasing the operating temperature of water electrolyzers; (ii) using electrode materials of higher surface area, and thus polarizing at less anodic potential to achieve a desired current density; and (iii) introducing a secondary cation into nickel oxide films (e.g., $NiCo_2O_4$).

3. Electrocatalysis of the Oxygen and Hydrogen Electrode Reactions

Oxide catalysts with a high surface area were prepared using a freeze drying technique. These powders were then used in the preparation of Teflon bonded electrodes. Teflon bonded Ba_2MnReO_6 electrodes were tested as oxygen electrodes over the temperature range 23-140°C in KOH for oxygen evolution and exhibited a Tafel slope of 0.7-0.8 RT/F. In general, catalytic effects of this perovskite were poor. With nickel cobalt oxide ($NiCo_2O_4$) which has a spinel structure, there was no change in the mechanism of oxygen evolution over the temperature range from 0° to 240°C. This oxide was tested as an oxygen electrode in single cells for water electrolysis over 500 hours. The rate of increase of overpotential with time was less with $NiCo_2O_4$ than with Ni (Figure 5). However, Teflon bonded nickel cobalt oxide electrodes showed poor structural stability at higher temperatures (>100°C) and current densities (>200 mA/cm²).

A promising material for use as a hydrogen electrode in alkaline electrolyte is nickel boride(9). Nickel boride electrodes, obtained from Deutsch Automobile Gesellschaft in Stuttgart, Germany, were evaluated as hydrogen electrodes in water electrolysis cells over the temperature range from 25-120°C and for over 500 hours. The overpotential on this electrode is less than on a comparable nickel screen electrode by up to 400 mV at a current density of 333 mA/cm² (Figure 6).

The effect of magnetic properties on the electrocatalysis of lithiated nickel oxide for the OER was investigated. Preliminary studies indicate a change of mechanism at about 180°C, which is close to the Neel temperature. In a related study(10), the temperature dependence of the Tafel behavior for oxygen evolution in alkaline solution was determined on Ni-Cu alloys, Ni₇₅Cu₂₅ and Ni₇₀Cu₃₀. The Curie temperatures for these alloys are 70°C and 50°C, respectively. There is a distinct change in the transfer coefficient for the oxygen evolution at a temperature close to the Curie temperature (Figure 7). Higher transfer coefficients are observed below the Curie temperature, under which conditions the alloys are ferromagnetically ordered.

4. Evaluation of Materials for Separators and Other Cell Components

Single cells have been designed and fabricated for long term evaluation of materials used in the construction of cells. Provision is also made in the cell design for measurements of half cell potentials of the hydrogen and oxygen electrodes as a function of time. All measurements were made in alkaline solution and materials for separators, gaskets, seals and cell frames have been evaluated in single cells, operating at desired current densities and at temperatures up to 150°C. The stress of this work has been on finding suitable separator materials. At least fifty materials have been screened and the more promising ones evaluated in long term studies. Summarizing conclusions on the usefulness or otherwise of these materials are presented in Table 2. Polysulfone will be suitable for fabrication of cell frames but has to be annealed properly to avoid stress cracking. Ethylene-propylene seals are satisfactory at temperatures below 120°C.

5. Measurement of Coulombic Efficiency for Electrolytic Hydrogen Production as a Function of Temperature and Pressure

In both acid and alkaline water electrolysis technologies, there is a need to increase the operating temperature to about 120-150°C to reach the goal of a cell potential of 1.47 volts (thermoneutral potential) at the highest possible current densities. To minimize ohmic losses, it is desirable to minimize the interelectrode spacing. Further, the hydrogen gas is generated at pressures of 40 atmos or higher for use in the chemical industry, hydrogen storage as hydride and in some applications as a fuel (e.g., natural gas supplementation). Pressure electrolysis is more economical than electrolysis at low pressures and subsequent external compression. All these factors increase the rates of diffusion of small amounts of the evolved gases from one electrode to the other, where it is consumed, and consequently reduces the coulombic efficiency in the cell.

An experimental cell was designed and constructed for measurement of the coulombic efficiencies for hydrogen production as a function of temperature and pressure. The preliminary results indicate that there is a loss of 2% coulombic efficiency at 120°C as compared with 25°C. Experiments to make these measurements as a function of operating temperature, pressure and interelectrode spacing are in progress.

6. Proposed Studies for FY 1978

The three major tasks in FY 1978 will include research and development of (i) solid polymer electrolyte water electrolyzers; (ii) advanced alkaline water electrolyzers; and (iii) advanced concepts. In the first area, efforts will be concentrated on the stabilization of ruthenium based electrocatalysts for the oxygen electrode, investigation of the usefulness of electrochemically conducting oxide materials (e.g., doped titanates) as anode current collectors and determination of coulombic efficiencies for hydrogen production as a function of operating temperature and pressure (this last subtask will also apply to the second task). The second task will involve the long term evaluation of cell construction materials (electrodes, separators, gaskets, seals, cell frames, etc.), particularly in the test rig being fabricated at Teledyne Energy Systems. A strong area of interest in the third task will be a continuation of the investigation of mixed oxides (spinel, perovskites) as oxygen electrodes. Correlations will be drawn between electrocatalytic activities and electronic, magnetic or morphologic properties. There is increasing interest in the use of anode depolarizers (e.g., carbonaceous materials) to considerably reduce the electric energy consumption in water electrolysis cells. Experiments will be initiated in this direction. The substitution of a hydroxyl ion transporting membrane for Nafion in SPE cells will help in the solution of finding non-noble metal electrodes and low cost current collectors. The general opinion to date is that hydroxyl ion transporting membranes are unstable. An examination of methods to stabilize hydroxyl ion transporting membranes may lead to promising approaches.

References

1. Srinivasan, S., Kissel, G., Lu, P. W. T., Kulesa, F. and Davidson, C. R., Proceedings of the DOE Contractors' Review Meeting on Chemical Energy Storage and Hydrogen Systems, Airlie, Virginia, November 8-9, 1977, p. 33.
2. Gottesfeld, S. and Srinivasan, S., J. Electroanal. and Interf. Electrochem., in press.
3. Schultze, J. W., Z. Phys. Chem., NF 73, 29 (1970).
4. Buckley, D. N. and Burke, L. D., Faraday Transaction I, 72, Part II, 2431 (1977).
5. Tseung, A. C. C. and Jasem, S., Electrochim. Acta, 22, 31 (1977).
6. Lu, P. W. T. and Srinivasan, S., paper presented in 151st Meeting of the Electrochemical Society, Philadelphia, Pennsylvania, May 8-13, 1977.

7. Davies, D. E. and Barker, W., Corrosion, 20, 47t (1964).
8. Conway, B. E. and Satta, M. A., J. Electroanal. Chem., 19, 351 (1968).

9. Benczúr-Ürmösy, G., paper presented at the Symposium on Novel Electrode Materials, Brighton, England, September 25-26, 1975.
10. Orehotsky, J., Huang, H. and Srinivasan, S., to be published.

Table 1. Kinetic Parameters for Oxygen Evolution on Pretreated Nickel Electrodes

Pretreatment	$d_f, \text{\AA}$	Tafel Slope, b(mV)		Exchange c.d., i_o (A/cm ²)	
		high η	low η	high η	low η
(1) Preanodization at 1.5 V, 2 hrs	~ 230	---	39	---	3.8×10^{-12}
(2) Preanodization at 1.8 V, 24 hrs	~ 620	170	43	4.2×10^{-6}	1.1×10^{-11}
(3) Preanodization at 2.0 V, 6 hrs	~ 1400	167	40	6.2×10^{-7}	2.2×10^{-12}
(4) Rejuvenation at 1.5 V, 2 hrs	~ 620	---	38	---	1.1×10^{-12}

Table 2. An Analysis of the Usefulness of Various Types of Materials as Separators for Alkaline Water Electrolysis at Temperatures in the Range of 80-150°C

Materials-Class or Type	Comments
Asbestos Material	Ideal separator under 100°C in alkali
Woven	Asbestos works well used commercially. Boron nitride - not stable in alkali especially above 100°C.
Potassium Titanate Paper (Teflon Binder)	Very good in alkali above 100°C.
Nafion	Very good in acid at all temperatures; works well in 20% NaOH at 100°C and above.
Non-woven (felts)	Low resistance material but limited life at elevated temperature. Also possible higher diffusion of gases.
Battery Separator	Works well as separator material. Most are of polyethylene base - not suitable for higher temperature.
Cationic Membrane	With the exception of Nafion, found to be suitable in regard to resistance but as a rule, short life above 100°C.
Anionic Membrane	Very high resistance and short life.
Porous Membrane	Teflon base, excellent durability above 100°C. All have high resistance (2 to 10 times asbestos).

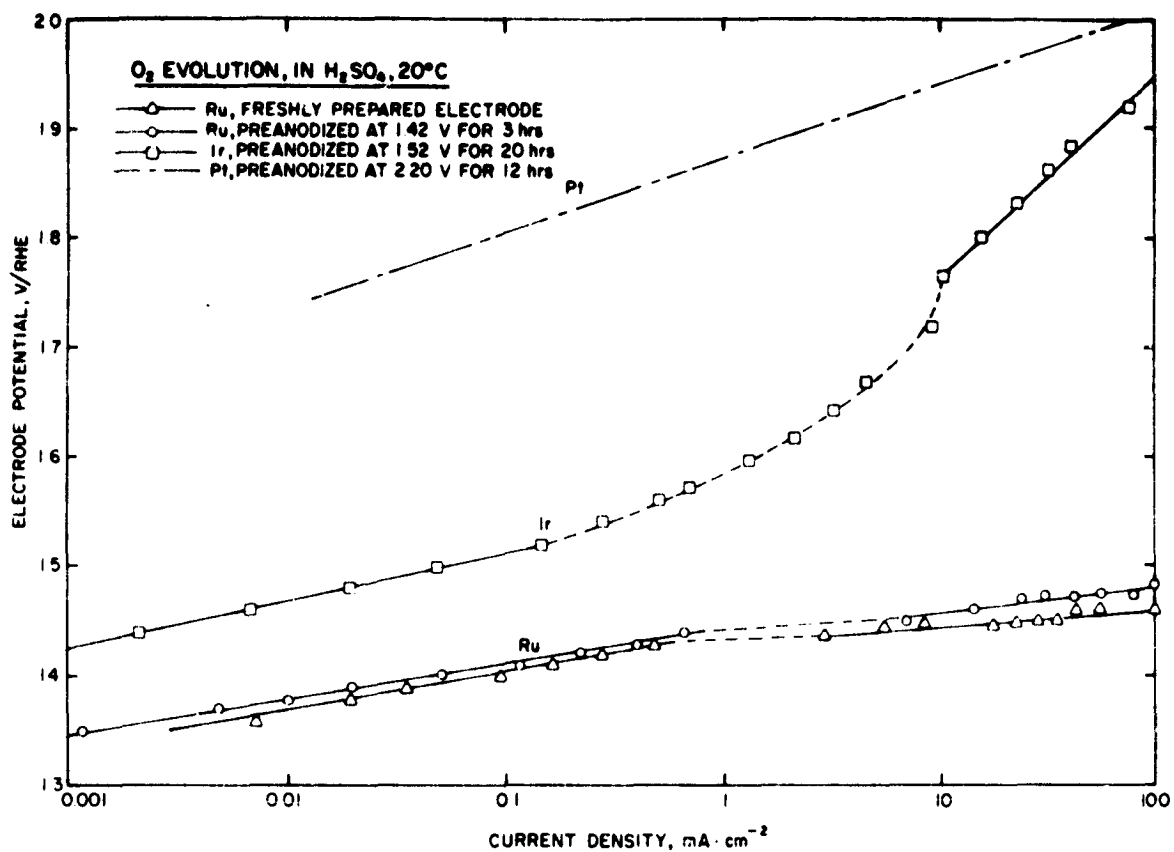


Figure 1. Tafel plots for oxygen evolution on Pt, Ir and Ru electrodes in 1N H₂SO₄ at 20°C

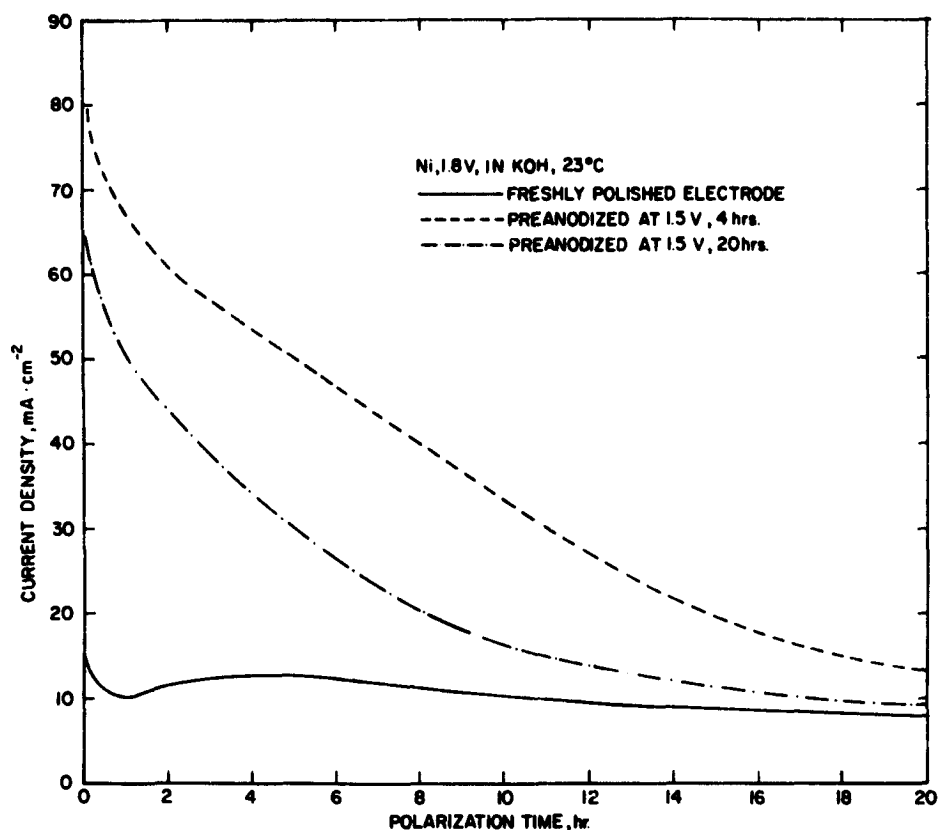


Figure 2. Effect of preanodization at 1.5 V on the current density for oxygen evolution on nickel electrodes in 1N KOH at 23°C

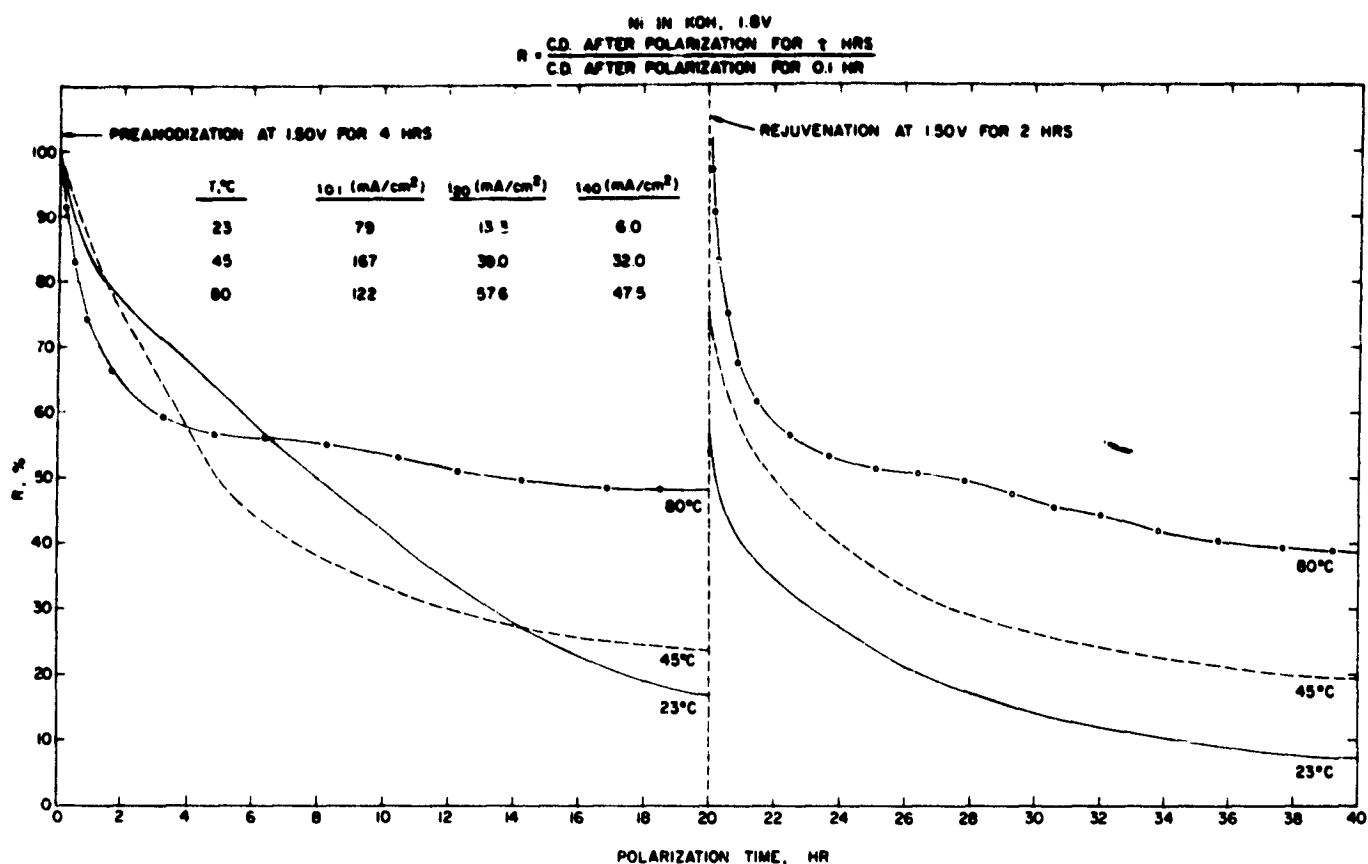


Figure 3. Effect of temperature on the rate of current decay for the oxygen evolution reaction on preanodized and rejuvenated nickel electrodes

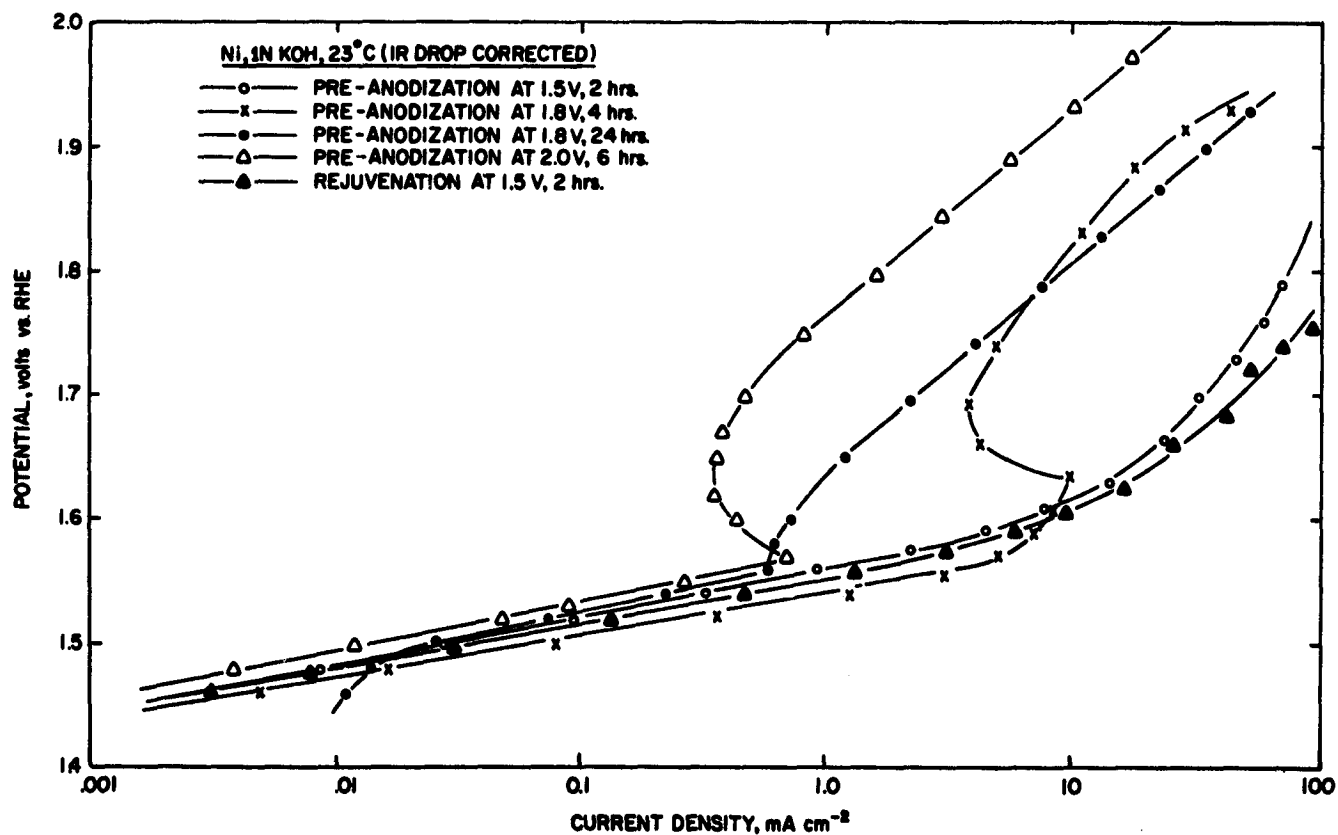


Figure 4. Tafel plots for the oxygen evolution reaction on various pretreated nickel electrodes in 1N KOH at 23°C

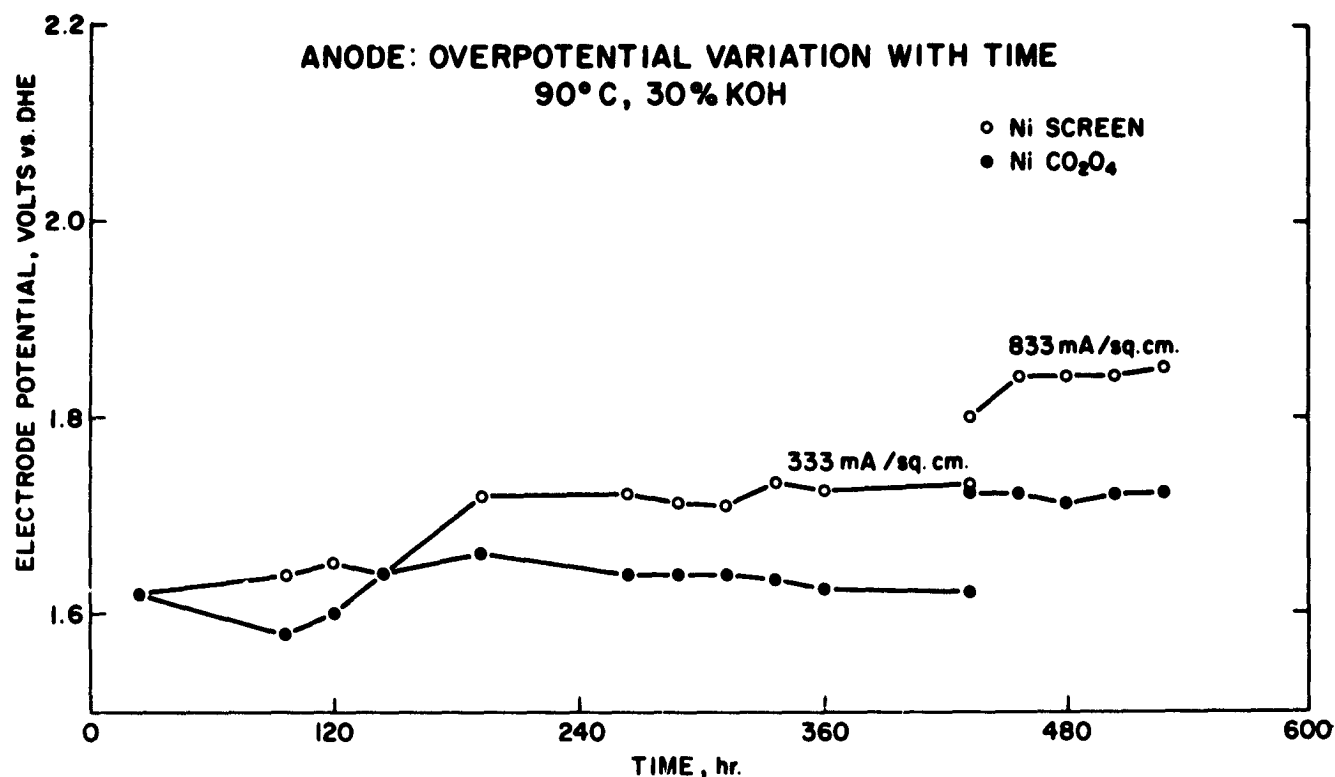


Figure 5. Variation of electrode potential with time for oxygen evolution on Teflon-bonded NiCo₂O₄ and Ni screen in 30% KOH at 90°C

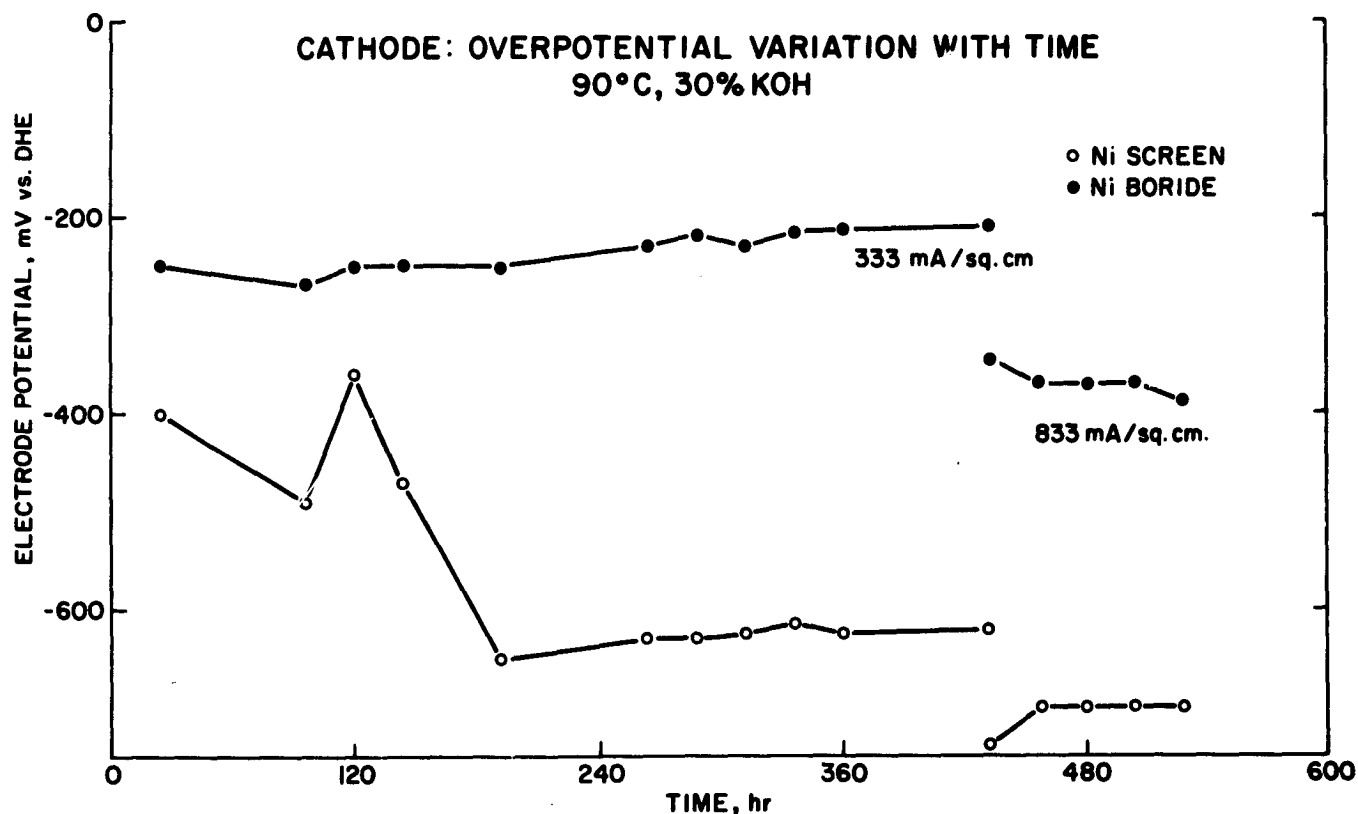


Figure 6. Variation of electrode potential with time for hydrogen evolution on nickel boride and nickel screen in 30% KOH at 90°C

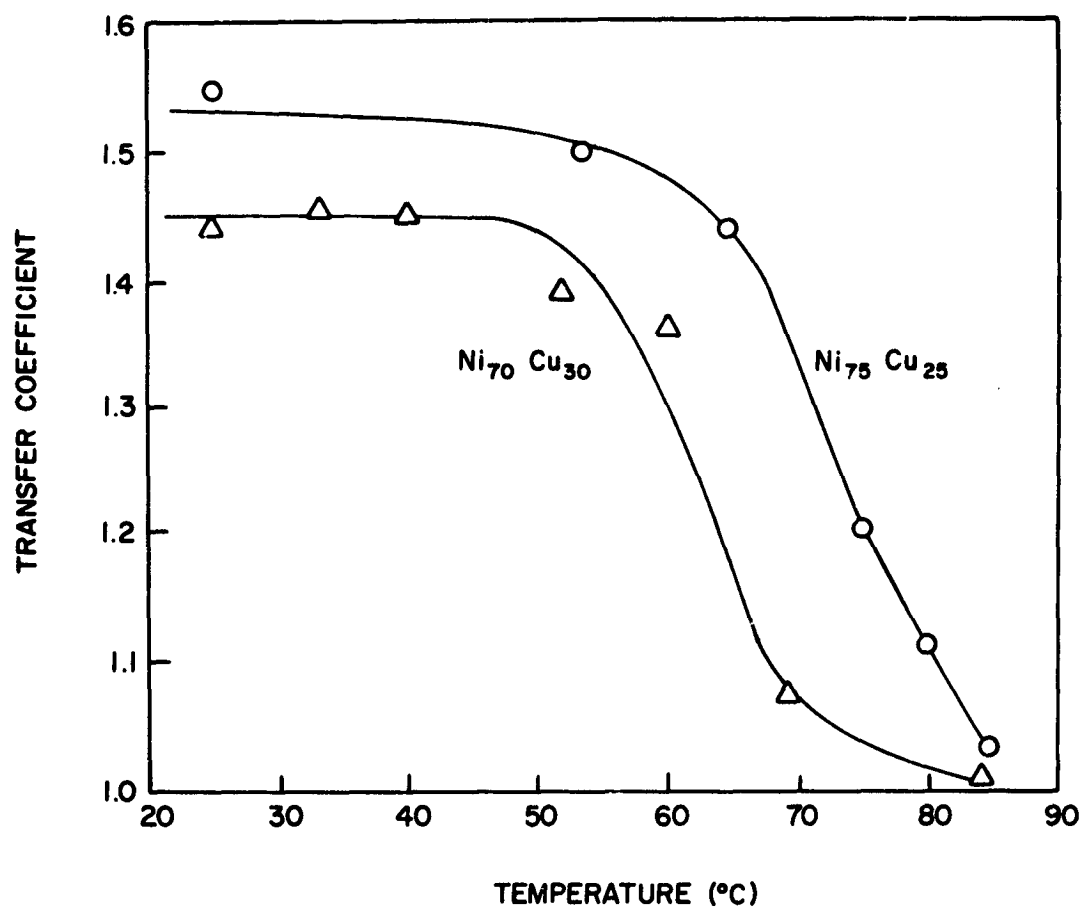


Figure 7. Temperature dependence of the transfer coefficient for oxygen evolution on two Ni-Cu alloys

**ADVANCED ALKALINE ELECTROLYSIS
CELL DEVELOPMENT**

**J.N. Murray and M.R. Yaffe
Teledyne Energy Systems
110 West Timonium Road
Timonium, Maryland 21093**

Abstract

The general approach and test results are presented from the Task One screening of thermoplastic polymers as potential electrode separators for use in alkaline solution electrolysis systems. The program has now proceeded into the (Task Two) design and fabrication of a high temperature, applied research test system. The general description of the test system is given and an outline for the upcoming program is discussed.

The production of hydrogen via direct current electrolysis of water from an alkaline solution has applicability in today's economy and an outstanding future coupled with many proposed energy schemes. This latter statement is of course tempered by the need for improving the operating efficiencies while maintaining or decreasing the low capital investment. The program at Teledyne Energy Systems, sponsored by Brookhaven National Laboratory under Contract BNL-380750-S, is directed to improving both the energetics and the economics of this classic process for hydrogen production. As discussed previously,⁽¹⁾ two approaches are being evaluated. First, higher operating temperatures lower the electrochemical electrode overpotentials as well as the ionic resistivity, leading to lower input cell voltages. Second, development of improved electrode structures incorporating improved electrocatalysts is being given limited attention. Rather than review the overall efforts, this report will be more of a program status report. Discussions on overall hydrogen production economics and detail of the technical experimental program are available for the interested reader in References 2, 3 and 4.

Current commercial alkaline water electrolysis processes are limited in operating temperatures to approximately 80°C (180°F) because of the life limitations of the asbestos mineral, chrysotile, electrode separator. At these conditions, cell operating voltages are reported to be between 1.8 and 2.2 volts per cell depending on operating applied current as well as the sophistication of the catalyst systems involved. These values represent upper process efficiencies of 67 to 82% relative to the thermoneutral input requirement of 1.48 volt (68.3 Kcal/mole). In general, improvements of roughly 3 mv per degree C are observed with a variety of electrode structures. With stable materials, one can then foresee process efficiencies of up to 93% without the need of noble metal catalysts by operating cells at 150°C.

The search for stable materials has been focused on the electrode separator. Four thermoplastics which had previously⁽⁵⁾ shown applicability in structural polymer applications were selected for the high temperature evaluation. Phase One A of this program, essentially completed in March 1977, involved the evaluation of polysulfone and polyarylsulfone, prepared into yarn/thread form by solvent spinning into 16 and 12 μ m diameter fiber respectively by FRL.* The overall approach to evaluation is presented as Figure One. The detail/results are available in a technical summary report⁽⁴⁾ and will not be discussed in this text. The general findings were essentially three. The polyarylsulfone (Astrel 360 from Carborundum Plastics) fiber was completely attacked by the 150°C (300°F) caustic environment within the 500 hour test period. Polysulfone fiber (essentially Udel P-1700 from Union Carbide) survived the 500 hour, 150°C caustic electrolyte testing although tensile strength was somewhat reduced. The oxygen/KOH was a more harsh environment than the hydrogen/KOH media. The second major finding was that the critical polymer surface tension of the polysulfone fiber separator was low. This in turn requires a significantly smaller pore size to be fabricated than predicted from capillary law theory. The same approximate effect and value was observed with the polyarylsulfone samples. The general test electrolysis cell results were found to behave in a predictable fashion as has been observed with

*formerly Fiber Research Laboratory, Dedham, Mass.

asbestos test cells. In general, superior test cell results were demonstrated with the porous polysulfone separator at 125°C compared to the input values for the asbestos separator cell at the recommended upper temperature limit for the asbestos/alkaline system.

The second pair of the thermoplastics is currently being evaluated. Polyphenylene sulfide, supplied by Phillips Fibers Corporation using hot melt spinning to produce both fiber and staple form, is being tested for chemical stability, mechanical stability and surface wettability characteristics. The fiber itself is too large (approximately 25 μ m) for small pore size matrix tests. Polyethersulfone, purchased from ICI United States, Inc. will be melt spun into approximately 3 μ m staple only for evaluation as a porous separator. The mechanical characteristics under different stress levels have been reasonably well documented by the manufacturer. A fifth potential polymer, polybenzimidazole (PBI), manufactured by Celanese Research Co. is reported⁽⁶⁾ to be available in sub-micron diameter size in the near future. Development of the PBI polymer fiber for fuel cell applications is being funded by NASA Lewis and chemical stability is reported to have been demonstrated up to 100°C. Testing of this material in the electrolysis cell environment should be possible by early 1978.

Part of the program with BNL has involved interfacing with the BNL sponsored matrix development program at the University of Virginia under Dr. Glenn E. Stoner and P. J. Moran. Three asbestos matrix with various degrees of treatment⁽¹⁾ prepared at the University were recently submitted to TES for evaluation. Although the initial test data appear encouraging, the experiments were not completed at the time of this writing.

Electrode and electrocatalyst development has recently been restarted. The primary interest is in the anode electrocatalyst NiCo_2O_4 discussed in a series of papers by Tseung et al and currently under study at BNL⁽⁷⁾. In particular, the freeze-dry approach to catalyst preparation appears to offer a specific approach to an ordered (spinel type) oxide which may have a stable, lower surface conductivity than the in situ formed nickel oxides found in commercial alkaline electrolyte electrolyzers. The requirement for a hydrophobic binder such as PTFE emulsions is of particular interest with respect to a gas evolution electrode reaction and will be pursued as time permits.

The primary effort in the Task Two portion of the contract now underway is the design and construction of the high temperature applied research electrolysis system. The unit will be in effect a small version of the anticipated commercial production equipment with sufficient instrumentation and controls to allow parametric studies as well as life testing of the various components which may feature potential improvements. The system will consist of three cabinets, the power conversion cabinet, the mechanical/electrochemical components cabinet and the instrumentation cabinet. In general, the system which will incorporate a 5 cell test module, will have sufficient input current (and voltage) to allow production of approximately 25 SLM (Standard Liters per Minute) of hydrogen. With the particular cell selected for the test program, electrode characteristics and stability can be studied up to current densities of 2500 ma/cm² without resorting to electrode masking techniques.

The power supply cabinet is a self contained, air cooled, solid state AC to DC converter. The SCR/diode package rectifies the 460 VAC, 3 phase input to DC to provide up to 750 ampere and 18 volt DC continuously. Although most life testing is anticipated to be in the 500 to 1000 ma/cm² region, the hardware capability was preselected to allow observations of, for example, changes in limiting current densities.

The mechanical cabinet contains the electrolysis module itself, the fluids support subsystems and the gas pressure control system. The design of the equipment is centerlined to accommodate testing up to 150°C (300°F). As the water vapor pressure at this temperature could be 3 atmospheres, operation at a moderate pressure of 7.8 atm (100 psig) is featured to minimize water losses via the product gases. The general mechanical schematic is shown as Figure Two. The anode and cathode compartments of the electrolysis module are supplied with filtered, temperature controlled, potassium hydroxide electrolyte from the respective anolyte (O₂) and catholyte (H₂) reservoirs by means of individually controlled electrolyte pumps. The fluids pass adjacent to the gas generating electrodes within the electrolysis module, entrain the evolving gas and pass back to the individual electrolyte reservoirs where gas/liquid separation occurs. The liquid flow rate is determined by the heat transfer requirements and with this value as the parameter, only a small portion (~1%) of the fluid stream is the required water to be electrolyzed. The gas content within the module effluent is also kept at a relatively low level at the normal operating range, however, the gas content could become appreciable at the highest current (82v/o at 750 amp) with the lowest preselecte pumping rate. The water consumed by the electrolysis process is replenished into the catholyte (H₂) reservoir by means of a pump on a signal provided by the lowering of the catholyte liquid level as measured by a differential pressure transducer (DPX-1).

Because the gases are generated at up to 100 psig, a fail-safe type gas pressure control scheme was designed, and successfully demonstrated. The approach, shown in Figure Two, allows close control of both the overall system pressure as well as the differential gas pressure imposed onto the electrolyte reservoirs and electrolysis module. In general terms, the overall system pressure is established (when the system is generating gas) by setting the oxygen back pressure via regulator BPR-1. The hydrogen pressure is then controlled by regulation of the hydrogen flow rate to maintain a preset gas differential pressure as monitored by DPX-2. During either normal or emergency system shutdown, the oxygen is removed from the system in a controlled fashion via shutdown regulator (SR) as the hydrogen bleeds out through the shutdown valving SV-3 and MV-5. Again, the differential gas pressure is maintained at quite close to zero.

The module itself will be a "conventional" modern bipolar plate, series aligned, 5 cell unit. The frame/seal design, established under a previous program incorporates polysulfone as the primary structural component with PTFE (teflon) seals. The electrodes as well as electrode separator are conventional commercial components, namely Nickel 200 wire cloth electrodes and "Iron free, type 1945, fuel cell grade asbestos board". A variety of experiences with these materials in the Teledyne Energy Systems commercial HG and HS Series of Hydrogen generators have shown these materials are stable beyond 13,000 continuous operating hours. The temperatures of the modules in these commercial units are normally maintained at less than 82°C and only limited electrolysis module test experience has been accumulated in the operating temperature range above 100°C. The next proposed task for the contract is the establishment of data at (at least) 125°C for a period of up to 2000 hours or three months.

The instrumentation cabinet or console features the meters for the display of electrical data as well as temperature data and contains the safety shutdown relays, resets, etc. A keylighted flow chart is provided which allows the operator quick reference to the various measurements in progress. The only data not available at the instrumentation console will be the gas pressures and the fluid flow rates, these in line process instruments being located in the mechanical cabinet.

The construction and verification testing of the high temperature test fixture constitutes the key segment of the Task Two effort. On completion of the fixture, a moderate systems and materials compatability test of up to 2000 hours (and/or three months) is anticipated as the Task Three effort. This data as well as the data from a proposed Task Four test of similar length with advanced technology module components will then be utilized in an economic evaluation of total hydrogen costs. For this economic study a plant size of 5 MW will be utilized to allow direct comparison of the various cost factors with previous studies by BNL. With economics of the advanced technology established as favorable, design and construction of a demonstration pilot plant of 1 MWe would proceed to verify this sensible means of production of hydrogen for the many present needs as well as future requirements.

Acknowledgements: The authors are pleased to thank BNL and the DOE for their continued interest in and sponsorship of the program. The authors are also pleased to acknowledge the efforts of M. C. Miller and S. A. Macarevich in the design of the test rig, T. H. Mullinix for his contributions to the experimental tasks, and to thank Ms. Carol Cheek for her patience in the preparation of this report.

REFERENCES

1. CONF 761134, Proceedings of the ERDA Contractors Review Meeting on Chemical Energy Storage and Hydrogen Energy Storage Systems, 8 and 9 November 1976, Airlie, Virginia.
2. Laskin, J. and Feldwick, R., "Recent Development of Large Electrolyte Hydrogen Generators," Proceedings of the 1st World Hydrogen Energy Conference, Miami Beach, Florida, 1-3 March 1976.
3. Kincaide, W. and Williams, C., "Storage of Electrical Energy through Electrolysis", presented at the 8th I.E.C.E.C., Philadelphia, Pennsylvania.
4. Murray, J.N., "Phase One A, Final Report, Evaluation of Polysulfone and Polyarylsulfone", TES-BNL-8, BNL Contract 380750-S, March 31, 1977.
5. Murray, J.N., "Stability of Thermoplastics and Fiber Reinforced Thermoplastics in KOH/O₂ Environments", Proceedings of 34th Annual Technical Conference, Society of Plastics Engineers, April 26-29, 1976.
6. Interagency Advanced Power Group Project Brief, PIC 3120, June 1977.
7. BNL-50714, "Electrolysis Based Hydrogen Storage Systems", Annual Report, 17 January 1976 to 31 December 1976 (in printing).

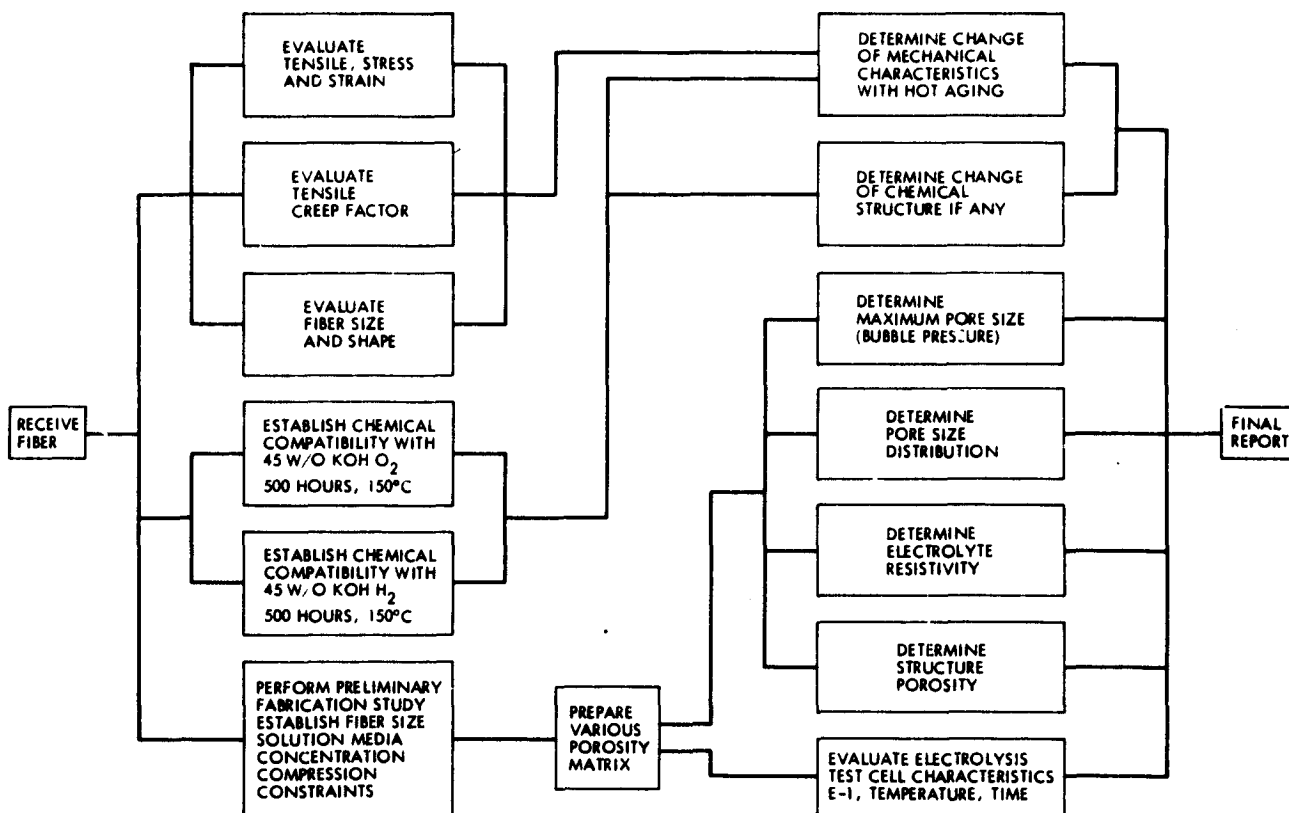


Fig. 1. Work Flow for Preliminary Evaluation of Porous Polymers

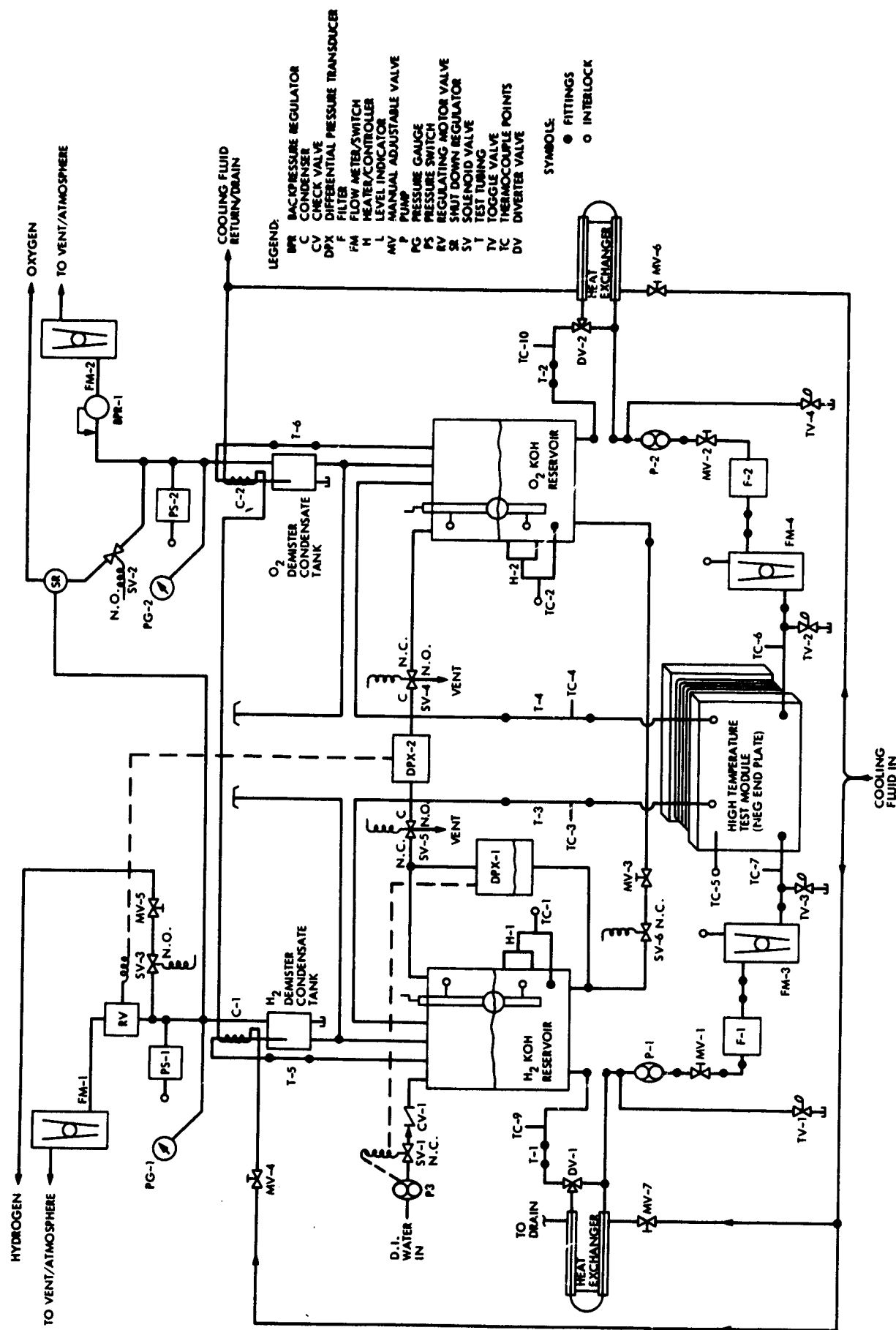


Fig. 2. Mechanical Schematic of High Temperature Test System

SELECTION AND CHARACTERIZATION OF MATERIALS FOR ADVANCED WATER ELECTROLYZERS;
ASBESTOS DIAPHRAGM FAILURE AND CATHODE KINETICS

P. J. Moran, G. L. Cahen, Jr., and G. E. Stoner

Department of Materials Science
University of Virginia
Charlottesville, VA 22901

ABSTRACT

Two problems which adversely affect performance of alkaline electrolyzers are matrix failure and time dependent increases in cell voltage. Observations of both of these phenomena have been documented and measured as functions of operating conditions. Several possible explanations are proposed for these two effects, and possible solutions are under investigation.

I. ASBESTOS DIAPHRAGM FAILURE

The failure of asbestos diaphragms in alkaline water electrolysis cells is a debated subject. One common hypothesis attributes the failure to chemical dissolution of the silica by the KOH electrolyte. However, other references state that the dissolution is slow¹, that the electrolyte can be saturated with K silicates without harmful effects to the electrolyte¹, and that a protective layer of MgO (MgOH?)² forms around the asbestos fibers, thus protecting the silicas from dissolution. No reference exists in the open literature that explains the dissolution mechanisms and the resultant failure in detail.

Investigative research conducted at the University of Virginia³, funded by ERDA through BNL (contract BNL 412533-S) indicated other possible failure mechanisms of the diaphragms. These mechanisms are of a physical nature and operate independent of the chemical dissolution. The relative severity of the physical vs. chemical mechanisms has not been resolved as of yet. A paper was presented concerning the research on the physical failure mechanisms at Airlie. The following section summarizes the important conclusions:

- (1) Gas pockets have been observed within the asbestos diaphragms, the origin being: entrapped gas upon insertion into electrolyte, nucleated gas on hydrophobic impurities in the asbestos diaphragm, or diffusion of electrolysis product gasses into the diaphragm.
- (2) Other gas pockets are observed near the electrode screens which are caused by diffusion or entrapment of electrolysis product gasses.
- (3) The internal gas pockets increase in size with temperature, while those nearer the electrode screens increase with both temperature and time during electrolysis.
- (4) The hypothesis suggests that a pinhole eventually develops by the linking of various gas pockets across the diaphragm (Fig. 1) allowing passage of product gasses, resulting in product gas contamination, which can cause additional complications or matrix failure. A second phase of the project at the University of Virginia was aimed at avoiding or reducing the physical failure

mechanisms. This was done by the addition of an appropriate wetting agent which reduced significantly the number of nucleation sites within the diaphragm.

One successful candidate was found. Tin hydrosol, an inorganic polymeric and relatively uncommon wetting agent, stabilized the diaphragm in accelerated nucleation tests and increased the wet strength of the diaphragm significantly. Initial commercial evaluation indicated that the presence of the treated diaphragm had increased the cell voltage by about 5%. Since that time two modifications have been performed. First, studies were undertaken to determine the minimum effective loadings of the wetting agent so that the increase in diaphragm resistance could be minimized (if that is where the increase is). Secondly, by treating the asbestos in a slurry and recasting the diaphragm, a more continuous coating is achieved. Previous treatment had been administered to as-cast diaphragms.

In August 1977, modified diaphragms were submitted for further commercial evaluation. Recently an observation which supports the physical failure mechanism theory has arisen. Stereo microscopic observation of electrode screen-asbestos interface, which has been operating for several days, indicates about 20% of the individual screen openings contain large spherical pockets. This observation must be conducted before disturbing the interface. Figure 2 is an illustration of what is visible.

The potential benefit of Sn hydrosol is still unanswered, but a conclusive decision is anticipated following interpretation of the commercial evaluation results.

The theory of physical failure mechanisms, however, is independent of the Sn hydrosol and is apparently gaining new support.

II. CATHODE KINETICS

An interesting problem was uncovered during the tin hydrosol program. Measurement of diaphragm resistance in an operating electrolysis cell was hindered by the lack of a stable cell voltage. Further investigation revealed the following:

- (1) The cell voltage increases approximately linearly with log t as illustrated in

Fig. 3. This is a continual decrease in voltage efficiency.

- (2) Upon shorting the cell for several minutes and then continuing electrolysis, the cell voltage repeats the initial cycle (Fig. 4).

After several logs of time the ΔV is small enough to consider the cell voltage stable. However, starting from a shorted cell at $t = 0$, a stable cell voltage has not been seen over a log of t . These phenomena indicate that some type of current cycling or interruption will increase the cell voltage efficiency. The following relationships were also found:

- (1) $\Delta V/\Delta t$ is \uparrow for $\uparrow T$
- (2) $\Delta V/\Delta t$ is \uparrow for $\uparrow i$
- (3) Both anode and cathode have initial overpotential changes. However, we have found the cathode's to be dominant in the cell voltage increase with t .
- (4) The cathode turns to a blackish color. SEM micrographs of before and after cathodes indicated no major change in surface area. The blackish color is stable in air and disappears when the cell is shorted. Initial analysis showed nothing unusual; however, more extensive analysis is underway.

Research efforts at Virginia are continuing in this area. A technique such as current interruption may be useful on a large scale to achieve a voltage efficiency increase.

If the source of the problem could be isolated, then the problem could be directly addressed. Perhaps a solution other than current cycling could be employed. Our present goal is to identify and/or alleviate the problem.

REFERENCES

1. Godin, P., Graziotti, R., Damien, A., and Masniere, P., "Study of the Corrosion of Asbestos in a Mixed Solution of Concentrated Potash as a Function of Temperature," paper presented at First World Hydrogen Energy Conference, Coral Gables, Florida, March 1976.
2. Akzo Zout Chemie Nederland, Hengelo, (O) Netherlands "Transport of OH^- Ions Through Asbestos Diaphragms" 1976 "Fundamentals of Diaphragm Performance"
3. Moran, P. J., Study of the Physical Failure Mechanisms of Asbestos Separator Material, Master's Thesis, University of Virginia, December 1976.

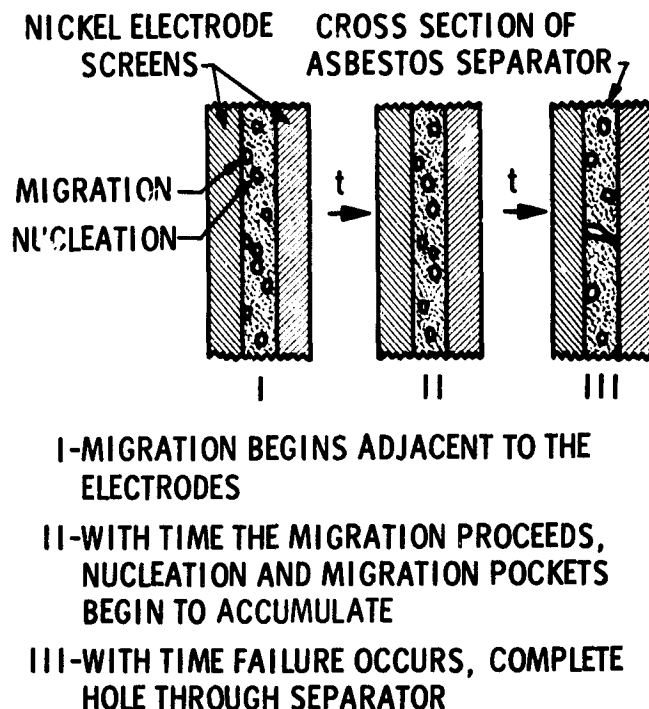


Fig. 1. Physical failure mechanism of asbestos separators in electrolysis cells

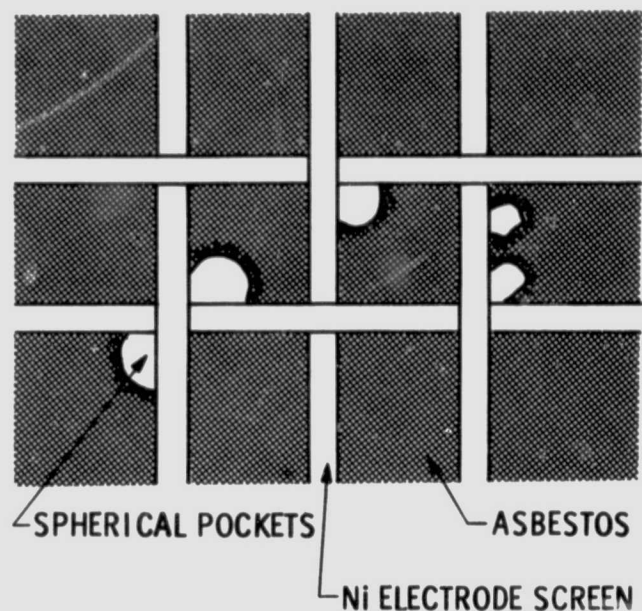


Fig. 2. Electrode screen-asbestos interface showing spherical pockets. The regions appear compressed or compact as if some force existed in the pocket, i.e., gas bubble

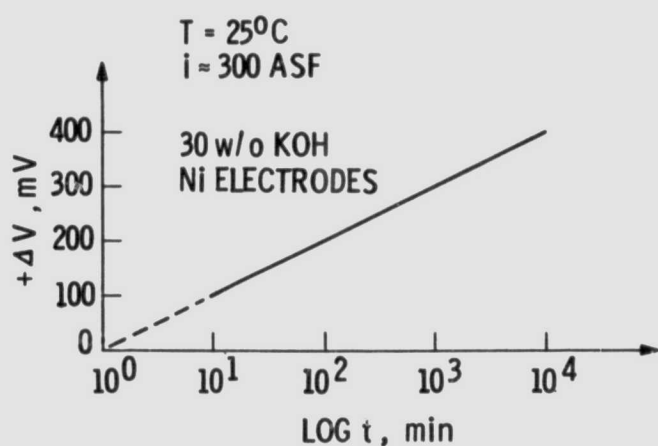


Fig. 3. Change in cell voltage with time

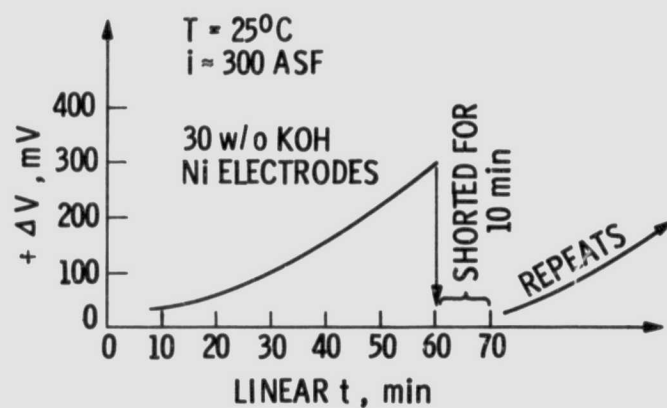


Fig. 4. Effect of shorting on cell kinetics

OPTICAL INVESTIGATION OF THE OXIDES OF RUTHENIUM
AND IRIUM IN RELATION TO THEIR ELECTROCATALYTIC
ACTIVITY*

Fred H. Pollak
Physics Department
Belfer Graduate School of Science
2495 Amsterdam Avenue
New York, N.Y. 10033

Abstract

It has been suggested that the problem of current decay with time in the oxygen evolution reaction in water electrolysis is connected with the continuous growth of a poorly conducting oxide film on catalyst surface. Optical techniques can yield valuable information concerning the dynamics of oxide formation as well as the nature of the oxide. The highly sensitive technique of the rotating light pipe reflectometer can be used to investigate the time and spectral dependence of reflectivity change on Ru and Ir catalyst surfaces in conjunction with electrochemical determinations. These materials have been shown to be superior to Pt. In addition this optical technique can be employed to evaluate the intrinsic reflectivity of RuO_2 and IrO_2 in the range 0.5-10 eV to gain information concerning the d -electrons of these materials.

* Supported by Brookhaven National Laboratory, Upton, N.Y.

I. Introduction

At the present time there is considerable interest in developing high efficiency and low cost water electrolyzers to meet the demands of hydrogen required by the chemical industry and as a fuel in fuel cells and gas turbines. The development of advanced technology for water electrolyses is essential to minimize the cost of hydrogen. The efficiency of water electrolysis systems depends critically on the behavior of the oxygen electrode. For oxygen evolution reaction (OER) on metals or alloys at constant potentials, the continuous decrease of current densities with time is one of the more difficult problems in water electrolysis. The time variation of current density has been pointed out by Schultze [1] in the anodic evolution of oxygen on platinum. More recently, similar behavior has been observed on iridium [2] and on nickel [3] anodes. It has been suggested that the current decay with time is connected with the continuous growth of a poorly conducting oxide film, which retards the electron transfer or inhibits the radical reaction on the film surfaces [2,3].

The OER always takes place on electrodes which are covered with an oxide layer. The "catalytic activity" of a metal-oxide-electrolyte system in the OER may be described quantitatively in terms of the exchange current density (i_0) and the Tafel slope ($b = \partial \eta / \partial \log i$). A good electrocatalyst is associated with a high value of i_0 and a low value of b . Little is understood about the properties of the oxide phase and, especially, about the properties of the oxide-electrolyte interface which are required to achieve improved performance in the OER. Evaluation of a number of metals and alloys as electrocatalysts for the oxygen evolution reaction, leads to nickel as a preferred anode material for the OER in alkaline solutions and to noble metals and their alloys as electrocatalysts for the OER in acid solutions. Among the noble metals, the performance of Ru, Ir and their alloys was found to be much superior to that of a pure Pt anode. Thus, the potential at which a steady state oxygen evolution current density of 1 mA cm^{-2} (real) is obtained on Pt at room temperature is about 1.8 V vs. RHE, while at an Ir anode this potential is only about 1.5 V [4]. It is obvious, therefore, that analysis of the surface layer formed on Ir prior to and during the evolution of oxygen, revealing the relationship between properties of this layer and the performance of the Ir/aqueous solution interface in the OER, may be an important key to the role of oxide layers in electrocatalysis.

A novel design for water electrolysis has recently been proposed by the General Electric Company using solid polymer electrolyte fuel cells [5]. In this type of water electrolysis cell a solid sheet of perfluorinated polymer (Nafion) serves as the electrolyte. The electrocatalysts are platinum on the cathode side and iridium, ruthenium or binary and ternary alloys of these metals with transition metals on the anode side. Hence there is considerable interest from a practical point of view in gaining a better understanding of nature of electrocatalyst/electrolyte interface for these particular materials.

II. Experimental Approach

The interest in the exact properties of the surface layer present on Ir, Ru or the alloys mentioned above has recently prompted an examination of the film formed by multicycling using various methods including ellipsometric and reflectometric techniques. These investigations have already yielded valuable information concerning the nature of the oxide and the dynamics of its formation [6,7]. However, they have been performed at only one wavelength, i.e. 5461 Å.

The wavelength limitation in the investigation of the dynamics of oxide formation and the properties of the oxide itself can be overcome by use of the highly sensitive technique of the rotating light pipe reflectometer (RLPR) [8]. A schematic diagram of the RLPR system is shown in Fig. 1. In this device, the quartz light pipe rotating at $\sim 100 \text{ Hz}$, captures alternately the reflected (RI) and incident (I) light beams and transmits them to the detector by internal reflection. The RI and I beam amplitudes are extracted from the time⁰ dependent signal $I(t)$ by an electronic gating circuit which employs field effect transistors as switches for sample and hold measurements. A high voltage operational amplifier adjusts the photomultiplier gain to keep I constant. The reflectance $R = (RI)/(I)$ is then recorded continuously as the photon energy $h\nu$ or other parameters such as oxidation times are varied. The rapid comparison between incident and reflected beams produces a high stability in R , so that reflective changes at least as small as $|AR/R| \approx 10^{-4}$ can be detected. Because the optical alignment is unchanged as the oxide layer is formed or removed, the full sensitivity of the technique can be exploited in such an investigation. Finally, the mechanical design of the light pipe produces a rather large duty cycle which makes possible a response time of the system sufficiently short ($\sim 1 \text{ sec.}$) that reflectance changes due to oxide formation or dissolution can be observed as they occur.

The sensitivity of the RLPR technique has been clearly demonstrated by the work of Rubloff et al. [9] on optical studies of chemisorption. Their results show that the technique can measure dynamical changes in reflectance due to the formation of one monolayer of adsorbate and that it is possible to make identification of the nature (i.e., species) of the adsorbate by measuring the spectral dependence of AR/R .

The RLPR method is not limited to one wavelength as is the case in the previous ellipsometric and reflectometric investigations 6,7. Using the RLPR it is possible to study the dependence of oxide formation as a continuous function of incident photon energy in the range 0.7 - 6 eV, the limitations being imposed by the absorption of the electrolyte and the window of the electrolytic cell.

In addition to evaluating the variations in reflectivity in relation to catalytic activity it would also be of considerable interest to determine the intrinsic reflectivity of RuO_2 and IrO_2 .

Measurements of the spectral dependence of semiconductors and metals have been extremely valuable in elucidating their electronic band properties. For example, recent work in the spectral range 0.5 - 10 eV on the transition metal oxides Ti_2O_3 and Nb_2O_5 has allowed an energy level scheme of d-electrons to be assigned [10]. These measurements were performed with the RLPR presently operative at Yeshiva University. A similar study on RuO_2 and IrO_2 will be compared with the recent band structure calculations of Mattheiss [11] and hence give valuable information concerning the d-electrons in these materials.

III. Planned Research

As discussed previously the RLPR method can be utilized to detect the small changes in reflectivity that occur during the process of oxide formation on a catalyst, both as a function of time and photon energy. We plan an investigation of both of these parameters in relation to the changes in reflectivity that occur on various catalysts. Specifically we intend to study RuO_2 , IrO_2 and Pt in various acidic solutions including HNH_4SO_4 and CF_3SO_3H acids. In addition binary and ternary alloys of transition metals in Ru will be investigated.

We also plan to observe the changes in reflectivity that occur at a fixed wavelength with time during the cycling process and to correlate these changes with the catalytic activity. Hence it will be necessary to perform electrochemical measurements in tandem with the reflectivity observations. The second phase of this program will consist of observing the changes in reflectivity that occur at different wavelengths in the range 0.7 - 6 eV. These determinations should yield valuable information concerning the nature of the species of the formed oxide. For example it is believed that the problem of the continuous decrease of current densities with time is related to the transformation of RuO_2 to RuO_3 . An investigation of the wavelength dependence of the oxide formation may be valuable in confirming this postulate. This second phase will also be done in tandem with electrochemical measurements.

The spectral dependence of the intrinsic reflectivity of RuO_2 and IrO_2 in the range 0.5 - 10 eV will be studied in order to gain information about the distribution of the d-electrons by comparison with the band structure calculation of Mattheiss [11].

References

1. Schultze, J.W., *Z. Phys. Chem.*, Vol. NF73, p.29, 1970.
2. Buckley, D.N., and Burke, L.D., *Faraday Transactions I*, Vol. 72, part 11, p. 2431, 1976.
3. de Zoubov, N., and Pourbaix, M., *Atlas of Electrochemical Equilibrium in Aqueous Solutions*, ed. by Pourbaix, M., p. 2431, Pergamon Press, London, 1963.
4. Hoare, J.P., *The Electrochemistry of Oxygen*, p. 107, Interscience, New York 1968.
5. Nuttal, L.J., "Review of Solid Polymer Electrolyte Water Electrolysis Technology" in *Proceedings of the First International Energy Agency Water Electrolysis Workshop*, ed. by Salzano, F.J. and Srinivasan, S., Brookhaven National Laboratory, Sept. 1975; Nuttal, L.J. and Titterton, W.A., "Hydrogen Generation by Solid Polymer Electrolyte Water Electrolysis" in *The Hydrogen Economy*, Miami THEME Conference, Feb. 1974.
6. Lu, P.W.T., and Srinivasan, S., to be published in the *Proceedings of the Spring 1977 Meeting of the Electrochemical Society*.
7. Gottesfeld, S., and Srinivasan, S., Brookhaven National Laboratory document #22027, to be published in *Electrochimica Acta*.
8. Gerhardt, U., and Rubloff, G.W., *Appl. Optics*, Vol. 8, p. 305, 1969.
9. Rubloff, G.W., Anderson, J., and Stiles, P.J., *Surface Science* Vol. 37, p. 75, 1973.
10. Lu, S.S.M., Shin, S.H., Pollak, F.H. and Raccach, P.M., in *Proceedings of the Thirteenth International Conference on the Physics of Semiconductors, Rome, 1976*, ed. by Fumi, F.G., p. 330, Tipografia Mares, Rome 1976.
11. Mattheiss, L.F., *Phys. Rev.*, Vol. 13B, p. 2433, 1976.

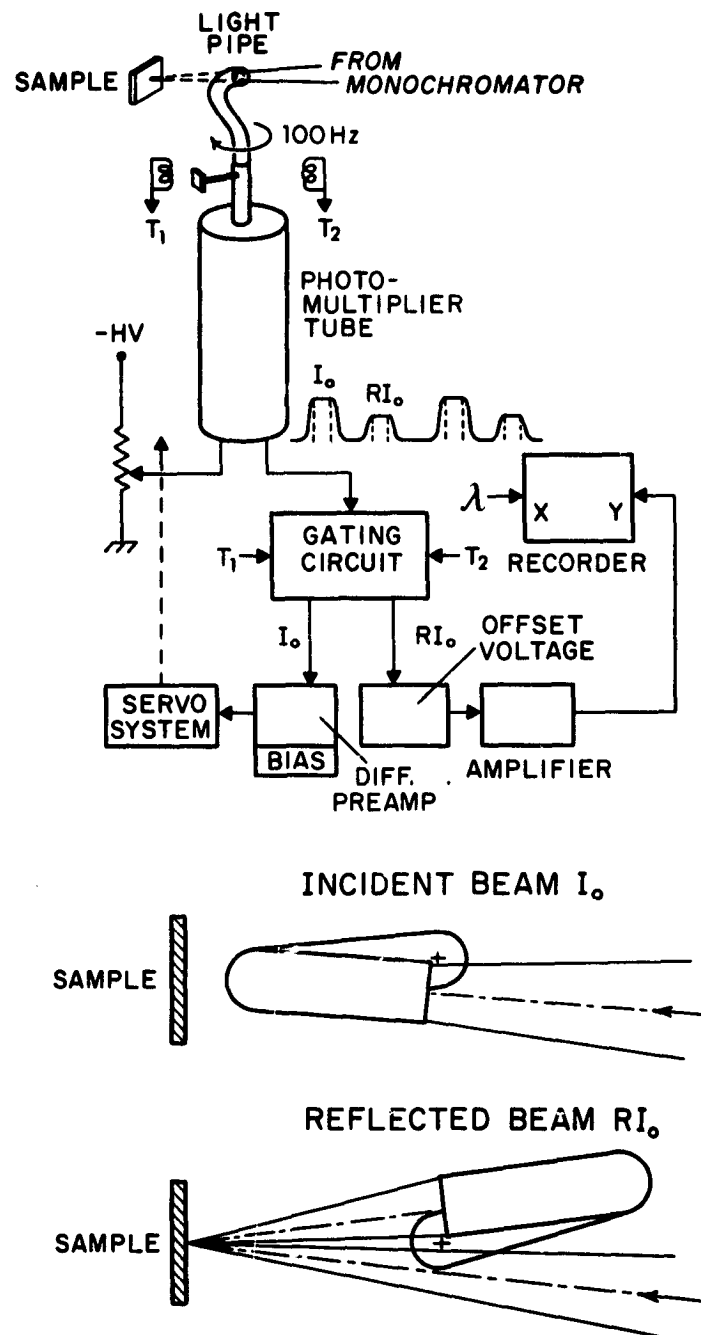


Fig. 1 Schematic diagram of the rotating light pipe reflectometer and associated electronics. Bottom portion shows the geometry of the sample in relation to the bent light pipe.

THE HYDROGEN-CHLORINE ENERGY STORAGE SYSTEM†

J. McBreen, R. S. Yeo, A. Beaufrere,
D-T. Chin* and S. Srinivasan

Department of Energy and Environment
Brookhaven National Laboratory
Upton, N. Y. 11973

Abstract

The electrochemically regenerative hydrogen-chlorine system is being considered for large scale energy storage. It offers many of the advantages of batteries with fluid reactants such as elimination of the problem of electrode morphology changes with cycling and the possibility of independently designing the system for energy and power. Hence, it can be used for both the daily and weekend utility cycles. Recent work includes an extensive heat and mass balance analysis for the system, measurements of Nafion membrane resistivity as a function of HCl concentration and temperatures, and diffusivities and permeation rates of chlorine through Nafion membranes. Results of these studies indicate that an overall electric-to-electric efficiency of 75% or greater can be projected for the system.

1. Introduction

The electrochemically regenerative hydrogen-chlorine system is being considered for large scale energy storage. Work at Brookhaven started in the Summer of 1975(1). Several workers had considered the system previously(2-4). However, only low current density cells were developed. Their characteristics are compared in Table I. In this program high current density operation has been achieved (270 mA/cm² @ 1.0V)(5). High current density operation is important since it reduces the separator and current collector areas and thus has a major effect on the overall system cost.

Table I. Current Density at 1.0V for Various H₂/Cl₂ Cells

Author and Year	Current Density at 1.0V (mA/cm ²)	Reference
Foerster (1923)	3.3	2
Yoshizawa, et al (1962)	10	3
Bianchi (1964)	50	4
McElroy (1976)	270	5

The present cell has a Nafion membrane separator. The electrodes are bonded to each side of the membrane. During discharge, hydrogen gas is fed into the cathode compartment. On charge, provisions have to be made for hydrogen and chlorine storage.

†This work was performed under the auspices of the U.S. Department of Energy

*Visiting Scientist at BNL from Clarkson College of Technology, Potsdam, N.Y., in the Summer of 1977

The hydrogen-chlorine cell has fluid reactants and products. Thus, the electrode morphology changes that often plague batteries with solid reactants are avoided. Cross migration of reactant species through the membrane does not constitute a permanent loss to the system, such as would occur in a battery with dissolved reactants and products.

Batteries with fluid reactants are attractive for energy storage applications because they can be independently designed for energy and power. Cell stacks can be optimized for power, efficiency and cost. The latter is strongly dependent on the current density and the number of cell parts. Energy storage subsystems can be sized for the particular application. This permits designs for either the daily or weekend utility cycle. One benefit that accrues from this ability to design independently for energy and power is a reduction in separator requirements. A battery with 10 hours of storage discharging at 270 mA/cm² has an energy density of 2.7 Wh/cm². This energy density is an order of magnitude higher than that found in batteries with solid reactants: so separator requirements are reduced accordingly. Circulating electrolytes also simplify thermal management.

At this early stage, there are many developing allied technologies which could help in the development of the hydrogen-chlorine energy storage systems. These are the solid polymer electrolyte electrolyzers and electrolysis of water, hydrochloric acid and brines, and the large scale manufacture of Nafion membranes for the chlor-alkali industry.

2. Overall System Considerations

The electrochemically regenerative hydrogen-chlorine energy storage system consists of a cell stack and subsystems for reactant and electrolyte storage. In the present conceptual design, chlorine is evolved as a gas during charge and is then separated from the acid and condensed as a liquid at 40°C using external cooling water. Hydrogen is stored either as iron-titanium hydride or as a compressed gas. This scheme of reactant and electrolyte storage is outlined schematically in Figure 1. The relative areas are proportional to the relative volumes of the subsystems. Table II gives the characteristics of a 10MW/85 MWh energy storage system with this design.

Table II. Characteristics of a 10MW/85MWh H₂/Cl₂ Energy Storage System

Characteristic	Value
Current Density (A/ft ²)	200-300
Energy Density Reactants+Water (Wh/kg)	239
Total Electrode Area (ft ²)	4.9x10 ⁴
Reactant Volume	
Chlorine/Hydrochloric Acid (ft ³)	1.15x10 ⁴
Metal Hydride (ft ³)	1.22x10 ³

The above calculations are for a current density of 209 ASF, an average discharge voltage of 0.97V and operation with hydrochloric acid concentrations in the range of 5-35 w/o.

The hydrogen-chlorine cell differs from most batteries in that the open circuit voltage varies appreciably with temperature and depth of discharge. An empirical relationship has been developed between the open circuit voltage and the cell variables:

$$E_o = 1280 - 9.6 (w-10) - 1.7 (T-25) + AP, \quad (1)$$

where E_o is the open circuit potential in mV, w the hydrochloric acid concentration in w/o (for concentrations above 10 w/o), T is the temperature in $^{\circ}\text{C}$, P the chlorine pressure in atmospheres and A is a constant that is close to 1.

The temperature variation of the open circuit potential reflects the large negative entropy of formation of hydrochloric acid. This yields a $T\Delta S$ value of 8.77 k cal/mole at room temperature. This corresponds to a voltage of 0.38V. Since the charging overvoltage is only about 0.15V, there is a cooling effect on charge and a heating effect on discharge.

This year we carried out a detailed heat and mass balance analysis for the system. A computer program was written for this purpose. This analysis took into account the variation in the physical and thermodynamic properties of all chemicals during cycling. The analysis also took into account variations in electrolyte temperature and concentration and the variation in operating cell voltages. Thus, the overall electric-to-electric efficiencies could be calculated. A standard method for non-isothermal heat balance analysis was used(6). Calculations were done for constant current operation at various overvoltages. Typical results are shown in Figure 2. Calculated electric-to-electric efficiencies are given in Figure 3. Electric-to-electric efficiencies of greater than 70% can be achieved if overvoltages can be maintained below 0.17V.

One salient feature of the present conceptual design is that no energy is required to maintain storage such as for heating or refrigeration. The system pressure is 150 psi which is within the pressure rating of most of the shelf equipment. Pressurized operation increases the solubility of chlorine in the electrolyte. Chlorine solubility in hydrochloric acid increases with increasing acid concentration, in the concentration ranges used in the system. This behavior is the opposite to what one finds in other inorganic chloride electrolytes where there is a salting out effect. High chlorine solubilities enhance mass transport on discharge and minimize electrolyte circulating requirements.

3. Nafion Membrane Resistivity and Electric-to-Electric Efficiency

Since the kinetics of the electrochemical reactions are fast, voltage efficiencies will be largely determined by the Nafion resistivity. Nafion resistivities have been measured as a function of HCl concentration and temperature. The method used was a simple DC method(7). The results are given in Figure 4. These results were used in

conjunction with the results of the heat and mass balance analysis to calculate the overall electric-to-electric efficiency for the system. The polarization losses due to the Nafion membrane depend upon the degree of cooling during charge. The latter is a function of the method of reactant storage, external cooling and the degree of heat exchange between the electrolyte and reactant storage subsystems. The greater the degree of cooling the higher the polarization losses due to the Nafion membrane. Figure 5 gives plots of several calculated cell voltage parameters. It was assumed that all polarization losses were due to iR losses in the Nafion membrane. A membrane thickness of 0.10" and the maximum possible degree of cooling were assumed. The calculated voltage is 74.5%. It is fortuitous that system temperature, acid concentration and Nafion resistivity vary in such a way that iR losses remain relatively constant with cycling. Thinner membranes and less cooling during charge would yield even higher efficiencies.

4. Chlorine Diffusivity in Nafion and Coulombic Efficiency

System coulombic efficiency will depend on the rate of reactant diffusion through the Nafion membrane. Figure 6 is a schematic of a cell for measurement of chlorine diffusivities and permeation rates. The cell consists of two compartments that sandwich a Nafion membrane with a chlorine electrode bonded to one side of the membrane. This electrode is potentiostated at 0.4V positive to the reversible hydrogen electrode in a hydrochloric acid electrolyte. A hydrochloric acid electrolyte containing chlorine is introduced into the other compartment. The chlorine diffuses into the membrane and is reduced on contact with the chlorine electrode. The chlorine electrode current transient reflects the buildup of the concentration gradient in the membrane and the steady state current is an indicator of the self discharge rate for that particular concentration of chlorine, temperature and Nafion membrane thickness. The ratio of the transient current to the steady state current (J_t/J_o) is related to the diffusivity (D) membrane thickness (L) and time (t) as follows:

$$\frac{J_t}{J_o} = \frac{2}{\pi^{1/2}} \frac{L}{(Dt)^{1/2}} \sum_{n=0}^{\infty} \frac{(-1)^n}{n!} e^{-\{L(2n+1)\}^2/4Dt} \quad (2)$$

The first term of the above equation gives results that are valid up to 96.5% attainment of the steady state, i.e.,

$$\frac{J_t}{J_o} = \frac{2}{\pi^{1/2}} \frac{L}{(Dt)^{1/2}} e^{-L^2/4Dt} \quad (3)$$

The diffusivity can be calculated from the current transient and the steady state permeation can be read from the steady state current. Preliminary data yield a chlorine diffusivity in Nafion of $2.1 \times 10^{-7} \text{ cm}^2 \text{ sec}^{-1}$ at 25°C . The steady state permeation using 14 w/o HCl and atmospheric pressure is about 1 mA for a 0.010" membrane. Data will be obtained as a function of temperature and HCl concentration. At present, indications are that the coulombic efficiency will be high. Self discharge on stand is not a concern since only a small fraction of the reactant is stored in the cell.

5. Subcontractor Activities

In FY 1977, there were subcontracts at GE, EDA and Bechtel. GE will soon deliver a 0.05 ft² cell with a chlorine/hydrochloric acid storage system capable of operating at elevated pressures and temperatures. EDA has been carrying out chlorine electrode studies, chlorine/hydrochloric acid subsystem studies and investigations of fluoroplastics for tank liners. Bechtel has carried out a preliminary techno-economic assessment.

6. Future Work

The 0.05 ft² cell and storage system will be used to determine cell performance as a function of HCl concentration, temperature, pressure and flow rates. These data will be used in defining systems processes and for optimizing the system and for designing larger systems. Materials studies will focus on materials for current collectors, hydrogen electrode electrocatalysts, cost effective reactant storage and materials for reactant circulating systems and seals.

References

1. Gileadi, E., Srinivasan, S., Salzano, F. J., Braun, C., Beaufriere, A., Gottesfeld, S., Nuttall, L. J., LaConti, A. B., J. Power Sources, in press.
2. Foerster, F., Z. Elektrochem., **29**, 64 (1923).
3. Yoshizawa, S., Hine, F., Takahara, Z., Kanaya, Y., J. Electrochem. Soc. (Japan), **30**, E10 (1962).
4. Bianchi, G., Mussini, T., Ric. Sci. Rend., **6A**, 37 (1964).
5. Beaufriere, A., Yeo, R. S., Srinivasan, S., McElroy, J., Hart, G., Proc. 12th IECEC Meeting, paper #779148, American Nuclear Society, LaGrange Park, Illinois (1977).
6. Chin, D-T., Yeo, R. S., McBreen, J., Srinivasan, S., to be published.
7. Lander, J. J., Weaver, R. D., in Characterization of Separators for Alkaline Silver Oxide Zinc Secondary Batteries, J. E. Cooper and A. Fleischer, editors, Air Force Aero Propulsion Laboratory, Dayton, Ohio (1964).

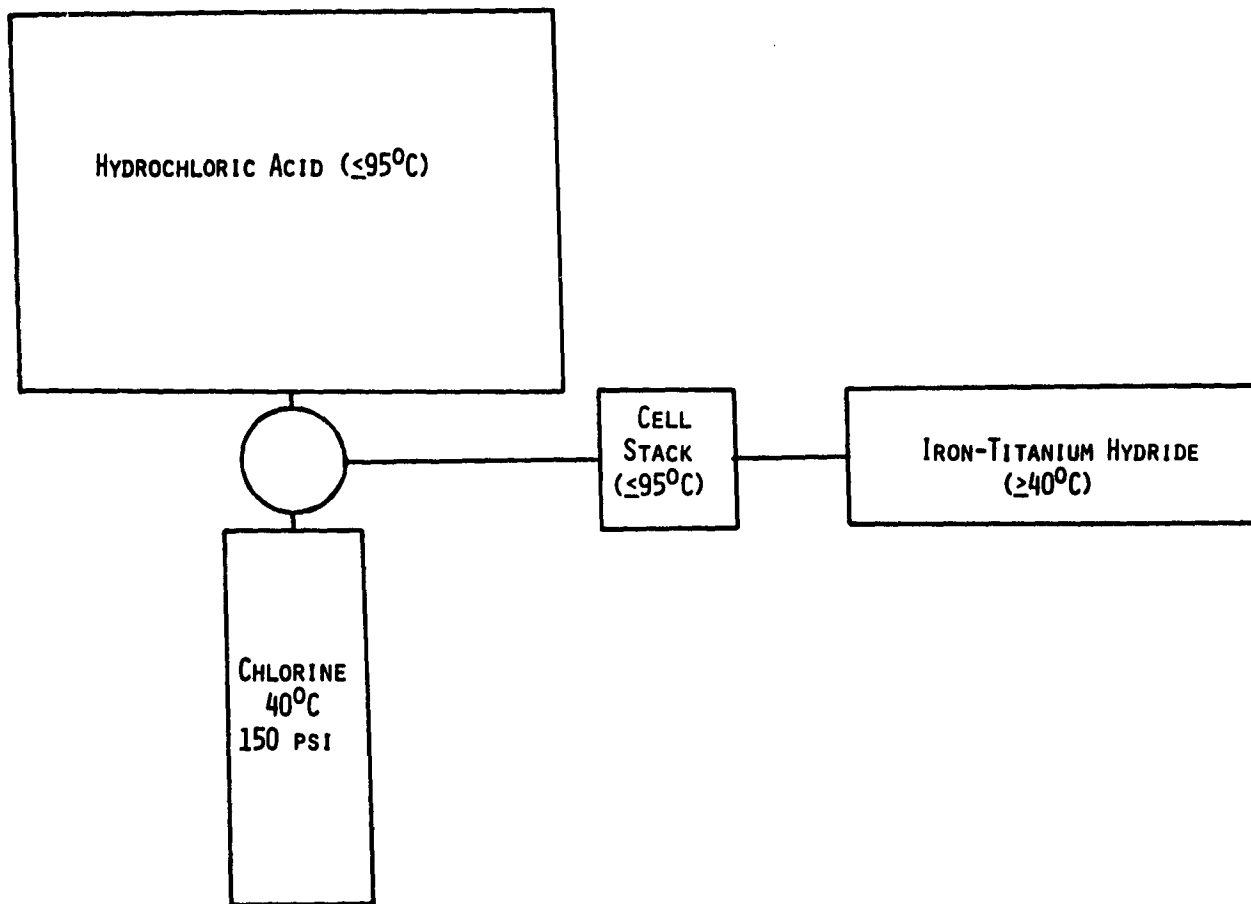


Figure 1. An Electrochemically Regenerative H₂/Cl₂ System

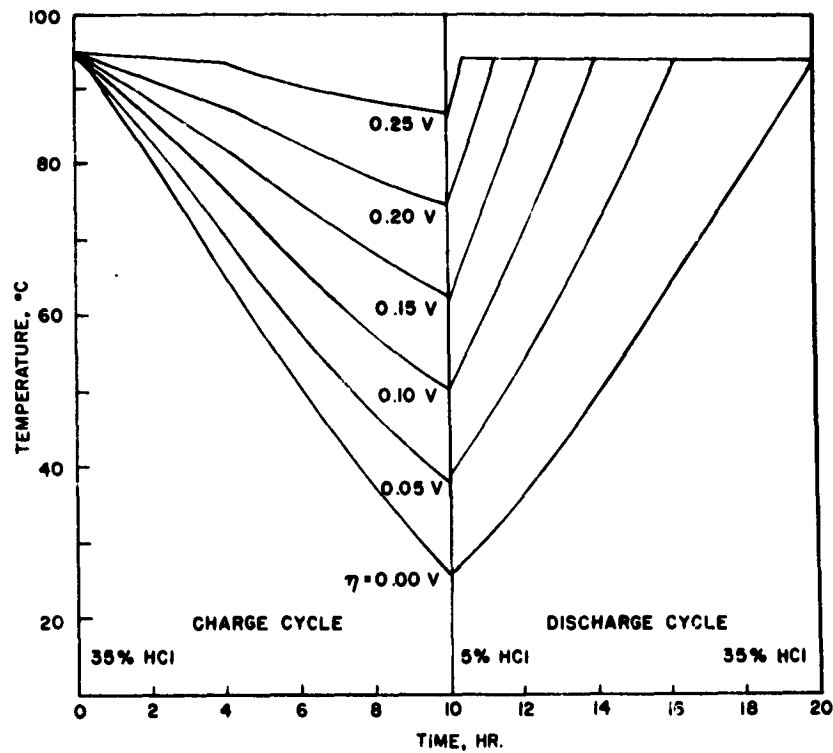


Figure 2. Electrolyte Temperature in a 1MW/10MWh H_2/Cl_2 System. Charge and Discharge Currents = $10^6 A$.

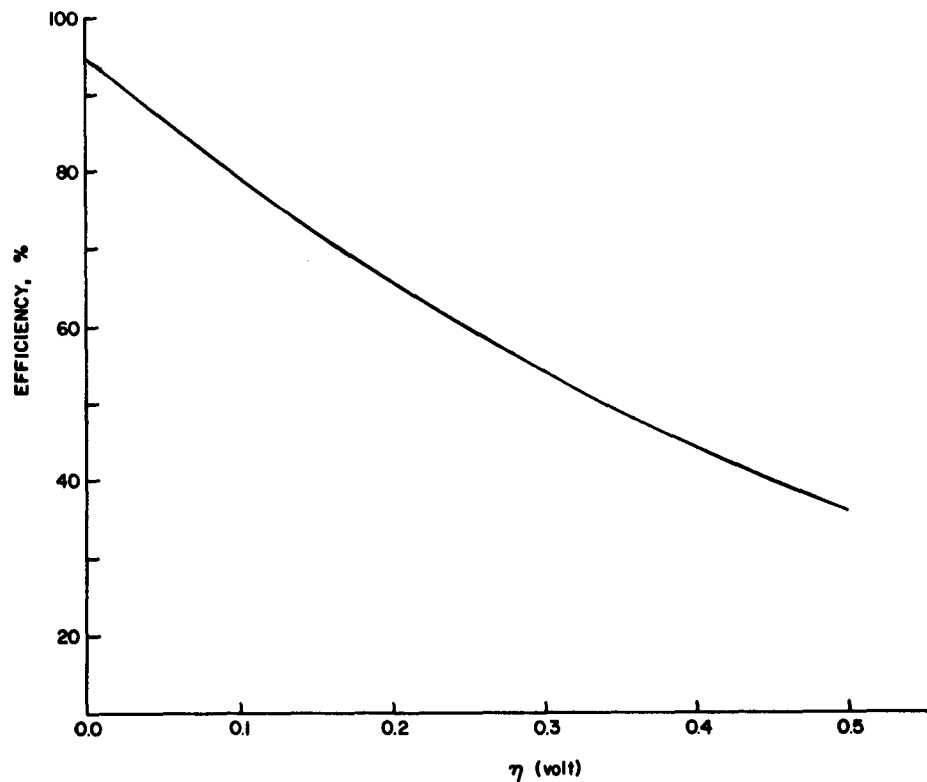


Figure 3. Calculated Electric-to-Electric Efficiencies as a Function of Cell Overvoltage for a 1MW/10MWh System Operating at $10^6 A$

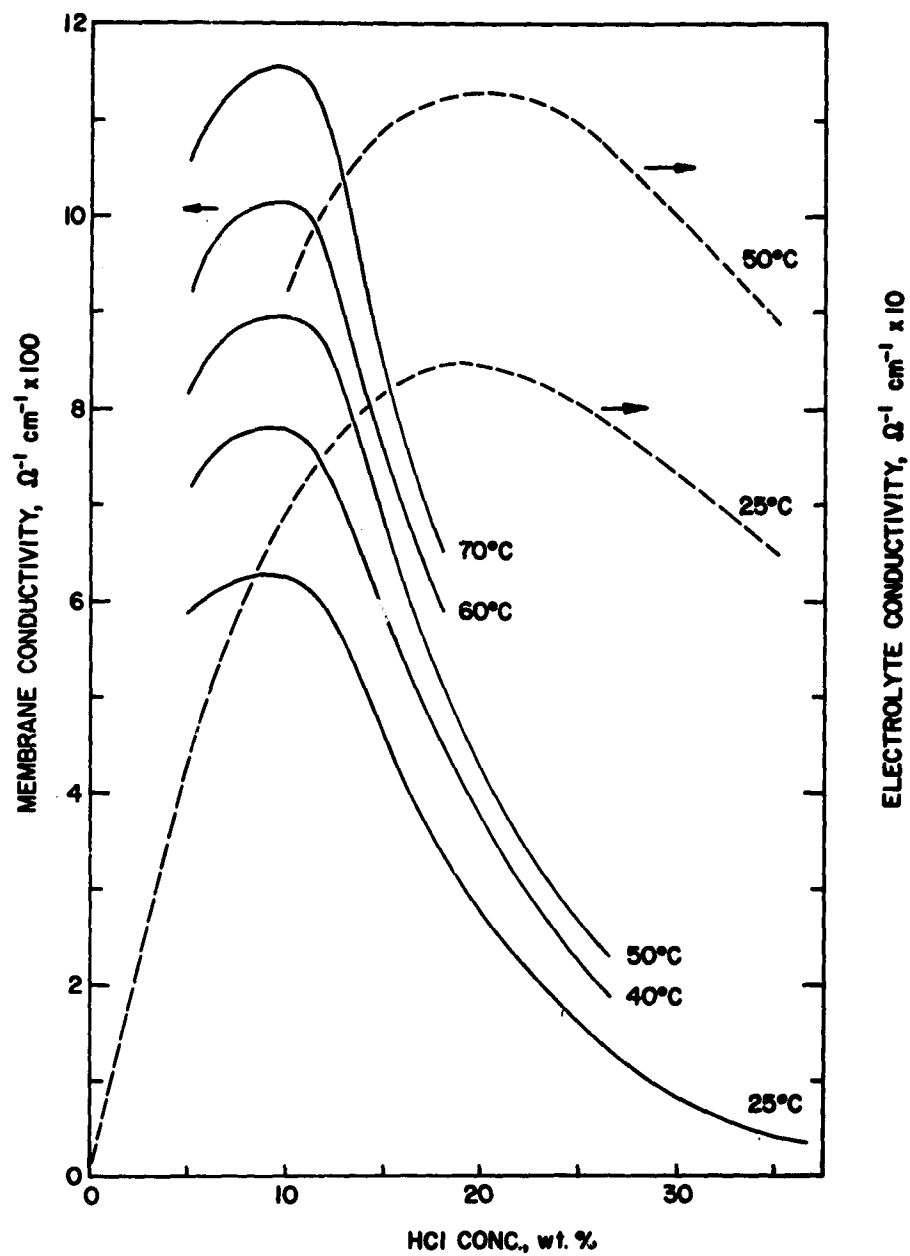


Figure 4. Nafion Membrane Resistivity Data as a Function of HCl Concentration and Temperature. HCl Electrolyte Conductivity at 25°C and 50°C Also Given.

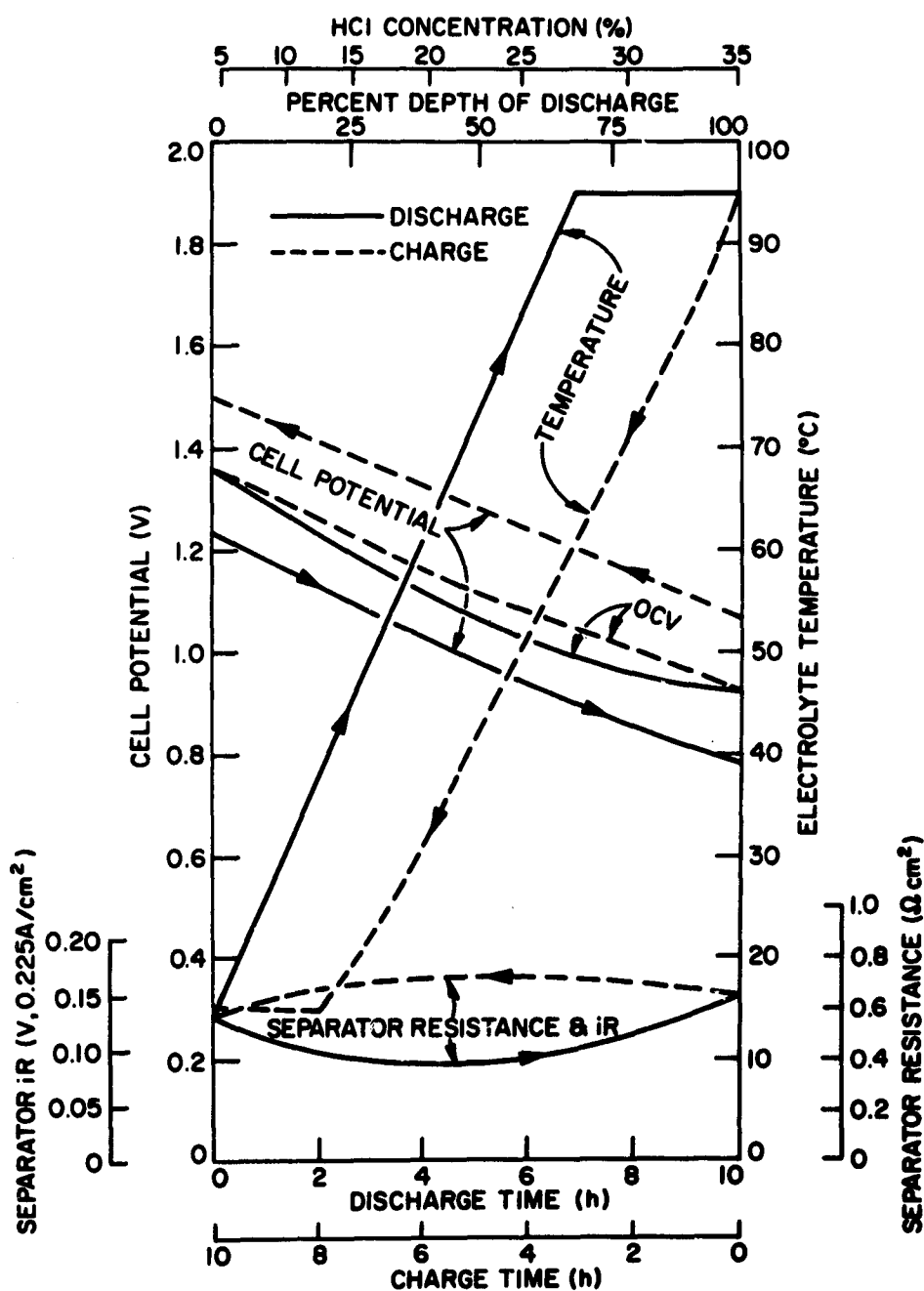


Figure 5. Calculated Voltage Parameters for a H_2/Cl_2 System Operating at $0.225 A/cm^2$

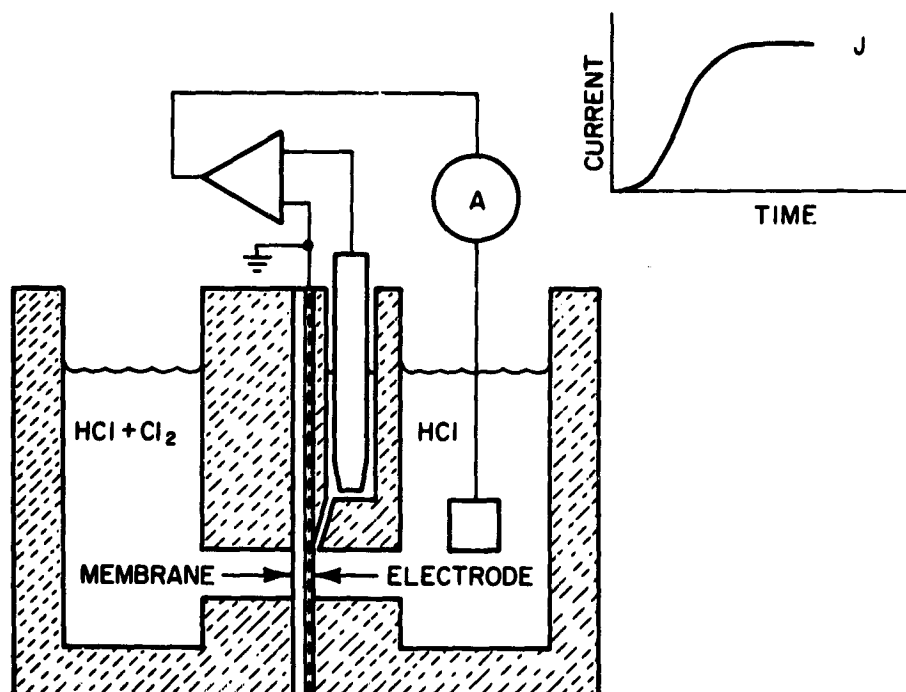


Figure 6. Schematic of Cell for Cl_2 Diffusivity Measurements in Nafion Membranes. Inset Indicates Shape of the Permeation Current Transient.

SESSION II
HYDROGEN PRODUCTION

B. THERMOCHEMICAL CYCLES

THE SULFUR CYCLE WATER DECOMPOSITION SYSTEM

G. H. Farbman

Westinghouse Electric Corporation

**CURRENT STATUS OF THE THERMOCHEMICAL WATER-SPLITTING
PROGRAM AT GENERAL ATOMIC**

J. D. de Graaf, J. L. Russell, J. H. Norman, T. Ohno, P. W. Trester,
and K. M. McCorkle

General Atomic Company

ASSESSMENT OF THERMOCHEMICAL HYDROGEN PRODUCTION

J. R. Dafler, S. E. Foh, and J. D. Schreiber

Institute of Gas Technology

THERMOCHEMICAL HYDROGEN PRODUCTION REVIEW PANEL

J. E. Funk

University of Kentucky

**THE LASL THERMOCHEMICAL HYDROGEN PROGRAM STATUS ON
OCTOBER 31, 1977**

K. E. Cox and M. G. Bowman

University of California Los Alamos Scientific Laboratory

**REVISED FLOWSHEET AND PROCESS DESIGN FOR THE ZnSe
THERMOCHEMICAL CYCLE**

O. H. Krikorian and H. H. Otsuki

Lawrence Livermore Laboratory

STATUS OF EUROPEAN THERMOCHEMICAL HYDROGEN PROGRAMS

M. G. Bowman

University of California Los Alamos Scientific Laboratory

THE SULFUR CYCLE WATER DECOMPOSITION SYSTEM

Gerald H. Farbman
Westinghouse Electric Corporation
Advanced Energy Systems Division
P. O. Box 10864
Pittsburgh, Pennsylvania 15236

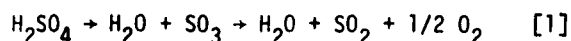
Abstract

The objective of this program is to assess the technical and economic feasibility of a hydrogen generation process, called the Sulfur Cycle Water Decomposition System, based upon the electrolysis of sulfurous acid. To do this, a multi-task program is being carried out to experimentally determine the operating characteristics of the key process steps in the hydrogen generating cycle and to develop the technology to the point where a bench scale integrated process development unit, operating at conditions similar to those expected in commercial plants, can be designed, built, and operated by Fiscal Year 1983.

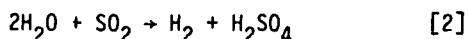
The experimental programs being conducted and discussed are concerned with the sulfurous acid electrolysis, materials for handling high temperature sulfuric acid and $\text{SO}_3/\text{SO}_2/\text{O}_2$ /steam mixtures, and sulfur trioxide reduction. In addition, performance characteristics of the process are presented.

The objective of this program is to assess the technical and economic feasibility of a hydrogen generation process, called the Sulfur Cycle Water Decomposition System, based upon the electrolysis of sulfurous acid. To do this, a multi-task program is being carried out to experimentally determine the operating characteristics of the key process steps in the hydrogen generating cycle and to develop the technology to the point where a bench scale integrated process development unit, operating at conditions similar to those expected in commercial plants, can be designed, built, and operated by Fiscal Year 1983.

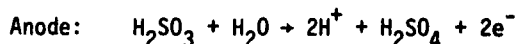
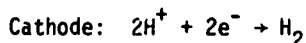
The Sulfur Cycle Water Decomposition System is a two-step hybrid electrochemical/thermochemical cycle for decomposing water into hydrogen and oxygen. The process, in its most general form, consists of two chemical reactions - one for producing oxygen and the other for producing hydrogen. The production of oxygen occurs via the thermal reduction of sulfur trioxide obtained from sulfuric acid.



The equilibrium for Reaction 1 lies to the right at temperatures above 1000K. Catalysts are available for accelerating the rate of sulfur trioxide reduction to sulfur dioxide and oxygen. The process is completed by using the sulfur dioxide from the thermal reduction step to depolarize the anode of a water electrolyzer. The overall reaction occurring electrochemically is:



This is comprised of the individual reactions:



The net result of Reactions 1 and 2 is the decomposition of water into hydrogen and oxygen. Sulfur oxides are involved as recycling intermediates. Although electrical power is required in the electrolyzer, much smaller quantities than those necessary in conventional electrolysis are needed. The theoretical voltage to decompose water is 1.23 V, with many commercial electrolyzers requiring over 2.0 V. The power requirements for Reaction 2 (0.17 volts at unit activity for reactants and products) are thus seen to be theoretically less than 15 percent of those required in conventional electrolysis. This can dramatically change the heat and work required to decompose water and lead to improved thermal efficiencies.

The process is shown schematically in Figure 1. Hydrogen is generated electrolytically in an electrolysis cell which anodically oxidizes sulfurous acid to sulfuric acid while simultaneously generating hydrogen at the cathode. Sulfuric acid formed in the electrolyzer is then vaporized, using thermal energy from a high temperature heat source. The vaporized sulfuric acid (sulfur trioxide-steam mixture) flows to an indirectly heated reduction reactor where sulfur dioxide and oxygen are formed. Wet

sulfur dioxide and oxygen flow to the separation system, where oxygen is produced as a process co-product and the sulfur dioxide is recycled to the electrolyzer.

The cycle has the potential for achieving high thermal efficiencies while using common and inexpensive chemicals. The product hydrogen and oxygen streams are available under pressure and at high purity. As a result, these may be pipelined and used without detrimental environmental effects and without jeopardizing processes which employ the gas.

Experimental studies are being conducted in those areas important to the success of the process. These studies are concerned with the sulfurous acid electrolyzer, materials for handling high temperature sulfuric acid and $\text{SO}_3/\text{SO}_2/\text{O}_2$ /steam mixtures, and sulfur trioxide reduction. In addition, engineering evaluations of the process, its performance as a function of operating parameters, and its economics have been performed.

Electrolyzer

The effort in the electrolyzer area has, in atmospheric ambient temperature test cells, considered anode materials, cathode types, and catholyte anolyte separatory membranes over a range of sulfuric acid concentrations and current densities.

An electrolytic test cell is shown schematically in Figure 2. The use of a membrane to separate catholyte and anolyte, as well as catholyte overpressure to preclude the diffusion of sulfurous acid to the catholyte with resulting preferential production of sulfur rather than hydrogen - have been incorporated in this design. The electrode on which gassing is shown is the cathode. The liquid level in this compartment is higher than in the anode compartment to maintain the desired overpressure level. Sulfuric acid solution, saturated externally with sulfur dioxide, is circulated through the anode compartment. The use of $\text{Hg}/\text{Hg}_2\text{SO}_4$ probe electrodes to monitor polarizations at the cathode and anode (and current-interruption techniques) permits detailed exploration of the causes of cell voltage variations with cell temperature, current density and experimental procedures. Sulfur deposition, if it occurs, is readily observable at the cathode due to the use of transparent PVC face plates in the cell, the rest of which is constructed of Teflon.

Initial testing of anodes used platinized platinum and platinized carbon flooded electrodes. Anode voltages ranged between 450 mV to 650 mV against the Standard Hydrogen Electrode (SHE) at current densities to 200 mA/cm^2 , with the platinized carbon showing much more reproducible results. To improve on the performance, tests were then performed on flow-through anodes, which would insure delivery of the dissolved SO_2 to the entire body of the anode at a concentration for optimum anode potential. Flow-through anodes constructed of monolithic porous graphite were evaluated at current densities up to 400 mA/cm^2 . These showed substantial improvements in voltage compared to the best of the flooded electrodes.

The overall cell performance capability reflects the summation of the individual components of anode,

cathode, and resistivity losses. Table 1 depicts the performance levels currently demonstrated in the test facility of Figure 3, and foreseen for the cell. Substantial progress has been made towards demonstrating the cell voltages of interest to a commercial process, and the areas where improvements are yet to be made have been identified and programs to accomplish them defined and underway. Work is proceeding at present, in evaluating electrocatalysts, other than platinum, for their effectiveness and in examining the effects of different anode porosities and sulfuric acid concentration on the achievable cell voltage.

Materials

As in most advanced technologies, materials of construction are challenged by the water decomposition process. The most critical structural and heat transfer materials problem is in the containment of boiling sulfuric acid, at pressures to 2069 kPa (300 psi) and temperatures to 724K (845°F), during the vaporization prior to SO₃ reduction. These conditions are beyond those normally used in the manufacture or use of sulfuric acid and therefore materials data is generally unavailable. Work is underway to screen various candidate materials to determine their suitability or need for new alloy development. This work is proceeding in the test facility shown in Figure 4, where material compatibility with concentrated sulfuric acid will be determined in precious metal lined autoclaves containing a given quantity of acid and a number of material test specimens. The specimens will be exposed for time periods up to 5000 hours at various pressure and temperature levels. At periodic intervals the samples will be removed from the test environment, inspected, weighed, and returned to test.

The concern with the suitability of structural materials for the high temperature SO₃ reduction reactor has resulted in the construction of the additional test facility to expose candidate material to the environment they will see in the reactor. The purpose is to test materials under isolated conditions with only the reactants, i.e., superheated steam, SO₃, SO₂, and/or O₂ present, and at temperatures to 1144K (1600°F).

Sulfur Trioxide Reduction

The thermal decomposition of sulfur trioxide into sulfur dioxide and oxygen proceeds very slowly unless catalyzed. The economics of the process can, therefore, be substantially affected by the choice of catalyst. Ideally, a catalyst will possess high activity and long life. Catalyst activity is important, since the ability to achieve equilibrium conversions at high space velocities leads to compact reactors. Similarly, the ability of a catalyst to maintain high activities for extended periods of time lowers maintenance and catalyst replacement costs. Most often trade-offs between activity and life are required, and these are reflected in an optimization of the capital and operating costs associated with the chemical reactor.

Several catalysts have been tested to determine their suitability to the SO₃ reduction step. Vanadium pentoxide, for instance, has been examined over the temperature range of interest to space velocities of 60,000 hr⁻¹. Equilibrium conversions were achieved over a space velocity range up to 10,000 hr⁻¹.

These activities were excellent, but 1000 hour life test, showed a reduction in conversion of about 7 percent at 1123K (850°C). A platinum catalyst was also tested which had poorer initial activity, but showed no reduction in activity over the same 1000 hours at 1123K (850°C). Further work, using the facility shown in Figure 5, will explore additional catalysts and extend the testing parameters for all catalysts to allow an economic judgment to be made on the most attractive catalyst. The process fluid to be reduced, in this facility, will contain SO₃ and water vapor in varying proportions to simulate the inlet conditions for a range of sulfuric acid concentrations. This provides a more realistic testing environment than the earlier experimental work which employed an SO₃/inert gas flow stream.

Process Flow Sheet Development

Process flow sheets have been developed under an earlier NASA contract (Ref. 1) and a prior ERDA contract (Ref. 2). The latter provided an iteration which allowed improvements to be made in the areas of:

- SO₂/O₂ Separation - The cryogenic separation system previously used was replaced by a less energy intensive scrubbing system for removing SO₂ from the oxygen co-product stream.
- Acid Vaporization - The pressure, and temperature, of the acid vaporization system was increased.
- Stream Matching - A great deal more attention has been paid, in the revised flow sheet, to the matching of process heating and cooling streams to maximize the use of hot fluids and minimize both the need for external heat inputs and the amount of heat ultimately rejected from the process plant.

The evaluation of the process flow sheets were all done on the same sizing basis, i.e., a hydrogen production rate of 380 x 10⁶ SCFD, so that comparisons can readily be made.

To provide a process evaluation without regard to the source of thermal energy to drive the process, two cases were considered with a "generalized heat source." These cases do not identify the source of heat, but only indicate the energy requirements and temperature levels of the process heat source. For comparison with the NASA sponsored conceptual design study (Ref. 1), two cases were considered with a Very High Temperature Nuclear Reactor (VHTR) integrated with the process plant. The VHTR provides all the energy requirements, i.e., thermal and electrical, for the entire plant.

The four cases, with the NASA flow sheet as a base, are compared in Table 2. In that table, Cases 1 and 3 reflect a self-sufficient process plant balanced to generate only that amount of power required for on-site consumption. As such, a quantity of elevated temperature heat in the process cannot be used and must therefore be rejected. Cases 2 and 4 are balanced to avoid this process heat loss by using the otherwise wasted heat in the electric generating plant to help produce electrical power in excess of plant requirements. With the use of this "waste" heat to supplement external heat inputs to the steam turbine generators, the "excess" electricity is

produced at an incremental thermal efficiency of 46 to 49 percent.

REFERENCES

The experimental and analytical work being performed on the Sulfur Cycle Water Decomposition System continues to support the technical and economic potential of the system as an efficient cost effective way to produce hydrogen in the post-1985 time period, using as energy inputs any reasonable high temperature heat source, such as nuclear or solar energy or a high temperature "waste" heat from an industrial process.

1. NASA-CR-134976, "The Conceptual Design of an Integrated Nuclear-Hydrogen Production Plant Using the Sulfur Cycle Water Decomposition System," Westinghouse Electric Corporation, April 1976.
2. FE-2262-15, "Hydrogen Generation Process - Final Report," Westinghouse Electric Corporation, June 1977.

TABLE 1

ELECTROLYTIC CELL PERFORMANCE⁽¹⁾

	CURRENTLY DEMONSTRABLE	PROJECTED
ANODE POTENTIAL	460 mV	300 mV ⁽²⁾
CATHODE POTENTIAL	10 mV	10 mV
CELL RESISTIVITY	130 mV ⁽³⁾	100 mV ⁽⁴⁾
	600 mV	410 mV

NOTES:

- (1) At 50 percent H₂SO₄ concentration, 200 mA/cm², atmospheric pressure, and temperature 323K (50°C).
- (2) Improved electrocatalyst, optimized anode porosity and internal surface area.
- (3) Total of membrane (25 mil microporous rubber) and other cell IR losses.
- (4) Total of membrane (15 mil microporous rubber) and other cell IR losses. Increase of cell temperature would reduce this by virtue of reduced sulfuric acid resistivity with increased temperature.

TABLE 2

PROCESS VARIATIONS

CASE	FLOW SHEET	HEAT SOURCE	H ₂ PRODUCTION	"EXCESS" POWER	OVERALL EFFICIENCY
BASE	NASA	VHTR	380 x 10 ⁶ SCFD	0	45.2%
1	REVISED	GENERALIZED	380 x 10 ⁶ SCFD	0	54.5%
2	REVISED	GENERALIZED	380 x 10 ⁶ SCFD	285,550 KWe	53.5%
3	REVISED	VHTR	380 x 10 ⁶ SCFD	0	54.1%
4	REVISED	VHTR	380 x 10 ⁶ SCFD	179,010 KWe	53.1%

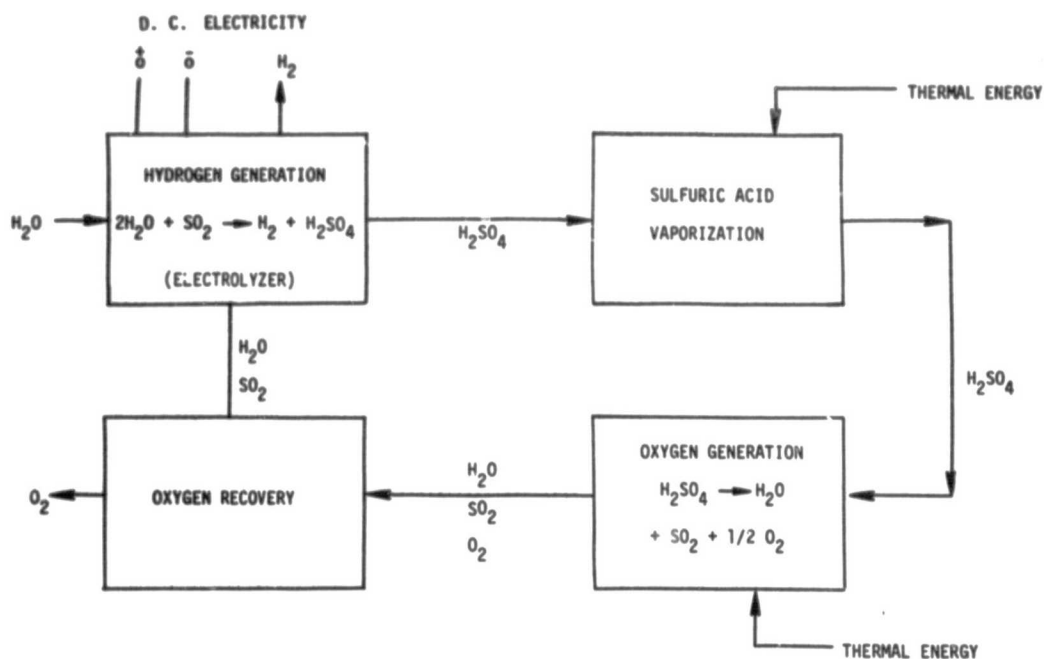


Figure 1. Hydrogen Generation Schematic Diagram

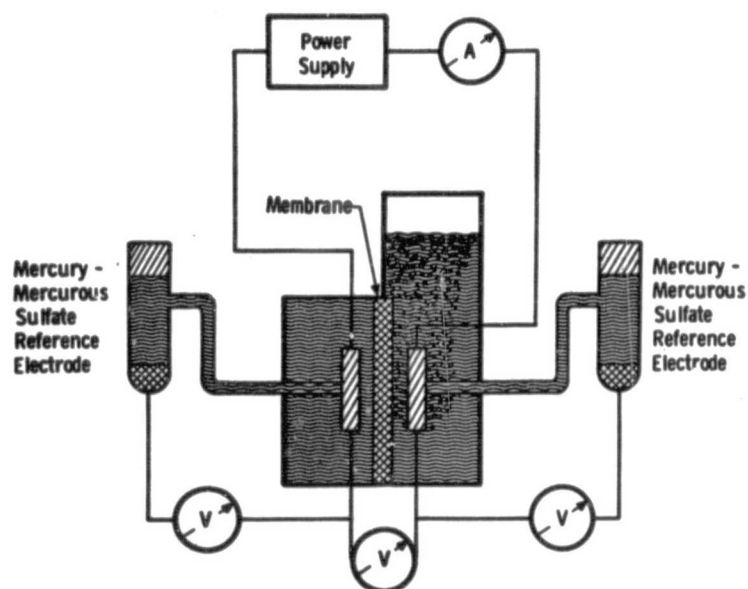


Figure 2. Schematic of Sulfur Dioxide-Depolarized Electrolytic Cell for Hydrogen Generation

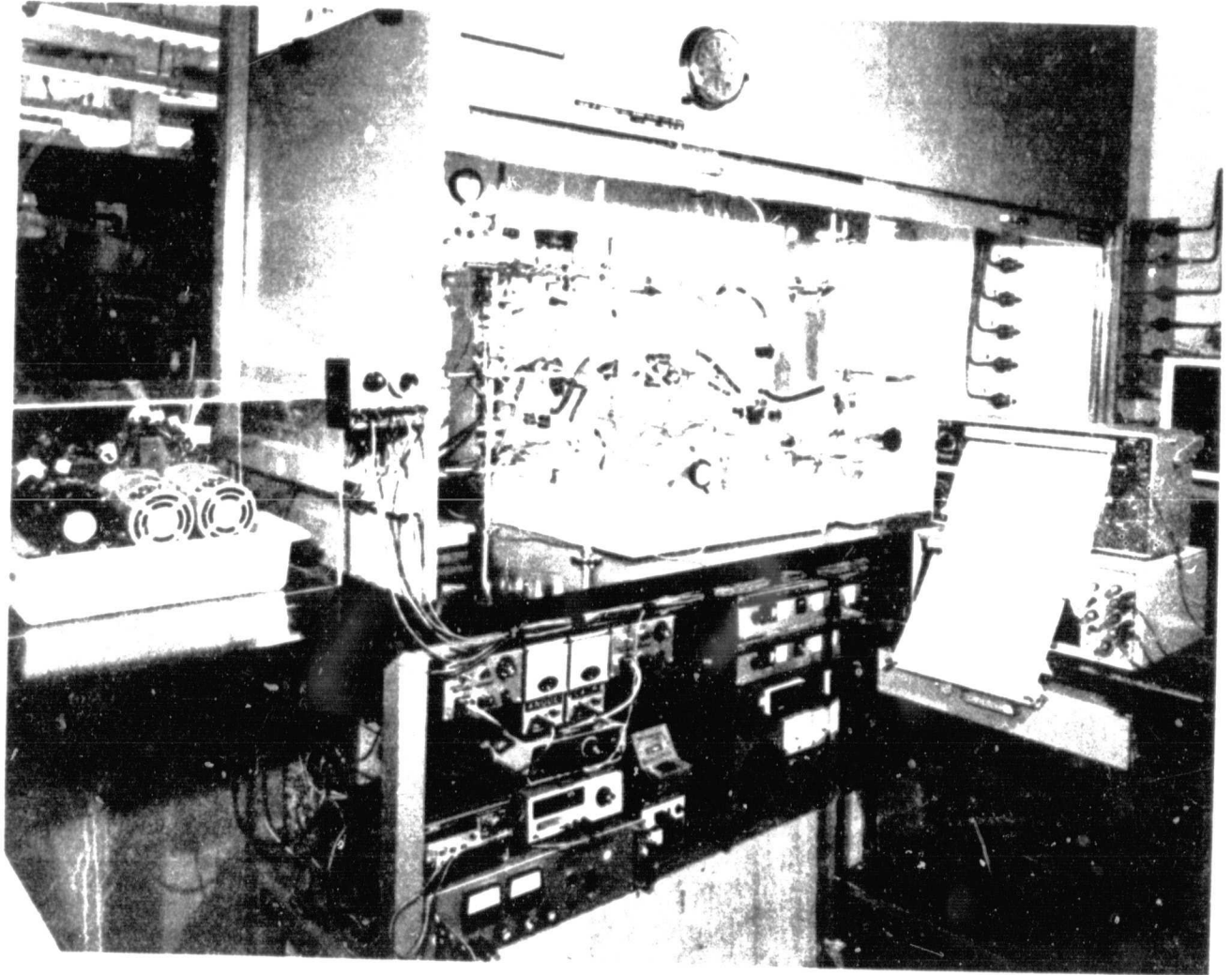


Figure 3. Cell Demonstration Facility

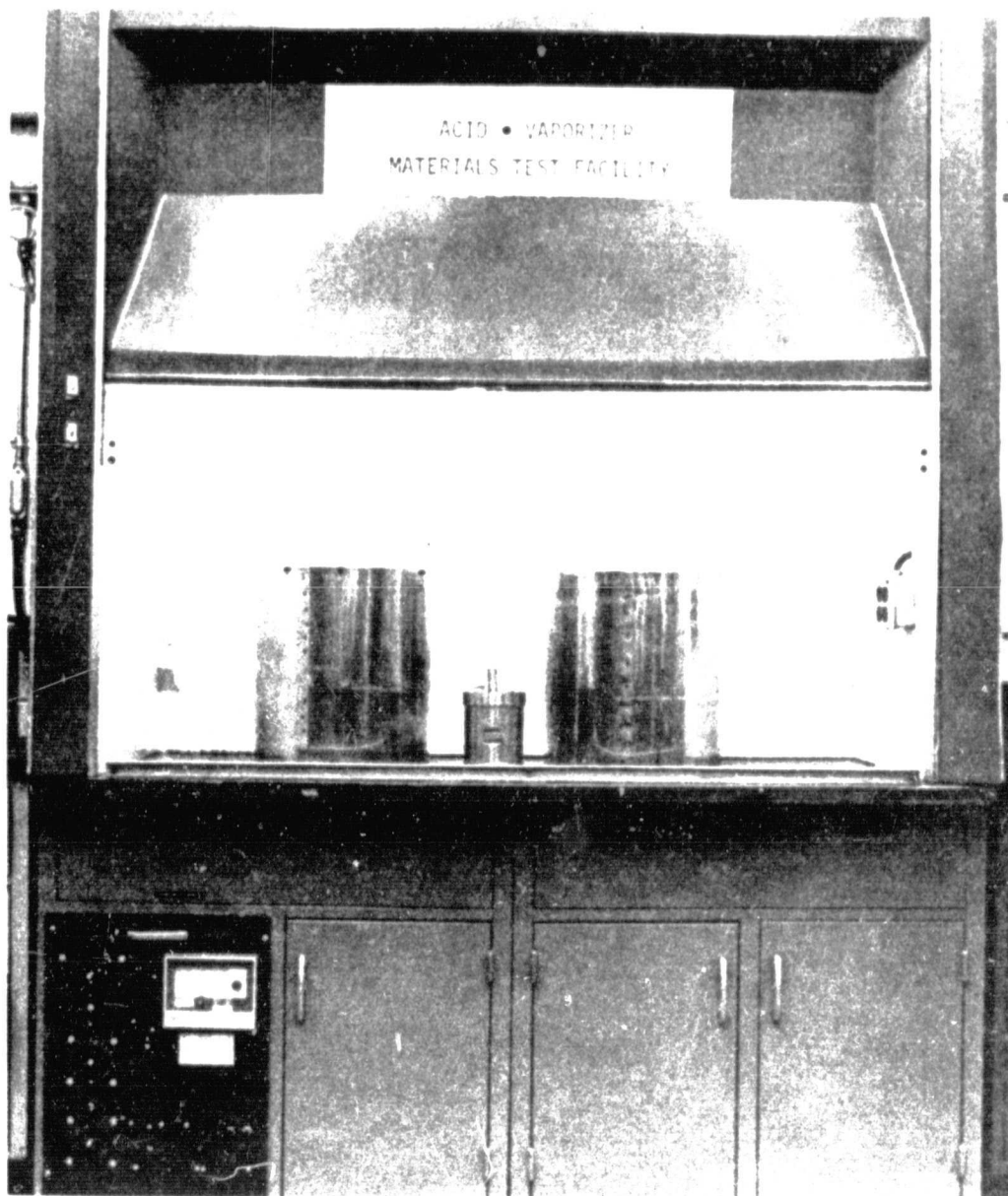


Figure 4. Acid • Vaporizer Materials Test Facility

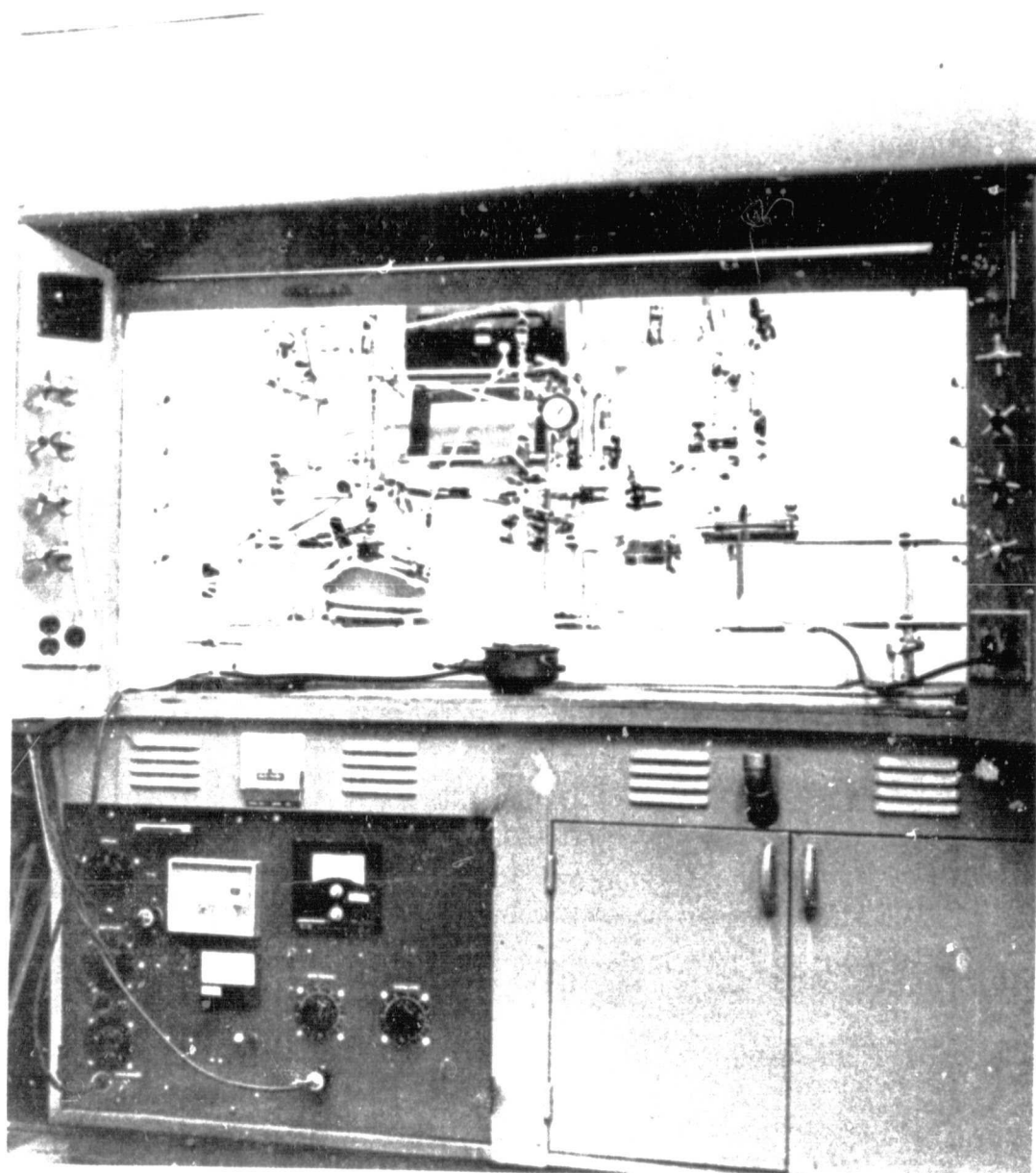


Figure 5. SO_3 Reduction Catalyst Screening Test Facility

CURRENT STATUS OF THE THERMOCHEMICAL WATER-SPLITTING
PROGRAM AT GENERAL ATOMIC

J. D. de Graaf, J. L. Russell, J. H. Norman,
T. Ohno, P. W. Trester, K. M. McCorkle

General Atomic Company
San Diego, California

ABSTRACT

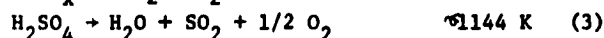
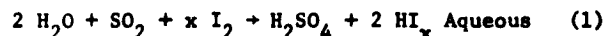
General Atomic's thermochemical water-splitting program is in its sixth year of development. It is presently a cooperative effort with support from the U.S. Department of Energy and the American Gas Association. Since the selection of the cycle in 1974, research on a broad basis has been carried out and considerable progress in the area of chemistry, process engineering, as well as material investigations, has been made.

Under DOE contract EY-76-C-03-0167, Project Agreement 63, GA is conducting bench scale technology validation studies and process engineering. The bench scale investigations are aimed at engineering approaches for conducting the chemical reactions and separation processes as continuous operations. For these investigations the process is broken up into three subunits: 1) the main solution reaction unit, 2) the sulfuric acid unit, and 3) the hydrogen iodide unit. The first unit has been built and is ready for testing. The second unit has been designed, while the third unit is still in the conceptual stage. The development of a third generation process flowsheet is in progress. Recent improvements found in the chemistry will be incorporated, and also major friction pressure losses will be taken into account. In this work the process simulator code DESIGN/2000 from the Chemshare Corporation will be applied.

1. INTRODUCTION

General Atomic's thermochemical water-splitting program is in its sixth year of development. It is presently a cooperative effort with support from General Atomic (GA), the American Gas Association (AGA), soon to become Gas Research Institute (GRI) and the U.S. Department of Energy (DOE). The DOE support for FY 1977 has been \$200,000 and funding at an equivalent level for FY 1978 is expected.

After a computer-aided search supported with scouting chemical investigations, the so-called Sulfur-Iodine cycle was selected. The abbreviated chemical description of the cycle, which was first described by Russell (Ref. 1) is:



where the HI_x represents the mixture of several polyiodides formed in the initial solution. Separation of the H_2SO_4 and HI_x takes place under gravity, as the two acids are almost immiscible. The upper phase contains most of the H_2SO_4 , and the lower phase contains most of the HI_x .

The main attributes of the cycle are as follows: 1) it has a high expected thermal efficiency (approximately 50%); 2) it has heat requirements that match the output capability of the very high-temperature gas-cooled reactor (VHTR); and 3) it can be conducted as an all-liquid and gas-phase process, which is a characteristic that should give it considerable engineering advantage over any cycle requiring solids handling.

The cycle is at this moment in the process development phase which concentrates on chemical investigations, bench-scale investigations, process engineering, and containment materials evaluations. Under a DOE contract, bench-scale investigations and the process engineering have been carried out.

The present paper summarizes the accomplishments in these two areas over FY 1977.

2. PRESENT STATUS

An extensive update on the current status of the program has recently been given by Schuster (Ref. 2) and we will summarize here only the main accomplishments.

Chemical investigations have established that the two acids formed in the main solution reaction (1) do separate quickly in two distinct phases if iodine is present in excess. A good understanding of the effect of iodine content and temperature on the yield of this reaction has been obtained by defining a figure of merit (FOM). The FOM is an appropriate measure of the energy required to recover unconverted reactants per mole of H_2SO_4 net produced. FOM isothermal plots vs initial $\text{I}_2/\text{H}_2\text{O}$ are shown in Fig. 1. These studies have also shown that separation of the acids improves with increasing iodine content: this

decreases the amount of back reaction after separation of the acids and is part of the reason for the increase in net yield.

The use of phosphoric acid as an agent to break the $\text{HI}-\text{H}_2\text{O}$ azeotrope in an extractive distillation is under investigation, and results so far are favorable. Work on the separation of HI from the $\text{HI}_x-\text{H}_2\text{O}$ phase by high pressure distillation, however, has been terminated due to unfavorable results.

Bench-scale investigations have been initiated. They are an essential development phase between small-scale laboratory experiments and larger scale pilot plant testing. The next section will discuss this further.

The effect of pressure on the azeotropic composition of $\text{H}_2\text{SO}_4-\text{H}_2\text{O}$ has been investigated at pressures up to 25 bar. A shift in composition has been found; however, the effect on the overall process efficiency is expected to be minor.

Studies have been conducted to survey catalysts to reduce SO_3 to SO_2 in the presence of H_2O vapor (decomposed vapor of the azeotrope of $\text{H}_2\text{SO}_4-\text{H}_2\text{O}$). Several prospective catalysts have been found which allow high conversion at residence times less than 1 sec.

Studies on the catalytic decomposition of HI at reasonably low temperatures (450-550 K) are in progress. Several catalysts have been tested and results so far indicate that 80% approach to equilibrium at 525 K and 4 sec residence time is practical.

The process engineering goal is to design a hydrogen production process based on GA's sulfur-iodine cycle. As heat source for the process, GA's VHTR is assumed,* and the process design aims at matching the process to this heat source in both a cost efficient and energy efficient way. By mid-1976, a full process engineering design was completed which showed a thermal efficiency of about 41%, defined as the ratio of the HHV of hydrogen produced and the heat put in by the heat source. Table 1 shows how much of the reject heat can be attributed to each of the major steps in the process. It is important to note that 20% of the heat put in must be rejected because of the characteristics of the heat source itself, this is independent of the type of thermochemical cycle used or the way it is engineered. Further development in this area is discussed in the next section.

Materials investigations are directed to screening and qualifying materials of construction for the various process environments and supplying engineering data on materials for design purposes. Design of components for the process will require stringent consideration of materials for corrosion compatibility. In many subsystems corrosion aspects are complicated by high temperature. At the current stage of process development and conceptual design, both materials engineering and research are being undertaken to select and screen candidate materials for use in the fluids under the severest predicted cycle operating conditions.

* Other high temperature heat sources could also be suitable.

These fluids can be grouped into two categories, H_2SO_4 and its decomposition products and HI phases. Results so far have identified as potential candidate materials Incoloy 800H with an aluminized diffusion coating for containment of the SO_3 decomposition at temperatures up to 1173 K, and zirconium-base and/or titanium-base alloys for containment of HI_x at temperatures from 295 K up to 475 K.

3. DOE PROGRAM FY 1978

Bench-Scale Investigations

The goal of bench-scale investigations is to construct, test, and operate a system into which water is fed and within which other chemicals are cycled and H_2 and O_2 are produced continuously. The only emphasis on energy efficiency at the bench level is in general to select components of such type that they can potentially perform efficiently on a large scale; for instance, a cocurrent flow reactor may be selected over a stirred vessel.

For these investigations, the process is broken up into three subunits which, after they separately have proven to operate satisfactorily, can then be linked together to operate as one water splitting entity. The three subunits are described below:

1. The main solution reaction subunit. In this unit the main solution reaction (1) is performed, the two acids H_2SO_4 and HI_x are separated and unreacted SO_2 is removed from the HI_x phase. Design and construction are complete except for the part which degasses HI_x from SO_2 and the SO_2 recycle system. Figure 2 presents the flow diagram of the unit and Figure 3 shows a photograph of the assembly.

The iodine is delivered from either of two 4-liter holding vessels as a liquid. Its delivery rate is measured with a manometer-orifice. It enters the reactor above metered supplies of H_2O and SO_2 . The combined feeds move up the entrance tube into the reactor, where the HI_x and H_2SO_4 are created during the residence of the fluids in the reactor. The required mixing is accomplished by alternating spiral glass vanes and the temperature is stabilized by passing a coolant in a jacket around the midsection of the reactor. The reactor effluent passes into a gas separation chamber where excess SO_2 that was used to drive the fluids through the reactor is separated from the liquid stream and bled to a recycle system (not yet installed). The two liquid phases are taken from the bottom of the gas-liquid separator and fed into a central point in a liquid-liquid separator where they are allowed to separate. The lighter H_2SO_4 phase is drawn off the top of this separator while the heavier HI_x phase is drawn off the bottom. Flow metering control valves adjust flow. A principal control method is to adjust the liquid level in the gas liquid separator to keep the liquid below the mixed fluid injection

point but well above the liquid takeoff point. The liquid-liquid interface in the liquid-liquid separator does hold at approximately 373 K at the entrance (mid) point.

The equipment needs to be operated at approximately 373 K for best product yields. The iodine delivery system will be operated at approximately 393 K to keep the iodine as a liquid. Heating, cooling and control systems are being installed to maintain these temperatures.

As of this writing, a cold flow test of the system has been made using CCl_3-CH_3 saturated with iodine as a substitute for $I_2(l)$ and N_2 as a substitute for SO_2 . Successful tests of the delivery systems, flow monitoring systems, reactor flow conditions, and separators were made at and above design conditions. Hot flow tests with actual process fluids will be made soon.

2. The sulfuric acid subunit. This unit will concentrate sulfuric acid (eventually received from the main solution reaction subunit), decompose it at high temperature (1144 K), and separate undecomposed H_2SO_4 , and the reaction products H_2O , SO_2 and O_2 (see the block diagram on Fig. 4). The design of this subunit is in its final stage and construction and testing of it is expected early in FY 1978.
3. Hydrogen iodide subunit. This unit will separate HI out of the lower phase product of the main solution reaction, and thermally decompose it into H_2 and I_2 . The conditions for these steps have not yet been fixed; however, most likely H_3PO_4 will be used for the HI separation step and the HI decomposition will be done catalytically at moderate temperatures.

Process Engineering

The design of a flowsheet of a thermochemical water-splitting process is not a simple straightforward operation. Due to the requirement to seek a high thermodynamic efficiency the design becomes an iterative process. This means that often an equipment arrangement or a process condition in one section has to be changed so as to accommodate conditions in another. During the previous flowsheeting for instance, it was clear that certain specific, preselected approaches could be improved upon, but time precluded starting over on that flowsheet to incorporate the improvements.

We are now preparing a third generation flowsheet of the GA process. It will incorporate efficiency improvements found by chemistry and will proceed into sufficient further detail to permit estimating the major friction pressure drops and their associated additional power requirements. In order to possibly expedite this work and to enable some optimization we intend to use in portions of the flowsheet, the process simulator code DESIGN/2000 from the Chemshare Corporation.

Property data in the thermochemical water-splitting area in general is scarce and not very well suited for the application of general equations, in contrast, for example, with the area of petroleum refining. However, we feel that DESIGN/2000 does provide a suitable method of inserting users data and subroutines, features which are essential to describe some of our unit operations which are not modeled in the code. We have now started writing these subroutines.

Flowsheeting is still in progress; therefore, new diagrams are not presently available. However, the following changes over the previous flowsheet can be indicated:

1. The main solution reaction will be operated at about 95°C and at higher iodine content than previously. This will result in a 20% increase in yield, while it also obviates the need for refrigeration.
2. For the separation of HI from the aqueous HI_x phase a more energy efficient, extractive distillation with H_3PO_4 will be used.
3. The concentration of sulfuric acid will be done by a multiple flash evaporation rather than by distillation. Optimization with Chemshare is planned here.
4. In the decomposition of H_2SO_4 higher pressures will be employed in order to

allow for pressure drops. This decreases the conversion per pass of the SO_3 decomposition reaction, but it is expected that this, at least partly, will be offset by a considerable reduction in size of the high temperature heat exchangers.

5. The decomposition of HI will be performed at lower temperatures through the use of catalysts.

4. ACKNOWLEDGEMENT

The work described in this paper was conducted under the sponsorship of the American Gas Association (Contract No. IU126-1), the U.S. Energy Research and Development Administration (ERDA) (now DOE) (Contract No. EY-76-C-03-167, PA No. 63), The University of California Los Alamos Scientific Laboratory (Order No. L46-48844-1), and General Atomic Company.

5. REFERENCES

1. Russell, J. L., et al., "Water-Splitting - a Progress Report," First World Hydrogen Energy Conference, Proceedings, Vol. 1, Miami Beach, Florida, March 1976.
2. Schuster, J. R., et al., "Status of Thermochemical Water Splitting Development at General Atomic," Paper presented at 9th Synthetic Pipeline Gas Symposium, October 31 - November 2, 1977 (Chicago, Ill.).

TABLE 1
PROCESS HEAT REJECTION IN GA SULFUR IODINE CYCLE
1976 FLOWSHEET

	Fraction of Process Input Heat
Ideal Heat Rejection of Assumed HTGR Heat Source ^(a)	0.161
Primary-to-Secondary Helium Heat Exchanger ΔT	0.141
Heat Source-Related Reject Heat (subtotal)	0.202
Secondary Helium-to-Process Heat Exchangers ΔT	0.076
Internal Energy Transfer Inefficiencies (by difference)	~ 0.257
Waste Heat Rejection Inefficiencies ^(a) (due to transfer ΔT)	0.037
Process-Related Reject Heat (subtotal)	~ 0.370
Input Heat-Equivalent of 50 atm H_2 Product Pressure	$\sim 0.014^{(b)}$
Heat Recovered on Std. HHV of H_2 (The "Thermal Efficiency")	0.414
Fraction of Input Heat Appearing in the H_2 Output (subtotal)	~ 0.428
	TOTAL 1.000

(a) Assuming heat is rejected isothermally to the general environment at 85°F (300 K).

(b) The standard [77°F (298 K), 1 atm] higher heating value of combustion of H_2 is 172,940 Btu/lb-mole (68,317 kcal/g-mole) of H_2 , but the process makes H_2 at 50 atm, not 1 atm. This pressure has a valuable work equivalent in it (which required input heat to generate), but there is no uniquely preferred way to account for the pressure-to-work-to-input-heat equivalence.

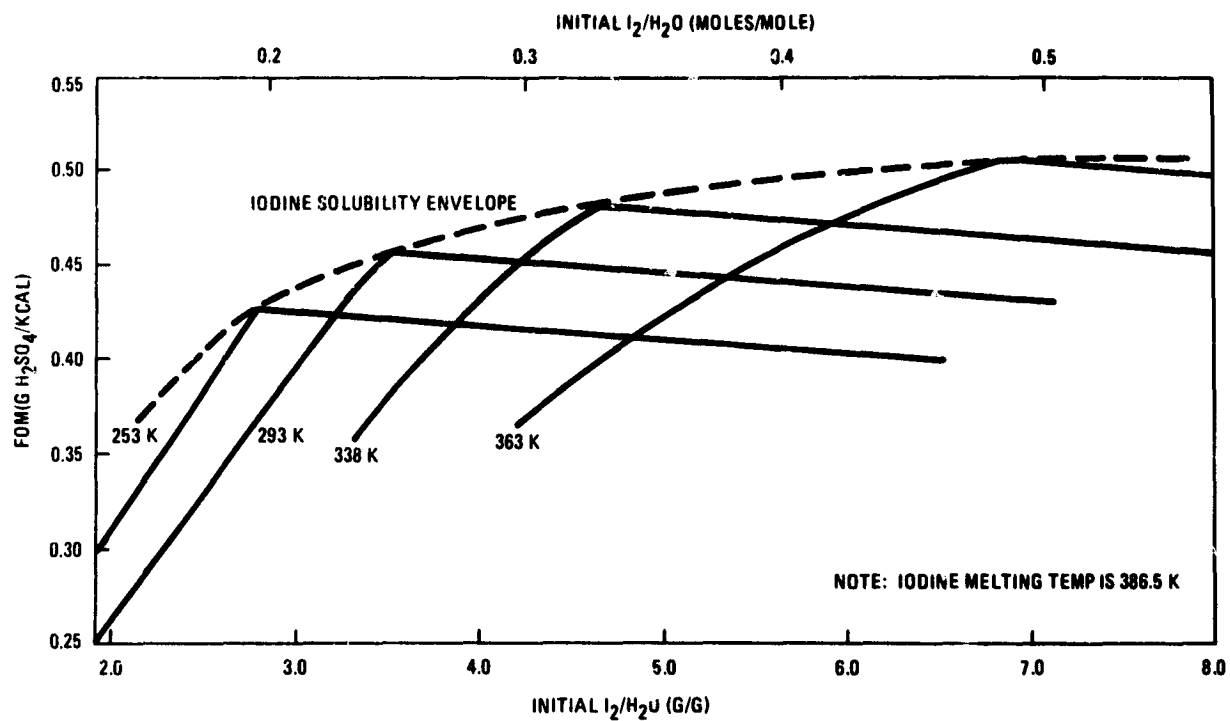


Figure 1. Main solution reaction figure of merit for various iodine-to-water ratios

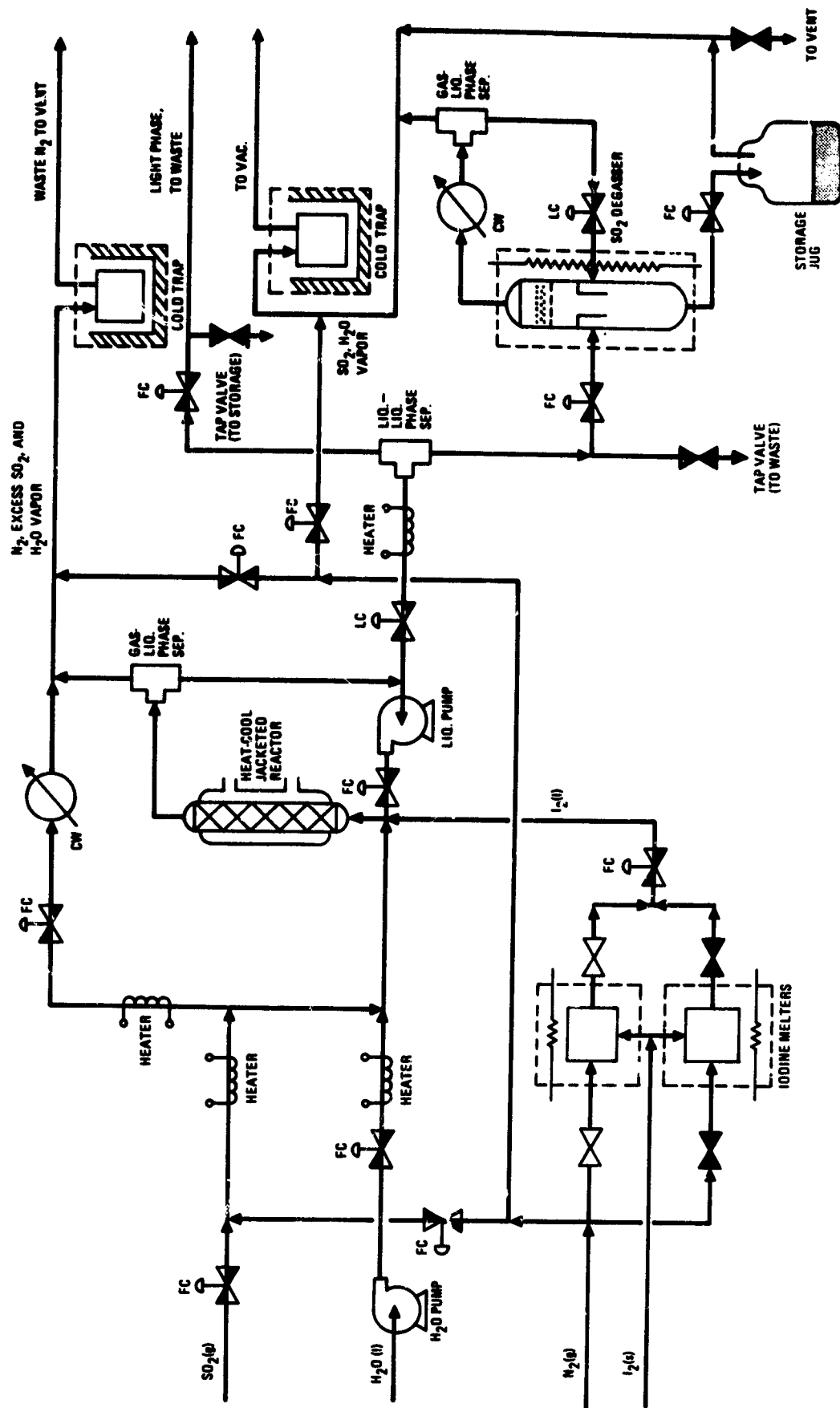


Figure 2. Flow diagram of main solution reaction bench-scale unit

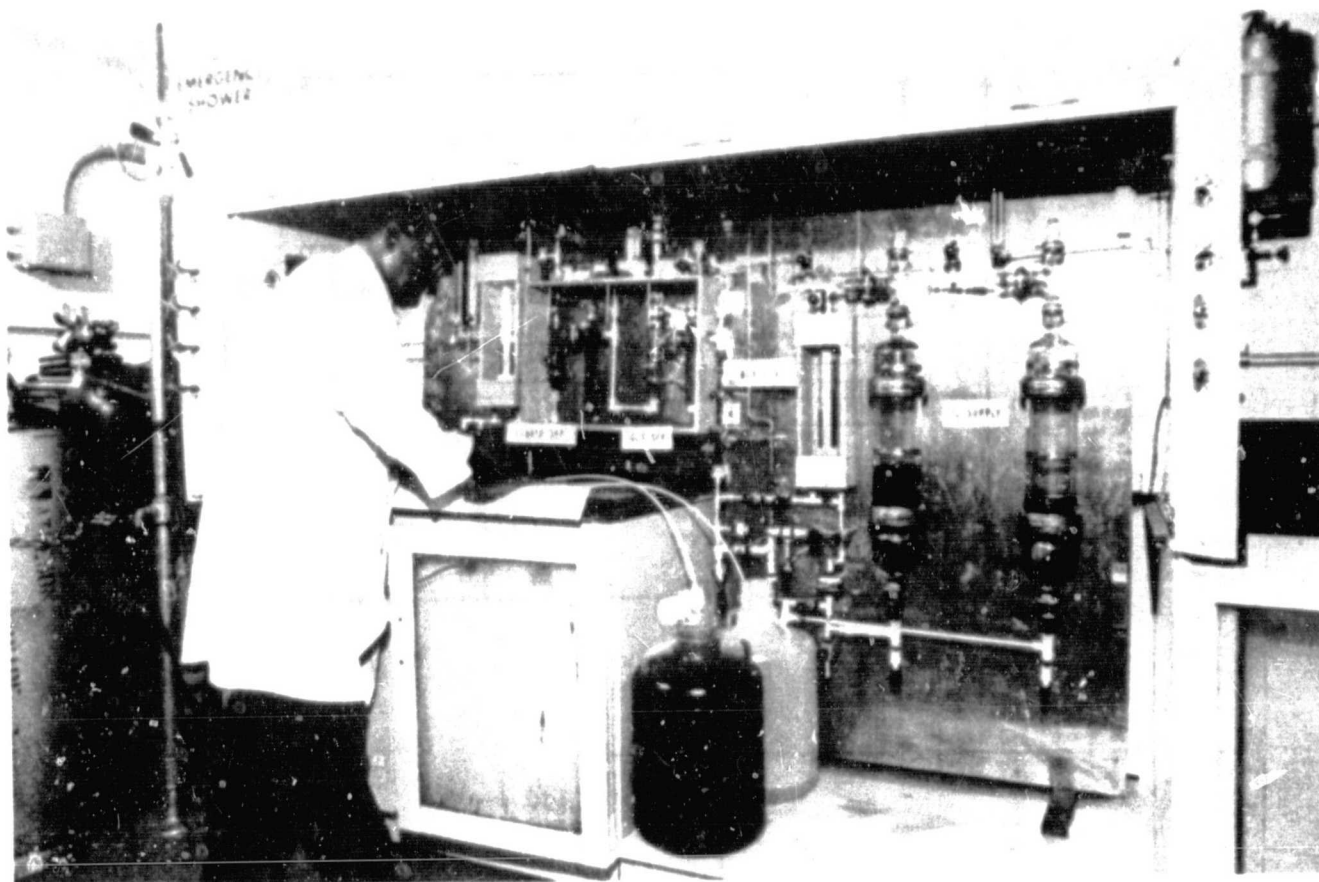
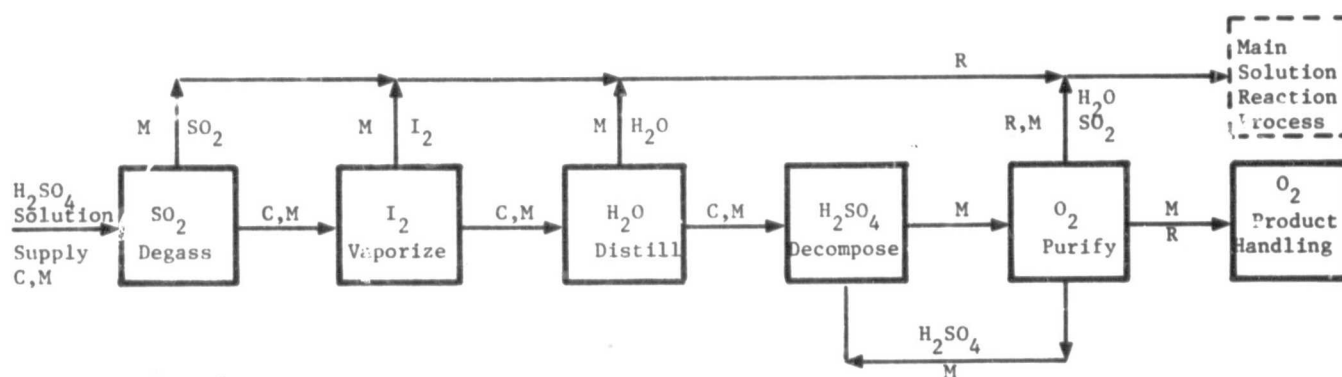


Figure 3. Main solution reaction bench-scale unit



C - Central Valve
 M - Metering
 R - Pressure Regulation

Figure 4. Block diagram of sulfuric acid bench-scale unit

ASSESSMENT OF THERMOCHEMICAL HYDROGEN PRODUCTION

James R. Daft¹, Stephen E. Foh, and James D. Schreiber

Institute of Gas Technology
Chicago, Illinois

Abstract

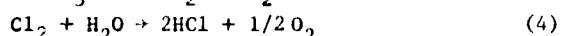
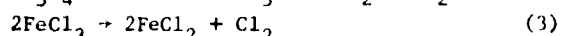
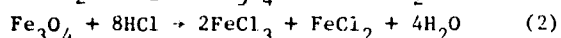
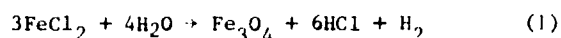
A base-case, or first-cut, flowsheet for IGT Cycle B-1 has been completed. Calculation of the energy balance has allowed us to define the worst problem areas in the overall process, and optimization effort has been directed to these parts of the process. Operation of the FeCl_2 -hydrolysis at pressures sufficient to interface with projected hydrogen transmission lines will apparently necessitate higher hydrolysis temperatures. Higher pressure, however, favors some of the critical separation steps.

The work of Schuetz and others on electrolysis and on the thermodynamics of the $\text{HBr-H}_2\text{O}$ system is being reviewed. Work plans for this part of the contract effort are summarized.

Task 1. Evaluation of Load-Line Efficiencies

Introduction

Cycle B-1 (1) represented by Reactions 1-4, is the Institute of Gas Technology's most developed thermochemical water-splitting cycle:



and one of the published cycles that has been completely demonstrated with recycled materials (2). This type of demonstration is a primary part of cycle development programs at IGT: Reaction operating conditions determined in the laboratory should be based on actual materials available from other reactions in the cycle if they are to accurately reflect process conditions.

The Base-Case Flowsheet

We have prepared a base-case flowsheet for Cycle B-1 designed to identify the portions of the process that will benefit the most from concentrated research and development effort. The base-case scheme was kept as simple as possible by assuming 1) atmospheric pressure reaction conditions, 2) equilibrium yields from all reactions, and 3) 298 K, 1 atm (101.3 kPa) condensed-phase separations of all $\text{HCl-H}_2\text{O}$ gas mixtures. Figure 1 is a schematic of the flowsheet, and Table 1 provides a summary of the molar flow rates based on the production of 1 gram-mole of hydrogen.

A large part of the process shown in Figure 1 involves separations. Reactions 1, 2, and 4 produce gaseous product streams (S-1, S-7, and S-14) whose primary components are H_2O and HCl , which must be separated for recycling. The HCl -rich overhead from D-1 (95 mol % HCl) is used as feed to Reaction 2. The water-rich bottom is the azeotrope (11.1 mol % HCl) and is used as feed to the hydrolysis steps (Reactions 1 and 4) and as a stripping medium at T-1

and T-2. Thus, there is constant recycling of two types of aqueous HCl streams: 1) the still bottoms, which contain 11.1 mol % HCl (azeotrope), and 2) the condenser and stripping tower effluents, which are saturated (25.9 mol % HCl) at 298 K and 1 atm (101.3 kPa).

Analysis of the Base Case

Table 1 indicates that the mass fluxes for the base case are too large. The dominant factors are 1) aqueous HCl liquid streams involved in the $\text{H}_2\text{O-HCl}$ separation, mixed to form Stream S-24; and 2) the large quantities of excess steam required for Reaction 1. An enthalpy balance around the base-case flowsheet has identified the largest internal heat transfer burdens. The largest contributor to this load is the distillation of the large quantities of liquid at D-1.

Analysis of the base-case flowsheet has identified the two areas that will most benefit from intensive engineering analysis. These are the $\text{HCl-H}_2\text{O}$ separation scheme and the steam-rich conditions for the FeCl_2 hydrolysis (H_2 -production) reaction.

Modifications to the Base Case

We have investigated physical adsorption and pressurized distillation as alternative $\text{HCl-H}_2\text{O}$ separation schemes. It is doubtful that better overall thermal efficiency will be obtained with physical absorption processes than with distillation.

Efficiency consideration aside, we have not found an adsorbent suitable for application to highly acidic conditions. Molecular sieves are definitely not compatible with the acid nature of our $\text{HCl-H}_2\text{O}$ streams. We will study other adsorbents including activated carbon to determine their suitability for this application.

Enough data has been acquired to evaluate high-pressure distillation. At elevated pressures the mole fraction of HCl in the azeotrope is reduced and the heat of vaporization of H_2O drops. Figure 2 is a plot of mole fraction HCl in the azeotrope as a function of system pressure. For example, at 35 atm (3.55 MPa) the azeotrope contains only 3.3 mol % HCl as compared with 11.1 mol % at 1 atm (101.3 kPa). In addition, the heat of vaporization of H_2O is about 75% of its value at 1 atm (101.3 kPa). Because a more complete separation of the $\text{HCl-H}_2\text{O}$ stream is possible at elevated pressures, high-pressure distillation reduces the required mass and heat fluxes for the overall process.

Equilibrium Effects

Pressurized operation of all reactions in Cycle B-1 was studied to determine effects on equilibrium yields. The yields from Reaction 2 are increased by pressure. The low operating temperature (about 475 K), however, limits to about 15 atm (1.520 MPa) the

pressure at which the reaction may be run without condensing the steam product. For hydrolysis of FeCl_2 (Reaction 1), the equilibrium mole fraction of hydrogen falls off rapidly with increasing pressure. However, a process designed to produce hydrogen for pipeline transmission at 70 to 100 atm (7.09 to 10.13 MPa) must yield hydrogen at pressure to avoid capital and energy penalties (3) for compression to transmission levels. The trade-off for operating Reaction 1 at elevated pressure is shown graphically in Figure 3, a plot of the equilibrium $\text{H}_2\text{O}/\text{H}_2$ product mole ratio versus temperature for pressures up to 100 atm (10.13 MPa). Since HCl impurity in the feed to Reaction 1 is also a reaction product, the presence of HCl impurity lowers the fraction of hydrogen in the product.

Conclusions

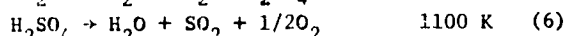
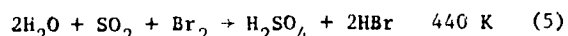
Our engineering study of Cycle B-1 indicates that proper modifications to the base-case flowsheet will improve the most troublesome process problems. The separation of HCl- H_2O mixtures can be made more complete by pressurized distillation, and the effects of producing H_2 at pressure can be minimized by higher temperatures and purer feeds. (We will use a minimum pressure figure of 30 atm.) These modifications, however, will probably result in a process requiring higher temperature process heat than formerly assumed.

Task 2. Hydrogen Bromide Electrolysis

The hydrogen-halide thermochemical cycle studied by Schuetz (4) is related to Hallett's earlier work (5). Hallett's cycle, a two-step HCl electrolysis sequence that employed the reverse Deacon reaction, had attractive economics, though not sufficiently attractive to lead to reasonable plant amortization terms. Also, it was a free-water system with the usual, difficult H_2O -HCl separations.

Schuetz's cycle is an extension of the Hallett cycle and related to other hybrid cycles presently undergoing intense development (6, 7).

Labeled Mark-13 at the Euratom Ispra Establishment, the cycle is represented by



Efforts to achieve thermochemical hydrogen production in Step 3 (Equation 7) have been unavailing (4). The principal difficulty in the hybrid step has been the achievement of high anode current densities. Cathode efficiencies are reported to be quite good, with high current densities obtained at elevated temperatures and pressures on platinum electrodes (4).

This should be an attractive cycle because it involves workable chemistries (Equations 5 and 7) and

* Electrolytic step.

an oxygen-producing step that is currently being aggressively developed (6, 7). It should be possible to separate HBr relatively cleanly in Step 1 (Equation 5) because the HBr will vaporize and entrain only small amounts of SO_2 and H_2O .

No experimental work has been performed as yet. We intend to investigate electrode reactions on three substrates as defined in the work statement. These are:

- Viteous graphite
- Porous carbon
- Platinum black/platinum.

We want to define whether special requirements in cell separation or proximity are required. We also wish to do the electrolysis in media representative of a functioning cycle with the aim of achieving an element design that maximizes anode efficiency.

Task 3. Maximum Attainable Thermal Efficiency of a Specific Bromine Hybrid Cycle

No work was done on this task to this time.

References

1. Pangborn, J. B., Gregory, D. P., and Gahimer, J. S., "Thermochemical Hydrogen Production - State of the Art, 1976," paper presented at the A.G.A. Synthetic Pipeline Gas Symposium No. 8, Chicago, Ill., October 18-20, 1970.
2. Gahimer, J., Mazumder, M., and Pangborn, J. B., "Experimental Demonstration of an Iron Chloride Thermochemical Cycle for Hydrogen Production," 11th Intersociety Energy Conversion Engineering Conference Proceedings, pp. 933-939, AIChE, New York, 1976.
3. Konopka, A. J., and Wurm, J., "Transmission of Gaseous Hydrogen," 9th IECEC Proceedings, pp. 405-412, ASME, New York, 1974.
4. Schuetz, E. H., "Hydrogen Producing Cycles Using Electricity and Heat - Hydrogen Halide Cycles: Electrolysis of HBr," Int. J. Hydrogen Energy, Vol. No. 4, pp. 379-388, 1974.
5. Hallet, N. C., "Study, Cost and Systems Analysis of Liquid Hydrogen Production," NASA-CR-73-226, 1968.
6. Schuster, J. R., et al., "Development of a Sulfur-Iodine Thermochemical Water-Splitting Cycle for Hydrogen Production," 12th IECEC Proceedings, pp. 920-927, ANS, LaGrange Park, Ill., 1977.
7. Farberman, et al., "Development Progress on the Sulfur Cycle Water Decomposition System," 12th IECEC Proceedings, pp. 928-932, ANS, LaGrange Park, Ill., 1977.

Table 1. Molar Flow Rates for the Flowsheet Shown in Figure 1

Stream	Composition, mol	Temperature at Source, K	Stream	Composition, mol	Temperature at Source, K
S-1	1 H ₂ (g) 6.94 HCl (g) 3.54 H ₂ O (g)	1150	S-17	0.50 O ₂ (g) 0.068 Cl ₂ (g)	298
S-2	3.54 H ₂ O (l) 1.23 HCl (aq)	298	S-18	0.50 O ₂ (g)	298
S-3	1 H ₂ (g) 5.71 HCl (g)	298	S-19	0.068 Cl ₂ (g)	298
S-4	1 Fe ₃ O ₄ (s)	1150	S-20	7.79 H ₂ O (l) 2.72 HCl (aq)	298
S-5	9.04 HCl (g) 0.48 H ₂ O (g)	333	S-21	11.0 H ₂ O (l) 3.86 HCl (aq)	298
S-6	2 FeCl ₃ (s) 1 FeCl ₂ (s)	425	S-22	25.49 H ₂ O (l) 8.89 HCl (aq)	298
S-7	4.48 H ₂ O (g) 1.04 HCl (g)	425	S-23	36.56 H ₂ O (l) 12.76 HCl (aq)	298
S-8	4.48 H ₂ O (l) 1.04 HCl (aq)	298	S-24	40.09 H ₂ O (l) 13.99 HCl (aq)	298
S-9	3 FeCl ₂ (s)	575	S-25	39.62 H ₂ O (l) 4.96 HCl (aq)	381
S-10	1 Cl ₂ (g)	575	S-26	32.08 H ₂ O (l) 4.01 HCl (aq)	381
S-11	1.08 Cl ₂ (g)	575	S-27	7.54 H ₂ O (l) 0.94 HCl (aq)	381
S-12	1 H ₂ O (l)	298	S-28	28.81 H ₂ O (l) 3.60 HCl (aq)	381
S-13	3.27 H ₂ O (l) 0.41 HCl (aq)	381	S-29	3.32 H ₂ O (l) 0.41 HCl (aq)	298
S-14	0.50 O ₂ (g) 0.068 Cl ₂ (g) 2.41 HCl (g) 3.27 H ₂ O (g)	1150	S-30	25.49 H ₂ O (l) 3.19 HCl (aq)	298
S-15	3.27 H ₂ O (l) 1.14 HCl (aq)	298	S-31	1 H ₂ (g)	298
S-16	0.50 O ₂ (g) 0.068 Cl ₂ (g) 1.27 HCl (g)	298			

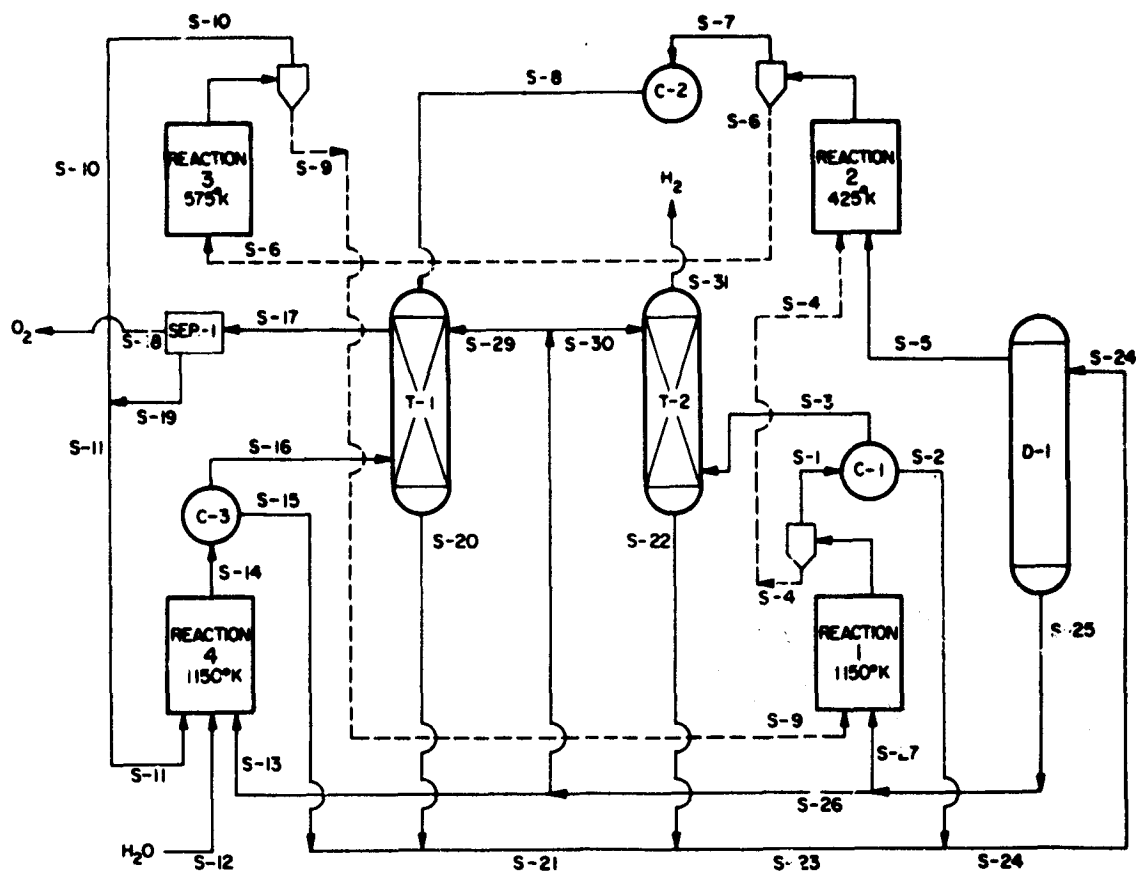


Figure 1. Schematic Diagram of the Base-Case Flowsheet for Cycle B-1

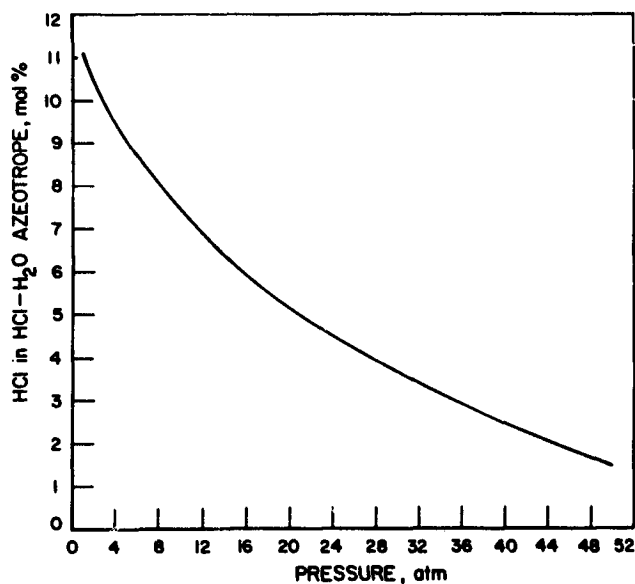


Figure 2. HCl-H₂O Azeotrope Composition as a Function of Pressure

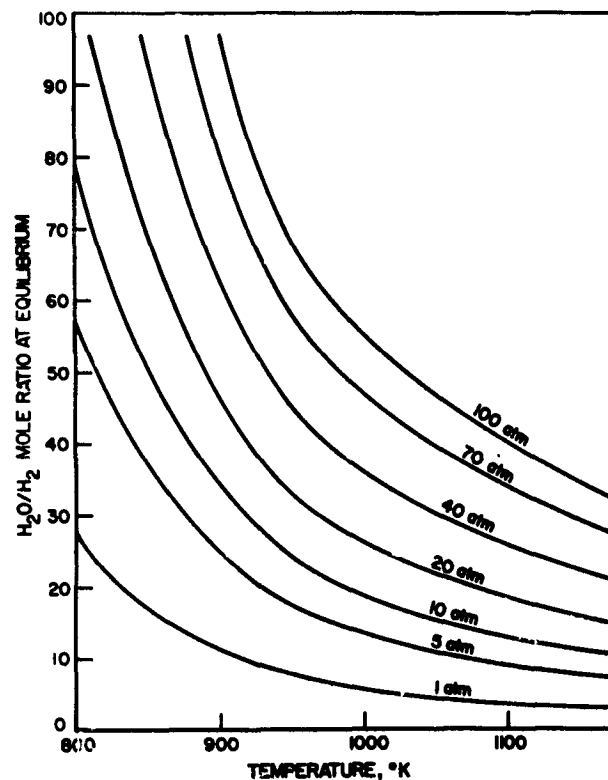


Figure 3. Ferrous Chloride-Steam Reaction: Equilibrium H₂O/H₂ Mole Ratio as a Function of Temperature, HCl/H₂O Feed Ratio = 0.00

THERMOCHEMICAL HYDROGEN PRODUCTION REVIEW PANEL

James E. Funk
University of Kentucky
Lexington, Kentucky 40506

This project involves the establishment of a review panel to evaluate various thermochemical processes for the production of hydrogen from water.

Objective:

To Review and Evaluate Engineering Flow Sheets for Various Cycles Designated by DOE.

Areas of Concern:

- 1) Chemistry
- 2) Flow sheet and efficiency - heat penalty analysis
- 3) Materials
- 4) Cost

First Process - Hybrid Sulfuric Acid

The Composition of the panel and the area of responsibility for each individual are shown in Table 1. The first meeting of the panel will be held in Washington, D.C. on November 17, 1977. The most recent information on the hybrid sulfuric acid process (1), as being developed by Westinghouse, has been distributed to the panel and will be discussed at the November 17th meeting.

A preliminary heat penalty analysis of the process has been completed and the results are shown in Table 2 and Figure 1. These results are subject to change as the analysis is performed in more detail.

(1) Farbman, G.H., and Koump, V., "Hydrogen Generation Process Final Report," FE-2262-15, prepared for ERDA under Contract EX-76-C-01-2262, June, 1977.

Table 1

Thermochemical Hydrogen Production Panel

	<u>Area of Responsibility</u>
Douglas Benion Electrochemical Technology Corp. 3935 Leary Way, NW Seattle, Washington 98107 206/632-5965	Electrochemical steps in the process
Kenneth E. Cox University of California Los Alamos Scientific Lab P.O. Box 1663 Los Alamos, New Mexico 87544 505/667-7059	Overview of field and relative position of the process
Jack DeVan Oak Ridge National Lab Nuclear Division P.O. Box X Oak Ridge, Tennessee 37830 615/483-8611 ext. 36891	Materials
Meng Teck Eng The Lummus Company 1515 Broad Street Bloomfield, New Jersey 07003 201/893-2927	Overall process design and cost estimates
James E. Funk University of Kentucky College of Engineering Lexington, Kentucky 40506 606/257-1688	Panel chairman - heat penalty analysis
Daniel D. Perlmutter Professor of Chemical Engineering University of Pennsylvania Towne Building/D3 Philadelphia, Pennsylvania 19104 215/243-8350	Chemical process design and engineering

Table 2
Preliminary Heat Penalty Analysis

	APRIL 1976		JUNE 1977	
	Heat Penalty MW	Direct Cap. Cost 10 ⁶ \$	Heat Penalty MW	Direct Cap. Cost 10 ⁶ \$
<u>Battery</u> ⁽³⁾				
G - Electrolyzer, Power Supply & Auxiliaries	243	155	114	200
H - Sulfuric Acid Vaporiza- tion & Decomposition	470	113	185	168
I - SO ₂ Separation	281	43	217	24
J - Power Generation	263	37	346	57
A - E - Heat Source	266	274	108	276
Total Heat Penalties	1523	622 ⁽¹⁾	970 ⁽⁴⁾	725 ⁽²⁾
Ideal Heat Requirement	1822		1820	
Primary Energy Source	3345		2790	
T _m , K	962		1028	
Process Thermal Efficiency, %	45		54	

(1) Mid 1974 Dollars

(2) Mid 1976 Dollars

(3) Offsites allocated to Batteries G-J

(4) Preliminary results

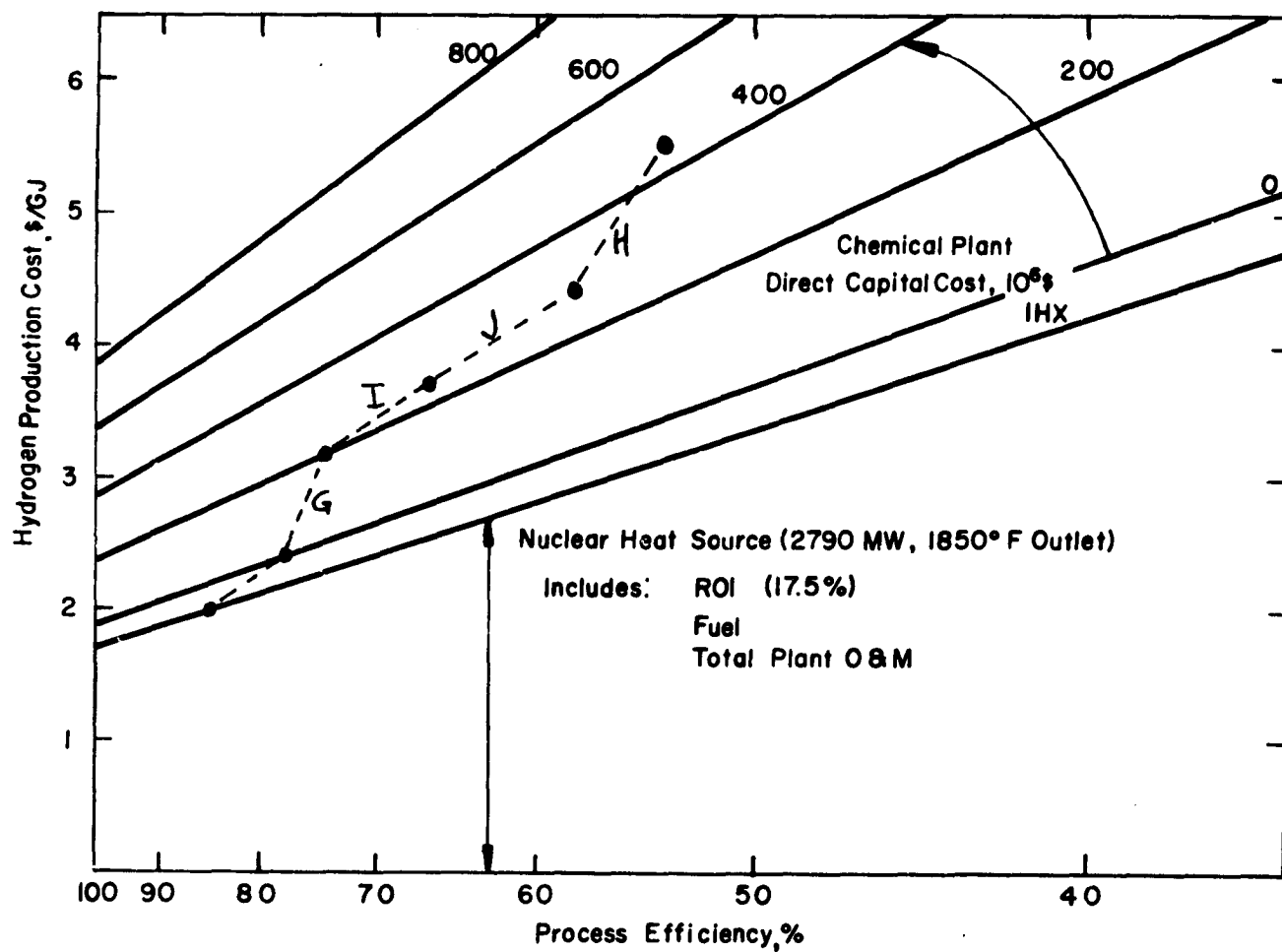


Figure 1. Preliminary Heat Penalty Analysis

THE LASL THERMOCHEMICAL HYDROGEN PROGRAM
STATUS ON OCTOBER 31, 1977

Kenneth E. Cox and Melvin G. Bowman

University of California
Los Alamos Scientific Laboratory
Los Alamos, New Mexico 87545

Abstract

The LASL Hydrogen Program is continuing its investigation of practical schemes to decompose water thermochemically for hydrogen production. Efforts were and are being devoted to process improvements in cycles that use sulfuric acid as an intermediate. Sulfuric acid-hydrogen bromide cycles are being studied as a means of overcoming the heat penalty in drying acid solutions. An alternate approach involves the use of insoluble bismuth sulfate that is precipitated from acid solution.

Preliminary energy balances indicate a significant increase in cycle efficiency for both these options.

Introduction

In the development of practical thermochemical cycles for hydrogen production from water, the approach adopted by the Los Alamos Scientific Laboratory has been to verify proposed cycle reaction schemes by experiment. This verification involves the careful determination of yields, rates and equilibria as well as the thermochemistry of the individual reactions in a cycle under a wide variety of operating conditions. After demonstration of a cycle's scientific feasibility, a preliminary engineering analysis is attempted to evaluate cycle efficiency and cost. Further experimentation is carried out to optimize the cycle as indicated by the above analysis. Typically, enhanced reaction yield leads to lower internal recycle rates and thus to a smaller energy expenditure involved in the separation of reaction products. Increase in reaction velocity lessens residence times within a reactor and thus contributes to lower capital cost for the overall cycle.

If a cycle should appear promising after the initial evaluation described, a final phase of process development would involve a bench-scale, closed loop test that provides data for more realistic engineering evaluation and cost analyses.

Together with these activities, an attempt is being made to match the heat requirements of the cycle to potential heat sources which could be derived from either fission, fusion or solar energy.

Much of the work done in the LASL program has been described by members of the hydrogen group in both publications and presentations at national and international scientific meetings.(1-7) The program was also recently summarized at the Thermochemical Hydrogen Contractors' Review Meeting held at DOE-HQ in October.(6)

The process development and engineering analysis activities have been directed primarily to

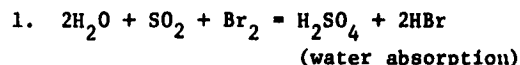
experimental studies of reactions relevant to cycles employing sulfuric acid as an intermediate substance. These cycles include the sulfuric acid-hydrogen bromide cycle, the hybrid sulfuric acid cycle (Westinghouse) and the sulfuric-acid-iodine cycle (General Atomic). The rationale for this work is to avoid the large heat penalties incurred on drying sulfuric acid solutions. The approach taken in the case of sulfuric acid-hydrogen bromide cycle has been to devise means of decomposing anhydrous hydrogen bromide which is produced with essentially pure sulfuric acid in one of the cycle steps making water evaporation unnecessary. In the work supporting the development of the hybrid cycle and the iodine cycle, the approach is slightly different. The use of an insoluble, non-hydrated, metal sulfate precipitated from sulfuric acid solutions as a means of recovering sulfur trioxide (and hence sulfur dioxide) without having to dry the acid is being continued. Efforts have been devoted to the engineering design and analysis of these modifications which produce smaller heat penalties as compared to the existing forms of the cycles. Results are an expected increase in cycle efficiency.

A preliminary view of cycles having maximum reaction temperatures in the 1500-1700 K range is being undertaken. These temperatures may be attained in magnetic fusion energy schemes. Magnetic fusion energy may thus incorporate thermochemical cycles in the production of synthetic fuels.

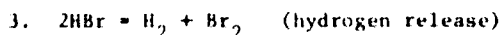
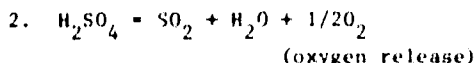
The Sulfuric Acid-Hydrogen Bromide Cycle

The conceptual cycle can be best described by the following reactions:

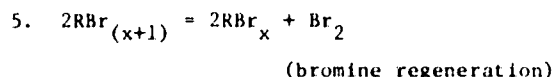
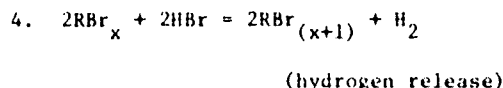
Low Temperature Heat-Rejecting Reactions



High Temperature Heat Absorbing Reactions



In practice, as reaction 3 does not proceed as written except electrochemically, it is usual to substitute the following sequence.

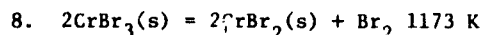
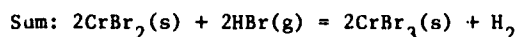
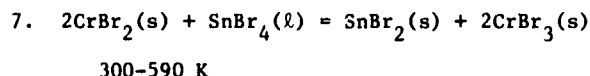
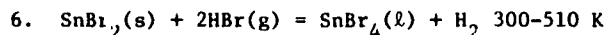


In principle, this cycle could be more efficient than the other sulfuric acid cycles under consideration. Reaction 1 yields nearly 100% H_2SO_4 rather than 50% H_2SO_4 as formed in the other cycles. Thus the rather large heat requirements for drying sulfuric acid can be avoided. In addition, typical ΔS° values for metal bromide decompositions are very near the value required for an "ideal" two-step decomposition of hydrogen bromide.

A preliminary energy balance illustrates this point further. This balance is shown in Table I. The products of reaction 1 are H_2SO_4 (liq.) and anhydrous HBr, the ΔH° for HBr decomposition is +72.8 kJ (for 2 mols of HBr); however, the ΔG° for this reaction is +107.1 kJ. As Table II indicates, it is possible to use twice or three times the theoretical heat (of reaction) in a sulfuric acid-hydrogen bromide cycle and still obtain a thermal efficiency of the order of 50%.

From literature data, the VBr_2 - VBr_3 couple and the CrBr_2 - CrBr_3 couple have ΔG° values near the value required for the efficient decomposition of HBr. However, in both cases the reaction of HBr with the lower bromide (to evolve H_2) is far too slow.

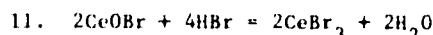
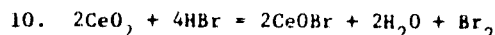
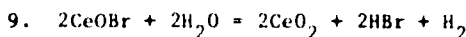
Earlier, satisfactory reaction rates were demonstrated for reactions involving chromium bromide hydrates (3). Consequently, in an attempt to promote the chromium bromide reactions in the absence of water, reactions 6 and 7 of the following sequence were investigated.



The thermochemical properties of the SnBr_2 - SnBr_4 couple would permit it to act as an oxidation-reduction catalyst to achieve the summation reaction. Reactions of HBr with mixtures containing known amounts of SnBr_2 , CrBr_2 , and CrBr_3 at a temperature of 516 K (in the presence of palladium black) resulted in hydrogen formation. Details of these experiments are given in reference 5. Use of this sequence in a practical cycle would depend on

increased reaction rates and more efficient use of the palladium catalyst.

A second halide hydrolysis sequence was also evaluated as a possible subcycle for HBr decomposition. The cycle is composed of reactions 9 and 10 in the following sequence.

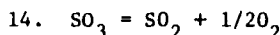
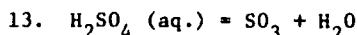
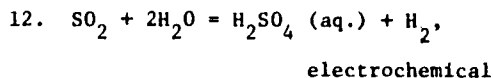


Reaction 10, conducted at temperatures between 775 and 875 K produced a solid CeOBr phase and bromine. Reaction 9, the hydrogen releasing reaction, was studied at temperatures from 1070-1250 K in order to obtain equilibrium data as well as kinetics. In these experiments measured quantities of H_2O were passed over CeOBr at the reaction temperature and the rate of hydrogen evolution was determined. Values of $\log K_p$ ranging from -5.5 to -3.0 were obtained over the temperature range investigated.(5) The ΔH° for the cerium oxybromide hydrolysis was found to be in the +250 kJ region. At practical reaction temperatures, this set of reactions for HBr decomposition exhibits a positive ΔG° value. Thus they constitute a "hybrid" cycle for HBr decomposition in which mechanical work is used in the place of electrical work in the more familiar electrochemical-thermochemical hybrid cycle. The total positive ΔG° requirement will be reduced by an important $\Delta T \cdot \Delta S^\circ$ term, however, and will be significantly lower than the room temperature ΔG° for HBr decomposition.

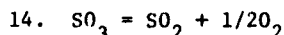
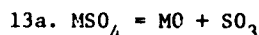
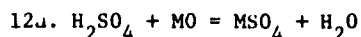
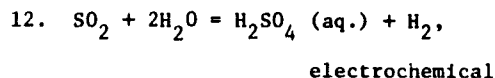
Despite the above, a successful HBr sub-cycle has not yet been achieved, work with other compounds is continuing.

Use of Metal Sulfates in the H_2SO_4 Cycles

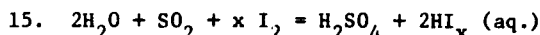
In the H_2SO_4 hybrid cycle (reactions (12-14) large amounts of heat are needed to dehydrate the sulfuric acid for the acid concentrations currently

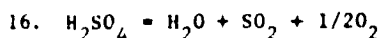


produced in reaction 12. A significant saving in energy might be achieved by forming a suitable metal sulfate from the H_2SO_4 . The alternative hybrid cycle may be represented by

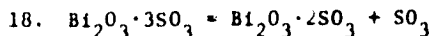


The same is true for the H_2SO_4 - I_2 cycle (reactions 15-17)





in which sulfuric acid produced in reaction 15 and phase separated from HI_x is dehydrated prior to thermal decomposition. The sulfate should have low solubility and form an anhydrous sulfate. An oxide sulfate may replace metal oxide in reaction 12. A survey and assessment of the literature were made for antimony and bismuth, both of which satisfy the first two criteria.



$\text{Bi}_2\text{O}_3 \cdot 3\text{SO}_3$ decomposes with increasing temperature to SO_3 and a series of oxide sulfates terminating in Bi_2O_3 itself. The equilibrium SO_3 pressure for reaction 18 is 1 atm at 860 K, and for reaction 19 is 1 atm at 1050 K. Final decomposition to form Bi_2O_3 occurs at higher temperatures. The options for generating SO_3 over a temperature range that includes intermediate temperatures (in addition to the high temperatures for SO_3 decomposition in reaction 14) should be useful in achieving efficient extraction of heat from the circulating helium gas of a high-temperature gas-cooled nuclear reactor. Experiments are being run to measure SO_3 pressure in the $\text{Bi}_2\text{O}_3 \cdot \text{SO}_3$ system.

Additional experiments are being carried out to obtain equilibrium concentrations and rates of reactions for bismuth oxide and bismuth oxysulfate with ~ 50 wt% sulfuric acid solutions.

A preliminary evaluation of the energy efficiency of the bismuth sulfate alternate to the hybrid sulfuric acid cycle has been completed. The hybrid cycle has been described in the literature. (8) A process sensitivity study (9) using a simplified flow sheet seen in Fig. 1 illustrated the action of process variables on the cycle's efficiency. Data taken from this study were used as a basis for comparison with the modified process involving an insoluble bismuth sulfate. The flow sheet for this latter case is seen in Fig. 2. The sulfuric acid stream leaving the electrolyzer was assumed to be at 50 wt% concentration in both cases. An equilibrium yield of 75% was calculated for sulfur tri-

oxide decomposition at 1100 K based on published thermodynamic data (JANAF Tables).

Tables III and IV illustrate the potential benefits to be gained on adopting the bismuth sulfate method of solution concentration. Reduction in the heat requirements for the acid concentration step as well as for the acid decomposition step show a potential gain of 12% in efficiency.

Future Research

In the LASL hydrogen program, we will continue to test reactions in cycles that are potentially suitable for different heat-source temperatures that also appear reasonable from the point of view of thermochemistry. From our laboratory experience, it is increasingly apparent that the most attractive cycles are usually impractical because of slow reaction rates for the low-temperature steps.

One method of improving kinetics is to utilize solution chemistry for low-temperature steps. We plan to examine more closely solution chemistry as a method for promoting otherwise attractive cycles. We also hope to identify and incorporate precipitation reactions in order to minimize solution-drying operations. We hope the use of solution reactions will also give added flexibility and lead to the discovery of cycles that are less corrosive.

The preparation of flowsheets, together with engineering design activities, is continuing for the modified sulfuric acid cycles. Irreversibility analysis is being applied to these problems as well as the problem of gas separations with support in this area being given to the DOE Thermochemical Review Committee under the direction of Dr. J. E. Funk.

Thermochemical cycles capable of utilizing heat at high temperatures (1500-1700 K) are being investigated. These cycles, containing two or three steps, and involving perhaps an oxide or a sulfate decomposition, may be a means of producing a synthetic fuel (hydrogen) from magnetic fusion energy. Scoping studies and a few preliminary experiments are envisioned at this time. This work should also be applicable to high temperature heat derived from solar energy.

References

1. Bowman, M. G., "Chemistry of Thermochemical Cycles from U.S.A. Programs," Proceedings of the A.I.M. International Congress on Hydrogen and its Prospects, Liege, Belgium, 15-18, Nov. 1976.
2. Mason, C. F. V., "The Reduction of Hydrogen Bromide using Transition Metal Compounds," International Journal of Hydrogen Energy, Vol., I, No. 4, pp. 427-434, Jan. 1977.
3. Mason, C. F. V., "The Use of Chromium Bromide Hydrates in the Sulfuric Acid-Hydrogen Bromide Cycle for the Production of Hydrogen Thermochemically," in press, International Journal of Hydrogen Energy, Aug. 1977.
4. Cox, K. E., "Irreversibilities in Thermochemical Cycles for Hydrogen Production by Water Decomposition," Proceedings of the 12th Intersociety Energy Conversion Engineering Conference, Paper 779144, pp. 947-950, Washington, D.C., 28-Aug. - 2 Sept. 1977.
5. Cox, K. E., "Thermochemical Processes for Hydrogen Production, 1 Jan. - 31 Jul. 1977," LASL Progress Report, LA-6970-PR, Oct. 1977.
6. Cox, K. E., "Progress in the Los Alamos Scientific Laboratory Program to Develop Thermochemical Processes for Hydrogen Production," presentation at DOE Contractors Review Meeting, Thermochemical Cycles Element, Hydrogen Energy Storage Program, DOE Headquarters, Washington, D.C., 5 Oct. 1977.
7. Bowman, M. G., "Thermochemical Production of Hydrogen from Water," to be published in the Proceedings of the International Symposium on Energy Sources and Development, Barcelona, Spain 19-21 Oct. 1977.
8. Brecher, L. E., Spewock, S., and Warde, C. J., "The Westinghouse Sulfur Cycle for the Thermochemical Decomposition of Water," Proceedings First World Hydrogen Energy Conference, Vol. I, pp. 9A1-16, Miami Beach, Florida 1-3 March, 1976.
9. Carty, R., Cox, K. E., Funk, J. E., Soliman, M., and Conger, W., "Process Sensitivity Studies of the Westinghouse Sulfur Cycle for Hydrogen Generation," ibid, pp. 9A17-28.

TABLE I

HEAT BALANCE FOR THE SULFURIC-ACID
HYDROGEN BROMIDE CYCLE(Units = kJ/mol H₂)

Step	Heat Requirement	Heat Available
1. H ₂ SO ₄ (l) Heating	47	
2. H ₂ SO ₄ Vaporization	56	
3. H ₂ SO ₄ (g) Heating	$\frac{64}{167}$	
4. H ₂ SO ₄ Decomposition (1100 K)	231	
5. Products Cooling		96
6. SO ₃ /SO ₂ /O ₂ Separation	126	
7. SO ₂ /Br ₂ /H ₂ O Reaction		18*
8. HBr Decomposition	$\frac{73}{597}$ (Theor.)	114

* Heat not available for matching

TABLE II

ESTIMATED EFFICIENCIES FOR THE SULFURIC ACID-
HYDROGEN BROMIDE CYCLEBasis: (1,2,3,) x Heat of Reaction,
HBr Decomposition(Units = kJ/mol H₂)

Efficiency 1	=	$\frac{286}{524 + 73 - 114}$	=	0.59
Efficiency 2	=	$\frac{286}{524 + 2(73) - 114}$	=	0.51
Efficiency 3	=	$\frac{286}{524 + 3(73) - 114}$	=	0.45

TABLE III

HEAT BALANCE FOR HYBRID SULFURIC ACID CYCLE

(Units = kJ/mol H₂ Produced)

Step	Power (Heat Eq.)	Heat Required	Heat Available
1. Electrolysis	42(126)		42 ^a
2. Acid Vaporization		648	
3. Acid Heating		314	
4. Acid Decomposition		285	
5. Acid Cooling			305
6. Acid Condensation			402
7. Steam Condensation			264 ^a
8. SO ₂ /SO ₃ /O ₂ Separation	42(126)		
	84(252)	1247	707 306 ^a
	286		

$$\text{Efficiency} = 252 + 1247 - 707 = 0.361$$

^a Heat unavailable for matching.

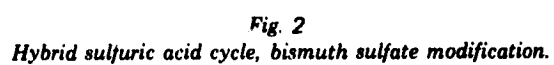
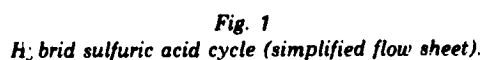
TABLE IV

HEAT BALANCE FOR BISMUTH SULFATE MODIFIED HYBRID
SULFURIC ACID CYCLE(Units = kJ/mol H₂ Produced)

Step	Power (Heat Eq.)	Heat Required	Heat Available
1. Electrolysis	42(126)		42 ^a
2. Bismuth Sulfate Formation			13-26 ^a
3. Bismuth Sulfate Decomposition		167-251 (estimated)	
4. SO ₃ Decomposition		96	
5. SO ₃ /SO ₂ /O ₂ Separation	42(126)		
	84(252)	263-347	55-68 ^a
	286		

$$\text{Efficiency} = 599 \text{ (max)} = 0.478$$

^a Heat unavailable for matching.



duf'

REVISED FLOWSHEET AND PROCESS DESIGN FOR THE ZnSe THERMOCHEMICAL CYCLE *

Oscar H. Krikorian and Henry H. Otsuki

Lawrence Livermore Laboratory
Livermore, CA

Abstract

We have completed a preliminary process design, flowsheet, and an economic analysis of an improved version of the ZnSe cycle for hydrogen production. The amount of ZnSO₄ that needs to be decomposed at high temperatures has been reduced by a factor of 2 in this revised cycle, thereby both lowering overall heat requirements and spreading out the prime heat required over a broader temperature range than before. Corresponding improvements have been achieved in both cycle efficiency and equipment costs. Assuming a VHTR nuclear reactor heat source and incorporating special equipment designs for critical steps in the cycle, we now obtain an overall cycle efficiency of about 40% and a hydrogen production cost of about \$13/GJ. We believe that this cost is conservative at this point of cycle development because the input data on reaction rates and equipment lifetimes have been conservative, and the analysis has not been optimized.

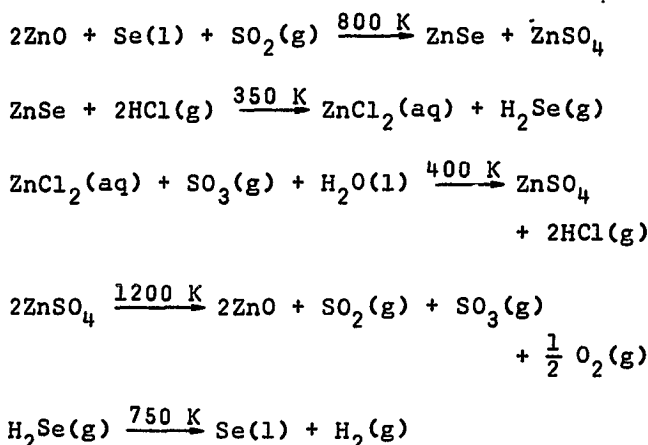
* Work performed under the auspices of the U.S. Department of Energy under contract No. W-7450-Eng-48.

I. INTRODUCTION

During the past three years, under funding provided by the DOE Division of Basic Energy Sciences, we have established scientific feasibility and have conducted both exploratory (1) and some detailed chemical experimentation (2) on a ZnSe cycle. More recently, under funding by the DOE Division of Energy Storage Systems, we expanded our studies to include the process design, flowsheeting, and economic analysis of the ZnSe cycle. This latter study was concluded at the end of FY-1977, and we report here our findings.

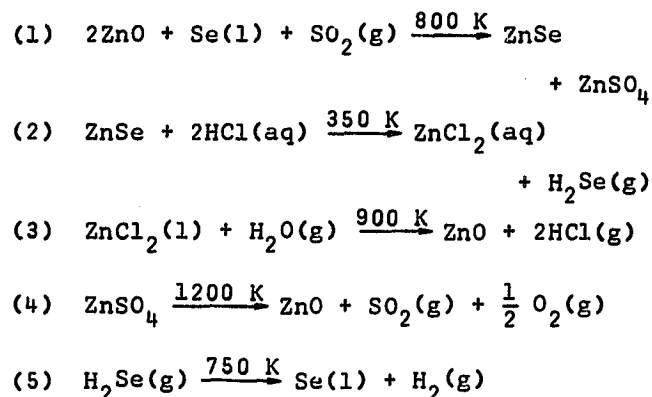
II. CYCLE CHEMISTRY

Until recently, the ZnSe cycle was developed on the basis of the following major reaction steps:



All but the ZnSO₄ decomposition step are exothermic, and the ideal thermal efficiency for the cycle is 49%. This cycle has several inherent advantages. Laboratory experimentation has shown that each of the steps clearly works. Reaction rates are fast (about 5 to 15 min.), conversions are high and free of undesirable by-products, and there is little separative work. In particular, the H₂ generation step (decomposition of H₂Se) gives far higher yields, i.e. 60% decomposition in 5 minutes at 750 K, than analogous steps in other cycles that depend upon decomposition of gases such as H₂S, HI, HBr, and HCl. An engineering disadvantage of this cycle is that most of the primary heat requirement is for decomposition of ZnSO₄, and is needed over a narrow temperature range. This small temperature differential makes it difficult to efficiently transfer heat out of a nuclear reactor. In view of this, the cycle has recently been modified to convert ZnCl₂ directly to ZnO. This has halved the amount of ZnSO₄. In the modified version we not only spread the primary heat input over a broader temperature range, but also increase the ideal thermal efficiency of the cycle.

The modified version of the ZnSe cycle, the one that we will be reporting on here, is described by the following major reaction steps:



The detailed heat balances for these and other reaction steps needed to close the cycle are summarized in Table 1. The status of the chemistry of these reactions will be reviewed next.

A. The ZnO/Se/SO₂ Reaction

Reaction (1) takes about 15 minutes for completion at 800 K with SO₂ pressures of ~500 kPa (~5 atm) and gives yields ranging from 60 to 95%. The yield depends primarily on the intimacy of mixing of ZnO and Se. The reaction rate is accelerated by either increasing the temperature or SO₂ pressure. The reaction appears to be free of side reactions at temperatures above ~720 K. Additional work is yet needed to identify the mechanism of the reaction and to better define the reaction parameters. We believe that significant increases in reaction rates and yields are achievable.

B. The ZnSe/HCl Reaction

We have found in small batch-type experiments that ZnSe in reaction (2) is rapidly hydrolyzed (~95% yield in 5 min.) by either dilute or concentrated aqueous HCl solutions. We have also learned that more of the ZnSO₄ produced from reaction (1) must be separated from ZnSe prior to hydrolysis since high concentrations of sulfate in acidic solution would oxidize Se²⁻ to Se.

C. The ZnCl₂/H₂O Reaction

Thermodynamic calculations based upon literature data (Wagman (3), Kelley (4), Cubicciotti (5)) indicate that reasonable yields of HCl(g) are to be expected for reaction (3) at about 900-1000 K by reacting steam with molten ZnCl₂, i.e., $(P_{\text{HCl}})^2/P_{\text{H}_2\text{O}} = 3 \text{ kPa (0.03 atm)}$ at 900 K and 13 kPa (0.13 atm) at 1000 K. We have recently carried out exploratory transpiration experiments to obtain approximate rate and yield data. In these experiments, a carrier gas, N₂, saturated with H₂O(g)

near room temperature, was bubbled through molten ZnCl_2 with a contact time of a few seconds. The unreacted $\text{H}_2\text{O}(\text{g})$ was absorbed by an in-line $\text{Mg}(\text{ClO}_4)_2$ trap. Product $\text{HCl}(\text{g})$ was collected, its volume measured, and its purity determined by infrared analysis. Results of these experiments indicate that equilibrium is readily attained at temperatures above 800 K.

D. The ZnSO_4 Decomposition Reaction

Although substantial literature exists on reaction (4) (Stern (6)), the literature work is not directly applicable to this cycle. Heat and mass transfer effects limit the interpretation of the literature work, both in regard to equilibrium and kinetic data. The decomposition of ZnSO_4 appears to occur in two stages. Initially, ZnSO_4 is decomposed to an oxysulfate, probably $\text{ZnO} \cdot 2\text{ZnSO}_4$, which then further decomposes to ZnO . An equilibrium decomposition pressure of one atmosphere is expected at ~1160 K, with an SO_2/SO_3 molar ratio of ~6/1. Consequently, conversion of SO_3 to SO_2 is also required to close our cycle. We plan to study the decomposition rate of ZnSO_4 under conditions that are not heat or mass transfer limited.

E. The H_2Se Decomposition Reaction

We have recently studied the kinetics of thermal decomposition of H_2Se , reaction (5), in the temperature range 673-748 K (see Fig. 1), and expect to publish the details of this work in the near future. The kinetics of decomposition are quite rapid above 750 K, but yields per pass are limited to ~60% at the higher temperatures. If a suitable catalyst can be found, we will operate at a lower temperature where higher yields can be obtained because of the more favorable equilibrium constant. Decomposition of H_2Se is exothermic at all temperatures of interest.

III. PROCESS DESIGN

The ZnSe thermochemical cycle for hydrogen production has been studied in the laboratory and has been shown to be scientifically feasible. The key reaction step in the cycle is the reaction of solid ZnO with liquid selenium and gaseous SO_2 , reaction (1), to produce a mixture of ZnSe and ZnSO_4 . This is followed by hydrolysis of ZnSe to yield H_2Se , reaction (2). The remaining reactions in the cycle are those used to generate hydrogen and oxygen and to regenerate the starting materials.

A simplified flow diagram (shown in Fig. 2) was used to develop the process flow. Only the principal unit operations in each of the batteries are identified. Detailed descriptions of each of the batteries are given below.

A. Battery A

The principle function of Battery A is to carry out reaction (1), $2\text{ZnO} + \text{Se}(\text{l}) + \text{SO}_2(\text{g}) = \text{ZnSe} + \text{ZnSO}_4$. Laboratory exper-

iments have shown us that this reaction will go to near completion in about 15 minutes at 800 K under an SO_2 pressure of about 500 kPa (5 atm) when ZnO and selenium are intimately mixed. To ensure that each ZnO particle is surrounded by selenium, we will use excess selenium in this step. The reaction is exothermic (-161 kJ per mole of selenium reacted) and liberates substantial heat for other process use. The major equipment in Battery A is a high temperature reactor equipped with a heat exchanger. The reactants, ZnO and selenium, are premixed in the injector/extruder system prior to introduction to the reaction chamber (see Fig. 3). Sulfur dioxide is maintained at 500 kPa pressure in the reaction chamber at all times to ensure a rapid reaction rate. The product $\text{ZnSe}/\text{ZnSO}_4$ with excess selenium is collected at the bottom of the reactor and screw conveyed out. Loss of SO_2 pressure through the screw conveyor is minimized by maintaining a balancing pressure of steam at the outlet to the conveyor. The $\text{ZnSe}/\text{ZnSO}_4/\text{Se}$ mixture is picked up and transported to Battery B in a stream of superheated steam ($T = 450 \text{ K}$). Flow rate of the steam is controlled to deliver the $\text{ZnSe}/\text{ZnSO}_4/\text{Se}$ mixture to Battery B at about 525 K.

B. Battery B

This battery is designed to separate ZnSO_4 from ZnSe by hot water leach prior to ZnSe hydrolysis. Solubility of $\text{ZnSO}_4 \cdot \text{H}_2\text{O}$ is temperature dependent. It is at its maximum at 325 K and decreases rapidly with increasing temperature. According to Von G. Bruhn (7), above 525 K, $\text{ZnSO}_4 \cdot \text{H}_2\text{O}$ can be considered insoluble (see Fig. 4). The integral heat of solution of ZnSO_4 is quite substantial. The heat of formation of $\text{ZnSO}_4 \cdot \text{H}_2\text{O}$ is -79.8 kJ/mol and the heat of solution of $\text{ZnSO}_4 \cdot \text{H}_2\text{O}$ in 14 H_2O is -35.3 kJ/mol for a total of -115.1 kJ/mol.

In setting up Battery B we assigned high priority to recovering as much of the hydration heat as possible for other process use. Water and anhydrous ZnSO_4 are contacted at 525 K to form $\text{ZnSO}_4 \cdot \text{H}_2\text{O}$ without solution formation. The heat of formation of the monohydrate goes to generate steam at 525 K. Sufficient water is added to the resultant $\text{ZnSO}_4 \cdot \text{H}_2\text{O}/\text{ZnSe}/\text{Se}$ slurry to form a saturated ZnSO_4 solution at 325 K, and excess heat is removed through a heat exchanger. The insoluble ZnSe/Se is separated and transported to Battery C for hydrolysis. The saturated solution of $\text{ZnSO}_4 \cdot \text{H}_2\text{O}$ is then reheated to 525 K to precipitate and recover $\text{ZnSO}_4 \cdot \text{H}_2\text{O}$, which is subsequently dehydrated in a rotary kiln. Anhydrous ZnSO_4 is directed to Battery F for decomposition. Steam generated in the dehydrator is used for process heat before it is returned to the hydrater, thus recovering a portion of the heat of dehydration.

C. Battery C

Hydrolysis of ZnSe is performed in Battery C. The reaction is: $\text{ZnSe}(\text{s}) + 2\text{HCl}(\text{aq}) = \text{ZnCl}_2(\text{aq}) + \text{H}_2\text{Se}(\text{g})$. Hydroly-

sis is rapid in both dilute and concentrated aqueous HCl solution. To minimize evaporative heat load in the later ZnCl_2 recovery step, we've selected concentrated HCl (about 15-20 N) for our hydrolysis reaction. If the hydrolysis operation were to be conducted in a conventional stirred tank reactor in concentrated HCl solution, the product gas, H_2Se , would entrain large quantities of HCl (about 25%) and present a difficult separation problem. We have, therefore, designed a hydrolyzer column (shown in Fig. 5) in which H_2Se gas can be generated relatively free of HCl. ZnSe particles are introduced high in the column and allowed to migrate down through a packed region and react with HCl to generate H_2Se . H_2Se , being insoluble in water, will form tiny bubbles, which coalesce and rise to the surface. Bubbles as they form would still contain about 25% HCl gas. However, much of the HCl will be extracted as the bubbles encounter less concentrated HCl solution during their ascent to the surface. Traces of HCl still remaining with the product gas are scrubbed in a water spray tower before H_2Se is piped to Battery E for decomposition. The HCl consumed in the hydrolysis reaction is fed in the primary reaction zone.

Other equipment items in Battery C are filters, an evaporator, and a crystallizer. Excess selenium is separated from ZnCl_2 solution via filtration and returned to Battery A. The ZnCl_2 solution is sent to the evaporator where it is concentrated and on to the crystallizer, where the solution is cooled to ~300 K. The ZnCl_2 precipitate is separated and sent to Battery D for ZnO regeneration. Liquid is recycled back to the evaporator.

D. Battery D

Battery D's main function is to regenerate ZnO from ZnCl_2 formed in Battery C. Zinc chloride is first dried, then transferred to a high temperature hydrolyzer where molten ZnCl_2 is reacted with steam to yield ZnO(s) and HCl(g) (reaction temperature is about 900 K). Solid ZnO is separated from molten ZnCl_2 (any ZnCl_2 adhering to ZnO particles is removed by further reaction with steam) and returned to Battery A where it joins ZnO from Battery F to start the cycle over again.

The $\text{HCl/H}_2\text{O}$ stream from the high temperature hydrolyzer goes to the distillation unit in Battery C for fractionation. The concentrated HCl(aq) stream goes to the ZnSe hydrolyzer, while a near azeotropic mixture from the reboiler goes back to the high temperature ZnCl_2 hydrolyzer.

E. Battery E

In Battery E we decompose H_2Se to its constituent H_2 and selenium. The decomposition reaction is exothermic and proceeds rapidly at temperatures above ~550 K. At 750 K, our proposed operating temperature, decomposition is 60% complete in

5 minutes, which necessitates recycle of undecomposed H_2Se . Separation of the $\text{H}_2\text{Se-H}_2$ mixtures is accomplished by pressurization and cooling to 100 K. The hydrogen product stream is scrubbed free of H_2Se (for toxicity reasons) and compressed to 3 MPa (30 atmosphere) for pipeline or chemical feedstock use. Liquid selenium is recycled to Battery A to complete the selenium part of the cycle.

F. Battery F

Battery F is where we perform the high-temperature thermal decomposition of ZnSO_4 . Since ZnSO_4 decomposition is an endothermic reaction requiring some 308 kJ/mol of ZnSO_4 , the decomposition reactor is provided with primary process heat from the VHTR via a high pressure high temperature helium stream. Another major equipment item in this battery is the cyclone separator used to separate ZnO particulates from the gaseous decomposition products.

The number of moles of ZnSO_4 decomposed per mole of hydrogen produced have been reduced from two to one in the current modified cycle, the second mole of ZnO being regenerated through direct hydrolysis of ZnCl_2 in Battery D. Although this reduction eases the problem, ZnSO_4 decomposition remains one of the critical process steps, and we have given considerable thought, not only to the design, but also on heat transfer and kinetic aspects of the process.

We have examined the experimental results reported by Pechkovskii (3,9) on the decomposition rate of ZnSO_4 in a stream of air as a function of temperature and believe that the decomposition rate he reports is governed by heat transfer to the decomposing particles. Radiation is the dominant mode of heat transfer at temperatures greater than 1000 K. Therefore, if the ZnSO_4 particles were dispersed, heat transfer would not be limiting, and we believe total decomposition can be achieved in times much less than 1 minute at ~1160 K. We plan to verify this experimentally, but assuming it for now, we visualize the following process. ZnSO_4 particles (100-200 μm in size and preheated to 1000 K) are dropped through the decomposer, get heated rapidly via radiation heat transfer to ~1160 K, decompose, and emerge as ZnO. The heat transfer tube surfaces are coated with catalyst to assure that $\text{SO}_2/\text{SO}_3/\text{O}_2$ equilibrium is established. ZnO, separated from the decomposition gases, is sent on its way to Battery A to start the cycle over again, while the gaseous decomposition product goes to Battery G for processing.

G. Battery G

Battery G provides for separation of the $\text{SO}_2/\text{SO}_3/\text{O}_2$ mixture obtained from the ZnSO_4 decomposition. Design of the separation plant resembles that of the Westinghouse Sulfur Cycle, which requires a similar separation, Farbman (10). Sulfur dioxide and

SO₃ are separated from O₂ by compression and cryogenic cooling. Refrigeration is provided by an NH₃ refrigerator and from the cold (172 K) O₂ produced through adiabatic expansion of compressed O₂ prior to venting. The SO₂-SO₃ fractionation is accomplished by simple distillation. The SO₃ stream is heated and passed through a catalytic converter at 1200 K, which decomposes SO₃ to SO₂ and O₂. The equilibrium mixture joins the gas stream from Battery F for further separation. The SO₂ stream is evaporated and returned to Battery A under pressure to complete the cycle.

IV. PROCESS THERMAL EFFICIENCY

The major endothermic and exothermic heat loads of the ZnSe cycle are shown in Table 1. It is very important from an efficiency standpoint to match process heat requirements with the available heat from exothermic steps in the cycle. Major process power requirements for the cycle are also listed in Table 1. We have assumed an efficiency of 34% for thermal to electrical conversion.

Although one mole of ZnSO₄ is decomposed per mole of hydrogen produced in the improved cycle as compared to two moles in the original ZnSe cycle, the decomposition step of Battery F still represents the largest single heat/energy consumer of the cycle at 399 kJ/mol of H₂ produced. Prime heat of 329 kJ/mol at 1200 K is required for ZnSO₄ decomposition, and an additional 70 kJ/mol is needed for electrical power to drive the compressors which circulate the heat transfer fluid, helium. Battery D is the next largest energy consumer. It requires 234 kJ/mol of H₂ produced. The high temperature ZnCl₂ hydrolysis step requires 215 kJ/mol also of prime heat, but at 900 K. The balance of the heat requirement, 18.8 kJ/mol, goes toward preheating ZnCl₂. The HCl-H₂O evaporator in Battery C is the other large heat consumer requiring some 207 kJ/mol of recovered process heat. Since little of the latent heat of evaporation of HCl-H₂O can be recovered for reuse due to low temperature, it is extremely important to minimize the amount of HCl-H₂O that has to be evaporated in the ZnCl₂ recovery. The net energy requirements in Battery E and G are for separative work and for compressing the product hydrogen to 3 MPa (30 atm) for pipeline or feedstock use.

The overall energy input to produce 1 mol of hydrogen for delivery at 3 MPa via the ZnSe cycle is 678.6 kJ. Using the higher heating value for hydrogen of 286 kJ/mol we estimate our overall efficiency as 42%.

V. HYDROGEN PRODUCTION COST

For the purpose of the economic analysis, the ZnSe thermochemical hydrogen production plant was assumed to use process heat at 1200 K from a VHTR nuclear reactor, and the hydrogen production rate was fixed at 27.3 Mg (60,000 pounds) of hydrogen per

hour to set the plant size. Thus, when operating for 7000 hours a year (capacity factor of 80%), this plant will produce 2.12×10^9 standard cubic meters of hydrogen per year. Costs are based on mid-1976 dollars. An additional constraint set for the plant design was that all equipment items in the plant would be rail transportable, i.e., no more than 3.6 m (12 feet) in diameter for process equipment. Appropriate numbers of each item are used to meet the load demand for each process step.

Since we are at an early stage in our process development, at a stage where we are still developing conceptual designs for process equipment, we have not yet optimized our process. Process optimization is an important first step in obtaining meaningful cost analysis. This is particularly true for thermochemical methods, which are very sensitive to internal heat matching. Our cost figures here will, therefore, be tentative and conservative.

Costs of the individual batteries (see Table 2) are based on conventional engineering estimation practice. Costs of major equipment items in each battery were summed, then increased by 105% of the equipment cost for costs of structures, installation, plumbing, insulation, and instrumentation. The total plant cost is estimated to be 855×10^6 \$, and allowing for contingencies and indirect costs, gives a total capital investment of 1.228×10^9 \$. The annual operating cost is placed at 280×10^6 \$, i.e., about 23% of the capital cost assuming major equipment lifetimes to be between 10 and 20 years. The cost of hydrogen, exclusive of nuclear heat cost, is \$0.124/m³ or \$9.86/GJ (\$10.40/10⁶ BTU) based on a heating value of hydrogen of 12.9 MJ/m³.

Accepting the cost figure of 443.6 $\times 10^6$ \$ for the 3426-MW thermal VHTR derived by Westinghouse Electric Corporation, Farbman (10) and adjusting to 1976 \$ by escalating the cost 17%, we have 519×10^6 \$ for the capital cost of the reactor. With an annual fixed charge rate of 15% for utility ownership (77.8×10^6 \$) plus nuclear fuel costs of 21×10^6 \$, and operation and maintenance costs of 6×10^6 \$, we have an annual reactor operating cost of 104.8×10^6 \$. The cost of process heat at the reactor is about \$1.24/GJ (\$1.30/10⁶ BTU) based on an 80% capacity factor.

For a hydrogen production rate of 27.3 Mg/h and thermal efficiency of 42%, the nuclear heat requirement is actually 2430 MW thermal. We will assume the same unit heat cost for the 2430 MW as for the 3426 MW thermal reactor. This translates to about \$2.94/GJ (\$3.10/10⁶ BTU) of produced hydrogen, and an overall hydrogen cost of \$12.80/GJ (\$13.50/10⁶ BTU).

VI. CONCLUSION AND SUMMARY

All thermochemical hydrogen cycles contain at least one high temperature endo-

thermic step, and the ZnSe cycle is no exception. The high temperature step in the ZnSe cycle is the decomposition of ZnSO₄ at 1160 K.

In the modified cycle we have reduced the amount of ZnSO₄ to be decomposed from 2 moles per mole of hydrogen produced to 1 mol. The second mole of ZnO is regenerated through direct hydrolysis of ZnCl₂ at 900 K. This improves the cycle in two ways:

- (1) it extends the temperature range over which the prime heat is delivered, and
- (2) it improves the ideal thermal efficiency of the cycle from 49 to about 63%.

With equipment specifically and innovatively designed for each process step, we can perform difficult cycle operations with a minimum of processing problems, and conserve heat for reuse in other process steps. We have achieved a thermal efficiency of 42% in the current design, with prospects for further improvement through process optimization. Laboratory investigations of reaction rates and yields, and development of alternative chemical approaches are needed to attain this optimization. Furthermore, with new developments in high temperature materials and fabrication techniques in the future, we might realize greater than the 10 to 20 year plant equipment life which was assumed, with a corresponding reduction in hydrogen production cost.

VII. REFERENCES

1. Dreyfuss, R. M. and Krikorian, O. H., "Exploration of a Selenium-Based Cycle for the Thermochemical Production of Hydrogen from Water," Lawrence Livermore Laboratory Report UCRL-51741, Feb. 1975.
2. Pearson, R. K., et al., "Reactions in the ZnSe Thermochemical Cycle for Hydrogen Production," Ind. Eng. Chem., Prod. Res. Dev., **16**, 73 (1977).
3. Wagman, D. D., et al., "Selected Values of Chemical Thermodynamic Properties, Tables for the First 34 Elements in the Standard Order of Arrangement," National Bureau of Standards, Technical Note 270-3 (1968).
4. Kelley, K. K., "Contributions to the Data on Theoretical Metallurgy, XIII. High-Temperature Heat-Content, Heat Capacity, and Entropy Data for the Elements and Inorganic Compounds," Bureau of Mines Bull. 584 (1960).
5. Cubicciotti, D. and Eding, H., "Heat Contents of Molten Zinc Chloride and Bromide and the Molecular Constants of the Gases," J. Chem. Phys. **4**, 978 (1964).
6. Stern, K. H. and Weise, E. L., "High Temperature Properties and Decomposition of Inorganic Salts, Part I. Sulfates," National Standard Reference Data Series, National Bureau of Standards, NSRDS-NBS-7 (1966).
7. Bruhn, Von G., et al., "Untersuchungen über die Löslichkeiten von Salzen und Gasen in Wasser und wässrigen Lösungen bei Temperaturen oberhalb 100°C," Z. für anorgan. allgem. chemie, **337**, 68 (1965).
8. Pechkovskii, V. V., "Thermochemical Decomposition of Zinc Sulfate," J. Inorgan. Chem. USSR (English translation) **11**, 1467 (1957).
9. Pechkovskii, V. V., "Decomposition of Zinc and Cobalt Sulfates in Current of Sulfur Dioxide and Air," J. Appl. Chem. USSR (English translation) **31**, 1130 (1958).
10. Farbman, G. H., "The Conceptual Design of an Integrated Nuclear Hydrogen Production Plant Using Sulfur Cycle Water Decomposition System," Westinghouse Electric Corporation Report NASA-CR-134976 (1976).

Table 1. Process energy balance.

Battery	Process step	Power (heat equiv.), kJ/mol H ₂	Heat req't, kJ/mol H ₂	Heat avail., kJ/mol H ₂
A	Selenium preheater		8.9 @ 725 K	
	ZnSe/ZnSO ₄ generator			166.1 @ 775 K
	Sensible heat of products			52.0 @ 525 K
	Injector/extruder power	1.0		
B	ZnSO ₄ ·H ₂ O former			35.8 @ 525 K
	ZnSO ₄ solution heater		30.1 @ 525 K	
	ZnSO ₄ ·H ₂ O dehydrator		79.4 @ 525 K	
	Steam			40.6 @ 500 K
C	HCl-H ₂ O evaporator		207.1 @ 400 K	
D	ZnCl ₂ preheater		18.8 @ 550 K	
	ZnCl ₂ -Steam hydrolyzer		150.0 @ 900 K	
	HCl-H ₂ O superheater		65.3 @ 900 K	
E	H ₂ Se decomposer			16.3 @ 700 K
	H ₂ -H ₂ Se separator			22.9 @ 550 K
	H ₂ product compressor	30.1		
F	ZnSO ₄ decomposer		329.0 @ 1200 K	
	He heater transfer			
	fluid circulator	70.0		
G	SO ₂ -SO ₃ -O ₂ process power	51.5		
	Steam			67.8 @ 600 K
	SO ₂ -SO ₃ -O ₂ separator	77.6		
	Turbo expander		10.4 @ 1000 K	49.3
Total		230.4	899.0	450.8

Net nuclear heat requirement = 230.4 + 899.0 - 450.8 = 678.6 kJ/mol H₂

Thermal efficiency (η) = 285.8/678.6 = 0.421

Table 2. H₂ production plant cost (1976\$).

Plant size is 27.3 Mg H₂/h
(60,000 lbs. H₂/h).

Battery	Operations	10 ⁶ \$*
A	ZnSe/ZnSO ₄ generation	20.0
B	ZnSO ₄ separation	152.0
C	ZnSe hydrolysis	141.0
D	ZnCl ₂ conversion	215.0
E	H ₂ Se decomposition	24.0
F	ZnSO ₄ decomposition	218.0
G	SO ₂ /SO ₃ /O ₂ separation	63.0
Off-site		
General		7.0
Off-site		
Direct		15.0
		855.0

* Including 105% for structures, installation, etc.

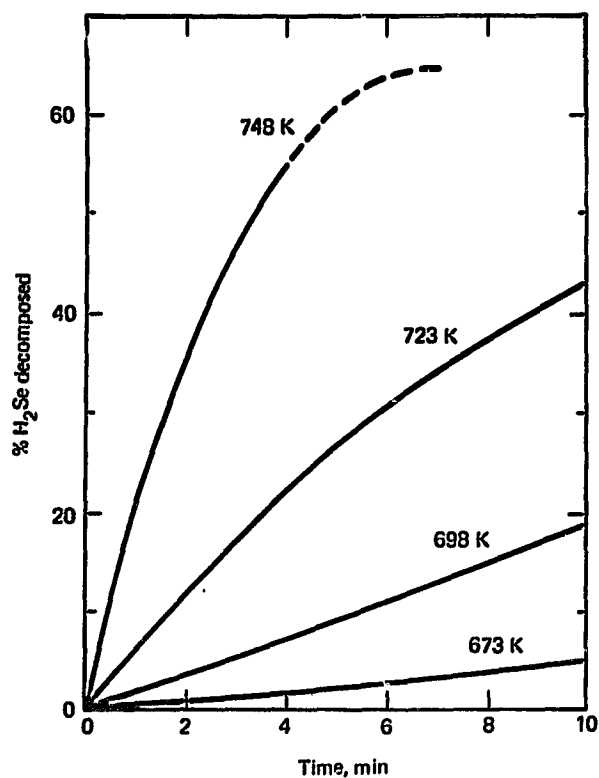


Fig. 1. Temperature dependence of H_2Se decomposition. 60% of H_2Se decomposes in 5 min. at 748 K.

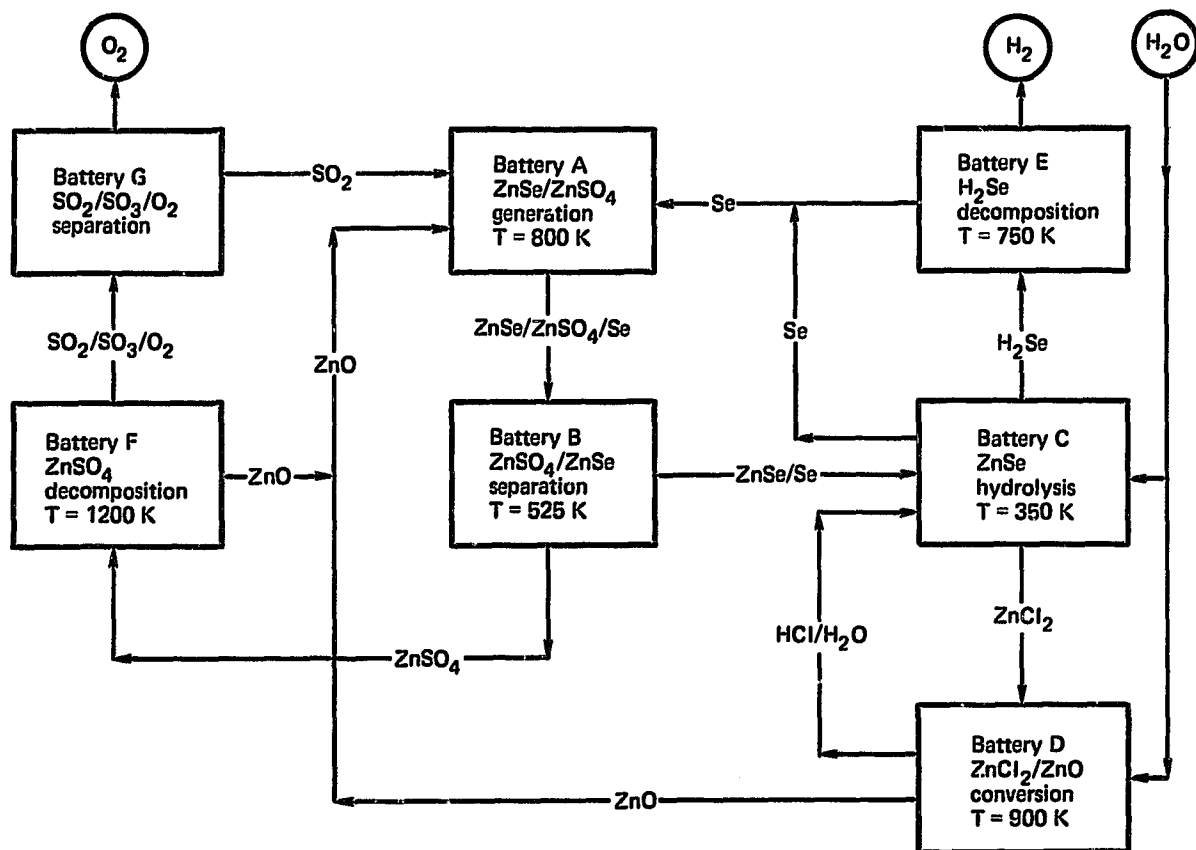


Fig. 2. Simplified schematic flow diagram of ZnSe cycle.

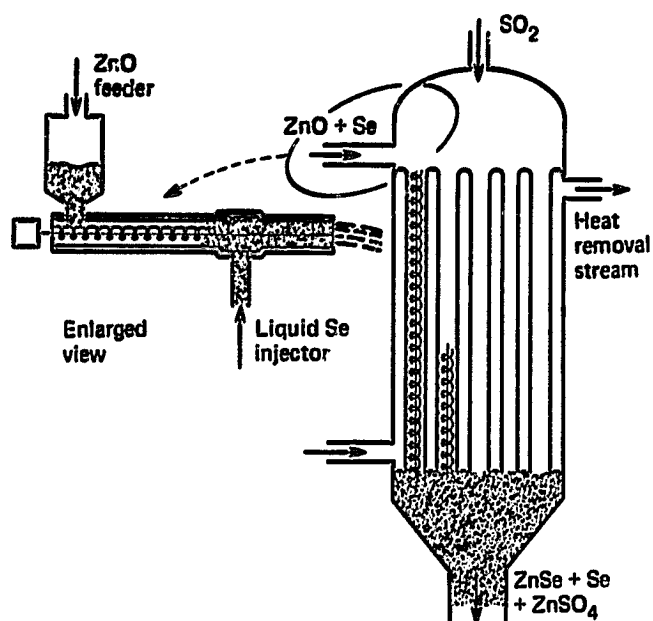


Fig. 3. ZnO-Se-SO₂ reactor. Intimate mixing of ZnO-Se is accomplished with injector-extruder type feeder.

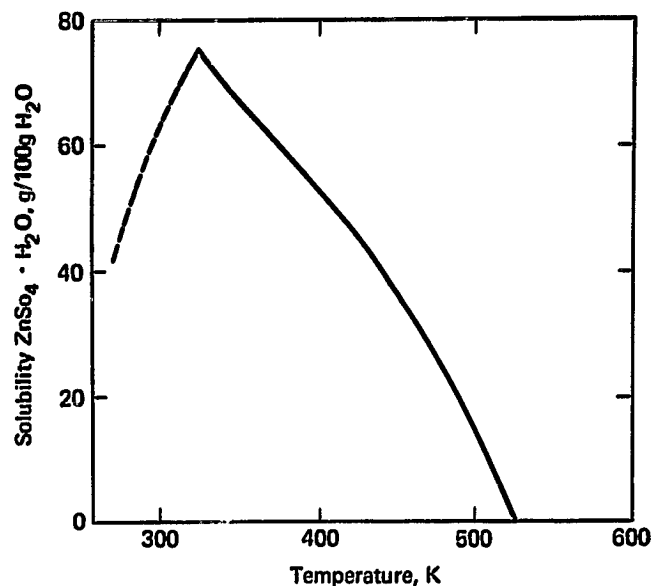


Fig. 4. Favorable ZnSO₄ solubility relation allows separation and recovery of ZnSO₄ without boiling of solutions.

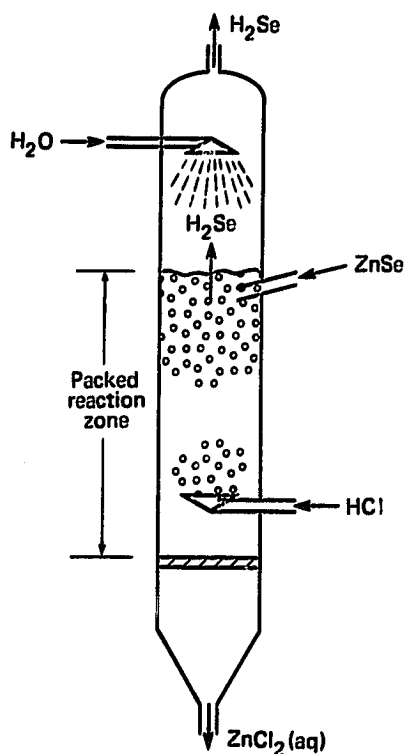


Fig. 5. ZnSe hydrolyzer. Packed column design allows better HCl concentration control in the hydrolyzer.

STATUS OF EUROPEAN THERMOCHEMICAL HYDROGEN PROGRAMS

Melvin G. Bowman

University of California
Los Alamos Scientific Laboratory
Los Alamos, New Mexico 87545

Abstract

An invited paper on Thermochemical Hydrogen Production was presented at an International Symposium on Energy Sources and Development held in Barcelona, Spain, October 19-21, 1977. Visits were then made to the following European Laboratories engaged in thermochemical hydrogen research: (1) The Euratom Central Research Center, Ispra, Italy. (2) The Center for Nuclear Research at Saclay, France. (3) The Rheinisch-Westfälische Hochschule in Aachen, Germany. (4) The Jülich Nuclear Research Center at Jülich, Germany.

The visits to the listed laboratories were primarily to learn the scope of the different programs and the general areas of information expected to be made available under the recently signed International Energy Agency Implementing Agreement on the Production of Hydrogen from Water. From observations made during these visits, the following conclusions were reached: (1) It is clear that the Europeans are directing their efforts towards relatively short term development of better methods for the production and utilization of hydrogen. (2) The European effort on thermochemical hydrogen research and development is significantly greater than the total of U.S. programs. (3) It will be advantageous for the United States to cooperate in information exchange activities under the I.E.A.

The description of the different visits is given in the format of a trip report.

The Barcelona Meeting

Abstracts of papers were distributed to participants. Complete texts of papers will be published in the "Proceedings" of the Symposium. This should be available by March 1, 1978. The executive secretary for the symposium was Dr. J. Plana, Banco Urquijo, Servicio de Estudios, Paseo de Gracia, 27 Barcelona 7 Spain.

The organizers of the symposium expressed the hope that it might lead to a Spain-U.S. exchange with meetings held in alternate years in Spain and the U.S. Informal discussions were held on Saturday, Oct. 21, 1977 to consider the possible meeting in the U.S. next year. No actual decisions were reached and further discussions will be held during visits of Spanish scientists to the U.S. in 1978.

The Ispra Visit

I presented a seminar at the Ispra Laboratory and summarized progress in U.S. programs on

thermochemical hydrogen production. Achievements and capabilities were described and it was stated that the large volume of specific information and experimental details would be available under the information exchange program.

I toured the experimental facilities at Ispra and I was impressed by the progress made in their programs. For the most part, I did not probe for details and data not included in the presentations. However, it is clear that valuable data and information will be included in reports and working papers that will be available under the information exchange agreement.

Essentially all of the Ispra work is concerned with three cycles. These are: (1) the sulfuric acid-hydrogen iodide cycle (this is the General Atomic Prime Cycle that Ispra has named Mark 16), (2) the sulfuric acid hybrid cycle (named Mark 11 by Ispra), and (3) the sulfuric acid-hydrogen bromide hybrid cycle (called Mark 13). This last cycle has been chosen for their "closed circuit" experiment.

It may be described by the reactions:

- I. $\text{Br}_{(2\ell)} + \text{SO}_2 + 2\text{H}_2\text{O} \rightarrow \text{H}_2\text{SO}_4 + 2\text{HBr(g)}$
- II. $\text{H}_2\text{SO}_4 \rightarrow \text{H}_2\text{O} + \text{SO}_2 + 1/2 \text{O}_2$ (high temperature)
- III. $2\text{HBr} \rightarrow \text{H}_2(\text{g}) + \text{Br}_{2(\ell)}$ (electrolysis)

There seems to be a group of 4-5 people working on each of the first two reactions. There are two groups working on the third reaction. One of these groups is designated "physical chemistry" and is concerned with developing the data base on electrode materials, electrode catalysts, and voltage versus current density curves as functions of temperature and pressure. The second group is developing bipolar cells and associated equipment in preparation for the closed circuit experiment. I was told that they have achieved a current density of 2000 A/m² at a cell voltage of 0.75 V for reaction III using graphite electrodes. I probed for more information on the graphite and was told that it is a "special" graphite that is only 20% more expensive than regular graphite.

In addition to the groups working on the above reactions, there is a group performing very extensive corrosion tests on a variety of materials. Most of this work is done under the various conditions associated with drying, decomposing and condensing the decomposition products of sulfuric acid. I was told that they have demonstrated at least one satisfactory material for each of the different conditions. It is clear that Ispra believes corrosion problems can be solved.

In addition to their experimental program, the Ispra personnel are engaged in preparing extensive and detailed flow-sheets and process design efforts on each of the cycles described above and on the iron chloride cycle. These conceptual designs are being used in attempts to estimate costs associated with thermochemical hydrogen production. As part of this effort, Ispra has given a contract to a large chemical engineering firm (Technipetrol, Inc., Rome) to examine the detailed flow-sheets and identify and furnish cost data for known industrial equipment and processes that can be used for each of the flow-sheet operations. The data from the chemical engineering firm will be used with the Ispra computer code in attempts to effect some optimization of process parameters and to obtain integrated cost figures. In this way, they expect to obtain realistic capital and operating costs for a plant that could be built. It is realized, of course, that these costs will be higher than those associated with the still unspecified plant that should be built.

Dr. Beghi (as the "operating agent") and I (as the U.S.A. "technical contact") discussed problems associated with the logistics of information exchange and also the workshop specified by the I.E.A. agreement. Relevant extracts from the agreement have been made as follows:

Means

- (a) Each Participant as indicated below will undertake an experimental or analytical programme on at least one of the following eight steps that apply specifically to

the sulphur-iodine and iron-chlorine cycles, but also apply in general to other cycles that incorporate the decomposition of sulphuric acid, a metal sulphate or hydroiodic acid:

- (1) Thermal decomposition of H_2SO_4 .
- (2) Thermal decomposition of a metal sulphate.
- (3) Hydrolysis of FeCl_2 .
- (4) Liquid separation of $\text{H}_2\text{SO}_4/\text{HI}$ from solution.
- (5) Reverse Deacon reaction.
- (6) Decomposition of HI .
- (7) Decomposition of FeCl_3 .
- (8) Electrochemical production of H_2SO_4 and H_2 from SO_2 and H_2O .

Although the Participants undertake a commitment to work only on at least one of the above steps, they are interested in pursuing the work in all of them.

- (c) Within the first year of the implementation of this Annex, each Participant will provide to the Operating Agent publications in its possession which have relevance to the objectives of this Task. In addition, each Participant will provide to the Operating Agent copies of such internal reports and working papers resulting from the work outlined in paragraph 2 (a) as may be of interest to the other Participants. Further, each Participant on an annual basis will prepare a progress report on its work under way and submit it to the Operating Agent.
- (d) The Operating Agent will compile and submit to the Executive Committee a work programme for the first year. The Executive Committee, acting in unanimity, shall approve a work programme for the first year, no later than three months after signature of this Annex. The work programme (including patent considerations) will outline the respective contributions of each Participant for accomplishing the objectives of the Task.
- (e) At the end of the first and second years, a 3-4 day workshop will be held to discuss progress reports and to formulate the next year's detailed work programme. Organization of the workshop shall be the responsibility of the Operating Agent.
- (f) Each Participant will designate for the Operating Agent technical contacts for each of the reaction or operation steps undertaken pursuant to paragraph 2 (a).

Time Schedule

Three years (1st November, 1977-31st October, 1980). Workshops planned: Summer 1978, Summer 1979.

In discussing the logistics problem Dr. Beghi and I noted that there are seven participants in the agreement, six countries and the European

community as a separate organization. Each participant (or country) will designate a technical contact or contacts. We decided on an initial procedure as follows:

- (1) Dr. Beghi will obtain the reports and documents described in Paragraph 2-c above from the technical contacts named by each of the countries. He will send one copy of each document to me and send a copy of the transmittal letter to Dr. John Gahmer who is the DOE headquarters contact for the Thermochemical Hydrogen Annex. I will make copies of these documents for headquarters and for each of the U.S. organizations working on the identified tasks. In the meantime, I will receive similar documents from the U.S. organizations and send eight copies of each document to Dr. Beghi (and a copy of the transmittal letter to Dr. Gahmer). Dr. Beghi will distribute these documents to each technical contact who in turn, presumably, will arrange for distribution to the active organizations in his country.

Dr. Beghi and I discussed various possibilities for the format and organization of the workshop described in paragraph 2-(c) of the agreement. No conclusions were reached. I agreed to discuss the subject with U.S. workers and then send suggestions by letter. We recognized that late August 1978 just after the Hydrogen Conference in Zurich, would be a convenient time for the first workshop.

The Saclay Visit

A small group of chemists, under the direction of Dr. Etienne Roth, are engaged in reactions of potential value in thermochemical cycles. They have been interested in cycles based on carbonate chemistry in attempts to identify less corrosive processes. They have not been successful in this particular area, but it is an interesting and well conceived program. They have also performed experimental studies on reactions and cycles considered at LASL. It is clear that information exchange can benefit both laboratories. Since the French are not participants in the I.E.A. agreement, the exchange will consist of papers at the pre-print stage, progress reports (hopefully) and infrequent visits.

I presented a seminar describing U.S. thermochemical hydrogen programs. I was surprised to learn that some of the audience were from the Reactor Division. After the seminar, I was given a very interesting tour of the large facility used to test components designed for their HTGR reactors. Their interest in thermochemical hydrogen was explained by the statement that HTGR reactors in France are to be used only for high temperature process heat applications and not for the production of electricity.

The Visit to RWTH-Aachen

Professors Knoche, Cremer and Schulten directed and performed imaginative work in the conception, testing, chemical engineering design and analysis as well as cost analysis of several very interesting cycles. The laboratory work has been stressed less than the analysis activities, but some reactions have been verified experimentally. At the present time, much of their work is centered around the iron chloride cycle and their experimental

and analytical results will become available under the I.E.A. agreement. They have developed a versatile and comprehensive computer code to guide process design associated with gas separation steps in the iron chloride cycle. It seems probable that the cycle will appear better after their optimization efforts, but I think their present opinion is that it will not be competitive with the best cycles. Nevertheless, the methodology they are developing should be extremely valuable when applied to other cycles.

The other cycles under investigation by this group are not covered by the I.E.A. agreement, but we have agreed to an informal exchange of information on our respective programs. Professor Knoche expressed an interest in performing some design optimization and analysis of the LASL cerium chloride cycle.

I presented a seminar on LASL thermochemical hydrogen research to an interested and informed group of graduate students and professors.

The Visit to Jülich Nuclear Research Center

Dr. Heiko Barnert will (presumably) act as the Operating Agent for Annex II of the I.E.A. hydrogen agreement, although he hasn't been formally notified that he has been designated. Annex II is concerned with problems of interfacing a High Temperature Reactor with a Thermochemical Hydrogen Plant. Dr. Barnert had been asked (by the Executive Committee Member from Germany) to prepare a detailed work statement on Annex II for the Executive Committee meeting to be held in Paris on November 8-9, 1977. Dr. Barnert had prepared a statement based only on the Jülich Program and was uncomfortably aware that the other participants in the Annex might not concur. However, until my visit, he had not been given the name of the designated technical contact for any of the countries. I informed him that Dr. John Gahmer will act as the DOE headquarters contact and that I will assist in technical matters. We agreed to initiate the exchange of reports and documents specified in the Exchange Agreement. We were both aware that there is an existing bi-lateral agreement between the U.S. and Germany for information exchange on high temperature reactors. Therefore, the selection of information to be made available under the I.E.A. agreement must be compatible with the bi-lateral agreement.

It seems quite clear that valuable information will be generated in the Jülich thermochemical hydrogen program. Approval has been given in principle for a 10 year experimental and theoretical program for the development of thermochemical processes and also for the development of metal hydrides for hydrogen storage. The funding level is projected to be between 60 and 80 million DM over the 10 year period. The specific objectives include the construction and operation of a "semi-technical" plant (about 100 kW level) for the production of hydrogen from water using a thermochemical cycle. At the present time, the cycle is projected to be the sulfuric acid hybrid cycle and most of the experimental effort is on the cycle. A second objective is the design and construction of a "semi-technical" plant for hydrogen storage. Currently there are six people (some part time) engaged in developing the electrolysis step in the hybrid cycle. This work is directed by Dr. Struck. He was very reluctant to give details of progress since part of the

program is funded by Euratom and he felt that specific permission was required before he could give information. There are three people working on the high temperature thermal decomposition of sulfuric acid. This work is directed by Dr. Hammeke and is still in the initial stages of equipment design and procurement. There are three people engaged in an activity called HTR coupling-economics. This program is directed by Dr. Barnert and it includes the development and comparison of methodologies for estimating the costs associated with thermochemical cycles coupled to high temperature reactors. There are, at present, two people engaged in metal hydride research.

Conclusions

It is clear that the Europeans are quite serious in relatively short term development of better

methods for the production and utilization of hydrogen. The effort on thermochemical hydrogen research and development in Europe is significantly greater than the total of the U.S. programs. In my opinion, the short range objectives are overemphasized and not enough attention is given to the conception and evaluation of alternative cycles. Thus, attention is concentrated on only two or three possibilities. In the past, this has resulted in a great deal of development work on cycles that finally had to be abandoned. At the present time, large scale development efforts are directed toward three cycles that were first identified in U.S. programs. Nevertheless, it seems quite clear that it will be advantageous for the United States to participate in information exchange activities under the I.E.A. and, indeed, in bi-lateral information exchange on cycles not yet formalized in the I.E.A. Agreement.

SESSION II
HYDROGEN PRODUCTION

C. ADVANCED CONCEPTS

APPLICATIONS OF SOLUBILITY PARAMETERS -- PART I

D. D. Lawson
Jet Propulsion Laboratory

**HYDROGEN PRODUCTION BY PHOTOELECTROLYTIC DECOMPOSITION
OF WATER USING SOLAR ENERGY**

R. D. Rauh, T. F. Reise, and S. Alkaitis
EIC Corporation

**DEVELOPMENT OF A PRACTICAL PHOTOCHEMICAL ENERGY STORAGE
SYSTEM**

C. Kotal, R. R. Hautala, and R. B. King
University of Georgia

APPLICATIONS OF SOLUBILITY PARAMETERS

PART I

D. D. Lawson

Jet Propulsion Laboratory
California Institute of Technology
Pasadena, California 91103

ABSTRACT

The long range objective of this work is to create a simple means of quantitatively dealing with the physicochemical nature of the interaction of hydrogen (atomic or gaseous forms) and other fluids with materials used in hydrogen production and/or storage environments. In the following sections, definitions and related data will be presented as a starting point to achieve the above objective.

The Solubility Parameter

The prime movers of the solubility parameter (δ) concept are Professors Joel H. Hildebrand and Robert L. Scott.(1) The solubility parameter of a material is a measure of the intermolecular forces in a given substance and is a fundamental property of all matter. The basic assumption in the solubility parameter is that there is a correlation between the Cohesive-Energy Density (CED) that is potential energy per unit volume and mutual solubility of materials.(2)

The potential energy of a mole of material (E) is:

$$E = Nv \quad (1)$$

when N is Avogadro's number and the potential energy of a molecule or a single atom is v. The cohesive-energy density is thus numerically equal to the negative potential energy of one cubic centimeter of the material:

$$CED = \frac{-E}{V} \quad (2)$$

where V is the molar volume or atomic volume.

It is convenient when solute-solvent systems are to be studied to define the square root of cohesive-energy density as the solubility parameter (δ).

$$CED = \delta^2 = \frac{-E}{V} = \frac{-Nv}{V} \quad (3)$$

The vaporization of a material can be imagined as a process involving the transport of all molecules or atoms from their equilibrium distance relative to each other, so that the potential energy of each molecule or atoms is reduced to zero.

In the case of metals, the heat of sublimation or the heat of atomization is the thermodynamic term used. The heat of vaporization or sublimation per mole (E) is thus the term used to compensate both for the potential energy per mole (E) and for the volume work, which for a vapor phase obeying ideal gas laws is RT, where R is the molar gas constant and T is the absolute temperature (at 25° this is 592 calories) then:

$$\Delta H_v = -E + RT \quad (4)$$

It follows that the CED can then be obtained from the heat of vaporization or sublimation (ΔH_v) and the molar volume (V)

$$CED = \delta^2 = \frac{\Delta H_v - RT}{V} \quad (5)$$

The units for the solubility parameter (δ) are cal^{1/2} cm^{-3/2} and is named a Hildebrand (Hb) in honor of Professor Joel Hildebrand.(2) Most organic materials have Hb values between 5 and 23.4 (water), whereas most metals have values from 30 to 180 Hbs.

Hildebrand's Mixing Rule and Miscibility

The real usefulness of the solubility parameter is that by the use of the Hildebrand mixing rule an

estimation of the solubility parameter (δ) of a mixture of materials can be calculated. This assumes that the materials are completely miscible with each other and are somewhat chemically inert to each other. The effective solubility parameters (δ_m) of a mixture of components 1 and 2 with $\delta_{1,2}$ and $\phi_{1,2}$ volume fraction is:

$$\delta_m = \phi_1 \delta_1 + \phi_2 \delta_2 \quad (6)$$

where

$$\phi_1 = \frac{V_1}{V_1 + V_2} \text{ and } \phi_2 = \frac{V_2}{V_1 + V_2} \quad (V = \text{volume})$$

Equation 6 rearranged in terms of Volume is:

$$V_2 = \frac{\delta_m}{\delta_2 - \delta_1} - \frac{\delta_1}{\delta_2 - \delta_1} \quad (7)$$

$$V_1 = 1 - V_2$$

In general, solubility, or miscibility, of two substances is to be expected if there is a decrease in the free energy of mixing, viz.,

$$\Delta F_{mix} = \Delta H_{mix} - T\Delta S_{mix} \quad (8)$$

In as the entropy of mixing ΔS_{mix} is positive (i.e., $-T\Delta S_{mix} < 0$), the enthalpy of mixing ΔH_{mix} will determine solubility. The latter term (for non-polar substances) is positive and its magnitude is proportional to the differences of the respective solubility parameters (δ) (i.e., square root of the cohesive energy density)

$$\Delta H_{mix} \sim (\delta_1 - \delta_2)^2 \quad (9)$$

Thus, the closer the solubility parameter values, the smaller the ΔH_{mix} will be and, consequently, the greater the decrease in ΔF_{mix} . However, mutual miscibility will exist for a range of values in the vicinity of the substance's solubility parameter. This range will depend on where in the δ continuum, i.e., organics 5 to 23 Hb or the metals up to 180 Hb, the material falls. In the organic region a value of ± 2.5 Hb is the generally used value and at the higher δ values it is 25 to 30 Hb for metallic materials.

In Table I is given data for materials commonly encountered in some thermochemical cycles for the production of hydrogen. In Table II is the δ data for the elements with atomic numbers of one through ninety two.

References:

1. Hildebrand, J.H. and R.L. Scott, "The Solubility of Nonelectrolytes" ACS Monograph series #17 (1950).
2. Barton, Allan F.M. Chem Reviews **75** 731-753 (1975).

Table I

MATERIALS THAT ARE ENCOUNTERED IN SOME THERMOCHEMICAL CYCLES FOR HYDROGEN PRODUCTION

Compound	T(K°)	V _T (cm ³)	ΔH_T^V (Kcal/mole)	δ_T (Hb)
Cl ₂	239	46	4.88	9.8
Br ₂	298	51	7.34	11.5
I ₂	298	59	11.73	14.1
HCl	187	30.5	4.58	12.25
HBr	185	19.2	5.05	13.14
HI	222	44.9	5.49	11.06
S ₈	298	135	21.77	12.7
SO ₂	263	44	5.95	11.0
α SO ₃	298	41.6	11.8	16.84
β (SO ₃) ₂	298	81.3	12.8	12.57
H ₂ SO ₄	298	53.3	18.0	18.39
SO ₂ Cl ₂	298	80.9	7.8	9.80
H ₂ O	298	18.0	10.0	23.53

NOTE: The δ will decrease as the temperature is increased. For more details see Ref 1, Ch XV.

Table II
SOLUBILITY PARAMETERS AND ATOMIC VOLUMES OF THE ELEMENTS

Element	Atomic Number Z	Atomic Volume cc/gram- atom	Solubility Parameters [cal/cc] ^{1/2}	Standard Deviation of the Solubility Parameter	Temperature K°	Symbol
Actinium	39	22.56	67.9	(A)	298	Ac
Aluminum	13	10.00	88.03	1.20	298	Al
Antimony	51	18.21	58.26	4.69	298	Sb
Argon	18	23.86	7.93	(A)	28	Ar
Arsenic	33	13.10	72.79	(A)	298	As
Astatine	85		(D)			At
Barium	56	39.24	32.91	0.30	298	Ba
Beryllium	4	4.38	126.00	0.60	298	Be
Bismuth	83	21.33	48.40	0.20	298	Bi
Boron	5	4.65	169.10	1.20	298	B
Bromine	35	(25.53)	32.37	0.02	298	Br
Cadmium	48	13.00	45.37	0.02	298	Cd
Calcium	20	25.97	40.31	0.17	298	Ca
Carbon	6	5.34	179.06	0.24	298	C
Cerium	58	20.70	68.67	(A)	298	Ce
Cesium	55	70.05	16.40	0.18	298	Cs
Chlorine	17	(19.30)	38.5	(A)	298	Cl
Chromium	24	7.23	114.62	0.85	298	Cr
Cobalt	27	6.67	123.66	0.86	298	Co
Copper	29	7.11	106.8	(A)	298	Cu
Dysprosium	66	19.00	59.17	3.00	298	Dy
Erbium	68	18.27	62.04	3.12	298	Er
Europium	63	28.98	38.34	0.32	298	Eu
Fluorine	9	(10.30)	42.82	1.60	298	F
Francium	87	73.0	15.75	(A)	298	Fr
Gadolinium	64	20.01	64.21	0.27	298	Gd
Gallium	31	11.80	74.16	(A)	298	Ga
Germanium	32	13.64	81.00	(A)	298	Ge
Gold	79	10.20	92.67	0.52	298	Au
Hafnium	72	13.64	110.94	4.67	298	Hf
Helium	2	19.53	1.06	(A)	1	He
Holmium	67	18.75	61.19	0.37	298	Ho
Hydrogen	1	(6.70)	124.2	(A)	298	H
Indium	49	15.71	60.40	0.22	298	In
Iodine	53	(25.68)	31.50	(A)	298	I
Iridium	77	8.54	136.47	0.51	298	Ir
Iron	26	7.10	118.68	0.84	298	Fe
Krypton	36	32.00	8.50	(A)	121	Kr
Lanthanum	57	22.44	67.35	1.03	298	La
Lead	82	18.27	50.61	0.76	298	Pb
Lithium	3	12.99	54.50	0.40	298	Li
Lutetium	71	17.77	74.55	2.14	298	Lu

Table II

SOLUBILITY PARAMETERS AND ATOMIC VOLUMES OF THE ELEMENTS (Continued)

Element	Atomic Number	Atomic Volume cc/gram-atom	Solubility Parameters [cal/cc] ^{1/2}	Standard Deviation of the Solubility Parameter	Temperature K°	Symbol
Magnesium	12	13.97	50.48	(A)	298	Mg
Manganese	25	7.39	95.58	0.69	298	Mn
Mercury	80	14.82	31.45	0.01	298	Hg
Molybdenum	42	9.39	129.51	(A)	298	Mo
Neodymium	60	20.61	60.56	0.34	298	Nd
Neon	10	16.76	5.12	(A)	24	Ne
Nickel	28	6.59	124.59	0.54	298	Ni
Niobium	41	10.83	127.12	1.28	298	Nb
Nitrogen	7	(11.40)	99.1	(A)	298	N
Osmium	76	8.43	149.10	0.51	298	Os
Oxygen	8	(8.50)	83.57	0.19	298	O
Palladium	46	8.88	100.73	0.71	298	Pd
Phosphorus	15	16.92	67.70	1.39	298	P
Platinum	78	9.09	121.86	0.12	298	Pt
Polonium	84	22.62	39.05	(A)	298	Po
Potassium	19	45.47	21.74	0.05	298	K
Praseodymium	59	20.82	64.08	0.64	298	Pr
Promethium	61	20.33	56.11	(B)	298	Pm
Protactinium	91	15.00	93.81	(B)	298	Pa
Radium	88	38.80	32.90	(B)	298	Ra
Radon	86	50.45	29.19	(A)	208	Rn
Rhenium	75	8.85	145.13	0.33	298	Re
Rhodium	45	8.29	126.76	0.67	298	Rh
Rubidium	37	55.87	18.78	0.45	298	Rb
Ruthenium	44	8.29	136.38	0.44	298	Ru
Samarium	62	20.07	49.86	(A)	298	Sm
Scandium	21	15.06	73.32	0.43	298	Sc
Selenium	34	16.48	54.75	0.78	298	Se
Silicon	14	12.06	94.80	1.85	298	Si
Silver	47	10.27	81.61	(A)	298	Ag
Sodium	11	23.67	33.10	0.13	298	Na
Strontium	38	33.70	34.08	0.03	298	Sr
Sulfur	16	15.49	65.46	1.39	298	S
Tantalum	73	10.90	130.59	0.45	298	Ta
Technetium	43	8.63	133.37	0.93	298	Tc
Tellurium	52	20.45	47.73	1.45	298	Te
Terbium	64	19.26	68.20	1.19	298	Tb
Thallium	81	17.25	50.07	0.20	298	Tl
Thorium	90	19.90	82.85	(A)	298	Th
Thulium	69	18.15	56.53	0.28	298	Tm
Tin	50	16.30	66.46	(C)	298	Sn

Table II
SOLUBILITY PARAMETERS AND ATOMIC VOLUMES OF THE ELEMENTS (Continued)

Element	Atomic Number	Atomic Volume cc/gram-atom	Solubility Parameters [cal/cc] ^{1/2}	Standard Deviation of the Solubility Parameter	Temperature K°	Symbol
Titanium	22	10.63	102.96	0.64	298	Ti
Tungsten	74	9.53	144.87	0.51	298	W
Uranium	92	12.48	100.07	1.70	298	U
Vanadium	23	8.35	121.22	3.49	298	V
Xenon	54	36.81	9.43	(A)	166	Xe
Ytterbium	70	24.87	40.10	(A)	298	Yb
Yttrium	39	19.88	70.14	(A)	298	Y
Zinc	30	9.17	58.51	0.41	298	Zn
Zirconium	40	14.06	101.90	0.49	298	Zr

(A) A single value available in the literature.

(B) Estimated data.

(C) Gray form of tin.

(D) No data available.

The atomic volumes in brackets are the single atom values.

**HYDROGEN PRODUCTION BY PHOTOELECTROLYTIC DECOMPOSITION
OF WATER USING SOLAR ENERGY**

**R. David Rauh, Terrence F. Reise and Saul Alkaitis
EIC Corporation
55 Chapel Street
Newton, Massachusetts 02158**

Abstract

The conversion of light to chemical energy can be effected through the photoelectrolysis of water to produce H_2 and O_2 . The aim of this program is to discover semiconducting photoelectrode materials which have optimal band gaps, electron affinities and stabilities for this application.

I. INTRODUCTION

When a semiconductor and redox electrolyte of different work function are brought into contact, their equilibration through electron exchange and surface reactions results in the formation of a rectifying barrier. This effect has long been known in connection with the study of electrochemistry at semiconductor electrodes (1). However, it was not until the published experiments of Fujishima and Honda (2) in 1972 that it was realized that irradiation of the semiconductor-aqueous electrolyte interface, in an electrochemical cell, would result under some conditions in the decomposition of H_2O into H_2 and O_2 . As in photosynthesis, a method was provided for directly converting solar energy into a storable fuel.

The purpose of this program is to demonstrate materials which maximize the efficiency of photoelectrolysis in inexpensive polycrystalline configurations. The ideal electrode should have a band gap with good solar collection efficiency. As described below, the bands must also be in the proper orientation with respect to the H^+/H_2 redox energy level of the electrolyte, and with respect to the vacuum. In addition, the water decomposition half reaction occurring on the photoelectrode must be preferred over electrode decomposition, on thermodynamic or kinetic grounds. Finally, the quantum yield for current production must be high, i.e., the photoreaction must compete favorably with the recombination of excited minority carriers produced under illumination.

II. ENERGETIC REQUIREMENTS OF PHOTOELECTROLYSIS

Figure 1A shows a typical configuration for a photoelectrolysis cell. The photosensitive electrode consists of an n or p doped semiconductor with an ohmic contact to its back surface. In this single photoelectrode embodiment, the counter electrode is a metallic conductor, such as Pt or graphite.

Figure 2 illustrates the energetics of an ideal n-type electrode under short circuit conditions of H_2O photoelectrolysis. The n-doping causes the work function to be lower than that of the electrolyte. Consequently, when the two are placed in contact, the SC releases some of its electrons to the electrolyte. Unlike a metal, a semiconductor has a limited number of electrons per unit volume - hence the depletion region extends well into the bulk of the electrode. This is manifested by a bending of the semiconductor valence and conduction bands over the depth required for equalization of the potentials of the two phases. Additional variations of the semiconductor potential applied via the ohmic contact using an external bias will result in an increased band bending for positive applied potentials and vice versa. The applied potential necessary to decrease the bending to zero is termed the flat band potential, ΔE_{fb} . Under most conditions, ΔE_{fb} for n-type electrodes is negative (as in Fig. 1), and positive for p-type materials.

It should be noted that the energy of the conduction band at the interface is equal to the electron affinity of the semiconductor, since very little depletion of electrons can occur within only a few angstroms of the surface. Thus, in the absence of surface adsorbents or ionizable

functional groups, the values of E_c and E_v are locked into place by the physical properties of the electrode material.

The interface energetics in the dark are determined by the presence and concentrations of redox species in solution. As pointed out by Nozik (3), the "Fermi level" of the solution is not very reproducible, being very sensitive to solution composition. The reversible potentials for H_2 and O_2 evolution are also shown in Figure 2, and are a function of pH. The energy of the normal hydrogen electrode (NHE), whose position is shown in Figure 2, is approximately 4.5 eV with respect to vacuum. The photoelectrode, solution and counter electrode are shown in chemical equilibrium.

On illumination of the semiconductor in Figure 2, electrons are excited from the valence band to the conduction band. Electrons placed into the space charge region of the conduction band are swept into the interior by the built-in field, while the valence band holes migrate to the surface. The increased population of minority carriers in the conduction band results in a negative displacement of the Fermi level, and thus, under short circuit conditions, in the potential of the counter electrode. In the absence of other more reducible species, electrons will reduce H^+ at the counter electrode. At the semiconductor, holes will oxidize H_2O . The counter electrode in Figure 2 is assumed to be of high surface area and, under illumination, to fix the equilibrium potentials of the two electrodes at E_{H^+/H_2} .

The positions of the redox levels relative to the bands are ideal in Figure 2. It is shown that the band gap, ΔE_g , must be at least 1.23 eV. However, the band bending required for electron-hole separation (ΔE_{EB}) and the overpotential for O_2 evolution (ΔE_{OVER}) must also be considered. In reality, then (4),

$$\Delta E_g \approx 1.23 \text{ eV} + \Delta E_{EB} + \Delta E_{OVER} \quad (1)$$

The actual requirements of ΔE_g in this single-photoelectrode configuration is debatable. In our opinion, there are insufficient experimental data to warrant a projected lower limit to ΔE_g for semiconducting electrodes used in the photoelectrolysis of H_2O . However, band gaps larger than ideal for solar energy power conversion (~1.5 eV) may be unavoidable.

Several alternative configurations to that shown in Figure 1A are possible. Figure 1B shows a single photoelectrode cell operating in series with an external power supply. Operation of this cell would constitute the photoassisted electrolysis of H_2O . The efficiency compared to a spontaneously operating cell would be decreased by the energy supplied by the external source. However, acceptance of this configuration can extend the range of possible materials for photoelectrodes, as the energetic positions of the bands with respect to the redox levels become less restrictive. In practice, the use of lower band gap materials may become possible, offsetting through more efficient solar collection some of the losses due to the power supply.

Figure 1C illustrates a cell in which both electrodes are photoactive. In this configuration, E_v on the n-side must lie deeper than $E(O_2/H_2O)$,

while E_c on the p-side must be higher than $E(H^+/H_2)$. Ideal energetics for such a p-n cell are illustrated in Figure 3. Clearly, it is possible to obtain non-assisted photoelectrolysis with electrodes having optimal band gaps for solar conversion.

III MATERIALS CONSIDERATIONS

In designing electrode materials for photoelectrolysis, it is evident from Figure 2 that we must consider the band gap and electron affinity of the semiconductor. Of equal importance, however, is stability under operating conditions. For the n-type semiconductor shown in Figure 2, the decomposition potential must be positive of the O_2/H_2O potential. Alternatively, decomposition may be very slow compared to electron transfer.

In general, the best materials for n-type oxygen photoanodes are fully oxidized compounds. These at least will not be susceptible to formation of higher oxides under conditions of O_2 evolution. However, anodic dissolution reactions can occur. At pH = 0, the most negative standard decomposition (E_p°) for TiO_2 is +1.18V, while $E^\circ(O_2/H_2O)$ is +0.99V vs. SCE. The separation becomes greater as the pH is increased (5). Thus, TiO_2 shows stability as an O_2 -evolving photoanode over a wide pH region. ZnO , on the other hand, is oxidized to Zn^{+2} and O_2 at +0.65V, and undergoes some even more negative decomposition reactions with OH^- . ZnO has been shown to decompose anodically under illumination, rather than act passively in an electron transfer reaction from H_2O (6). Similar arguments can be made for reductive decomposition reactions which may occur on p-type photocathodes.

Another concern of stability involves the doping of the semiconductor electrode. Oxide semiconductors doped by virtue of oxygen deficiency (e.g., TiO_{2-x}) may not retain their doping under conditions of O_2 evolution. Wold and co-workers (7) have reported the stabilization of WO_{3-x} by adding F^- for vacancy compensation. It is also possible, of course, to dope semiconductors in other ways, e.g., by incorporating donors as acceptors in stoichiometric compounds, or by the use of mixed oxides.

IV. THE DESIGN OF PHOTOELECTRODES

It is clear that the materials chosen for H_2O photoelectrolysis need not be selected from among commonly researched semiconductors. For a single n-type photoanode (Configuration 1A or 1B), we require a material of low electron affinity. For a semiconductor MX, the electron affinity is roughly manipulated by the more electropositive element, M, while the electrons in the valence band tend to be associated with the more electronegative component. Butler and Ginley (8) have used electronegativities to predict the properties of various metal titanates, but the principles can be applied to any semiconductor. For example, we may write

$$EA = \bar{\chi}_{SC} - (\Delta E_G/2) \quad (2)$$

where $\bar{\chi}_{SC}$ is the geometric mean of the electronegativities of the constituent elements (9). The individual electronegativities are given by

Mulliken (10) as $(IP + EA)/2$, and are about 2.8 times the Pauling electronegativities (11).

Using this model, let us compare SnO_2 with $SrTiO_3$. For SnO_2 , $\Delta E_G = 3.5$ eV, $\chi(Sn) = 4.8$ eV and $\chi(O) = 7.55$ eV. Hence,

$$EA(SnO_2) = \left[(4.8)(7.55)^2 \right]^{1/3} - 3.5/2 = 4.7 \text{ eV}$$

Similarly, for $SrTiO_3$, $\Delta E_G = 3.2$ eV, $\chi(Sr) \approx 2.7$ eV, $\chi(Ti) \approx 3.7$ eV, so that

$$EA(SrTiO_3) = \left[(2.7)(3.7)(7.55)^3 \right]^{1/5} - 3.2/2 = 3.7 \text{ eV}$$

The results agree remarkably well with the experimental value for SnO_2 (12) and qualitatively with the large difference in flat band potentials between the two compounds (13). Since the energy of the NHE is ≈ 4.5 eV, the model also predicts the observed contrast of these two materials for photoelectrolysis of H_2O . $SrTiO_3$ will decompose H_2O spontaneously in the single photoelectrode configuration (14), while SnO_2 , because of its positive flat band potential, always requires an external bias (15). In designing an n-type oxide photoelectrode, then, it is important to have metals with low electronegativities, and to have fully oxidized compounds preferably with O:M ratios of ≤ 1.5 . This will ensure a small χ_{SC} term, and hence a low EA.

For the p-n configuration, the EA on the n-side can be about 5 eV, and the band gap should be ≈ 1.5 eV. This tends overall to allow for the use of higher electronegativity metals in forming metal oxides. The p-electrode should have an EA ≤ 4.5 eV, and $E_g \approx 1.5$ eV. We need not use oxides, although there is a danger of auto-decomposition for materials whose anodic E_p° values are too negative (5). Of course, the p-materials must also exhibit good cathodic stability.

Our general approach involves the recognition that a very large number of semiconductors can be synthesized with control of the band gaps and of the electron affinity. For example, it should be possible to attain a variety of band gaps through the synthesis of mixed valence oxides, or by making solid solutions of large and small band gap semiconductors of similar crystal structures (16). As a guide, we will employ theoretical considerations (e.g., equation (2)) to predict electron affinities, and use free energies of formation to predict E_p° .

V. ELECTROCHEMICAL EVALUATION OF PHOTOELECTRODES

Electrodes will be constructed using materials synthesized according to the considerations of the previous section. Polycrystalline electrodes will be used in most cases, in order to expedite the evaluation of a large number of substances. These will be constructed either by hot-pressing (17) or, where appropriate, by chemical vapor deposition (18).

Evaluation of electrodes will involve half-cell studies of photocurrent quantum yield (ϕ) vs. electrode polarization and of the fraction of the photocurrent going into the appropriate gas-forming reaction. The ideal current-voltage behavior for an n-type electrode is shown in Figure 4. Here

it is seen that overlap of O_2 evolution potential regions on the photoelectrode and H_2 evolution potential regions on the counter electrode is the major criterion for spontaneity. Of course, this overlap will be enhanced by the use of a high surface area counter electrode. Similarly, p and n photoelectrodes can be compared which show high overlap of their respective photocurrent-potential curves. As can be seen from Figure 4, maximum full cell photocurrents can be predicted from these half-cell studies, as can the ultimate quantum yield for their operation.

REFERENCES

1. Gerischer, H., "Semiconductor Electrochemistry" in Physical Chemistry, Vol. 9A, p. 463 (ed. by H. Eyring, D. Henderson, W. Jost), Academic Press, New York, 1970.
2. Fujishima, A. and Honda, K., "Electrochemical Photolysis of Water at a Semiconductor Electrode," Nature **238**, 37 (1972).
3. Nozik, A. J., "Energetics of Photoelectrolysis" in Semiconductor Liquid-Junction Solar Cells, p. 272 (ed. by A. Heller), The Electrochemical Society, Inc., Princeton, 1977.
4. Butler, M. A., "Photoelectrolysis and Physical Properties of the Semiconducting Electrode WO_3 ," J. Appl. Phys. **48**(5), 1914 (1977).
5. Bard, A. J. and Wrighton, M. S., "Thermodynamic Potential for the Anodic Dissolution of n-Type Semiconductors," Ref. 3, p. 195.
6. Pettinger, B., Schoppel, H. R., Yokoyama, T. and Gerischer, H., "Tunnelling Processes at Highly Doped ZnO -Electrodes in Aqueous Electrolytes. Part II," Ber. Bunsenges. Phys. Chem. **78**(10), 1024 (1974).
7. Derrington, C. E., Castro, C. A., Godek, W., Sanchez, R. L. and Wold, A., "Tungsten Oxy-fluoride Photoanodes," Ref. 3, p. 254.
8. Butler, M. A. and Ginley, D. S., "Correlation of Photosensitive Electrode Properties with Electronegativity," Chem. Phys. Letters **47**(2), 319 (1977).
9. Sanderson, R. T., Chemical Periodicity, Reinhold, New York, 1960.
10. Mulliken, R. S., J. Chem. Phys. **2**, 782 (1934); **3**, 537 (1935).
11. Douglas, B. E. and McDaniel, D. H., Concepts and Models of Inorganic Chemistry, p. 84ff, Blaisdell Publishing Co., Waltham, Mass., 1965.
12. Feucht, D. L., "Heterojunctions in Photovoltaic Devices," J. Vac. Sci. Technol. **14**(1), 57 (1977).
13. Schwerzel, R. E., Brooman, E. W., Craig, R. A. and Wood, V. E., "Optimal Electrode Properties and the Selection of Stabilizing Electrolytes," Ref. 3, p. 293.
14. Wrighton, M. S., Ellis, A. B., Wolczanski, P. T., Morse, D. L., Abrahamson, H. G. and Ginley, D. S., "Strontium Titanate Photoelectrodes. Efficient Photoassisted Electrolysis of Water at Zero Applied Potential," J. Am. Chem. Soc. **98**, 2774 (1976).
15. Wrighton, M. S., Morse, D. L., Ellis, A. B., Ginley, D. S. and Abrahamson, H. B., "Photo-assisted Electrolysis of Water by Ultraviolet Irradiation of Antimony Doped Stannous Oxide Electrode," J. Am. Chem. Soc. **98**, 44 (1976).
16. Hill, R., "Energy Gap Variations in Semiconductor Alloys," J. Phys. C: Solid State Phys. **7**, 521 (1974).
17. Miller, B., Heller, A., Robbins, M., Menezes, S., Chang, K. C. and Thomson, J., "Solar Conversion Efficiency of Pressure Sintered Cadmium Selenide Liquid Junction Cells," J. Electrochem. Soc. **124**, 1019 (1977).
18. Hardee, K. L. and Bard, A. J., "Semiconductor Electrode. I. The Chemical Vapor Deposition and Application of Polycrystalline n-Type Titanium Dioxide Electrodes to the Photosensitized Electrolysis of Water," J. Electrochem. Soc. **122**, 739 (1975).

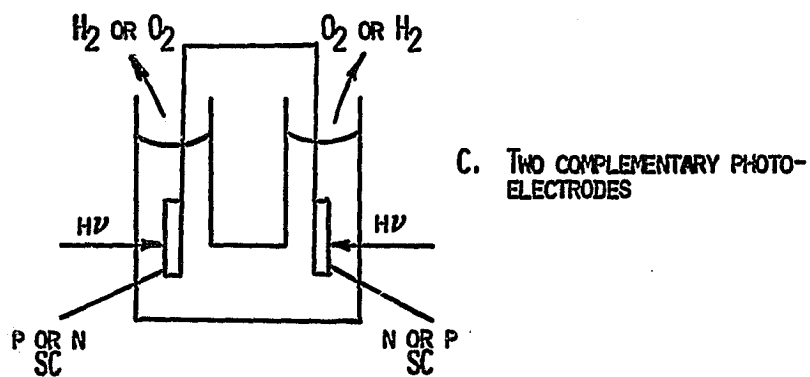
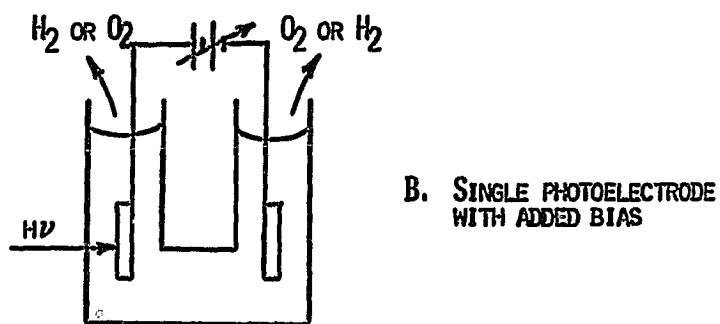
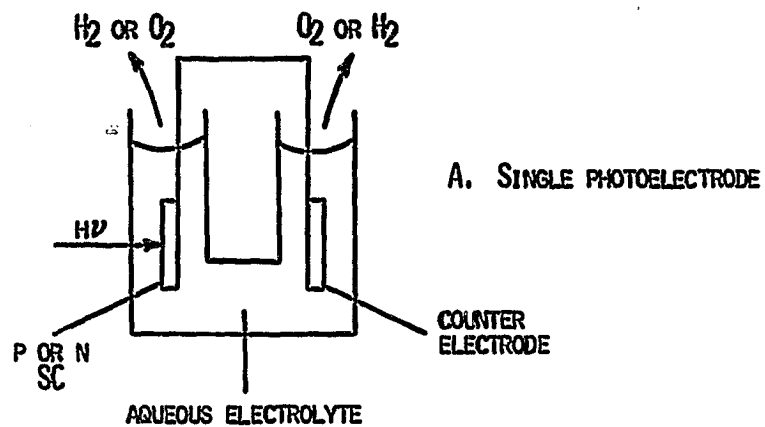


Fig. 1. Cell configurations for water photoelectrolysis.

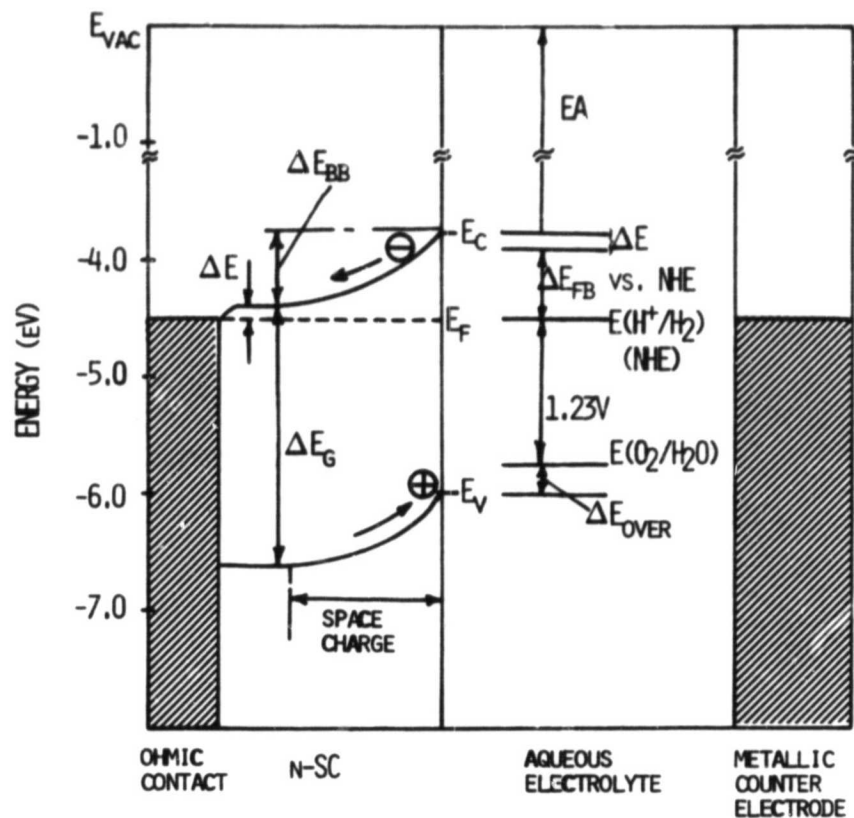


Fig. 2. Energetics of the semiconductor electrolyte and counter electrode-electrolyte interfaces in a photoelectrochemical cell. The cell can operate spontaneously under closed circuit conditions (no external bias).

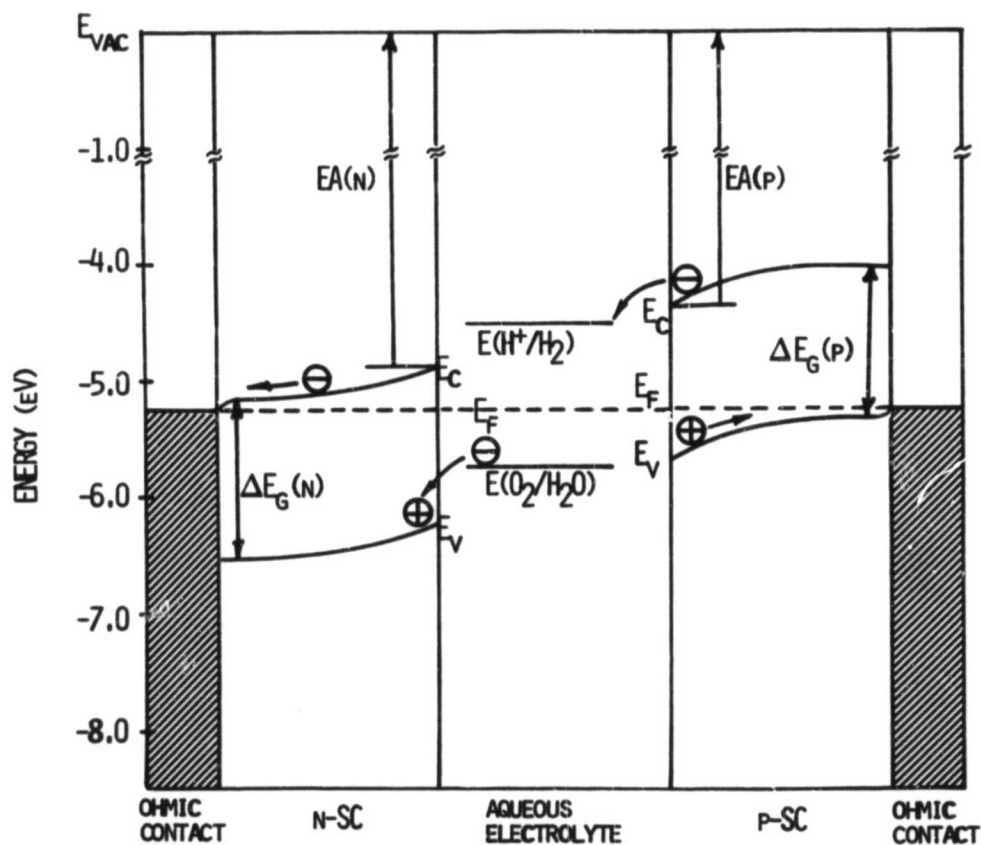


Fig. 3. Energetics of a p,n photoelectrochemical cell, operating spontaneously under short circuit conditions.

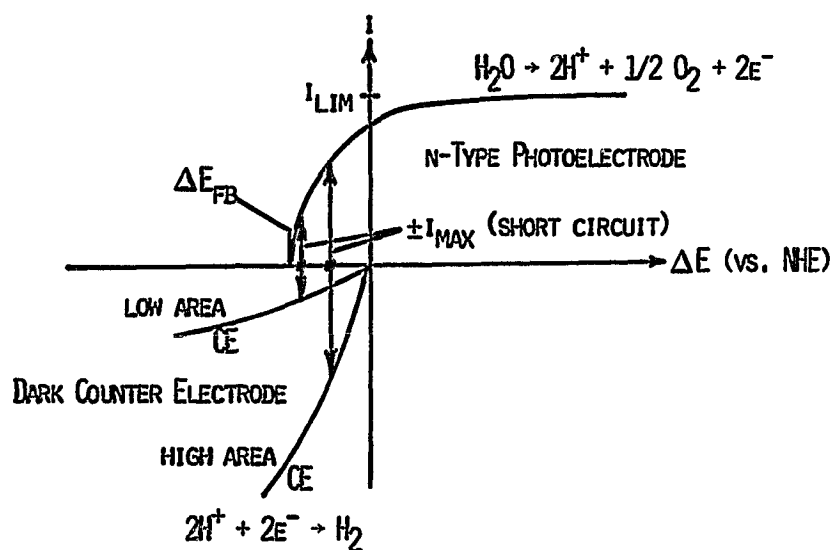


Fig. 4: Ideal current voltage curves for half cells comprising a spontaneously operating photoelectrochemical cell, utilizing one n-type photoelectrode and an inert counter electrode. The limiting photocurrent is a function of light intensity. Note that ΔE_{fb} corresponds to the onset of photocurrent, and is well negative of the H^+/H_2 (NHE) equilibrium potential.

DEVELOPMENT OF A PRACTICAL PHOTOCHEMICAL ENERGY STORAGE SYSTEM

Charles Kutal, Richard R. Hautala
and R. Bruce King
Department of Chemistry
University of Georgia
Athens, Georgia 30602

Abstract

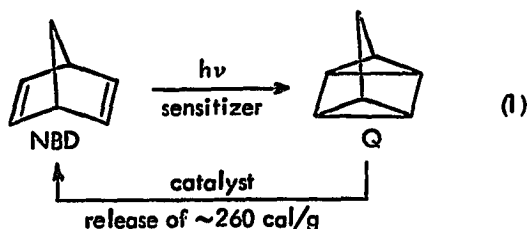
A solar energy storage system based upon the interconversion of norbornadiene and quadricyclene possesses several attractive features, including high specific energy storage capacity, kinetic stability of the energy rich photoproduct in the absence of suitable catalysts, and relatively inexpensive reactants. Two steps are required in this cyclical system: (1) Energy storage through the sensitized photolysis of norbornadiene to quadricyclene in an endothermic reaction; (2) Energy release through the catalyzed reconversion of quadricyclene to norbornadiene in an exothermic reaction. Introduction of the sensitizer and catalyst onto separate polymeric supports facilitates the construction of an actual device in which the energy storage and energy release steps are sequentially coupled. An energy storage system based on these principles could result in the practical use of solar energy for heating buildings and related applications.

I. INTRODUCTION

The use of sunlight induced photochemical reactions to generate storable products of high energy content which are reconvertible at will to the original material offers an attractive approach to the long term storage of solar energy. The net effect of cycling the energy storage-energy release steps is to convert sunlight to a more controllable, and thus usable form without consuming any nonrenewable resources. Ideally the recyclable storage medium should possess the following characteristics:

- (i) significant absorption of incident solar radiation
- (ii) high quantum efficiency of the photochemical energy storage step
- (iii) high specific energy storage capacity (heat stored per gram of photoproduct formed)
- (iv) absence of destructive side reactions
- (v) ease of handling (can be readily cycled in a storage device)
- (vi) synthesis from readily available and inexpensive starting materials

Because of these stringent requirements the number of currently known photochemical reactions which possess any promise for use in a cyclical energy storage system is understandably small. Among the most attractive candidates is the norbornadiene (NBD)-quadricyclene (Q) interconversion (Reaction 1). Both compounds are liquids with boiling



points and densities similar to water. Although NBD itself does not absorb light in the wavelength region of available solar radiation (>300 nm), the photoreaction does occur in the presence of an appropriate spectral sensitizer with an overall efficiency of Q production approaching 100% in optimal cases (1). The photoproduct, while containing some 260 cal/g (1.1×10^6 joule/kg) excess energy over NBD, is stable toward thermal reversal because of orbital symmetry constraints. Exposure to certain transition metal catalysts, however, allows for the clean and rapid conversion of Q to NBD with the release of the excess energy (2). NBD is an attractive storage medium from a cost standpoint, since it is prepared from commonly available chemicals (acetylene and cyclopentadiene).

The characteristics of a NBD-Q based energy storage system recommend its use as a source of low-grade ($\sim 100^\circ\text{C}$) heat. Some readily apparent applications along this line are the heating, cooling, and hot water production in buildings. Roughly 20% of all energy (primarily from fossil fuels) currently consumed in the United States is used for these purposes.

The Solar Energy Storage Program at the University of Georgia has been directed toward the evaluation and development of this promising system. Several related research areas have been under investigation:

A. Sensitizer Development

At the outset of the project, there was limited information available on the sensitized conversion of NBD to Q. The sensitizers that had been reported were generally weak absorbers of solar radiation, inefficient, or prone to de-

composition. Thus our efforts have concentrated on (i) surveying a wide variety of potential organic and inorganic candidates and (ii) studying the mechanism of sensitization in order to intelligently design new candidates offering improved characteristics.

B. Catalyst Development

While several catalysts for the reverse reaction are known, it would be advantageous to have ones which are relatively inexpensive and which would offer a range of catalytic activity in order to select the optimal rate for the reversion at ambient temperature. We have therefore been searching for new structures of high catalytic activity, high product specificity, and low cost.

C. Polymeric Anchoring of Sensitizers and Catalysts

The need to physically constrain the catalyst for the heat-releasing reaction to the catalytic chamber is obvious. Similar confinement of the photosensitizer to the irradiation chamber reduces the required amount of this component. Polymer immobilization also precludes undesirable interactions between the catalyst and sensitizer, and facilitates their replacement in an actual device.

D. Recycling Studies

The requirement that the NBD-Q energy storage system can be repeatedly cycled without degradation of the key components (sensitizer, catalyst, storage medium) is quite stringent. For this reason the ability of the system to be recycled is being examined using a small scale laboratory apparatus.

Our initial efforts in each of these areas have been described previously (3). In the present article we focus upon our most recent results as well as our future plans.

II. SENSITIZER DEVELOPMENT

a. Organic Sensitizers

Our recent activities in this area have been directed toward (i) evaluation of the sensitization performance of various graft copolymers of polystyrene relative to the homogeneous monomeric counterparts, (ii) evaluation of the performance of polymeric sensitizers related to the type of polystyrene and to the method and extent of chemical functionalization, (iii) durability and performance of the polymeric sensitizers which are subjected to repeated cycling, (iv) synthesis and evaluation of potential sensitizers with improved solar absorption characteristics, and (v) evaluation of glass beads as an improved matrix for immobilizing photosensitizers.

A variety of organic sensitizers have been studied in both monomeric and polymeric forms (3). For certain sensitizers, the polymeric forms have been found to be decidedly inferior. Most notable among these are the polymeric counterparts of benzophenone and acetophenone. The poor performance of these polymers has been tentatively ascribed to competitive hydrogen abstraction (from the polymer backbone). For other polymeric sensitizers, however, efficient sensitization, equalling or exceeding that of the monomeric counterpart, has been achieved. Most attention has been directed at the graft copolymer of N, N-dimethylaminobenzophenone and polystyrene. For this polymer (Polymer N) we have examined the effects of cross-linking, extent of functionalization, solvents, polymer pore size, and dependence on norbornadiene concentration. High quantum efficiencies have been observed for polymer N over a wide range of experimental variables.

We have observed a gradual deterioration of Polymer N in our recycling experiments. At present we do not have sufficient information to speculate on the nature of the decomposition.

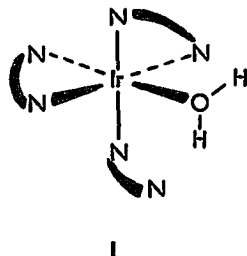
Our recent investigation involving the discovery of new classes of photosensitizers has been concentrated on thiocarbonyl derivatives. Very inefficient sensitization has been observed for thiobenzophenone and di-*t*-butyl thio ketone. We are currently involved in the syntheses of a series of thio esters, the most promising candidate of which is O-ethyl-1-thionaphthoate (4).

We have recently begun preliminary experiments involving the functionalization of glass surfaces as a means of immobilizing our sensitizers. The principal reasons for exploring this approach involve an expected decrease in reflected light for the glass surfaces (in contrast to polymeric surfaces) and a higher degree of stability of the sensitizer.

b. Inorganic Sensitizers

We recently reported the first detailed studies of the transition metal sensitized conversion of norbornadiene to quadricyclene (5-7). Thus simple CuX salts (X is Cl, Br, I, or C₂H₅O₂) and phosphine containing compounds such as Cu[P(C₆H₅)₃]₂BH₄ and Cu[P(C₆H₅)₂CH₃]₃BH₄ were found to be quite effective sensitizers when excited with 313 nm radiation. The lack of absorption of longer wavelength light, however, severely limits the usefulness of these compounds in a practical energy storage system. For this reason, our recent strategy in designing Cu(I) sensitizers has centered upon the incorporation of a strongly absorbing chromophore into the sensitizer molecule. Tetrameric [CuXPR₃]₄ clusters, for example, are cleaved by heterocyclic nitrogen bases to form colored complexes of the type CuXPR₃(N-N) (typically X is Cl, Br, I, R is an alkyl or aryl group; N-N is 1,10-phenanthroline or 2,2'-bipyridine). By employing bulky R substituents (e.g. *n*-butyl), it should be possible to labilize PR₃ toward substitution by other ligands present in solution while retaining the Cu(N-N) chromophore. This raises the possibility of producing an (N-N)XCu-NBD complex which is strongly absorbing in the visible wavelength region. Absorption of a photon by this complex may then result in the conversion of norbornadiene to quadricyclene, in analogy to the situation which obtains for simple CuX sensitizers (6).

We have recently discovered that certain transition metal compounds containing ligands with delocalized π systems can function as very effective sensitizers. In particular, [Ir(bipy)₂(OH₂)(bipy')]³⁺ (Structure I), whose



absorption spectrum appreciably overlaps the wavelength region of available solar radiation, sensitizes the conversion of NBD to Q with a quantum efficiency of ~0.7 (70%) when irradiating with 366 nm light. Another attractive feature of this compound (or any charged sensitizer) is the ease with which it can be immobilized onto a polymeric support. We have recently prepared a sulfonated resin using macroreticular (20% crosslinked) styrene-divinylbenzene copolymer beads. Immobilization is accomplished by

equilibrating a solution of [Ir(bipy)₂(OH₂)(bipy')]³⁺ with the resin. Quantitative studies concerning the effects of various parameters (such as NBD concentration, percent loading of the sensitizer on the polymer, polymer porosity, etc) on the quantum efficiency of the polymer bound sensitizer are underway.

III. CATALYST DEVELOPMENT

At the present time the following five major types of catalysts for the conversion of quadricyclene to norbornadiene are known: (i) rhodium(I) complexes (8); (ii) palladium(II) complexes (8, 9); (iii) metalloporphyrins of iron(II), cobalt(II), and nickel(II) (10); (iv) triphenylcyclopropenyl-nickel complexes (11); (v) molybdenum dithiolates such as [(CF₃)₂C₂S₂]₃Mo (11). Recently the latter two types of catalysts, which were discovered during an earlier phase of this research program, have been studied in some detail. In connection with the chemistry of triphenylcyclopropenyl-nickel complexes a variety of new compounds of the stoichiometries (C₆H₅)₃C₃NiL₂Cl and (C₆H₅)₃C₃NiLCl have been prepared and their catalytic activities examined for the conversion of quadricyclene to norbornadiene. The most active catalysts appear to be the previously reported (12) carbonyl halides [(C₆H₅)₃C₃Ni(CO)X]₂ (X = Cl and Br). Substitution of the carbonyl groups by trivalent phosphorus ligands appears to reduce or eliminate their catalytic activity. In the near future we plan to investigate by means of phosphorus-31 n.m.r. spectroscopy the reactions of [(C₆H₅)₃C₃Ni(CO)Cl]₂ with various trivalent phosphorus ligands in an attempt to characterize better the resulting complexes and understand the reasons for their reduced catalytic activity.

The trigonal prismatic molybdenum compound [(CF₃)₂C₂S₂]₃Mo (13) is highly active as a catalyst for the conversion of quadricyclene to norbornadiene provided non-coordinating solvents such as benzene or dichloromethane are used. However, the catalytic activity is lost if coordinating solvents such as methanol or pyridine are employed. Studies of the electronic spectra of the resulting solutions indicate that reduction of [(CF₃)₂C₂S₂]₃Mo to the corresponding monoanion occurs in these latter solvents. A pure sample of the tetraphenylarsonium salt [(C₆H₅)₄As][[(CF₃)₂C₂S₂]₃Mo] of this monoanion (14) was shown to be catalytically inactive in benzene solution.

In connection with the development of new catalysts for the conversion of quadricyclene to norbornadiene we plan to investigate new types of coordinately unsaturated metal complexes. A particularly interesting recently reported possibility is the five-coordinate molybdenum(0) complex (diphos)₂MoCO (diphos = (C₆H₅)₂PCH₂CH₂P(C₆H₅)₂).

In a recyclable solar energy storage system it is necessary to have the catalysts immobilized onto polymers. We have developed polystyrene-anchored cobalt(II) tetraarylporphyrin complexes which show considerable activity for the conversion of quadricyclene to norbornadiene (15). Such polymer-anchored catalysts undergo a slow loss of activity upon repeated recycling in open systems. However, such deactivated catalysts can be regenerated with reducing agents such as titanium(III) suggesting that this difficulty is due to traces of oxygen. An actual solar energy storage device would be closed and therefore after the polystyrene-anchored cobalt(II) catalyst removed the reactive oxygen from the solution with some loss of the initial activity further deactivation would not be likely to be serious. Furthermore, these polystyrene-anchored cobalt(II) catalysts have such a high activity that considerable loss of activity could occur before the activity became too small for the catalyst to be useful.

We are now interested in exploring possible modifica-

tions of the cobalt tetraarylporphyrin catalyst to reduce the susceptibility towards this troublesome deactivation through oxidation. The first thing that we plan to try is the synthesis of polystyrene-anchored cobalt(II) phthalocyanine catalysts in order to compare the susceptibility of the phthalocyanine and tetraarylporphyrin systems towards loss of activity through oxidation. After we have fundamental information on the catalytic activity of the polystyrene-anchored cobalt(II) phthalocyanines as well as the polystyrene-anchored cobalt(II) tetraarylporphyrins discussed above, we can then decide which of the two types of systems are most suitable for further development.

IV. RECYCLING STUDIES

Sensitizer and catalyst candidates which appear to function cleanly and efficiently on the basis of single runs may prove to be unsatisfactory upon numerous repetitions of the energy storage-energy release steps. For this reason it is of prime importance to test the long term stability of the chemical components of the system. Toward this end we have constructed the small scale recycling apparatus pictured in Figure 1. The unit operates in alternating modes as follows:

Energy Storage

NBD in the storage vessel is circulated by means of a pump (foreground, middle) to the photoreactor which consists of a circular tube containing a polymer immobilized sensitizer. Light from a bank of lamps is absorbed by the sensitizer, which subsequently interacts with NBD and converts it to Q. The newly formed Q is then returned to the storage vessel.

Energy Release

By switching a valve, Q can be routed from the storage vessel to the reversion reactor which contains a stainless steel U-tube filled with a polymer immobilized catalyst. Upon exposure to the catalyst, Q is rapidly reconverted to NBD with the release of heat. (Since the U-tube is immersed in water, the amount of heat released is readily determined by measuring the rise in temperature of the water.) NBD is then returned to the storage vessel where it can be routed through another energy storage step.

The long-term performance of promising sensitizer and catalyst candidates is currently being tested in this apparatus. The information obtained from these studies should be valuable in suggesting improvements in the design and functioning of the energy storage system.

REFERENCES

- (1) Murov, S. and Hammond, G. S., "Mechanisms of Photochemical Reactions in Solution. LVI. A Singlet Sensitized Reaction", *J. Phys. Chem.*, Vol. 72, No. 11, pp. 3797-3801, 1968.
- (2) Bishop, K. C., "Transition Metal Catalyzed Rearrangements of Small Ring Organic Molecules", *Chem. Revs.*, Vol. 76, No. 4, pp. 461-486, 1976.
- (3) Hautala, R. R., Little, J., and Sweet, E., "The Use of Functionalized Polymers as Photosensitizers in an Energy Storage Reaction", *Solar Energy*, Vol. 19, No. 5, pp. 503-508, 1977.
- (4) Gisin, M. and Wirz, J., "An Efficient Photosensitizer: O-Ethyl-1-Thionaphthoate", *Helv. Chim. Acta*, Vol. 58, p. 1768, 1975.
- (5) Schwendiman, D. P. and Kutal, C., "Transition Metal Photoassisted Valence Isomerization of Norbornadiene. An Attractive Energy-Storage Reaction", *Inorg. Chem.*, Vol. 16, No. 3, pp. 719-721, 1977.
- (6) Schwendiman, D. P. and Kutal, C., "Catalytic Role of Copper(I) in the Photoassisted Valence Isomerization of Norbornadiene", *J. Amer. Chem. Soc.*, Vol. 99, No. 17, pp. 5677-5682, 1977.
- (7) Grutsch, P. A. and Kutal, C., "Use of Copper(II) Phosphine Compounds to Photosensitize the Valence Isomerization of Norbornadiene", *J. Amer. Chem. Soc.*, Vol. 99, No. 19, pp. 6460-6463, 1977.
- (8) Hogeveen, H. and Volger, H. C., "Valence Isomerization of Quadricyclene to Norbornadiene Catalyzed by Transition Metal Complexes", *J. Amer. Chem. Soc.*, Vol. 89, No. 10, pp. 2486-2487, 1967.
- (9) Gassman, P. G. and Patton, D. S., "The Acid-Catalyzed Rearrangement of Quadricyclanone and Quadricyclanone Dimethyl Ketal. Product Dependency on Carbon Protonation vs. Oxygen Protonation", *J. Amer. Chem. Soc.*, Vol. 90, No. 26, pp. 7276-7282, 1968.
- (10) Manassen, J., "Catalysis of a Symmetry Restricted Reaction by Transition Metal Complexes. The Importance of the Ligand", *J. Catalysis*, Vol. 18, pp. 38-45, 1970.
- (11) Quarterly report SRO-893-10 for ERDA Contract E(38-1)-893, June 15, 1977.
- (12) Gowling, E. W. and Kettle, S. F., "A π -Cyclopropenyl Derivative of Nickel Carbonyl", *Inorg. Chem.*, Vol. 3, No. 4, pp. 604-605, 1964.
- (13) King, R. B., "Organosulfur Derivatives of the Metal Carbonyls. III. The Reaction Between Molybdenum Hexacarbonyl and Bis-(trifluoromethyl)-dithietene", *Inorg. Chem.*, Vol. 2, No. 3, pp. 641-642, 1963.
- (14) Davison, A., Edelstein, N., Holm, R. H., and Maki, A. H., "Synthetic and Electron Spin Resonance Studies of Six-Coordinate Complexes Related by Electron Transfer Reactions", *J. Amer. Chem. Soc.*, Vol. 86, No. 14, pp. 2799-2805, 1964.
- (15) King, R. B., Sweet, E. M., and Hanes, R. M., "Attached Metal Complex Catalysts for a Solar Energy Storage System", Preprints *Div. Petrol. Chem.*, Vol. 22, p. 1201, 1977.

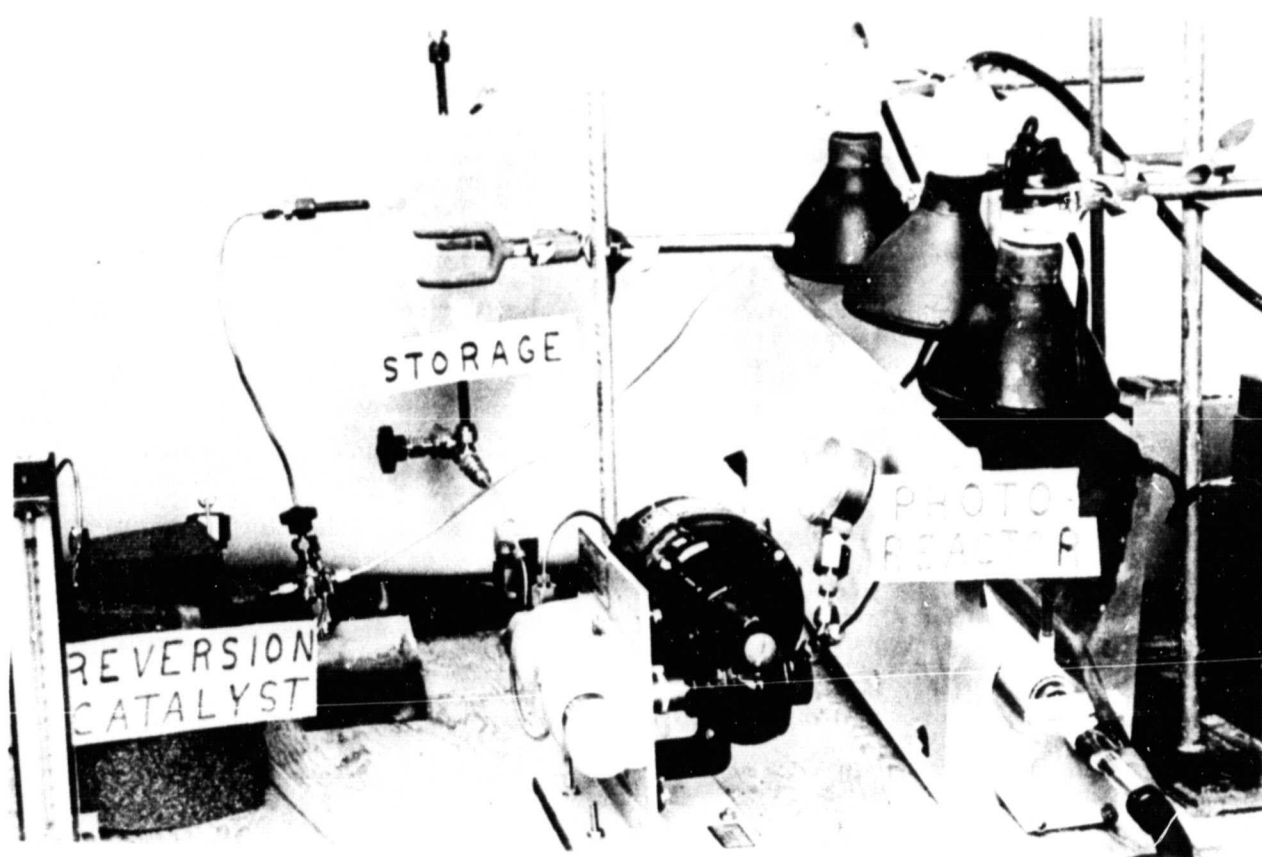


Fig. 1. Recycling apparatus to test the NBD-Q energy storage system

SESSION III
TRANSPORT AND CONTAINMENT MATERIALS

NASA EXPERIENCE WITH GASEOUS HYDROGEN

R. Hagler, Jr.
Jet Propulsion Laboratory

**STUDY OF THE BEHAVIOR OF GAS DISTRIBUTION EQUIPMENT IN
HYDROGEN SERVICE: UPDATE -- 1977**

J. S. Pangborn, D. G. Johnson, and W. J. Jasionowski
Institute of Gas Technology

HYDROGEN-METAL INTERACTIONS

H. G. Nelson
NASA-Ames Research Center

**HYDROGEN COMPATIBILITY OF STRUCTURAL MATERIALS FOR
ENERGY STORAGE AND TRANSMISSION APPLICATIONS**

S. L. Robinson
Sandia Laboratories

EFFECT OF STRESS STATE ON HYDROGEN EMBRITTLEMENT PROCESSES

M. R. Louthan, Jr., and R. P. McNitt
Virginia Polytechnic Institute

**EVALUATION OF LASER WELDING TECHNIQUES FOR HYDROGEN
TRANSMISSION**

J. A. Harris, Jr., and J. Mucci
Pratt & Whitney Aircraft Group

BLANK PAGE

NASA EXPERIENCE WITH GASEOUS HYDROGEN

Ray Hagler, Jr.

Jet Propulsion Laboratory
California Institute of Technology
Pasadena, California

ABSTRACT

A survey of NASA agencies and private companies who have had experience with gaseous hydrogen facilities was conducted by JPL during FY'77. This report identifies facility capability and attempts to assess the current status of the equipment. The majority of the hydrogen experience was found to cluster within the agencies and companies who have been active in the LH₂/LOX Rocket Engine Programs (Apollo, Centaur, and Space Shuttle).

I. Introduction

The Interagency Agreement between ERDA and NASA (EG-77-A-31-1035) requires NASA to document related technologies and identify existing facilities that have been utilized during recent NASA programs for the transmission and distribution of gaseous hydrogen (GH₂). A plan for the accomplishment of this data-gathering process was devised and executed as follows:

1. A list (Table 1) of NASA agencies and private companies who have had experience with gaseous hydrogen facilities was established. Most of the expertise was determined to be clustered within the LH₂/LOX Rocket Engine Programs (Apollo, Centaur, and Space Shuttle) wherein GH₂ was used for propellant (LH₂) tank pressurization, manifold purging, and component testing.
2. A telephone contact was made with a knowledgeable individual (Table 1) at each location. A letter stating NASA goals and indicating the desired information was sent to each individual.
3. When appropriate and possible, a personal visit to each location (Table 1) was arranged to personally review collected data and inspect existing facilities.

The data-gathering process took place during April, May, and June of 1977.

II. Summary

NASA agencies and their predecessors have had a long association with hydrogen. The unique properties of this lightest element have been exploited in a wide spectrum of uses which range from buoyancy for airships to fuel for the large booster rockets which launched the Apollo spacecraft. During these many programs, NASA has conclusively demonstrated that gaseous hydrogen (GH₂) can be safely contained and stored at pressures as high as 15,000 psig and safely transported by pipelines (manifolds) from the storage sites to the areas where required for use. Whereas most of the GH₂ manifolds are considerably shorter and smaller than conventional, natural gas pipeline lengths and diameters, the results from the NASA GH₂ experience should be directly applicable to any storage and distribution network. With the exception of conventional "K" bottles and "tube" tanks, most of the GH₂ storage and transmission systems are pressurized to maximum operating pressures only during usage periods which, generally, represent a small fraction of the total time that these systems have been in existence. During standby periods between operations, the systems are usually maintained with pad pressures of only a few atmospheres. Control components for GH₂ systems with operating pressures less than 5000 psig are readily available but components for higher pressure systems must be selected with care to ensure satisfactory performance.

III. Discussion

Pressure Vessels (Tanks)

A laminated-wall pressure vessel using a liner or inner section of compatible, austenitic stainless steel (CRES) or mild steel (A.O. Smith Type 1146a) can be considered the standard for the storage of larger quantities of GH₂ at high pressures. The A.O. Smith laminated tank design using Type 1146a steel for the inner lamina is in general usage by NASA and private companies at GH₂ pressures below 5000 psig. One bank of six of the 15,000 psig-rated, A.O. Smith design tanks is in derated service at NASA-MSFC for GH₂ pressures as high as 10,000 psig. Another group of five of these A.O. Smith design tanks was built with 304L CRES liners by Chicago Bridge and Iron Co. for Pratt and Whitney and are used at GH₂ pressure as high as 10,000 psig. Rocketdyne has many laminated, low-carbon steel tanks in service at pressures which range from 2000 to 5000 psig, and, in addition, has installed 316L CRES liners inside 4-foot diameter, 10,000 psig-rated, laminated tanks to upgrade GH₂ storage capability to 15,000 psig for their test facility at Santa Susanna. Operating pressure in these larger tanks is maintained only when needed for testing of rocket engines and control components. Whereas the tanks are repeatedly pressurized to the operating pressure, the total time that this pressure is maintained is only a small portion of installed lifetime.

Smaller quantities of GH₂ are conventionally stored in banks of "K" bottles and "tube" tanks at pressures as high as 6000 psig. These tanks utilize seamless construction techniques and are made from mild steel; usually Type 4130. The operating pressures are maintained for lengthy periods of time and the tanks are periodically refilled. The levels at which these seamless tanks are stressed during operation are well below the yield strength of Type 4130 steel and appear sufficiently low to preclude problems from interaction with the high pressure GH₂ that they contain.

One group of ten "tube" tanks (18 inches OD) was built by U.S. Steel for use at the National Space Technology Laboratory in Bay St. Louis, Mississippi for an operating pressure of 10,000 psig. At this time, the tanks have been tested and used with helium but have not been used with GH₂.

Manifolds

NASA routinely uses austenitic stainless steels (CRES) for distribution manifolds at pressure levels below 10,000 psig, and mild steel (A106B;T1) at pressures below 5000 psig. The longest manifolds are only several thousand feet in length. Highest pressure (15,000 psig) manifolds are made from Type 21-6-9 CRES. Low-carbon content CRES (304L, 316L) is used when manifolds are joined by welding. Post-weld heat-treatment of the welds in mild steel manifolds is desirable to eliminate weld-induced stresses. Commercial connectors (Grayloc, Autoclave, Swagelok, and MS flared (37-1/2°) type) are considered satisfactory for mechanical joints. Copper, aluminum, and nickel cone seals are used with the 37-1/2° flared connectors. Teflon-coated (TFE) sealing rings (Grayloc) and CRES/TFE (Flexitallic) spiral gaskets are used in commercial flanges.

Some manifold fabrication procedures prohibit bending of the tubing to ensure that associated cold-working and deformation do not affect material properties when containing GH_2 . Since most manifolds have some bends in the tubing, the "no-bend" criteria appears overly restrictive but it does indicate the desirability for minimizing material deformation during assembly of GH_2 systems.

Components

Commercial components have proven reliable either "as designed" or with minor modifications for GH_2 systems with pressures less than 5000 psig. TFE, Kel-F, Nylon, and Vespel have proven satisfactory for seat seals with no more restraints than those normally observed when designing for the seal loading inherent with high pressure applications. Metal-to-metal "hard" seats are generally used for the higher pressure applications. TFE "chevron" seals have been proven satisfactory for stem seals and normal elastomers (Butyl, Neoprene, Viton, etc.) have been used for "O" rings in the lower pressure systems. Some problems have been experienced with the shafts and shaft seals of commercial valves in 10,000 psig systems. Rocketdyne has designed and fabricated "ball" valves for minimum flow resistance in the 15,000 psig system at Santa Susanna. A routine practice involves the use of helium for the pressurization of dome-loaded GH_2 regulators. Gages should incorporate austenitic CRES Bourdon tubes. Pressure transducers should incorporate austenitic CRES sensing membranes.

Compressors

The diaphragm-type compressor (Corblin) can be considered the standard for compressing small quantities of GH_2 to pressures as high as 10,000 psig. One company, Rocketdyne, uses conventional (piston-type) compressors to stage GH_2 pressure from 80 to 15,000 psig. The more universal method for obtaining pure GH_2 at high pressure is to pressurize liquid hydrogen to some intermediate pressure and gasify at that pressure to supply GH_2 to the suction side of the high-pressure compressor. Facilities which have no compressors utilize banks of "K" bottles or "tube" tanks, usually on trailers, to supply high-pressure GH_2 to the test setups.

Safety

Safety precautions are necessary because of the flammability of hydrogen. Due to the low specific gravity of GH_2 , air or GN_2 ventilation is usually adequate to ensure that GH_2 concentrations associated with small leaks or permeation are kept below the ignition limit. Vent stacks are used for disposition of larger quantities of GH_2 associated with manifold purging or the relieving of system pressure. Some vent stacks incorporate propane burners but burning is optional in open areas. Explosion-proof, electrical wiring should be utilized for facility electrical distribution circuits but this practice is not always compatible with instrumentation circuits. Ventilation can be utilized to ensure that instrumentation containers do not accumulate flammable concentrations of GH_2 .

The major safety considerations for GH_2 are those associated with any high-pressure gas. One further precaution precludes direct venting of high-pressure GH_2 to ambient air. The heat generated by the shock

at large pressure differentials can ignite the released hydrogen.

IV. Facilities

Aerojet Liquid Rocket Company

The Aerojet Rocket Test Facility at Sacramento, California, has had extensive experience with GH_2 and has the capability to operate GH_2 systems at pressures up to 10,000 psig. Two GH_2 systems utilize conventional CRES manifolds with welded or mechanical joints. Carbon steel tanks with CRES liners are used to store approximately 60 cubic feet of high-pressure GH_2 . A high-pressure, diaphragm-type compressor is used to increase the GH_2 pressure from a storage trailer pressure (2200 psig) to the desired test pressure (10,000 psig; maximum). Conventional control components are used throughout the systems. Both systems are operable but neither is presently being used for hydrogen service.

Boeing Company

The Boeing Tulalip Test Facility at Marysville, Washington, has the capability to test materials in a GH_2 environment at pressures up to 10,000 psig. This facility utilizes conventional small-diameter CRES manifolds and control components which are joined by mechanical fittings. The system is utilized intermittently and is disassembled and stored when not in use.

General Dynamics/Convair

The GD/Convair Sycamore Canyon test site at San Diego, California, is used for component and sub-system testing with LH_2 or GH_2 . Stored LH_2 is compressed, gasified, and stored as GH_2 at 2000 psig, in A.O. Smith type, laminated tanks. The manifolds and control components are conventional CRES with both welded joints and mechanical fittings. The GH_2 system is presently being operated as designed and has provided satisfactory service for eight years.

Lockheed Research Laboratory

The Lockheed Palo Alto Research Laboratory operates LH_2 and GH_2 test facilities at Palo Alto, California, for thermal properties evaluation and at Santa Cruz, California, for hot-gas generation which is used in ascent/re-entry simulation testing. The Palo Alto GH_2 systems are used to control boil-off gases from LH_2 containers under test. These systems use conventional CRES manifolds and control components which are joined by mechanical fittings. Operating pressures are only a few torr above local ambient. The Santa Cruz system is used to feed GH_2 at 2500 psig and -320°F to a GH_2/LF_2 burner where hot gas is generated and directed at test materials to simulate the heating that the materials will experience during the ascent or re-entry phase of missile flight. This GH_2 system uses conventional CRES manifolds and control components which are assembled by welding or Grayloc mechanical fittings. The control components are specially designed for capability to perform at -320°F . The system is presently operable.

Martin Marietta/Denver Division

The Martin Marietta Hazardous Test Facility at Denver, Colorado, has operated GH_2 test systems at pressures up to 3000 psig on an intermittent basis for testing rocket engines and control components. The systems were assembled from conventional CRES manifolds and control components using mechanical fittings. The systems were assembled when needed for test and subsequently dismantled and stored.

NASA-Johnson Space Center

The JSC Test Facility at Clearlake, Texas, is utilized for fuel cell (GH_2/GO_2) operation. Ultrapure GH_2 is delivered in "tube" tank trailers and regulated to desired system pressure of approximately 60 psig. The GH_2 system is assembled with conventional CRES manifolds and control components using mechanical (AN flared) fittings with nickel cone seals. The system is operable and has been in existence for approximately two years. JSC also has the capability for materials compatibility studies in GH_2 environments as high as 1000 psig. This test setup is used on an intermittent basis when needed for materials evaluation. GH_2 is furnished from "K" bottles and regulated to desired system pressure. Construction of the compatibility test system is similar to the fuel cell test system.

NASA - J.F. Kennedy Space Center

The KSC facility at Cocoa Beach, Florida, furnishes GH_2 at 6000 psig to the Shuttle launch pad where the pressure is regulated down to the desired pressure for use in the GH_2/GO_2 fuel cells. The GH_2 is stored in seamless U.S. Steel tanks until needed for cell operation. The GH_2 system is assembled with conventional CRES manifolds and control components using mechanical fittings. The JFK assembly procedure does not permit bending of the manifold tubing. The manifold is constructed of 2 inch OD x 3/16 inch wall Type 316 CRES tubing and is approximately 1800 feet long. The system is operable and will be used for Shuttle launches.

NASA - Langley Research Center

LaRC has two GH_2 facilities in Hampton, Virginia; one system is used for supersonic combustion studies for ramjets, and the other system is used to feed an expansion tube for hypervelocity testing. The GH_2 for the ramjet combustion research system is stored in a 2400 psig "tube" tank trailer and regulated down to 720 psig for burner operation. The main manifold is conventional carbon-steel pipe (3 inch OD; schedule 40) joined by welding and mechanical fittings. Smaller manifolds and control components are conventional CRES which are joined by mechanical fittings. The ramjet test facility is operable and in daily use. The GH_2 for the expansion tube system was stored in "K" bottles and fed to the 5000 psig system as needed. The system was assembled with conventional CRES manifolds and control components using superpressure mechanical fittings. This system was dismantled and stored in 1973.

In addition to current GH_2 effort, LaRC provided an interesting, historical background from the Nerva program which was terminated in 1972. The Nerva concept used GH_2 to cool a nuclear reactor. After cooling the reactor, the heated GH_2 was expelled through a nozzle to produce thrust. Much of the data about materials and control components which

were used for the Nerva program are still applicable to present day technology.

NASA - Lewis Research Center

The LeRC GH_2 facility at Cleveland, Ohio, is used to test rocket engines. Stored LH_2 is pressurized and gasified to provide 4000 psig GH_2 which is stored in a bank of low-carbon steel tanks. Approximately 100 feet of low-carbon steel pipe (4 inch OD; schedule 40) is used to manifold the tanks. The primary system manifold and the control components are constructed from conventional CRES and the system is assembled with welded and mechanical joints. The system is operational and is currently being used for testing rocket engines.

NASA - Marshall Space Flight Center

MSFC has a multipurpose test facility at Huntsville, Alabama, which consists of over 2 miles of 1.5 to 3.0 inch OD carbon-steel and CRES pipe and 40 pressure vessels capable of storing approximately 3,000,000 cubic feet of GH_2 at operating pressures ranging from 3100 psig to 10,000 psig. All GH_2 storage tanks are the A.O. Smith design, laminated construction. The GH_2 facility was developed to test rocket engines and rocket engine components for the Apollo boosters and the Shuttle main rocket engine programs. The GH_2 is used to purge the fuel (LH_2) tanks and manifolds prior to loading and used for tank pressurization after loading. MSFC uses welding for joining manifold pipes of similar materials and uses Grayloc fittings for the mechanical joints between dissimilar materials and for control component installation. All carbon-steel manifolds have been derated from 5000 to 3100 psig to account for the effects of contained hydrogen. The 5000 psig-rated manifolds are constructed from Schedule 160; Type 304 CRES. The 10,000 psig-rated manifolds are constructed from heavy-wall, Type 304L CRES. The facility is fully operable and will be used for verification of Shuttle components.

Pratt and Whitney Aircraft, Government Products Division

The Pratt and Whitney (P&W) facility in West Palm Beach, Florida, is utilized to test LH_2/LOX rocket engines and components. Development of this facility was started during the late 50's and has been expanded and used continuously since that time for the Centaur RL10 engine program and for research and development of several other rocket engines (including Shuttle) and related components. The facility routinely compresses LH_2 to desired pressures and gasifies at that pressure for GH_2 in the range from 3000 to 5000 psig. Higher pressure GH_2 (up to 10,000 psig) is obtained by compressing the 5000 psig GH_2 with a diaphragm-type compressor. Lower pressure GH_2 (less than 3000 psig) is obtained by regulating down from the 3000 to 5000 psig storage tanks. The Air Force originally supplied LH_2 to the facility from an on-site liquefaction plant which is presently inactive. LH_2 is now transported by truck, as needed, from New Orleans, Louisiana. P&W stated that the basic facility would probably remain intact but the high-pressure (10,000 psig) system was scheduled for dismantling because of their loss of the Shuttle main rocket engine competition.

The basic facility capability would be available for any GH_2 testing including component and

materials evaluation. The P&W low-pressure GH₂ facility utilizes laminated low-carbon steel tanks for storage of 730,000 cubic feet at 3150 psig and 275,000 cubic feet at 5500 psig. The high-pressure system uses CRES liners in A.O. Smith design, laminated tanks to store 1,200,000 cubic feet of GH₂ at 9300 psig. The manifolds for the low-pressure system are low-carbon steel with welded and mechanical (Grayloc) joints. Any branches from the basic manifold are usually CRES tubing with mechanical joints. The control components for the low-pressure system are CRES with mechanical joints (Grayloc) for installation. The high-pressure manifold and all control components are conventional CRES with welded joints whenever possible.

Rockwell International - Rocketdyne Division

Two Rocketdyne facilities were visited; the Main Propulsion Test facility (Santa Susanna) in California and the Shuttle Rocket Engine Test facility at NSTL, Bay St. Louis, Mississippi.

The Santa Susanna Laboratory has the most extensive GH₂ capability of any identified during the survey. The facility has 124 tanks for GH₂ storage in the pressure range from 3000 to 5000 psig and 11 (7 active) tanks for GH₂ storage at pressures as high as 15,000 psig. Three low-pressure (approximately 80 psig) tanks with a combined volume of 258,000 cubic feet are used for recovery of GH₂ after passing through the test manifolds at the various test stands. Appropriate piston-type compressors are used to stage the GH₂ from stored pressure (80 psig) to the desired test pressures (3000 to 15,000 psig). The low-pressure tanks are fabricated from low-carbon steel. Laminated tanks are used for the 5000 psig rated tanks and for some of the 3000 psig rated tanks. The balance of the 3000 psig rated tanks are welded, A212; grade B, low-carbon steel. The manifolds for all systems with pressures less than 5000 psig are low-carbon steel with welded joints for permanent connections and mechanical fittings (Grayloc) for test branches. Most of the test manifolds and all control components are conventional CRES with mechanical joints for installation.

The highest pressure (15,000 psig) system manifolds and control components are fabricated from Type 21-6-9 CRES. The manifolds are from one to six inches ID with appropriate wall thickness to withstand the 15,000 psig pressure. All manifold joints are welded and Grayloc fittings are used for installation of the control components. Rocketdyne fabricated the ball-type valves which are used in the two- and six-inch ID manifolds to minimize pressure-drop during flow. The balance of the valves are commercially available with only the necessary modifications for use in high-pressure hydrogen. All valves are remotely operated by a control system using 3000 psig, hydraulic-fluid actuators. The GH₂ systems are all operable at this time but some uncertainty as to future usage

may lead to dismantling and some of the capability could be lost.

Rocketdyne is testing the Shuttle main engine (LH₂/LOX) at the A2 test stand at the National Space Technology Laboratory in Bay St. Louis, Mississippi. The GH₂ for this testing is furnished from a central location where LH₂ is pressurized to 2500 psig and gasified at that pressure and stored in tanks until needed at the test stand. A 1.5 inch OD, Type T1 steel manifold is used to transport the GH₂ from the central "tank farm" to the test stand. The GH₂ is regulated down to desired pressure for fuel (LH₂) system purge (before filling) and tank pressurization during the rocket engine firing. A diaphragm-type compressor and ten 18-inch OD "tube" tanks to provide GH₂ at 10,000 psig are on-site if needed for cooling instrumentation. To date, this system has only been used for storing helium since the requisite high-pressure GH₂ for transducer cooling is being bled from the rocket engine manifold during operation.

Rocketdyne International - Space Division

Two space division GH₂ facilities were visited; the Control Components Test laboratory in Downey, California, and the Main Propulsion Test facility at the National Space Technology Laboratory in Bay St. Louis, Mississippi.

The test facility in Downey has the capability to operate with GH₂ at pressures up to 2500 psig and at temperatures from -420 to +100°F. Manifolds range from 0.25 to one inch OD and are constructed from aluminum or conventional CRES using mechanical fittings and flanges.

Space Division has had significant experience with conventional components in gaseous hydrogen service which indicates that the major precautions necessary with the use of aerospace-quality components involve safety considerations for the high-pressure and the flammability limits. Two secondary precautions require the use of austenitic CRES for highly-stressed membranes and bellows and the minimum use of elastomers when permeability is a concern. Acceptable elastomers for hydrogen service include Buna "N", Neoprene, Viton, Teflon and Vespel. The use of metal (copper, aluminum, CRES, nickel, etc.) is preferred when possible.

Space Division GH₂ systems are assembled when required for test and dismantled and stored between periods of usage. The GH₂ for testing is contained in "K" bottles until needed for testing. After testing, the GH₂ is burned in vent stacks.

The NSTL facility is used to test the integrated tanks and main rocket engines for the shuttle. The facility uses LH₂ for fuel to the rocket engine but uses helium for purging and pressurization. The only GH₂ system is the vent system for disposal of the vapors.

Table 1

GASEOUS HYDROGEN FACILITIES

Facility	Contact
Aerojet Liquid Rocket Co. P.O. Box 13222 Sacramento, Calif. 95813	Richard Simonson (FTS) 454-2408 Dept 1280 Bldg. 3308
Boeing Company Tulalip Test Site 3202 116 Street NE Marysville, Washington 98270	Norman Wise (206) 342-2121 Site manager Ext. 261
General Dynamics Convair Division P.O. Box 80847 San Diego, Calif. 92138	"Bob" Tuttobene (FTS) 891-8900 42-6611 Ext. 2276
Lockheed Palo Alto Research Laboratory 3251 Hanover Street Palo Alto, Calif. 94304	George Cunningham (FTS) 493-4411 5232 Ext. 45136 Bldg. 205
Martin Marietta Corporation Denver Division P.O. Box 179 Denver, Co. 80201	C. A. Hall (FTS) 329-0111 0480 Ext. 4049
NASA Johnson Space Center Houston, Texas 77058	Clarence Propp (FTS) 525-4991 EP 6
NASA John F. Kennedy Space Center Florida 32899	W. H. Boggs (FTS) 823-3626 DE-A NASA
NASA Langley RC Hampton, VA 23665	R. D. Witcofski (FTS) 928-3838 249A
NASA Lewis RC 2100 Brook Park Road Cleveland, Ohio 44135	J. W. Gregory (FTS) 294-6644 500-318
NASA Marshall Space Flight Center Redstone Arsenal, Ala 35812	W. D. Powers (FTS) 872-2813 PS03 892-2817
NASA Jet Propulsion Laboratory 4800 Oak Grove Drive Pasadena, Calif. 91103	Ray Hagler (FTS) 792-3970 125/224 792-3941
Pratt and Whitney Aircraft Government Products Division P.O. Box 2691 W. Palm Beach, Fla. 33402	J. A. Daley (305) 844-7311 B 52 Ext. 3613
Rockwell International Rocketdyne Division 6633 Canoga Ave Canoga Park, Calif. 91304	"Bob" Davis (FTS) 984-2582 EB06
Rockwell International Rocketdyne Division; NSTL A2 Test Stand Bay St. Louis, Miss 39629	R. J. Smutny (FTS) 494-3026
Rockwell International Space Division 12214 Lakewood Blvd Downey, Calif. 90241	"Jim" Liston (FTS) 985-2653 CA 04
Rockwell International Space Division; NSTL Mississippi Main Propulsion Test Bay St. Louis, Miss 39629	John Plowden (FTS) 494-3555 ZM01

STUDY OF THE BEHAVIOR
OF GAS DISTRIBUTION EQUIPMENT
IN HYDROGEN SERVICE
UPDATE - 1977

J. B. Pangborn, D. G. Johnson and W. J. Jasionowski
Institute of Gas Technology
IIT Center, 3424 S. State Street
Chicago, IL 60616

Abstract

The Institute of Gas Technology is conducting an experimental program to identify problem areas that could occur with the use of conventional natural gas distribution equipment in hydrogen service. Funded by DOE, there are 15 manufacturers and gas distribution companies which are participating by loaning or donating equipment and services. Three model test loops have been constructed and are operational: a Residential/Commercial loop with smaller sized components, an Industrial loop with larger sized components, and a small test loop for special (created) leakage tests. We are measuring flow rates and energy delivery, and leakage rates, and we will note apparent problems in materials compatibility. Baseline data on natural gas operation are just becoming available.

Introduction

This program is part of a multi-year effort to supply needed information about hydrogen delivery in natural gas distribution equipment. The overall program will identify operating, safety, and materials problems associated with the use of hydrogen in conventional distribution systems. One of the major incentives behind (nonfossil-based) hydrogen as a future supplement and eventual replacement for natural gas is the expectation that the existing gas delivery system can be used without major modifications. This is primarily a financial incentive for the continued delivery of energy in the form of fuel gas. The embedded capital investment in the gas distribution industry now exceeds 20 billion dollars, and this includes over 650,000 miles of distribution mains which carry gas to about 45,000,000 customers. Further, most equipment and lines now being installed are expected to last 50 years or longer. If it is practical to carry hydrogen safely in this existing gas distribution equipment, then hydrogen is indeed an attractive form for energy delivery in the future. If moderate problems are identified, then we have sufficient time now to define and develop "fixes" or alternative operating procedures. If, however, serious problems are found, then other alternatives (besides hydrogen) must be weighed against major system modifications.

Construction of Test Loops

After site facility preparation, IGT proceeded during 1977 to construct three model test loops using equipment loaned or donated by 15 manufacturers and gas utility companies. The 15 companies that are program participants (along with the DOE) are listed in the Appendix to this report. We estimate that these organizations have donated collectively over \$35,000 worth of equipment and services to this program. The three test loops have been constructed in general accordance with the (simplified) diagrams presented in last year's report to this conference.¹ All construction was done in accordance with gas industry procedures and requirements, in fact, a field construction

welder from Northern Illinois Gas Co. welded the necessary steel joints with standard field equipment. All subassemblies were leak tested prior to integration into a total assembly or test loop. Each subloop and loop were then further leak checked.

Residential/Commercial Test Loop

The Residential/Commercial model loop consists of four subloops and a bypass. The pipeline materials of construction are 1) steel, 2) copper, 3) plastic (high-molecular-weight, high-density polyethylene), and 4) cast iron. This model contains components and equipment normally installed in typical residential and/or commercial service. Figure 1 is a photograph of the completed Residential/Commercial test loop. In operation, a single-stage compressor feeds 15 SCF/min of natural gas or hydrogen to the model at a pressure between 60 and 65 psig. The compressed gases pass through an aftercooler to reduce gas temperature to ambient and then through a surge tank to dampen pulsations. A regulator reduces pressure to about 50 to 60 psig, simulating pressures in the distribution mains and the service lines to commercial or residential consumers. In the case of cast-iron subloop, the pressure is reduced further by another pressure regulator to 6 inches water column. At the simulated building line (that is, the termination of the service line), the distribution pressure (50 to 60 psig) is reduced further by a service regulator to 6 inches water column. The gases then pass through a gas meter to the inlet of the compressor and are recompressed and recycled. Flow is controlled and proportioned through the subloops with valves and the bypass.

Industrial Test Loop

The Industrial model consists of one loop and a bypass. The pipeline material is steel. This model contains components and equipment normally installed in typical industrial service. Figure 2 is a photograph of the Industrial model. In operation, a two-stage compressor feeds 15 SCF/min of natural gas or hydrogen to the model at a pressure between 170 and 175 psig. The compressed gases pass through an aftercooler to reduce gas temperatures to ambient and through a surge tank to dampen pulsations. A line regulator installation reduces the pressure to 60 psig, simulating pressures in the distribution main. Another regulator downstream, in series, reduces the pressure further to 8 psig, simulating the operating service pressures of industrial components. The gases then pass through several industrial gas meters (for example, diaphragm, rotary, or turbine) connected in series, to the inlet of the compressor, and are recompressed and recycled. Flow is controlled and proportioned with valves and the bypass.

Safety Test Loop

The Safety Test model consists of one loop with a leak zone and a bypass. The leak zone provides a space for testing and defining problems associated with mechanical or corrosion leaks, leak clamps, and ruptures. The pipeline material is steel except at the leak zone. Figure 3 is a photograph of the Safety Test model. In operation, a single-stage compressor feeds 10 to 15 SCF/min of natural gas or hydrogen to the Safety Test model at a pressure between 50 and 60 psig. The compressed gases pass through an aftercooler to reduce gas temperatures to ambient and through a surge tank to dampen pulsations. The gases then pass through the experimental setup in the leak zone to the inlet of the compressor and are recompressed and recycled. If excess leakage is a problem, the gas flow will terminate in the leak zone and the gases will be vented to the outdoors.

Special Measurement Procedures

The three reciprocating piston compressors were installed to recycle and compress natural gas and/or hydrogen to the operating design conditions of the model test loops. The Residential/Commercial loop and the Industrial loop have each been operated for about two weeks to gain baseline data on flow and leakage with natural gas. Measurements with hydrogen are now beginning for the Industrial loop.

As the gases pass through various regulators or stations in the two major loops, the operating pressures are reduced from the feeder main (150 to 200 psi), to the distribution main (50 to 60 psi), and to the point of service (5 to 10 psi for Industrial and 6 to 10 inches water column for Residential/Commercial). Meters are installed either in series or in controlled subloops so that comparative flow measurement data (on natural gas and hydrogen) can be taken. At a simulated building line, the gases are filtered, recompressed, and recycled to the loops. The Residential/Commercial and the Industrial models are designed to operate continuously, whereas the Safety Test model will operate intermittently. Using local pressure and temperature measurements, all gas flows are reduced to gas industry standard cubic feet (SCF, 60°F, 1 atm).

Eleven components (couplings, unions, a pressure regulator, a flow meter) were enclosed with sheet metal or Plexiglas enclosures to monitor and compare leakage of natural gas and hydrogen from these specific components. Figure 4 is a photograph of a pressure regulator sealed in a Plexiglas enclosure. Volumetric displacement and gas analysis (by gas chromatography or mass spectrograph) were the methods selected to measure the leak rates of these components.

Total system leakage is being determined by measuring makeup gas additions to the high-pressure side of the test loops (after the compressor). The makeup gas quantities are being determined by pressure decay from calibrated cylinders.

A 40-hour shakedown test was performed with the Residential/Commercial and Industrial models at design conditions using nitrogen gas. The systems operated satisfactorily, and leak rates of the components and model were characterized. During this operation it was again assured that the systems and the individual components, fittings, and connections met industry requirements for leak-tightness.

Preliminary Results and Conclusions

Both the Residential/Commercial model loop and the Industrial model loop have suffered excessive compressor gas leakage problems. The compressors are reciprocating piston machines with Teflon rings and Teflon dynamic seals for oil-free operation in natural gas and/or hydrogen service. They were selected over diaphragm models on the basis of costs and delivery time. Both compressors have been serviced by the supplier to replace the dynamic seals (Residential/Commercial loop) and the head gasket (Industrial loop). Natural gas leakage became quite large after short compressor operating periods, and the relatively large volume of lost gas obscured the test loop leakage. In order to determine the leakage of a test loop, the compressor leakage must be subtracted from the combined system leakage.

Figure 5 presents simplified cumulative leakage data for the Industrial loop over a 500-hour test with circulating natural gas. This baseline test shows three notable aspects of system leakage --

1. Compressor leakage apparently decreased with time (possibly as rings and seals "wore in")

2. The model loop leakage rate is quite small, about 0.07 SCF/hr
3. Loop leakage is relatively constant and no significant new leakage appears to be developing with time.

Figure 6 presents simplified cumulative leakage data for the Residential/Commercial loop over a 150-hour test that is now in progress with circulating natural gas. Although incomplete, this test indicates some similarities to leakage in the Industrial loop, but the compressor is not behaving well.

1. Compressor leakage is continually worsening (possibly the seals are failing; this compressor will have to undergo further servicing)
2. The model loop leakage rate is quite small, about 0.12 SCF/hr
3. Loop leakage is relatively constant and no significant new leakage appears to be developing with time.

The data for individual component leakage are currently being processed. Comparative flow meter readings in the Industrial loop are presented below (534-hour cumulative test on natural gas). All meters are of a different brand (manufacturer); the mean value of the average flow rates is 236.7 CF/hour.

<u>Meter Type, Capacity</u>	<u>Cumulative Reading, CF</u>	<u>Average Flow Rate, CF/hr</u>	<u>% Deviation From Mean</u>
Turbine, 4000 CF/hr	124,718	233.5	-1.4
Diaphragm 1000 CF/hr	129,678	242.8	+2.6
Diaphragm 1000 CF/hr	115,250*	235.7	-0.4
Diaphragm 1000 CF/hr	124,260	232.7	-1.7
Rotary 3000 CF/hr	127,513	238.8	+0.9

* Not included in test for first 45 hours; cumulative reading and rate for 489 hours of service.

In the very near future we will be completing the baseline natural gas tests on the Residential/Commercial test loop provided that the compressor can be made to operate with satisfactorily small leakage rates. This loop will then be switched to hydrogen for a 6-month period of operation. The Industrial test loop is now undergoing the change-over to hydrogen. At the end of the 6-month operating period, selected parts and components will be examined to identify any apparent materials problems or effects from the hydrogen exposure. It is hoped that the test facility will be further utilized, beyond the 6-month hydrogen exposure test, to better define problem areas and operating procedures for natural gas equipment in hydrogen service.

Reference

1. Pangborn, J. B. and Jasionowski, W. J., "Study of the Behavior of Gas Distribution Equipment in Hydrogen Service." Paper presented at the Information Meeting for Contractors in the ERDA Hydrogen Energy Program, Airline, Virginia, November 8-9, 1976.

APPENDIX

Companies Participating in the Experimental Study of Gas Distribution Equipment in Hydrogen Service at IGT

The Peoples Gas Light & Coke Company
Chicago, Illinois

Northern Illinois Gas Company
Aurora, Illinois

American Meter Division of Singer
Philadelphia, Pennsylvania

Municipal and Utility Division of
Rockwell International
Pittsburgh, Pennsylvania

Kerotest Manufacturing Corporation
Pittsburgh, Pennsylvania

Mueller Company
Decatur, Illinois

The Sprague Meter Company
Bridgeport, Connecticut

Dresser Measurement Division of
Dresser Industries, Inc.
Houston, Texas

Phillips Products Company, Inc.
Dallas, Texas

Fisher Control Company
Marshalltown, Iowa

Dresser Manufacturing Division of
Dresser Industries, Inc.
Bradford, Pennsylvania

E.I. duPont de Nemours and Company
Wilmington, Delaware

Republic Steel Corporation
Cleveland, Ohio

Rego Company
Chicago, Illinois

Flow Control Division of
Rockwell International
Pittsburgh, Pennsylvania

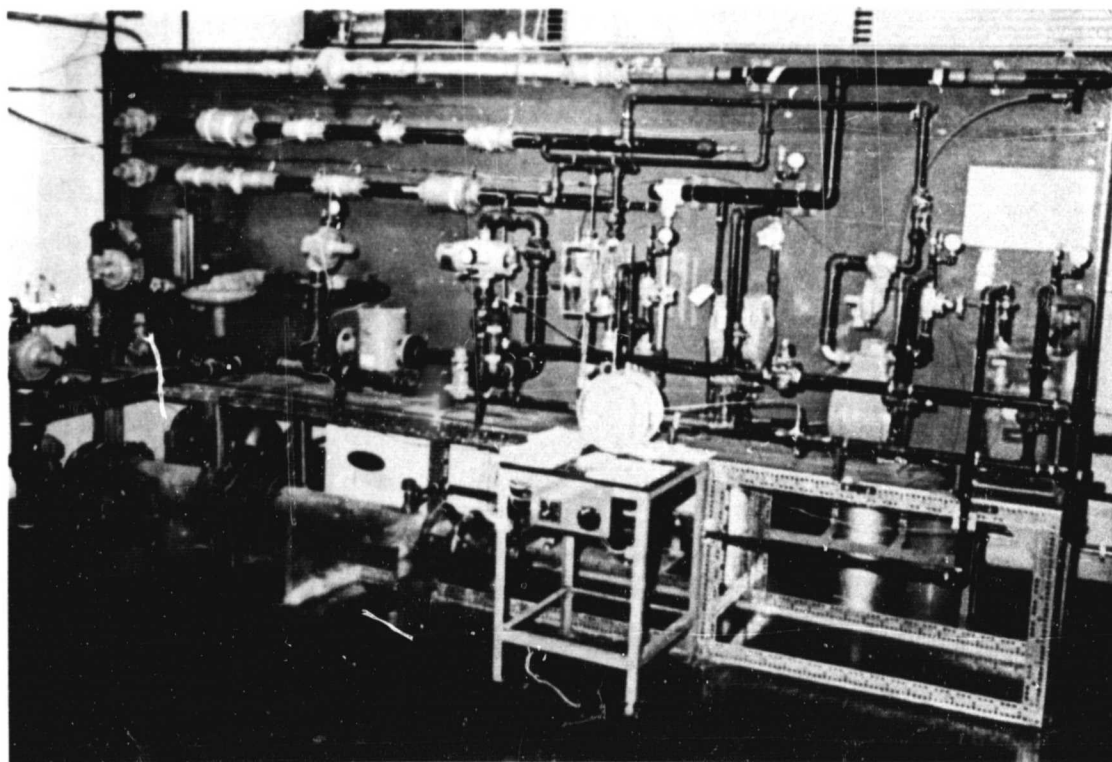


Fig. 1. Residential/Commercial test loop

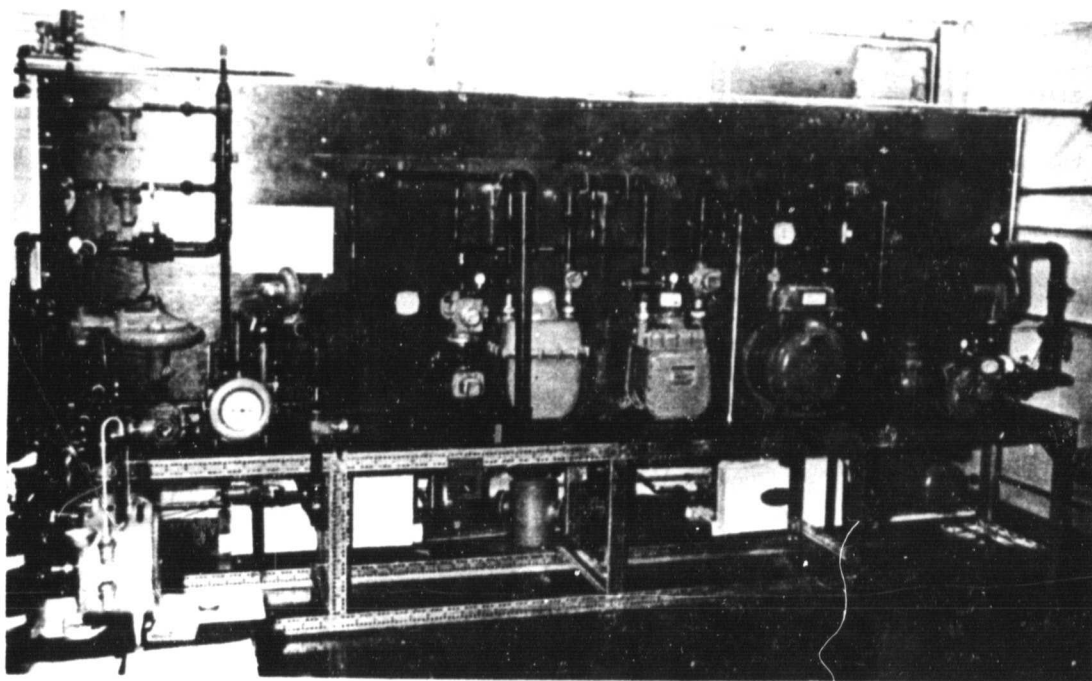


Fig. 2. Industrial test loop

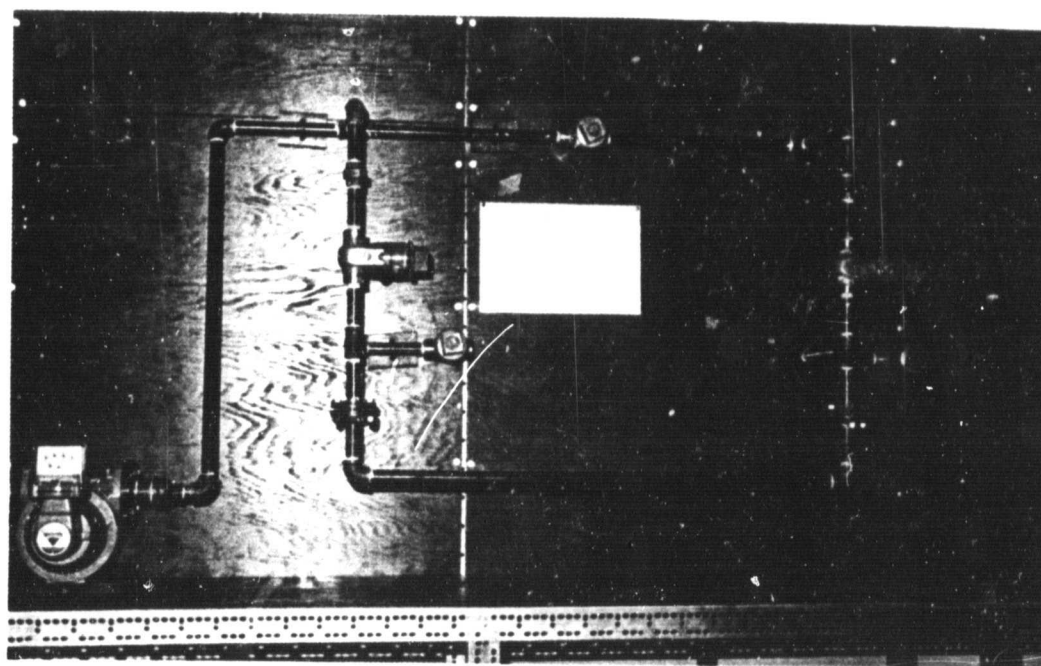


Fig. 3. Safety test loop

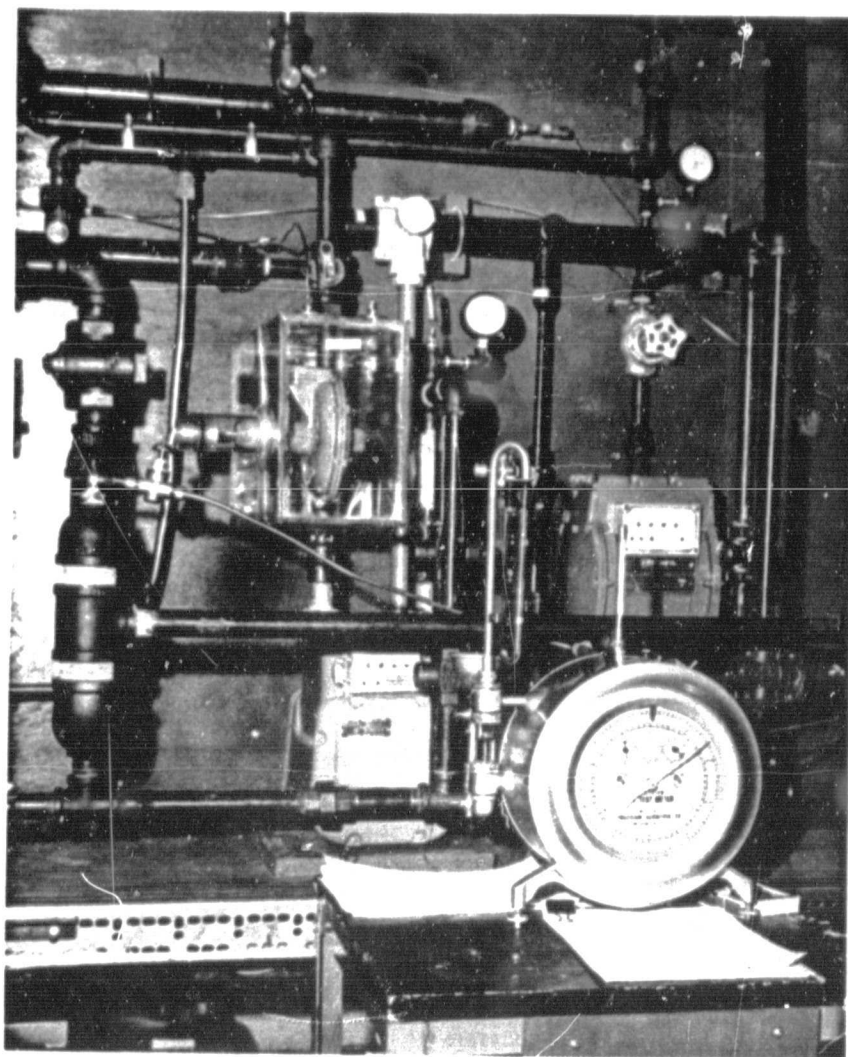
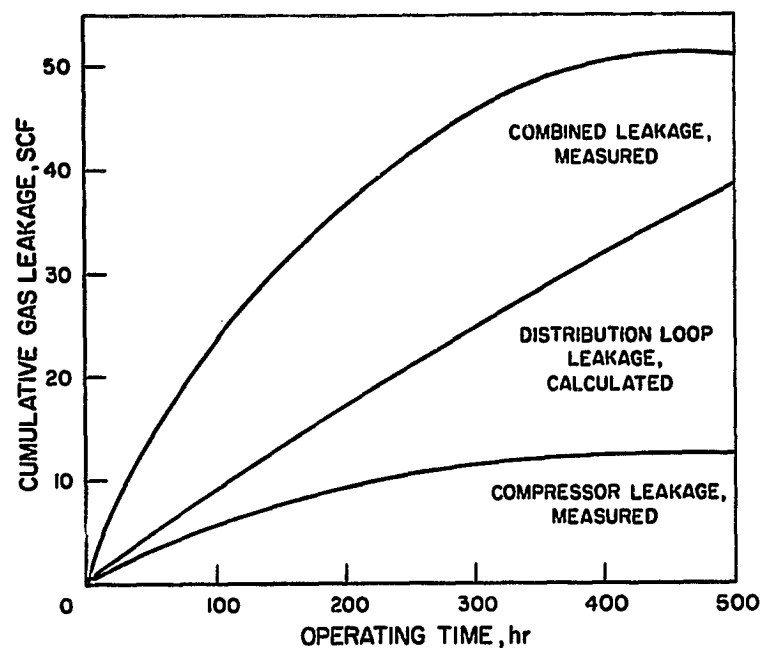
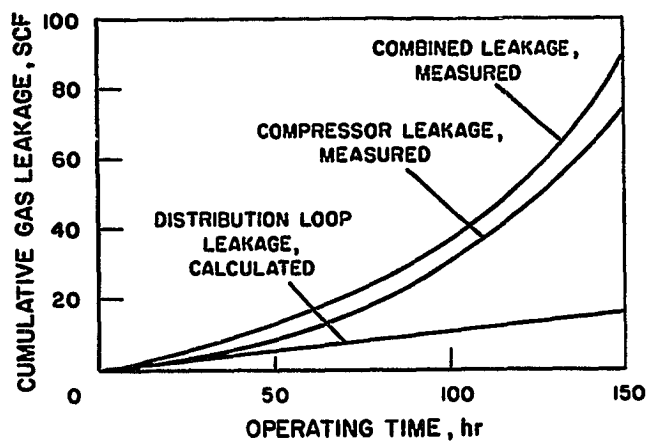


Fig. 4. Pressure regulator in enclosure



A77112464

Fig. 5. Baseline natural gas leakage for Industrial distribution test model



A77112463

Fig. 6. Baseline natural gas leakage for Residential/Commercial test model

HYDROGEN - METAL INTERACTIONS

Howard G. Nelson
NASA-Ames Research Center
Moffett Field, CA 94035

Abstract

The NASA-Ames Research Center program consists of three tasks: 1) identify the influence of hydrogen/methane blend on the fracture behavior of carbon steel; 2) establish the kinetic of hydrogen entry into carbon steel from the dissociation of FeTiH_x ; and 3) establish the kinetics of hydrogen entry from a methane environment. In hydrogen/methane blends, fatigue crack growth rate of the ferritic steel was found to increase as a function of the partial pressure of hydrogen with the presence of methane having no apparent influence. At a hydrogen partial pressure of MPa crack growth rate is as much as 20 times more rapid than that observed in air and 100 times more rapid than observed in vacuum.

I. INTRODUCTION

The NASA-Ames Research Center program in the area of hydrogen containment materials is designed to fill some of the apparent gaps in the Hydrogen Containment Materials Element of the DOE Hydrogen Energy Storage Program. As such, it consists of three separate tasks having the objectives: 1) to define the influence of hydrogen/methane blends on the fracture behavior of a plain carbon, ferritic steel, 2) to establish the influence of the dissociation of FeTiH_x on the kinetics of hydrogen entry into a plain carbon steel, and 3) to establish the kinetics of hydrogen entry into a plain carbon steel from a methane environment over a broad range of temperature.

II. HYDROGEN/METHANE BLENDS

As discussed at the previous review meetings, an Ad Hoc committee has been in existence to study the feasibility of hydrogen as a supplement to our present natural gas supply [1]. Hydrogen is an attractive supplement in that our present natural gas distribution system could be adapted to distribute hydrogen/methane blends in the short term and pure hydrogen in the long term [2].

Very little information is available to reliably establish the compatibility between low strength carbon and low alloy pipeline steels and methane blends containing hydrogen. Recent work in high-purity, high pressure hydrogen environments suggest that hydrogen compatibility may not exist. Limited observations by Chandler and Walter [3] indicate some degradation in unnotched tensile ductility of SAE 1020 and 1042 carbon steels tested in a 10,000 psi hydrogen environment at ambient temperature. Under conditions of cyclic loading, Walter and Chandler [4] have observed increases in crack growth rate greater than an order of magnitude in ASME SA-105 Grade II steel exposed to high pressure hydrogen. Likewise, Nelson [5] has observed a similar enhancement in SAE 1020 plain carbon steel exposed to less than one atmosphere of gaseous hydrogen with further enhancement observed at high pressures [6]. Additionally, in a hydrogen/methane blend containing 15 volume percent methane, Nelson [5] observed enhanced fatigue crack growth equal to that which would be anticipated for hydrogen alone, thus suggesting that methane may not have an inhibiting effect on the degradation incurred by the presence of hydrogen.

The present study was initiated to evaluate the influence of hydrogen/methane blends containing 30% or less hydrogen on the fatigue crack growth behavior of SAE 1020 carbon steel (a steel similar in microstructure to most mild steels used in transmission service). Fig. 1 shows the logarithm of fatigue crack growth rate (da/dN) as a function of applied alternating stress intensity ($\Delta K = K_{\text{max}} - K_{\text{min}}$) observed in vacuum, air, high purity hydrogen and methane blends of 30 percent and 10 percent hydrogen. Crack growth rates in the blends were observed to be equal to those observed in a hydrogen environment alone at equivalent hydrogen partial pressures, and are as much as 20 times more rapid than that observed in air and 100 times more rapid than that observed in vacuum. Fatigue fracture in air occurred by a transgranular mode and was associated with large amounts of plastic deformation. In hydrogen

and hydrogen/methane blends fracture was also transgranular but was associated with very little deformation.

III. KINETICS OF HYDROGEN ENTRY FROM FeTiH_x

The storage of hydrogen in the form of metal hydrides appears to be a viable process and requires long-term containment over a very large number of hydriding/dehydriding cycles. Evidence suggests that for at least some metal hydrides hydrogen activity in material in intimate contact may be significantly altered. The present study was initiated to determine the influence of the dissociation of FeTiH_x in intimate contact with SAE 1020 steel on the kinetics of hydrogen uptake.

Fig. 2 is a plot of the logarithm hydrogen permeation rate as a function of the reciprocal of temperature observed using a gas-phase permeation apparatus [7]. Hydrogen permeation from a high purity hydrogen environment and from a hydrogen environment containing FeTiH_x , during the dissociation cycle, were observed to be essentially identical. It appears then that the kinetics of hydrogen entry into a carbon steel or hydrogen activity at the steel surface is unaltered by the simultaneous dissociation of FeTiH_x .

IV. KINETICS OF HYDROGEN ENTRY FROM CH_4

Many energy conversion systems involve the containment of methane rich environments over a broad range of temperatures and pressures. The dissociation of methane on a metallic surface may release hydrogen which could enter the metal lattice and cause hydrogen embrittlement at low temperatures or hydrogen attack at high temperatures. The purpose of the present investigation was to establish the rate of hydrogen uptake by SAE 1020 steel from a high purity methane environment over a broad range of temperature.

Hydrogen permeation rates, as a function of the reciprocal of absolute temperature observed from a high purity hydrogen environment and from hydrogen/methane blends of 33 percent and 20 percent hydrogen, are shown in Fig. 3. As can be seen, all data are identical, suggesting permeation is controlled by the hydrogen partial pressure and methane is inert to the process over the temperature range investigated (375°C to 100°C).

At temperatures above 400°C methane was found to dissociate on the carbon steel membrane releasing hydrogen. Hydrogen permeation through a fresh membrane at temperatures just above 400°C exhibited an energy of activation of approximately 164 KJ/mole and was approximately directly proportional to pressure to the first power, as shown in Figs. 4 and 5. At some methane pressure, decreasing with increasing temperature, hydrogen permeation rate increased rapidly to levels much greater than would be expected from an extrapolation from the lower methane pressures. These anomalously high permeation rates remained so over all future temperature (Fig. 4) and pressure variations until the methane environment was removed from the membrane surface and the surface was exposed, briefly, to a vacuum.

REFERENCES

1. Steinmetz, G. F., "Work of the Ad Hoc Committee Evaluating the Use of Hydrogen as a Supplement to Natural Gas," ERDA Contractor's Review Meeting, Nov. 1976, Airlie, Virginia.
2. Guerra, C. R., Griffith, J. E., Kelton, K. and Nielson, D., "Blending of Hydrogen in Natural Gas Distribution Systems," ERDA Contractor's Review Meeting, Nov. 1976, Airlie, Virginia.
3. Chandler, W. T. and Walter, R. J., Hydrogen Energy (T. N. Veziroglu, ed.), pp. 1057-78, Plenum Press, New York, 1975.
4. Walter R. J. and Chandler, W. T., "Cyclic-Load Crack Growth in ASME SA-105 Grade II Steel in High Pressure Hydrogen," Effect of Hydrogen on Behavior of Materials (Thompson and Bernstein, ed.), AIME, pp. 23-86, 1975.
5. Nelson, H. G., "Hydrogen-Induced Slow Crack Growth of a Plain Carbon Pipeline Steel under Conditions of Cyclic Loading," Effect of Hydrogen on Behavior of Materials (Thompson and Bernstein, ed.), AIME, pp. 602-11, 1975.
6. Nelson, H. G., "On the Mechanism of Hydrogen-Enhanced Crack Growth in Ferritic Steels," Proc. ICM-II, ASM, pp. 690, 1976.
7. Johnson, D. L. and Nelson, H. G., "Determination of Hydrogen Permeation Parameters in Alpha Titanium Using the Mass Spectrometer," Met. Trans. 4, pp. 569-573, Feb. 1973.

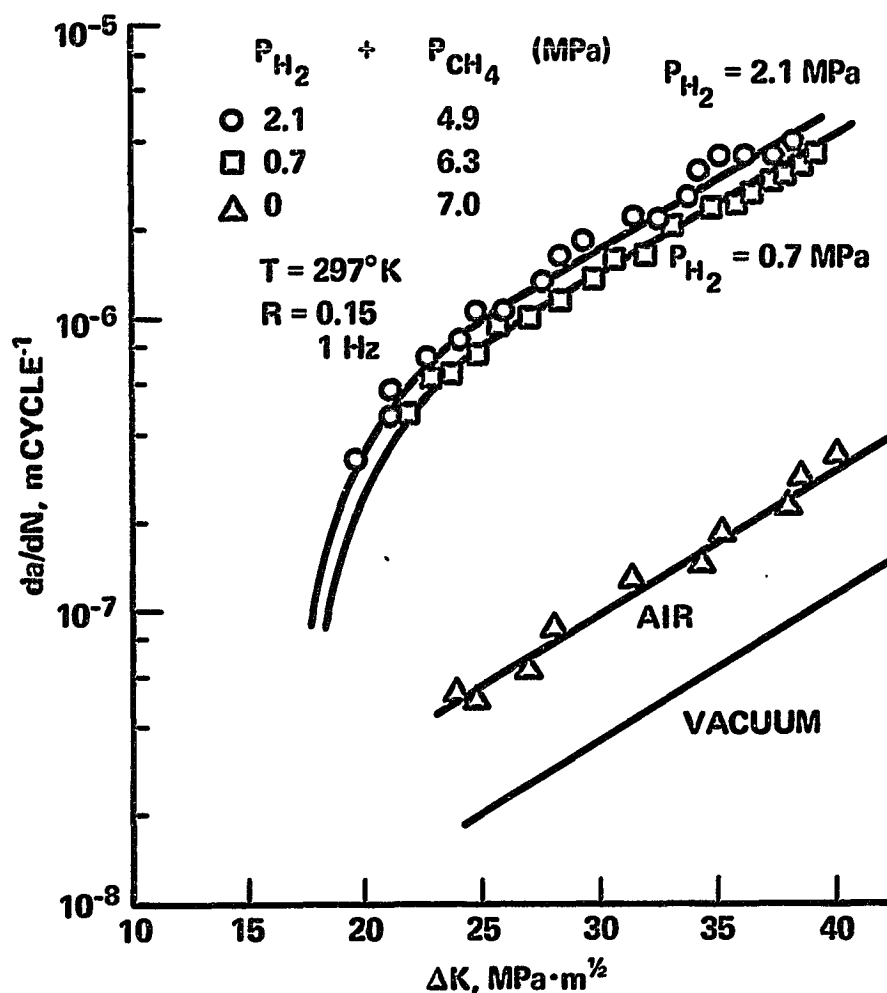


Fig. 1. Fatigue crack growth of SAE 1020 steel in H_2 - CH_4 blends

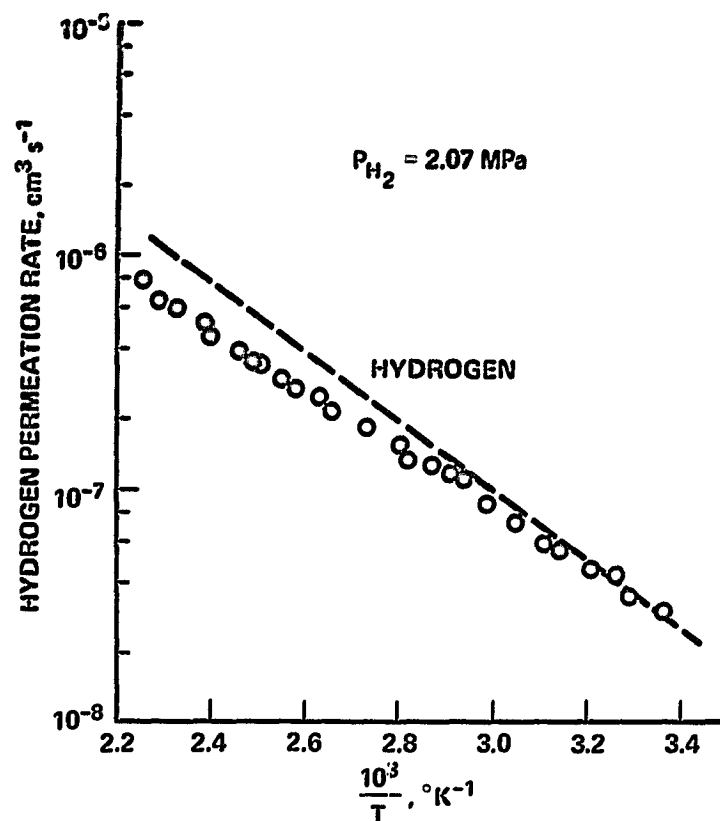


Fig. 2. H₂ permeation through SAE 1020 steel in contact with FeTiH_x

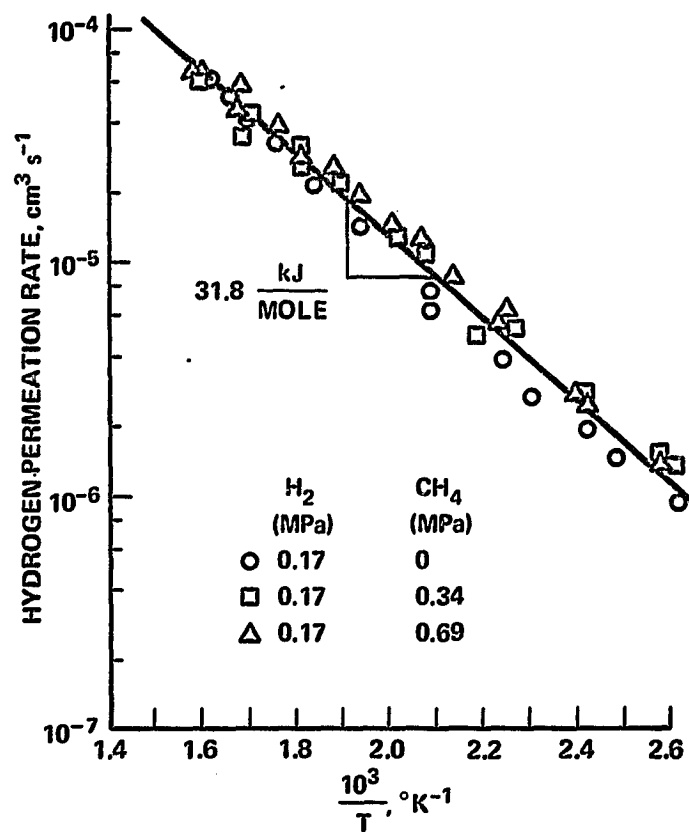


Fig. 3. H₂ permeation from CH₄-H₂ blends through a 1020 steel

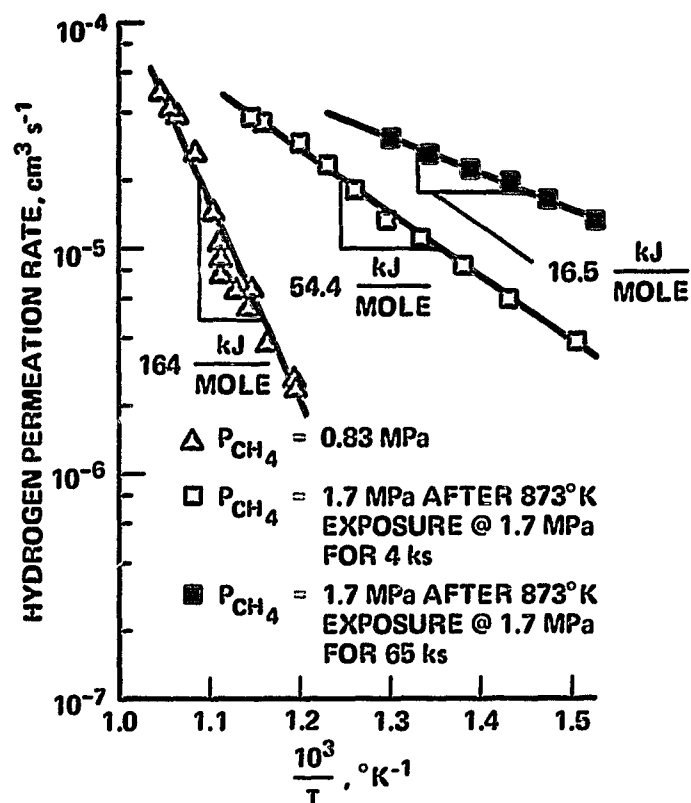


Fig. 4. Temperature dependence of H_2 permeation from a CH_4 environment

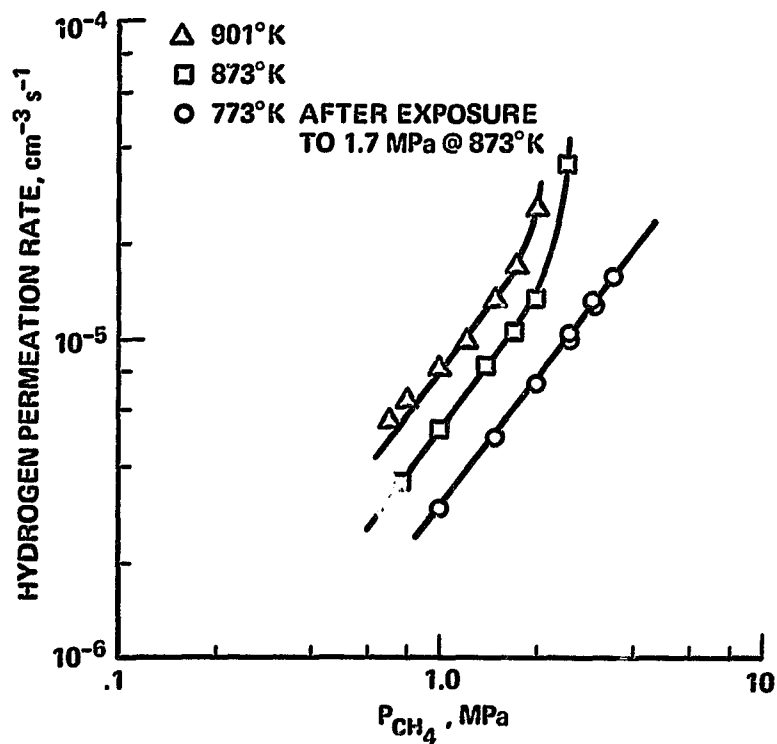


Fig. 5. Pressure dependence of H_2 permeation from a CH_4 environment through a 1020 steel

HYDROGEN COMPATIBILITY OF STRUCTURAL MATERIALS FOR ENERGY
STORAGE AND TRANSMISSION APPLICATIONS

Steven L. Robinson
Sandia Laboratories
Livermore, California

Abstract

The suitability of structural materials for service in hydrogen energy storage and transmission applications is being investigated in several ways. The goal is to provide performance data for cost effective safe structures, and to improve the hydrogen environment performance of structural steels.

Material performance in hydride containment vessels has been characterized by in-situ tests of tensile specimens, vessel bulging phenomena have been analyzed, and fatigue cracking hazards assessed. The use of existing natural gas pipeline systems for hydrogen transmission is being explored through an experimental hydrogen pipeline, which will be used to assess the sensitivity of pipeline materials to defects and flaws. The performance of carbon-manganese mild steels have been improved by alteration of the metallurgical processing methods and by minor alloying additions. In addition, the effects of microstructural modifications upon hydrogen compatibility of pipeline steels are being assessed.

Introduction

Sandia Livermore Laboratory has an active role in three areas of the study of structural materials for hydrogen service. These are: (1) hydride storage support, (2) materials for hydrogen pipeline service (the experimental hydrogen pipeline), and (3) advanced metallurgy of hydrogen compatibility in structural steels. The goals are: to provide performance data so that designers may choose cost effective and safe materials, to characterize the performance of existing storage and transmission systems, and to assist in developing economical improved materials for future hydrogen energy systems.

Hydride Storage Support

Our principal activity in this area has been to support Brookhaven National Laboratories' work on iron-titanium hydride by characterizing the behavior of steels in hydrogen/hydride environments. Our support for BNL has consisted of three phases: (a) postmortem of a stainless steel vessel which has undergone 4254 cycles of hydride cycling; (b) a test matrix of self-loaded tensile specimens, subjected to hydriding cycles, was analyzed; and (c) fatigue flaw growth in structural steel vessels was analyzed numerically.

A 304 stainless steel was analyzed after 4254 cycles of hydriding. Plastic deformation of 0.4% had been observed in one region of the vessel, a 1 inch diameter tube 12 inches long. This deformation was due to the iron-titanium alloys' volume swelling of 15% upon hydriding, cracking of particles and a mechanical interlocking producing a wedging effect(1). Fusion analysis of the dissolved gases gave a figure of 11.8 w/o H₂, or more than 50% higher than thermal diffusion of hydrogen could account for alone. Analysis of the internal surface by scanning electron microscopy (SEM) showed longitudinal surface gouging and striations as shown in Figure 1. Particles of SiO₂ and FeTi were found imbedded in the vessel wall, along with unidentified particles bearing aluminum, chlorine and phosphorous. The transport of extra hydrogen into the metal by plastic deformation and the abrasion by the hydride present no significant additional hazard in the case of 304 stainless steel, but could be hazardous in ferritic structural steel hydride vessels.

The self-loaded tensile specimens for exposure to hydride cycling were of the configuration shown in Figure 2. The test matrix of 80 specimens is given in Table I. These specimens were placed in a hydride bed and exposed to 821 cycles of hydride charging and discharging (21 cycles between FeTiH_{0.1} and FeTiH_{1.27}, and 800 cycles between FeTiH_{0.146} and FeTiH_{0.189}). Following exposure, the hydrogen was discharged, the specimens and chamber were outgassed for several days and the specimens removed and transported from BNL to Sandia Livermore. The lengths of the loaded specimens were measured to determine the degree of relaxation of the applied tensile load. Some relaxation had occurred, but no pattern was evident. The specimens were then removed from the fixture and tensile tested to failure in air. (Due to the experimental limitations, it was not possible to test specimens with the hydrogen still in them.)

Fracture surfaces were examined by SEM and compared to tensile fractures of unexposed and H₂ exposed specimens. Tensile data was also compared to the unexposed and H₂ exposed data.

During cycling, the specimens were exposed to thermal cycling, abrasion by fine hard particles, high purity dry hydrogen up to 3.5 MPa (500 psi), and possible atomic hydrogen charging during hydride discharging and charging. No failures occurred in ferritic alloy specimens while in reactor and no significant stress relaxation was observed. One welded aluminum specimen failed at a weld flaw, although this was probably not a hydrogen-assisted failure. Post-reactor tests on aluminum were hindered by the galling of thread and fixture, with most specimens failing due to removal torque, although lubricants had been applied after removal from the hydride bed. No difficulties were experienced in removing ferritic specimens.

Tensile data of the outgassed material showed no degradation after the exposure to FeTiH_x. Fractographic examination also showed no significant deviations from normal fracture appearances. Small amounts of secondary microcracking were observed on the fracture surfaces of the Cr-Mo steel (Figure 3), but not in A516 and A106 steels.

The data may be interpreted in terms of delayed failure phenomena with the use of a schematic diagram (Figure 4). The first curve, t_1 , is an applied stress-damage time curve, at which time irreversible damage has been done to a specimen. The second curve is the failure stress-time curve. The time between the two curves is the time in which flaws grow to critical size and cause failure. Testing at two stress levels and with smooth and notched specimens should put us at or above the threshold stress. Tensile testing after hydride exposure should detect significant irreversible damage as degraded properties, and altered fracture surface appearance. The conclusion to be reached from the postmortem test results is that, for the stated experimental conditions, the applied stress is either below the threshold stress, or that more hydride cycles are necessary to produce irreversible damage that can be detected by tensile tests and/or fractographic analysis. Additionally, we have gained confidence that ferritic structural steels may be used for reasonable lifetimes in hydride containment vessels.

The growth of fatigue cracks during service in hydrogen is a potential hazard to the structural integrity of a hydride vessel. Although previous work has established that low strength ferritic materials such as A106-B and A516 grade 70 do not exhibit sustained load cracking in hydrogen(3,4), they do exhibit accelerated fatigue crack growth in gaseous hydrogen environments. Fatigue data for steels similar to these to be used in BNL's HYTACTS vessel is shown in Figure 5. A frequency effect is noted for SA-105 steel tested at 15,000 psi in which fatigue cracks grow faster in low frequency fatigue environments. For purposes of setting NDT acceptance standards and assessing the lifetime of prototype hardware, a calculation was made of expected fatigue crack propagation rates using an extrapolation of the data in Figure 5 for low frequency conditions similar to service conditions,

shown on the dotted line. In order to provide a degree of conservatism in the calculations, the following conditions were assumed:

- a. Extrapolation of da/dn vs. ΔK at $f = 0.001$ Hz to $\Delta K \sim 2$ MPa \sqrt{m} . (Very severe assumption.)
- b. Use of an R ratio = 0.15 ($R = K_{min}/K_{max}$, which is more severe than the actual duty cycle.
- c. Use of data for $P_{H_2} = 15,000$ psi, which may result in overly pessimistic growth rates at $P_{H_2} = 500$ psi in the assumed duty cycle.
- d. Flaw orientation of maximum severity.
- e. Two flaw calculations were considered:
 - 1) a large sharp flaw in the body of the vessel.
 - 2) a small sharp flaw in the body of the vessel.
- f. Failure was assumed to occur when flaw penetration reached 90% of the wall thickness.
- g. Approximations in the equations of fracture mechanics were biased in the conservative direction.

The large sharp flaw was calculated to have a lifetime of 2000 cycles while the small flaw had a lifetime in excess of 14,000 cycles, following the growth curve shown in Figure 6. Thus, even severe flaws could last significant periods of time in these steels. Note also that approximation (a) is very severe, assuming no threshold for fatigue cracking when in fact a threshold might exist. It is concluded that prototype hardware can be built and safely operated for reasonable lifetimes.

A number of questions are left unanswered by the experiments and calculations performed. The effect of a discharging $FeTiH_x$ powder in contact with sharp fatigue cracks and the potential effects of atomic hydrogen charging were not completely answered by the experiments in the hydride reactor. The fatigue crack growth rates at low stress levels, the presence of a threshold stress and its magnitude, and confirmation or denial of a frequency effect for fatigue cracking, all need to be addressed in appropriate materials in the hydrogen pressure regimes of interest. Sandia Laboratories is currently initiating test programs to address these issues.

Experimental Hydrogen Pipeline

The experimental hydrogen pipeline began operating September 15, 1977. The pipeline is constructed of A106 grade B pipe steel except for stainless steel flexhoses between "pump" chamber and pipeline, which take up accumulated misfit. The pipeline is a square 6 meters long per side, with test modules in which materials experiments take place. The schematic layouts of both pipeline and modules are shown in Figures 7 and 8. Two modules, incorporating high stresses and both girth and longitudinal welds with flaws, are in place during the 4-month "shakedown" period. Operating pressure is 6.9 MPa (1000 psi) of hydrogen gas. Before introduction of hydrogen, evacuation to <100mm Hg and backfilling with nitrogen to 0.69 MPa (100 psi) is performed three times. Pressure is provided by cascading 6-packs of hydrogen into the

pipeline until 6.9 MPa pressure is reached. The gas is analyzed for oxygen by mass spectroscopy, and the centrifugal blower is turned on to provide circulation.

A linear gas velocity of 2.25-2.5 meters/second is obtained by the blower. Temperature and pressure excursions of 55°C and 0.5 MPa have been noted, as a consequence of direct solar heating of the pipeline. Consequently, a sunshade has been designed and is under construction to limit ΔT to lower levels. Other modifications under consideration include addition of an oxygen analyzer to assure that oxygen poisoning of embrittlement does not occur.

Materials tests to be performed in the experimental modules include performance of mechanical flaws and weld defects. The first generation of tests, to go into test January 1978, is internal notches ranging from 10 to 25 cm. in length and at three stress levels approaching the gross section yield stress of the A106-B test material. Burst tests in both hydrogen and in inert environments will establish baseline properties of these flawed pipe sections.

Future aspects of the program include the characterization of common pipeline defects, and assessment of their behavior in gaseous hydrogen environments. Tests of state-of-the-art pipeline materials are also anticipated, including API specification steels in seamless, spiral, and longitudinal welded forms, up to grade API-SLX-65.

To support the experimental pipeline test program and to enhance our understanding of the behavior of welds in pipeline steels in a hydrogen environment, a program has been initiated to characterize the microstructures obtained when these steels are welded under various conditions. These microstructures will be evaluated for hydrogen compatibility to enable the determination of the most desired microstructures for hydrogen service.

Metallurgy Studies

Metallurgy studies include methods of improving the properties of structural steels in hydrogen. These studies have included 1) thermomechanical treatment and alloying of low cost structural steels for hydrogen service, 2) permeation barriers and permeation studies, and 3) studies of effects of gaseous inhibitors.

The thermomechanical treatment of the alloys is the process known as warm working, which involves mechanical deformation of iron alloys above the $\gamma \rightarrow \alpha$ transformation temperature over a range of temperatures, followed by working just below the transformation temperature, to produce a fine grain size, reduced carbide sizes and produce a dislocation substructure. Alloying considerations are two fold. First, the heavy reductions in these sulfur bearing steels tend to produce elongated MnS inclusions which are very detrimental to transverse properties. Secondly, additions of precipitate forming elements tend to refine the grain size and produce precipitation strengthening while reducing the volume of pearlite in the alloy matrix. Both of these factors are conducive to improve hydrogen compatibility.

Fortunately, both approaches can be applied simultaneously by slight additions of Ce or Ti.

An experimental alloy of 0.1 w/o cerium added to A516 grade 70 steel was cast and worked. After forging to 2.5 cm thickness, it was held in air at 1100°C for 1 hour, reduced from 2.5 cm to 1.5 cm in 0.25 cm passes while cooling to 600°C, held at 554°C for 3 minutes and reduced to 1 cm thickness by 4 passes of 0.125 cm. The microstructure produced is shown in Figure 9. Pearlite colonies and cementite decorate the grain boundaries and only a slight grain elongation occurred. The grain size is about 25 microns. Globular cerium-sulfur compounds (confirmed by x-ray analysis; oxygen not detectable) are observed, rather than 30-50 micron long stringers which would be expected if no Ce addition had been made. Thus, the cerium addition successfully controlled the shape of the sulfide inclusions.

Tensile testing results confirm the effectiveness of the cerium/warm working combination. Table II summarizes the results. A small but definite anisotropy exists, with the yield strength varying 9% between longitudinal and long transverse orientations. The ductility properties in hydrogen are encouraging; for the transverse orientation, no significant loss of % RA (reduction in area) occurred. The test data reported are for single specimens, since only a limited amount of material was available from the initial laboratory heats.

Equally significant is the fracture behavior (Figure 10). Very little embrittlement appears to have occurred since the fracture was highly ductile with dimpling and tear ridges. No significant amount of cleavage was observed in the cerium-modified steel, while some cleavage was found in the unalloyed, warm-worked steel. These results, if reproducible, represent a significant improvement in the hydrogen compatibility of mild steels.

Tensile test data for 0.3 w/o Ti and 0.1 w/o Ti-modified and warm worked A516 are tabulated in Table III. Small titanium additions appear to have significant potential as hydrogen traps in carbon steels, as shown by permeation studies⁽⁵⁾ and ion implantation and profile studies⁽⁶⁾. In addition, vanadium has potential as a grain refiner in the warm working process due to its low precipitation temperature.

The initial results from these small alloying additions and the thermochemical processing have been encouraging. Therefore, 20 lb. heats of 0.1 w/o Ce, 0.1 w/o Ti, and 0.1 w/o V are being prepared. These larger heats will provide sufficient material to confirm the initial results and to optimize the thermal mechanical processing schedule.

An alternative method of providing improved performance of structural materials is to occlude hydrogen from contact with the steel. This may be done by means of either a) interposing a barrier layer of low hydrogen permeability between the metal and the gas, or b) an inhibitor which occludes hydrogen from the surface. Extensive work has been done on brushplating or selective electroplating, plasma spraying, and chemical pyrolysis for the application of hydrogen permeation resistant

coatings to susceptible substrates. These results were reported in June to the American Electroplaters Society conference and submitted for publication. In summary, the concept was found to be applicable to pressure vessels but probably not applicable to large systems such as pipelines, due to factors of the operating environment, the economic factors and difficulties of quality assurance. This work on permeation barriers have been discontinued until such time that their practical viability is evidenced.

The effect of potential gaseous inhibitors of hydrogen embrittlement was briefly studied in a series of notched bar tensile tests using mixtures of SO₂ and CO in hydrogen. The experimental results are tabulated in Table IV. Small percentages of SO₂ are effective at improving ductility in hydrogen; larger amounts of CO are required for equivalent effects. A more detailed evaluation of this concept should be conducted.

Summary of Sandia Livermore's Program Status

1. Tests to evaluate the effects of hydride discharging on the toughness and fatigue crack growth rates at frequencies much less than 1 Hz have been initiated.
2. The Experimental Hydrogen Pipeline is operational and the first internally flawed test sections will begin test in January, 1978.
3. Efforts to improve the hydrogen compatibility of pipeline steels through minor alloying additions and thermochemical processing will be expanded.

References

1. Personal communication, G. Strickland, Brookhaven National Laboratories.
2. Bernstein, I. M., Garber, R., Pressouyre, G.M., p. 37 in "Effect of Hydrogen on Behavior of Metals," Thompson, A. W., Bernstein, I. M., Eds., AIME 1976.
3. SAND76-8255, Sandia Laboratories Energy Report, "Hydrogen Compatibility of Structural Materials for Energy Storage and Transmission Applications," Robinson, S. L., December 1976.
4. Loginow, A. W., Phelps, E. H., Corrosion - NACE, 31, (1975), 404.
5. Pressouyre, G. M., Doctoral Dissertation, "The Role of Trapping on Hydrogen Transport and Embrittlement" Carnegie-Mellon University, June 1977.
6. Myers, S. M., Robinson, S. L., Stoltz, R. E., Sandia Laboratories, work in progress.

TABLE I - Test Matrix for Long-Term In-Situ Self-Loaded Tensile Specimens

Condition	Material						
	A106 Proof Stress	A106 Design Stress	A516 Proof Stress	A516 Design Stress	6061 Proof Stress	Cr-Mo Proof Stress	304 Proof Stress
Smooth Matrix	2	2	2	2	2	2	2
Notch Matrix	2	2	2	2	2	2	2
Smooth Weld	2	3	2	2	2	2	2
<u>Notched Weld</u>							
Heat Affected Zone	2	2	2	2	1	2	2
Fusion Zone	2	2	2	2	2	2	2
<u>Coated (Sn-Pb)</u>							
Smooth Weld	2	1	2	1		2	
Notched Weld	2	1	2	1		2	

TABLE II Preliminary Tensile Results on Cerium Modified Warm-Worked A516 Steel, Heat No. 102776

Specimen	Orientation	Test Condition	0.2% Yield Strength (MPa)	Ultimate Strength (MPa)	% Reduction of Area
7	Longitudinal	Uncharged/ Air Test	596	649	57.9
8	Transverse	Uncharged/ Air Test	546	611	56.6
11	Transverse	Uncharged/ 4.2 MPa H ₂	550	603	56.5

All data are single specimen.

**Table III Preliminary Tensile Results on Titanium
Modified Warm-Worked A516 Steel**

Heat #011077 0.1 w/o Titanium

Specimen	Orientation	Test Condition	0.2% Yield Strength (MPa)	Ultimate Strength (MPa)	% Reduction of Area
19	Longitudinal	Uncharged/ Air Test	715	759	60.1
21	Longitudinal	Charged/ 4.2 MPa H ₂	742	768	51.8
22	L. Transverse	Uncharged/ Air Test	708	722	57.4
23	L. Transverse	Charged/ 4.2 MPa H ₂	727	766	53.3

Heat #011477 0.3 w/o Titanium

Specimen	Orientation	Test Condition	0.2% Yield Strength (MPa)	Ultimate Strength (MPa)	% Reduction of Area
13	Longitudinal	Uncharged/ Air Test	708	738	59.9
15	Longitudinal	Charged/ 4.2 MPa H ₂	678	701	60.6
16	L. Transverse	Uncharged/ Air Test	680	694	61.9
18	L. Transverse	Charged/ 4.2 MPa H ₂	695	733	55.8

**TABLE IV Notched A516 Tensile Bar Tests in Mixtures
of Inhibitor Gas and Hydrogen**

Test	0.2% Yield Strength (Notched Bar) MPa	Ultimate Strength MPa	%RA
4.2 MPa H ₂ + 28%CO	667	808	20.5
+ 0.25%SO ₂	675	827	24.4
+ 0.5%SO ₂	700	845	34.0
+ 1.0%SO ₂	716	851	25.0

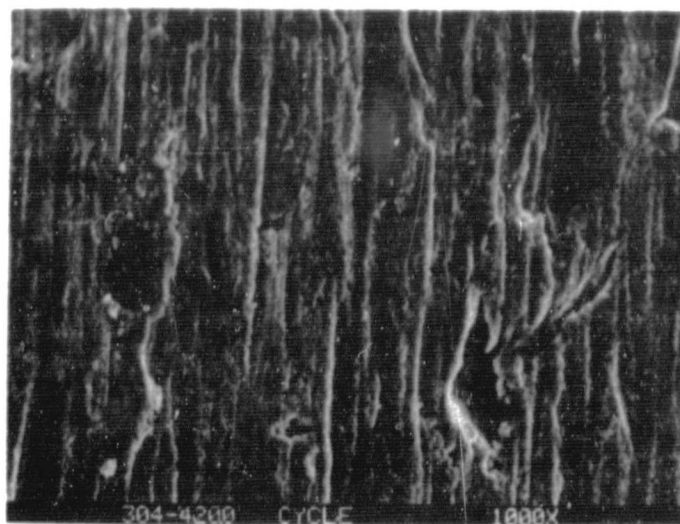


Figure 1 Surface damage in a 304 stainless steel vessel which had undergone 4254 hydride cycles. The particle at left is an FeTi particle from the hydride bed, which has become imbedded in the vessel wall.

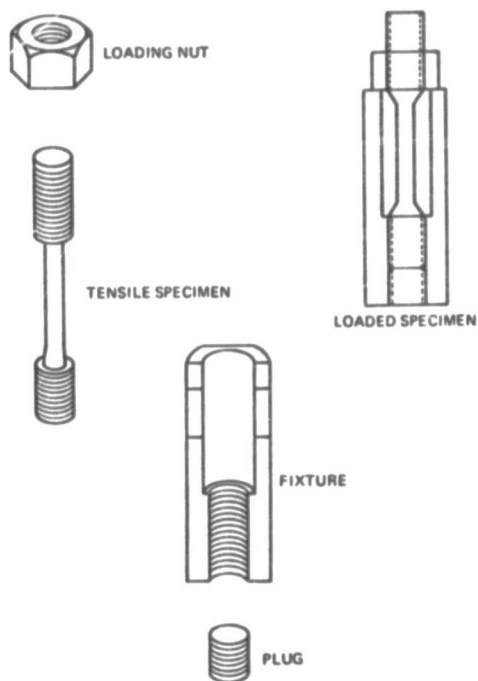


Figure 2 Self-Loading Test Specimen

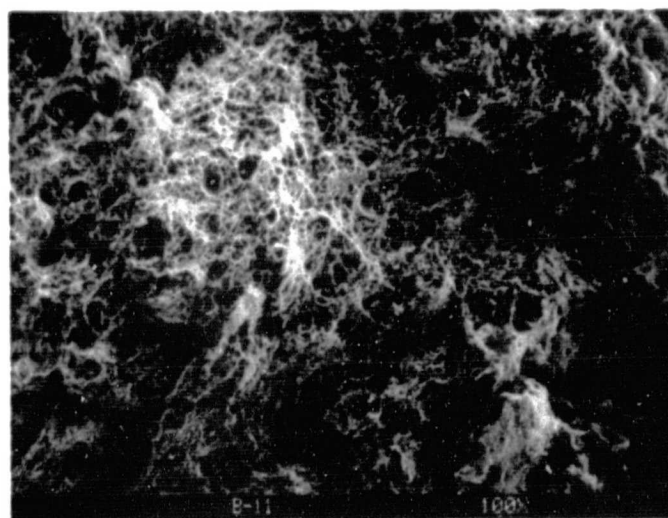
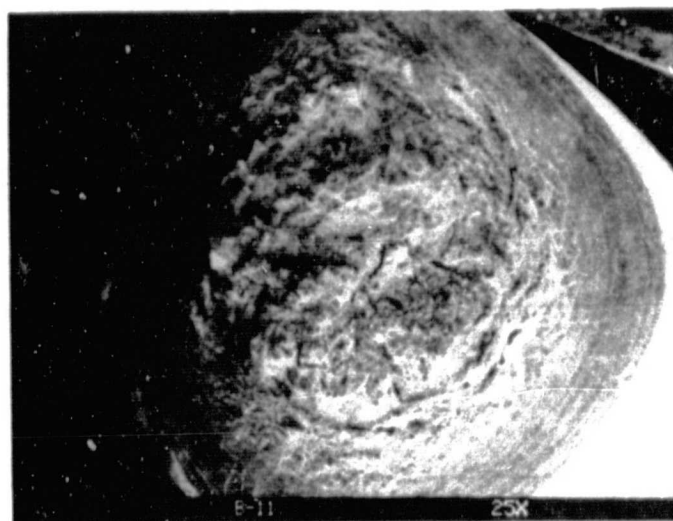


Figure 3. Fracture Surface of Specimen B-11, 2 1/2 Cr - 1 Mo Steel Exposed to FeTiH_x Environment.

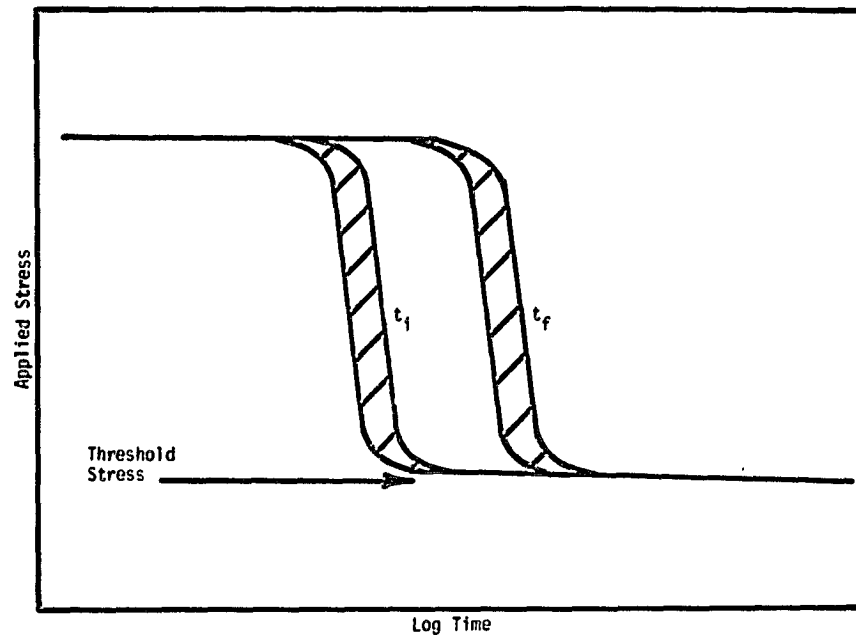


Figure 4. Schematic Delayed Failure Curve.

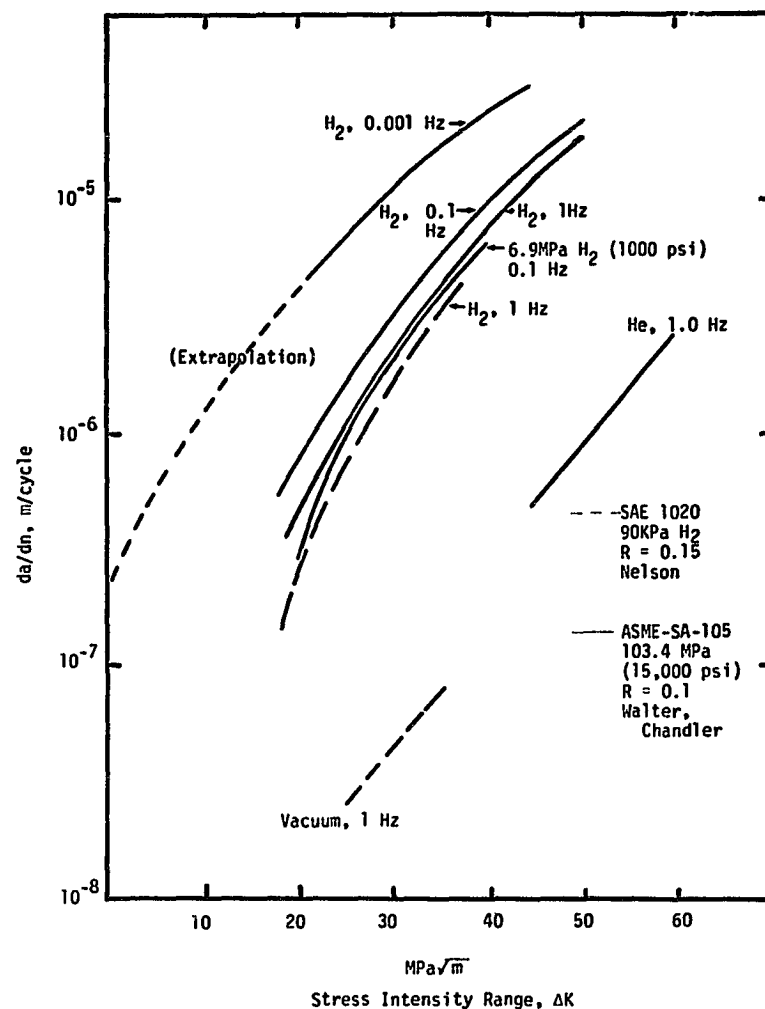


Figure 5 Collected Cyclic Flaw Growth Data for Manganese-Carbon Mild Steels in Hydrogen Gas Environments

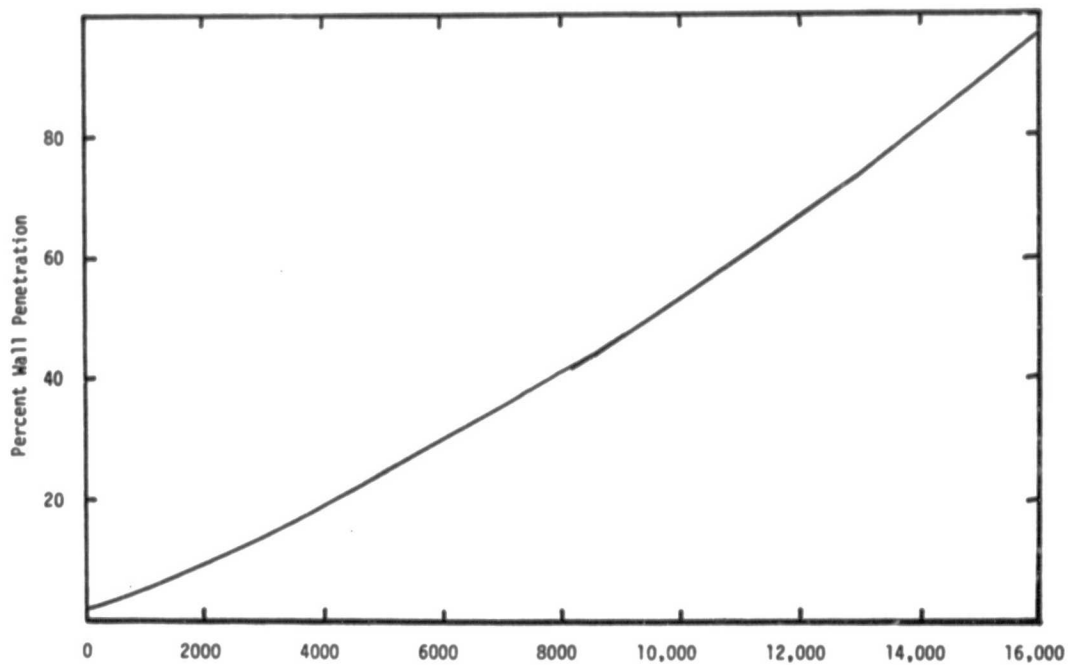


Figure 6 Thumbnail Crack Growth Curve

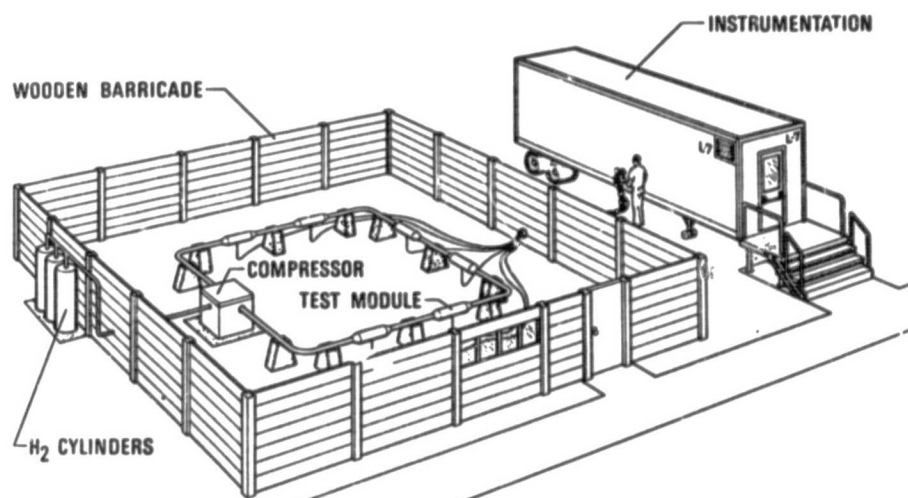
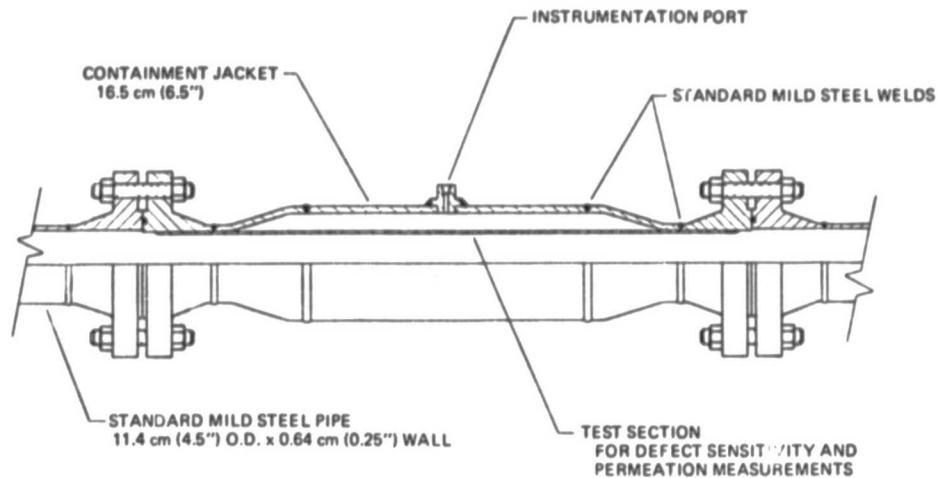


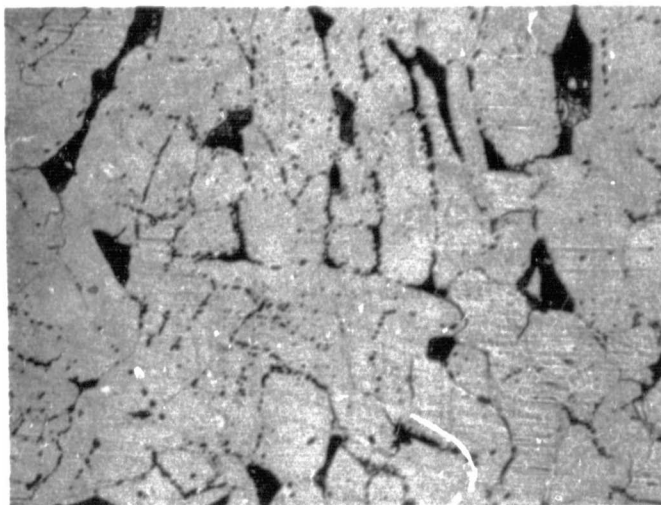
Figure 7 Experimental Hydrogen Pipeline Facility



DESIGN INFORMATION

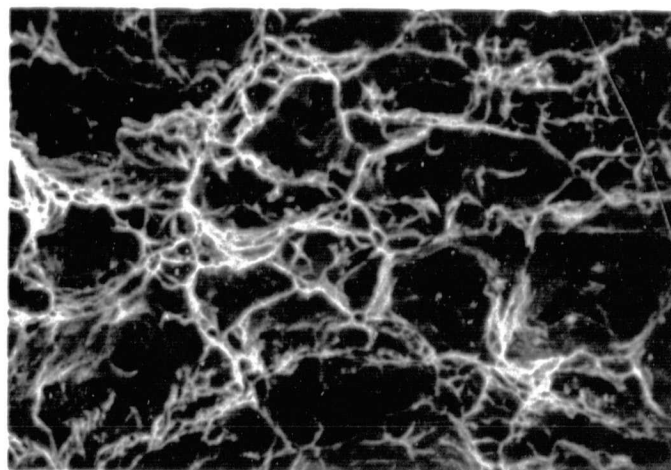
- *HYDROGEN GAS PRESSURE = 6.9 MPa (1000 psi)
- *ALL MILD STEEL CONSTRUCTION
- *MATERIAL STRESS LEVELS \approx 25% of YIELD STRENGTH
(EXCEPT TEST SECTION \approx 75%)

Figure 8 Modular Section of Pipeline



400X

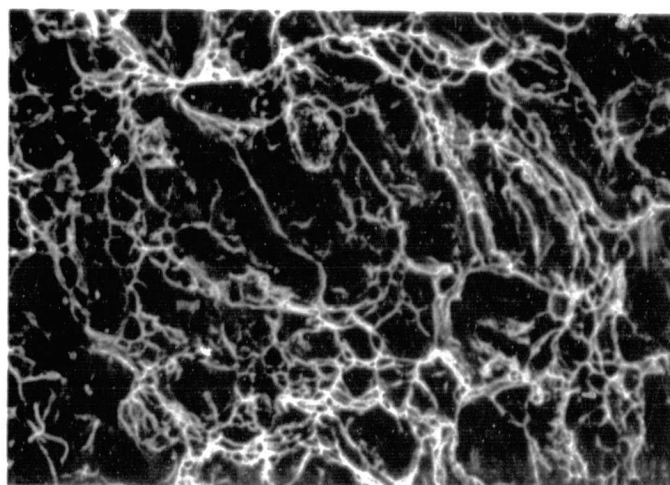
Figure 9 Optical Microstructure of the 0.1 w/o cerium modified and warm worked A516 steel, heat #102776.



Air Test

(A)

1000X



(B)

1000X

Figure 10. Fracture surfaces of long transverse smooth tensile bars of the cerium modified warm worked A516 steel. (A) is the air test, (B) is a 4.2 MPa (600 psi) H₂ gas test.

EFFECT OF STRESS STATE
ON
HYDROGEN EMBRITTLEMENT PROCESSES

M. R. Louthan, Jr. and R. P. McNitt
Virginia Polytechnic Institute
Blacksburg, Virginia 24061

Abstract

Delayed failure hydrogen embrittlement studies in high pressure gaseous hydrogen show that the susceptibility to embrittlement progressively increases as the stress state changes from uniaxial to biaxial to triaxial. This contrasts the results of dynamic tests in similar atmospheres where embrittlement is favored by uniaxial stress states. These results show that design considerations of material compatibility in hydrogen environments must include analysis of the stress-state and loading-rate during exposure. Such considerations are difficult, at present, because of (1) difficulties in extrapolating data from short-time dynamic tests to predict long time compatibility under static loads, and (2) very little definitive work on the role of macroscopic stress state in hydrogen embrittlement processes has been reported.

Introduction

Hydrogen compatibility may be a critical criteria in evaluating structural materials for use in energy storage and transmission. Correspondingly the tensile properties and fracture characteristics of many candidate materials have been studied before, during, and after exposure to various hydrogen environments. Such studies have stimulated a tabulation of metals and alloys as either susceptible, mildly susceptible or immune to hydrogen embrittlement. This type of categorization is fraught with difficulties because all too often alloys found to be relatively immune to embrittlement in one type of test are found to be highly susceptible to embrittlement in other tests. Furthermore, whenever a single test shows that a material displays a "high degree of susceptibility," that particular test can effectively eliminate the potential for using that material in hydrogen service even though different testing modes have indicated that the alloy has a reasonable hydrogen compatibility.

Delayed failure hydrogen embrittlement has received increasing attention in recent years primarily because of the accelerating usage of high strength components in aggressive environments. The concept that "maximum triaxiality" plays a vital role in the embrittlement process is primarily based on the interpretation of "static fatigue" or delayed failure tests. This concept assumes that hydrogen is localized at or near crack tips or other regions of maximum hydrostatic (or triaxial) stress. Most investigators agree that some minimum local hydrogen concentration is required to cause embrittlement (1-5). Under static loading conditions localization is diffusion controlled and the steady-state hydrogen content, C , in a region of hydrostatic stress, σ_n , at equilibrium is given by

$$C = C_0 \exp(V_0 \sigma_n / RT)$$

where C_0 = bulk hydrogen content, V = partial molar volume, and T = temperature. Whenever C is greater than the critical concentration required for embrittlement, delayed failure may occur. However, because hydrogen diffusion is slow at or near room temperature, delayed failure tests often require lengthy tieups of experimental equipment. Consequently when investigations of "unexposed" samples tested under dynamic conditions seemed to show results similar to the lengthy delayed failure studies, the use of such short time tests began to increase. Justification for the use of dynamic tests was enhanced by mechanistic studies which suggested that the embrittlement mechanism responsible for hydrogen induced degradation was the same in both delayed failure and dynamic studies. However, careful analysis indicates that, even if the "same mechanism" hypothesis is correct, test technique and stress state play critical roles in determining whether embrittlement is observed.

Hydrogen localization by classical diffusion through significant diffusion distances cannot occur during dynamic testing because of insufficient time. Under such dynamic test conditions hydrogen localization has been attributed to transport by mobile dislocations. Dislocation motion requires localized shear, not hydrostatic, stresses; therefore test conditions which favor embrittlement under static (and hence many real life) exposures are not necessarily those conditions which favor embrittlement under dynamic testing (or application). Analysis of the two methods for localizing the hydrogen indicates that a uniaxial stress state, with the attendant shear stress = $\frac{1}{2}$ tensile stress, should maximize embrittlement under dynamic conditions while, as previously shown, triaxial stresses should maximize embrittlement under static conditions.

Experimental Techniques and Results

Selection of AISI 4340 steel and A-106 steel as the materials to be studied in the program was based on discussions with staff members of DOE, SLL and VPI. The AISI 4340 steel represented an alloy known to be highly susceptible to hydrogen induced delayed failure while the A-106 represented a candidate pipeline material and was not regarded as easily embrittled. The A-106 steel (available only in tubular stock) being tested was supplied by Sandia Laboratories-Livermore and is from the stock they are testing in their hydrogen pipeline. The AISI 4340 was purchased in both tubular and plate form.

Static Tests

Right circular cylinders were fabricated from both types of steels and have been tested under various stress states. The basic design requires that the 1.27 cm wall of the 7.62 cm outside diameter pipe be reduced to 0.075 cm in the gage section. The test specimen is sealed to end caps by crushing an O-ring between the end of the specimen and the back surface of the cap. The interior cavity of the specimen is filled with an aluminum dummy block (Figure 1) to minimize the energy stored in the specimen during test. The end caps are machined to accept standard high pressure fittings and the specimen is filled to the desired hydrogen pressure (35 MPa maximum) through a valve controlled connector. Each specimen under

test is also equipped with a standard 35 MPa rupture disk on a safety head and a 35 MPa gage (Figure 2). The stress state is controlled by axial loads applied to the test specimen by means of a universal tensile machine or a creep frame when sustained, long time loading is required. Failure data to date (Figure 3) indicate that none of the standard failure theories explain the hydrogen embrittlement process.

The susceptibility of notched precharged AISI 4340 samples heat-treated to approximately 1400 MPa yield to hydrogen embrittlement was studied in delayed failure tests. The tests showed that the susceptibility to embrittlement was reduced as the constraint (and hence triaxiality) at the crack tip was reduced. The specimens contained a 60°V notch in 1.27 cm diameter rods. The notch reduced the throat diameter to 0.90 cm. The root radius of the notch was 0.005 cm. Constraint at the crack tip was controlled by drilling axial holes with a gun bore drill; increasing the hole diameter decreased the constraint and increased the resistance to delayed failure. These effects were apparent in macroscopic observations which showed the effect of both constraint and hydrogen on the shear lip which developed in delayed failure tests (Figure 4). Fractographic studies showed that even in the flat fracture region of the hydrogen charged samples, failure was occurring by both microvoid coalescence and intergranular rupture. Assuming that the intergranular rupture represents embrittlement (5), the scanning electron microscopy supports the conclusion that embrittlement is caused by hydrogen diffusion to points of maximum hydrostatic stress. In all cases, examination of near crack tip area showed a region of microvoid coalescence near the starter crack and intergranular fracture deeper in the sample. In several cases areas of intergranular fracture completely surrounded by microvoid coalescence were observed (Figure 5). These observations are in agreement with diffusion controlled, stress induced development of hydrogen concentration profiles such as shown in Figure 6 and support the argument that stress induced hydrogen transport is the major factor causing hydrogen localization during delayed failure.

The importance of stress state in controlling delayed failure hydrogen embrittlement during exposure to high pressure gaseous hydrogen was also evaluated by testing smooth plate specimens. These samples were stressed in either a four point loading apparatus (Figure 7) which simulated uniaxial loading, or in an in-house designed clamped plate assembly (Figure 8) to simulate biaxial loading. The stressed specimens were placed in a high pressure autoclave (Figure 9); the autoclave was cycled through a series of evacuations and back filling with hydrogen before being pressurized. The susceptibility of these flat plate samples to delayed failure depended on heat-treatment, stress-level and stress state. No failures were observed in 200 hours exposure of any low strength steel sample regardless of stress state during exposure. However, delayed failure in less than 90 hours was observed in the 4340 samples heat treated to 1750 MPa yield and stressed biaxially, to a calculated maximum stress of 1400 MPa (Figure 10). The companion samples stressed to 1600 MPa in

uniaxial tension did not fail. Microscopy and fractographic studies of these samples showed both microvoid coalescence and intergranular fracture.

The complex nature of the crack pattern shown in Figure 10 indicates the difficulty in determining the stress state during crack propagation in the biaxially stressed samples. Analytical techniques to improve our ability to determine the stress state-crack path interactions need to be developed so that the role of stress state can be better assessed.

The common assumption that intergranular fracture represents the surface topography formed by delayed failure hydrogen embrittlement in 4340 steel may be true; however, examination of the notched hollow round samples which had the least constraint at the crack tip and failed in delayed failure tests showed almost no evidence of intergranular fracture. This result indicated that hydrogen induced microplasticity could be involved in the fracture process. Such plasticity arguments have previously been advanced but this model for embrittlement has received very little support. Because of this "new" evidence (lack of intergranular fracture on the low constraint samples), and earlier arguments based on the Onsager principle, tests were conducted to determine the effect of hydrogen uptake on yielding in high strength steel samples. These tests were made by increasing the dead weight loading of a 4340 steel sample in a creep frame until plastic deformation was initiated. The sample was then held under load for times sufficient to insure that no further deformation was occurring. The sample was then exposed to high hydrogen fugacity. The hydrogen exposure caused plastic deformation to resume. Results which looked similar to the hydrogen induced crack growth curves of Johnson were obtained (Figure 11). Careful examination of the exposed samples did not reveal any evidence of cracking. This result indicates that one mechanism of delayed failure may be hydrogen diffusing to a region of high stress (in the notched round samples these regions were generally high triaxial stresses) and lowering the yield strength in that region. Fracture mechanics considerations show that the critical plastic zone size at the onset of failure depends on the yield strength. The size of the plastic zone is dependent on the applied stress intensity at the crack tip; thus lowering the yield stress lowers the required stress intensity for fracture and hydrogen diffusion to a crack tip could induce failure. The mode of failure is not defined by this model and could be either intergranular rupture (high triaxial stresses) or microvoid coalescence (minimal triaxial stresses). However, in either event failure is initiated because of hydrogen diffusion to regions of high lattice dilation. The tendency for such diffusion is clearly enhanced by triaxial stresses and thus such stresses enhance delayed failure hydrogen embrittlement.

Dynamic Tests

The effect of stress-state on the susceptibility of steels to hydrogen embrittlement under dynamic test conditions was examined via a disk rupture system designed and fabricated for that purpose. By controlling the radius around which

the edge of the pressurized clamped plate was allowed to bend, the location of failure initiation can be controlled. A large radius at the clamped surface caused failure to initiate under almost biaxial stress conditions (Figure 12a) in the center of the plate while a sharp radius caused failure to initiate in regions tending towards "uniaxial" tension conditions (Figure 12b). The exact stress states in the disk rupture samples have not been determined because the required elastic-plastic analysis of such a clamped plate has not been made. However, both elastic analysis and intuition indicate a large difference in stress states under the two burst conditions. The effect of stress state on the susceptibility to dynamic hydrogen embrittlement was then determined by comparing the burst pressures of nearly identical samples in oxygen and hydrogen. The pressure ratio p_{O_2}/p_{H_2} is then used as a measure of embrittlement.

The results of the burst tests indicate that under dynamic rather than static loading conditions, hydrogen embrittlement is enhanced by uniaxial rather than biaxial (or triaxial) loadings. Burst tests in the disk rupture system demonstrated that when samples were ruptured in biaxial tension the burst pressure was not significantly affected by the test gas. Tests of similar samples under more uniaxial conditions, however, showed that when hydrogen was used as a burst gas, the burst strength was reduced by 20%. This result was expected because, as described in the introduction, dynamic tests were thought to require dislocation transport and hence high shear stresses to localize hydrogen.

Conclusions

The most significant conclusion of these tests is the obvious difficulty in using short time dynamic tests to predict the effects of hydrogen on long time behavior under static loads. Clearly different variables control the hydrogen localization mechanism in the two types of tests and extrapolation of data obtained under one set of test exposure conditions to any other set of service (or potential service) conditions should be made carefully. These results also point out the need for continuing (and increased) effort to determine the role of stress state in hydrogen embrittlement process so that data and models can be developed to permit the maximum use of the large body of hydrogen embrittlement information in design considerations.

Acknowledgments

These studies have, in part, been possible due to the financial support of DOE through Contract E(40-1)5255. The authors wish to thank T. S. Sudarshan and J. Murali for their assistance on this project.

References

- 1) Rice, J. R., "Hydrogen and Interfacial Cohesion", Proceedings of conference on Effects of Hydrogen on Behavior of Materials (A. W. Thompson and I. M. Bernstein, eds.) TMS-AIME, New York, p. 455 (1976).
- 2) Louthan, M. R. and McNitt, R. P., "Role of Test Technique on Evaluating the Mechanism of Hydrogen Embrittlement", Proceedings of conference on Effects of Hydrogen on Behavior of Materials, TMS-AIME, New York, p. 559(1976).
- 3) Beachem, C., "A New Model of Hydrogen-Assisted Cracking," Met. Trans., Vol. 3, p. 437 (1972).
- 4) Oriani, R. A., "A Mechanistic Theory of Hydrogen Embrittlement of Steels", Ber. Bunsenges Phys. Chem., Vol. 76, p. 848 (1972).
- 5) Thompson, A. W. and Bernstein, I. M., Reviews on Coatings and Corrosion, Vol. 2, p. 3 (1975).

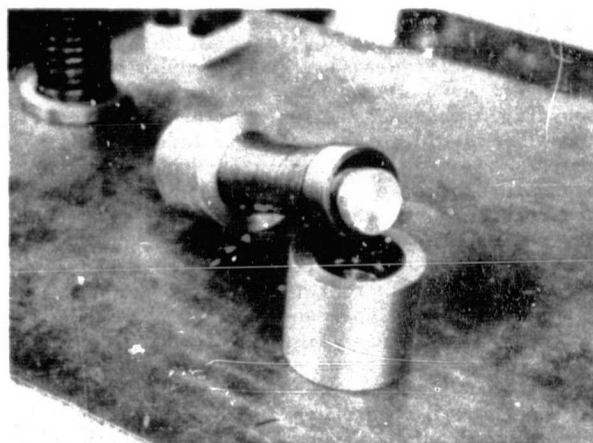


Figure 1. Cylindrical test specimen for evaluation of the effects of stress state on susceptibility to hydrogen embrittlement.

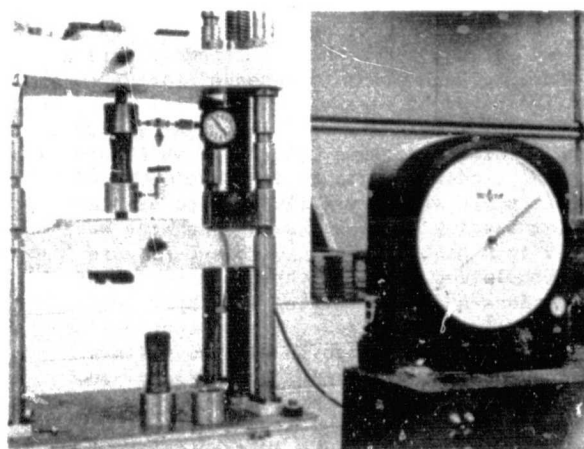


Figure 2. Cylindrical specimen in instron tensile machine.

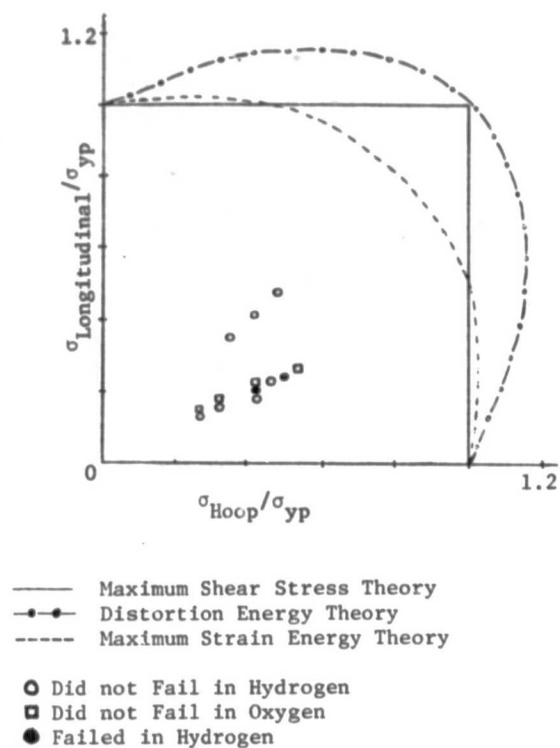


Figure 3. Delayed failure data for specimens tested under biaxial, $\sigma_H = \sigma_L$, and standard cylinder, $\sigma_H = 2\sigma_L$, states of stress.

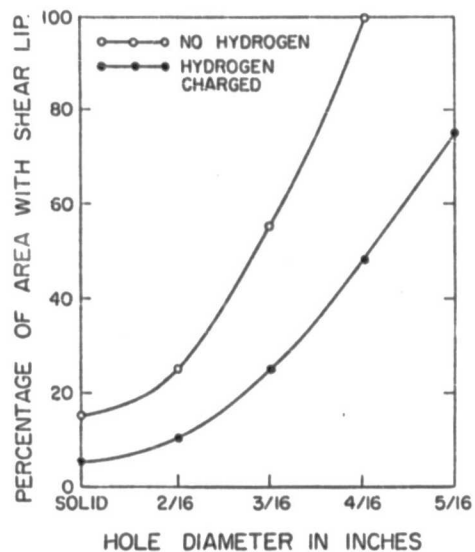


Figure 4. Effect of constraint and hydrogen on shear lip in notched hollow round samples.

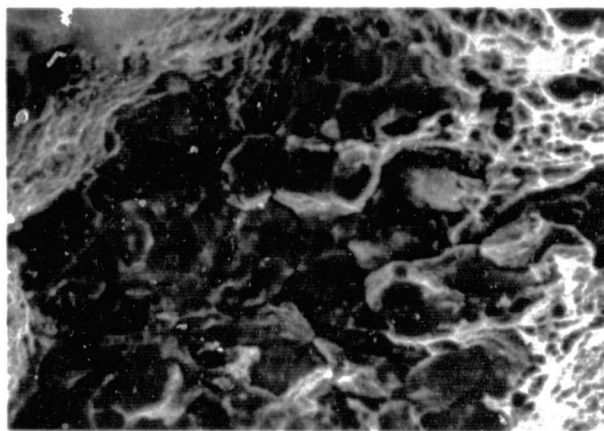


Figure 5. Intergranular fracture and microvoid coalescence on fracture surface of sample failed in delayed failure test.

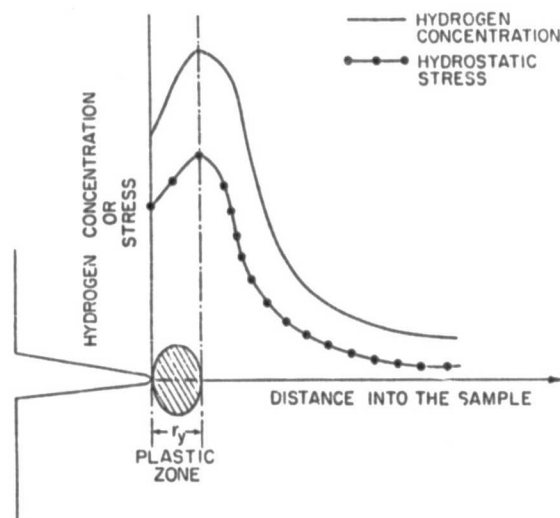


Figure 6. Predicted hydrogen concentration profiles at crack tip.



Figure 7. Four point loaded sample and test apparatus.

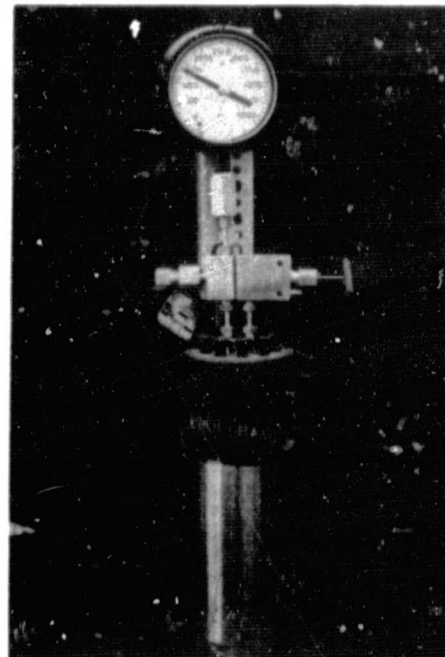


Figure 9. High pressure hydrogen autoclave for exposing delayed failure samples.

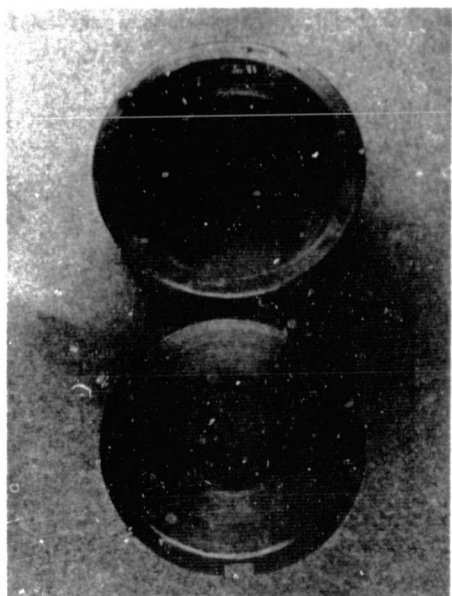


Figure 8. Clamped plate assembly for testing sheet specimens in biaxial tension.



Figure 10. Failed biaxially loaded sample.

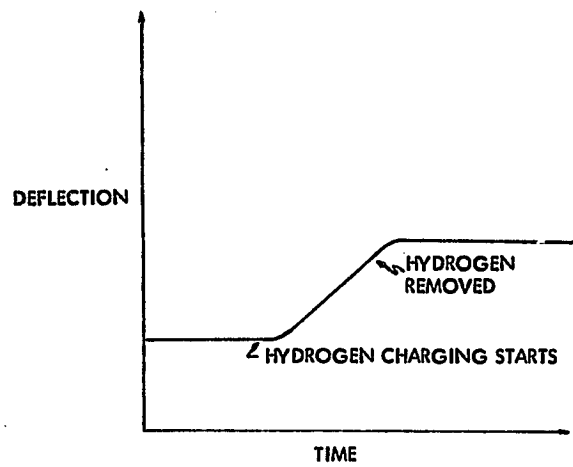


Figure 11. Effect of hydrogen charging on tensile strain in smooth bar tensile sample.

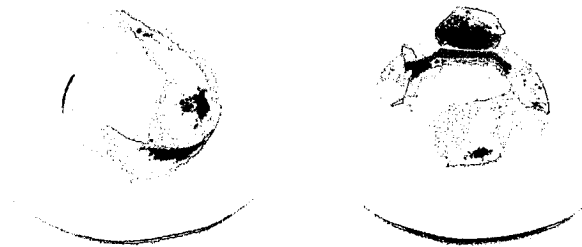


Figure 12. Disk rupture test specimens from biaxial and "uniaxial" loadings.

EVALUATION OF LASER WELDING TECHNIQUES FOR HYDROGEN TRANSMISSION

J. A. Harris Jr. and J. Mucci
Pratt & Whitney Aircraft Group
Government Products Division
West Palm Beach, Florida

Abstract

This program will evaluate the smooth and notched tensile, low-cycle-fatigue and fracture toughness properties of two pipeline materials, ASTM A312 Grade AISI 304L and ASTM A106 Grade B, in parent and welded (Laser, Electron Beam and GTA) conditions. Testing in air and 13.8 MPa (2000 psig) gaseous hydrogen will establish the susceptibility of the materials to hydrogen environment effects. Metallurgical analysis of the weldments and fractographic evaluations of failed test specimens will be conducted to supplement the mechanical property characterizations and aid in determining if laser welding is feasible for hydrogen transmission pipeline application. The program started on 30 September 1977. This paper discusses the program objectives, approach and status to date.

I. Introduction

The evolution of a hydrogen energy system will require major technology development programs. Regardless of the means of production, transmission and storage of hydrogen will be required. Current gas transmission pipeline technology will form the base from which hydrogen transmission will grow. However, unlike natural or hydrocarbon gases, hydrogen has a unique effect upon most metals in that it embrittles or degrades properties. This effect upon material properties has been studied most extensively in the development of hydrogen-fueled rocket engines. For space applications, use of expensive, highly alloyed materials is justified. The economics of gas transmission systems, however, require the use of lower cost, more plentiful structural materials.

Mild and low alloy steels are being considered because of the economic factor. A problem exists, however, in that most ferritic steels are susceptible to degradation of structural properties resulting from hydrogen exposure over a wide range of conditions. Since numerous welded joints are required in the fabrication of transmission pipelines and storage systems, an additional problem exists: weldments appear more susceptible to hydrogen degradation (embrittlement) than the parent alloys. Moreover, various welding processes may yield different degrees of susceptibility. In general, welding processes that minimize fusion and heat-affected zones tend to produce high integrity welds that are less susceptible to hydrogen degradation and also produce joints that maintain many of the characteristics of the parent material.

Research at the United Technologies Research Center (UTRC) indicates that laser weldments possess these desired qualities. The Pratt & Whitney Aircraft Government Products Division has conducted extensive parent and welded material evaluations in gaseous hydrogen environments. These divisions of the United Technologies Corporation will determine the feasibility of laser welding as a viable means of fabricating and/or joining hydrogen transmission piping. The process for obtaining results and conclusions from this study is diagramed in Fig. I-1.

This program is being conducted under Department of Energy (ERDA) Contract EC-77-C-02-4355, sponsored by Dr. James H. Swisher, Assistant Director, Physical Storage Systems, Washington, DC under the technical cognizance of Dr. Howard G. Nelson, NASA-Ames Research Center, Moffitt Field, California. Mr. Joe Mucci is the Pratt & Whitney Aircraft Group, Government Products Division program manager.

John A. Harris Jr. and Joe Mucci are Project Materials Engineer and Assistant Project Materials Engineer respectively in the Materials and Mechanics Technology Laboratory of the Pratt & Whitney Aircraft Group, Government Products Division of the United Technologies Corporation, P. O. Box 2691, West Palm Beach, Florida, 33402.

II. Program Approach

This program consists of smooth and notched tensile, low-cycle-fatigue (LCF) and fracture toughness tests of two pipeline materials in the parent and welded (laser, electron beam and gas tungsten arc) conditions. Comparison of test results in air and 13.8 MPa (2000 psig) gaseous hydrogen will establish the susceptibility of the materials to hydrogen environment effects. The program is diagramed in Fig. II-1. The tests to be conducted and the environmental conditions are listed in Table II-1.

A. Materials and Welding

The test materials, ASTM A312 Grade 304L stainless steel and ASTM A106 Grade B carbon steel, to be evaluated have been procured in the form of No. 5 Schedule 160 Seamless Pipe [141.3-mm (5.562-in.) outside diameter, 15.9-mm (0.625-in.) wall thickness]. Weldments will be produced by the Automatic Gas Tungsten Arc (GTA), electron beam and laser processes by joining two 50.8-mm (2.0-in.) lengths of pipe (Fig. II-2).

Gas tungsten arc and electron beam welding will be performed using current process schedules and specifications. Calibration welds will be made to verify and/or select process parameters and then the pipe samples will be welded. Visual, radiographic, and fluorescent penetrant inspection will be performed to ensure soundness.

Laser welding will be performed by the UTRC. Since laser welding is a relatively new process, weld schedules for specific materials and thicknesses have not been developed. Therefore, appropriate laser welding parameters will be determined for the ASTM A106B and AISI 304L steels that are to be used in this program. Initial parameters will be selected on the basis of general penetration-speed-power information, which has been established for laser welding. It is anticipated that a laser power level of approximately 12 to 14 kW will be required; welding speed at this power level will be varied from about 63.5 to 127.0 cm/m (25 to 50 in./m). Bead-on-plate penetrations will be formed in the materials and subjected to visual inspection.

The conditions at which optimum bead-on-plate penetrations are formed will be used to form direct butt welds between pipe sections. These welds will be subjected to visual, radiographic, and selected metallographic inspection. The latter is important for selection of weld parameters since the nature of the weld bead shape and grain structure have been related to the mechanical properties. Attempts will be made to generate a weld bead exhibiting a uniformly-tapering cross section from top to bottom. This weld bead shape, which would be expected to promote progressive solidification from bottom to top, also would be expected to promote expulsion of gases from the weld zone. A weld shape that exhibits a narrow waist, on the other hand, often leads to trapped gases in the lower weld zone.

regions, as well as to the generation of shrinkage cracks. Within the limitations imposed by bead requirements weld parameters will be selected at the highest corresponding speed (i.e., with the lowest specific energy input) to attain the smallest possible grain size.

Sample weldments will be formed in the subject materials using the selected parameters. Direct butt welds will be made between 50.8-mm (2.0-in.) pipeline sections using inert gas shielding provisions to prevent atmospheric contamination of the welds. Slope-out procedures will be employed at the end of the weld to eliminate the termination defect that occurs in deep-penetration welds without this procedure. Welds will be inspected visually and radiographically, and then forwarded to the Government Products Division for evaluation of mechanical properties in a hydrogen environment.

B. Specimens

Solid, externally pressurized specimens will be used for each test. These specimens will be machined from the pipe sections illustrated in Fig. II-2. Test specimens are shown in Fig. II-3 and described briefly in the following paragraphs.

1. Tensile Specimens

Smooth and notched specimens will be used for this testing. Smooth specimens will have a 6.40-mm (0.252-in.) gage diameter and a reduced section length of 27.0-mm (1.062-in.). Notch specimens ($K_t=8.0$) have a larger diameter of 9.5-mm (0.375-in.) and a notch diameter of 5.9-mm (0.234-in.) machined in the center of the specimen reduced section at a 60-deg angle, with a 0.038-mm (0.0015-in.) radius at the apex of the notch. The welded materials specimen blanks will be given a light etch and the gage section oriented such that the notch will be positioned in the center of the fusion or Heat Affected Zone (HAZ) areas.

2. Fracture Toughness Specimen

A 1w, 12.7-mm (0.50-in.) thick, compact tensile specimen, conforming to ASTM E-399-74 specifications, will be used for the fracture toughness tests. The welded specimen starter notch will be oriented so that the fatigue precrack will be located in the fusion or HAZ areas.

3. LCF Specimen

The LCF specimen incorporates integral machined extensometer collars. A calibration procedure has been established to relate the maximum strain-to-collar deflection during both the elastic and plastic portion of the strain cycle. The specimen design and calibration procedure were verified both experimentally and analytically.

All specimens will be cleaned and packaged prior to testing to protect them from surface contamination.

C. Testing and Evaluation

The test effort for this program consists of the mechanical properties tests listed in Table II-1 and described below:

1. Smooth tensile tests will be conducted in air and gaseous hydrogen at ambient temperature using applicable ASTM E-8 procedures.
2. Notch tensile tests will be conducted in air and gaseous hydrogen at ambient temperature using applicable ASTM procedures. The notch will have a stress concentration factor (K_t) of 8.

3. Low-cycle fatigue tests (completely reversed-mean strain of zero, -axial strain controlled) will be conducted in air and gaseous hydrogen.

4. Fracture toughness tests will be conducted at ambient pressure in air at ambient temperature using ASTM E399 procedures where applicable. In the event valid K_{IC} conditions are not met, J integral methods will be used to obtain fracture toughness values.

All of the hydrogen testing will be conducted in 13.8 MPa (2000 psig) gaseous hydrogen. This is the pressure projected for economical transmission of hydrogen (Ref. 1). In this program, it is proposed to go directly to the anticipated operating pressure and establish feasibility based upon performance in that environment. The effects of potential hydrogen pickup during welding, or thermally charged specimens will not be investigated as they appear more academic in light of the anticipated operating environment and scope of this program.

Metallurgical evaluation will be conducted to characterize the parent material and welds. This evaluation will include macroetch, microhardness profiles, and phase identification. In addition, metallographic and fractographic evaluation will be conducted on representative samples of failed test specimens to aid in explaining test results.

III. Test Facilities

The Government Products Division of Pratt & Whitney Aircraft maintains a dedicated facility for conducting materials property evaluations in high pressure gaseous environments. The facility was originally established to perform materials properties tests for space propulsion systems with various gaseous environments at pressures to 34.5 MPa (5000 psig) and temperatures to 1144°K (1600°F). The testing equipment includes machines for performance of tensile, fracture toughness, fracture mechanics, high and low cycle (strain controlled) fatigue and creep/stress rupture tests. Basically the machines are closed loop servo-controlled systems with programmable controllers, located in isolated test cells with the associated gas handling systems.

The test facilities have been described in detail in previously published works (Ref. 2-8), and will not be described in this paper.

IV. Status

We are currently in the first month of this eight (8) month program. The AISI 304L and ASTM A106B materials in the form of seamless pipe have been procured, and test facilities are being prepared.

References

1. Gray, H. R., and H. G. Nelson, et. al., *Potential Structural Materials Problems in a Hydrogen Energy System*, NASA TM X-71752 NASA Lewis Research Center, Cleveland, Ohio, June 1975.
2. Van Wanderham, M. C., and J. A. Harris, Jr., "Low Cycle Fatigue of Metals in High Pressure Gaseous Hydrogen at Cryogenic, Ambient and Elevated Temperatures," 1971 WESTEC Conference, Los Angeles, California. I coming

3. Harris, J. A., Jr., J. F. Schratt, and M. C. Van Wanderham, "Creep Rupture Properties of Materials in High Pressure Hydrogen at Elevated Temperatures," Proceedings of Third National SAMPE Technical Conference, Huntsville Alabama, October 1971.
4. Harris, J. A., Jr., and M. C. Van Wanderham, "Various Mechanical Tests Used to Determine the Susceptibility of Metals to High Pressure Hydrogen." *Hydrogen Embrittlement Testing*, ASTM Special Technical Publication 543, American Society for Testing and Materials, Philadelphia, Pennsylvania, 1974 pp. 198-221.
5. Harris, J. A. Jr., and M. C. Van Wanderham, "Properties of Materials in High Pressure Hydrogen at Cryogenic, Room, and Elevated Temperatures," FR-5768, Contract NAS8-26191, Marshall Space Flight Center, Alabama, July 1973.
6. Harris, J. A., Jr., and M. C. Van Wanderham, "Influence of Gaseous Hydrogen on the Mechanical Properties of Incoloy 903," FR-7175, Contract NAS8-30744, Marshall Space Flight Center, Alabama, September 1975.
7. Mucci, J., and J. A. Harris, Jr., "Influence of Gaseous Hydrogen on the Mechanical Properties of High Temperature Alloys," FR-7746, Contract NAS8-30744, Marshall Space Flight Center, Alabama, July 1976.
8. Mucci, J., J. R. Warren, and J. A. Harris, Jr., "Mechanical Properties of Several Nickel Alloys in Hydrogen at Elevated Temperatures," FR-8971, Contract NAS8-30744, Marshall Space Flight Center, Alabama, September 1977.

Table II-1. Experimental Test Outline to Determine the Susceptibility of Welded Pipeline Materials to Hydrogen Degradation

Material	Weld Type	Environment ^a	Mechanical Properties Tests			
			Smooth Tensile	Notch Tensile ^b	Low-Cycle Fatigue	Fracture Toughness
AISI 304L	Parent Material	Air	2	2	2	2
		Hydrogen	2	2	2	
	GTA	Air	2	2		2
		Hydrogen	2	2	2	
	GTA (HAZ)	Air		2		2
		Hydrogen		2		
	EB	Air	2	2		2
		Hydrogen	2	2	2	
	EB (HAZ)	Air		2		2
		Hydrogen		2		
	Laser	Air	2	2		2
		Hydrogen	2	2	2	
	Laser (HAZ)	Air		2		2
		Hydrogen		2		
AISI 304L	Total	Air	8	14	2	14
		Hydrogen	8	14	8	
ASTM A106B	Total	Air	8	14	2	14
		Hydrogen	8	14	8	
Total Specimen Tests - 136			32	56	20	28

^aAir Tests at 297°K (75°F), 1 atmosphere

Hydrogen Tests at 297°K (75°F); 13.8 MPa (2000 psig)

^bStress Concentration Factor, $K_T = 8.0$

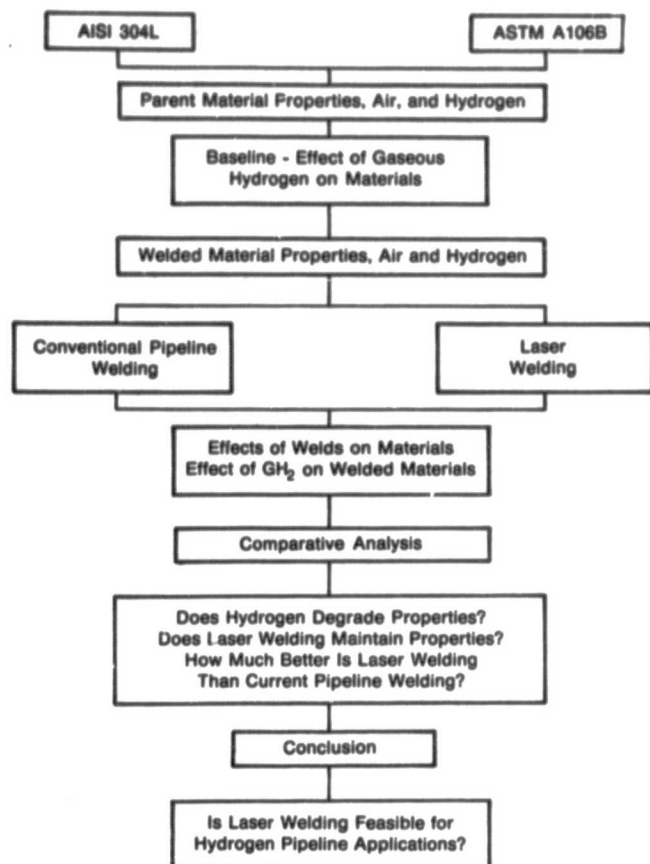


Fig. I-1. Process for Obtaining Program Results and Conclusions from the Laser-Welded Hydrogen Transmission Pipeline Evaluation

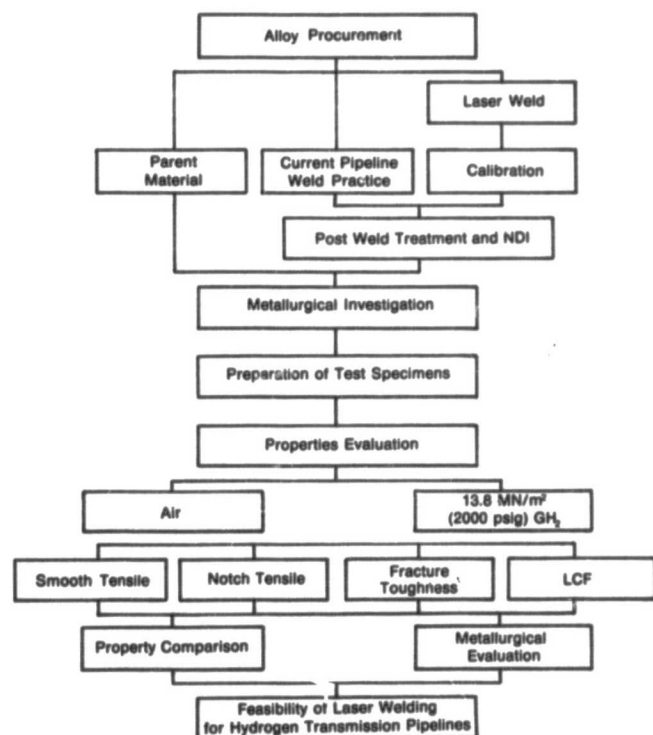


Fig. II-1. Program for the Evaluation of Laser-Welded Hydrogen Transmission Pipelines

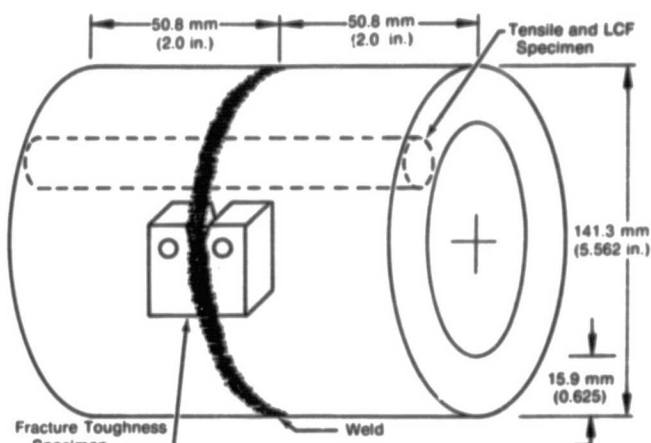


Fig. II-2. Pipe Weldment Showing Specimen Orientation

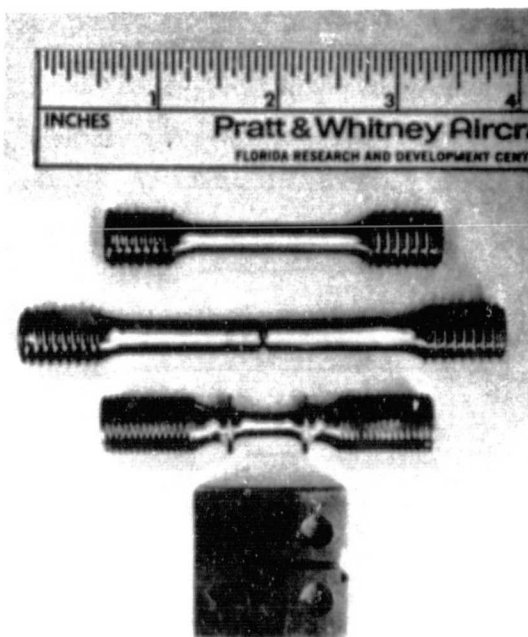


Fig. II-3. Test Specimens for Evaluating Laser-Welded Hydrogen Transmission Pipeline Material-Top to bottom: Smooth Tensile, Notch Tensile, Low Cycle Fatigue and Fracture Toughness

SESSION IV
HYDROGEN STORAGE - HYDRIDES

**THE METAL HYDRIDE DEVELOPMENT PROGRAM AT BROOKHAVEN
NATIONAL LABORATORY**

J. R. Johnson and J. J. Reilly
Brookhaven National Laboratory

HYDROGEN-TECHNOLOGY EQUIPMENT TEST PROGRAM AT BNL

G. Strickland, A. H. Beaufreire, and M. J. Rosso
Brookhaven National Laboratory

**HYCSOS: A CHEMICAL HEAT PUMP AND ENERGY CONVERSION
SYSTEM BASED ON METAL HYDRIDES**

D. M. Gruen, I. Sheft, G. Lamich, and M. H. Mendelsohn
Argonne National Laboratory

DRI RESEARCH PROGRAM ON IMPROVED HYDRIDES

C. E. Lundin, F. E. Lynch, and C. B. Magee
Denver Research Institute

**A THERMODYNAMIC AND ECONOMIC STUDY OF VARIOUS TECHNIQUES
FOR THE LARGE SCALE PRODUCTION OF HYDRIDING GRADE FeTi**

C. J. Trozzi and G. D. Sandrock
The International Nickel Company, Inc.

**STATIONARY HYDRIDE VESSEL OF LARGE DIAMETER --
PROGRAM PLAN**

R. E. Billings, R. L. Woolley, and J. H. Ruckman
Billings Energy Corporation

142

THE METAL HYDRIDE DEVELOPMENT PROGRAM
AT BROOKHAVEN NATIONAL LABORATORY

J. R. Johnson and J. J. Reilly
Division of Basic Energy Sciences
Brookhaven National Laboratory
Upton, N.Y. 11973

Abstract

This program is in the nature of a progress report through the period September 30, 1976 to September 30, 1977. The following subjects will be discussed: the influence of the free energy change and the metal atom mobility upon the reaction of intermetallic compounds with hydrogen; the properties of a ferro-titanium alloy hydrides formulated for a specific application (H_2 - Cl_2 dual mode cell); the effect of cyclic hydriding and dehydriding on FeTi; the $TiCr_2$ -H system and its properties.

I. Introduction

Over the past year our metal hydride development program has focused on the following areas: (1) a general consideration of the reaction of intermetallic compounds and alloys with hydrogen; (2) the properties of ferro-titanium alloy hydrides; (3) a definition of the $TiCr_2$ -H system; (4) properties of substituted $TiCr_2M_n$ alloy hydrides; (5) management responsibilities for several DOE contracts in this area. This report will be concerned with items 1-4. It should also be noted that items 1, 2 and 3 are areas which also received support from the Division of Basic Energy Sciences which has contributed in part to the results presented herein.

II. On the Reaction of Intermetallic Compounds with Hydrogen

It is rather difficult to predict a priori whether an intermetallic compound will react with hydrogen or which reaction path will be followed and what products will form. However, some empirical predictive theories have been developed, of which the most notable is the theory of Reversed Stability as proposed by Miedema et al. [1]. This theory has been quite useful in systems involving AB₅ alloys, but it has enjoyed only limited success in those involving first row transition intermetallic compounds (e.g., FeTi, $TiCr_2$). We have found, however, that intermetallic-hydrogen systems, without exception, will obey three rather simple rules. They are as follows:

1. In order for an intermetallic compound to react directly and reversibly with hydrogen to form a distinct hydride phase, it is necessary that at least one of the metal components be capable of reacting directly and reversibly with hydrogen to form a stable binary hydride.

2. If a reaction takes place at a temperature at which the metal atoms are mobile, the system will assume its most favored thermodynamic configuration.

3. If the metal atoms are not mobile (as is the case in low temperature reactions), only hydride phases can result, which are structurally very similar to the starting intermetallic compound.

Rule 1 is purely empirical. It is based on our own and other's experimental observations [2]. The latter two rules are firmly based on established thermodynamic and structural principles. They are, obviously, not new concepts. They refer to two temperature dependent variables, the free energy and the metal atom diffusion rate, either one of which may be the dominant factor in system behavior. We have found their explicit statement to be quite useful and have altered both our experimental procedures and program direction substantially.

III. Ferro-Titanium Alloy Hydrides

In this area we have focused primarily on synthesizing a hydride of the type $TiFe_xMn_yH_2$ which would have optimized properties in relation to the H_2 - Cl_2 dual mode electrolytic cell [3]. The target requirements for this material are as follows:

Effective H storage capacity	1.5 wt %
Maximum activation temperature	<100°C
Minimum discharge press @ 60°C	3 atm
Maximum charging press @ 40°C	34 atm
(for stated storage capacity).	

A number of alloys were formulated which satisfy the above criteria; their composition and pertinent properties are given in Table 1. At this time we consider the alloy having the composition $TiFe_{0.85}Mn_{0.15}$ to be optimum for the H_2 - Cl_2 unit. Its pressure-temperature-composition relationships are summarized in Figure 1. It is worth noting that hysteresis in this system is considerably reduced compared to that of the $TiFe$ -H system as shown in Figure 2.

We have previously reported that the activity of FeTi towards hydrogen is a sensitive function of the concentration of oxygen in the gas phase and as little as 10 ppm O_2 in H_2 has a detectable effect [4]. During the past year we investigated the effect of chlorine in hydrogen gas. The results of these experiments are summarized in Table 2. They differ from those obtained in the oxygen contamination experiments in the following respect: there was no detectable effect at an initial concentration of 10 ppm Cl_2 ; there were substantial effects at higher concentrations and at these levels the samples could not be completely reactivated. It should also be noted that Cl_2 may transform to HCl under the experimental conditions, whether it does so in fact is probably of academic interest only.

Iron titanium hydride is metastable with respect to the formation of TiH_2 and Fe_2Ti . In several long term experiments we have subjected FeTi to ~30,000 hydriding-dehydriding cycles with no detectable deterioration in performance. One sample was given particular scrutiny in this respect. It was cycled ~13,000 times over a six-month period. Each cycle was 12 minutes long during which the temperature was varied from ~-70°C to +110°C and the pressure from 32 to 34 atm. The average composition change, in terms of the atom ratio, H/Ti, was 1.1 per cycle. No deterioration in performance was detected as a function of time or cycles as measured by the constancy of

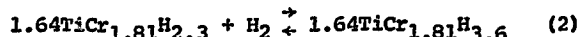
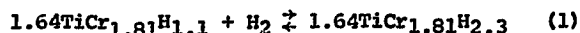
$\Delta(H/Ti)$ per cycle. Further, there was no evidence of the presence of any TiH_2 or Fe in the alloy upon removal of the sample from the system as determined by x-ray diffraction analysis. A small amount of Fe_2Ti was present in the original alloy which, as far as could be determined, did not increase over the course of the experiment. However, there was a large change in the magnetic susceptibility as shown in Figure 3 [5]. Such an effect has been observed by Hempelmann and Wicke [6] and they attributed it to the formation of small iron clusters formed by the exchange of Ti and Fe atoms in the ordered CsCl lattice. This exchange is made possible even at low temperatures ($\sim 100^\circ C$) because of the distortion of the metal lattice caused by dissolved hydrogen. It is noteworthy, however, that the change in magnetic properties for the highly cycled sample was no greater than that observed in the sample of Hempelmann and Wicke which had undergone only several cycles over a period of 6 weeks.

While no significant disproportion of $FeTi$ has been noted even at elevated temperatures ($\sim 450^\circ C$), other Ti intermetallic compounds, which form ternary hydrides at room temperature, have been observed to do so. Yamanaka, et al. [7] report the following alloys disproportionate, at the indicated temperature, in the presence of hydrogen; $TiNi$ ($500^\circ C$), Ti_2Ni ($250^\circ C$), $TiCu_3$ ($500^\circ C$), $TiCu$ ($200^\circ C$) and Ti_2Cu ($200^\circ C$). We have also noted the disproportion of Ti_2Cu at $> 350^\circ C$.

IV. Ti-Cr Alloy Hydrides

The Ti-Cr alloy system exhibits one intermetallic compound, $TiCr_2$, of which there are two temperature dependent allotropes [8]. Both are Laves phases, the low temperature form having the cubic $MgCu_2$ (C15) structure while the high temperature form has the hexagonal $MgZn_2$ (C14) structure. Both forms will react with hydrogen to form hydride phases but only the $TiCr_2$ (C15)-H system has been defined [9].

At room temperature the limits of homogeneity for the C15 phase have compositions corresponding to $TiCr_{1.71}-TiCr_{1.92}$. At $-78^\circ C$ and 60 atm pressure, the hydrogen saturated C15 phase will react sequentially with hydrogen to form two distinct hydride phases:



The product of reaction (2) represents the highest hydrogen content of the solid phase observed to date.

A p-c-t diagram for the system is shown in Figure 4. It should be mentioned that in order to obtain single phase C15 alloy samples a rather extensive and complex annealing treatment is required. If mixed phase samples are used, reproducible data are not easily obtained and the isotherms are distorted as shown in Figure 5. This system is notable for the all but non-existent hysteresis effect as illustrated in Figure 6. It will be noted that there is $1^\circ C$ difference between the sorption and desorption isotherm, if both isotherms were determined at the same temperature they probably would be, within the experimental error, coincident.

Whereas the theory of Reversed Stability would predict the formation of stable hydrides from $TiCr_2$ they are, in fact, very unstable, even to the point of limited utility for practical applications. However, as with other alloy hydrides it is possible to modify their properties by composition changes. An example of such modification is shown in Figure 7, in which Mn has been substituted in part for Cr. The difference in behavior between the annealed and the as-cast alloy is striking. The sloping plateau is attributed to small concentration gradients in the alloy which can be removed by annealing. Lynch has found this effect to be common in such substituted alloys [10].

Finally, as would be expected, both ternary hydrides are metastable with respect to formation of TiH_2 and Cr. However, upon short term exposure of $TiCr_{1.2}$ (C15) to hydrogen at $450^\circ C$ there was no indication of any formation TiH_2 and/or Cr.

Table 1

HYDROGEN STORAGE CAPACITY OF $TiFe_xMn_y$ ALLOYS UNDER PROJECTED H_2 - Cl_2 CELL OPERATING CONDITIONS

Alloy Composition	Effective H Storage Capacity Wt%
$TiFe_{0.9}Mn_{0.096}$ (INCO #4)	1.65
$TiFe_{0.9}Mn_{0.1}$	1.7
$TiFe_{0.85}Mn_{0.15}$	1.7
$TiFe_{0.8}Mn_{0.2}$	1.5
$TiFe_{0.932}Mn_{0.094}$ (INCO)	1.55

Table 2

EFFECT OF Cl_2 IN H_2 GAS ON THE ACTIVITY OF $TiFe_{0.9}Mn_{0.1}H_x$

Initial Cl_2 Content ppm	Activity Loss %	Reactivation Temp. $^\circ C$	Activity Recovered %
10	--	--	--
100	50	110	88
1000	75	110	63*
1000	75	300	75*
		400	75*

* These are maximum values. After exposure to high Cl_2 concentrations there was a slow deterioration in performance after reactivation.

References

1. Van Mal, H. H., Bushow, K. H. J. and Miedema, A. R., "Hydrogen Absorption in $LaNi_5$ and Related Compounds: Experimental Observations and Their Explanation," *J. Less-Common Metals* 35, 65 (1974).

2. Reilly, J. J. and Wiswall, R. H., "Annual Report Nuclear Engineering Dept.", p. 36, U.S.A.E.C., BNL-50023(s-69), Brookhaven National Laboratory, Upton, N.Y., 1966; Van Mal, H. H., "Stability of Ternary Hydrides and Some Applications," Thesis, 1976.
3. Srinivasan, S., Yeo, R. S. and Beaufre, A., "The Hydrogen-Halogen Energy Storage System: Preliminary Feasibility and Economic Assessment," 12th Intersociety Energy Conversion Engineering Conf., Washington, D.C., August 1977.
4. Proceedings of the ERDA Contractors Review Meeting on Chemical Energy Storage and Hydrogen Energy Systems, Airlie, Va., November 1976.
5. Sandrock, G., Final Report to Brookhaven National Laboratory Subcontract, BNL-352410S, August 1977; The Interrelations Among Composition, Microstructure, and Hydriding Behavior for Ferro-titanium Alloys, International Nickel Co., Suffern, N.Y.
6. Hempelmann, R. and Wicke, E., "Irreversible Change of the Magnetic Properties of TiFe by Hydrogenation," *Ber. Bunsenges. physik. Chem.* **B81**, Nr. 4, 1977.
7. Yamanaka, K., Saito, H. and Someno, M., "Hydride Formation of Intermetallic Compounds of Ti-Fe, Ti-Co, Ti-Ni and Ti-Cu," *Nippon Kagaku Kaisha (J. Chem. Soc., Japan)*, 1975, No. 8, 1267.
8. Faner, P. A. and Marzolin, H., "A Reinvestigation of the Chromium-Rich Region of the Ti-Cr System," *Trans. Met. Soc. AIME* **227**, 1342 (1963).
9. Johnson, J. R. and Reilly, J. J., "The Reaction of Hydrogen with TiCr₂, Abstract 172nd Meeting American Chemical Society," San Francisco, September 1976; manuscript to be submitted to *Inorganic Chemistry*.
10. Lynch, F., Denver Research Institute, Denver, Colorado, personal communication.

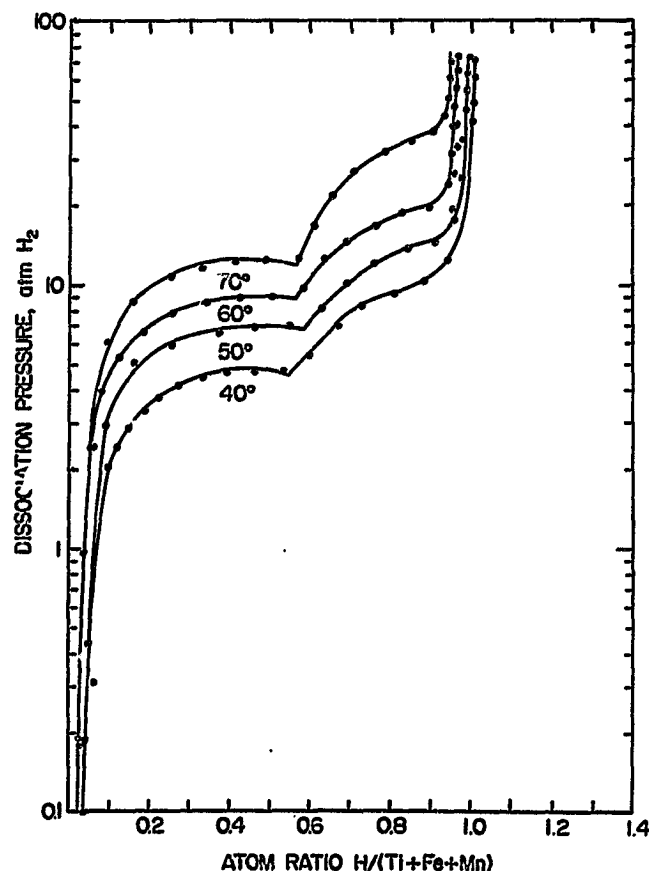
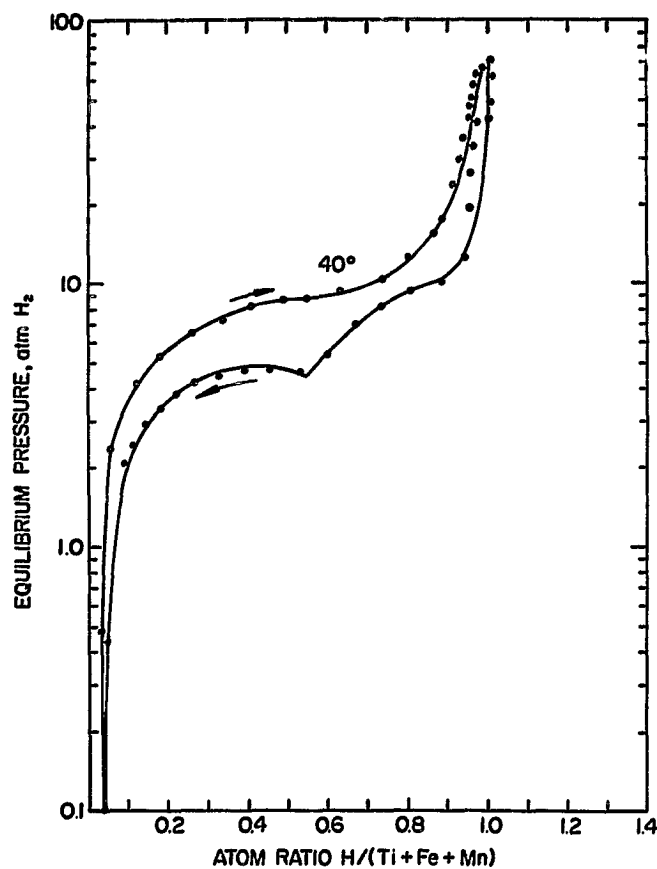
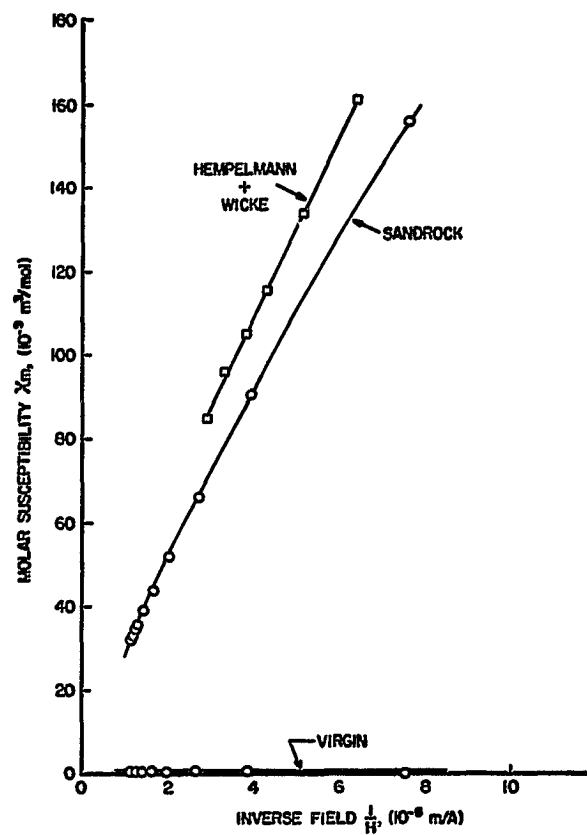


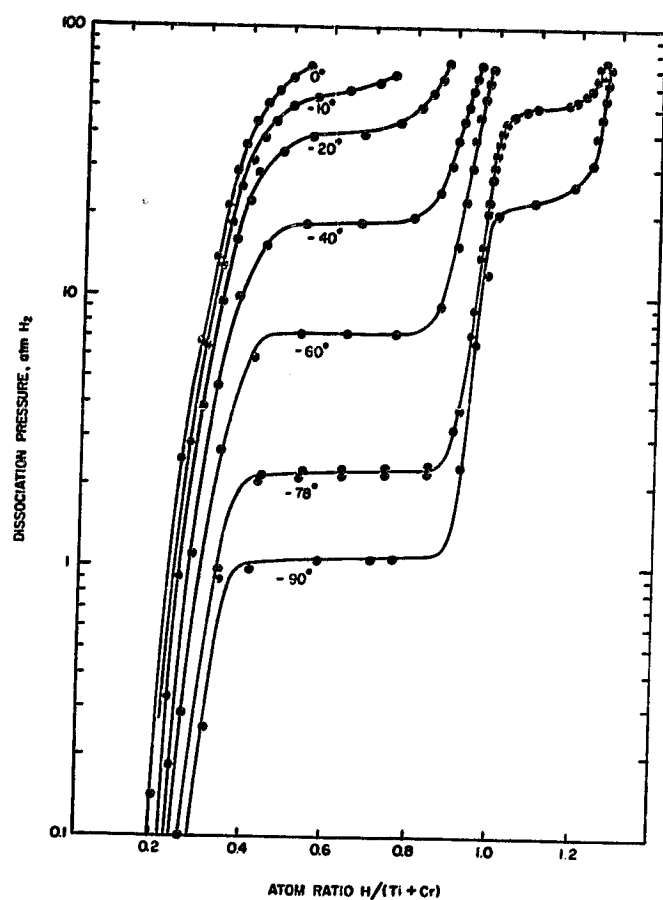
Fig. 1 Pressure-Composition isotherms for the TiFe_{0.85}Mn_{0.15}-H₂ system. This material is considered to have optimum properties for the H₂-Cl₂ dual mode cell.



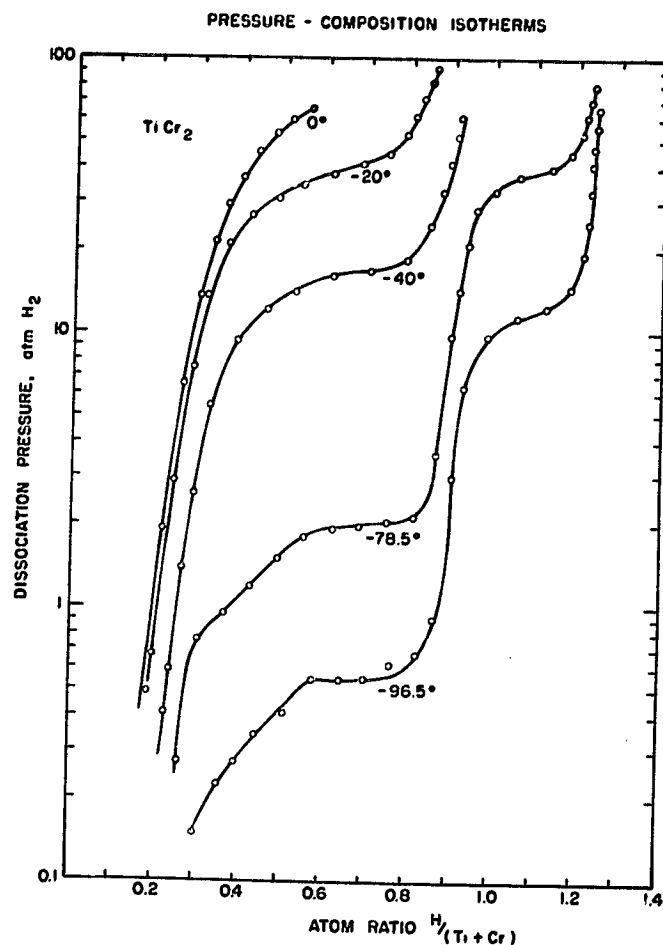
2. Hysteresis in the $TiFe_{0.85}Mn_{0.15}-H$ system.



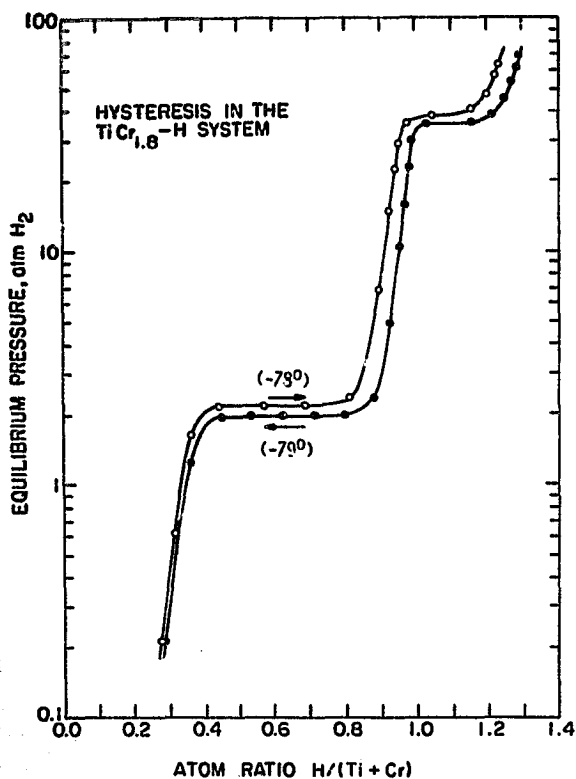
3. Magnetic susceptibility of $FeTi$ after hydriding.



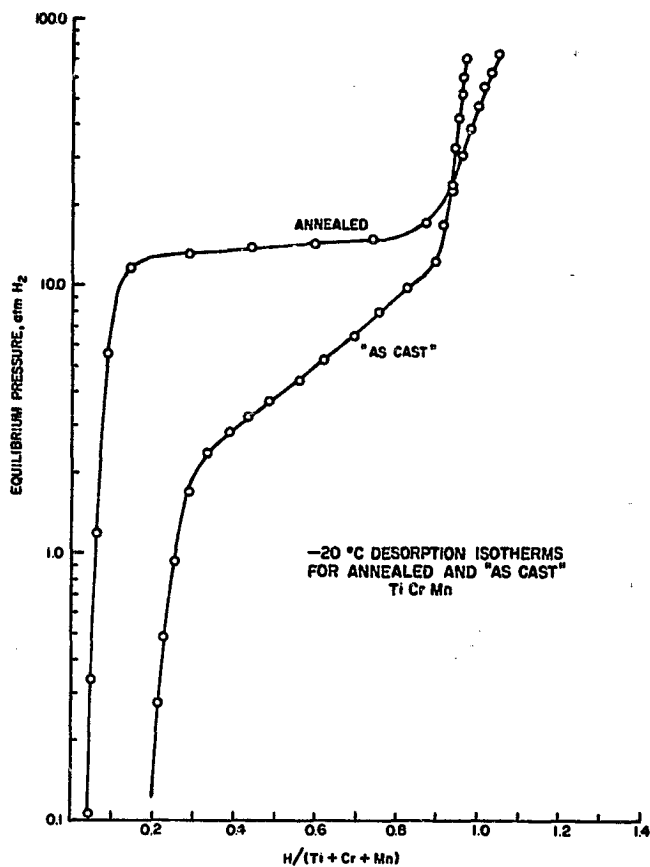
4. Pressure-Composition isotherms for the TiCr_{1.8} (C15)-H system.



5. Pressure-Composition isotherms for the as-cast TiCr_{1.8}-H system.



6. Hysteresis in the $\text{TiCr}_{1.8}(\text{Cl5})$ -H system.



7. Pressure-Composition isotherms for the TiCrMn -H system using annealed and as-cast alloy samples.

JAP

HYDROGEN-TECHNOLOGY EQUIPMENT TEST PROGRAM AT BNL

Gerald Strickland, Albert H. Beaufrere and
Matthew J. Rosso
Brookhaven National Laboratory
Upton, New York 11973

ABSTRACT

In furthering the development of hydrogen energy technology it is essential to test both major and supporting components on a practical scale. The Hydrogen-Technology Advanced-Component Test System (HYTACTS) is being constructed to fulfill this need. Components for production of hydrogen by electrolysis, storage of hydrogen as a metal hydride, and use in several types of energy conversion devices will be tested and evaluated. The first application to be evaluated uses hydrogen as an energy carrier in an electric-energy storage system. Off-peak or spinning-reserve power is used to electrolyze hydrochloric acid; the hydrogen and chlorine are stored for recombination in the same cell when the demand for power exceeds the system capacity. Hydrogen stored in containers of hydride will also be tested for use as an automotive fuel. The program phases are described along with some details on the equipment to be tested in the hydrogen storage section of the system now being constructed.

INTRODUCTION

The future of hydrogen as a major energy carrier is highly dependent upon developing methods of production, storage and conversion which can become competitive with comparable energy sources. Because the cost of hydrogen energy is relatively high today, there is an incentive to develop ways of lowering that cost. The energy required to make use of hydrogen energy must be reduced by making improvements in efficiency. New materials and components must be developed, tested and evaluated in this search.

The size and variety of components now being developed for applications involving hydrogen production, storage and use have grown to the point where an integrated service system is required for performance testing of the components. This need is being satisfied by construction of the Hydrogen-Technology Advanced-Component Test System (HYTACTS). The components are those used in electrolytic hydrogen production, storage of the hydrogen as a metal hydride, and use of the released hydrogen for electric power generation in a fuel cell, or for use as a combustible fuel. Also to be evaluated is the performance of the related control equipment, sensing elements, in-

strumentation, and the materials of construction. The skills of various industrial organizations are being used in this development work so that they can acquire new knowledge and thus assume a responsible role in furthering the development.

PROGRAM PHASES

Work will be done first on components of an Electric Energy Storage System. Here power which is produced at minimum cost is stored for use when the cost of production is appreciably higher. That is, off-peak or spinning-reserve power is stored for use when the demand for power exceeds the system capacity. The system now under development is known as the Hydrogen-Chlorine Energy Storage System. This system operates as a closed chemical loop and is based on use of a reversible electrochemical cell being developed by General Electric Co. The working fluids are hydrochloric acid in the electrolyzer mode and hydrogen and chlorine in the fuel-cell mode. Details on cell development are presented in another section of the Proceedings.

The hydrogen storage section of the HYTACTS is being constructed first because this technology is in a more advanced state of development than the electrochemical technology. Here the tasks deal with heat transfer and hydride expansion in the particle bed as well as behavior of materials and components in contact with hydrogen and the hydride. Two 0.6M (2 ft)-diameter vessels having different features will be tested initially under conditions suitable for stationary applications. They are called Variable-Parameter Test Units (VPTU) because the internal assemblies can be replaced by modified units. The first VPTU is only 0.9M (3 ft) long and will be used primarily for hydride expansion work as explained below. The second VPTU is 2.16M (7 ft) long and will be used primarily for obtaining data on hydrogen charging and discharging (transfer) rates and for tests of the Electric-Energy Storage System. Subsequently a scaled-up version of the storage vessel, perhaps 0.9M (3 ft) in diameter and 6.16M (20 ft) in length, will be tested. It will be a preprototype sub-module designed for use at an electric utility site as part of the Hydrogen-Chlorine Energy Storage System. Vessels of this type could also be used as substitutes for propane containers used in rural areas.

Concurrently, work on design, fabrication and installation of the other components of the Hydrogen-Chlorine Electric Energy Storage System will be undertaken in conjunction with a qualified organization.

Later on, work will commence on design and testing of reservoirs and a control system for use in automobiles. Designs suited for various drive cycles will be developed and tested using FeTi-based and high-Mg hydrides, or other suitable storage media. This work is of prime environmental importance because the main product of hydrogen combustion is water. It is also challenging because the storage system must have a

tolerable weight, in addition to being potentially competitive with liquid fuels.

HYDRIDE TEST PROGRAM

The main physical problem to be solved for hydrogen stored as a hydride deals with the accommodation of hydride expansion. Operating experience and specific studies have shown the Fe-Ti based hydride (FeTiH_x) can cause permanent deformation of the container (1). The value of x has a typical range of 0.2 - 1.6 under dynamic conditions. In beds of hydride particles more than $\sim 0.15\text{M}$ (~ 6 in.) deep, it appears that the volumetric expansion ($\sim 10\%$) which occurs during hydriding, and the subsequent contraction during dehydriding, gradually cause a reduction in the void space. At some point the angularly shaped particles become "locked-in" and have limited movement; then expansion of the container occurs. Two means of avoiding damage to the container will be tested. The first technique consists of providing a means of briefly loosening the bed, prior to hydriding, by very rapid addition of hydrogen to induce incipient fluidization. The second method avoids the problem by limiting the bed depth so that the hydride can freely expand upward.

In order to sustain hydrogen transfer in a hydride bed, heat must be removed during hydriding and provided during dehydriding. Several styles of heat exchangers utilizing water will be tested; namely, U-tube (plain), embossed-plate, and water-jacketed (canned hydride). After testing of these units, there will be sufficient information to develop a scaling correlation for future designs.

A simplified flow diagram for the hydrogen storage section of the HYTACTS is shown in Figure 1. Hydrogen will be supplied either by a tube trailer (99.8% min. purity) or a water electrolyzer. In the purifier the level of contaminants is reduced to about 0.0005% by means of a deoxidizer, which converts residual oxygen to water, and a molecular-sieve drier. A compressor is used to repressurize the hydrogen for storage in the bank of 24 tubes ($\sim 37\text{M}^3$ or $\sim 1000\text{Ft}^3$ at STP). During charging the hydrogen is reduced in pressure, and flow to the hydride bed is controlled and integrated. At the start of charging the same components provide a very high flow rate for a few seconds in order to loosen the bed. During discharging, hydrogen flows through a flow controller-integrator to the compressor and back to the supply tanks. The gas analyzer will be used to check purity of the hydrogen.

Both storage vessels are being fabricated of suitable carbon steels and have flanged heads. Materials which passed screening tests in 4.1 MPa (600 - psi) hydrogen at Sandia Laboratories (SL) were subjected to an FeTiH_x environment at BNL in the form of self-loaded tensile specimens. An evaluation of their performance at SL has confirmed the suitability of the selected materials (2). Details of the test results are reported by S. L. Robinson in another section of the Proceedings. The vessel shell and nozzles are made of seamless steel pipe (ASTM Spec. A106-B) and the

caps and flanges are made of similar material: steel plate (ASTM Spec. A-516 Grade 70) is recommended for a rolled and welded shell made from plate.

The first VPTU, which is being fabricated at BNL, is shown in simplified form in Figure 2. It has six porous metal tubes (PMT) for use in loosening the hydride bed, and three other PMT for normal hydrogen flow in or out of the vessel. The thermal load is handled by four embossed heat-transfer panels made of carbon steel. Two flat panels with double embossing are located on opposite sides of the vertical centerline, and two curved panels with single embossing fit against the sidewall. A temperature-controlled stream of cold or hot ethylene glycol solution is circulated in a closed loop by a pump.

The second and longer VPTU is being designed and fabricated by Foster Wheeler Energy Corp. (FWEC) under a subcontract to BNL. A simplified sketch of this vessel is shown in Figure 3. It has panels of porous metal sheet for hydrogen distribution and filtration. A new feature to be tested is a hollow center body which is designed to collapse before the vessel expands beyond the yield point, if the hydride bed becomes packed too tightly. The thermal load in this VPTU is handled by a U-Tube heat exchanger which has the tubes aligned vertically in order to minimize interference during loosening of the bed. The nominal power rating of this vessel is 50kW for 10 hours (500 kWh).

It is also planned to test a stack of vertical trays in the second VPTU. The vessel will be mounted with its axis in a vertical plane; and the tray depth will be close to 0.15M (6 in.) An embossed heat-transfer panel will be used for the bottom of each circular tray.

Both vessels and the HYTACTS piping for the storage section are now being constructed. It is expected that the first tests will be started near mid-1978.

REFERENCES

1. Strickland, G., "Some Observations on the Effects of the Volumetric Expansion of Iron-Titanium Hydride on Vessels Built at BNL," BNL Report 23130, Aug., 1977.
2. Robinson, S. L., Sandia Laboratories, Livermore, California, Private Communication to G. Strickland, Oct. 27, 1977.

HYDROGEN STORAGE SECTION OF HYTACTS

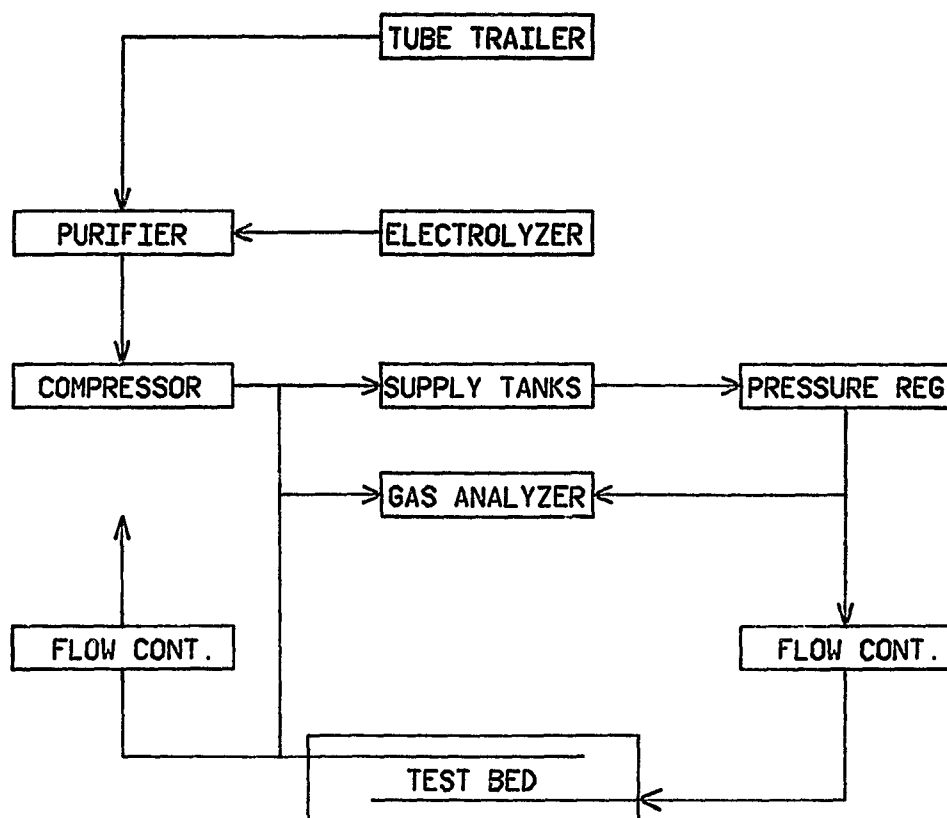


Fig. 1 Simplified Flow Diagram

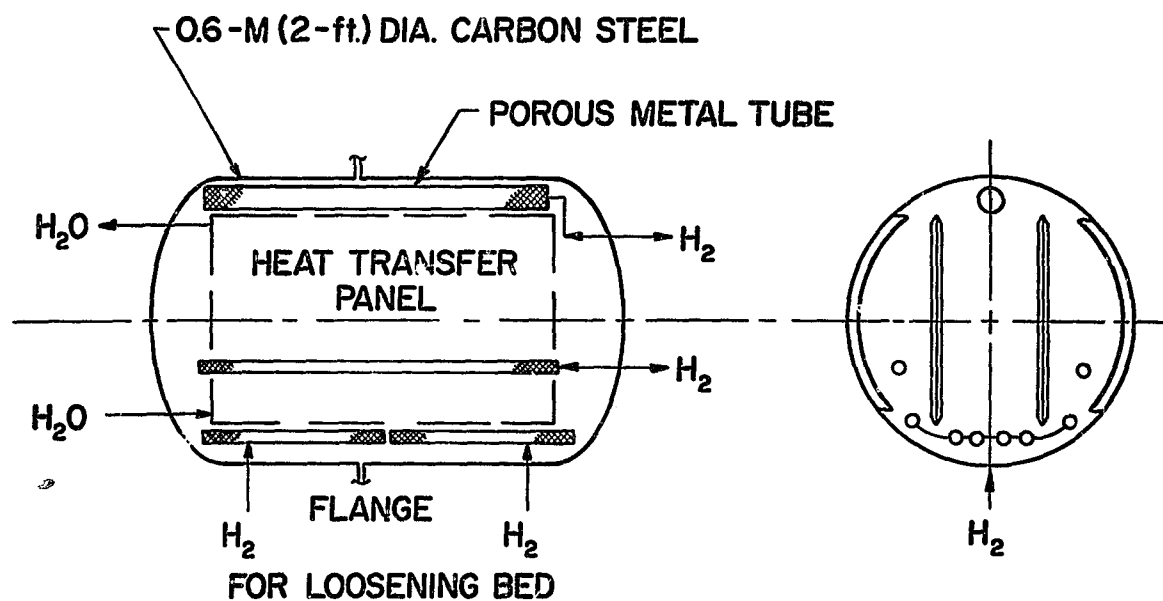


Fig. 2 Sectional views of BNL Variable-Parameter Test Unit showing major components.

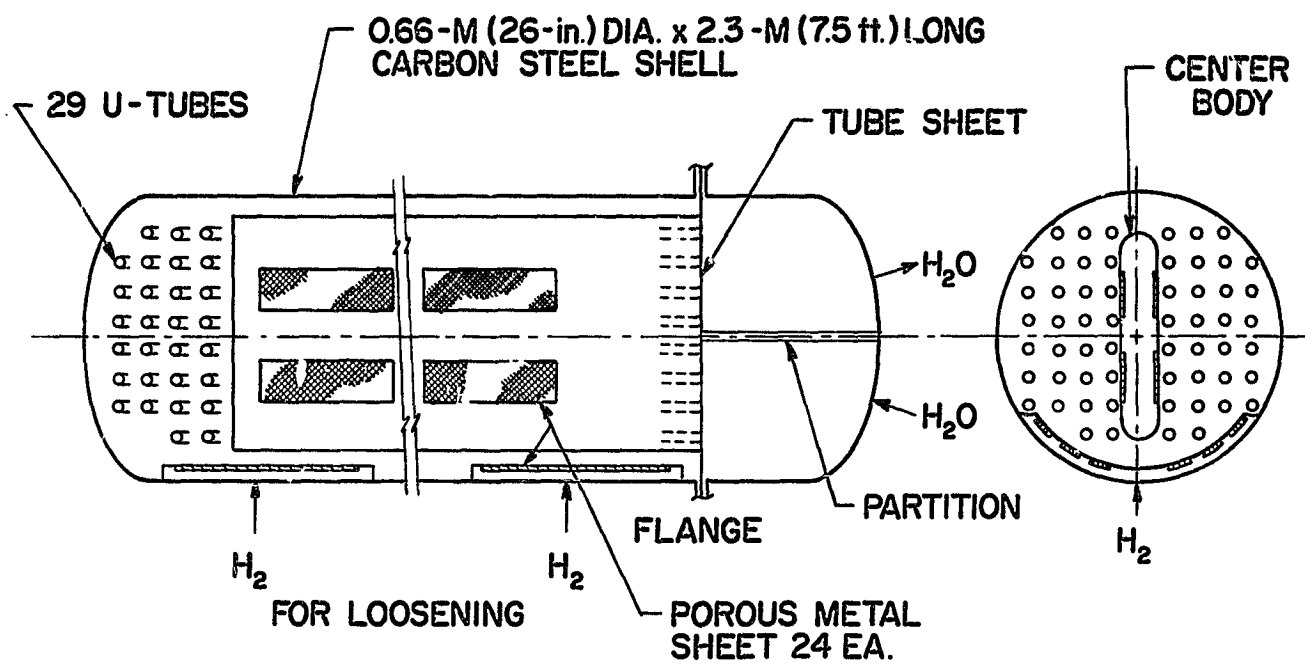


Fig. 3 Sectional views of FWEC Variable-Parameter Test Unit showing major components.

HYCSOS: A CHEMICAL HEAT PUMP AND ENERGY CONVERSION SYSTEM BASED
ON METAL HYDRIDES*

Dieter M. Gruen, Irving Sheft, George Lamich, and Marshall H. Mendelsohn
Chemistry Division
Argonne National Laboratory
9700 South Cass Avenue
Argonne, Illinois 60439

Abstract

Design and construction features of the ANL demonstration test facility which utilizes four stainless steel tanks holding 10 lbs. each of either LaNi_5 or CaNi_5 are given. The operation, instrumentation and control of the system is detailed with the aid of photographs, drawings and a system layout diagram.

Initial operation of the system has shown that 33 moles of hydrogen can be transferred from LaNi_5 at $\sim 8^\circ\text{C}$ to reform CaNi_5H_4 at 40°C with cycle times approaching 2 minutes for 50% hydrogen transfer. The relevant data pertaining to these experiments are given in graphs and tables. The program for FY1978 includes work on a fully automated and insulated system to establish a firmer data base, obtain power balances and determine optimum operating parameters. In order to achieve these goals in a reasonable time frame, a data display and handling system is being installed. A second generation heat exchanger based on aluminum foam technology will be tested.

A materials development program is being carried out concurrently with HYCSOS operations. Significant process is being made in the development of new, ternary alloy systems, based on the composition $\text{LaNi}_{5-x}\text{Al}_x$ which display superior properties for heat pump action. An economic and performance analysis is being carried out to evaluate the potential of the HYCSOS system for commercialization.

*Work performed under the auspices of the Division of Energy Storage, USDOE.

I. Introduction

The Argonne HYCSOS system, a two hydride concept for the storage and recovery of thermal energy for heating, cooling and energy conversion in an integrated system, is operational and preliminary results are described with the help of heat transfer fluid and hydrogen gas flow diagrams. Initial descriptions of the overall concept [1], and a thermodynamic analysis of the efficiency of the energy conversion cycle have appeared [2] and the overall systems concept has been described [3]. Operating parameters for the HYCSOS demonstration system have also been detailed elsewhere [4,5,6].

Equations for chemical heat pump action for a two metal hydride system have been developed [7]; the hydrogen decomposition pressures of a series of compositions in the new $\text{LaNi}_{5-x}\text{Al}_x$ ternary alloy system have been measured [8]; and the relationship between the configurational entropies and the stabilities of intermetallic alloys have been clarified [9,10].

In its simplest form a hydride heat pump would consist of two hydride beds, each containing a different hydride. The beds would be interconnected to allow hydrogen gas to flow between them. Means would be provided for the input of high temperature heat from solar concentrating collectors; for heat rejection to or heat acquisition from the atmosphere; and for heat input to or heat rejection from the building.

To provide a near-continuous heat pumping action the HYCSOS concept uses four hydride beds, two with LaNi_5H_n and two with CaNi_5H_n . The respective beds can exchange heat during the temperature change periods and with the exception of these periods the heat pumping action is continuous.

At present, work is proceeding on an engineering design concept and analysis of a small residential-sized HYCSOS chemical heat pump system [11]. This system will use aluminum foam heat exchangers of novel design and a halocarbon refrigerant for heat transfer with boiling and condensing heat exchange. The use of the halocarbon will enable the system to operate as a heat pump in the winter because it will not freeze. The condensing and boiling heat transfer occur at very small temperature drops so that the system efficiency is increased. Because a large portion of the heat transfer fluid is in the gaseous phase in both the evaporating and the condensing process, the inert thermal mass which degrades the system performance for a water heat transfer fluid will be much less. In addition, the enthalpy change per unit volume of fluid pumped is greater than for sensible heat transfer with water. For the same heat transfer rates, this results in reduced inert thermal mass, reduced cost for fluid lines, and reduced pumping power.

In addition to providing air conditioning in summer and heating in winter by chemical heat pump action, the system will provide electrical power during the spring and fall or with electrical power input, operate as a conventional heat pump.

At present, the work on the small chemical heat pump/air conditioner/electrical power/heat pump system is directed toward producing an automated set of design and performance programs

because the variables involved in the design calculations require many iterations. Some results on the system will be available by the end of this year, but preliminary indications are that it will be cost-competitive with small $\text{LiBr-H}_2\text{O}$ absorption refrigeration systems.

The technological "fit" between this system and concentrating collectors is very good. This system takes the high thermodynamic availability of the high-temperature heat output of the concentrating collector and uses it to provide a larger amount of lower grade heat to the residence or cooling or electrical power. The ability of the system to use solar thermal input during periods when little heating or cooling is required means that the cost of the collectors can be amortized over the whole year.

II. System Design Description

A. General

A demonstration test facility has been constructed, experimentally, to evaluate the HYCSOS chemical heat pump and energy conversion concept. The test facility enables one to transfer hydrogen gas from tanks containing a metal hydride bed of one composition to tanks containing a metal hydride bed of another composition, under the influence of a thermal gradient. The heat of formation of the metal hydride (CaNi_5H_6) and sensible heats associated with system heat capacities are supplied, at a specific temperature which is commensurate with the hydrogen pressure required to decompose the M1 hydride and drive the hydrogen to the other metal (LaNi_5), where the hydrogen is absorbed.

The test facility, jointly designed by the Argonne Chemistry and Engineering Divisions, consists of four reservoirs (tanks) of approximately one-half gallon volumetric capacity each, containing two different types of metal powders or metal hydride powders. The reservoirs and hydrogen piping system are made of 316 type stainless steel. For the heat storage and refrigeration tests, two of the reservoirs contain lanthanum-nickel and/or its hydride, the other two reservoirs contain calcium nickel and/or its hydride. For the power generation tests, only three reservoirs are used containing either lanthanum-nickel or calcium-nickel.

Internal heat transfer surfaces are provided in each of the hydride bed reservoirs in the form of coiled tubing; the heat transfer cooling or heating fluid circulates inside the tubing. Safety relief valves, filters, flowmeters, shutoff valves, and manifolds between the hydride beds are provided in the hydrogen process system. The heat transfer fluid (water) is heated electrically in this demonstration system, with automatic variable power input controls, to simulate a solar heat source. Tap water is used as the heat sink in a heat exchanger system. Pressures, temperatures and flowrates are measured remotely, monitored and recorded using a digital data acquisition system.

The size of the demonstration unit was chosen as a compromise to permit large enough flow rates within the process fluids so standard flowmeters can be used, and pumping and heating power

requirements to be met from available laboratory supplies. Heat losses are kept to a minimum with proper insulation and by keeping heat transfer fluid volumes to a minimum. For personnel safety considerations, the hydride tanks are surrounded by a well ventilated hood through which a large volume flowrate of air (2000 CFM) is drawn and exhausted outdoors. Continuous hydrogen concentration monitoring, with an alarm set below the flammability limit, is provided to warn of potential danger.

Design of the hydride beds internal heat exchange surface configuration, line sizes and pumping rates were dictated by design goal cycle response times. The power generation mode has the shortest characteristic design cycle time (12 minutes) which requires individual bed thermal transients to be completed in approximately 2 minutes. These times are design goals. Thermal response limitations of associated components (thermal inertia of lines, pumps, valves, and heaters), which were not considered in detail in the design analysis, are expected to degrade the achievable cycle response time of the individual hydride bed to perhaps 4 minutes. The heat storage mode and refrigeration modes of operation have design goal cycle times one-half hour and 4 to 8 minutes, respectively, so these modes are not design limiting. It will be seen that in the initial operations design cycle times are approached. Figure 1 gives an overall view of the test facility.

B. Heat Transfer Fluid System

Three fluid heat transfer loops, Fig. 2, are available and can be remotely valved and pumped to the appropriate tanks. The solar or other suitable low temperature thermal energy input, loop A, is simulated by an 18 KW electric heater. Loop B, a water cooled heat exchanger of 25 KW heat transfer capacity, represents the space being heated in winter and serves for ambient heat rejection during cooling cycles. A heat exchanger cooling water circuit is provided from the building water supply. A third fluid loop, loop C, with a 6 KW electric heater is the refrigeration heat load in the cooling cycle and the ambient heat supply during the recovery cycle.

The heat transfer system contains water in all three heat transfer fluid loops. The valves which control the flow of water through the hydride tank heat exchangers are double acting air actuators controlled by solenoid operated air valves. The water plumbing system is 3/4 inch x .065 wall hard copper tubing with soft-soldered (50/50 type) socket joint fittings.

Each flow loop incorporates a one gallon fluid expansion and surge tank of type 304 stainless steel and rated for 400 psig operation. Each surge tank has a sight gauge to show liquid level, nitrogen pressurization valve, a relief valve and a water fill valve.

The heating loop "A" has three electric heater assemblies for heating the water. These heaters, arranged in parallel flow, consist of a 240 VAC Watlow "Firerod" cartridge heating element 5 feet long of 6 KW capacity encased within 1 1/8 inch OD type K hard copper tubing. The heat transfer fluid outlet is in line with the axis of the assembly at the opposite end from the inlet.

A bypass throttling valve (VTA) is used to manually vary the flow rate of heat transfer fluid through the hydride beds. Flow loop A incorporates a bypass relief valve to protect the pump in the event that all inlet valves are closed. A manual bronze ball valve is incorporated at the low point in the loop to drain the system. The pump is a turbine type rated at 6.2 gpm at 65 psid, and is driven by a 1/2 hp electric motor.

Cooling loop "B" features a water to water heat exchanger for cooling the recirculated process fluid. Tap water from a 1 1/2 inch, 60 psig laboratory supply is used to cool loop B fluid. The water pump is a turbine type having a rating of 12.4 gpm at 65 psid and using a 1 1/2 hp electric motor drive. The loop has a water bypass relief valve (VBB) and a throttling bypass valve (VTB).

The water pump for the water cooling loop associated with loop B is also a turbine type. Two bypass flow loops around the water pump are provided. One with a pressure relief valve to protect the pump in case of operator error and the second bypass loop allows for adjustment of the water sink temperature in the heat exchanger, and the consequent heat exchanger heat load capacity, by manual adjustment of throttling valves.

The refrigeration loop "C" features a single electric heater of 6 KW capacity, which serves as the equivalent heat load of this circuit. The turbine type pump is rated at 6.2 gpm at 65 psid and is driven by a 1/2 hp electric motor. Detailed fluid system requirements are shown for each circuit (Tables 1, 2, and 3).

Table 1. Heat Transfer Fluid Loop A

Maximum Fluid Temperature	135°C (275°F)
Design Temperature Range	21°-135°C (70-275°F)
Design Pressure (max)	120 psig
Relief Pressure	110 psig
Static Pressure	40 psig
Pump Pressure (Head)	60 psid
Flow Rate (max)	6 gpm
Heat Transfer Fluid	water
Power Input (Heating)	0-18 KW
Heater Voltage	0-208 (3φ) VAC
Pump Power	0.50 hp

Table 2. Heat Transfer Fluid Loop B
Primary Loop

Maximum Fluid Temperature	61°C (142°F)
Design Temperature Range	25-50°C (77-122°F)
Design Pressure (max)	100 psig
Relief Pressure	110 psig
Static Pressure	40 psig
Pump Pressure (Head)	60 psid
Flow Rate	12 gpm
Heat Transfer Fluid	water
Heat Transfer Capacity	25 KW (70°F sink, 122°F source)
Pump Power	1.5 hp
Heat Exchanger Cooling Water Circuit	
Maximum Temperature	21°C (70°F)
Design Pressure	120 psig
Static Pressure	60 psig
Pump Pressure (Head)	60 psid
Flow Rate (max)	6 gpm
Heat Transfer Capacity	25 KW (70°F/21°C sink, 122°F/ 50°C source)
Pump Power	0.50 hp

Table 3. Heat Transfer Loop C

Maximum Temperature	61°C (142°F)
Design Temperature Range	-31° to 21°C (-24 to 70°F)
Design Pressure (Max)	100 psig
Relief Pressure	110 psig
Static Pressure	40 psig
Pump Pressure (Head)	60 psid
Flow Rate (max)	6 gpm
Heat Transfer Fluid	water
Power Input (Heating)	0-6 KW
Heater Voltage	0-208 (3φ) VAC
Pump Power	0.50 hp

C. Hydrogen System

The hydrogen system consists of hydride tanks with internal heat exchangers, piping and valving.

Four metal/metal-hydride filled tanks are used in the demonstration system as shown in the system layout. Each of these tanks is constructed as shown in Fig. 3. The tank cylindrical wall is a 9 1/4 inch length of 4 inch SCH 10 type 316L stainless steel pipe. The tank heads are 4 inch SCH 10-IPS type 316L stainless steel pipe caps. Stainless steel tabs are welded to the side of the cylinder for mounting the tank in a vertical orientation.

A number of coils of tubing form a heat exchanger inside of each hydride tank. External shaped tubing cooling/heating coils attach to the outside of each tank. Internal manifolding for the cooling/heating coils is provided by a Tee shaped tubular assembly which connects to the outlet manifold head.

Each tank was constructed so that all pressure boundary welds were 100% radiographed and dye penetrant checked. The tanks were hydrostatically tested to 1000 psig. Each tank was constructed with the top hydrogen outlet and the bottom water-glycol inlet and outlets having compression type fittings such that any of the tanks can be readily removed from the system for changing hydride material. The hydride material which fills each tank approximately 2/3 full is poured in or out through the top hydrogen line.

A hydrogen filter is incorporated immediately above the hydride tank to preclude particulate, transfer of hydride through the lines into the valves, which could cause leakage, and contamination of the other type hydride material. The cylindrical pressure shells are 2 inch SCH 10 type 316 stainless steel pipe containing a cylindrical porous sintered 316 stainless steel filter element having 0.25 sq. ft. surface and a 1 micron absolute filtration retention. All pressure boundary welds were 100% radiograph and dye penetrant tested. The filters were hydrostatically tested to 1000 psig.

The hydrogen piping between each hydride tank and its filter is 1/2 inch diameter type 316 stainless steel tubing having .049 inch wall thickness. Above the filters, all of the hydrogen lines are 3/8 inch diameter type 316 stainless steel tubing having .035 inch wall thickness. The tubing

sections and components in the hydrogen flow system are connected together using Swagelok fittings.

The remote actuated hydrogen valves are nominal 3/8 inch bellows sealed type 316 stainless steel valves with air to open, spring closed actuators. The manual hydrogen valves for filling and venting the hydrogen system and the relief valves are also 3/8 inch bellows sealed type 316 stainless steel. Design requirements for the hydrogen system are shown in Table 4.

Table 4. Hydrogen System

<u>Hydrogen Loop</u>	
Design Pressure (max)	750 psig
Design Pressure (min)	30 psig
Relief Pressure	825 psig
Design Temperature (max)	135°C (275°F)
Design Temperature (min)	-31°C (-24°F)
Hydrogen Flow Rate (max)	0.55 gm/sec
The hydrogen shall be filtered to 1 micron absolute size at the outlet of each hydride tank.	

<u>Hydride Tanks</u>	
Design Pressure (max)	750 psig
Design Pressure (min)	30 psig
Relief Pressure	825 psig
Design Temperature (max)	135°C (275°F)
Design Temperature (min)	-31°C (-24°F)
Free Internal Volume	2.5 liters
Hydride Volume	1 to 1.5 liters/tank

D. Hydrogen System Instrumentation

The instrumentation and control functions which are required for operation of the demonstration unit, for the most part, are separate from the experimental apparatus. Air operated remote valves in the hydrogen system were specified to eliminate spark and explosion potential.

Flow from each hydride tank is measured using a Brooks heated tube mass flowmeter. Remote recording of flow rate and integrated flow is done with a digital data logger. Remote readout is on a graphic display panel. The hydrogen flowmeters are located on the "clean side" of the filters to minimize contamination from the fine hydride particles. Four hydrogen flowmeters are provided.

Hydrogen absolute pressure level is monitored at a position in the system immediately above the filter (on the clean side) using Sensotec metal diaphragm, type transducers rated from 0 to 1000 psia. Four hydrogen pressure transducers are provided. The pressure drop through the filter during hydrogen flow conditions is accepted as a known system error for initial phases of operation. Temperature of the hydrogen is monitored at a position above each filter using immersion type copper/constantan thermocouples inserted into the flow stream. Temperatures are recorded on the digital data logger which provides automatic reference temperature compensation.

E. Heat Transfer Fluid Transport System Instrumentation

Temperatures of the water heat transfer fluid and water coolant are measured using immersion type copper constantan thermocouples and are recorded on the digital data logger. Heat transfer fluid temperatures are measured at the inlet and

outlet of each of the four hydride beds (e.g., T1A1 and T1A2 for bed HT1; see Fig. 2). In heating loop A, heat transfer fluid temperatures are measured at the inlet and outlet of the electric heater (TA1 and TA4). In cooling loop B, heat transfer fluid temperatures are measured at the inlet and outlet of the heat exchanger (TB1 and TB2). In the water cooling circuit, the temperature of the supply water (TW1) and the temperatures of the water at the inlet and outlet of the heat exchanger (TW2 and TW3) are measured. In refrigeration loop C, the temperatures of the heat transfer fluid at the inlet and outlet of the electric heater (TC1 and TC4) are measured.

Heat transfer fluid flowrates are measured at the inlet to each hydride bed heat exchanger (e.g., FIAB), using turbine flowmeters. The signal from each of these flowmeters is recorded by the digital data logger and also displayed on the remote graphic panel. The bypass flows of heat transfer fluid in loops A, B, and C and the recirculation flow of water in the water cooling circuit are measured locally with Rotameters. Water flow through heat exchanger (HXB) is measured using a turbine flowmeter and is recorded on the digital data logger and displayed on the remote graphic display panel.

Pressure levels in the heat transfer fluid flow circuits are measured with local indicating gauges. The gas pressure above each surge tank (in loops A, B, and C), the heat transfer fluid pressure on the downstream side of the pump in each circuit (loops A, B, and C) and the laboratory water supply pressure are measured locally.

F. Fluid Transport System Controls

The valves which control the water heat transfer fluid flow through the hydride bed heat exchangers are air actuated solenoid valves. Sets of solenoid valves associated with a given hydride tank are controlled by a single switch to prevent a tank from being simultaneously open to more than one fluid loop. The bypass throttle valves (VTA, VTB, and VTC) in loops A, B, and C, which control the net flowrate of heat transfer fluid through the hydride bed heat exchangers, and the water supply valve are manually operated.

The electrical heater for the heat transfer fluid in loop A can be controlled from the graphic panel, in either a constant power mode or in a constant output fluid temperature mode of operation. Power level or fluid temperature level is adjustable from the remote control panel. The constant temperature mode of operation for the heater in loop A operates with feedback control of temperature as monitored by thermocouple TA2 located downstream of the heater. The fluid heater for loop A has an interlock to shut off power when flow through the system is below a set level as determined by flowswitch (FSA). If the set heater outlet fluid temperature is exceeded or the power to pump PA is lost, a safety interlock shuts off the heater power.

An identical electrical heater control system is provided for flow loop C. Thermocouple TC2 controls output fluid temperature via heater control HC. Overtemperature of the output fluid is precluded via interlock (HC) using thermocouple TC3. Flow switch FSC shuts off the heater power if the flow rate is too low. The pump (PC) must

be energized before the heater can be energized. Controls for the two aforementioned heater and pump functions are mounted on the remote panel along with indicators of the specific functions (i.e., status lights and panel meters for set point temperatures and power levels). Flow loop B and the water coolant recirculation pump have an on-off switch for pump power. The energy usage for each heater and pump is recorded by the data logger. Heater powers are displayed on the graphic panel.

G. Data Logger

The short HYCSOS cycle times necessitate an automatic data logger to record all of the pertinent system variables for analysis. The data logger used is a John Fluke Mfg. Co. Model 2240 A with 30 wide range voltage input channels, and 15 alarm limits. The data logger currently samples input data at the rate of three channels/second and prints output information on paper tape.

H. Hydrogen Safety

Because of the wide explosive and flammability limits of air-hydrogen mixtures, the hydrogen containing system is housed in a well ventilated enclosed structure, with an air flow of 2000 CFM. This flow is sufficient to maintain the hydrogen concentration below the 4 volume percent flammable limit in a maximum credible accident, the release of the total 43 SCF of hydrogen during the two minute thermal transient excursion of the energy conversion mode. The sloping top of the enclosing and continuous hydrogen concentration monitoring prevent unknown accumulation of hydrogen. Limit pressure alarms on each tank warn of potential hydrogen buildup in the tanks. Pressure relief valves on each tank are set 10% below the design pressure limit.

III. Hydride Materials

The Argonne HYCSOS concept requires pairs of hydrides having pressure-temperature relationships which permit reversible hydrogen transfer at appropriate temperatures. Alloys of the form AB_5 are eminently suitable for this purpose. By varying the materials A and B and the ratio B/A, pressure-temperature relationships over wide ranges are obtainable [12].

Calcium nickel hydride and lanthanum nickel hydride are being used for the initial HYCSOS tests. The pressure temperature relationships of these hydrides are illustrated in Fig. 4. A new generation of alloys based on the $LaNi_{5-x}Al_x$ or the $MnNi_{5-x}Al_x$ system has recently been developed and will be used in the next phase of the HYCSOS program [8].

IV. Results and Discussion

In order to evaluate heat balances in the various hydriding and dehydriding cycles, it is necessary to know base-line thermal characteristics of the HYCSOS system. Using measured integrated heater power inputs, preliminary heat capacity values have been determined for empty uninsulated portions as follows:

Heater Loop A+ Tank 2 = 7.1 kcal/deg.

Heater Loop C+ Tank 3 = 1.9 kcal/deg.

The heat equivalent of the pump power input under typical operating conditions is about 200 watt hours, sufficient to raise the heat transfer fluid in the uninsulated loop by approximately 25°C. These and other measurements will be re-run on the insulated system.

Because of ready availability in sufficient quantity, CaNi_5 and LaNi_5 have been used in the first series of tests. Five kilograms (11.561 moles) of LaNi_5 (Molycorp.) was put through a #12 sieve (1.68 mm) and added to tank 3 through the hydrogen gas tube. Approximately half the charge was fine powder obtained by ballmilling oversize pieces. An equivalent hydrogen capacity amount of sieved CaNi_5 , 5.8 Kg (17.341 moles), (Novamet Corp., International Nickel Co.) was added to tank 2. Determination of the bulk density by reduction of gas volume in the tanks after addition of the alloys, 8.9 gm/cc for LaNi_5 and 6.9 gm/cc for CaNi_5 , compares favorably with the crystal density measurements of 8.3 gm/cc for LaNi_5 and 6.7 gm/cc for CaNi_5 .

Approximately thirty-seven moles of ultra high purity hydrogen (Matheson, 99.999%) were added in five to ten mole batches at 600 PSI to initially hydride and activate the LaNi_5 . The final composition was $\text{LaNi}_5\text{H}_{6.10}$ at 16.3°C and 124 psi. Hydrogen to activate the CaNi_5 was transferred from the $\text{LaNi}_5\text{H}_{6.1}$ at 78°C to the CaNi_5 at 12°C to form $\text{CaNi}_5\text{H}_{3.4}$ at 21.7 psi leaving $\text{LaNi}_5\text{H}_{7.4}$ as the residual composition of the LaNi_5 hydride. Calcium nickel hydride was decomposed in the storage mode by circulating water at 100°C through its bed and absorbing the hydrogen on the LaNi_5 , cooled to remove the heat of hydride formation. Typical data collected on the data logger for the storage mode is shown in Fig. 5. Figure 6 is a linear plot of the integrated power required to maintain the temperature of the dissociating CaNi_5 hydride at a relatively constant 100°C. The intercept of the extrapolation to the vertical axis, the start of hydrogen transfer, is the energy actually used to decompose the $\text{CaNi}_5\text{H}_{3.66}$ and give up approximately 25 moles of H_2 . The determined value, 0.225 KWH, gives a calculated heat of dissociation of CaNi_5H_4 of 7.7 kcal/mole H_2 , to be compared with a literature value of 7.5 kcal/mole H_2 . A typical recovery mode is shown in Fig. 7.

A summary of the data obtained in three cycles in the storage mode, the high temperature decomposition of CaNi_5 hydride and formation of LaNi_5 hydride and three cycles in the recovery mode, the low temperature decomposition of LaNi_5 hydride and formation of CaNi_5 hydride are shown in Table 5 and Table 6, respectively. The data represent the first 15 minutes of a 45 minute cycle when 75%-90% of the hydrogen was transferred. ΔH_B is the heat of formation or decomposition for the amount of hydrogen involved expressed as a positive quantity. The heat recovered or heat added is the product of the temperature difference across the appropriate tank, taken at one minute intervals, and the fluid flow during that interval. The initial hydrogen flow when the valve was first opened was so large as to exceed the instrumentation limits and may also account for loss in heat measurements in the first minute interval. Except for the high

temperature dissociation of CaNi_5 hydride, no attempt was made in these preliminary experiments to maintain isothermal conditions and together with heat loss in the initial interval measurement could account for the incomplete heat balances. The temperature rise of the decomposing LaNi_5 hydride after seven minutes, Fig. 7, is due to heat input from the pump.

All of the runs up to now have been made in the absence of insulation. The next phase of operation will be to determine heat balances and cycle times with thermal insulation in place and with the system operated automatically using a data handling and display package.

It can be concluded that the system is meeting design specifications and that the scientific feasibility of the HYCSOS concept has been demonstrated.

Table 5. Storage Mode Hydrogen Transfer: CaNi_5 Hydride to LaNi_5

Run	H_2 Moles	CaNi_5 HYDRIDE			LaNi_5 HYDRIDE		
		ΔH_B kcal	Heat added kcal	Heat Add. ΔH_B %	ΔH_B kcal	Heat Rec. kcal	Heat Add. ΔH_B %
6	20.65	154.88	177.20	115	148.68	135.03	91
8	22.59	169.42	203.36	120	162.65	122.66	75
10	21.09	158.18	164.60	104	151.85	124.22	82

Table 6. Recovery Mode Hydrogen Transfer: LaNi_5 Hydride to CaNi_5

Run	H_2 Moles	CaNi_5 HYDRIDE			LaNi_5 HYDRIDE		
		ΔH_B kcal	Heat Rec. kcal	Heat Rec. ΔH_B %	ΔH_B kcal	Heat Added kcal	Heat Add. ΔH_B %
7	23.36	175.20	149.75	85	168.19	119.09	71
9	18.10	135.75	137.22	101	130.32	97.04	74
11	21.91	164.32	164.30	100	157.75	157.75	76

References

- (1) Gruen, D. M., and Sheft, I., "Metal Hydride Systems for Solar Energy Conversion and Storage", Proc. NSF-ERDA Workshop on Solar Heating and Cooling of Buildings, Charlottesville, Va., April, 1975.
- (2) Gruen, D. M., et al., Proc., First World Hydrogen Conference, Miami Beach, Fl., March, 1976.
- (3) Gruen, D. M., et al., Proc. of the 11th IECEC, p. 681, September, 1976.
- (4) Gruen, D. M., Sheft, I., Lamich, G. and Mendelsohn, M., ANL-77-39, June, 1977.
- (5) Sheft, I., Gruen, D. M., Lamich, G., Carlson, L. W., Knox, A., Nixon, J. and Mendelsohn, M., "HYCSOS: A System for Evaluation of Hydrides as Chemical Heat Pumps", Proc. Int. Symp. on Hydrides for Energy Storage, Geilo, Norway, August, 1977 (In press).

- (6) Sheft, I., Gruen, D. M., Lamieh, G., Carlson, L. W., Knox, A., Nixon, J. and Mendelsohn, M., "Performance Characteristics of the HYCSOS Chemical Heat Pump System Based on Rare Earth Transition Metal AB₅ Hydrides", Proc. 13, Rare Earth Res. Conf., Oglebay Park, W. Virginia, October, 1977 (In press).
- (7) Gruen, D. M., Mendelsohn, M. and Sheft, I., "Metal Hydrides as Chemical Heat Pumps", Solar Energy (In press).
- (8) Mendelsohn, M. H., Gruen, D. M. and Dwight, A. E., "LaNi_{5-x}Al_x: A Versatile Alloy System for Metal Hydride Applications", Nature, Vol. 269, 45 (1977).
- (9) Gruen, D. M. and Mendelsohn, M. H., "Configurational Entropies and the Stabilities of Intermetallic Hydrides", J. Less Common Metals, Vol. 55, 149 (1977).
- (10) Gruen, D. M., Mendelsohn, M. H. and Dwight, A. E., "Stability Considerations of AB₅ Hydrides in Chemical Heat Pump Applications with Particular Reference to the New LaNi_{5-x}Al_x Ternary System", Advances in Chemistry Series, American Chemical Society (In press).
- (11) Gorman, R. and Akridge, W. L., "Hydride Heat Pump System for Building Air Conditioning Using High Temperature Solar Input", Proceedings of Concentrating Solar Collector, Conf. Exhibit Workshop, Georgia Institute of Techn., September, 1977 (In press).
- (12) van Vucht, J. N. H., et al., Phillips Res. Reports, Vol. 25, 133-140 (1970); Buschow, K. H. J. and van Mal, H. H., J. Less Common Metals, Vol. 29, 203 (1972).

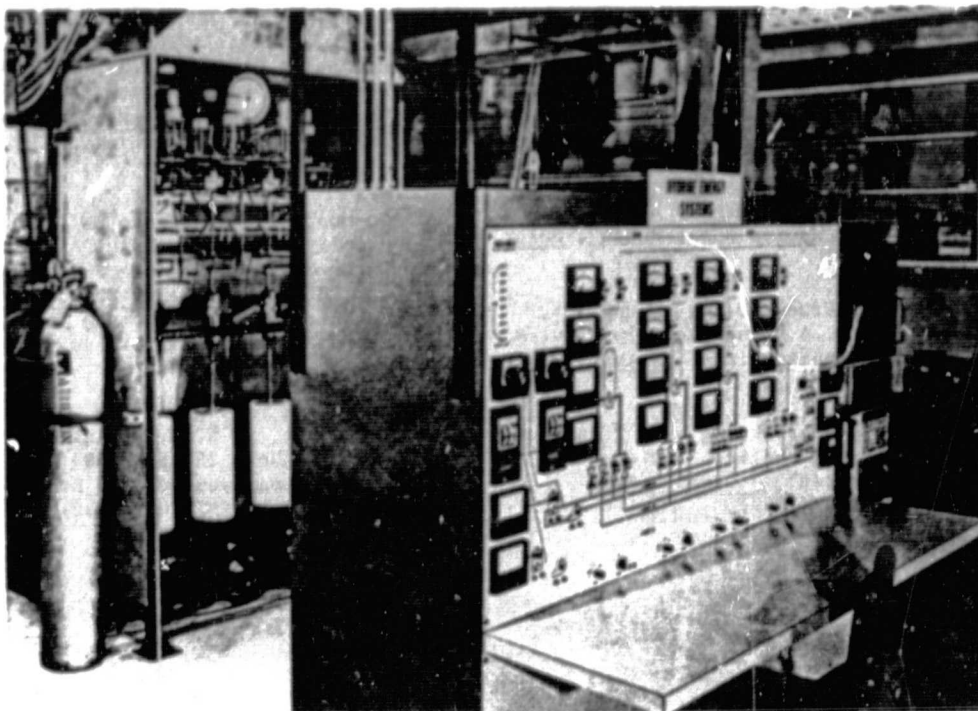


Fig. 1. HYCSOS Demonstration Test Facility

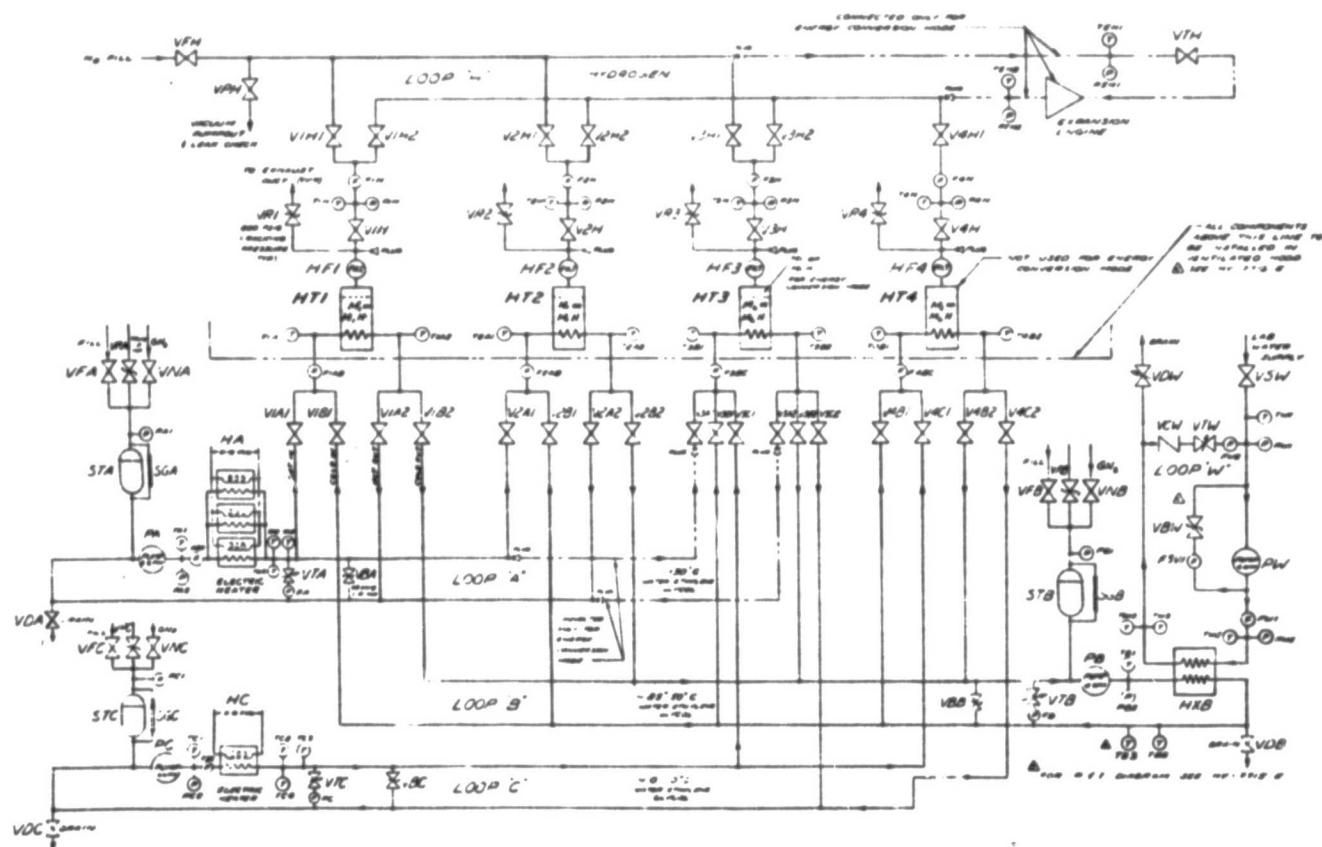


Fig. 2. HYCSOS System Layout

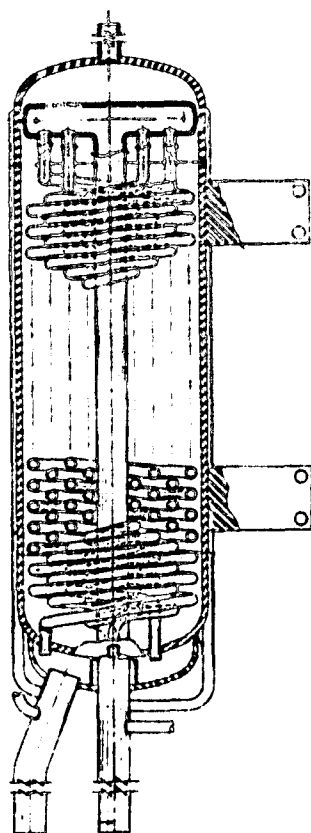


Fig. 3. Metal Hydride Storage Tank

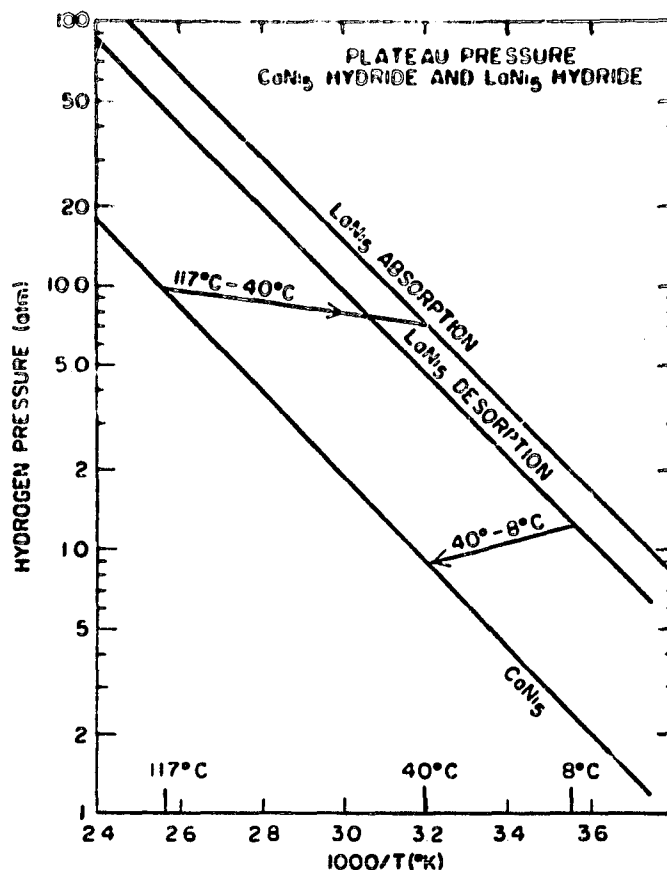


Fig. 4. Plateau Pressure: CaNi_5 Hydride and LaNi_5 Hydride

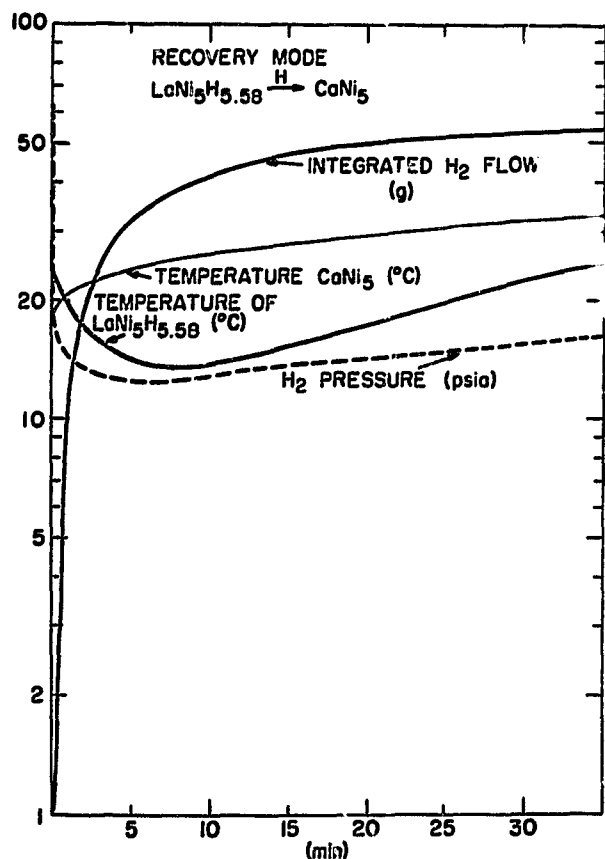


Fig. 5. Recovery Mode: $\text{LaNi}_5\text{H}_{5.58} \xrightarrow{\text{H}} \text{CaNi}_5$

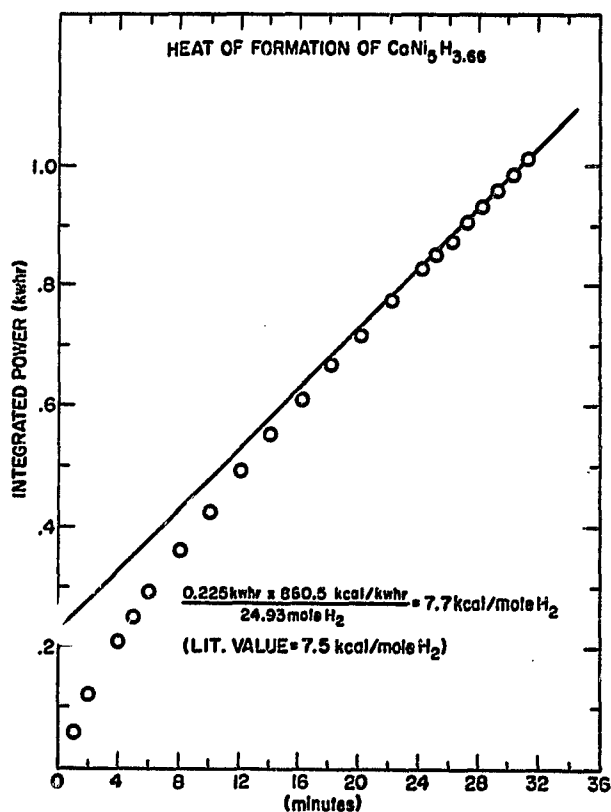


Fig. 6. Heat of Formation of $\text{CaNi}_5\text{H}_{3.66}$

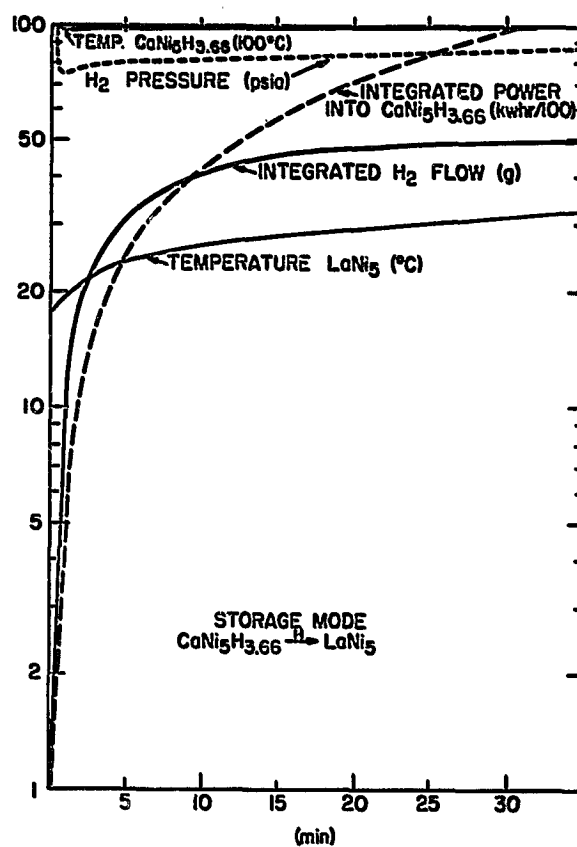


Fig. 7. Storage Mode: $\text{CaNi}_5\text{H}_{3.66} \xrightarrow{\text{H}} \text{LaNi}_5$

DRI RESEARCH PROGRAM ON IMPROVED HYDRIDES

C.E. Lundin, F.E. Lynch, and C.B. Magee
Denver Research Institute
University of Denver
Denver, Colorado 80208

ABSTRACT

The emphasis in this research program is to develop new and improved hydride storage materials. The approach will be to employ DRI developed predictive techniques to select candidate systems. Those systems with potential will be fully characterized and ultimately optimized by alloy addition. The goal is to develop hydrides with more than 3 weight percent hydrogen.

The studies during this review period were devoted principally to five subject areas. These were: (1) studies of AB₂ Laves phases and their hydriding characteristics, (2) the analysis of hysteresis effects in hydride storage materials and the development of a rationale for hysteresis effects, (3) hydriding studies of ANi₅ systems in which Ni was partially replaced with two neighboring elements, (4) hydriding studies of titanium-base, beta solid solution alloys, and (5) design, procurement, and construction of a new Sievert's apparatus and an activation apparatus.

I. Introduction

A research program was initiated approximately four months ago between the Brookhaven National Laboratory and the Denver Research Institute, University of Denver to develop hydrogen storage materials for application to energy needs. The principal program objectives are to develop hydrides with hydrogen capacities of at least three weight percent. The general approach to selection of materials will rely heavily on a predictive criterion developed in our laboratories⁽¹⁾. The criterion to be employed is a correlation of the free energy of formation of the hydride with the interstitial hole sizes in the metallic lattice. Attention will also be given to establishing the following properties: 1) decreased materials cost, 2) contamination resistance, 3) minimized hysteresis, 4) maximized kinetics, 5) good thermal conductivity, 6) safe handling properties, and 7) long-term recyclability. Ultimately, a series of fully characterized, hydrogen storage materials should be made available for various applications.

II. Research Progress

During the period covered by this project review, five separate subject areas of study have been initiated. These are:

A. Experimental study of the hydriding characteristics of selected AB_2 compounds of the Laves phase type including an analysis of the general structural and geometric characteristics of the Cl_4 and Cl_5 Laves phases and the type and number of interstitial sites for hydrogen occlusion.

B. Literature review of hysteresis effects in hydrides, development of a rationale from an analysis of prior theories that would be applicable to current lesser stable hydrides of interest, and preparation of a paper summarizing the significant findings to promote a better understanding of hysteresis effects for presentation at the International Symposium on Hydrides for Energy Storage in Gjeilo, Norway during August 14-19, 1977.

C. Initiation of hydriding studies on ANi_5 compounds where Ni is partially replaced by two neighboring elements.

D. Initiation of hydriding studies on titanium-base, beta solid solution alloys.

E. Design, procurement, and construction of a new Sievert's apparatus and design, procurement, and construction of an activation apparatus.

As stated in the Introduction, the selection of candidate materials is not to be left to intuitive or statistical sampling as has been the case in many previous studies. Several selection rules have evolved which are generally known and accepted. These will be employed as required. For instance, compounds which hydride are those in which one of the elements is a former hydride itself. Earlier studies⁽¹⁾ at DRI have also provided a better understanding of the hydrogen occlusive process. These studies resulted in the development of a useful predictive criterion⁽²⁾. The criterion entails a linear correlation between the standard free energy of formation of the hydride (or logarithm of the plateau pressure) and

the interstitial hole size of the metallic compound lattice. The correlation teaches that the larger the interstitial hole size, the more stable the hydride, basing the comparison at a constant temperature (usually 25°C). The correlation for each structure type is different and must be established first with experimental hydriding and lattice parameter data for several representative compounds. The stabilities of unknown compounds with the same structure type can then be determined by converting lattice parameter data into the interstitial hole size and obtaining the stability from the correlation plot. With more complex structure types, where the hole size is difficult to locate or calculate, atomic volumes can be used. The atomic volume is roughly proportional to the volume of the interstitial holes.

The stability-size correlation has been verified by data from many investigators as well as by our own. Also, it has been demonstrated with many different structure types. Only a few exceptions have been observed. This predictive tool is not only useful for locating new storage compounds, but also for adjusting or tailoring the stability of known materials to higher or lower pressure levels by the properly selected alloy addition.

The experimental study of AB_2 Laves phase inter-metallic compounds, was initiated first with the pseudo-binary system, Fe_2Y-Fe_2Ti . These two binary systems were selected first for several reasons. The 66.7 atomic percent Fe in the AF_2 compound is an inexpensive component with a relatively large fraction of the metallic content. The Ti at 33.3 atomic percent is somewhat more expensive, but is the lightest weight transition metal (other than Sc). Yttrium is more expensive, but hopefully a small amount would be required. Yttrium is also light-weight. Hypothetically, if the $Fe_2Ti_{.75}Y_{.25}$ alloy forms an AB_2H_4 hydride, the hydrogen content would be about 2.4 weight percent, which is considerably better than $FeTi$ and $LaNi_5$ hydrides. The Fe_2Y compound is the Cl_5 (cubic) Laves phase, whereas the Fe_2Ti compound is the Cl_4 (hexagonal) Laves phase. The Fe_2Ti compound melts congruently, while the Fe_2Y compound is formed peritectically. In the studies of Sandroock, Reilly, and Johnson⁽³⁾ it was found that, under the experimental conditions employed, the Fe_2Ti phase did not hydride. The Fe_2Y phase has been found to hydride to Fe_2YH_4 by Van Mal, et al.⁽⁴⁾ It is postulated by DRI investigators that Fe_2Ti does hydride under the proper experimental conditions. Ultra-high pressures at low temperatures would be expected to cause hydriding to an AB_2 -hydride. On the other hand, the Fe_2Y is very stable and readily forms a hydride with extremely low equilibrium pressures at ambient temperatures. These factors can be readily predicted from the stability-size correlation. The atomic volume of Fe_2Ti was calculated to be $38.4A^3$ (per formula weight), and the atomic volume of Fe_2Y was calculated to be $49.8A^3$ (per formula weight). According to the correlation the smaller volume should be very unstable, whereas the larger volume should be very stable, as is the case. The experimental AB_2 data of Shaltiel, et al.⁽⁵⁾ were plotted in conformance with the size-stability correlation. It was found that the stability range of 1 to 10 atm plateau pressure corresponded to about $45A^3$ atomic volume. Thus, the Fe_2Ti-Fe_2Y pseudo-binary system should bracket the right pressure range, namely 1 to 10 atmospheres. The

obvious next step was to prepare alloys in the Fe₂Ti-Fe₂Y pseudo-binary intermediate range in an attempt to form an appropriate atomic volume in between 38.4A³ and 49.8A³. First, the Fe₂Ti and Fe₂Y alloys were prepared and subjected to hydriding to verify the previous studies. Hydriding attempts with Fe₂Ti up to about 120 atm were unsuccessful in the formation of a hydride phase, whereas the Fe₂Y reacted immediately at room temperature to form a hydrided alloy. The composition was not readily determined, because the as-cast sample was not single-phase due to the peritectic solidification. Next, a series of alloys were melted in the Fe₂Ti-Fe₂Y pseudo-binary system. These have been examined metallographically, since a two-phase region was expected in which the C14 and C15 phases co-existed. It was hoped that considerable solubility existed at either end of the pseudo-binary system to allow adjustment of the size factor and, in turn, stability. However, the two-phase region was found to be extensive, covering between about Fe₂Ti_{0.85}Y_{0.15} and Fe₂Ti_{0.15}Y_{0.85}. One alloy in the two-phase region was hydrided to determine what the hydriding characteristics of the dual phase combination were. The alloy was the Fe₂Ti_{0.75}Y_{0.25} composition. The Fe₂Ti phase with Y in solution did not hydride appreciably, while the Fe₂Y phase with Ti in solution was still very stable. The composition of the Fe-Y base hydride was estimated to be about 4.5 H/AB₂. This system had to be abandoned due to the extensive two-phase region and the gross stability and instability of the two phases in equilibrium in the two-phase region.

The next related pseudo-binary system which was felt to allow more possibilities for adjustment to the proper hydriding properties was the Fe₂Zr-Fe₂Y system. Should an Fe₂Zr_{0.75}Y_{0.25} alloy form an AB₂H₄ hydride, the hydrogen content would be about 2 weight percent. This may then be used as a starting phase to modify in the direction of increased hydrogen capacity. In this case, the two Laves-phase structures are of the C15 (cubic) type. Complete solid solubility is expected. The atomic volumes are 44.2A³ for Fe₂Zr and 49.8A³ for Fe₂Y, which are closer together compared to the Fe₂Ti-Fe₂Y systems. Also, the atomic volumes still bracket the estimated 45A³ atomic volume for AB₂ structures which is projected to give the correct stability range. The Fe₂Zr compound was subjected to hydriding first. Pressures up to about 120 atm did not cause hydriding. Obviously, the size of the lattice or interstices is still too small to allow a sufficiently high degree of stability. Alloys have been made, and hydriding characteristics are being determined in the pseudo-binary system. So far, alloys in the compositional range from Fe₂Zr_{0.9}Y_{0.1} to Fe₂Zr_{0.5}Y_{0.5} appear to be single-phase alloys. An alloy at Fe₂Zr_{0.7}Y_{0.3} was found to hydride at room temperature. Alloys in this compositional region are currently being studied to establish the total saturation and the pressure-temperature-composition relationships.

An associated topic of study with the AB₂ Laves phases was concurrently initiated. An analysis is being made of the general structural and geometrical characteristics of the C14 (hexagonal) and C15 (cubic) type Laves phases in conjunction with the pseudo-binary system hydriding investigation.

In the AB₂ compounds there are three types of tetrahedral holes encompassed by metallic atoms as follows: B₄, A₂B₂, and AB₃. Current analyses are directed toward characterization of these holes as follows: 1) Determination of the radii of these holes in the AB₂ compounds as a function of the lattice parameters; and 2) Determination of the number of each of these types of holes, and the relative geometric positions of these holes in the crystal lattices of these compounds. The following correlations are being made: 1) Experimentally determined hydrogen concentration with number of available holes; 2) Experimentally determined hydride stabilities with hole type and size; and 3) Occupancy and stability with the electronic structures of the A and B elements involved.

The unit cell of the cubic AB₂ (C15) compound contains 8 A atoms and 16 B atoms. The relative positions are best understood by looking at a three dimensional model. Close packing within this structure requires that the atomic distances (closest approach) satisfy the following criteria:

$$A-A: \frac{2\sqrt{3}}{8} a,$$

$$B-B: \frac{2\sqrt{2}}{8} a,$$

$$A-B: \frac{\sqrt{11}}{8} a,$$

where a is the lattice parameter of the crystal.

The relative positions of the atoms and the specifications of interatomic distances presented above have been used to calculate the "hard sphere" radii of the three types of tetrahedral holes that are found in this structure. The radii of the spheres that touch the four encompassing atoms are given below:

B₄ tetrahedron (4 touching B atoms):

$$R_s = \frac{a}{8} (\sqrt{3} - \sqrt{2}) = \frac{a}{8} (0.31784)$$

AB₃ tetrahedron (three touching B atoms, A-B distance ($\sqrt{11}/8$)a):

$$R_s = \frac{a}{8} \left(\frac{\sqrt{3}}{\sqrt{6}+2} \right)$$

$$R_s = \frac{a}{8} (0.38927)$$

A₂B₂ tetrahedron (B atoms touching, A atoms touching, and A-B distance ($\sqrt{11}/8$)a):

$$R_s = \frac{a}{8} \left(\frac{3}{1+2\sqrt{6}} \right) \{ -(\sqrt{3}+\sqrt{2}) + \sqrt{2}(3+2\sqrt{6})^{\frac{1}{2}} \}$$

$$R_s = \frac{a}{8} (0.42129)$$

The coordinates of the three different types of holes closest to the origin of the cell are given below:

$$B_4: x=2\left(\frac{a}{8}\right), y=2\left(\frac{a}{8}\right), z=-2\left(\frac{a}{8}\right)$$

$$AB_3: x = \left(\frac{\sqrt{3}}{2}\right)\left(\frac{a}{8}\right), y = \left(\frac{\sqrt{3}}{2}\right)\left(\frac{a}{8}\right),$$

$$z = -\left(\frac{\sqrt{3}}{2}\right)\left(\frac{a}{8}\right)$$

$$x = -\frac{a}{8} (1.2247) = y$$

$$z = -\frac{a}{8} (1.2247)$$

$$A_2B_2: x = y = \frac{a}{8} (1.5223)$$

$$z = -\frac{a}{8} (0.044634)$$

Along certain planes the holes are arranged in clusters, each with one B_4 and $2AB_3$ and 2 A_2B_2 holes. Counting the holes in these clusters gives 5 B_4 , 20 AB_3 , and 16 A_2B_2 holes. This number of holes is reported by Pebler and Gulbransen⁽⁶⁾. However, there are many A_2B_2 holes in the cell which are not contained in these planar clusters. Three-dimensional clusters about each of the B_4 holes accounts for a total of 5 B_4 , 20 AB_3 , and 48 A_2B_2 holes. This counting of A_2B_2 holes does not take into account those holes originating from clusters outside the unit cell but shared by the cell. Depending on how these holes are considered to be shared by adjoint unit cells, there can be as many as 40 additional A_2B_2 holes per unit cell.

The second area of study involved the hysteresis effects observed almost universally in these hydrogen storage materials. A large hysteresis results in a reduced thermodynamic efficiency when employed cyclically in various applications and dilutes the argument that hydrides are safer than high pressure hydrogen systems. Thus, it is important both scientifically and technologically to understand the phenomenon of hysteresis. Considerable effort was expended to conduct a literature survey of hysteresis effects in hydrides, develop a rationale from an analysis of prior theories that would be applicable to current hydrogen storage materials, and prepare a paper⁽⁷⁾ summarizing the significant findings, all to promote a better understanding of hysteresis effects. The paper was then presented during August 14-19, 1977 at the International Symposium on Hydrides for Energy Storage in Norway.

The salient features of the rationale are presented in this review paper. Briefly, the rationale proposes that strain effects are the fundamental cause of the hysteresis. The hysteresis effects are thought to be manifested at the atomic level, thus powder particle size would have little effect on hysteresis. The hysteresis appears to be an irreversible property in these materials. Thus, no single path in absorption-desorption should be possible. The desorption plateau is regarded as the closest approach to "equilibrium" conditions since the strain is irreversible plastic deformation. Localized compressive strain is imposed on the unfilled interstitial sites during hydrogen absorption in the metal solid-solution region, and during the large expansion on absorption in the two-phase region. The α and β phases are thus subject to plastic deformation at the micro level. On desorption from the β phase, the elastic portion of the strain is relieved on approaching the two-phase region and through the two-phase region which causes the desorption plateau pressure to fall below that of the absorption plateau pressure. The pressure difference is attributed to the effect observed in the size stability correlation wherein

the stability of the hydride decreases (higher pressure plateau) due to the compressive strain reducing the size of the unfilled sites. On relief of strain during desorption, the size of the sites is increased which increases the hydride stability (lower pressure plateau). The strain sensitivity of stability for these hydrides is extremely large, so only a small amount of strain is necessary to cause hysteresis.

A relationship was found which describes the hysteresis pressure difference in any one system as a function of temperature. This was expressed as $\ln(P_2/P_1) = \text{constant}$. A survey of the experimental data from the SmCo_5 , LaNi_5 , and FeTi hydride systems supports this relationship rather well.

The case of hysteresis in CeCo_5 and CeNi_5 hydrides was given special attention. Although the Co and Ni atoms are similar in all respects, their AB_5 compound hydrides react very differently. The CeNi_5 shows an enormous hysteresis; 240 atm in absorption and 50 atm in desorption at 25°C, whereas the CeCo_5 has only a fraction of one atmosphere difference in the absorption-desorption plateau pressure at 25°C. Also, the hydriding characteristics are quite different. CeCo_5 forms a CeCo_5H_3 hydride, whereas CeNi_5 forms a CeNi_5H_6 hydride. The small hysteresis of CeCo_5 hydride and the large hysteresis of CeNi_5 hydride are attributed to their different capacities to promote 4f electrons into the conduction band. The large hysteresis observed in MischmetalNi_5 hydride is attributed to the Ce content as a result of this analysis and a former investigation⁽¹⁾ conducted for the Advanced Research Projects Agency. Removal of the cerium can be accomplished easily during the extraction process from the mineral concentrate. The cerium-free, Mischmetal pentanickel compound hydrides readily and is much more stable. The hysteresis has been almost entirely removed by eliminating the Ce.

The third area of study conducted during this period was with LaNi_5 as a base for alloy additions. The objectives were to substitute for the nickel component with less expensive elements such as Mn, Fe, Cu or Zn and, in doing so, to gain insight into the factors determining the extent of hydrogen capacity in metal hydrides. The substitution must be done with pairs of elements. The effect is somewhat analogous to forming ferromagnetic alloys, known as Heusler alloys, from Cu and Mn (which in themselves are non-ferromagnetic). They bracket Fe in atomic number and are alloyed to replace Fe, employing a size effect relationship of the CuMn solid solution that averages out to that of Fe. Since Mn, Fe, or Co and Cu or Zn bracket Ni in atomic number, respectively without much change in size, they could be substituted appropriately in pairs. Hopefully, one could prepare a hydride of less expensive materials and still not decrease hydride capacity, or maybe increase capacity. Thus, an alloy with the composition $\text{LaCo}_{1.25}\text{Ni}_{2.5}\text{Cu}_{1.25}$ was selected as the first candidate to test feasibility. The phase equilibria are such that an essentially single-phase alloy would be expected. Metallography was employed to verify that this was the case. The alloy hydrided readily at room temperature to the H/alloy ratio of 5.5, which is excellent considering the cobalt content. The plateau has considerable slope in the as-cast specimen. Heat treatment has, as yet, been

unsuccessful in developing a single plateau. It appears instead that two or three distinct hydrogen occlusion modes will develop in this system as they have in others, e.g., $\text{LaCo}_5\text{-H}$ and FeTi-H .

The fourth area of study is currently being initiated. This is the hydriding characteristics of Ti-base, beta solid solutions. Selection of alloys is to be made in terms of the predictive correlation. Once the binary, Ti-base alloy hydride has been optimized, ternary alloy additions will be made for further optimization. The first binary system to be investigated is the Ti-Mo, binary system. Alloys are currently being prepared to initiate hydriding studies.

The fifth area of project activity was as follows: Design, procurement, and construction of a new Sievert's apparatus, and design, procurement, and construction of an activation apparatus.

Although a Sievert's apparatus with provision for three reaction chambers already exists and has been used on prior projects, it was felt necessary to expand the capabilities for increased screening and characterization studies for the ERDA program. Improvements in design and pressure capability have been incorporated in the new system which is provided with three reaction chambers each of which can be operated concurrently. The apparatus is essentially completed and will be operative in about a month.

In conjunction with the Sievert's apparatus, another activation unit is being assembled. It will allow pre-activation and sample break-in prior to conducting the absorption and desorption isotherms on candidate samples. The system has three stations to activate three samples simultaneously. It is fitted with a hydriding bed which will provide activation and cycling for several cycles automatically. The samples can then be removed easily without disturbing the reaction chamber atmosphere and moved to the Sievert's apparatus where quantitative characterization of absorption and desorption isotherms can be conducted.

ACKNOWLEDGEMENTS

The authors are grateful for the support of the Brookhaven National Laboratory under Contract No. 414771-S. Also, recognition must be given for the assistance of Dr. J. Liu, and the laboratory technicians, R. Nye and Y. Shinton.

REFERENCES

- (1) Lundin, C. E. and Lynch, F.E., "Solid State Hydrogen Storage Materials for Application to Energy Needs", Denver Research Institute University of Denver, Final Report No. AFOSR-TR-76-1124, August 1976, Under Contract to ARPA, Order 2552.
- (2) Lundin, C.E., Lynch, F.E., and Magee, C.B., To be published in November 1977, Journal of Less Common Metals.
- (3) Sandroock, G.D., Reilly, J.J., Johnson, J.R., Technical Paper 936T-OP, 11th IECEC, Proceedings September 1976, Nevada.
- (4) Van Mal, H.H., Buschow, K.H.J., Miedema, A.R., Journal of Less Common Metals, 49(1976) 473-475.
- (5) Shaltiel, D., Jacob I., and Davidov, D., Journal of Less Common Metals, 53 (1977) 117-131.
- (6) Pebler, A., and Gulbranson, E.A., Trans AIME, 239 (1967) 1593.
- (7) Lundin, C.E. and Lynch, F.E., Proceedings of International Symposium on Hydrides for Energy Storage, Geilo, Norway, Institutt for Atom-energi, August 1977.

A THERMODYNAMIC AND ECONOMIC STUDY OF VARIOUS TECHNIQUES FOR THE
LARGE SCALE PRODUCTION OF HYDRIDING GRADE FeTi

C.J. Trozzi and G.D. Sandroek
The International Nickel Company, Inc.
Paul D. Merica Research Laboratory
Sterling Forest, Suffern, NY 10901

Abstract

The intermetallic compound FeTi has considerable potential as a hydrogen storage medium. This paper represents a survey of possible large scale production methods for FeTi and related compounds. Direct and indirect reduction of ilmenite ore is considered in thermodynamic and economic detail. Results show that thermodynamics, economics and impurity effects make the direct production of FeTi from ilmenite unlikely. For the foreseeable future FeTi will be made by the melting of primary sponge Ti and scrap steel at final selling prices slightly above \$2.00/pound.

INTRODUCTION

Work at Brookhaven National Labs has shown that the intermetallic compound FeTi, along with related alloys, has considerable potential for use as a rechargeable hydride. This is the result of two factors: (a) it has attractive hydrogen storage properties in the vicinity of room temperature(1) and (b) it has the lowest raw materials cost of any presently known rechargeable hydride. As large scale engineering applications for FeTi-base alloys develop, it becomes important to establish the basic information on the metallurgy and production of the system to optimize the properties on a practical, multiton basis. This paper provides a survey of the thermodynamic and economic feasibility of producing FeTi by employing direct or indirect reduction of ilmenite ore and the direct melting of Ti and Fe metal. The factors considered were raw materials, process thermodynamics, effect of residual elements on hydriding capacity, and economics.

It has been established that FeTi is quite complex metallurgically and that a number of compositional factors must be considered in its production(2). The basic roles of Fe/Ti ratio, effect of O, N, C and Si contamination and the role of a number of ternary transition element substitutions have been established. A survey of the technical aspects of conventional induction melting was conducted and two new quasi-conventional melting techniques for large scale FeTi production were developed(2,3).

The thermodynamic and rough economic analyses of techniques which might conceivably be used to produce FeTi directly or indirectly from an ore have been investigated, discussed in detail(4) and will be summarized here. The study also involved the examination of the technical and economic feasibility of directly melting elemental titanium and iron.

The study was directed toward the achievement of a good quality hydriding grade FeTi. By this we mean a homogeneous alloy of about 54 wt. % Fe and 46 wt. % Ti with oxygen content less than 0.1 wt. %. Such an alloy should be capable of hydriding to a capacity on the order of $H/M = 0.85$ or more. The effect of other impurities (e.g., Al or Si) will be considered in context where appropriate.

SURVEY APPROACH

The basic information for the thermodynamic and economic calculations made below were derived predominantly from the following:

1. Open literature.
2. Personal contacts within the primary titanium and ferrotitanium industries.
3. Internal Inco information for comparable metallurgical processes or procedures.

Various sources of information have been utilized in this study. In some cases a given piece of information can be referenced. Often it represents internal information or a composite from several sources that cannot be readily referenced. The numbers used in this study are felt to represent valid estimates for 1977. Of course, in a study of this sort, there are always technical unknowns which could affect the end result. These unknowns have been identified wherever possible.

The technical processes surveyed were the following:

- A. Direct Reduction of Ilmenite
 1. Gaseous Reduction
 - a. Hydrogen
 - b. Carbon Monoxide
 - c. Methane
 2. Carbon Reduction
 3. Metallothermic Reduction
 - a. Silicon
 - b. Magnesium
 - c. Calcium
 - d. Aluminum
- B. Indirect Reduction Processes
 1. Chloride (Kroll) Process
 2. Electrolytic
- C. Conventional Melting of Primary or Scrap Ti
 1. Air Induction Melting
 2. Vacuum Induction Melting
 3. Consumable Electrode Arc Melting

It should be recognized that FeTi is not necessarily the optimum alloy for a given application. Because of this, along with the fact that the composition of the ore will vary over wide limits,

remelting and composition adjustment is mandatory for any of the direct or indirect reduction processes considered.

Any reduction method employed would require a final remelting, composition adjustment, and mischmetal (rare earth) deoxidation of the alloy product(2,3). Oxygen (greater than 0.1 wt. %) has a deleterious effect on the hydrogen storage capacity of FeTi, so its removal is desirable. Similarly, FeTi directly melted from elemental Fe and Ti should also be mischmetal treated. The small additional cost assures a high hydrogen capacity for vehicular applications and minimum decrepitation for stationary applications, as well as aiding activation(2).

The final number presented for each analysis is the FeTi selling price in \$/pound. This involves a mark-up from the overall production costs. The mark-up used throughout this study is 42%, based on the assumption of a 50% tax on income and a 15% after-tax return on sales. This mark-up can vary slightly with a number of factors, but we feel it is representative of the metallurgical industry that would be called upon to produce multimillion pound quantities of FeTi for energy storage applications.

ORE SOURCES - RUTILE VS. ILMENITE

In order to survey various processes for producing FeTi, a survey of raw material resources was necessary.

Titanium originates from two ores: rutile (nominally TiO_2) and ilmenite (nominally $FeTiO_3$). Rutile (generally 96-98% TiO_2) is a higher grade ore than ilmenite, having a higher titanium content. Neither of these ores are totally free of other oxides. Ilmenite, however, contains more additional oxides than rutile. The U.S. has an abundance of ilmenite, but is dependent on Australia for rutile which is presently used in manufacturing pigment, welding rod coatings and titanium metal. The increased rutile consumption has placed increased demands on rutile reserves and is subsequently driving prices up(5).

Rutile is 59% titanium, while ilmenite is only 31.6% titanium. Although the purity of rutile may seem attractive, it lacks the iron necessary for the production of FeTi. Since ilmenite contains a considerable amount of iron (both in the ilmenite phase and in the form of various iron oxides), it would be beneficial to find a method of reduction which would yield both titanium and iron metal simultaneously.

In view of our future energy situation, future raw material availability is a critical factor. The limited quantity of rutile leaves ilmenite as the only long range alternative. There are a wide variety of grades of ilmenite but that of the highest purity is desired for FeTi production.

Some typical ilmenite compositions are shown in Table I and Reference 4. The ilmenite concentrate, used as a basis for the calculations, is only one of the many concentrates available. The mineral analysis can vary widely from grade to grade. Therefore, the material and heat balance for each ore will be different. The ore price varies depending on the ore grade and lot size.

DIRECT REDUCTION OF ILMENITE

The primary reduction reactions ($FeTiO_3 \rightarrow Fe + TiO_2 + 1/2O_2$) and secondary reduction reactions ($TiO_2 \rightarrow Ti + O_2$) with reducing agents such as C, H, CO, Si, Al, Mg and Ca have been examined using basic thermodynamics. When examining the feasibility of applying each reducing agent, the following questions need to be asked: Is the reaction thermodynamically possible? How effectively does it reduce ilmenite? And in doing so, how much of the reducing agent residual is left in the alloy? Does this residual have a deleterious effect on its hydriding properties? How pure is the product?

The equation $\Delta G^\circ = -4.574 T \log K$ illustrates that at a given temperature ($^\circ K$) the equilibrium constant (K) and hence, the equilibrium state is determined entirely by the standard free energy change, ΔG° . Quantitative information on the chemical equilibrium state is given by either K or ΔG° . A value of K greater than 1 corresponds to a negative value of ΔG° , which means that when reactants and products are present in their standard states the reaction will proceed spontaneously toward equilibrium, as written. Consequently, the larger the negative free energy change is for a given reaction, the more likely it is that that reaction will take place. The values and equilibrium constants for the primary and secondary reactions involving each reducing agent have been calculated (for details see Reference 4). The primary reduction reaction involving each reducing agent is thermodynamically possible; but the degree to which the reduction will take place will depend on which reducing agent is employed. Complications arise during the secondary reduction reactions due to the large affinity Ti has for oxygen. Figure 1(6) illustrates the $Ti + O_2 \rightarrow TiO_2$ oxidation reaction (reverse for the reduction reaction) and its relationship with the oxidation curves of the reducing agents considered. A basic thermodynamic rule can be applied while referring to Figure 1. All of those elements which have " ΔG° vs. T " curves lying below the curve of the oxide being reduced are eligible as reducing agents for that oxide (corresponding to a negative free energy change), and it follows that the larger the free energy gap, the more effective the reducing agent will be. Elements associated with " ΔG° vs. T " curves lying above the curve of the oxide being reduced are not potential reducing agents (corresponding to a positive free energy change). In other words, for those reducing agents under consideration, that which has the largest equilibrium constant for the reduction reaction is the most desirable.

Titanium's great affinity for oxygen is a major drawback of all of the reduction processes considered. The partial free energy change per mole of oxygen has been plotted by Kubashewski et al(7) as a function of oxygen content in the Ti-O system. This curve illustrates the affinity Ti has for oxygen. Upon careful examination of the O-Ti phase diagram one can observe that there is no significant change in phases occurring between 1000°C and 1500°C. Therefore, even though Figure 2 has been calculated at 1000°C, it is reasonable to assume that it would have a very similar shape at temperatures up to at least 1500°C.

The graph illustrates that a reducing agent that

can overcome the affinity of oxygen to TiO_2 , Ti_2O_3 , Ti_3O_5 and TiO may not produce pure titanium owing to the affinity of oxygen dissolved in the metallic titanium. Therefore, thermochemical calculations which do not account for the solution phase may fail, reduction being less complete than would be expected from the calculations(7).

The heat of oxide formation is another factor which will affect the manner in which the reduction is carried out. If the reaction is endothermic (positive heat of oxide formation), then an outside heat source will be required to carry out the reaction. If the reaction is exothermic (negative heat of oxide formation), an outside heat source is not required in order to carry out the reaction. Any reserve heat left after the ore oxides are dissociated can contribute to heating the charge.

The elements which thermodynamics predicted could not be effective reducing agents for TiO_2 were not considered further. Those elements which looked promising were examined more closely (for details of the material, equilibrium calculations, balance, economics and heat balance, see Reference 4). Once the technical feasibility was established, the most important factor was economic feasibility. Calculations made for the reduction reactions which proved to be economically unfeasible (due to the high cost of reducing agent) were not carried out in great detail.

The arrival and growth of the steel industry brought a need for ferroalloys (i.e., Fe-Ti, Fe-Si, etc.). The three production methods employed were carbon reduction, silicon reduction and aluminum reduction.

Gaseous Reduction

Hydrogen Reduction. Hydrogen is utilized as a reducing agent in only a few limited cases. Ferrotitanium cannot be produced by ferroalloy producers in this manner because its stable oxides are not reducible by hydrogen. The equilibrium constant for the critical reduction reaction is one of the lowest of all reduction reactions considered. At temperatures in the vicinity of the melting point of FeTi (1623°K), the free energy change remains positive. It has also been shown that the equilibrium constant for the secondary reaction $TiO_2 + 2 H_2 \rightarrow Ti + 2 H_2O$ is $K = 7.18 \times 10^{-11}$ at 1623°K(4). Under equilibrium conditions only iron is reduced by hydrogen, leaving rutile (TiO_2) unreduced(8). Therefore, if this method were employed, subsequent reduction of TiO_2 by some other method (i.e., metallothermic) would be required. Thus, direct hydrogen reduction of ilmenite is thermodynamically unfeasible. Partial reduction with H_2 followed by subsequent reduction of TiO_2 with a more powerful reductant, though unexplored technically, may be of interest. However, this procedure does not offer any hope of a major production cost breakthrough.

Carbon Monoxide Reduction. Carbon monoxide is the least likely candidate for ilmenite reduction from a thermodynamic standpoint. The free energy to drive the reaction is positive throughout the entire temperature range under consideration. The secondary reaction $TiO_2 + 2 CO \rightarrow Ti + 2 CO_2$ near the melting point of the alloy has a very unfavor-

able equilibrium constant $K = 7.14 \times 10^{-12}$ (4).

Examination of the possibility of ilmenite reduction by CO illustrates that even if the reaction were achieved under special conditions, the formation of carbide would be favored. As mentioned below, carbon ties up titanium as TiC, thus hindering FeTi's H-storage capacity.

Methane Reduction. Recently some success in reducing titaniferous magnetite (i.e., a magnetite-ilmenite mixture) with CH_4 has been reported(9) although the thermodynamics tend to favor the ultimate formation of TiC; there appears to be a critical time-temperature realm where some of the TiFe phase can form. This represents a possibility for the production of FeTi from ilmenite, but information at this time is not adequate to judge either economics or technical feasibility on a commercial scale.

Carbon Reduction

Carbon reduction of TiO_2 is possible at high temperatures (Figure 1 - at temperatures above 1600°C where the $2 C + O_2 \rightarrow 2 CO$ curve lies below the $Ti + O_2 \rightarrow TiO_2$ curve). Carbon is a poor reducing agent for ilmenite at low temperatures, requiring a large amount of heat and therefore must be carried out in an electric arc furnace. Equilibrium constants for the primary and secondary reactions are shown in Reference 4. As illustrated by the equilibrium values and Figure 3, the titanium carbide reaction will tend to predominate. This is indicative of the fact that ferrotitanium alloys produced carbothermally (by the ferroalloy industry) have a high carbon content (~3-8%)(10).

Though reduction of ilmenite with carbon is thermodynamically possible, its employment in FeTi production is undesirable due to the residual carbon which takes the form of TiC and would very seriously inhibit its hydrogen storage capacity. Each weight percent carbon would tie up about 4%Ti as TiC. Thus an 8%C alloy would have only about 46-4(8) = 14% free titanium left for the formation of the FeTi phase. The capacity would be further lowered by substantial amounts of residual oxygen. Carbon reduced ilmenite would probably have less than 20% of the H-storage capacity of high purity FeTi.

Metallothermic Reduction

The principle by which metallothermic reduction takes place is very basic. A metal oxide can be reduced to metal by a particular metal reducing agent if that chosen reducing agent has a greater affinity for oxygen than that of the metal to be reduced. A complex equilibrium occurs in which those metals with higher affinity for oxygen will be found in the slag phase and those that do not will be found in the metallic phase.

The following basic considerations(11) must be made in order to determine the feasibility of producing titanium and iron from ilmenite, in a metallothermic process according to the general chemical equation:



*The chemical equation will require balancing, depending on the oxide and reducing agent employed.

M is the metal to be reduced.
X is another metal used as a reducing agent.
Y is some non-metallic element or radical.

- (1) Is the driving force of the reaction sufficient?
- (2) Will the reaction proceed to within a reasonable approach of completion?
- (3) Will sufficient heat be evolved to melt the products of reaction?
- (4) Will the reaction products separate?

Metallurgical reduction processes are batch processes which guarantee a carbon-free product. When employing this kind of process, there are two kinds of approaches, both of which are self-propagating reactions(12): (a) top igniting a mixture of powdered charge (reducing agent, ore, flux and boosters) and allowing the reaction to complete by itself (in-furnace or out-of-furnace) and (b) preheat the reducing agent (i.e., ingot form) and add the powdered charge to the top of the heat, thus allowing the preheated reductant to ignite the reaction (in-furnace). In the former approach, the process begins from the top and the products of reaction travel by gravity through the mixture to the entire mass. In the latter approach*, the fresh mixture travels by gravity through the hot reaction products.

Once the reaction is complete for an out-of-furnace application, the vessel is allowed to cool and the ingot is knocked out. The resultant slag layer, which has protected the ingot from the atmosphere, can be knocked off.

After a complete reaction in-furnace, the alloy and slag must be removed from the furnace and allowed to solidify. Application of an in-furnace method would only require furnace power to initially heat the reductant. Once the reaction is ignited, it will proceed without assistance.

Thermodynamically, there is free energy sufficient to drive the reduction reaction of ilmenite using Al, Mg or Ca as reducing agents. Each of these has an oxide with a large exothermic heat of formation, but which is not totally sufficient to carry out reduction of ilmenite metallurgically out-of-furnace(4). Each reduction reaction would require a thermal booster plus excess reducing agent to react with the booster to produce extra heat. The reaction efficiency will improve with the reduction of slag/alloy volume ratio. If the reduction were carried out in an electric arc furnace, a thermal booster and excess reductant would not be necessary and therefore the slag volume would be considerably reduced. Though furnace production insures greater efficiency, there is a risk of refractory contaminants.

There is associated with each of these reduction reactions, a high equilibrium constant(4) in the temperature range in which the reaction will take place (1600-1800°C). But Ti has a high affinity for oxygen, which is responsible for equilibrium inevitably occurring with a high concentration of

Ti in the slag phase, rather than in the metallic phase. Two factors which will help decide the technical feasibility of a reducing agent are its boiling point and its melting point. A good reaction is one which occurs above the reductant's melting point and below its boiling point. This maximizes the activity of the reducing agent and minimizes its loss due to vaporization.

The calculations (heat and charge balance) made for metallurgical reduction of ilmenite are somewhat crude. It is not practical to burden the analysis with details which are subject to variations. Furthermore, for aluminothermic reduction of complex ores, calculations sometimes become unrealistic. In commercial practice the right proportions of the mixture are established by trial reductions on small batches.

In order to obtain a reasonable idea of production cost/lb FeTi, all calculations(4) have been based upon 100 kgs ilmenite concentrate (Chemalloy Co., Inc. ilmenite composition analysis as basis - Table I) the stoichiometric quantity of reducing agent, and 50% Ti recovery from the concentrate. The 50% Ti recovery assumption was based upon the thermodynamics extracted from the literature and industrial contacts. Economics has been considered only for those methods which have been proven thermodynamically feasible. In such cases the costs have been normalized to cost per pound of FeTi produced.

If a metallurgical process is employed, optimization will involve many variables(4).

Silicothermic Reduction. Silicon is an inefficient reductant for ilmenite and requires an electric arc furnace. There is enough free energy to drive the reaction to produce Fe and TiO₂(4); however, reduction of TiO₂ by Si (Figures 1 and 3) involves a positive free energy change. Si is apparently a very weak reducing agent for Ti oxides over the entire temperature range of interest. Even though the presence of iron facilitates reduction, the final product is a low Ti-high Si alloy (i.e., ~30%Ti, ~30%Si)(10). The hydriding capacity of FeTi will be hindered by Si residuals(4). Thus from an overall point of view, silicon reduction of ilmenite is thermodynamically unfeasible.

Magnesiothermic Reduction. Magnesium, from a heat of reaction standpoint is a more efficient reducing agent than aluminum(13). One of its most unattractive characteristics in this application is its low boiling point (1103°C), since the smelting temperatures will be in the vicinity of 1800°C (some Mg will be lost as vapor). The melting point of pure MgO oxide is 2800°C. The iron oxide and titanium oxide products are good fluxes for MgO. Therefore, it is not likely that any additional flux would be needed to lower the slag melt point and increase slag fluidity. The heat generated by Mg oxidation is greater than that generated by Al(4). The slag which is composed of predominantly MgO and TiO is not as massive as that produced by aluminothermic reduction. A very important factor to consider when dealing with Mg powder is safe transport and handling.

Although the technical aspects of the process make utilizing Mg as a reducing agent undesirable, the factor that makes it impossible is the economics.

*This procedure may prove to be more explosive.

Good quality Mg powder presently costs \$2.20/lb. The material cost of Mg/lb FeTi has been listed in Table II as \$1.70. In calculating this value(4) excess Mg, which is necessary to react with a thermal booster and possible material loss due to vaporization, has not been accounted for. After calculating all possible costs involved using the out-of-furnace approach, including a mark-up for profit and taxes, magnesiothermic reduction will produce a FeTi alloy at approximately \$4.59/lb (out-of-furnace method).

In an effort to reduce the cost, one might be inclined to alter the process, to avoid using costly fine Mg powder in a mixture of powdered charge materials. Alternatively, magnesium (ingot) could be melted (in furnace) and the flux-core mixture top charged into the molten Mg and subsequently allowing the reduction reaction to take place. Though it may not greatly improve the technical feasibility, it can improve the economic feasibility because the current price per pound of Mg ingot (\$.98/lb) is half that of Mg powder. The approximate cost per pound FeTi produced would then be approximately \$2.26. The actual cost will undoubtedly be higher because of excessive Mg volatilization.

Calciothermic Reduction. The most desirable feature of calciothermic reduction is calcium's large heat of oxide formation, its high equilibrium constant associated with its reduction of ilmenite, and its low solubility in Ti metal. Although these factors meet the criteria for deciding a material's effectiveness as a reducing agent, there is much else to be considered. The boiling point of Ca (1482°C) is below the temperature at which the process will be carried out (some Ca will be lost as vapor), and its oxide melting point is 2580°C. The efficiency of a metallothermic reduction process depends on these factors. When reducing with calcium, similar problems will arise, as did when reducing with Mg. Calcium produces more of a problem because it rapidly forms an oxide layer in air at room temperature which would interfere with its effectiveness in reducing ilmenite. Handling and transporting calcium powder would be hazardous and expensive, requiring an argon atmosphere.

An estimated calculation was made in order to obtain approximate material cost(4). The producer price/lb calcium powder* (6 mesh) is currently \$2.13. The cost of calcium per pound of FeTi produced would be \$2.67 without accounting for excess Ca to react with booster, loss due to vaporization and dust loss. The thermicity of this reaction is greater than that obtained by reducing with either Al or Mg, but is insufficient to run the reaction. Therefore, the reaction will require some thermal booster for extraneous heat and a flux (if necessary) to lower the slag melting point and increase slag fluidity. The estimated alloy cost/lb FeTi produced employing calciothermic reduction out-of-furnace will be \$6.59 (Tables II and III). An alternate approach which would reduce the cost of the reducing agent is to melt Ca (crowns or ingot) and top charge the flux and ore into the molten Ca. In this case, the Ca charge could be composed of the cheapest form of Ca (crowns - 99.5% pure) at \$1.49/lb*.

*Chas. Pfizer, Inc.

The cost of Ca/lb FeTi produced would then be \$1.87 (NOTE: this does not account for excess Ca additions), and consequently (in-furnace) the approximate cost/lb FeTi would be \$3.91. This modification would be slightly more technically feasible and less hazardous than using Ca powder. But the high cost of Ca still makes it economically unfeasible. Consequently, calciothermic reduction of ilmenite is neither technically or economically desirable.

Aluminothermic Reduction. The most efficient aluminothermic reactions which produce a high metal recovery occur when a pure oxide is reduced (subsequently producing alumina slag and metal). The reactions are very short and therefore a minimum amount of heat is lost(12). The more complex the ore is the more it is burdened with secondary reactions. The slag will contain reaction products which will absorb a considerable amount of heat from the reaction and thus decrease its efficiency. Even though the equilibrium constant for Al reduction of ilmenite is high, a low Ti recovery (~50%) is expected, due to titanium's high affinity for oxygen. The 50% Ti recovery assumed was in agreement with a ferroalloy producer(14) who due to past experience with ferroalloy production informed us that a 40-50% Ti ferrotitanium alloy could be expected by this method (this implies a ~50% Ti recovery from the ore). Al will reduce FeTiO_3 to TiO_2 (4). Analysis of the secondary reactions shows some TiO_2 reducing to TiO. The thermodynamics illustrates that the major reactions which take place insure Ti loss in the slag as oxide and Al residual in the alloy. The titanium recovery may be somewhat improved by reducing with Al in the presence of some nascent Fe (a good Ti solvent) which will help shift the equilibrium to the right(15).

An approximate slag and heat balance was calculated(4). The exothermic heat generated by the reaction is barely sufficient to dissociate the oxides in the concentrate. Therefore, a large amount of extra heat will be required to help reduce the ilmenite and melt the charge and slag. Assuming approximately a 30% heat loss in an out-of-furnace application, the final quantity of extra heat which is needed to carry out the reduction process must be supplied by an external heat source (booster or furnace).

A flux addition is necessary to reduce the Al_2O_3 -TiO slag melting point and to increase the fluidity. Lime was considered as the most appropriate flux. CaO is a more basic oxide than TiO and weakens its bond with Al_2O_3 , facilitating a more efficient reduction(10).

The aluminothermic reduction of ilmenite will take place above the melting point of Al (659°C) and below its boiling point (1800°C), where Al has a higher activity, making Al more technically attractive than any other reducing agent.

A stoichiometric Al addition will generally produce a 5-10% Al alloy (as produced by various ferrotitanium producers). As illustrated in Figure 4, Al greatly reduces the H-capacity of FeTi. Since the steel industry has little concern for the residual Al in ferrotitanium, the ferroalloy industry optimization requires maximizing Ti recovery. However, since our interests lie in producing a pure FeTi intermetallic compound with

good hydriding properties, the most critical factor involved in its production is the residual elements, especially Al. Therefore, optimization would involve minimization of the Al content, regardless of Ti recovery. Even if Al residuals as low as 1-2 wt. % were achieved by optimizing, the hydrogen storage capacity would be hindered. Any Ti deficiency could be corrected by adding Ti sponge during remelting.

Purity of the alloy product is questionable. Only experimental trials will indicate applicability of this process. It is doubtful that aluminothermic reduction will produce a pure enough product for hydriding purposes, even after remelting and deoxidation.

From an economic standpoint Al reduction of ilmenite is the least costly, and creates the fewest technical difficulties(4). The total price/lb FeTi has been estimated (Table II) to be \$1.93/lb FeTi (out-of-furnace method). Alternatively, in an effort to reduce the cost of Al/lb FeTi (\$.34), utilizing Al ingot in place of powder had been considered. This approach would involve melting Al ingot in a furnace, and top charging the ore, flux and thermal booster (mixture). The high temperature of the Al should ignite the mass. Al ingot is \$.51/lb, and therefore cost of Al/lb FeTi is reduced to \$.29/lb FeTi. The total estimated price/lb FeTi would then be \$1.62.

INDIRECT REDUCTION PROCESSES

Chloride (Kroll) Process

All primary sponge is made by the Kroll (or closely related Hunter) process. Usually rutile is chlorinated and the resultant chlorides purified to produce high purity $TiCl_4$. The $TiCl_4$ is then reduced with Mg to form Ti metal and $MgCl_2$ (Na is used as the reductant in the Hunter process). After leaching or inert gas purging out the $MgCl_2$ the result is Ti sponge which forms the basis of the metallurgical Ti industry.

It has been well established that ilmenite can be directly chlorinated and the resultant chlorides purified to produce a $TiCl_4$ that can be Mg reduced in a Kroll vessel to produce Ti sponge(16). Ilmenite will no doubt be the future feedstock for the Kroll process when rutile runs out.

For the purpose of producing FeTi directly, let us consider taking the unpurified mixed chloride product of ilmenite chlorination ($TiCl_4$, $FeCl_3$, plus various impurity chlorides) and Kroll reduce that with Mg to form a Fe-Ti alloy sponge. From a technical point of view it is not completely clear that this can be done because $FeCl_3$ first condenses as a solid and $TiCl_4$ condenses as a liquid so that the condensed mixed chlorides will be in a pasty form that may be hard to feed into a Kroll reaction vessel. It is felt that the resultant FeTi alloy will be very inhomogeneous and will certainly require remelting. A final technical unknown is the fact that impurity chlorides (e.g., those of Si, Mn, Mg, V and Al) will be produced along with $TiCl_4$ and $FeCl_3$ during the ilmenite chlorination process and will be incorporated into the final product.

Even if the above technical problems can be

overcome with the chloride process, there remain serious economic problems. A cost estimate based on this procedure is outlined in Table II. The final estimated FeTi price is high, about \$3.00/lb FeTi. The key problem, of course, is that a relatively expensive process and relatively expensive Mg is used to reduce the relatively cheap Fe component in addition to Ti. Thus, the mixed chloride process seems to be unfeasible from an economic point of view, if not a technical point of view. As will be shown later it offers no advantages over the direct production of Ti sponge and the remelting of that sponge with scrap Fe.

Molten Salt Electrolysis

It is possible to produce quality Ti by electrolysis. The process involves the electrolytic decomposition of $TiCl_4$ in a molten alkaline or alkaline earth electrolyte(17). No commercial size cells are yet in operation, although substantial pilot scale experience has been obtained by the Timet Division of The Titanium Metals Corporation of America(18). Electrolytic Ti production has an advantage over the Kroll process in that its operating costs are lower. However, capital equipment costs are significantly higher, the process requiring carefully constructed, gas-tight, high temperature cells. When both operating and capital cost considerations are taken into account, it is felt that the final selling price of electrolytic Ti could be about 10% lower than present sponge made by the Kroll process.

The question at hand is "Could FeTi be made directly by simultaneous electrolytic co-deposition of Fe and Ti using mixed $TiCl_4$ + $FeCl_3$ feedstock from chlorinated ilmenite?" Although it is impossible to completely answer this without extensive experimental study, the answer is probably "no" both from technical and economic points of view. First, from a technical point of view, it has been observed that as $FeCl_3$ is added to the $TiCl_4$ feedstock, the resultant electrodeposit becomes extremely fluffy with a high surface area(18). Such a structure is subject to corrosion and oxygen pickup during handling and can even be prophoric! The homogeneity of such a product is doubtful and would certainly require remelting. Finally, with respect to economics, we are saddled with an analogous problem to Kroll production of FeTi. In this case we are using expensive equipment and expensive electric power to produce the Fe component of FeTi. It is impossible to make an accurate cost estimate at this time. However, it seems reasonable to assume that electrolytic FeTi, if technically feasible, would cost at least 90% of the price of Kroll reduced FeTi, i.e., at least \$2.70/lb.

DIRECT MELTING OF ELEMENTAL Fe AND Ti

All of the FeTi production schemes discussed so far have components of doubt for technical and economic reasons. If a large market for hydriding grade FeTi developed tomorrow, the only certain way of producing it would be by direct melting of the elements. In this section we discuss the economics of melting. In all cases it will be assumed that the source of the iron would be scrap steel at \$0.05/lb (\$100/ton). We will consider both scrap and primary sponge for the Ti source.

Melting with Scrap Ti

The melting of FeTi from scrap Ti provides interesting problems in terms of scrap availability and price. At first glance it would seem that substantial quantities of scrap are available. The U.S. titanium industry produces more than 30 million pounds of scrap annually(19). However, virtually all of this is either recycled in the Ti industry or used in the steel or aluminum industry as an alloying element. Furthermore, most of the scrap is of an aerospace grade and contains a substantial amount of Al (e.g., the most common aerospace alloy is Ti-6Al-4V). Because of the extremely deleterious effect of Al on hydriding behavior (Figure 4), it appears that the Al-containing scrap, which probably constitutes more than 90% of the scrap, will be unusable for hydriding grade FeTi.

The remaining commercial purity (CP) grade scrap is in high demand and it commands a price premium over the rest of the scrap. The price of Ti scrap is rather volatile(4). CP grade scrap must be used in the melting of hydriding grade FeTi and its limited availability would support only a small level of FeTi production (at most only a few hundred thousand pounds) before driving the scrap price to near that of primary sponge Ti.

Cost estimates have been developed, bearing the above difficulties in mind, for the air induction melting of scrap Ti and scrap Fe using the 4% rare earth deoxidation procedure developed earlier in this contract(2,3). The basic calculations are shown in Reference 4 and the results outlined in Table II. The results of these calculations are shown as a function of scrap price (Ti) and recovery (R)(4). Based on an early 1977 CP scrap Ti price of \$1.55/lb and an anticipated recovery of 80%, a FeTi price of \$2.00/lb is calculated. Again bear in mind this price is artificial and would rapidly escalate if much additional demand were put on scrap CP titanium.

Melting with Sponge Ti

In the end it appears that the only guaranteed method of producing multimillion pound quantities of hydriding grade FeTi is the direct melting of primary Ti sponge and scrap Fe. The present U.S. sponge capacity is on the order of 50 million pounds per year with substantial additional quantities available as imports from Japan and the U.S.S.R.(19). At present most plants are operating below capacity so that a new market of several million annual pounds of FeTi could be tolerated without difficulty. If a substantially larger FeTi hydride market should develop, then new installed capacity would be required. It would probably be electrolytic and result in a slightly lower Ti price (perhaps 10%, as cited earlier).

Price estimates for the production of FeTi from sponge Ti and scrap Fe are outlined in Table II for: (a) air melting with mischmetal deoxidation(2, 3), (b) vacuum induction melting in a graphite crucible(2,3), and (c) consumable electrode, vacuum arc melting. Calculations are based on 10,000 pound melt sizes. The price we used for Ti sponge was \$2.50/lb [the present published price ranges from \$2.50/lb for imported sponge to \$2.75/lb for domestic sponge(20)]. For the vacuum melting no mischmetal is required for deoxidation

purposes; however, 1% was added to aid in activation(2).

Of the three techniques considered, air melting is more expensive, primarily because of the relatively low recovery associated with the rare earth deoxidation technique (see Ref. 2). Vacuum induction and vacuum arc melting are lower in cost and are almost the same, within the accuracy of the calculations (on the order of \$2.20/lb). These calculations assume the purchase of Ti sponge at the \$2.50 from a Ti producer by a melter who is not a Ti producer. If the melting were done by one of the major sponge producers (i.e., Timet, RMI, or Oremet), some of the profit may be absorbed in the primary sponge operation resulting in a somewhat lower effective markup than the 42% we used. However, it still seems unlikely to us that a price much lower than about \$2.00 for good hydriding grade FeTi can be expected.

SUMMARY AND GENERAL COMMENTS

All of the obvious methods of producing FeTi have been briefly examined from technical and economic points of view. To put things into perspective, the main results(4) for each method are summarized and compared in Tables II and III). The overall picture is pessimistic. The lowest FeTi price (\$1.64/lb) was obtained with aluminothermic reduction, although this result is rather clouded by the fact that the Al residual lowers hydrogen storage capacity greatly(4). The only sure procedures are vacuum induction and arc melting of primary Ti and scrap Fe which narrow down to a FeTi price slightly above \$2.00/lb.

Although ilmenite ore is very abundant and fairly cheap, we are dealing with a fundamental chemical problem of nature - the intensely strong bond between Ti and oxygen atoms. The energy required to break that bond is large and therefore the extractive metallurgy of Ti is expensive, just as it is with all other "energy intensive" metals. The problem is further complicated by the apparent fact that good hydriding grade FeTi is not tolerant of impurities, especially Al and O.

The solution to this dilemma is not obvious. There is always hope of a new breakthrough that will substantially lower the cost of Ti or FeTi extraction from ilmenite. Within the present state of the art there is little hope for an immediate or even long term cost reduction of any significant size. There are a number of things that can be examined further: CH_4 reduction, perhaps more thorough studies of electrolytic processes, a metallothermic reduction using a combination of reductants, quaternary additions to FeTi to counteract the negative Al effect, etc. In the end, however, what is needed is a radical new approach to the extractive metallurgy of Ti. Nature seems to have made this a very formidable task.

ACKNOWLEDGEMENTS

We are grateful to a number of individuals at Inco, Brookhaven, and numerous outside industrial organizations.

REFERENCES

1. Reilly, J.J. and Wiswall, Jr., R.H., *Inorganic Chem.*, 13 (1974), p. 218.
2. Sandrock, G.D., *Interrelations Among Composition, Microstructure, and Hydriding Behavior for Alloys Based on the Intermetallic Compound FeTi*, The International Nickel Company, Inc., Final Report, BNL Contract 352410S, June 30, 1976.
3. Sandrock, G.D., *New Melting Techniques for the Production of Hydriding Grade FeTi*, Proceedings of the ERDA Contractors Review Meeting on Chemical Energy Storage and Hydrogen Energy Systems, Airlie, VA, Nov. 8-9, 1976, ERDA Report CONF-761134, p. 143.
4. Sandrock, G.D. and Trozzi, C.J., "Thermodynamic, Economic, and Metallurgical Studies of Various Techniques for the Large Scale Production of Hydriding Grade FeTi and Related Compounds", Final Report, Contract BNL 352410S (Second Year), in preparation.
5. Elger, G.W., Kirby, D.E., Rhoads, S.C., and Stickney, W.A., *Synthesis of Rutile from Domestic Ilmenites*, Bureau of Mines, RI-7985, U.S. Department of Interior, 1974.
6. Richardson, F.D. and Jeffes, J.H.E., *J. Iron Steel Inst.*, 160, 261, 1948.
7. Kubaschewski, O., Evans, E. LL. and Alcock, C.B., *Metallurgical Thermochemistry*, Pergamon Press, 1967.
8. Shomate, C.H., Naylor, B.F. and Boericke, F.S., *Thermodynamic Properties of Ilmenite and Selective Reduction of Iron in Ilmenite*, Report of Investigations, Bureau of Mines, U.S. Department of Interior, May 1946.
9. Ajersch, F., *Ecole Polytechnique de Montreal*, private communication.
10. Elyutin, V.P., Paulev, Yu A., Levint, B.E., Alekseev, E.M., *Ferrotitanium, Production of Ferroalloys*, The State Scientific and Technical Publishing House, Moscow, 1957, p. 318.
11. Pargeter, J.K., *The Production of Ferroalloys by Exothermic Reduction of Metallic Oxides*, unpublished report.
12. Saklatwalla, B.D., *Thermal Reactions in Ferroalloy Metallurgy, the Basis of Alloy Steel Development*, Transactions of the Electrochemical Society, Vol. 84, 1944, p. 13.
13. Belitskus, D., *Aluminothemic Production of Metals and Alloys*, *Journal of Metals*, January 1972, p. 30.
14. Deeley, P., Spindelov, H. and Jennings, J., *Shieldalloy Corporation*, private communication.
15. Volsky, A., Sergievskays, E., *Theory of Metallurgical Processes*, (Russian) Translated by Ivan Saviu, MIR Publishers, Moscow 1971.
16. Dooley, III, G.J., *Titanium Production: Ilmenite vs. Rutile*, *Journal of Metals*, March 1975, p. 8.
17. Tukumoto, S., Tanaka, E. and Ogisu, K., *The Deposition of Titanium Metal by Fusion Electrolysis*, *Journal of Metals*, Nov. 1975.
18. Palmer, H.R., *Timet Research Labs*, Henderson, NV, private communication.
19. Wood, R.A., *The Titanium Industry in the Mid-1970's*, MCIC Report 75-26, Metals and Ceramics Information Center, Battelle, Columbus, OH, June 1975.
20. *American Metal Market*, Vol. 85, No. 108, Monday, June 6, 1977.

Table I

Chemical and Mineral Composition Analysis of Various Ilmenite Ores

Typical Analysis

Chemical Composition* (Wt. %)		Chemical Composition** (Wt. %)		Mineral Composition**	
TiO ₂	59.8	% TiO ₂	59.54	Ilmenite & Altered	
Fe ₂ O ₃	23.0	% Fe ₂ O ₃	25.11	Ilmenite	96.6
FeO	12.0	% FeO	9.19	Rutile	0.5
Al ₂ O ₃	2.0	Fe (Total)	24.63	Zircon	1.3
SiO ₂	1.2	Al ₂ O ₃	1.18	Sillimanite	0.4
Alkaline Earths	0.05	CaO	0.08	Garnet	0.3
S	0.03	MgO	0.88	Quartz	0.5
P	0.05	SiO ₂	1.19	Monazite	0.4
		MnO	0.42		100.0
		V ₂ O ₅	0.22		
		Cr ₂ O ₃	0.13		
		P ₂ O ₅	0.18		
		Nb ₂ O ₅	0.17		
		ZrO ₂	0.48		
		S	0.002		
		C	0.019		
		Loss on Ing. (900°C)	1.70		

*Chemalloy, Inc., Bryn Mawr, PA.

**N.L. Industries, Inc. [ore source - Quilon (India)].

Table II

Production Cost Estimates for FeTi(4) (in \$/Lb FeTi)

Cost Estimate for Reduction of FeTi by Metallothermic Reduction

Process	Total Material Cost/lb		Processing Cost/lb		Remelt & Deoxidation Cost/lb		Total Alloy Cost/lb		42% Markup/lb		Final Alloy Price/lb	
	Out*	In**	Out*	In**	Out*	In**	Out*	In**	Out*	In**	Out*	In**
Magnesiothermic	2.69	.98	.13	.20	.41	.41	3.23	1.59	1.36	.67	4.59	2.26
Calciothermic	4.05	2.09	.18	.25	.41	.41	4.64	2.75	1.95	1.16	6.59	3.91
Aluminothermic	.81	.59	.13	.20	.41	.41	1.35	1.14	.57	.48	1.92	1.62

Cost Estimate for Production of FeTi by the Chloride (Kroll) Process

Total Material Cost/lb	Processing Cost/lb	Vacuum Induction Melting & Deoxidation Cost/lb	Final Alloy Price/lb
1.00	.80	.31	3.00

Cost Estimates for Production of FeTi by Directly Melting Fe and Ti

Materials	Total Material Cost/lb	Processing and Melting Cost/lb	Total Cost/lb	Final Alloy Price/lb
Scrap Ti & Fe	.03 + .462 Ti***	0.38(Air Melt & 5%Mn Deoxidize)	0.41 + 0.462Ti R***	1.42(0.41 + 0.462Ti) R
Sponge Ti & Scrap Fe	1.19	0.42(Air Melt & 5%Mn Deoxidize)	1.62	2.87
Sponge Ti & Scrap Fe	1.19	0.31(Vac. Ind. Melt & 1%Mn Deoxidize)	1.52	2.20
Sponge Ti & Scrap Fe	1.19	0.37(Consumable Elec. Vac. Melt & 1%Mn Deoxid.)	1.56	2.26

TABLE III

SUMMARY OF FeTi PRODUCTION PROCESSES STUDIED

Technique	Estimated FeTi Price, \$/lb.	Technical Problems Anticipated
H ₂ Reduction of Ilmenite	--	Thermodynamically unfeasible.
CO Reduction of Ilmenite	--	Thermodynamically unfeasible.
CH ₄ Reduction of Ilmenite	?	Probably difficult to control on commercial basis to prevent TiC formation.
C Reduction of Ilmenite	--	Thermodynamically impractical. Strong tendency toward TiC formation.
Silicothermic Reduction of Ilmenite	--	Thermodynamically unfeasible.
Magnesiothermic Reduction of Ilmenite	2.26*/4.59**	High vapor pressure of Mg may make process impractical or result in very low recoveries.
Calciothermic Reduction of Ilmenite	3.91*/6.59**	High vapor pressure of Ca may make process impractical or result in very low recoveries.
Aluminothermic Reduction of Ilmenite	1.62*/1.92**	High Al and O residuals will probably lower hydrogen capacity.
Molten Salt Electrolysis	2.70?	Deposition problems when Ti and Fe chlorides mixed.
Chloride (Kroll) Process	3.00	Impurities may reduce capacity. May be difficult to handle mixed chlorides.
Air Induction Melting of Scrap Ti and Scrap Fe	2.00+	Requires CP Ti scrap of limited availability
Air Induction Melting of Scrap Fe and Sponge Ti (MM Deoxidation)	2.87	Recovery, slag handling, and crucible cleanup.
Vacuum Induction Melting of Scrap Fe and Sponge Ti (Graphite Crucible)	2.20	None.
Consumable Electrode Vacuum Arc Melting of Scrap Fe and Sponge Ti	2.26	None.

*Required for an out-of-furnace process (booster substitutes for furnace power).

**Required for an in-furnace process, without booster.

***Variable price of Ti and recovery R.

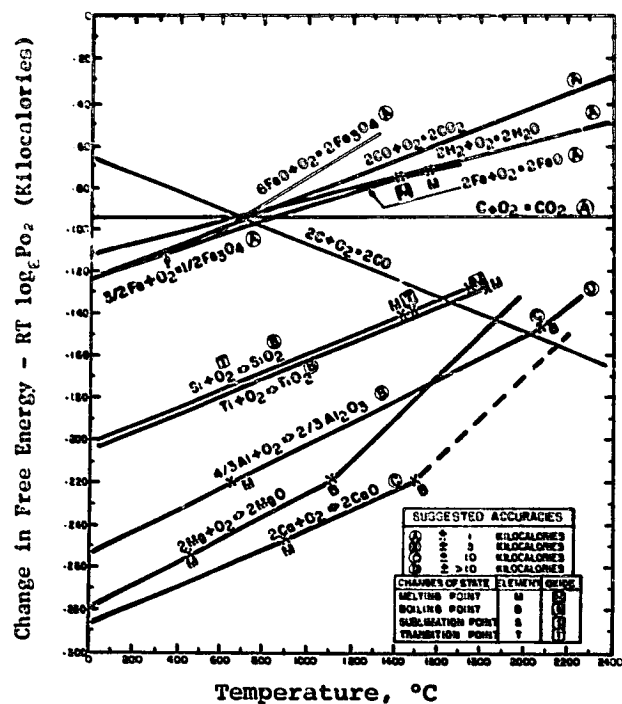


Fig.1. Standard free energy of formation of oxides(5,6)

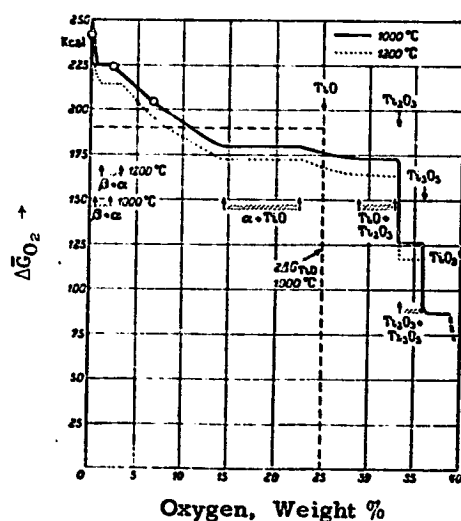


Fig.2. Partial free energies of dissociation of 1 mole oxygen in the titanium-oxygen system(7, p. 54)

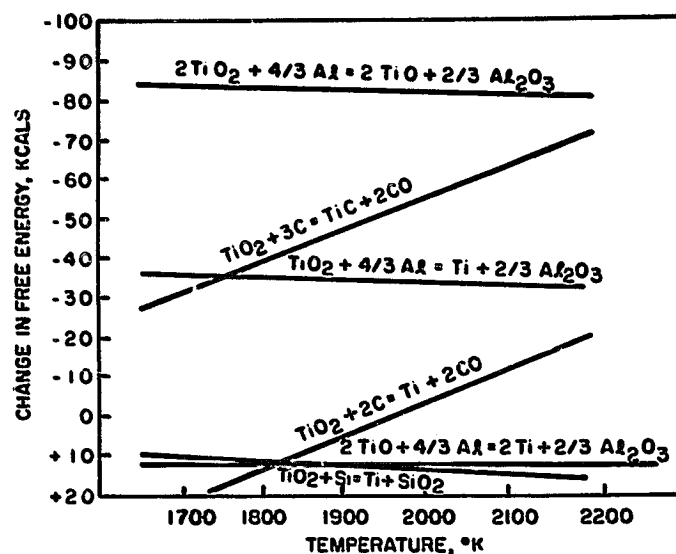


Fig.3. Dependence of the free energy of reduction of titanium oxides on the temperature(10)

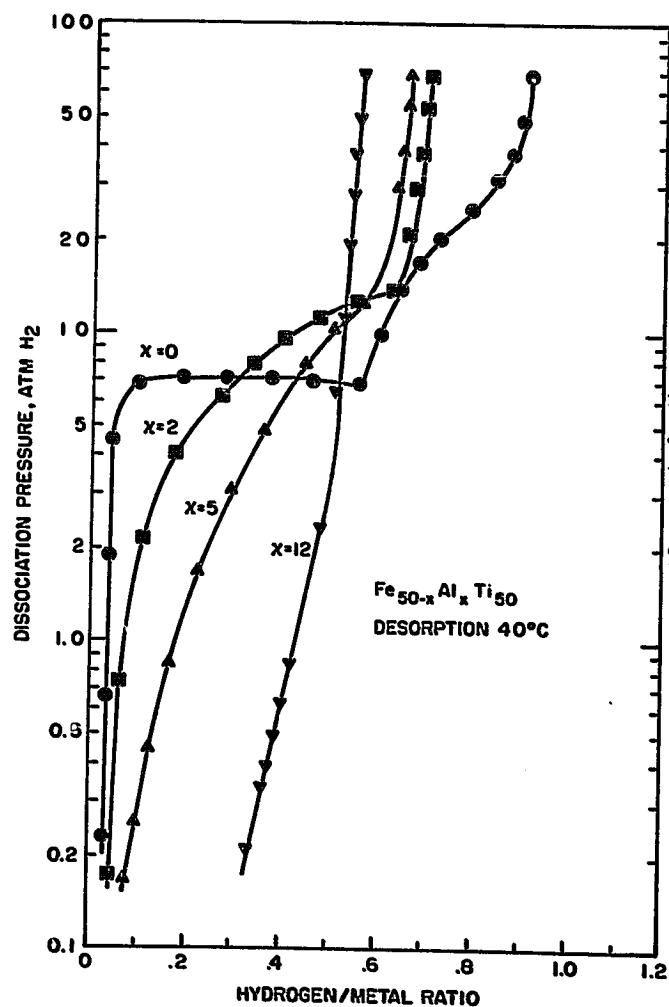


Fig.4. Effect of Al-content x on the 40°C desorption isotherm of Fe_{50-x}Al_xTi₅₀ alloys(4)

**STATIONARY HYDRIDE VESSEL OF LARGE DIAMETER-
PROGRAM PLAN**

**Roger E. Billings, Ronald L. Woolley and Jack H. Ruckman
Billings Energy Corporation
Provo, Utah 84601**

Abstract

A metal hydride vessel of engineering scale has recently been installed as a peak shaving component of the BEC "Hydrogen Homestead." Operational performance and vessel behavior are to be computer monitored for a one-year period. Of particular interest are heat transfer characteristics and the consequence of hydride packing in a large hydride vessel with a hemispherical end cap. This paper discusses planned experiments and operation of the vessel. Instrumentation debugging is now proceeding preparatory to the start of data collection.

I. INTRODUCTION

Hydrogen provides a common energy carrier that unites all energy resources with all energy users. The purpose of the "Hydrogen Homestead" is to demonstrate this fact with working hardware. A key component is a metal hydride storage vessel. Energy demand in a home fluctuates. Hydrogen production from many energy resources such as wind or solar energy is also nonuniform and may cease for several days. Storage of hydrogen is thus an essential part of a successful system.

II. SYSTEM DESCRIPTION

In the first phase of the homestead, hydrogen will be produced by electrolysis using electricity generated by hydroelectric, wind, coal, or solar energy (Fig. 1).

Hydrogen will pass through a water trap and then flow either directly to the homestead or into the hydride vessel, passing first through an oxygen catalyst and a molecular sieve dryer before entering. Homestead uses of hydrogen are as follows: 1) a Cadillac Seville that may be switched from hydrogen to gasoline while driving, 2) a Jacobsen lawn and garden tractor, 3) oven, 4) range, 5) barbecue, 6) fireplace log, 7) hot water supplementary heat when solar energy is inadequate, and 8) a hydrogen boiler to aid the heat pumps in the winter.

Low grade heat for dissociation of the hydrogen from the hydride will come from two sources: solar energy and reaction heat when the alloy is hydrided. Both energies will be stored in a 275 gallon (1041 l) water tank for later use. Water will be circulated continuously between the holding tank and a belt water jacket around the hydride vessel midriff in an attempt to maintain temperature uniformity at a level consistent with the solar collectors (approximately 131° F or 55° C). Temperature nonuniformity, pressure, tank expansion, and other data will be monitored and reduced by a BCC micro-computer.

A specially designed electrolyzer will produce 3 pounds/day (1.4 Kg/day) of hydrogen at a pressure of 500 psig (3450 KPa) continuously. At this supply pressure, the hydride will approach maximum loading even though the temperature is elevated. Starting from these nominal operating conditions of elevated temperature and pressure, the vessel should be capable of discharging three or more days of production without additional heat transfer because of the thermal capacity of the hydride. Discharge of the remainder of the contents will be limited by the heat exchange rate and by heat conduction within the hydride bed.

In order to monitor the temperature

nonuniformity, thermistor probes have been inserted into the hydride bed and placed around the vessel periphery. Pressure taps have been placed at four locations to monitor pressure drop through the bed. The pressure sensors will also reveal possible filter clogging.

The pressure vessel (Figure 2) consists of two hemispherical end caps joined by a cylindrical section (internal diameter=36.5 inches=92.7 cm, internal max height of bed=46.4 inches=118.4 cm). This low carbon steel vessel is fitted with pressure taps, a hydrogen flow port with a 5 micron filter, a hydride sample port, a sight glass (Figure 3), and a loosening jet arrangement at the base. Approximately 4,000 pounds (1814 Kg) of titanium-iron manganese-alloy is contained within the vessel ($Ti_{51}Fe_{44}Mn_5$). It was activated externally and then poured into the vessel at an overall vessel density of 190 lb/ft³ (3040 Kg/m³).

III. EXPERIMENTS

A number of experiments are planned to define the operating characteristics of the system and the behavior of the vessel. These are as follows:

1. Total hydrogen capacity at equilibrium.
2. Discharge capacity at constant flow rate (set by flow controller and mass flowmeter).
3. Change of hydride particle (Fig. 4) size and activity with time (sample removed periodically).
4. Pressure drop through the bed.
5. Pressure drop across the filter.
6. Temperature profile within hydride bed.
7. Temperature gradient on vessel surface.
8. Heat transfer to circulation water.
9. Filter clogging.
10. Alloy mobilization in the outlet gas stream.
11. Change in tank girth with pressure, temperature, and hydride packing.
12. Visual observation of hydride motion and size change.
13. Effectiveness of loosening jets in breakup of hydride packing and lock-up.
14. Effectiveness of circulation of heat-

ed hydrogen in discharging the vessel.

IV. CONCLUSIONS

Tests of the metal hydride storage vessel, a component in the BEC Hydrogen Homestead, will provide engineering scale information relative to the use of hydriding alloy in a pressure vessel. Data on heat transfer, pressure drop, working capacity, and changes in vessel dimensions

will be gathered in the program. The storage vessel represents practical application of new technology as an important part of an independent energy system.

V. ACKNOWLEDGEMENT

This program is sponsored by the U.S. Department of Energy under a subcontract with the Brookhaven National Laboratory.

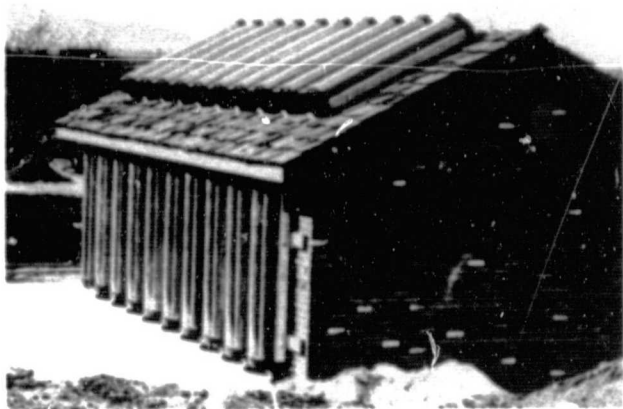


Fig. 1. Solar collectors on roof and side of energy shed

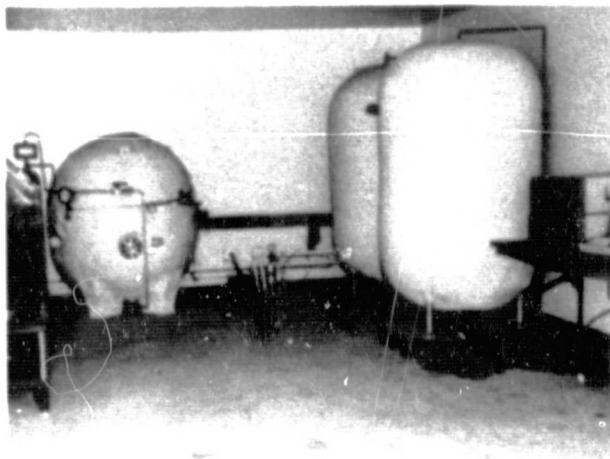


Fig. 2. Inside energy shed from L to R: electrolyser, metal hydride vessel, hot water storage tanks, and computer monitoring system



Fig. 3. Removing protective cover to expose sight glass

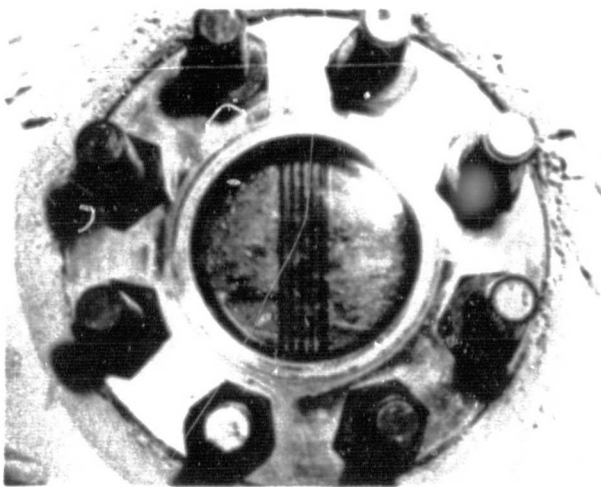


Fig. 4. Metal hydride particles within vessel

Page intentionally left blank

SESSION V
SYSTEM STUDIES

HYDROGEN AS A CHEMICAL FEEDSTOCK (STUDY AND WORKSHOP)

C. J. Huang

University of Houston

K. K. Tang

Jet Propulsion Laboratory

USE OF HYDROGEN ENERGY SYSTEMS TO IMPLEMENT SOLAR ENERGY

T. Fujita, C. Miller, K. H. Chen, G. Voecks, and W. Mueller

Jet Propulsion Laboratory

**SOLAR-CHEMICAL ENERGY CONVERSION AND STORAGE:
CYCLOHEXANE DEHYDROGENATION**

A. B. Ritter, G. B. DeLancey, J. Schneider, and H. Silla

Stevens Institute of Technology

**SYSTEM EVALUATION OF SUPPLEMENTING NATURAL GAS SUPPLY
WITH HYDROGEN**

W. S. Ku

Public Service Electric and Gas Company

**HYDROGEN FROM FALLING WATER: ASSESSMENT OF THE RESOURCE
AND CONCEPTUAL DESIGN PHASE**

W. J. D. Escher

Institute of Gas Technology

J. P. Palumbo

Pennsylvania Gas & Water Company

HYDROGEN ENGINE/STORAGE SYSTEM -- APPLICATION STUDIES

A. M. Karaba and T. J. Pearsall

Teledyne Continental Motors

Page intentionally left blank

**HYDROGEN AS A CHEMICAL FEEDSTOCK
(STUDY AND WORKSHOP)**

**C. J. Huang
University of Houston
Houston, Texas 77004**

**K. K. Tang
Jet Propulsion Laboratory
California Institute of Technology
Pasadena, California 91103**

Abstract

The objective of this study and workshop is to determine steps which can, and should, be taken to enable and encourage a shift in the chemical industries from natural gas and naphtha as hydrogen sources to other energy forms.

Preliminary findings of informal interviews conducted prior to the workshop are summarized for key segments of the hydrogen market. Plans for the workshop to be held in December, 1977 are discussed.

**HYDROGEN AS A CHEMICAL FEEDSTOCK
(STUDY & WORKSHOP)**

1. INTRODUCTION

Current hydrogen use in the U.S. is dominated by applications in the chemical and petroleum industries, with a projected annual growth during the next 25 years of between 6 and 12 percent. The supply of the traditional hydrogen feedstocks, principally natural gas, is becoming a problem. This will tend to increase the market penetration of hydrogen produced from feedstocks and techniques less affected by increasing scarcity and rising cost. New government energy policies may accelerate this trend toward non-traditional sources, particularly from coal in the near future.

The HEST study quantified the supply and use of hydrogen in the U.S., developed projections for the balance of the century, and identified alternatives to the present practices. The alternative High vs Low Merchant to Captive ratios for Hydrogen Supply scenarios were developed and documented in Hydrogen Tomorrow (Ch. III and IV). For each industry, the fractions of hydrogen which could be supplied as merchant were calculated. This was done based on extensive contacts with the industries involved in addition to, and as a basis for, our own analyses.

The present study is intended to determine steps which can, and should, be taken (particularly by the government) to enable and encourage a shift in the chemical industries from natural gas and naphtha as hydrogen sources to other energy forms. This may come about through merchant supplies of hydrogen, or through shifts in captive production to the other energy forms. The steps may include technology enhancement, further analyses or assessments, or recommended regulatory modifications. The technologies may be in the areas of hydrogen production, delivery or storage.

The study will interface closely with the University of Houston Workshop (see Sect. 3), using the workshop as a data source. It will concentrate on the chemical and petro-chemical industries but will consider other users of hydrogen as appropriate. Alternative hydrogen production from coal gasification, electrolysis, and heavy oil will be considered. For each industry, the needed mixtures of gases with hydrogen, and the value of hydrogen purity will be determined, as will the prospects of biproduct utilization.

It is anticipated that the workshop and study will identify and lead to approaches for significant conservation of natural gas and petroleum distillates. Based on the findings and recommendations of the Houston Workshop, a study contract will be issued to conduct the in-depth analysis in phase two during FY'78.

2. PRE-WORKSHOP FINDINGS

A series of informal interviews was conducted prior to the Houston workshop with various chemical industry representatives, to gain some insight into the issues of concern to the industry. The preliminary findings of these interviews are summarized below for several key segments of the hydrogen market.

A. AMMONIA AND METHANOL

Essentially all ammonia and methanol production in the U.S. uses natural gas as both feedstock and fuel. Together, these two markets account for about one-third of the natural gas consumed by the chemical and allied products sector in the U.S., or 3.3% of the total natural gas consumption in the nation.

The heavy dependence of these markets on natural gas as feedstock and fuel would lead one to believe that ammonia and methanol producers must be busily investigating alternative sources of feedstock and fuels. A survey of major ammonia producers by the IGT in 1975 revealed that "of the 30 plants responding, half have some concerns about meeting their natural gas requirements through 1985. 23 have experienced some form of service curtailment or interruption, and 16 have had to alter or cancel expansion plans because of a lack of natural gas. Almost half of these plants are developing background information on other kinds of processes not using natural gas, but only two are switching some of their fuel uses to oil."

A survey of major methanol producers by the IGT revealed a similar response regarding their natural gas supply situation. The consensus appears to be that our natural gas production will not increase significantly in the next decade. Demand projections for ammonia and methanol, on the other hand, range from 3% annual growth or higher. Translated to hydrogen demand, these two markets may well require twice the present 0.5 Quad of Hydrogen by 1990, at a 6% growth rate.

Our recent interviews with chemical industry representatives revealed that many economic studies are underway, particularly in the coal conversion area. One recently published report (Brookhaven-Exxon) concluded, on the basis of production economics studies, that coal gasification technology (improved K-T process) could become competitive with natural gas reforming for methanol production by 1982 and ammonia production by 1989. (A key assumption made in this report is that the cost of natural gas and petroleum products will escalate at 1.5% per year over the general inflation rate of 5%.) All of the new ammonia plants announced for construction by 1985 are based on the use of natural gas.

In an effort to survey the synthetic fuels industry, the Koppers Company sent questionnaires in 1976 to presidents or chief executive officers of 161 U.S. and 6 Canadian companies or research organizations, with an interest in coal gasification.

The survey was designed to provide meaningful answers in the following areas:

- the impact of the energy crisis to date on each organization
- the interest in alternate energy supply from coal
- the attitude toward energy allocation by the federal government
- the interest in government incentives for establishment of synthetic fuel plants

The response to Item No. 10 of the questionnaire is of particular interest, as it reflects the views of industry on the issue of government incentives. Of the six types of incentives listed, the survey revealed the following order of preference by the respondents:

- (1) Accelerated depreciation of facilities (3-5 years)
- (2) Increase of present investment tax credit
- (3) Ability to issue tax-free bonds
- (4) Loan guarantees by the federal government
- (5) Government equalizing prices of substitute fuels with that of imported oil
- (6) Government project financing with provision for lease to industry

The following comments from chemical companies may be noted:

"The most important government incentive, in our opinion, is price protection so that the synthetic gas from coal gasification plants does not incur the grave risk of being undermined by sudden reduction in OPEC oil prices. In conjunction with this type of price protection from the government, we feel that issuance of tax-free bonds and increasing the investment tax credit from say 10 to 20 percent would be the most effective incentives involving minimum subsequent government interference."

B. COAL LIQUEFACTION

Hydrogenation is a key conversion reaction of coal liquefaction processes. A coal liquefaction process, such as the H-Coal process, requires 18,600 SCFT of hydrogen for each ton of coal to be liquefied. Since one ton of coal is converted to 4.44 Bbls of Syncrude, a liquefaction plant with a daily capacity of 100,000 Bbls Syncrude demands 419 millions SCFT of hydrogen for hydrogenation, in addition to 50 million SCFT for desulfurization. In terms of mass, the hydrogen requirement of a 100,000 Bbl/day Syncrude plant is 2.64 million pounds per day. If this hydrogen requirements is to be met by a coal gasification plant affiliated with the liquefaction facilities, and if the hydrogen yield from coal is 4.9% by weight, the amount of coal required for the hydrogen production is 24,490 tons per day. Since the liquefaction facilities convert 22,520 tons of coal to Syncrude, it means that for each ton of coal converted to Syncrude, an additional ton of coal would be expanded to generate the necessary hydrogen. If and when the nation's capacity for coal liquefaction reaches one million Bbls per day, the annual requirement of hydrogen will be equal to 4 million tons. This is equivalent to 34.4% of the hydrogen required for methanol and ammonia syntheses in the year 2000. (4.5×10^{12} SCF/YR.)

The above figures also indicate that if the hydrogen requirement of 4 million tons can be met from other sources, then the coal required for this purpose can be converted to another million Bbls/day of Syncrude.

Technologically, coal liquefaction to produce syncrude has been proven. Its full industrialization is dependent on factors such as:

- (1) The nation's industrial capacity of fabricating the necessary process equipment
- (2) Code modification for the process equipment
- (3) Guarantee for raw material supply and its price
- (4) Guarantee for products sales and prices
- (5) Investment finance

C. DIRECT IRON REDUCTION

At the present time (November 1977), there are six direct reduction plants in operation in this country, with an annual production capacity of 1,260,000 metric tons. By 1980 the national capacity will be increased by 900,000 metric tons with the expected completion of an additional plant in Texas. Thus in 1980, the direct reduction capacity in this country will reach 2,160,000 metric tons per year. In four of the above seven plants, totaling the annual capacity of 2 million tons the reducing agents are manufactured by reforming natural gas or oil. The reductant gas mixture contains 74% hydrogen and it is estimated that approximately 100 pounds of hydrogen is required for each ton of the reduced product. By 1980, the hydrogen requirement for direct iron reduction will be 91,000 tons per year. This amount is relatively small compared with the other hydrogen requirements such as ammonia or methanol production. It is noted that a direct iron reduction plant becomes economically not competitive if its capacity goes beyond 1,000,000 tons per year. Furthermore, the national capacity of direct reduction is not expected to grow substantially in this country. For these reasons, the hydrogen consumption in this industrial sector is not significant. In contrast with the slow development in the U.S., Venezuela will expand its capacity for direct reduction from the present 1 million tons to 5 million tons a year in 1980.

D. PETROLEUM REFINING

Petroleum refining consumes approximately 47% of the total industrial hydrogen consumed in this country. Even though it is the largest sector in the hydrogen supply/demand picture, there seems to be a lack of fairly accurate quantitative data available. A petroleum refinery is a producer as well as a consumer of hydrogen and therefore it does not, in general, report its demand/supply data to the outside. This is a major reason for the lack of quantitative data. Furthermore, the hydrogen consumption in a refinery is determined by complicated and inter-related factors such as:

- (1) Quantity of crude oil processed
- (2) Quality and source of crude oil processed
- (3) Refining processes
- (4) Product-mix
- (5) Environmental constraints

Each petroleum refinery seems to have its own unique set of the above factors influencing its refining operation, and consequently its hydrogen requirements. However, as a good approximation to determine the national demand in this sector, it may be assumed that the catalytic reforming in refineries supplies enough hydrogen to meet the demands for desulfurization of light distillate and other minor hydro-treating operations. And that the hydrogen consumed by gas oil desulfurization, residue desulfurization and residue hydrocracking will be supplied with merchant hydrogen or specifically installed hydrogen production units such as steam reformer of natural gas or oil. There is another reason for the special hydrogen production units to supply hydrogen to these three operations. The processes require a hydrogen stream of high concentration (up to 95% purity) whereas the hydrogen stream from a conventional catalytic reforming unit is only 70 or 80% purity. The hydrogen requirement for these three refining processes, as reported in the Brookhaven-Exxon report, is approximately 2.75 million tons of hydrogen a year in 1990. The estimate is also based on another assumption that the residue treatment processes are characterized by "carbon removal" rather than "hydrogen addition". A definitive study of hydrogen requirements for petroleum refining operation is not available in the literature.

E. FUEL CELL ELECTRICITY GENERATION

Conversion of fuels to electricity by means of fuel cells can be accomplished in a highly efficient and environmentally acceptable manner. Two major areas of application are envisioned for fuel cells. Large multi-megawatt fuel cell power plants may be constructed within electric utility networks to complement large-scale systems. The generation needs of small private and public utilities may be provided by these power plants. Smaller size fuel cells may be installed at building locations to provide integrated electric and thermal service for commercial and industrial complexes. There are varying estimates of the market for liquid and gaseous fueled electric generation equipment. Its market growth is estimated to be in a range of 5% to 6.7%.

The penetration of fuel cell power plants into the market is clouded by uncertainties associated with the growth rate. Nevertheless, a specific market, i.e., replacement of retired generation plants in areas of fuel shortage and critical environment, appears extremely attractive. It is estimated that the market for fuel cell power plants will be largest in private utilities, followed by the on-site integrated energy system for commercial and industrial complexes. An estimate for the total fuel cell market for the five year period of 1980-1985

is between 26,800 and 82,300 MW. The annual demand of hydrogen required for these fuel cell plants is estimated to be between 2.4×10^{12} SCF to 6.9×10^{12} SCF. This is indeed a tremendous market for hydrogen, comparable to that needed for manufacturing ammonia and methanol.

Several other attractive benefits are associated with fuel cell application for power plants but its technological and economic feasibility should be demonstrated for commercial-scale facilities.

F. FOOD INDUSTRY

In the food industry, hydrogen is mainly used to hydrogenate fats and oils. The hydrogen requirement is rather small, approximately 17,000 tons per year. This hydrogen market has the following unique features:

- (1) Demand per plant is small, from 50 to 1,000 MSCF/day/plant
- (2) High purity hydrogen is required with pressure range of 60-200 psig
- (3) Hydrogen cost is insignificant in determining the final price of the products. (Thus, the industry is more concerned with its steady and easy access to hydrogen than with the hydrogen cost itself.)
- (4) Since hydrogen is not produced within its manufacturing processes, it is supplied by small-scale hydrogen production units on-site or by purchasing merchant hydrogen
- (5) Hydrogenating plants are located across the country, currently there are 50 plants in 20 states

3. WORKSHOP PLANS

The University of Houston has received a grant from ERDA to conduct a workshop on the "Supply and Demand of Hydrogen as Chemical Feedstock" on December 12-14, 1977, at the University. The workshop is being organized by Dr. C. J. Huang, Professor of Chemical Engineering.

The objectives of this workshop are:

- (1) to assess and predict the present and future demand and supply of hydrogen as a chemical feedstock,
- (2) to discuss and evaluate the available technology and economic feasibility of manufacturing hydrogen from sources other than oil or natural gas
- (3) to develop implementation scenarios and to formulate recommendations for obtaining chemical raw material hydrogen from sources other than oil or natural gas

Approximately sixty participants, including some from outside the U.S., have been invited. They include executives, plant managers, economic planners and process engineers from the:

- Oil refining industry
- Petrochemical industry
- Agricultural chemicals and other industry
- Potential hydrogen supplier industries
- Independent engineering consultants
- Chemical plant engineers and constructors

- Academic and non-profit research organizations
- Government agencies

A preliminary conference was held in September 1977 to work out the details of the workshop program. There will be a total of six sessions, with short papers on various key issues to be presented for discussion by all participants. The final session will conclude with recommendations on the future supply of hydrogen as chemical feedstock, following detailed discussion of alternative scenarios and their technical and economic feasibility. A report on the workshop will be submitted to ERDA by April 1978.

USE OF HYDROGEN ENERGY SYSTEMS
TO
IMPLEMENT SOLAR ENERGY

T. Fujita, C. Miller, K. H. Chen
G. Voecks and W. Mueller
Jet Propulsion Laboratory
Pasadena, CA

Abstract

As the first phase of a study to explore the use of hydrogen energy systems to implement solar energy, potential roles are broadly identified in terms of future markets and the formulation of implementation scenarios. By converting solar energy to hydrogen, an energy pathway is created whereby solar energy can supply major new markets comprising (1) production of chemicals such as ammonia and methanol, (2) total energy/cogeneration, (3) synfuel/chemical feedstock production, (4) direct fuel uses, and (5) other small but important uses such as ore reduction. These new market opportunities for implementing solar energy are predicated primarily on the unique role of hydrogen as a key element in the chemical/industry sector.

Implementation of solar-hydrogen systems to fulfill these new markets is analyzed in terms of key issues. By considering the renewable fuel era (estimated to start in ≈ 2030), where fossil sources are sharply declining, a critical and major role for hydrogen systems is identified. In the absence of fossil fuels, the survival of our entire hydrocarbon-based chemical industry requires use of solar (or other non-fossil sources) to generate hydrogen from water. The key issues then revolve about developing and implementing solar-hydrogen systems to effect a smooth transition directed toward fulfilling this ultimate role. Issues governing implementation include conservation policies, possible environmental impacts from carbon dioxide generated from continuing accelerated usage of fossil fuels, and emergence of large markets for byproduct oxygen. These issues are addressed in terms of their potential for accelerating implementation of solar-hydrogen systems.

I. Introduction

A major thrust in the Department of Energy's (DOE) overall program is to develop and support implementation of solar energy systems to conserve rapidly depleting natural gas and petroleum reserves. By combining solar energy with hydrogen systems, new possibilities may be uncovered which could enhance the implementation of solar energy. In such solar-hydrogen energy systems, solar energy is used to generate hydrogen from water. This hydrogen is then transmitted, stored, and used in myriad ways, e.g., it can be used as a fuel to generate electrical energy or as a chemical feedstock to produce ammonia and methanol.

The overall objective of the present effort is to examine roles for solar-hydrogen systems as a basis for projecting which roles are likely to be fulfilled and in what sequence. Emphasis is placed on roles which utilize unique characteristics of hydrogen systems since these roles are considered to have a greater likelihood of being implemented. That is, unique roles are capable of creating new opportunities for enhancing the implementation of solar energy.

A. Approach

As shown in Fig. 1, the effort is divided into two phases and the present paper covers only the first phase which was completed in FY77. This Phase 1 activity identifies potential roles for solar-hydrogen systems. The follow-on Phase 2 effort will examine solar hydrogen systems in terms of practicability and required technology development to fulfill the roles identified in Phase 1.

The approach to identifying roles/options involved the delineation of future markets in terms of potential size as a function of time. Then, implementation scenarios were formulated in terms of timeframe, key issues, and alternatives.

A basic premise for the Phase 1 effort is that technology for both solar and hydrogen systems will be successfully developed and that goals in terms of performance and cost will be achieved per present development program schedules. The identified roles and implementation scenarios from Phase 1 only show potential for solar-hydrogen systems and do not address the likelihood of achieving this potential or consider ultimate efficiencies.

The Phase 2 effort (Fig. 1) will examine system options primarily in terms of technology status and associated uncertainties in projected costs and performance. The effect of these uncertainties on expected implementation will be evaluated in terms of estimated R&D requirements (both time and funds) and relative technical risks. Basic steps involved in the Phase 2 activity and their interaction are depicted on Fig. 1. The technical development activities which will potentially provide the greatest contribution toward implementation of solar-hydrogen systems will be delineated to serve as an input for DOE's Hydrogen Storage Systems program.

B. Scope

Solar energy systems are in a very early stage of development and are not commercially competitive with fossil and nuclear systems for large

scale power generation. The rate of implementation of solar energy systems will be governed by depletion rates (and associated price escalations) for fossil fuels, the viability of solar systems vis-à-vis other renewable or large energy source alternatives such as nuclear fusion, ocean thermal gradient geothermal, etc., and the degree of success in developing solar energy systems tailored to meet application system/end-use requirements.

The implementation of solar energy systems and in particular solar-hydrogen systems is therefore dependent on the complex interrelations of overall energy usage and the evolving policies which will govern this usage. Projections of energy usage range from simple extrapolation of current use pattern and growth rates to reduced consumption based on conservation and development of more energy-efficient systems and processes.

Within the scope of the present study, the many different energy futures and their complex ramifications on implementation of solar-hydrogen systems cannot be assessed in detail. The effort is thus limited to the well-established energy futures which were previously used as the basis for projecting hydrogen demand (Ref. 1). The rationale inherent in these futures provides a framework within which specific issues relating to implementation of solar-hydrogen systems can be analyzed.

The energy futures employed in Ref. 1 stressed conservation of fossil resources by use of technically improved and more efficient devices and the shifting of energy sources from natural gas and petroleum to coal and nuclear energy. The futures covered a period up to the year 2000 during which depletable resources of natural gas, petroleum, and coal play major roles. Renewable sources such as solar energy will of necessity assume the dominant role when these depletable sources become scarce. Baseline projections of solar energy implementation to the year 2020 for the present study are derived from ERDA-49 (Ref. 2).

Thus, when identifying roles for solar-hydrogen systems, it is necessary to extend the energy futures of Ref. 1 and look beyond the depletable fossil fuel era. Within the scope of the present study, major roles that were identified for solar-hydrogen systems in the post fossil or renewable fuel era could only be explored in terms of basic first order considerations; however, the existence of potentially major roles in the post fossil era provides a perspective regarding technology development activities. The development effort during the fossil era should be regarded as a transitional phase where specific activities will be ordered to provide a smooth transition in meeting the requirements of the post fossil era.

II. Solar-Hydrogen Systems

A solar-hydrogen system is herein defined as a system where solar energy is collected and used to generate hydrogen which is then transmitted, stored, and supplied to end-use markets.

A. Utility Hydrogen Energy Storage

Hydrogen energy systems were initially directed primarily towards being an energy

transmission and storage medium for electric utilities (Ref. 3). The basic system is shown in Fig. 2 (Ref. 4). Off-peak utility power in the form of electricity and/or heat is used to decompose water into hydrogen and oxygen. The hydrogen can then be stored and used in fuel cells or turbines to generate electrical energy during peak power demand periods. As indicated on Fig. 2, the byproduct oxygen can be either sold to oxygen users or used as the oxidant for the fuel cells and turbines.

A major feature of this storage system is flexibility with regard to the location of components. For the usually considered case of electrolytic decomposition of water, the electrolyzer can be located near available water since electrical energy can be supplied from the central power plant via electric transmission lines. The hydrogen can then be transported in pipelines to another site such as an underground storage reservoir. From the storage reservoir, the hydrogen can again be piped to a conversion plant located, e.g., within the load center.

B. Solar Energy Systems

Solar energy systems encompass a wide spectrum which is broken down into the following two basic categories (Ref. 5):

- Natural Collection - Indirect Use
 - Photosynthetic processes in plants
 - Generation of winds and waves
 - Creation of ocean thermal gradients
- Engineered Collection - Direct Use
 - Conversion of photons to electricity
 - Conversion of insolation to thermal energy
 - Use for heating needs
 - Convert to electricity via heat engines
 - Thermionic

All of the above methods of collecting solar energy are being pursued (Ref. 6). Biomass systems are based on photosynthetic processes. Programs to use wind power and ocean thermal gradients to generate power (OTEC - Ocean Thermal Energy Conversion) are underway (Ref. 2). Engineered collection systems are focused on photovoltaic systems (photons to electricity) and solar thermal power systems. A 10 MW solar thermal power plant is presently being developed for installation at Barstow, CA. The concept involves a central receiver mounted on a tower. A field of two-axis tracking mirrors (or heliostats) reflects energy on the receiver in which steam is generated. The steam is then used to power a steam power plant as shown on Fig. 3.

C. Solar-Hydrogen Production Pathways

The solar-hydrogen production pathways corresponding to natural and engineered solar collection systems are presented on Figs. 4 and 5, respectively. For natural collection systems of Fig. 4, the photosynthesis process embodies several options. First, the green plants, produced from photosynthesis can be either burned directly to produce heat or they can be processed (chemical conversion) to form products such as methanol which can be used as a fuel for combustion or a chemical feedstock. The thermal energy of combustion can be used to drive either a thermochemical plant which uses heat to split water via a series of

closed loop chemical reactions or a power conversion (heat engine) system to produce electrical power which is fed to an electrolysis plant.

The pathway for wind power involves only electrolysis since the energy is initially in mechanical form. The OTEC plant uses small differential temperatures of $\sim 20^\circ\text{F}$ to drive a heat engine cycle which is coupled to an electrolysis plant. The wind power plant can employ storage such as batteries or flywheels to smooth out wind speed variations and thereby allow the electrolysis plant to be sized for operating loads that are lower than peak wind energy loads. The OTEC plant is expected to generate a steady load so that storage ahead of the electrolysis plant is not needed.

For engineered collection systems (Fig. 5), the photovoltaic plant directly converts solar energy to electricity and is therefore coupled to an electrolysis plant for hydrogen production. Solar-thermal plants have two optional pathways involving power conversion - electrolysis or thermochemical plants. Photolytic plants capture photons and directly split water via electrochemical processes. Compared to the photovoltaic approach, the intermediate step of generating electricity is avoided, but the photolytic approach is in the early research stage, whereas photovoltaic and solar-thermal systems are in the development and design phase. The thermochemical plant is also considered to be in the early research stage.

D. Basic Roles for Hydrogen Systems

After hydrogen is produced from solar energy via any of the spectrum of pathways shown on Figs. 4 and 5, the major role of hydrogen systems involves energy storage and transmission of energy to users as illustrated on Fig. 6. For the system on the upper portion of Fig. 6, electricity is generated on the outskirts of the load center and the electrical distribution network is used to transmit energy within the load center. A portion of the hydrogen is also supplied to large industrial users. For the system on the lower portion of Fig. 6, hydrogen is distributed via pipelines within the load center and electricity is generated by small substations within the load center where waste heat from electrical production can be used to meet heat loads.

In the context of large scale implementation of solar energy, two features of hydrogen systems are particularly attractive. Pipeline transmission coupled with underground gas storage has potential for achieving low-cost, long distance delivery of energy (Ref. 4). As shown on Fig. 7, the region of highest insolation is in the Southwest and this energy could be transported to major load centers via hydrogen pipelines with storage accomplished in underground reservoirs which generally exist near major load centers. Present underground natural gas reservoirs as shown on Fig. 7 will become available for hydrogen storage as natural gas is depleted and additional new reservoirs could be found and/or developed.

III. Future Markets

The primary thrust of present engineered solar collection system programs is to supply heat and electrical energy markets. Hydrogen energy systems

permit solar energy to supply major new markets as shown on Fig. 8.

A. Chemical Markets

Hydrogen is a basic feedstock for producing essential chemicals such as ammonia for fertilizers and methanol for the plastic industry. It also has a major role in petroleum refining. As indicated in Ref. 1, this market accounts for ~90% of present hydrogen usage which is of the order of $\sim 3 \times 10^{12}$ SCF/year.

Over ~70% of present hydrogen requirements are supplied by natural gas via steam reforming. As natural gas reserves become depleted, shifts to other sources such as coal are anticipated. As governed by conservation policies, environmental impacts, and related issues, solar may initially make some penetration into this market.

For both coal and solar, the possibility of supplying this chemical market via externally-generated merchant hydrogen exists. That is, hydrogen can be generated in large coal or solar plants and then be shipped via pipelines to industrial users. A factor which could stimulate a move toward merchant hydrogen is the possibility of capital cost savings for chemical plants via removal of equipment associated with the captive (on-site) hydrogen generation. As shown on Fig. 9, a major portion of present ammonia plants is associated with the generation of hydrogen and nitrogen. If external hydrogen is supplied, this equipment (inside the dashed box) can be removed and this will reduce capital costs by ~50%. A nitrogen plant will have to be added, but a substantial net cost savings will result.

B. Total Energy/Cogeneration

The use of total energy and cogeneration systems, where electrical and heat needs are provided by an on-site conversion plant, is being pursued by DOE since high overall energy efficiencies are possible. Basically, the reject heat from electrical generation is used for heat needs and detailed matching of heat and electrical loads is required. Cogeneration and total energy both involve the concept of reject heat utilization, but cogeneration has the added flexibility that part of the electrical power generated on-site can be supplied to the utility grid.

The near term emphasis for total energy/cogeneration systems involves the use of fossil fuel energy. The use of on-site solar-thermal total energy systems is also being investigated (Ref. 7). The solar-hydrogen pathway can provide several major advantages. The on-site location of a solar-thermal total energy system requires substantial land area for solar collection and this could rule out some potential applications, particularly in crowded industrial centers. With solar-hydrogen systems, the solar collection plant can be located at an off-site location while the more compact energy conversion components can be located on-site. Hydrogen can be supplied via pipelines from the solar collection plant to the industrial or commercial use site. Hydrogen can also be stored, e.g., in underground reservoirs, and when fossil fuel reserves become depleted, total energy/cogeneration plants using fossil fuels can be converted to use solar-hydrogen.

Markets for total energy/cogeneration systems are shown in Table 1 (Ref. 8). The process heat requirements listed in Table 1 could be supplied by reject heat from electrical generation, where the reject heat must be supplied in the application temperature range shown. As shown in Table 2, hydrogen/oxygen and hydrogen/air fuel cells and gas turbines can furnish reject heat temperatures suitable for a large portion of the process heat needs of Table 1.

C. Synfuel/Chemical Feedstock Production

As natural gas and petroleum reserves are depleted, fossil sources such as coal, oil shale, tar sands, and also biomass can be processed to produce synfuels. Processes for synthetic natural gas (SNG) and liquid fuels require hydrogenation since the source feedstocks are hydrogen deficient in relation to the output product. A sizable fraction of the synfuel process is therefore devoted to the production of the required hydrogen using the source feedstock as an energy source.

If the required hydrogen were supplied from an external solar-hydrogen source, the capital costs of the synfuel plants could be reduced. Additionally, the product yield per unit feedstock source would increase and carbon dioxide emissions would be reduced. These benefits are presented on Table 3 for coal-based processes. For the same product yield, coal savings of the order of 50% to 60% are indicated for SNG and synthetic gasoline production. The reduction in carbon dioxide emissions is approximately the same as the coal savings. Substantial capital cost savings of at least 35% are indicated for these two processes. Lesser but significant savings of the order of ~8% accrue to the process for producing solvent refined coal (SRC).

Process diagrams for the SNG and liquid fuel (I. G. Farben) processes are shown on Figs. 10 and 11, respectively. It is indicated that substantial portions of the process plant can be removed when external hydrogen is supplied. The economic viability of using external hydrogen is of course governed by the cost of this hydrogen. However, the prospects of substantial savings in both capital and feedstocks tend to push for earlier entry of external hydrogen.

D. Direct Fuel Uses

Hydrogen from solar can also be supplied for direct fuel uses such as industrial process heat, transportation, and commercial/residential needs. When fossil fuels are in relatively plentiful supply, solar-hydrogen can only make a small penetration since it is more costly. Use of some hydrogen as a fuel is a possibility for uses requiring clean burning/low air pollution.

As fossil sources such as natural gas become scarce, hydrogen can potentially serve as a replacement where competitors will be other synfuels. The penetration of solar-hydrogen into the direct fuel market could initially be accomplished in a gradual manner by using hydrogen to supplement natural gas as shortfalls develop.

E. Other Small Uses

Hydrogen is needed for numerous small but important markets such as ore reduction, reducing

agent, heat transfer fluid, etc. When fossil sources for hydrogen production are no longer available, solar-hydrogen systems can supply the needed hydrogen to sustain these markets.

F. Potential Market for Solar-Hydrogen

The potential new markets for solar energy via hydrogen systems are dominated by chemical industry requirements. In the Hydrogen Energy Systems Technology (HEST) study of Ref. 1, projections of hydrogen demand were made for a Reference projection based on the Ford FTFB scenario (Ref. 9). For this Reference projection a high merchant supply option was formulated where energy policies based on conservation would tend to stimulate earlier introduction of solar (renewable) sources.

Results of projections for solar-hydrogen based on this HEST projection are shown on Fig. 12 as additions to solar projections for other markets per ERDA-49 (Ref. 2). It is seen that the potential solar-hydrogen markets (dashed lines) represent a substantial increase in the solar market. It is noted that the energy shown on Fig. 12 is in terms of source energy or the solar energy that has to be supplied. The actual energy delivered to the end use is a fraction of this energy as determined by the system efficiency.

In projecting solar-hydrogen to the year 2020, it was assumed that solar would displace all of the natural gas while assuming half of the percentage burden carried by petroleum in the year 2000. These trends follow from the expected depletion of natural gas and petroleum. It is noted that solar comprises ~1%, ~10%, and ~30% of the total source energy in the years 1985, 2000, and 2020, respectively. This provides a measure of the anticipated development timeframe for solar and the logical increase in implementation rate as fossil reserves decline.

IV. Implementation Issues

The rate at which solar-hydrogen systems will be implemented to fulfill the identified markets depends on three key issues which are:

(1) the timeframe, since availability of fossil fuels is declining, (2) existence of markets for byproduct oxygen, and (3) environmental impacts associated with an increase in atmospheric carbon dioxide.

A. Fossil Fuel Era

During the fossil fuel era, where fossil sources are dominant, the primary candidate energy sources are fossil, nuclear, and renewable/nonfossil. Energy carriers include electricity, hydrogen, and fossil fuels. Major end use categories are electric utilities, chemical industry, and fuel requirements.

The primary and secondary pathways for hydrogen during this fossil fuel era are shown on Fig. 13. The primary pathway involves the use of fossil fuels to generate hydrogen for use in the chemical industry. This pathway employs well-developed technology and is the most economical as long as fossil sources are available.

The secondary pathway involves nuclear and renewable sources with the possibility of some supplementation of natural gas in the latter portion of the fossil fuel era. This coincides with the projections of Fig. 12, where solar (renewable) sources begin to penetrate the market after 1985 and grow rapidly only after the year 2000.

B. Renewable Fuel Era

In the renewable fuel era (estimated to start in ~2030) where fossil sources are no longer dominant, a critical pathway involving hydrogen energy systems is identified on Fig. 14. In the absence of fossil fuels, the survival of our hydrocarbon-based chemical industry requires hydrogen from water and carbon from sources such as biomass/waste recycling. Thus, hydrogen systems provide a vital energy pathway between solar and other renewable energy sources and the chemical industry.

The identification of a critical future need for hydrogen systems using solar and other non-fossil sources provides a basic framework for a coherent development program and implementation plan. The development and implementation sequence can be structured to provide a smooth transition directed toward ultimately fulfilling the essential role of hydrogen systems in maintaining our chemical-based industrial complex.

As shown in Fig. 14, fuel requirements can be met by either hydrogen or other synfuels. However, hydrogen is required for production of synfuel. Hence, hydrogen systems also play a critical role with regard to satisfying fuel requirements.

C. Markets for Byproduct Oxygen

When hydrogen is produced via the decomposition of water, oxygen is formed as a byproduct. If this byproduct oxygen could be sold as a merchant gas, the costs of the solar-hydrogen system can be spread over both hydrogen and oxygen. The net effect will be a lower cost for hydrogen production and an associated greater market penetration.

As shown in Table 4, the potential market for merchant oxygen is projected to grow rapidly. Large new markets for waste water treatment and synfuel/feedstock production are identified. The byproduct oxygen associated with projected solar-hydrogen (Fig. 12) can satisfy a substantial portion of the oxygen demand as shown on Fig. 15. Thus, it appears that byproduct oxygen from solar-hydrogen systems can be sold at prices competitive with alternative sources of oxygen production such as air separation plants.

D. Increase in Atmospheric Carbon Dioxide

Potentially large and catastrophic environmental impacts are possible as a result of continued growth in atmospheric carbon dioxide concentration associated with fossil fuel usage (Refs. 10, 11, and 12). Based on detailed measurements of atmospheric carbon dioxide since 1958, a 13% increase has been observed.

For over 100 years, carbon dioxide emissions have increased at the rate of ~4.3% per year. The consequence of continued carbon dioxide emission is an increase in climatic temperatures which can cause impacts such as relocation of agricultural regions and melting of polar ice caps. When polar ice caps melt, there will be a rise in sea level and a modification of the shoreline.

Regarding this problem, society is faced with two choices. Fossil fuel rates can be allowed to

grow until impacts force a change. This involves a risk since the adverse effects will probably persist for long periods of time. The other course of action is to modify fossil fuel usage to control the severity of the impacts. This would require earlier usage of more costly renewable source energy systems for which solar-hydrogen systems could play a major role. This substitution would enable fossil sources to be used under conditions which would greatly reduce carbon dioxide emissions (e.g., Table 3).

REFERENCES

1. Kelley, J. H., "Hydrogen Tomorrow, Demands and Technology Requirements," JPL Report 5040-1, NASA/Jet Propulsion Laboratory, Pasadena CA., December 1975.
2. ERDA, "A National Plan for Energy Research, Development, and Demonstration," Washington, D.C., 1975.
3. Gregory, D. P., "The Hydrogen Economy," Scientific American, Jan. 1973, Vol. 228, No. 1.
4. Fujita, T., "Underground Energy Storage for Electric Utilities Employing Hydrogen Energy Systems," JPL Report 900-744, EM 342-339, Jet Propulsion Laboratory, Pasadena, CA., June 1976.
5. Reuyl, J. S., et. al., "Solar Energy in America's Future," Second Edition, ERDA Contract E(04-3)-115, SRI Project URU-4996, Stanford Research Institute, Menlo Park, CA., March 1977.
6. Bockris, J. O'M., Energy, The Solar-Hydrogen Alternative, John Wiley & Sons, New York, 1975.
7. Bush, L. R., "Solar Thermal Dispersed Power Program, Total Energy System Project," Technical Progress Report ATR-77(7692-01)-1, Aerospace Corp., El Segundo, CA., 1 August 1977.
8. Intertechnology, "Analysis of the Economic Potential of Solar Thermal Energy to Provide Industrial Process Heat," Intertechnology Report No. 00028-1, ERDA 000/2829-1, Dist. Category VC-596, Final Report, Vol. 1, 7 Feb 1977
9. Ford Foundation, Energy Policy Project, "A Time to Choose," Ballinger Publishing Co., Cambridge, Mass., 1974.
10. Baes, C. F., et. al., "The Global Carbon Dioxide Problem," Report ORNL-5194, Oak Ridge National Laboratory, Oak Ridge, TN, August 1976.
11. Bolin, B., "The Impact of Production and Use of Energy on the Global Climate," Annual Review of Energy, Vol. 2, Annual Reviews Inc., Palo Alto, CA, 1977.
12. "Energy and Climate," pp. 110 ff, National Academy of Sciences Report, November 1977.

Table 1. Markets for total energy/cogeneration

SUMMARY OF PROCESS HEAT DATA BASE BY INDUSTRY* AND PROCESS TEMPERATURE REQUIREMENTS

<u>INDUSTRY</u>	<u>PROCESS HEAT 10¹²Btu/YR</u>	<u>APPLICATION TEMPERATURE REQUIREMENTS, °F</u>
MINING	129.00	250-2500
FOOD & KINDRED PRODUCTS	319.00	100-550
TOBACCO PRODUCTS	1.40	~ 220
TEXTILE MILLS	116.00	200-275
LUMBER & WOOD PRODUCTS	172.00	212-300
FURNITURE	12.00	70-150
PAPER & ALLIED PRODUCTS	1,093.00	150-1900
CHEMICALS	534.00	80-2200
PETROLEUM PRODUCTS	2,640.00	250-1600
RUBBER	9.70	250-425
LEATHER	2.50	85-140
STONE, CLAY & GLASS	991.00	120-3300
PRIMARY METALS	3,770.00	100-2700
FABRICATED METAL PRODUCTS	.03	130-850
ELECTRICAL EQUIPMENT	1.60	150-1700
TRANSPORTATION	24.00	250-2650
TOTAL	9,815.00	

*REF: INTERTECHNOLOGY CORP, 1974 SURVEY

Table 2. Potential for total energy/cogeneration

WASTE HEAT AMOUNT AND LEVEL FOR H₂ FUEL CELLS AND TURBINES

	<u>WASTE HEAT % HHV OF H₂</u>		<u>WASTE HEAT TEMPERATURE °F</u>
	H ₂ /O ₂	H ₂ /AIR	
● FUEL CELLS			
● ACID ELECTROLYTE			
● STATE OF ART	56	58	325 ~ 375
● FUTURE	49	53	250 (1)
● BASIC ELECTROLYTE			
● FUTURE	40	48	ROOM TEMPERATURE (1)
● MOLTEN CARBONATE- SOLID OXIDE			
● FUTURE	53	55	1100 (2)
● TURBINES	40 ~ 47	~ 55	110 ~ 770 (3)

(1) JPL ESTIMATES

(2) FROM ATOMICS INTERNATIONAL

(3) BASED ON OPERATING CONDITIONS FROM NASA LeRC

**Table 3. Synfuels production
POTENTIAL SAVINGS VIA EXTERNAL SOLAR-HYDROGEN
(COAL-BASED PROCESSES)**

<u>PROCESS</u>	<u>COAL SAVINGS, %</u> (ALSO CO ₂ REDUCTION)	<u>CAPITAL COST SAVINGS, %</u>
● KOPPERS-TOTZEK (SNG)	~ 60	~ 35 ⁽¹⁾
● SOLVENT REFINING (SRC)	~ 8	~ 9
● I.G. FARBEN (GASOLINE)	~ 50	40-68 ⁽²⁾

(1) INCLUDES EXTERNAL OXYGEN SAVINGS OF ~ 31%

(2) RANGE BASED ON TECHNOLOGY STATUS

Table 4. Potential merchant oxygen market

PROJECTED CONSUMPTION, 10⁹ SCF

<u>PRESENT MARKETS</u>	<u>1972</u>	<u>1978</u>	<u>1985</u>	<u>2000</u>
● STEEL MAKING	251	289	342	488
● METAL FABRICATION	42	51	64	105
● CHEMICAL INDUSTRY	61	80	115	238
● OTHER/MISCELLANEOUS	4	25	54	108
SUBTOTAL	358	445	575	939
<hr/>				
<u>NEW MARKETS</u>				
● WASTE WATER TREATMENT	--	--	41	2,190
● SYNFUEL/FEEDSTOCK PRODUCTION				
LIQUID FUELS (SLF)	--	--	165	1,237
GASEOUS FUELS (SNG)	--	--	260	2,184
● DRINKING WATER PURIFICATION	--	--	--	61
SUBTOTAL	--	--	466	5,672
<hr/>				
TOTAL	358	445	1,041	6,611

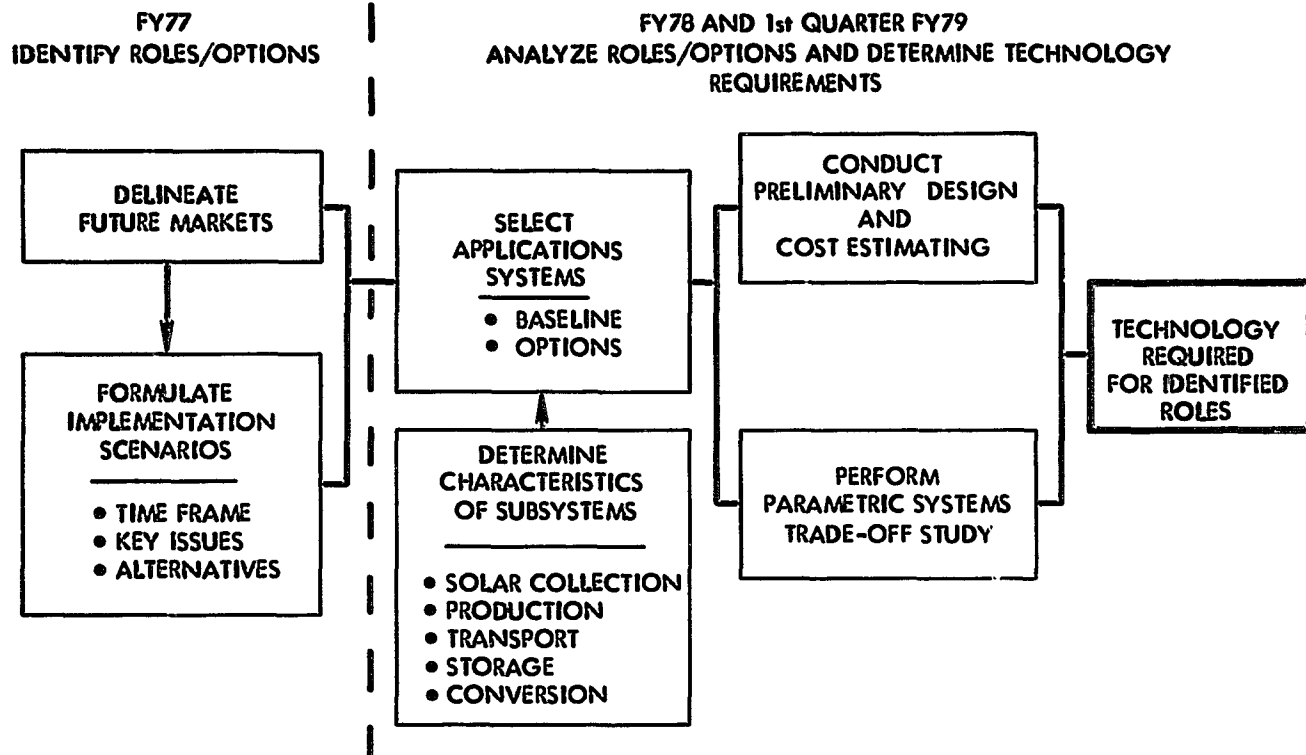


Fig. 1. Organization of Study Effort

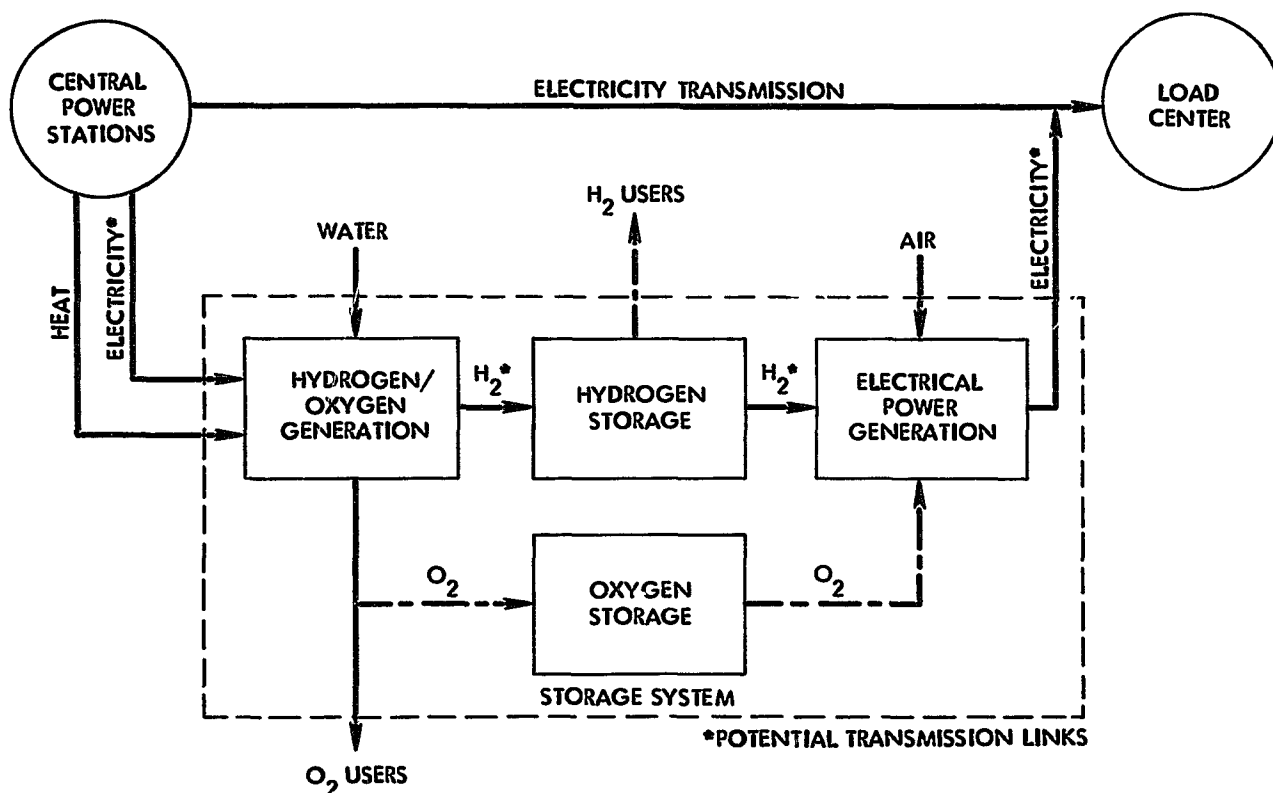


Fig. 2. Hydrogen Energy Systems for Electric Utility Energy Storage

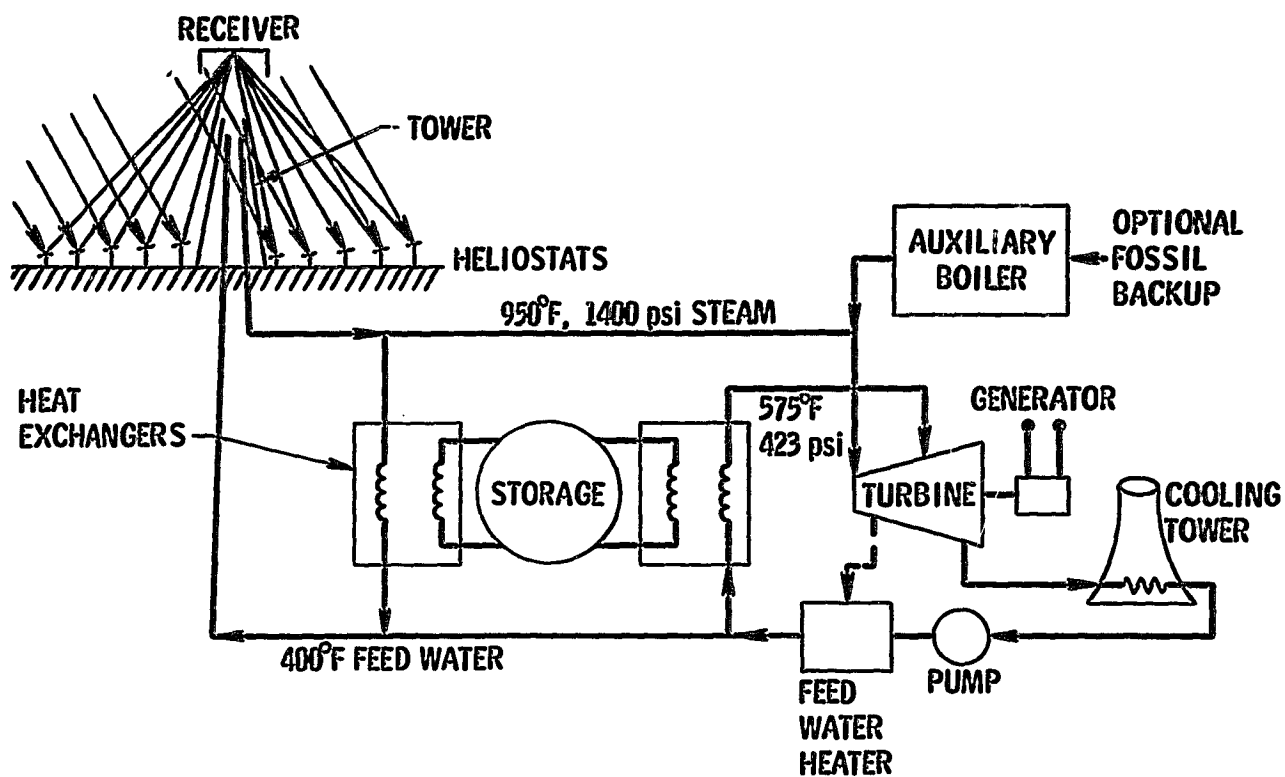


Fig. 3. Central receiver solar thermal-electric power plant

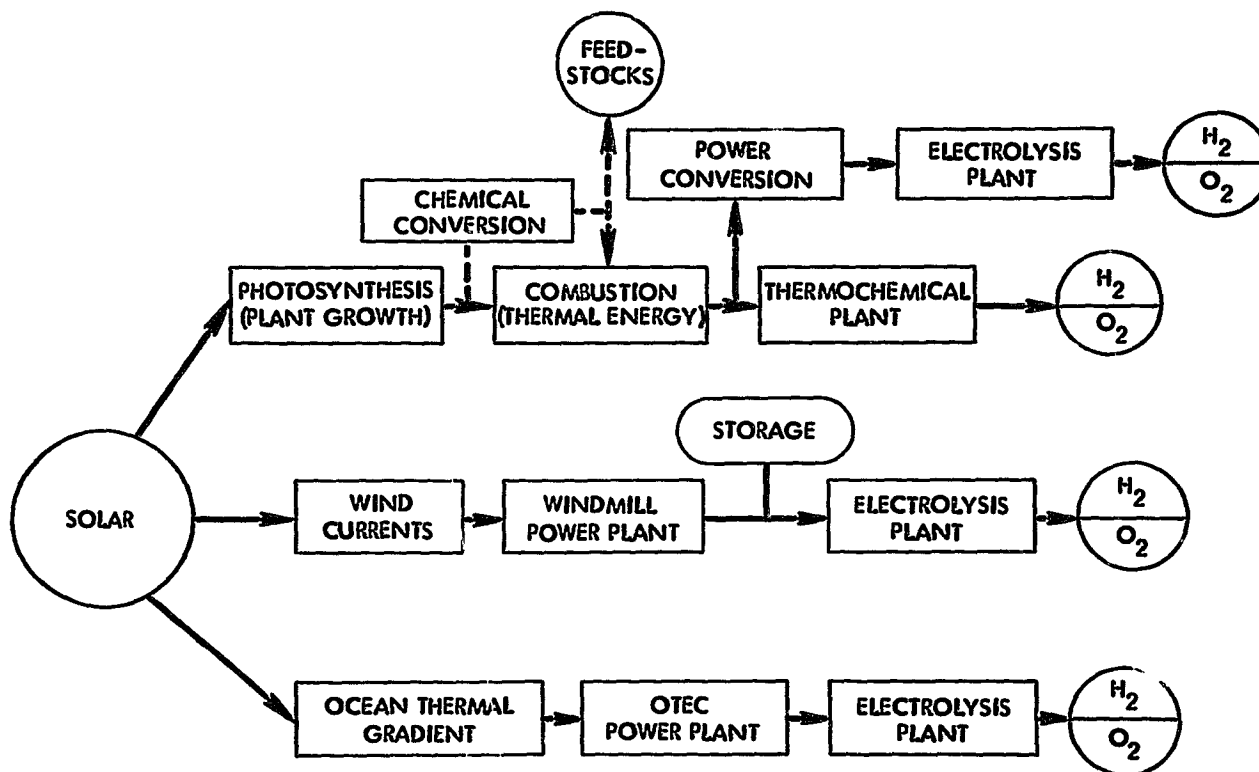


Fig. 4. Solar-hydrogen production pathways
natural solar collection systems

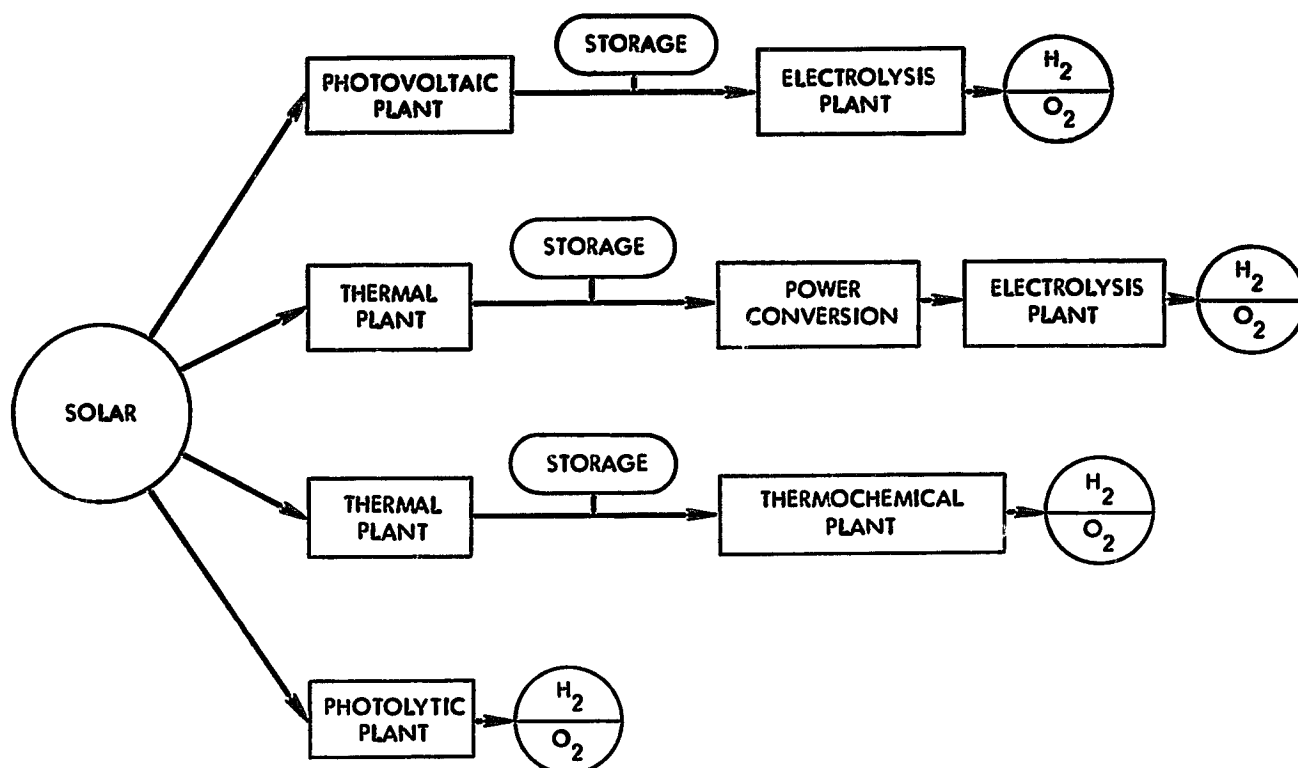


Fig. 5. Solar-hydrogen production pathways
engineered solar collection systems

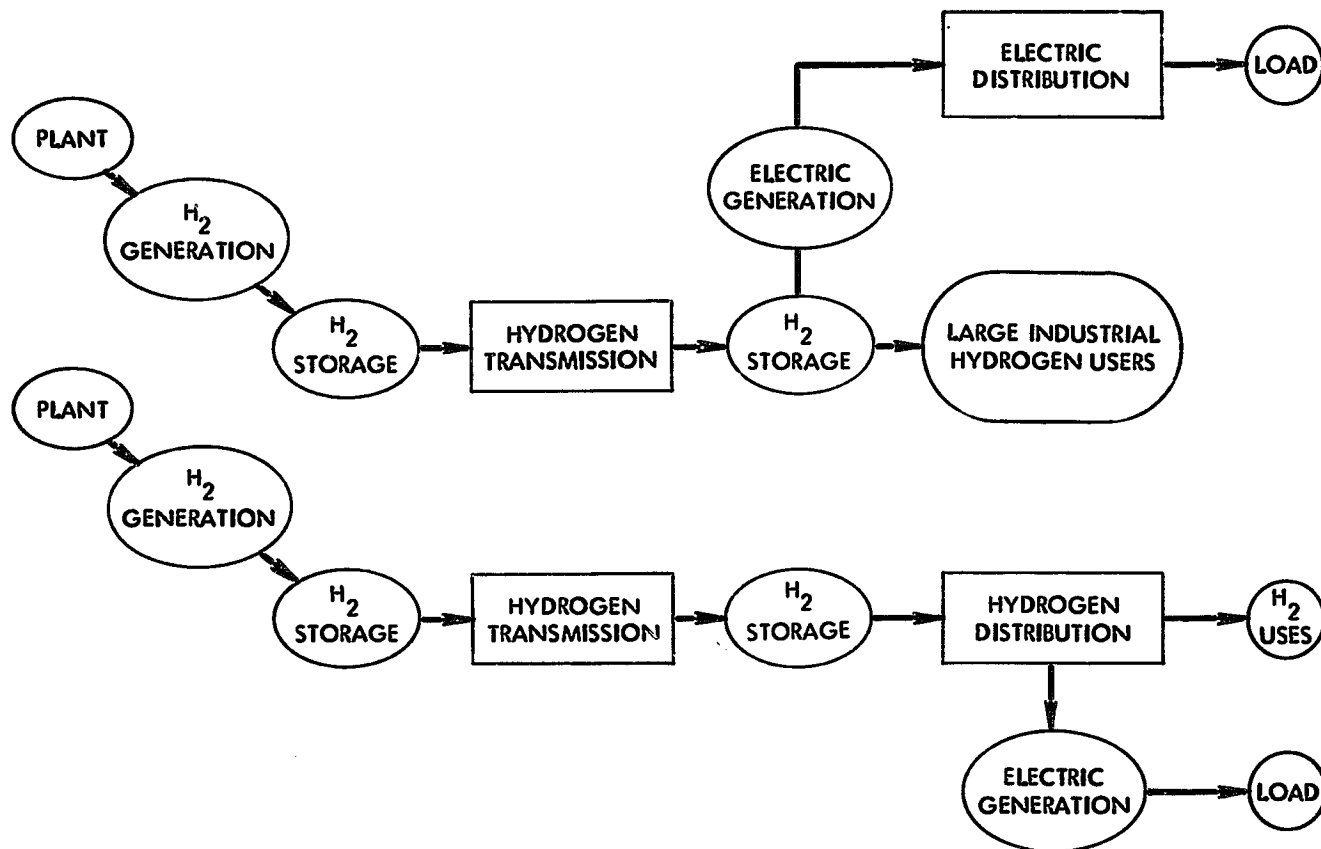


Fig. 6. Hydrogen transmission systems



Fig. 7. Potential for low cost bulk storage and transmission of solar-hydrogen

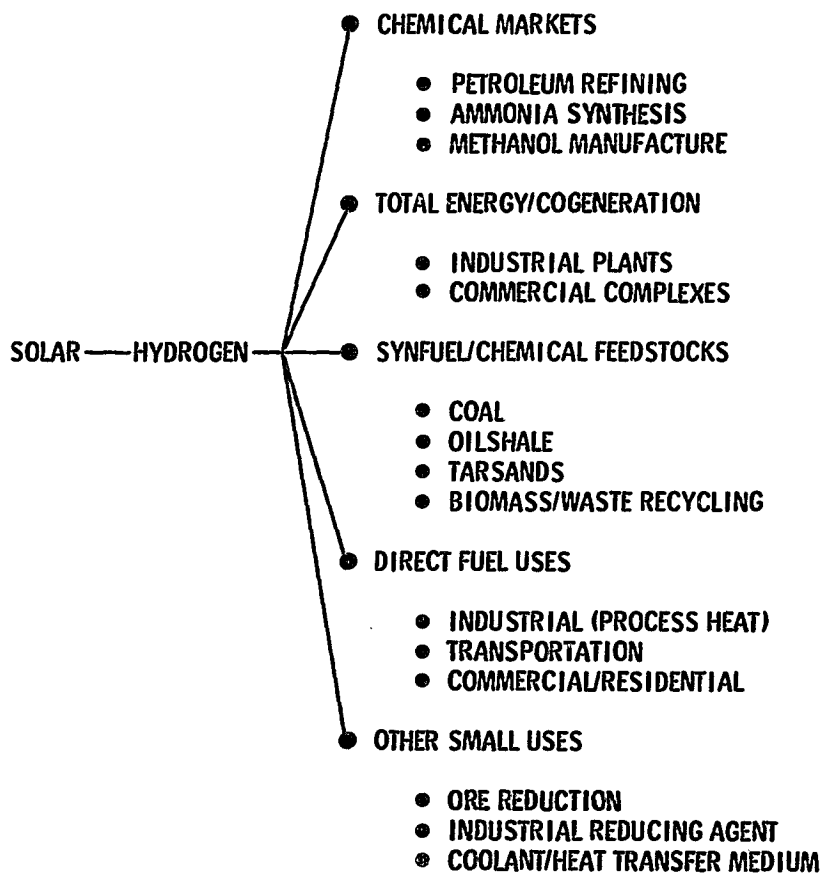


Fig. 8. Solar markets via hydrogen systems

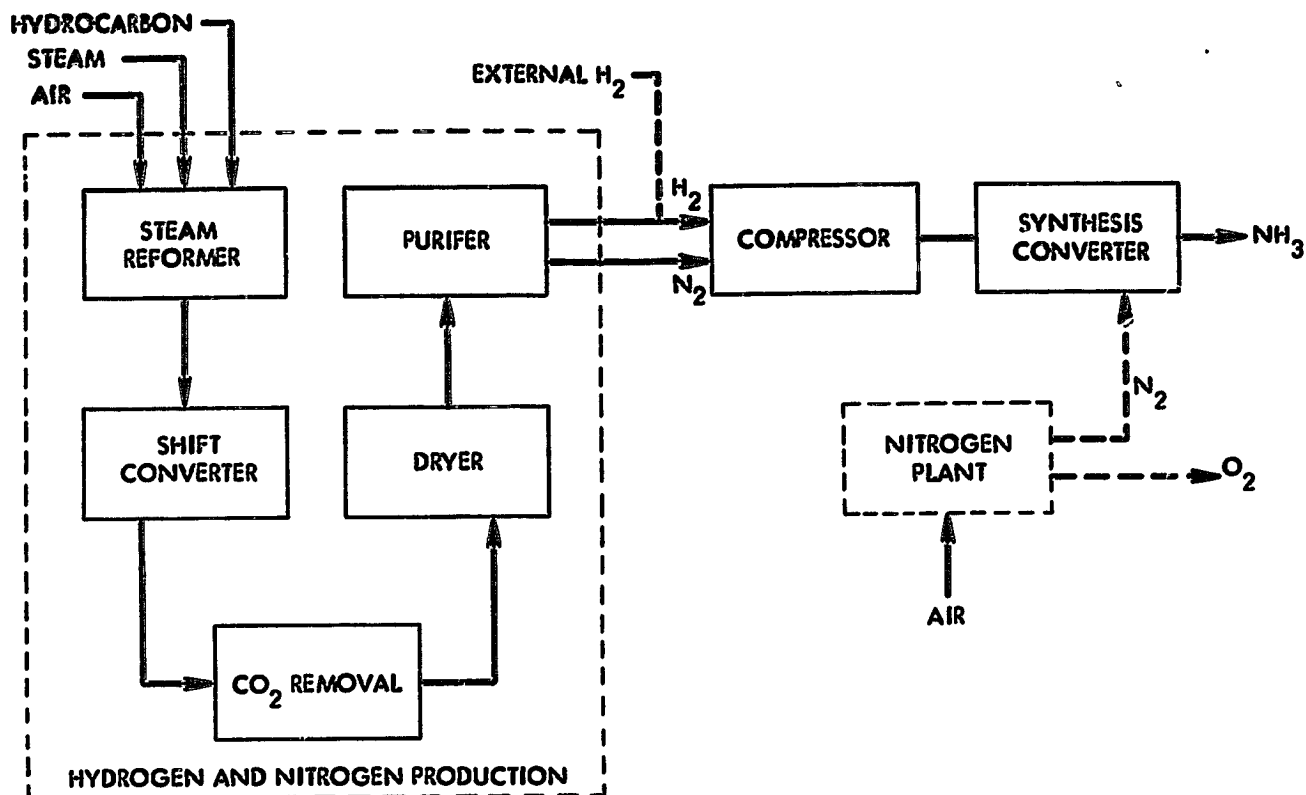


Fig. 9. Effect of external hydrogen on ammonia plant design

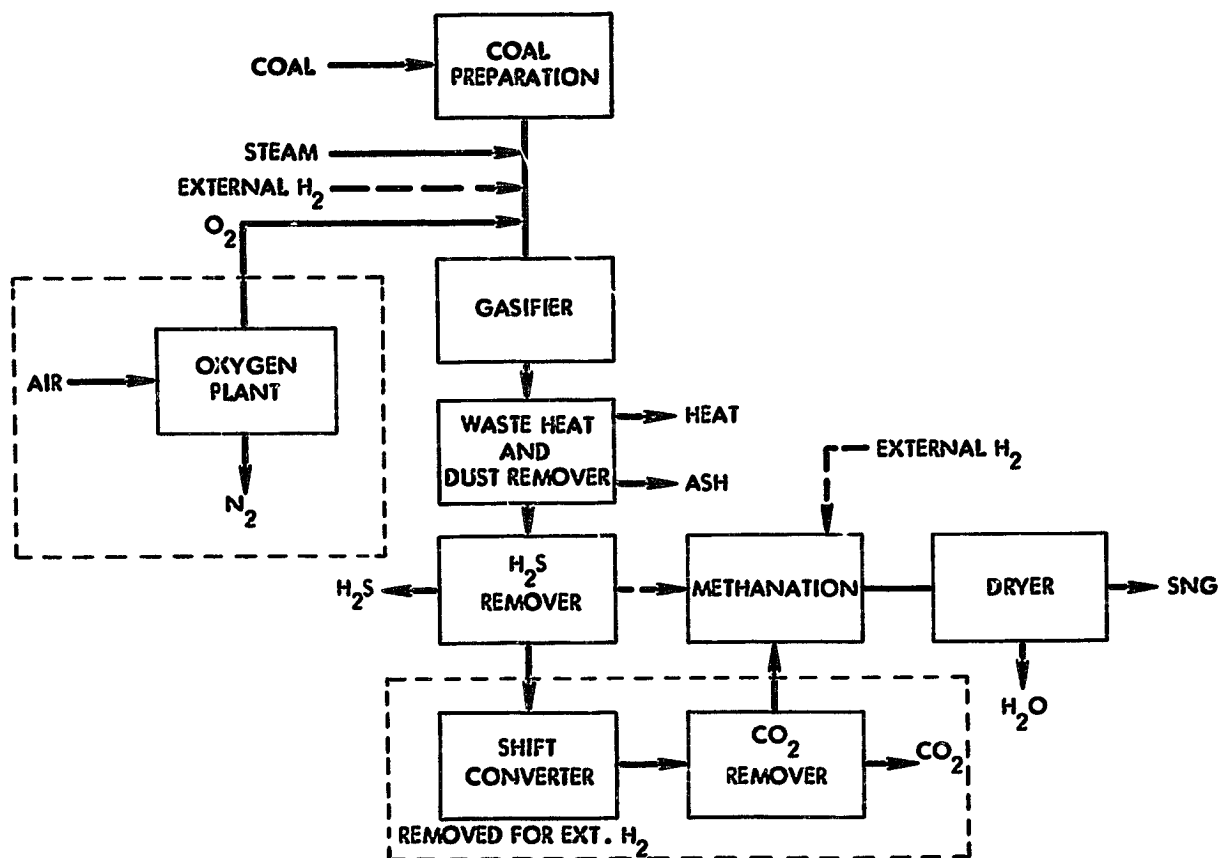


Fig. 10. Effect of external hydrogen on coal gasification (SNG) plant design

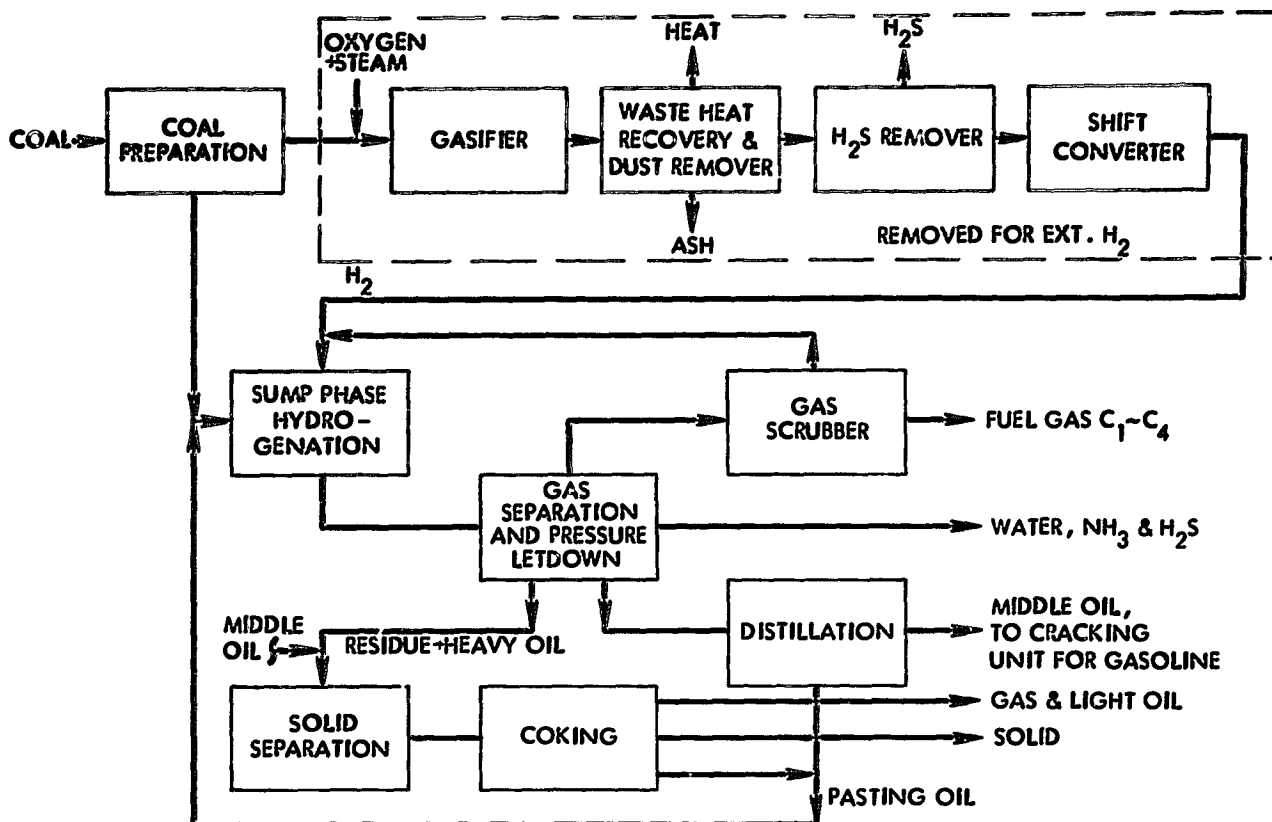


Fig. 11. Effect of external hydrogen on coal catalytic hydrogenation plant design (I. G. Farben)

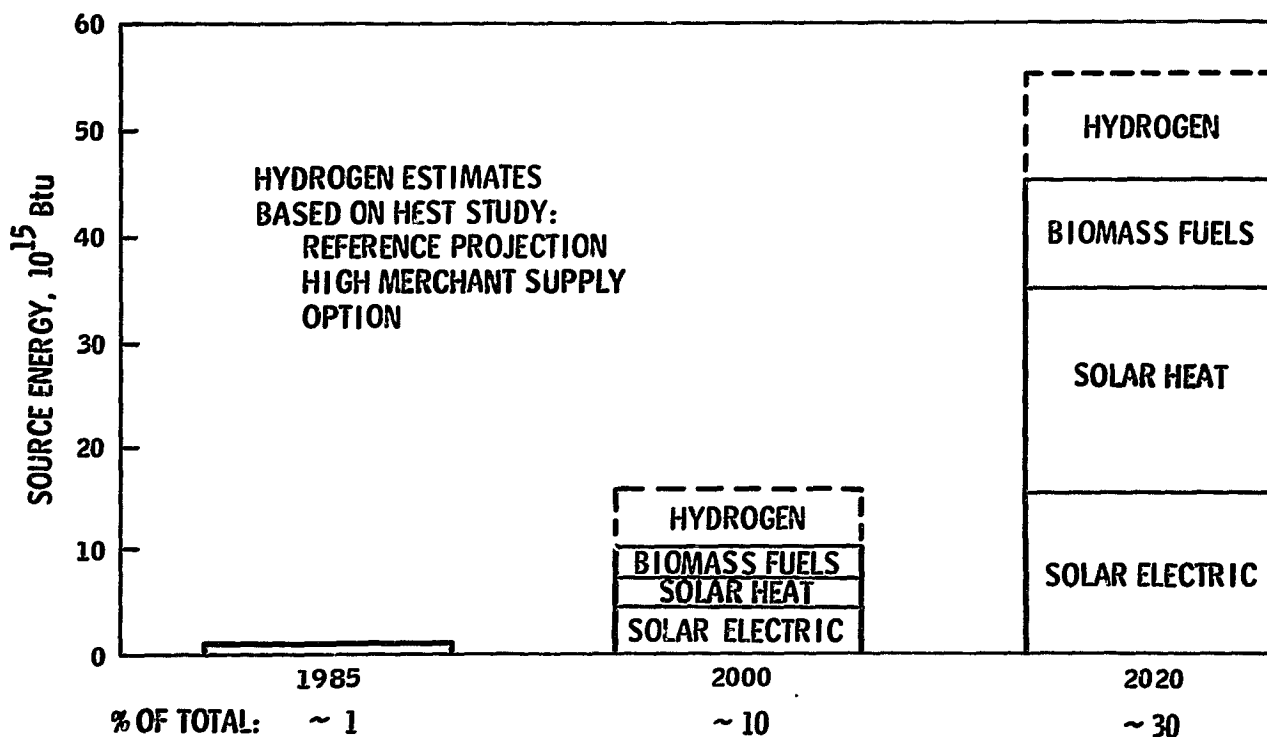


Fig. 12. United States solar energy projections (Baseline from ERDA-49)

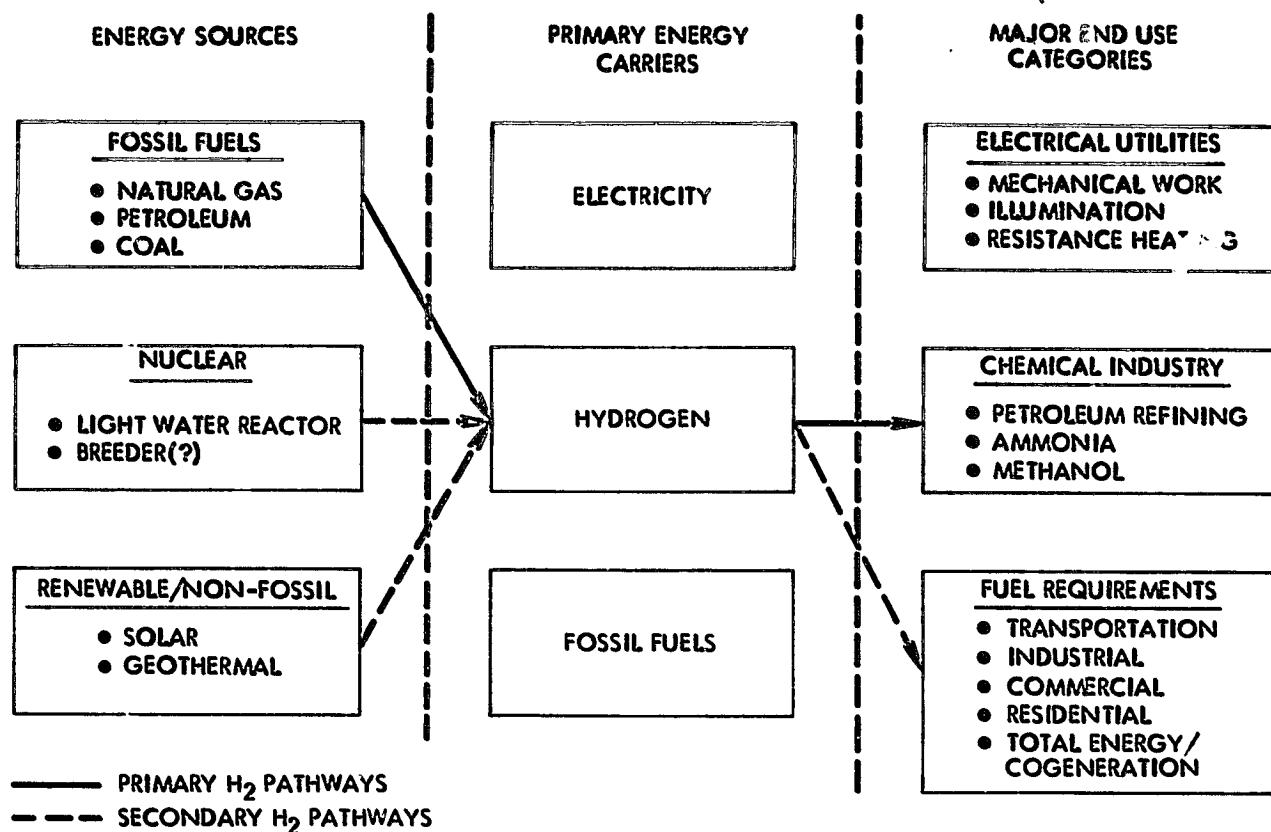


Fig. 13. Primary and secondary hydrogen pathways, fossil fuel era

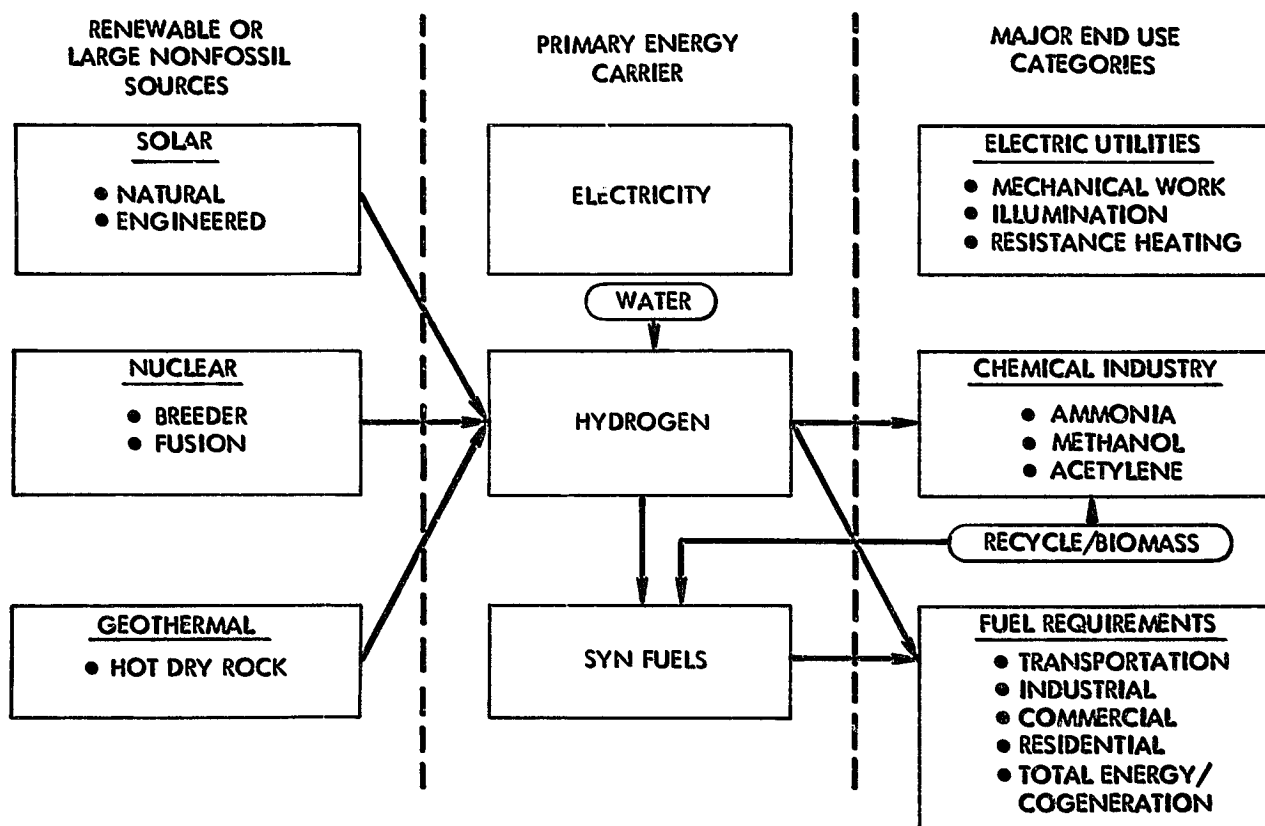


Fig. 14. Critical hydrogen pathways, renewable fuel era

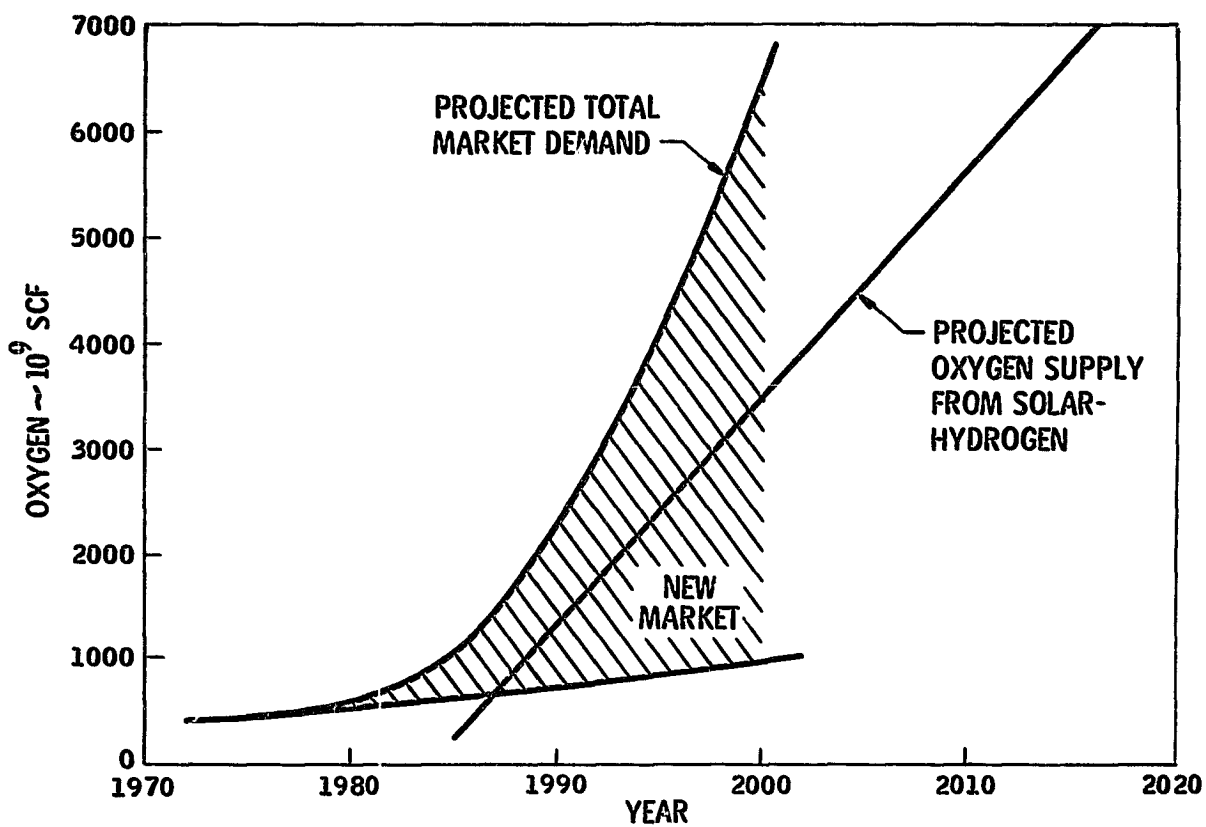


Fig. 15. Byproduct oxygen from solar-hydrogen, supply and demand

SOLAR-CHEMICAL ENERGY CONVERSION AND STORAGE:

CYCLOHEXANE DEHYDROGENATION

Arthur B. Ritter, George B. DeLancey,
James Schneider and Harry Silla

Department of Chemistry and Chemical Engineering
Stevens Institute of Technology
Hoboken, New Jersey 07030

Abstract

The concept of storing excess Thermal Energy as chemical bond energy and the subsequent recovery of this energy on demand by utilizing reversible catalytic chemical reactions shows great promise from an energy density point of view. In the intermediate temperature range (400-800°F) the cyclohexane-benzene reaction appears to be the most appropriate. While this reaction has been extensively studied in the exothermic direction, little useful design data exists for the endothermic reaction. We have studied the apparent kinetics of the gas-phase catalytic decomposition of cyclohexane to benzene in an internally recirculated (gradientless) reactor over the temperature range 400-600°F. At low space velocities (high conversions) a maximum of 0.2% of the product formed in a single pass over a commercially available naptha reforming catalyst is side products which may or may not be reversible. At high space velocities, there are significant mass transfer limitations on conversion. A test loop has been designed to enable us to study the buildup of side products and catalyst activity behavior during long term continuous cycling of the reversible reaction.

INTRODUCTION

The collection and storage of thermal energy through the destruction and reformation of chemical bonds is an attractive competitor to the utilization of sensible and latent heat effects as the energetics of chemical reactions are considerably more intense than the energetics of the latter two processes. In addition, and equally important, chemical energy storage offers the potential of low storage volumes and thermally efficient storage conditions at ambient temperatures. The basic principles on which chemical energy storage and transmission is based are broadly outlined in (7). Essentially, the chemical energy storage-recovery scheme we have developed involves a reversible gas-phase catalytic reaction which is endothermic in one direction and exothermic in the reverse direction. The endothermic step is driven by a source of excess thermal energy (e.g. solar) and the products of the reaction are stored until such time as the thermal energy is needed. Often it will be economically justifiable to store the reaction products at ambient temperatures since the sensible heat required to raise the temperature of the reactants up to the reaction temperature will only constitute a small fraction of the enthalpy of reaction. The presence of a catalyst is necessary for the reverse reaction to proceed so that the reaction products (and therefore the chemical bond energy they contain) can be stored indefinitely. Recovery of the thermal energy takes place on demand by running the reverse (exothermic) reaction over an appropriate catalyst. In a reversible reaction the products of the endothermic reaction are just the reactants for the exothermic reaction and vice-versa. The net result of this cyclic process is the storage of thermal energy during times when supply exceeds demand and recovery of the energy during times when demand exceeds supply. No net consumption of any of the reacting species occurs over the cycle. Furthermore, it is not necessary that the collection and utilization of energy take place at the same location. For example, the endothermic reaction (energy collection step) can be carried out at one location (e.g. where sunshine is plentiful and regular) and the reaction products shipped via the existing natural gas and/or petroleum pipeline distribution system to one or more users. At the utilization site, the exothermic reaction (energy recovery step) can then be carried out and the products of this reaction returned to the collection site, again, via the pipeline distribution systems. This is the so-called "Chemical Heat Pipe" concept (16).

Reaction Selection

A brief review of some of the reactions which have been suggested and at least partially evaluated is given in table 1. Chemical systems which have been proposed with the primary objective of hydrogen production have not been included. The emphasis here is on chemical storage cycles from a more general point of view. Reactions suitable for thermal storage applications fall into two basic categories: catalytic and thermal decomposition reactions (where the reactants and products exist in different phases). Reactions in both of these categories are susceptible to precise control which is required for efficient storage and/or transmission operations. The proposed thermal sources for all of these reactions are solar or

nuclear either via direct contact between the thermal source and the reactive system or via an intermediate heat transfer fluid. The primary focus of attention has been on reactions whose endothermic steps are operative in the temperature range 600-900°F as higher temperature sources such as gas cooled nuclear reactors (-1600°F) of the Pebble Bed Reactor (-2000°F) will not be readily available in the United States in the near future (4). The object here is to address the question of a suitable reaction which can absorb thermal energy at approximately 600°F and release this energy at a temperature of 400°F which is suitable for saturated process steam and electrical energy generation.

In searching for a suitable reaction, attention was focused primarily on catalytic reactions since such reactions very often exhibit high reaction rates which are important for the applications considered here and because this class of reactions is very extensive and includes many of the most energetic and thoroughly studied systems. In addition, the survey was not limited to the 400-600°F range of interest since little additional effort was required to include the high temperature regime. An abbreviated version of the results of a review of catalytic systems whose kinetics have been studied is given in table 1. The full table contains over 20 catalytic reaction systems which show some measure of potential for application to solar-chemical conversion systems and which have been studied to a sufficient degree that past experience has shown them technically worthy of consideration.

Once the desired temperature range has been selected, the choice from among the wide variety of catalytic reactions will be governed by the following general criteria:

1. The chemical capacity for energy storage should be large, i.e. the enthalpy change for the reaction should be large.
2. The system should exhibit significant conversions at the temperature extremes to effectively exploit the energy storage potential, although in some cases it may be more economically feasible to operate at lower conversions and recycle the unreacted product. If a gas phase reaction involves mole changes, as most do, the pressure at the energy absorption and desorption stages may be adjusted to enhance the equilibrium conversions.
3. The catalyst, which may be different for the reverse reaction, should be stable and inexpensive.
4. The rate of reaction should be large to minimize reactor volumes and heat transfer areas. The reaction should not proceed to any significant extent in the absence of the catalyst.
5. The selectivity of the catalyst in both endothermic and exothermic directions should be near 100%. However, side reactions which are reversible and do not cause deactivation of the catalyst can be tolerated.
6. The reactants and products should be economically stored at high energy densities.

7. Inexpensive materials of construction must be available that will not be attacked by the chemical species or act as unfavorable catalysts for the reaction(s) involved.

These characteristics are not independent and must be weighed together in the final selection of a catalytic reaction. Similar criteria have been proposed by others (5) (11).

One of the selection criteria requires the calculation of an energy density for the reaction. Since the reactions are reversible, the energy density can be based on the reactants, entirely on the products or some average of the two. Consequently in table 1, we present three different forms of the energy density. The first, e_r , is based entirely on the reactants. The second, e_p , is based on the products; while the third, e_t , is based on the average and is given by:

$$\frac{1}{e_t} = \frac{1}{e_r} + \frac{1}{e_p}$$

The value of e_p (for example) was calculated as:

$$e_p = \frac{(-\Delta H_R)}{\sum \frac{v_i}{\rho_i}}$$

products ρ_i

$(-\Delta H_R)$ - enthalpy change for the reaction

v_i - stoichiometric coefficient of species i

ρ_i - density of species i

The summation was taken over the reactants for the calculation of e_r . The energy densities are calculated for the storage conditions listed beneath the products and reactants. All species are assumed to be stored, stoichiometrically, at 300°K. Gases are supposed to be compressed to 100 atm.

Based on this and other information concerning the availability of catalysts and kinetic data, we can conclude that the following reactions show the most promise for successful application to chemical energy storage and conversion systems.

In the high temperature range (1000°F-1500°F), the oxidation of sulphur dioxide is the most appropriate. The kinetics of this reaction have been thoroughly studied (17) in the exothermic direction. Also, considerable process technology has been accumulated (3). The high energy densities are both due to the condensation temperatures of the sulphur oxides and low stoichiometric coefficient for oxygen. This reaction has been considered for energy storage by several investigators (1) (9) (14). A recent study in this laboratory (6) has indicated a pronounced hysteresis phenomenon in the temperature - conversion history of this system which must be studied further. However, it appears that, for this case, the hysteresis phenomenon is beneficial rather than detrimental from an energy storage point of view.

In the intermediate temperature range (400°F-

600°F), the hydrogenation of benzene appears to be the most appropriate. The most popular catalyst for the exothermic direction appears to be the Ni catalysts, although others are available (2). The reverse reaction can be catalyzed effectively with industrial reforming catalysts as well as carbides, silicates and sulphides of carbon (8). It should be noted that although the density for energy storage is large, the density would be appreciably increased if the hydrogen were stored in the hydride form (10) (15).

We have chosen to concentrate our efforts in the intermediate temperature range (400-600°F). In particular we believe that the benzene hydrogenation-cyclohexane dehydrogenation reversible catalytic reaction is the vehicle by which the chemical energy storage concept can be most readily demonstrated on a commercial scale. Some of the reasons for this position are given in (12). The primary technical questions that are associated with the current proposal lie in the reactor technology associated with the cyclohexane dehydrogenation reactor (energy collection step) and the possibility of detrimental side reactions concomitant to the dehydrogenation step. On the other hand, the technology for the benzene hydrogenation step (energy recovery) is well known and readily available on a commercial scale (18).

With respect to the dehydrogenation reactor, one must investigate the nature of the procedures required to effectively provide transient operation as opposed to the steady state technology that is available in the chemical industry. Start up and shut down algorithms must be developed. Such an investigation is most appropriately done computationally in the preliminary stages with engineering models of the reactor.

The chemical aspects of the dehydrogenation step must be investigated experimentally. The results of a preliminary investigation in this laboratory are presented below.

KINETIC STUDY OF C_6H_{12} DEHYDROGENATION

Flow System

We have measured the kinetics of the cyclohexane dehydrogenation reaction in the temperature range 400°F-750°F over a commercially available naphtha reforming catalyst (RD 150) manufactured by Englehard Industries in a fully instrumented internally recirculated (gradientless) stirred tank reactor built by Autoclave engineers. A schematic diagram of the experimental system is shown in figure 1.

Cyclohexane feed is introduced into the reactor by means of a Harvard constant infusion syringe pump. This is a positive displacement pump that provides very precise control of flow-rate over the range 0.025-38.2 ml/min depending on the size of the syringe used and the speed selected. A double syringe model is used along with a 3-way ball valve arrangement to insure virtually continuous precise flow of the cyclohexane feed to the reactor. The calibration of the pump has been checked at all speeds using a graduated cylinder and stopwatch. The reactor has a one gallon working capacity. The catalyst is supported in a cylindrically shaped bed approximately

5.8 cm in diameter by 13.0 cm long located on the axis of the fan. The catalyst bed is an integral part of the fan system which is designed to circulate the gas phase through the catalyst bed to insure intimate contact between the gas and catalyst. A rheostat allows the fan speed to be adjusted over the range 1000-2100 rpm. The speed is measured by means of a strobetachometer. Two thermocouples located 2.0 from the top and 2.0 cm from the bottom of the catalyst bed allow us to monitor the temperature change across the bed. The location of these thermocouples can be adjusted to monitor the temperature at any two points along the catalyst bed. Temperature control is provided by means of three 650 watt resistance heaters located around the reactor. The three heaters provide 3 independently regulated zones of heat at the top, middle and bottom of the reactor. All 3 heaters are used for startup, while only the bottom heater is generally required for temperature control during operation. The reactor is well insulated and the temperature variation is usually less than $\pm 0.5^{\circ}\text{F}$ during a run. The pressure in the reactor is controlled manually by means of a needle valve and pressure gauge on the outlet line. The data in these studies were taken at a constant reactor pressure of 2.0 psig. The outlet from the reactor is split into two streams. The major part is passed through a total condenser. The cooling water for the condensor is provided by a refrigeration unit operating near 0°C (although capable of going to -10°C with the use of a heat transfer fluid such as Dowtherm). The condensed product (benzene and cyclohexane) is collected in glass containers and disposed of in a safe manner. Non-condensibles (mostly hydrogen saturated with benzene and cyclohexane vapors at 0°C) are vented through the laboratory hood system. A small portion of the outlet stream is piped directly to a Hewlett-Packard 5830A computer controlled gas chromatograph equipped with a heated, automatic, programmable gas sampling valve. The detector is a hydrogen flame ionization unit and excellent separation of benzene and cyclohexane is achieved by a $1/4" \times 6 \text{ ft.}$ column packed with carbowax. The chromatograph is calibrated both for concentration of cyclohexane and benzene and total sample size by injecting known amounts of carefully prepared mixtures of benzene and cyclohexane. A correction for sample size is required since at high conversions, large volumes of hydrogen are present in the product stream along with the cyclohexane and benzene. The hydrogen essentially acts as a diluent when the sample passes through the hydrogen flame ionization detector. The computer on the chromatograph automatically computes the total areas under all the curves (related to sample size) as well as the fraction of the areas under each curve. It should be emphasized that the experimental apparatus are flexible enough so that the kinetics of many gas phase catalytic reactions can be readily studied with only minor modifications to the system.

Experimental Procedure and Data

At the end of each days operation the flow system is thoroughly flushed with nitrogen and left overnight under a slight nitrogen positive pressure for safety. To start operation, the system is first brought up to the desired operating temperature, the nitrogen is shut off and cyclohexane feed is introduced at a liquid flowrate of about 2.75 ml/min to flush the reactor. After

approximately 5 residence times of flushing (-25 min.), the cyclohexane flowrate is adjusted to the desired experimental value. Conditions of temperature, pressure and flowrate in the reactor are maintained constant until the concentration of benzene leaving the reactor (as indicated on the gas chromatograph) reaches a constant value. The rule of thumb is to wait at least 5 residence times after any system changes have been made to insure that a steady-state condition has been reached.

The feed to the reactor is reagent grade cyclohexane. As each new bottle of cyclohexane is opened, its purity is checked by running several samples through the chromatograph. Occasionally trace quantities of toluene and other impurities are detected in the cyclohexane. The naphtha reforming catalyst is in the form of pellets approximately $1/16" \text{ D} \times 3/16" \text{ L.}$ The catalyst is weighed and loosely packed into the cylindrically shaped bed support. Layers of glass beads of several different sizes are randomly interspersed with the catalyst pellets to fill the unused portion of the bed with inert material and provide a matrix to insure adequate flow in and around each catalyst pellet and through the bed. Before each new set of runs the catalyst is activated by a nitrogen flush (to eliminate any oxygen present) followed by a hydrogen purge at 900°F for 2 hours. The catalyst activity is checked at the beginning and end of each set of runs by duplicating a high conversion ($>90\%$) data point at 600°F and comparing the conversion with the conversion obtained when the catalyst was fresh. We have used the same batch of catalyst over the past year and a half, including over 2 dozen reactivations and many start ups and shut downs (temperature cycling). As far as we can tell the catalyst activity has remained constant.

At each temperature and feedrate (space velocity), the reactor is run at several different agitator speeds to determine the effects of external mass transfer on the conversions. Figure 2 shows the results for several flowrates at 600°F . One can see that at low space velocities, where conversions close to equilibrium are obtained, the external mass transfer can keep pace with the (relatively low) reaction rate. However, as the space velocities are increased and the reaction gets farther from equilibrium, the external mass transfer can't keep pace with the (relatively rapid) reaction rate and so the mass transfer effects limit the observed conversion. Under these conditions the conversion becomes a function of the agitator speed and the "true" conversion must be obtained from the data by extrapolation to infinite agitator speed (elimination of external mass transfer effects). Figure 3 is a plot of the conversion of cyclohexane obtained over a range of space velocities, with temperature in the range $500-750^{\circ}\text{F}$ as a parameter. Figure 4 is even more descriptive in that it shows the reaction rate times the space velocity - vs - conversion at each temperature. The data in figure 4 clearly point out the effects of mass transfer limitation. The dashed line is data taken at 600°F at low agitator speeds. The data at each temperature approach the calculated equilibrium values at low space velocities.

By Products

At high conversions (low space velocities) and at temperatures above 540°F at 2 psig, several side products are produced along with the benzene and hydrogen over this catalyst. The total amount of these products is never more than 0.2% in a single pass through the reactor and is generally <0.1% except at the most severe conditions. Using a chemical ionization mass spectrometer (CIMS) we analyzed the components in the vapor phase leaving the condensor for one run at 600°F and a space velocity of 0.029 moles cyclohexane/g-catalyst-hr. The major side product has clearly been identified as toluene. Based on the gas-chromatograph data, when side products are produced, toluene constitutes somewhere between 60-100% of the side product formation. We have not, as yet, identified the remaining side products, although there is some evidence that methylcyclopentane may be present. However, this molecular weight is masked on the CIMS by the presence of cyclohexane. A peak at molecular weight 54 corresponds to 1 or 2 butene or might correspond to one of the fragmentation products produced in the spectrometer. Similarly, the presence or absence of C₁ to C₄ hydrocarbons in the product stream is masked by the fragmentation products of the spectrometer. Accordingly, we have ordered some pure methylcyclopentane and 1 and 2 butene. We will introduce these into the gas chromatograph and compare their retention time on the chromatograph column with our unknown peak. Similarly we have ordered a chromatograph column which will allow us to separate the C₁ to C₄ hydrocarbons to see if any are present in our product stream. It should be noted that toluene is reversible and methylcyclopentane is not reversible to cyclohexane over a suitable catalyst (13).

Table 2 summarizes the chemistry of the cyclohexane decomposition reaction as we have been able to determine it to date.

FUTURE PLANS

The questions we plan to answer in the next phase of our study center around the behavior of the system under long term cycling. In particular we must ascertain whether or not the side products produced are reversible and if not whether or not they reach an acceptably low equilibrium value under long term cycling. We must also study the behavior of the catalyst(s) under long term cycling to see what effects there are on such parameters as catalyst activity and attrition.

Accordingly, we have designed a test loop to study these and related questions. A schematic diagram of the test loop is shown in figure 5. The major pieces of equipment in the loop have been sized and will be purchased in the near future. This loop will allow us to continuously cycle the cyclohexane, benzene and hydrogen over both the reforming catalyst and a hydrogenation catalyst. Periodic sampling of the product streams in each loop and the catalyst beds should allow us to answer some of the questions posed above. The loop was designed on the basis of a hydrogen flow of 1 SCFM with a hydrogen surge-storage capacity of 10 minutes (1 ft³, 34 atm). The cyclohexane and benzene liquid flowrates were sized at a nominal value of 60 ml/min. with 10 gal. feed tanks. Except for the hydrogen compressor, the test loop will fit in one corner of our research laboratory (10 x

12 ft).

A second set of questions we expect to answer over the next year concerns the behavior of cyclohexane decomposition reaction at high pressure (up to 500 psig). Because hydrogen is produced in the decomposition reaction, higher pressures will tend to shift the equilibrium to lower conversions (hence lower energy storage capacities). However, for chemical heat pipe applications, it is desirable to operate the collector at higher pressures. This means increasing the operating temperature to compensate for the higher pressure. We also know that at higher temperatures greater quantities of the side products are produced and there is also the possibility of thermally cracking the benzene molecule. The answers to these and other questions related to the catalyst stability at the higher temperature and pressures will be pursued over the next year.

Finally, we have developed a mathematical model which describes the transient behavior of a gas phase catalytic reactor dedicated to the collection of thermal energy. The results have been reported previously (12). The model will prove useful in simulating startup, shutdown and in developing control algorithms for chemical energy storage systems. The model is being modified to take into account the mass transfer limitations we have observed in the cyclohexane decomposition reaction. Over the next several months we expect to develop the model to the point where we are able to simulate the transient behavior of the collector reactor in the test loop under varying conditions of startup, shutdown and changes in the thermal energy flux reaching the reactor.

ACKNOWLEDGEMENTS

We wish to thank Robert Yarrington of Englehard Industries who supplied us with the RD 150 naphtha reforming catalyst used in this study and the Union Carbide Corp. for their donation of the reactor. We also gratefully acknowledge the many long days and nights spent by Stevens undergraduates Mike Kosusko, Rochelle Chernikoff and Richard Jarosz in collecting and analyzing the data. Their enthusiasm, energy and good humor went far beyond the requirements of their work-study jobs. Also to Dominick Quagliato for his help with the Chemistry, and to Marianna Buzzerio and Abram Addonizo for their help in the lab. Finally, we would like to acknowledge the financial support given to Jim Schneider through the R.C. Stanley Fellowship fund at Stevens Institute of Technology and the Energy Research and Development Administration through ERDA grant no. E(11-1) 4031, which partially supported this research.

REFERENCES

1. Chubb, T.A., Solar Energy, 17, 129 (1975).
2. Dini, P., et al., "A Study of Platinum - Polyamide Catalysts. Catalytic Behavior in the Benzene Hydrogenation Reaction", J. Catalysis, 30, 1 (1973).
3. Duecker, W., West, J., The Manufacture of Sulfuric Acid, Reinhold Publishing Corp., New York, 1959.

4. Golibersfirch, D., F.P. Bundy, P.G. Kosby and H.B. Vakil, "Thermal Energy Storage for Utility Applications," Thermal Energy Storage Conference, NATO, Turberry, Scotland, March, 1976.
5. Hanneman, R.E., Vakil, H.B. and Wentorf, R.H., "Closed Loop Chemical Systems for Energy Transmission, Conversion and Storage", 9th IECEC, San Francisco, 435 (1974).
6. Kovenklioglu, S. and DeLancey, G.B. "A Study of the Apparent Kinetic of the Reversible Catalytic Oxidation of Sulphur Dioxide," Submitted to AIChE J (1977).
7. Kovich, E.G. (Ed.) "Thermal Energy Storage", report of a NATO Science Committee Conference held at Turberry, Scotland, March, 1976.
8. Krylov, O.V., in Catalysis by Nonmetals, translated by Happel, J., et al., Academic Press, New York, 1970.
9. Lynn, S., and Foss, A., "The Sulphur Dioxide System for Energy Storage", Proceedings of the ERDA Contractors review meeting, Brookhaven National Laboratory, April, 1976.
10. "On the Shelf: Scientists seek ways of Storing Electricity to Prevent Brownouts", Wall Street Journal, Vol. CLXXXIV, No. 4, July 5, 1974.
11. Prengle, H.W. and Sun, C.H., Solar Energy **18**, 561 (1976).
12. Ritter, A.B. and DeLancey, G.B., "Thermo-Chemical Energy Conversion and Storage", Proc. ERDA Contractors Review Meeting on Chemical Energy Storage and Hydrogen Energy Systems, ERDA CONF-761134, Airlie, Va., Nov. 8-9, 1976.
13. Personal Communication from Matthew Rosso, Jr. Brookhaven National Laboratory, Sept. 20, 1977.
14. Spewock, S., Brecher, L.E. and Talks, F., "The Thermal Decomposition of Sulphur Trioxide to Sulphur Dioxide and Oxygen", 1st World Hydrogen Energy Conference, Miami Beach, Fla., March 1-3, 1976.
15. "Solar Energy work Advancing Rapidly," Chem. and Eng. News, Sept. 16, 1974.
16. Vakil, H.B., "Energy Transmission by Chemical Heat Pipe," General Electric Technical Report No. 76CRD281, Schenectady, N.Y., 1976.
17. Weychert, S. and Urbanek, A., "Kinetic Equations for the Catalytic Oxidation of Sulphur Dioxide", Int. Chem. Eng., **9**, 396 (1969).
18. Thomas, C.L. Catalytic Processes and Proven Catalysts, Academic Press, New York (1970), p. 138-139.

Table 1

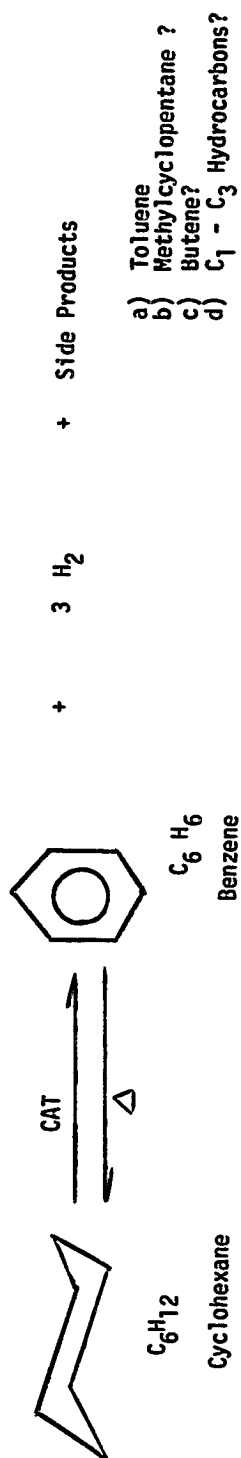
Review of Some Candidate Reactions Currently Proposed For Thermal Energy Storage Applications

Reaction (Exothermic)	$(-\Delta H_R)$ (Kcal/g-mole)	Energy Density (BTU/Ft ³) x 10 ⁻³			Energy Absorption			Energy Desorption		
		e_r	e_p	e_t	T (°F)	P (ATM)	CAT.	T (°F)	P (ATM)	CAT
$SO_2 + \frac{1}{2} O_2 = SO_3$ 11q. gas at 4.1 atm	23.5	15.8	63.5	12.6	1500- 1800	3	Pt	900- 1100	3	V_2O_5
$*CO + 3H_2 = CH_4 + H_2O$ $CO_2 + H_2 = H_2O + CO$ $H_2O = 11q$ at .03atm, rest = gases	53.0 -10.0	5.8 4.2	21.0 3.9	4.6 2.0	1500	40	N_i + EXCESS H_2O	950	40	Ru , N_i
$C_6H_6 + 3H_2 = C_6H_{12}$ 11q gas at 0.13atm	49.25	6.7	51.7	5.93	400- 600	1.0-1.5	N_i , Pt	300- 500	40	N_i , Pt
$CaO(s) + H_2O = Ca(OH)_2(s)$	12.2	-	-	-	950	1.0	NONE	950	1.0	NONE
$MgO(s) + H_2O = Mg(OH)_2(s)$ $H_2O = 11q$ at 0.03 atm.	18.5	-	-	-	500	1.0	NONE	500	1.0	NONE
$NH_3 + H_2O + SO_3 =$ 11q. 11q. 11q. $NH_4HSO_4(l)$ at at at 10 0.03 0.44 11q. at 147°D atm atm and 1.0 atm	80.4	-	-	-	1800 950	1.0 142.0	NONE NONE	900 790	1.0 1.46	NONE NONE

* The ADAM-EVA Chemical Energy Storage Process, seriously considered in Europe, involves only the first reaction. The combined set of reactions have been proposed for use in a chemical heat pipe system (5) (16).

Table 2

Summary of Cyclohexane Dehydrogenation Chemistry



Space Velocity = 0.03 g cyclohexane/g cat. hr.

Temperature (°F)	Conversion (% Benzene)	% Side Products
500	42.0	0.11 - Toluene < 0.01 - Other(s)
540	68.0	0.10 - Toluene < 0.01 - Other(s)
575	76.5	0.09 - Toluene 0.03 - Other(s)
600	84.0	0.09 - Toluene 0.09 - Other(s)

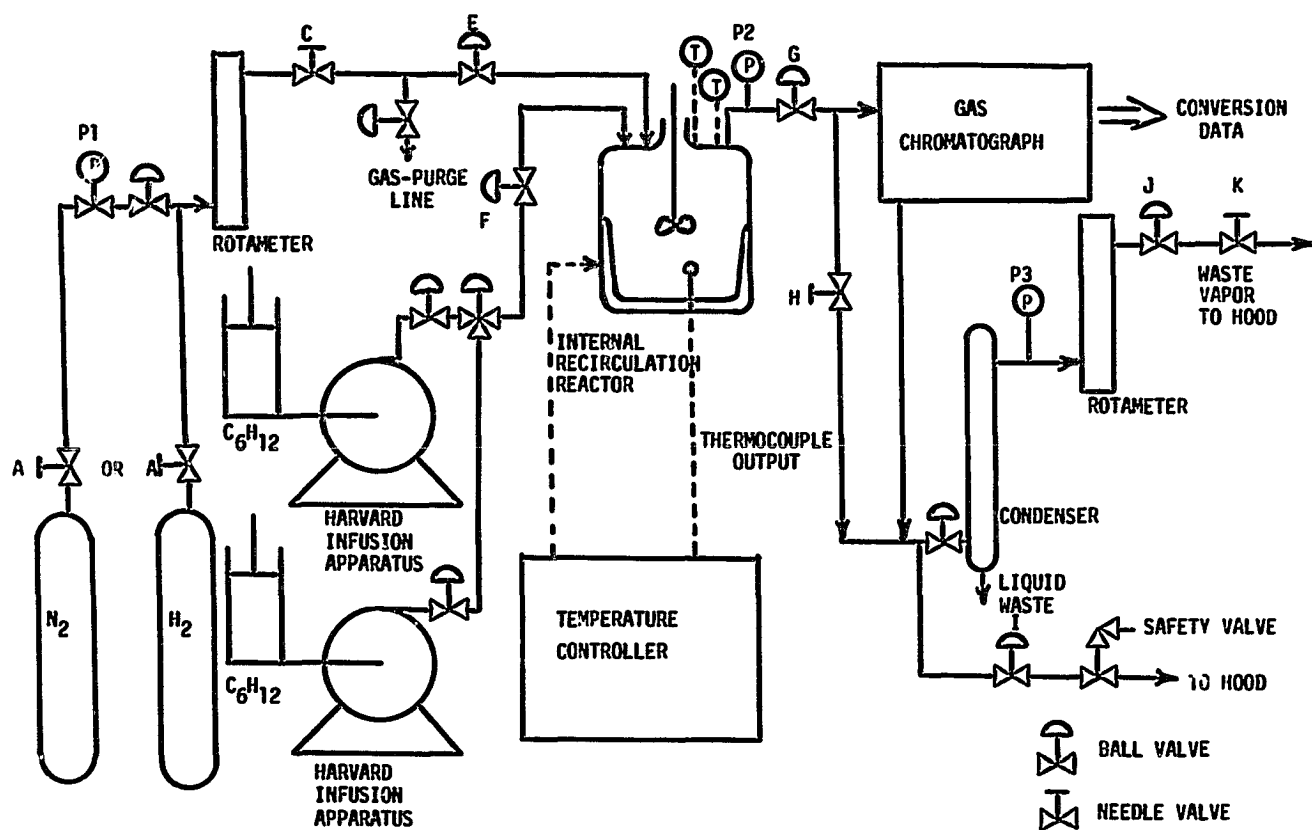


Fig. 1. The experimental flow system for studying the kinetics of gas phase catalytic reactions

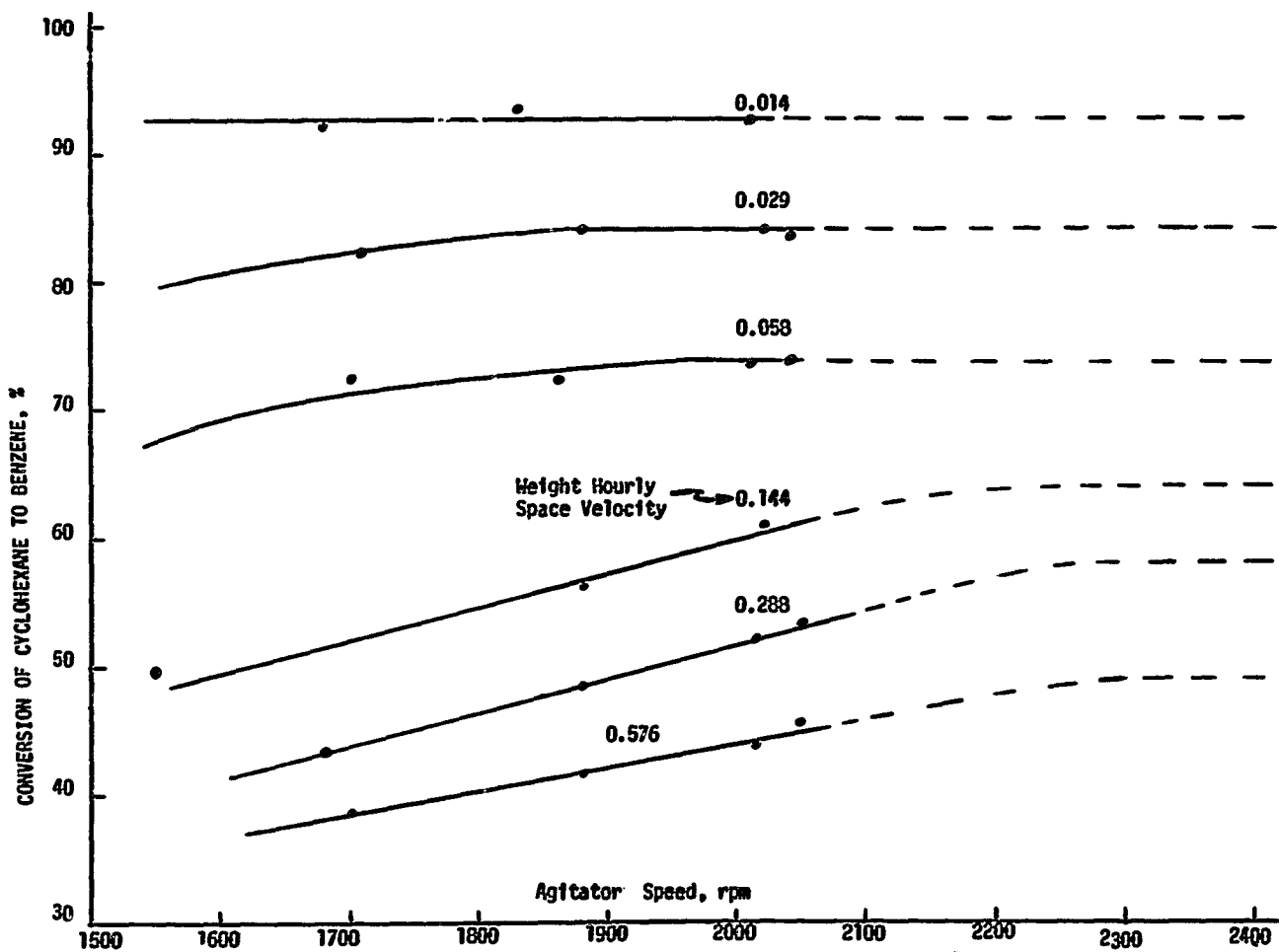


Fig. 2. The effects of external mass transfer on conversion at 600°F

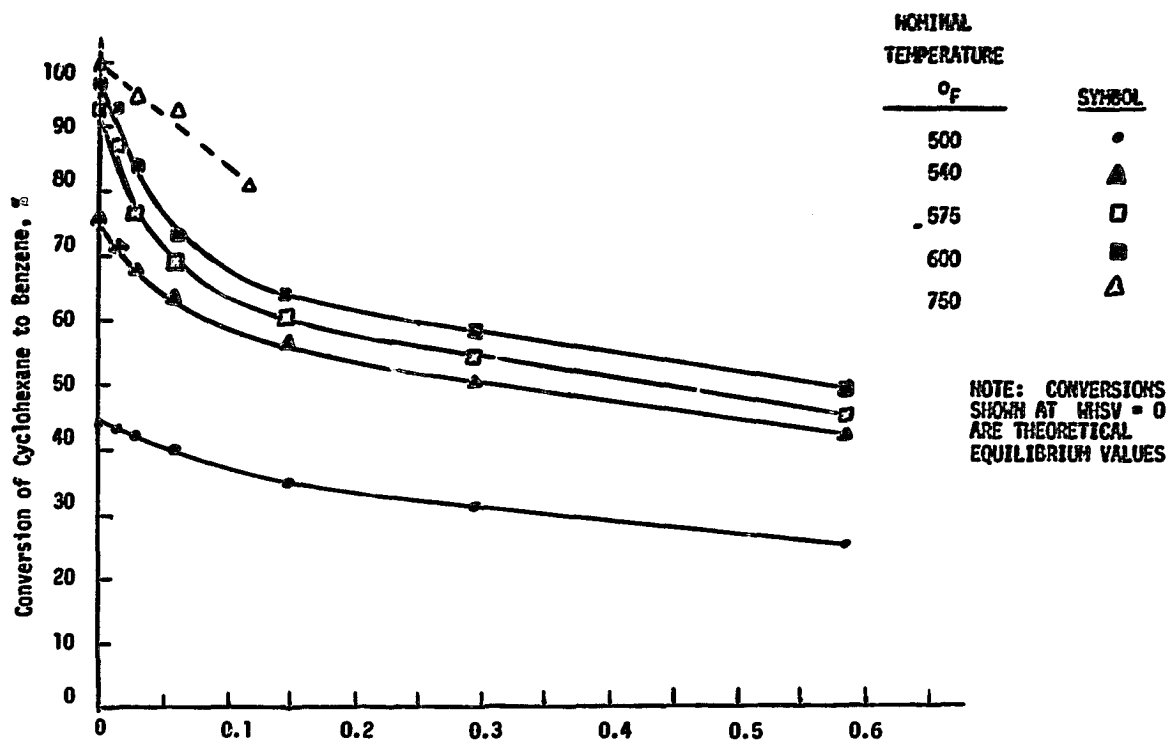


Fig. 3. Cyclohexane conversion vs weight hourly space velocity over the temperature range 500-750°F at 0.2 psig

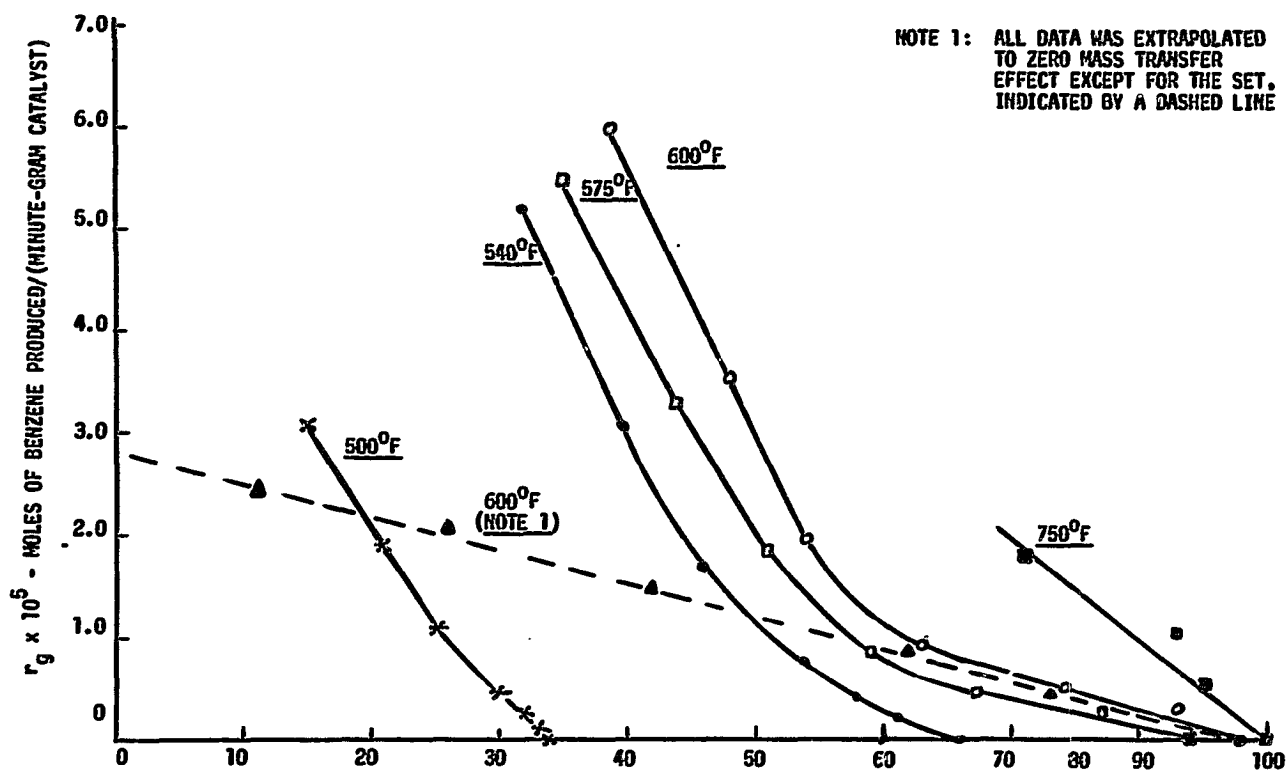


Fig. 4. Reaction rate times space velocity vs fractional conversion of cyclohexane over the temperature range 500-750°F

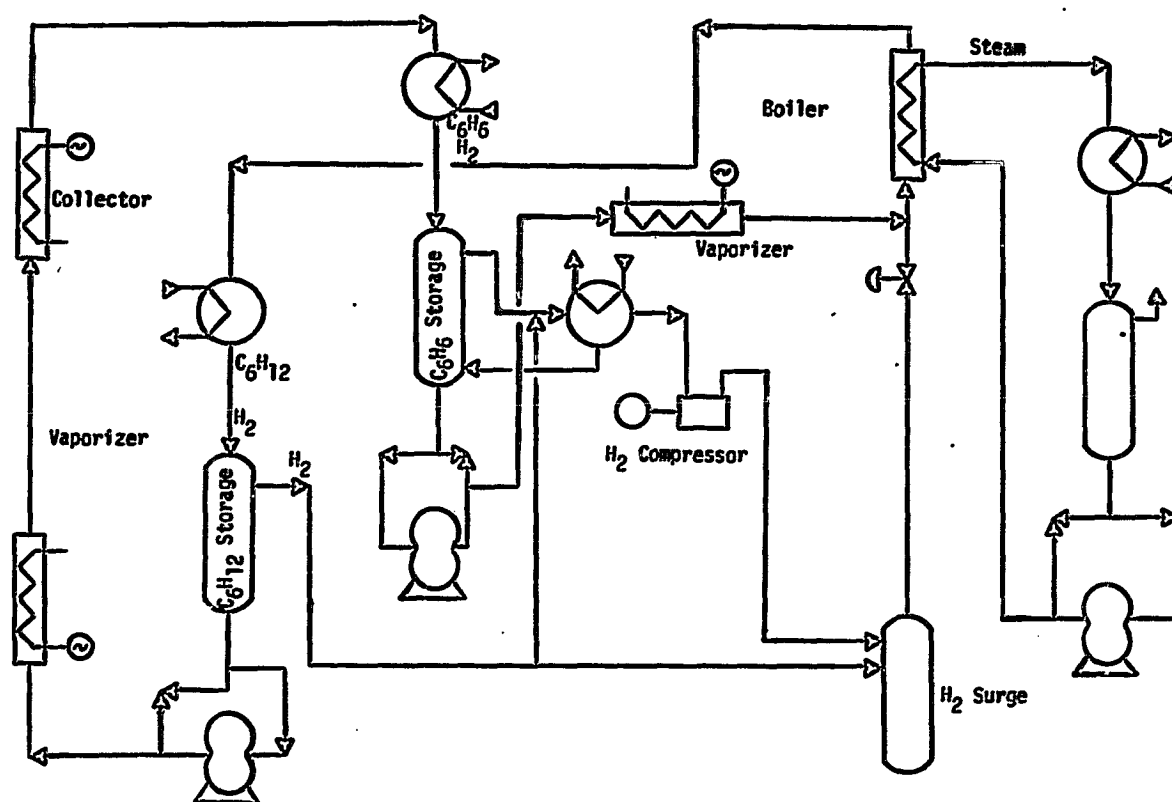


Fig. 5. The experimental flow system for studying long term cycling of the cyclohexane-benzene system

**SYSTEM EVALUATION OF SUPPLEMENTING
NATURAL GAS SUPPLY WITH HYDROGEN**

**W. S. Ku
Public Service Electric and Gas Company
Newark, New Jersey**

Abstract

The production of hydrogen by electrolysis using excess energy available from base-load electric generating units provides one potential means of supplemental future dwindling natural gas supply. Advanced electrolyzer technology now in the research stage was applied for the evaluation. A maximum of 15% volume blending of hydrogen was assumed. No hydrogen storage was applied. The results indicate that electrolytic hydrogen could become economically competitive in the 1990-2000 period with high-cost supplemental natural gas supply.

Introduction

With the natural gas supply picture becoming increasingly critical for future years, alternative technologies are being explored to provide supplemental gas supplies. One such potential means would be to blend hydrogen with natural gas if hydrogen could be economically produced.

Public Service Electric and Gas Company (PSE&G) under a contract with Associated Universities, Inc. and U. S. Energy Research and Development Administration, has completed a system evaluation study to investigate the economic potential of supplementing natural gas with hydrogen produced by electrolysis. The major objectives of the study are:

1. To determine the amounts and associated costs of off-peak electric energy available in typical electric utility systems that could be utilized for producing hydrogen.
2. To determine the economic competitiveness and feasible extent of utilizing electrolytic hydrogen in a "companion" gas utility system.

Study Scope and Guidelines

1. Selected Test Utility Systems - Four electric-gas utility system pairs were selected for the study. These systems are either of a combination company or of two different utilities serving a common territory and represent different geographical regions: A. Mid-Atlantic, B. Midwest, C. Northeast, D. Pacific Coast.
2. Basic Concept of Producing Electrolytic Hydrogen - The principle concept of making hydrogen from electrolysis is to utilize excess energy available from base-load electric generating units during off-peak periods. The base-load units are those with lower fuel costs and are expected to be operating around the clock delivering full-capacity energy output during most of these hours. In future years nuclear and coal-fired steam units are generally classified as base-load generation. The off-peak periods cover those weekday hours from late evening to early morning and most of the hours during weekends when average electric demands are substantially lower.
3. Electrolyzer Technology - Advanced electrolyzer technology, such as the General Electric's solid polymer electrolyzer concept, was considered as the basis for this evaluation. Based on the ERDA guideline, such electrolyzer was assumed to require a capital cost of \$150/kw (1975 dollars), including power conversion

and substation equipment, supervisory control, electric, gas and water connections, and installation. It has an efficiency of 90% and an average life of 20 years.

4. Hydrogen Blending - The companion investigation undertaken by PSE&G for ERDA revealed that with a 10% volume blending no problems are apparent. With a 15 to 20% blending, some modifications of gas burners appear required. For the purpose of this system evaluation study, a more conservative maximum permissible blending level of 15% was used.
5. Hydrogen Storage - One of the ERDA guidelines was not to consider the use of hydrogen storage in this study. Without storage, hydrogen produced electrolytically must be injected directly into the gas distribution system for immediate utilization.
6. Study Period - The period chosen for the study was 1985 through the year 2000.

Electric and Gas System Evaluation

1. Electric Phase

The electric load demand of a utility system varies from hour to hour, day to day, and season to season. Most utility systems now experience its annual peak demands during the summer season. Figures 1 and 2 show respectively the average summer and winter week load curves of a representative electric utility system.

The amount of base-load generating capacity installed will determine the extent of excess energy available from the base-load capacity during off-peak periods. Figures 3 and 4 illustrate this relation. For simplicity the available base-load generation is shown as a common straight line in both figures. The actual available amount of base-load generation in each week is determined by probabilistic analysis taking into account forced and maintenance outages of various units. The excess amounts of base-load energy available each hour can then be determined.

Table 1 shows the amounts of installed base-load capacity, in percent, of the four test systems. Table 2 shows the calculated total excess base-load energy expressed as a percent of total energy produced in that system.

2. Gas Phase

Similarly the gas demand of a utility system also varies continuously. The annual peak demands generally occur in winter. Figures 5 and 6 show respectively the average winter and summer week load curves of a representative gas utility system.

Based on the designated maximum volume blending of 15% hydrogen, the amount of hydrogen that can be absorbed hourly into each test system can be determined. If the selection of the overall electrolyzer capacity is based on the amount of hydrogen that can be absorbed during the minimum gas demand period of the year because of lack of storage, then the actual amounts of blending during other time periods will be substantially less. Tables 3 and 4 show respectively the average percents of hydrogen blending and associated electric energy utilized for the testing systems A and B.

The reason that only the results of two of the four test systems are shown is because the evaluation results of Systems A and B appear to be more meaningful. The other two systems did not provide sufficient future-system data and essentially all their excess base-load energy would be from non-nuclear units as indicated in Table 2.

3. Economic Evaluation

In determining the economic competitiveness of hydrogen supplementation against other forms of supplemental gas supply, the hydrogen cost based on the lowest fuel cost of available excess energy, namely nuclear, should be compared first with the highest-cost supplemental natural gas supply, such as naphtha-derived synthetic natural gas (SNG). Coal-fueled electric energy should be considered next and will increase the volume of hydrogen produced but also the average electric energy cost for producing such hydrogen.

Tables 5 and 6 show respectively the cost comparison between electrolytic hydrogen and supplemental natural gas supply for the test systems A and B. For the Mid-Atlantic system (System A), an annual escalation rate of 4% was applied for both electric system fuel and SNG costs. For the Mid-western system (System B), an escalation rate of 4% was used for electric fuel costs and 7% for natural gas cost.

Summary

1. Adequate amounts of excess electric energy are expected to be available

from base-load generating units of electric utility systems during off-peak periods for producing hydrogen by electrolysis which can be effectively utilized by their companion gas systems. However, the actual availability must take into account such energy uses by other forms of energy storage. Also, economics may justify only the utilization of that portion of available off-peak energy from the lowest fuel-cost units, such as nuclear.

2. The amount of excess energy available from base-load generation is a function of the relative amount of this installed base-load capacity as a percentage of total installed capacity of a system. Generally, this base-load level is in the order of 50 to 60%. With such a level, the excess base-load energy is available during off-peak periods only. On the other hand, if the base-load capacity level is raised to 80% or higher, then certain excess base-load energy would also be available during certain heavy-load time periods, resulting in more electric energy available for making hydrogen during more hours of each day.
3. About 35 to 50% of all excess base-load energy is available on weekends. Therefore without the application of hydrogen storage, a major portion of this electric energy could not be utilized for producing hydrogen.
4. Electrolytic hydrogen may become economically competitive in the 1990-2000 period with SNG on other forms of high-cost supplemental gas supply. Much will depend on:
 - (a) A breakthrough in electrolyzer technology particularly with regard to cost and efficiency,
 - (b) the extent of base-load electric generation in nuclear capacity, and
 - (c) the future cost escalation of SNG or other forms of supplemental gas supply, with respect to the cost escalation of electric generation fuels.

Acknowledgments

The author would like to acknowledge the valuable contributions provided by the following PSE&G personnel who participated in this study: D. C. Nielsen, J. Zemkoski, D. L. Leich, P. Yatchko, J. M. Torres and G. P. Gaebe (formerly with PSE&G).

TABLE 1
BASELOAD CAPACITY MIX
IN PERCENT OF TOTAL INSTALLED CAPACITY

<u>SYSTEM</u>	<u>YEAR</u>	<u>NUCLEAR (%)</u>	<u>COAL (%)</u>	<u>OIL (%)</u>	<u>TOTAL (%)</u>
A	1985	32	16	15	63
	1990	39	13	4	56
	1995	45	11	3	59
	2000	48	9	1	58
B	1985	45	36	0	81
	1990	47	38	0	85
	1995	50	39	0	89
	2000	50	40	0	90
C	1985	34	52	0	86
	1990	49	40	0	89
	1995	*	*	*	*
	2000	*	*	*	*
D	1985	23	6	17	46
	1990	31	11	14	56
	1995	*	*	*	*
	2000	*	*	*	*

*System data unavailable for study

TABLE 2
TOTAL ANNUAL BASE-LOAD OFF-PEAK
SPINNING RESERVE ENERGY

<u>SYSTEM</u>	<u>YEAR</u>	<u>PERCENT OF TOTAL SYSTEM ENERGY REQUIREMENTS</u>	<u>AMOUNT (Gwh)</u>	<u>PERCENT BY TYPE</u>		
				<u>NUCLEAR</u>	<u>COAL</u>	<u>OIL</u>
A	1985	11.4	4,918	0	25	75
	1990	9.5	4,942	13	58	29
	1995	11.4	7,278	28	52	20
	2000	10.1	7,872	40	50	10
B	1985	31.4	34,700	6	94	0
	1990	37.0	54,938	7	93	0
	1995	40.7	81,229	8	92	0
	2000	43.3	116,099	6	94	0
C	1985	31.1	5,285	0	100	0
	1990	41.2	8,530	5	95	0
	1995	*	*	*	*	*
	2000	*	*	*	*	*
D	1985	0.4	461	0	0	100
	1990	2.4	3,405	0	3	97
	1995	*	*	*	*	*
	2000	*	*	*	*	*

*System data unavailable for study

TABLE 3
STATUS OF ELECTROLYTIC HYDROGEN PRODUCED
(MID-ATLANTIC SYSTEM)

<u>YEAR</u>	<u>% BLENDING</u>	<u>ELECTROLYZER LOAD FACTOR %</u>	<u>% OF TOTAL AVAILABLE OFF-PEAK BASE- LOAD ELECTRIC ENERGY USED</u>
1985	1.6	42	7.3
1990	2.0	55	9.7
1995	3.0	60	10.7
2000	2.9	60	10.0

TABLE 4
STATUS OF ELECTROLYTIC HYDROGEN PRODUCED
(MIDWESTERN SYSTEM)

<u>Year</u>	<u>% Blending</u>		<u>Electrolyzer Load Factor %</u>		<u>% of Total Available Off-Peak Base-Load Electric Energy Used</u>	
			<u>*</u>	<u>**</u>		
1985	1.7	4.6	37	100	1.8	5.0
1990	2.1	4.6	45	100	1.4	3.2
1995	2.3	4.6	50	100	1.1	2.2
2000	2.2	4.6	48	100	0.7	1.5

* Utilizes nuclear only
** Utilizes nuclear and coal

TABLE 5

**COST COMPARISON BETWEEN ELECTROLYTIC
HYDROGEN AND SYNTHETIC NATURAL GAS
(MID-ATLANTIC SYSTEM)**

<u>PRODUCTION FACILITY</u>	<u>HYDROGEN AND SNG COSTS (\$/DEKATHERM)</u>			
	<u>1985</u>	<u>1990</u>	<u>1995</u>	<u>2000</u>
Electrolyzer (35% to 65% Load Factor)	13.25	12.75	13.50	14.75
SNG Plant (50% Load Factor)	7.30	9.30	12.00	15.50

1 Dekatherm = 1 million Btu

TABLE 6

**COST COMPARISON BETWEEN ELECTROLYTIC HYDROGEN AND SUPPLEMENTAL
NATURAL GAS SUPPLY
(MID-WESTERN SYSTEM)**

<u>Production Facility</u>	<u>Hydrogen and Natural Gas Costs (\$/Dekatherm)</u>			
	<u>1985</u>	<u>1990</u>	<u>1995</u>	<u>2000</u>
Electrolyzer (35 to 50%* Load Factor)	8.80	8.60	9.40	10.90
(100 Load Factor**)	7.20	8.20	9.90	12.50
Supplemental Natural Gas Supply	7.40	11.00	16.90	22.50

1 Dekatherm - 1 million Btu

*Utilizes nuclear only. The load factor increases from about 35% in 1985 to about 50% by 1995-2000.

**Utilizes nuclear and coal

FIGURE 1. SUMMER TYPICAL ELECTRIC LOAD CURVE

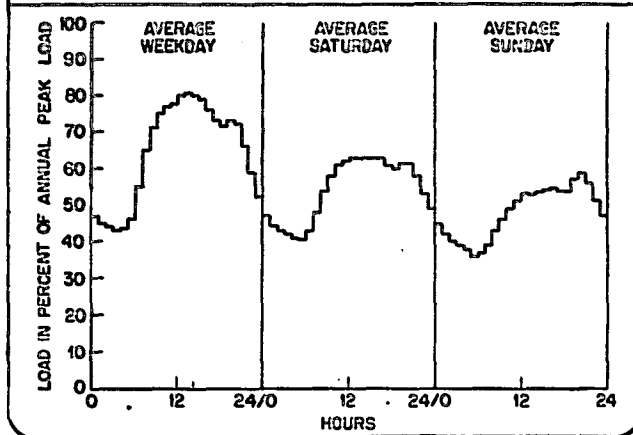


FIGURE 2. WINTER TYPICAL ELECTRIC LOAD CURVE

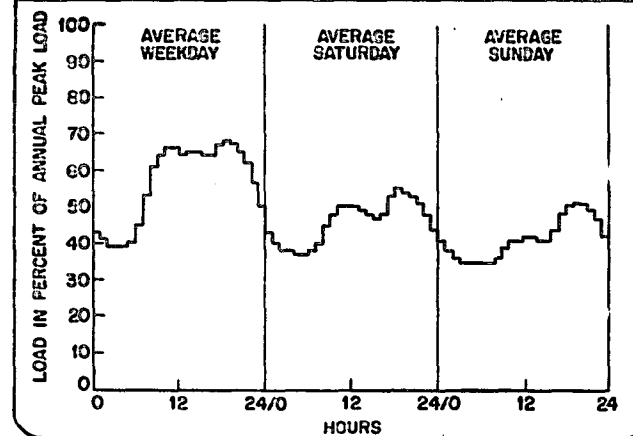


FIGURE 3. SUMMER TYPICAL ELECTRIC LOAD CURVE
(WITH EXCESS OFF-PEAK ENERGY SHOWN)

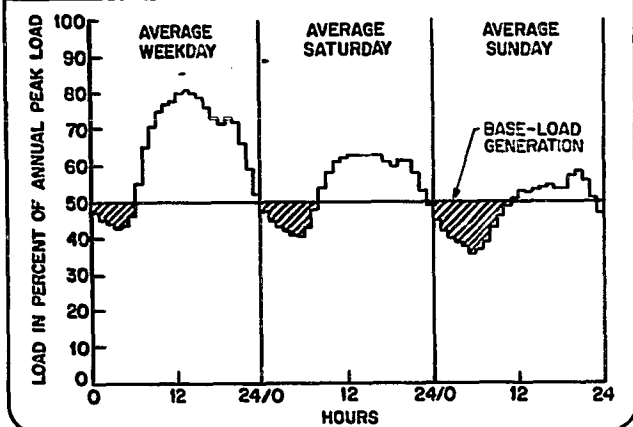


FIGURE 4. WINTER TYPICAL ELECTRIC LOAD CURVE
(WITH EXCESS OFF-PEAK ENERGY SHOWN)

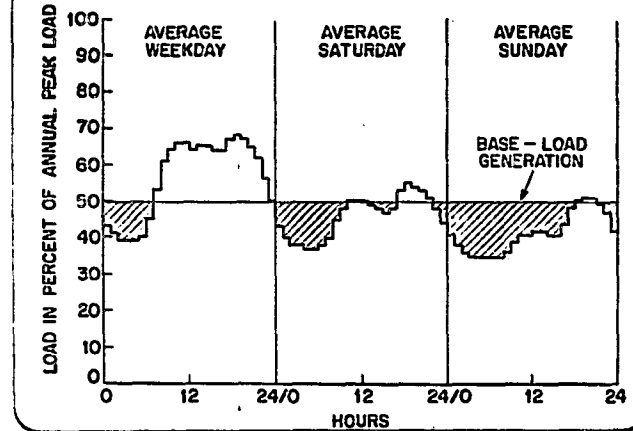


FIGURE 5. WINTER TYPICAL GAS SENDOUT

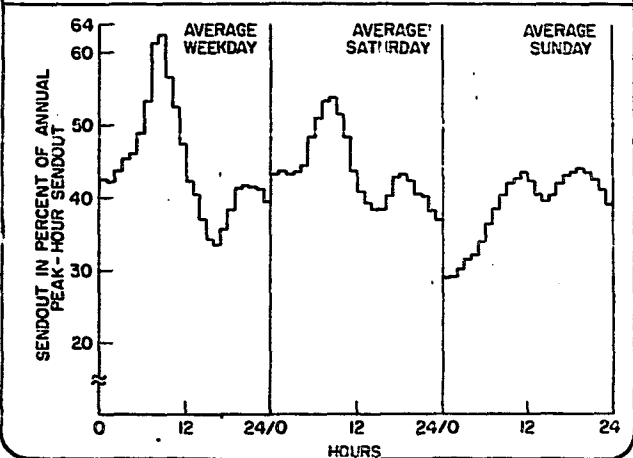
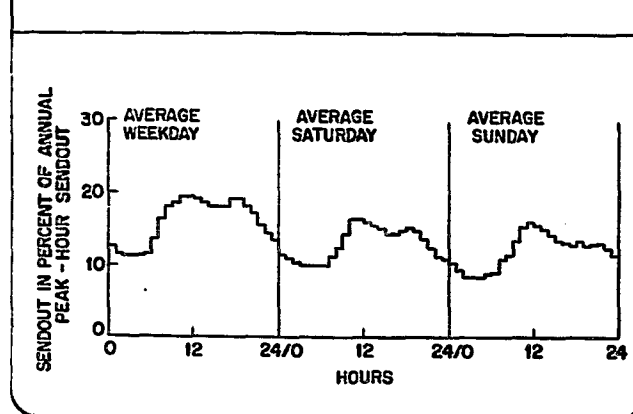


FIGURE 6. SUMMER TYPICAL GAS SENDOUT



**HYDROGEN FROM FALLING WATER:
ASSESSMENT OF THE RESOURCE
AND CONCEPTUAL DESIGN PHASE**

**William J. D. Escher
Institute of Gas Technology
Chicago, IL
and**

**James P. Palumbo
Pennsylvania Gas & Water Company
Wilkes-Barre, PA**

Abstract

A unique opportunity to develop a supplemental solar-hydrogen gas energy system presents itself in the many small, presently unused hydropower facilities in the United States. As opposed to generating conventional electricity, turbine-generators would be directly coupled to water electrolyzers for the production of hydrogen and oxygen. There appear to be significant advantages to this approach from the standpoint of delivering energy via a distribution system to the end user.

At present, an assessment of the falling water resource in terms of hydrogen energy potential is being conducted for the U. S. Northeastern states. Conceptual design efforts on the energy conversion station are also being carried out. If these initial results are favorable, the construction of an operating falling water to hydrogen energy conversion facility would be in order. Such a station might serve as a flexible R&D facility for further development of this approach at achieving new energy supplies from inexhaustible resources.

Introduction

In recent months, there has been expressed a great deal of interest in the potential of harnessing presently undeveloped or unused hydropower as a clean, domestically-available source of energy (1,2).

A special 3-month study was carried out at the request of the Administration by the Corps of Engineers which estimated that 159.3 kWh of hydropower annually is potentially available from such sites (3). Additionally, assessments have been, and are being made, at the state level.

Emphasis so far has been on generating conventional electricity, i.e. synchronized 60 Hz alternating current compatible with the electric utility grid.

Another approach, under investigation by the Institute of Gas Technology and Pennsylvania Gas & Water Company, sponsored by the U.S. Department of Energy, provides for the conversion of the work of falling water to hydrogen using water electrolysis. Because hydrogen is storable and, as a chemical energy form, flexibly applied to many use sectors, this concept may prove advantageous in capitalizing on the availability of such hydropower resources as a complement to conventional electricity generation.

Objective of the IGT/PG&W Study

Presently IGT and PG&W are carrying out a 4-month "Phase 0" step which is proposed to be followed up with further efforts, potentially leading to the development of a pilot facility useful for research and development of hydrogen from falling water.

The purposes of the present effort are primarily two-fold:

- (1) To assess the total undeveloped resource in terms of hydrogen energy production in the 9 Northeastern states of the U.S.
- (2) To a "concept-level", characterize in technical and economic terms the hardware systems which will be required for the production of hydrogen from small falling water resources.

The results of the effort are scheduled to be reported early in Calendar Year 1978.

Technical Concept

The essence of the technical concept being pursued is shown in the functional block diagram of Figure 1.

As shown in the figure, the energy of falling water (which is a function of water mass flow rate and differential pressure or head) is extracted in a water turbine. The resulting shaftpower operates an electrical generator, which, however, may be rather different from that used in conventional hydropower systems since it is used to power an electrolyzer as opposed to being fed into the utility grid. For example, it could be advantageous to use a dc generator which might be directly interfaced with the electrolyzer. Such might significantly reduce the equipment cost as well as avoid efficiency losses in rectification and power conditioning of ac power.

Feedwater provided to the electrolyzer, and the power input, produce hydrogen and oxygen gas. The hydrogen is shown to be delivered to the energy using sectors, and the oxygen as a coproduct.

In the particular example shown, in which the falling water derives from an upper reservoir and is to be used for municipal water supplies, such ultimate usage of the water is indicated. In such systems, which are illustrated by a number of reservoirs in the PG&W service area, the pressure "energy" is lost, sometimes intentionally in pressure regulator stations.

As to end-use of the hydrogen, a number of possibilities present themselves. Generally, there has been emphasis on "local use" of the energy product:

Natural Gas Supplement

Straight Hydrogen

Industrial gas use (non-fuel)
Direct fuel gas for residences
" " " " industries
Transportation fuel

Project Status of 1 November 1977

Work to date has focused mainly on the assessment of the falling water resource in the Northeast, with PG&W taking the lead. Telephone contacts and meetings have been held with representatives in all the states being canvassed. Documentation, not in hand at the beginning of the project (when it was first proposed), is being gathered from both federal and state organizations. Generally, more information than first supposed is proving to be available. Consequently, emphasis is now being applied to the cataloging step. IGT is providing its electronic data processing facilities to this task.

IGT, assisted by PG&W who carried out initial contacts, is surveying the applicable equipment manufacturers in support of the conceptual design.

Preliminary Summary of Findings

Following are some of the Project's initial findings:

- (1) The data-base on the falling water resource is fairly expansive, but definitely of uneven quality and quantity from region to region.
- (2) Electronic data processing appears to be an appropriate way to catalog the data so that it will be readily available for specific use.
- (3) As anticipated, we have found no manufacturers of equipment oriented to this application; this suggests the need for a special systems integration effort in which component suppliers are consulted in an iterative manner.
- (4) There do appear to be significant advantages for hydrogen (vis-a-vis electricity) in

tying the small hydro-energy resources into the distribution system, primarily a consequence of hydrogen's storability.

These preliminary findings are being followed up at present with results to be presented in the Project report early in Calendar Year 1978.

Reference

1. Lilienthal, D. E., "Energy from Waters," New York Times, December 1976
2. Christiansen, D., "Water Over the Dam," IEEE Spectrum 14, No. 2, February 1977
3. Anon., "Estimate of National Hydroelectric Power Potential at Existing Dams," U.S. Army Corps of Engineers, July 20, 1977

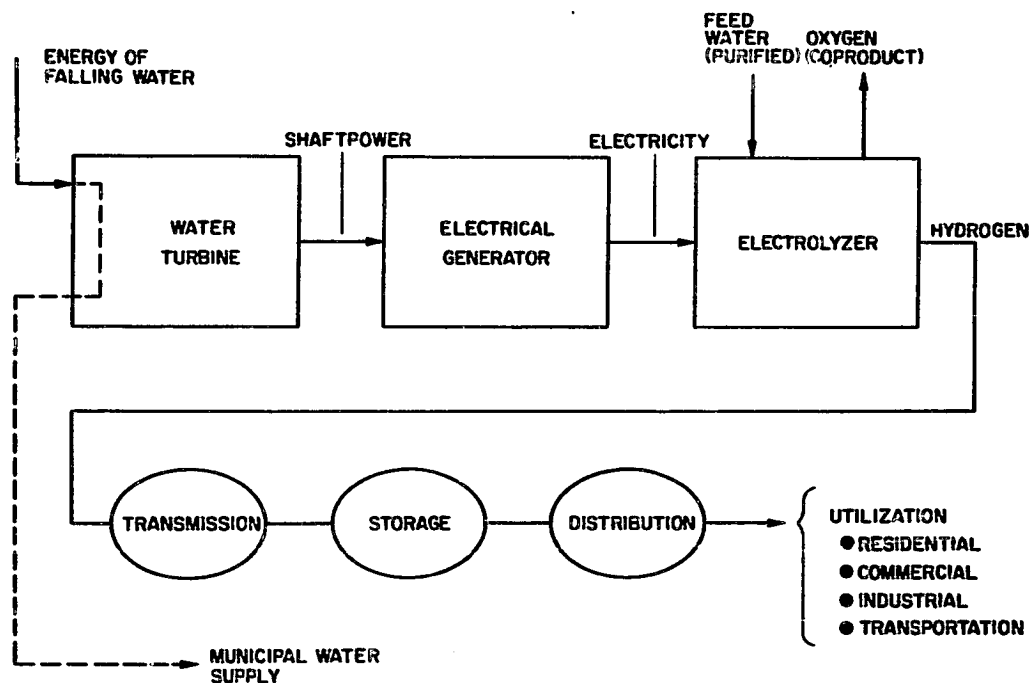


Figure 1. SYSTEM TECHNICAL CONCEPT

HYDROGEN ENGINE/STORAGE SYSTEM -- APPLICATION STUDIES

A. M. Karaba and T. J. Pearoall

Teledyne Continental Motors
Muskegon, Michigan 49442

ABSTRACT

The study addressed the unique problems associated with the storage and use of hydrogen. Criteria were established for evaluating potential applications, and a near-term candidate was selected and performance predictions were made. A hydride bed design was proposed, and engine modifications were outlined.

The costs to own and operate a hydrogen fueled engine were analyzed, and it was concluded that early applications will require incentives other than economic. Several practical problems need to be addressed now. An expansion of the present effort, including development of both components and integrated systems, was recommended.

PROGRAM OBJECTIVE

IDENTIFY AND DEFINE

**AN ATTRACTIVE EARLY VEHICLE APPLICATION FOR A
METAL-HYDRIDE STORAGE SYSTEM COUPLED TO A
HYDROGEN FUELED PISTON ENGINE.**

Contract No. 412123-S

Duration: July 1977 to November 1977

Contracting Organization: Brookhaven National Laboratories

Contractor: Teledyne Continental Motors General Products Division

Project Officer: Mr. Matt Rosso, Jr.

Principal Investigators: Messrs. A.M. Karaba and T.J. Pearsall

PROGRAM ELEMENTS

1. REVIEW BACKGROUND INFORMATION

- A. ENGINE TYPES**
- B. HYDRIDE TYPES**
- C. SAFETY ASPECTS**

2. ESTABLISH FUELING REQUIREMENTS

3. IDENTIFY AN EARLIEST APPLICATION

The study addressed practical methods of dealing with the unique problems of the storage, engine, and safety aspects of a near term installation.

STUDY RESULTS (GENERAL)

1. NEAR TERM APPLICATIONS MUST RELY ON LOCALLY GENERATED HYDROGEN
2. ELECTROLYTICALLY GENERATED HYDROGEN IS CONSIDERED THE ONLY PRACTICAL NEAR TERM SYSTEM
3. APPLICATIONS THAT CAN BENEFIT FROM THE LOWER INDUSTRIAL ELECTRICAL RATES APPEAR MOST ATTRACTIVE
4. INCENTIVES OTHER THAN ECONOMIC ONES WILL ESTABLISH THE FIRST SERIOUS APPLICATIONS

Teledyne Continental Motors General Products Division concludes that no near term application can rely on a low cost hydrogen source. Local generation electrolytically would favor industrial plants where electrical rates are typically 60 to 80 percent of residential rates. The higher fuel costs of H₂ mean that motivations, such as low emissions must provide the incentive for conversion.

EVALUATION OF CANDIDATES

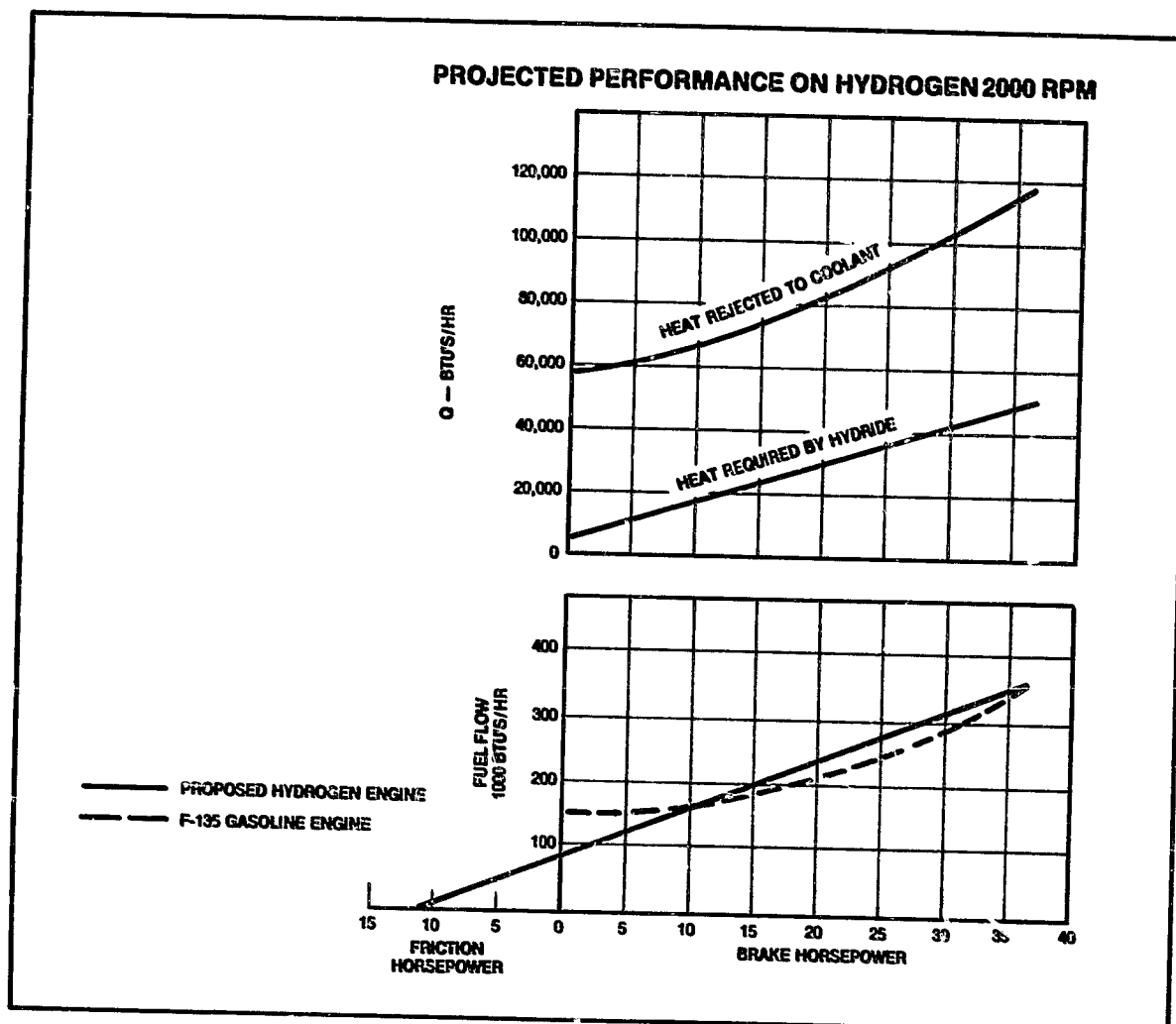
1.	2.	3.	4.	5.
WEIGHT IS AN ADVANTAGE	ECONOMIC OR ENVIRONMENTAL BENEFIT DERIVED	GOOD FLEET SIZE	CONSISTENT WITH CENTRAL FUEL STATION	DIFFUSION SPACE AVAILABLE
SWEEPERS LOADERS AGRICULTURAL TRACTORS RACK HOES ROLLERS SCRAPERS	SWEEPERS (IN-PLANT)		SWEEPERS (IN-PLANT)	AGRICULTURAL TRACTORS BACK HOES ROLLERS SCRAPERS
LIFT TRUCKS CRANES SHOVELS	LIFT TRUCKS	LIFT TRUCKS	LIFT TRUCKS	CRANES SHOVELS
OFF-HIGHWAY EQUIPMENT	DELIVERY VANS MAIL TRUCKS	DELIVERY VANS MAIL TRUCKS	DELIVERY VANS MAIL TRUCKS	OFF-HIGHWAY EQUIPMENT DELIVERY VANS MAIL TRUCKS
BULLDOZERS	TAXI CABS GOLF CARTS URBAN CAR URBAN BUS	TAXI CABS URBAN BUS	TAXI CABS GOLF CARTS URBAN BUS	BULLDOZERS TAXI CABS GOLF CARTS URBAN CAR URBAN BUS

Teledyne Continental Motors General Products Division established five criteria for evaluating potential applications. No candidate met all five criteria. The diffusion space criteria was weighted low because of the "enclosed" storage and control system to be employed. On that basis, the industrial lift truck appeared the most attractive.

INDUSTRIAL TRUCK SELECTION

- A. OPERATIONAL HOURS CAN BE ACCUMULATED RAPIDLY**
- B. OPERATION CAN BE CONTROLLED**
- C. CHANGES OR MODIFICATIONS CAN BE EASILY AND QUICKLY APPLIED**
- D. SKILLED MAINTENANCE PERSONNEL ARE ALWAYS CLOSE AT HAND**

In addition to the practical aspects identified as necessary to justify any application, considerations that relate to the technical and information gathering aspects of the program recommend an industrial application.



A 2000 rpm fuel hook comparing a 135 in 3 conventionally carbureted gasoline engine is shown compared to a hydrogen fueled engine of 20 percent more displacement to provide comparable horsepower.

The unthrottled hydrogen fueled engine can be expected to exhibit fuel flow versus horsepower similar to an unthrottled diesel engine. The obvious point to note is the significant reduction in required fuel energy at light load.

The figure also illustrates the heat rejection to the coolant as a function of load as compared to the heat required by the hydride bed for release of the fuel.

INDUSTRIAL TRUCK OPERATING MODES

MODE	RPM	PERCENT POWER	PERCENT TIME	BTU'S/HOUR	
				GASOLINE	H ₂
IDLE	600	0	40%	19,000	9,500
FULL POWER	2800	100%	5%	20,900	20,900
DECELERATION	2000/600	0	5%	2,400	1,200
LIGHT LOAD	2000	10%	25%	39,000	29,250
LIGHT LOAD	2000	40%	25%	45,000	48,750
				126,300	109,600

In quantifying fuel required for the hydrogen fueled vehicle we made use of the fuel hooks described in the previous chart.

Overall thermal efficiency of the gasoline truck is 14 percent with the hydrogen truck at 16 percent.

Vehicles employed in more rigorous service could be less attractive from a thermal efficiency point while light load applications with a high percentage of standby idle and light load could be more attractive.

HYDROGEN STORAGE

1. BED IS IMMERSSED IN ENGINE COOLANT AND RELEASE IS CONTROLLED BY COOLANT FLOW MODULATION
2. TUBE DIAMETER IS SMALL — APPROXIMATELY 3 INCHES I.D. FOR IMPROVED TRANSIENT PERFORMANCE
3. "START UP" BED IS EXHAUST HEAT ACTIVATED
4. EXTRUDED ALUMINUM HYDRIDE STORAGE VESSELS APPEAR MOST ATTRACTIVE
5. FeTiMn MATERIAL APPEARS MOST ATTRACTIVE BECAUSE OF INCREASED USABLE CAPACITY

The totally immersed bed proposed offers a practical system for insuring good heat transfer. Usable hydrogen in the bed was projected to be 1.4 percent by weight.

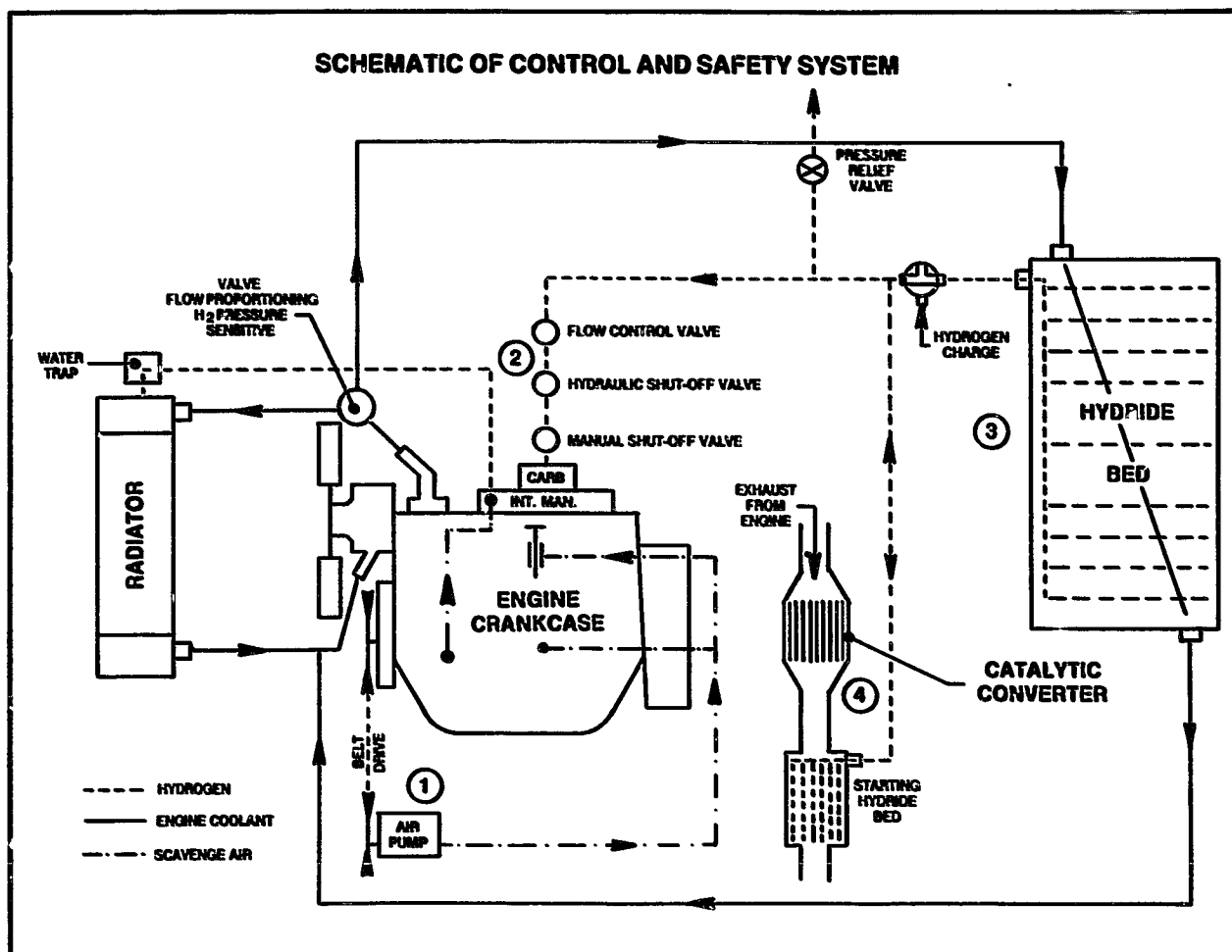
Cold start-up problems are addressed with an exhaust heated bed estimated to be 5 percent of the total. Cold start-ups will require a warm up period to bring the entire engine and hydride bed system up to temperature.

ENGINE CHANGES

- 1. ALUMINUM HEAD AND PISTON**
- 2. IMPROVED OIL CONTROL**
- 3. COOLED EXHAUST VALVE**
- 4. POSITIVE CRANKCASE VENTILATION**
- 5. EXHAUST DILUTION WITH CATALYST**

Engine changes are proposed to address these problems:

- 1. Both intake and exhaust backfire.*
- 2. Worn engines developing ignitable mixtures in the crankcase.*
- 3. Elimination of free hydrogen in exhaust.*



Significant features of the control system include:

1. An air pump employed to:

- (a) Cool the exhaust valves
- (b) Provide positive crankcase ventilation
- (c) Exhaust dilution

2. Fuel to the engine — limited by:

- (a) Ignition switch for positive shut-off
- (b) Oil pressure switch limits fuel delivery until cranking speed is achieved
- (c) Fuel flow modulation without throttling

3. Hydride bed controls include:

- (a) Flow control modulated by hydrogen pressure
- (b) Venting of the cooling system into the intake manifold insuring a hydrogen leak from the bed is routed thru the engine
- (c) Fuel shut-off does not stop ignition system which continues should a bed leak exist

4. Exhaust system incorporating:

A conventional catalytic converter with over temperature warning to indicate a defective ignition system.

COST SUMMARY (\$/YEAR)

	<u>GASOLINE</u>	<u>ELECTRIC TRUCK</u>	<u>LPG TRUCK</u>	<u>H₂ POWER [ELEC]</u>	<u>H₂ POWER [PIPELINE]</u>
COST TO OWN	1,669	3,417	1,739	2,247	2,247
COST TO OPERATE	1,822	759	3,220	5,534	1,922 **
COST TO MAINTAIN	2,529	1,877	2,529	2,529	2,529
TOTAL DOLLARS/YEAR	6,020	6,053	7,488	10,310	6,698

* BASED ON A 7.5 YEAR LIFE

** BASED ON H₂ COST OF \$5.00/10⁶ BTU'S

The economics of an industrial truck operating in a normal environment are strongly related to fuel cost.

Early applications that will not have the low fuel cost advantages ultimately projected and will require incentives other than economic.

CONCLUSIONS

1. SEVERAL APPLICATIONS FOR HYDRIDE STORAGE COUPLED TO A HYDROGEN FUELED PISTON ENGINE ARE ATTRACTIVE
2. THE ECONOMICS OF FUEL PRODUCTION COST RECOMMEND FIRST APPLICATIONS IN THE INDUSTRIAL FIELD WHERE LOWER ELECTRICAL COSTS AND ENVIRONMENTAL CONSIDERATIONS ARE BOTH ATTRACTIVE
3. A PRACTICAL AND SAFE SYSTEM CAN BE PUT INTO SERVICE TODAY

Engine/hydride systems have several practical problems that need to be addressed now. The evolution of practical systems capable of long term, trouble free and safe operation, requires performance of systems in real environments. An expansion of the present effort is recommended. That expansion should include both component and integrated system applications.

BLANK PAGE

SESSION VI
NATURAL GAS SUPPLEMENTATION

NATURAL GAS SUPPLEMENTATION WITH HYDROGEN
C. R. Guerra, J. E. Griffith, K. Kelton, and D. C. Nielsen
Public Service Electric and Gas Company

HYDROGEN AS A MID-TERM GASEOUS FUEL SUPPLEMENT BY
BLENDING WITH NATURAL GAS
G. F. Steinmetz
Baltimore Gas and Electric Company

NATURAL GAS SUPPLEMENTATION
WITH HYDROGEN

C. R. Guerra, J. E. Griffith, K. Kelton and D. C. Nielsen
Public Service Electric and Gas Company
80 Park Place
Newark, New Jersey 07101

Abstract

The potential supplementation of natural gas with hydrogen is being evaluated. The studies include: (1) combustion tests of gas blends in burners and appliances, (2) computation of capacity of a distribution network and system adjustments to deliver gas blends and (3) measurement of gas leakage from prototype joints of mains removed from a gas distribution grid.

The results show that main burners can burn blends with up to 20-25% hydrogen in natural gas, but target pilots limit the hydrogen concentration to 6-11%. After modification of pilot orifice or increase in gas supply pressure, blends with up to 20% hydrogen were found satisfactory for use in most burners and appliances. The flow studies indicate that natural gas with up to 20% hydrogen could be readily adapted to utility operations at the gas pressure and flows used in the distribution, utilization and service subsystems of the grid. The metering station appears to be the most suitable site for introducing hydrogen into the distribution system. Measurements of gas leakage from joints containing blends of hydrogen with natural gas are currently under way.

Introduction

The supplementation of natural gas with hydrogen is an attractive concept because, as a gas, hydrogen is readily adaptable to existing utility distribution systems and to the utilization equipment owned by gas users. Gas TSD pipeline networks and customer appliances and equipment represent, as an aggregate, a large investment with a productive life and usefulness highly dependent on the availability of natural gas and certain gas substitutes and supplements.

Hydrogen is pre-eminent as a natural gas supplement because it can be derived from various primary energy sources ranging from fossil to nonfossil sources, including fusion and solar energy. Gradual supplementation of natural gas with hydrogen is expected to be a key element in the smooth transition from fossil fuel dependence to the nonfossil economy of the future.

Under contract with ERDA and with funding support from Public Service Electric and Gas Company (PSE&G), various aspects concerning the delivery of blends of hydrogen with natural gas, via existing utility systems, are being studied. The program focuses on the following: (1) the limitations which the use of hydrogen blends may bring about in customer appliances and equipment, (2) the operation of a utility grid distributing hydrogen blends, (3) the selection of suitable points for injecting hydrogen into the distribution system, (4) the effectiveness in hydrogen containment by typical components of a utility grid and (5) certain nontechnical aspects related to safety and regulatory requirements.

Combustion Tests of Blends in Burners and Appliances

The objective of this investigation was to determine the maximum amount of hydrogen that could be blended in natural gas, maintaining the reliability and efficiency of typical utilization devices with minimal or no adjustment or conversion.

Although interchangeability criteria, which may be calculated from the gas analysis, are available, these methods are not mutually consistent and were developed over 20 years ago. Since that time, new varieties of burners have been developed, and others have been modified, and burners which were critical are no longer used. In addition, use of these criteria to predict ignition or extinction noise; flashback on rapid turn-down or short-cycling; faulty ignition performance, with either thermal elements or flash tubes; and unfamiliar gas odors have not been successful. The preferred method of assessing interchangeability is to (1) determine the possible interchangeable

mixtures using established criteria, (2) set up in a laboratory selected burners/appliances representative of the most critical types served and (3) operate the proposed mixtures on the critical burners/appliances.

A preliminary study, using Weaver Indexes of interchangeability, indicated that mixtures containing up to approximately 20% hydrogen should be interchangeable with natural gas. Of the five conditions which must be met for satisfactory interchangeability: (1) little change in burner input, (2) no lifting of flames, (3) no flashback of flames, (4) no excessive yellow tipping of flames, (5) no incomplete combustion, it appeared that these mixtures would be critical with respect to flashback. Laboratory tests were undertaken to substantiate the preliminary finding.

Test Methods and Equipment

Test gases were prepared by mixing natural gas and hydrogen in cylinders and the gas blends analyzed. Each test burner was adjusted on natural gas to obtain proper input and the best possible flame characteristics. The following parameters, where applicable, were then evaluated with natural gas and the substitute mixtures of natural gas and hydrogen:

1. Gas rate (input)
2. Inner cone height
3. Primary aeration
4. Occurrence of yellow-tipping
5. Thermocouple output
6. Occurrence of flashback
 - a. under steady state conditions
 - b. under modulating conditions
 - c. on ignition
 - d. on turndown
 - e. on extinction
 - f. on short cycling
7. Occurrence of lifting
8. Noise of extinction
9. Incomplete combustion

Where adjustment of the primary air was provided on burners, the above observations were also made with hard and soft flame adjustments.

The test equipment used in this investigation consisted of 11 pilot burners, 13 main burners, and 10 appliances. Tables 1, 2 and 3 summarize the type of gas utilization equipment tested.

Table 1
Pilot Burners Tested

<u>No.</u>	<u>Burner Type</u>	<u>Use</u>	<u>Safety Type</u>	<u>Input - Btu/Hr</u>
P 1	Primary Aerated	Boiler, Furnace	Thermocouple	1,505
P 2	Incinerating	Boiler, Furnace	Differential Expansion	742
P 3	Primary Aerated	Boiler, Furnace	Differential Expansion	1,705
P 4	Non-Aerated	Range Oven	Liquid Expansion	632
P 5	Non-Aerated	Range Oven	Liquid Expansion	351
P 6	Non-Aerated	Range Top	---	110
P 7	Target	Boiler, Furnace	Thermopile	1,753
P 8	Target	Boiler, Furnace	Thermocouple	912
P 9	Target	Boiler, Furnace	Thermocouple	852
P 10	Target	Boiler, Furnace	Thermocouple	740
P 11	Target	Water Heater	Thermocouple	833

Table 2
Main Burners Tested

<u>No.</u>	<u>Burner Type</u>	<u>Material</u>	<u>Use</u>	<u>Test Input - Btu/Hr</u>	<u>Rated Input - Btu/Hr</u>
B 1	Ribbon	Cast Iron	Boiler	18,878	20,000
B 2	Ribbon	Pressed Steel	Furnace	25,256	25,000
B 3	Drilled Port	Cast Iron	Boiler	76,339	75,000
B 4	Drilled Port	Pressed Steel	Water Heater	40,120	40,000
B 5	Drilled Port	Cast Iron	Water Heater	18,765	18,000
B 6	Slotted Port	Pressed Steel	Water Heater	40,120	40,000
B 7	Slotted Port	Pressed Steel	Furnace	24,332	25,000
B 8	Luminous Flame	Aluminum Alloy	Room Heater	32,413	30,000
B 9	Luminous Flame	Aluminum Alloy	Room Heater	45,711	45,000
B 10	Drilled Port	Cast Iron	Range Top	14,262	12,000
B 11	Slotted	Pressed Steel	Air Conditioner	18,697	18,000
B 12	Single Port	Pressed Steel	Clothes Dryer	28,074	25,000
B 13	Target	Pressed Steel	Clothes Dryer	25,109	25,000

Table 3
Appliances Tested

<u>No.</u>	<u>Appliance</u>	<u>Burner Type</u>	<u>Burner Material</u>	<u>Test Input - Btu/Hr</u>	<u>Rated Input - Btu/Hr</u>
A 1	Boiler	Single Port	Cast Iron	131,293	130,000
A 2	Furnace	Slotted Port	Pressed Steel	79,976	80,000
A 3	Water Heater	Drilled Port	Cast Iron	37,913	36,000
A 4	Furnace	Single Port	Cast Iron	70,712	75,000
A 5	Range Oven	Drilled Port	Cast Iron	18,599	16,000
A 6	Range Top	Slotted Port	Pressed Steel	10,152	12,000
A 7	Room Heater	Slotted Port	Cast Iron	20,839	20,000
A 8	Range Oven	Slotted Port	Pressed Steel	18,599	19,000
A 9	Range Top	Slotted Port	Pressed Steel	10,152	10,000
A 10	Clothes Dryer	Single Port	Pressed Steel	28,269	30,000

Conclusions

1. Gas blends containing more than 6-11% hydrogen (by volume) are the limiting mixtures for target type pilot burners.
2. Gas blends containing more than 20-22% hydrogen are the limiting mixtures for main burners operating in the open.
3. Gas blends containing more than 22-25% hydrogen are the limiting mixtures for main burners tested in appliances.
4. Modification of the orifice in target pilots or increasing the supply pressure to a minimum of seven inches water column will permit the use of gas blends with 20% hydrogen.
5. The limiting conditions result from the tendency of target type pilot burner flames to burn back at the orifice and not above it as designed, resulting in reduced thermocouple output.
6. Main burner performance was limited by flashback under turn down conditions with a tendency to noise when the flame was turned off.
7. Minor changes in burner adjustment such as adjustment of primary air has little effect on the amount of hydrogen which can be satisfactorily utilized.
8. Although no tests were performed on industrial equipment, the limiting percentages of hydrogen found for residential equipment should operate satisfactorily on industrial equipment because it is readily capable of adjustment to meet variations in gas composition. Some industries, such as glass, would probably welcome the addition of hydrogen to natural gas since a more clearly defined sharp flame results.
9. The Weaver Indexes of interchangeability do not accurately predict the interchangeability of hydrogen and natural gas mixtures. Additional work needs to be undertaken to modify these indexes to arrive at a method which is universally applicable.
10. A statistical analysis of the number of types of burners in use needs to be undertaken so that accurate predictions can be made as to the costs of conversion, and the extent of the problems which may occur with various substitute gases.

Determination of Gas Distribution System Flows

This study examines the ability of a typical utility distribution system to deliver hydrogen while conforming to the pressure limitations of a system designed for natural gas. Natural gas is distributed in the U.S. today by means of a well integrated network of transmission lines operated by pipeline companies and by the distribution systems of hundreds of utilities which carry the gas to the ultimate user. The moving force which causes the gas to flow from wellhead to customer is the difference in the pressure of the gas from one point in the system to another. Different gases, since they have different characteristics such as heating value and specific gravity, require different pressure differentials for the delivery of an equivalent amount of energy.

Methodology

The flow of gas in a pipe segment can be computed by well known flow formulae which give rate of gas flow (Q) as a function of gas pressure differential (P or h), specific gravity of the gas (S), length of pipe segment (L), and a factor (C) which takes into account pipe diameter and friction. Operating personnel rely on different formulae according to the gas pressure in the mains.

For intermediate pressures (1 psig to 60 psig)

$$Q = C \sqrt{\frac{P_1^2 - P_2^2}{SL}}$$

For utilization pressures (below 1 psig)

$$Q = C \sqrt{\frac{h_1 - h_2}{SL}}$$

Computing the flow in a given pipe for different types of gases is relatively simple; however, flow computations for complicated networks of mains such as those common in gas distribution systems can be quite tedious and time consuming. For this reason, PSE&G commonly conducts network studies on a Univac 1106 Digital Computer.

Table 4 lists the principal elements of the natural gas T&D system from the wellhead to the customer's appliance. In the network studies, two subsystems of primary concern with regard to the flow of gas blends were examined in detail:

(1) a distribution pressure subsystem involving a large PSE&G feeder main network and (2) a utilization pressure subsystem involving a medium sized PSE&G grid. Network analyses were carried out for 100% natural gas at peak load conditions and for blends containing 10% and 20% hydrogen at peak load conditions. Comparisons of the results were made to determine the system modifications needed to carry the different gas blends. The service pressure subsystem was only briefly examined because it is expected that excess capacity is available to accommodate the flow of gas blends.

Table 4

Principal Elements of the
Natural Gas T&D Network

Gas Well
Pumping Station
Underground Storage
Transmission Line
Metering Station
High or Medium Pressure Feeder Main
Distribution Regulator
Utilization Pressure Main
Service Main
Service Regulator
Customer Meter
Customer Line
Customer Appliance or Equipment

Distribution Pressure Subsystem

The network studied is made up of 300 miles of feeder mains ranging in size from 2" to 36". Approximately 142,000 customers in an area of 421 square miles are served by this system which receives gas from two meter stations and a regulating station. The estimated consumption of these 142,000 customers during the maximum hour of a zero degree day (winter of 1976/77) is about 9×10^6 cubic feet per hour of natural gas. The System is designed for 60 psig with a previous maximum operating pressure of 35 psig. It must operate at a maximum of 35 psig, unless it is uprated according to DOT (Department of Transportation) Operating Procedures. In accordance with PSE&G design criteria concerning minimum pressures, it can have no pressure below 3 psig.

If the flow studies show that the load on a zero degree day maximum hour results in pressures lower than the minimum allowable, then modifications of some type must be made to the system. These modifications could consist of one or more of the following:

a. Installing additional feeder mains at key points of the system to increase load carrying capacity.

b. Install additional supply points to the system.

c. Uprate the system to operate at higher pressures. Uprating consists of raising the pressure in stages and conducting extensive leakage tests at each stage. In some cases, some system components must be replaced with higher rated components before uprating begins. Uprating costs can vary widely from system to system, but generally uprating is the most economic method of correcting pressure problems.

Utilization Pressure Subsystem

The network chosen for computer analysis consists of about 18,000 feet of 3", 4", 6", and 8" cast-iron and plastic mains. There are 383 customers served by this system and most of them use gas for space heating. Gas is fed into this system from two distribution regulators. The estimated consumption of this system during the maximum hour of a zero degree day (winter of 1976/77) was about 29.4×10^3 cubic feet per hour of natural gas. The design criteria which must be met for this system is that the pressure at the lowest point cannot be below 4.2" water column, and the outlet pressure at the distribution regulator cannot exceed 7.5 inches water column under normal circumstances.

If the flow studies show that the load on a zero degree day maximum hour with maximum input pressures results in pressures at any point lower than the minimum allowable, then modifications of some type must be made to the system. These could consist of one or more of the following:

a. Increasing main sizes at key points in the system to increase load carrying capacity.

b. Installing additional distribution regulators to supply the system.

Conclusions

1. A maximum-design-hour load of about 9×10^6 cubic feet per hour of 100% natural gas could be handled by the distribution pressure system studied without violating any design criteria or requiring reinforcements. The lowest system pressures were estimated to be 3.5 psig on the basis of sendout pressures of 35 psig (7.9×10^6 CFH supply source A) and 31 psig (693×10^3 CFH supply sources B&C).

2. To distribute a blend of natural gas with 10% hydrogen in the system described in (1) above, it is required that the sendout pressure at all three supply sources (A, B, and C) be kept at 35 psig to maintain a minimum acceptable pressure of 3 psig at any point in the system.

3. To distribute a gas blend with 20% hydrogen in the system described in (1) on the preceding page, it is required that the conduit pressure at the supply points be 35 psig (7.86×10^3 CFH supply source A) and 38.4 psig (900×10^3 and 667×10^3 CFH supply sources B&C) to maintain a minimum pressure of 3 psig throughout the system.

4. A maximum-design-hour load of 29.4×10^3 CFH of 100% natural gas could be handled by the utilization pressure system studied without violating any design criteria or requiring reinforcements. The lowest system pressure was estimated to be 5.38 inches water column with the two regulators feeding gas at 6" pressure.

5. The system described in (4) above could distribute blends of hydrogen with natural gas and maintain the minimum allowable pressure of 4.2" throughout the system. Blends with 10% and 20% hydrogen resulted in minimum pressures of 5.35" and 5.32", respectively.

Points of Potential Hydrogen Admission

The selection of the points at which hydrogen should be admitted to a distribution system to supplement natural gas is closely related to the requirements of the State Utility Commission. Aside from safety considerations, the utility commission's chief concern will most likely be that customers receiving the lower heating value blend are billed accordingly. To this end, the commission will probably require that the limits of the area receiving the blend are clearly defined so that these customers can be easily identified. From the utility's standpoint, the simplest way to define these limits would be to supply the blend to an entire distribution system, or if this cannot be done, at least to some easily defined sub-section of the distribution system. This can be done most easily if the utility blends hydrogen into natural gas at the meter stations supplying a particular distribution system.

Impact of Regulatory Standards

An analysis of the Regulatory Commission rules in one state (New Jersey) reveals few problem areas with regard to distributing hydrogen blends, but certain topics need further study.

1. Possible conflicts with a variety of existing codes, including piping and plumbing codes, welding codes, electrical codes, and compressor station codes.

2. Gas detector calibration could be difficult when the percentage of hydrogen in the blend is constantly varying.

3. Odorizing hydrogen-natural gas blends could present problems.

4. Purging mains for hydrogen-natural gas blends may need development of special procedures.

5. Heating value calculations for billing purposes will be more complicated.

Regulatory standards regarding gas distribution and hydrogen handling may vary significantly among states and localities and further studies should be made in this regard.

Performance of Gas Distribution Equipment

The rate of gas leakage or hydrogen permeation through prototype utility pipes and joints will be measured using a special test facility. The facility circulates natural gas or blends at a rate of 3,000 cubic feet per day and pressures in the utilization and distribution ranges. Cast iron, plastic pipe and steel joints removed from the PSE&G system, after various service lives, are being tested for leakage. The facility has been used for baseline tests with dry natural gas and, presently, a dry gas blend with 10% hydrogen is being tried.

HYDROGEN AS A MID-TERM GASEOUS FUEL SUPPLEMENT
BY BLENDING WITH NATURAL GAS

G. F. Steinmetz
Baltimore Gas and Electric Company
Baltimore, Maryland

Abstract

The Ad Hoc Committee studied the potential for mid-term (1985-2000) commercial application of the use of hydrogen for blending into the present natural gas delivery system as an energy supplement. Successful development of advanced electrolyzer technology and the availability of low cost "off-peak" electric generating capacity are basic to this concept.

The Committee determined that a major, federally funded research, development, and demonstration program aimed at proving the technical feasibility is not justified within the next five years. Basic reasons are that even a completely successful RD&D program would not spur mid-term commercialization to:

- * Produce sufficient hydrogen to significantly alleviate the natural gas shortage on a national basis.
- * Produce hydrogen at a cost competitive with other supplemental gaseous fuels if present price projections hold true.
- * Provide the electric power industry with incentives to devote available generating capacity to this end in competition with various storage concepts, operating alternatives, and end uses under development.

The Committee found no overriding environmental, safety, legal, code, or regulatory considerations which would preclude the hydrogen-natural gas supplementation concept.

INTRODUCTION

Several divisions of the United States Energy Research and Development Administration (ERDA) support research efforts relating to the use of hydrogen as a medium for energy transmission and distribution. While the general consensus of technical experts projects hydrogen as an energy carrier in the long-term (beyond the year 2000), its prospective role as an energy delivery medium in the mid-term (1985-2000) must also be examined. Such analyses should be within the framework of U.S. Energy systems and emphasize comparison between hydrogen and competitive alternatives available and/or under development.

At the invitation of ERDA's Chemical and Thermal Storage Branch, Division of Energy Storage Systems, Office of Conservation, an Ad Hoc Committee was established to conduct this analysis and comparison. The Committee was charged with determining the potential of hydrogen supplementation for mid-term commercial development and the appropriateness of a major government supported research, development, and demonstration (RD&D) project. If the results were positive, the Committee was asked to present a plan for implementing such a program within five years. Production of electrolytic hydrogen from off-peak electric generating capacity was emphasized as the likely hydrogen sources.

Participation was solicited from a broad base of electric, electric and gas, gas transmission and distribution utilities, related trade associations, industry, government agencies, and national laboratories. Thus, a balance of diverse perspectives and views on the value of the proposed project was included.

This activity was formally instituted at an organizational meeting held at ERDA Headquarters on April 21, 1976. Work was essentially completed in January, 1977 and a report entitled "An Evaluation of the Use of Hydrogen as a Supplement to Natural Gas" (1) was finally edited for publication during the summer of 1977. This paper is a presentation of the significant findings of the Ad Hoc Committee.

EVALUATION OF CRITERIA

Four criteria were used by the Ad Hoc Committee to evaluate the potential for mid-term commercialization of the hydrogen - natural gas blending concept. These are discussed in turn below to explain the Committee's reasoning and judgement.

First Criteria - Volumes of hydrogen produced and utilized would make a significant contribution to alleviating the natural gas shortage on a national basis.

Inherent in this criteria are the dual questions of interchangeability and production potential. Interchangeability is defined as the ability to interchange one gas with another without incurring unacceptable performance of equipment. The prime aspects of performance are:

- * No incomplete combustion, i.e., the generation of carbon monoxide beyond acceptable limits.
- * No lifting of flames from burner ports.
- * No flash-back of flames into the burner.

- * No excessive velocity tipping of flames.
- * Little change in burner input (less than $\pm 10\%$).

The interchangeability of one gas with another on all the appliances and equipment connected to distribution pipelines is not subject to exact determination. Much work has been done over the past twenty-five years to develop approaches which are indicative of satisfactory performance but not conclusive. A brief treatment is given using the Knoy "C" Equation (2) approach to gain some perspective on the effect of hydrogen blending. Table 1 shows a typical natural gas analysis and the resultant change in heating value and specific gravity as hydrogen is introduced in various percentages by volume. The Knoy "C" Equation is a simplified approach to interchangeability which permits a rapid assessment based on a relationship of heating value and specific gravity. Its basic premise states that if "C" developed by the following formula for an adjustment gas remains constant within limits for substitute gases they will be interchangeable.

$$C = \frac{\text{Heating Value} - 175}{\text{Specific Gravity}}$$

Interchangeability results from the maintenance of a primary air-gas mixture of approximately 175 BTU/ft.³ within the burner head. On a plot of heating value versus specific gravity, a constant "C" or interchangeability line can be developed for the adjustment gas. A variation in "C" of $\pm 5\%$ is considered to be a tolerance band within which satisfactory appliance performance can be expected. A second tolerance band to $\pm 10\%$ variation in "C" indicates an area within which some degree of difficulty with appliance performance will be experienced and burner adjustments needed. Beyond this band, substitute gases cannot be considered for satisfactory performance. Figure 1 shows the Knoy "C" plot for the typical natural gas as the adjustment gas and the various hydrogen percentage mixtures as substitute gases.

Laboratory research done on a variety of gas appliances by actually imposing hydrogen mixtures has shown approximately 10% to be the limit for interchangeability which is in good correlation with the Knoy result. Higher mixtures result in flashback problems with certain burners. The indications are that with modification of equipment to some degree and at a commensurate cost a maximum of 25% hydrogen by volume might be distributed. None of the interchangeability techniques, even laboratory testing, are capable of giving broad consideration to the "in situ" condition of equipment regarding field adjustment, deterioration, accumulation of dirt and debris and venting conditions. Neither do they fathom the nuances of customers exposed to changes in the appearance or operation of appliances. Performance on an operating distribution system is the only conclusive index of interchangeability.

With an apparent 10% assured minimum to 25% doubtful maximum, it is important to consider the effects of hydrogen mixing on natural gas requirements. Since hydrogen has a heating value of only about one-third that of natural gas, any mixing of hydrogen will lower the heating value of the gas distributed. However, the system will require the

same total heat usage regardless of the gas distributed. Thus more cubic feet of the lower heating value gas will be required during a given time period. When the relative volumes of natural gas required to satisfy a given heat load are calculated for various percentage mixtures of hydrogen, the results produce Figure 11. A 10% mixture of hydrogen will decrease natural gas requirements by only 3.40% and a 25% mixture by 9.55%. Hydrogen blending then has a limited potential for alleviating natural gas shortages due to the interchangeability factor. In contrast, alternative gaseous fuels such as synthetic natural gas from either coal or naphtha and imported liquified natural gas are directly interchangeable on a cubic foot for cubic foot basis.

Although limited, the use of hydrogen would be worth pursuing if sufficient quantities were available at a competitive price. Production potential was explored by the Committee through a detailed review of possible sources. Possibilities considered and conclusions reached are summarized below:

a) Coal Gasification

SNG production from coal is more attractive than hydrogen production for natural gas blending from efficiency, cost, and compatibility viewpoints. Hydrogen production by coal gasification may be attractive for natural gas substitution in industries such as oil refining, ammonia manufacture, or production of methanol and other chemicals.

b) Renewable Resources

Of the nine possibilities examined, none appears to be feasible for large-scale application in the mid-term. There is little probability that a solar photovoltaic electrolyzer will be economically feasible in the mid-term unless breakthroughs in improved photovoltaic cell efficiency and at least a fifty-fold reduction in manufacturing costs occur. Because of high costs for electricity generation in a capital-intensive facility operating at a low annual capacity factor, there is also little hope for solar thermal electrolysis due to high cost of electricity generation and remote siting requirements. None of the photochemical concepts under development are realistically close to commercial operation by 2000, and more fundamental research is required before this concept can be adequately assessed. Bio-gasification favors methane production and anaerobic digestion of organic waste materials produces much more methane than hydrogen; reforming methane to hydrogen would be uneconomical. No prospects are seen for either solar or nuclear-based thermochemical hydrogen for commercial application before 2000. Also, considerable work remains to be done on the earth's magma as a potential hydrogen source before economic feasibility can even be assessed. Once technology is proven, wind electrolysis could be attractive under the right conditions and there is a slight chance for mid-term commercialization; however, because of regional applicability requirements, it could only be employed on a minor and very select basis.

c) Electrolytic Hydrogen from Installed Generating Capacity

Because there is presently no large-scale

electrolytic equipment industry in the United States, production on a megawatt scale requires acquisition of equipment from European manufacturers. Thus, the Committee firmly concluded that advanced electrolyzer technology is required to make mid-term commercialization feasible because burdens imposed by present technology in compression requirements and manned operations preclude any hope of competitive pricing. Table 2 presents an evaluation of present state-of-the-art electrolysis technology compared to postulated goals for advanced technology.

The General Electric Solid Polymer Electrolyte (GE-SPE) approach, now under development by the Electric Direct Energy Conversion Laboratory at Wilmington, Massachusetts with partial funding from ERDA and the Niagara Mohawk Power Company, is an advanced concept. This process employs a solid perfluorinated polymer as the electrolyte rather than aqueous KOH which is used in current systems. The GE-SPE electrolysis process is an outgrowth of the solid polymer electrolyte fuel cells supplied by General Electric for use on several aerospace vehicles.

Thus electrolytic hydrogen from "off-peak" electric generating capacity was found to be the only source capable of mid-term commercialization. Production potential then centers around the availability of "off-peak" power. Estimates by the Committee, using the advanced electrolyzer capability for hydrogen generation, were developed as follows:

Nuclear generating capacity in some geographical areas may be about equal to or slightly in excess of the base load by about 1985, and in the 1985-2000 period this excess nuclear capacity above the base load will probably gradually increase. The availability of off-peak nuclear generating capacity in the year 1995 for the contiguous 48 states has been estimated using future generating plant capacity and load data from 1976 reports filed with the Federal Power Commission by each of the nine electric utility regional reliability councils. This estimate indicates that by the year 2000 there may be as much as 72 billion kwhr of off-peak nuclear electricity that would be available about 12 hours per day at an incremental cost (fuel + O&M) of 0.6-0.8 ¢/kwhr (1975 \$). This off-peak nuclear electricity is likely to be available along the East Coast north of Virginia, in the Northern Mid-West, and on the Pacific Coast. This 72 billion kwhr/year would provide 0.2 Quad/year of electrolytic hydrogen at a cost of \$4.60-5.25/MBtu (1975 \$) including the utility rate of return on the electrolysis plant investment. This 0.2 Quad/year would be about 1% of the U.S. requirements for gaseous fuel.

The conversion of coal to electricity and then to hydrogen by electrolysis involves an overall thermal efficiency (coal to hydrogen) of about 34% compared to 60-65% for converting coal to SNG by the Lurgi process or by the newer coal gasification processes now being developed. However, in spite of this serious efficiency deficit, electrolytic hydrogen production from off-peak coal fired generating

capacity may be attractive at some locations. For example, the use of electrolysis would allow electric utilities to replace cycling type coal fired generators with high efficiency (low heat rate) plants that are not readily cycled.

Estimates have been made of the availability of off-peak electricity in the years 1985 and 1990 from hydro, nuclear, and low cost coal fired plants at a maximum incremental cost (fuel + O&M) of 1.1 ¢/kwhr (1975 \$). These estimates are based on data provided by two of the larger utility systems that represent 8.5% of the total U.S. generating capacity. These data indicate that this category of U.S. off-peak electricity may be 256 billion kwhr/year in 1985, 314 billion in 1990, and may reach 465 billion in the year 2000. This larger quantity of off-peak electricity includes the off-peak nuclear electricity, discussed above; it also is available about 12 hours/day and would vary somewhat from season to season. It was assumed that 260 billion kwhr/year of this 465 billion total could be used for electrolysis in the year 2000. This would provide 0.8 Quad/year of electrolytic hydrogen or about 4% of the U.S. gaseous fuel requirements in the year 2000. This electrolytic hydrogen would cost about \$6.20/MBtu (1975 \$) including return on the electrolysis plant.

While the estimates of future available electrolytic hydrogen are significant, up to 4.0% of U.S. gaseous fuel requirements in year 2000, the probability of actually achieving this output must be considered. This probability factor is rather low because low cost off-peak electricity may not be available due to greater than anticipated electrical demand or delays in the construction of nuclear power plants. It may not be attractive to use electrolysis if SNG from coal gasification develops more rapidly than is now anticipated. There is also the distinct possibility that, if available, the low cost off-peak electricity may be utilized in an energy storage system such as pumped hydro or underground compressed air or by the use of time-of-day electricity pricing or for the night-time recharging of electric vehicles. Obviously, the competition for this energy is real. Utility managements will determine the end use which is most apt to be directed toward optimum profitability and benefit for the electric system operation. There is no apparent strong incentive for the use of this energy as a natural gas supplement by producing hydrogen. Accordingly, the Committee judged that a factor of no more than 0.10 would be applicable. Such probability scales down the anticipated hydrogen production to an order of about 0.4% of U.S. gaseous fuel requirements in year 2000 and increases the expectation that it would be on a limited regional basis rather than having national effect. On this basis, using 20 quads of energy requirement annually, electrolytic hydrogen production for supplementation would approach 0.08 quads or 0.25 trillion cubic feet. This is less than 0.1 trillion cubic feet of natural gas equivalent but worth approximately 0.5 billion dollars at the calculated production cost of \$6.20 per million BTU.

Second Criteria - Hydrogen will be cost competitive with other supplemental fuels (all costs based on 1975 dollars).

Present electrolyzer technology and industry in the U.S. is not adequate for hydrogen generation on the required scale because MW capacity units are not available and hydrogen production costs are prohibitive.

Commercialization requires successful development of advanced electrolyzers such as the General Electric Solid Polymer Electrolyte (SPE) process. Granting such development, at an approximate cost of 20 million dollars, hydrogen production costs (1975 \$) range from \$4.60-\$5.25 per million Btu (from nuclear off-peak generation only) to \$6.20 per million Btu (from all off-peak generation up to 1.1 ¢/kWh in 1975 \$). The lowest hydrogen production costs are comparable to the highest supplemental gaseous fuel costs of past years, namely substitute natural gas from naphtha, at \$4.50 per million Btu. The major competitive gaseous fuel under development, substitute natural gas from coal (SNG) at a projected cost of \$3.50 per million Btu, shows hydrogen to be 77.1% higher, although these projections might be revised upward along the course of development to commercialization.

In order to arrive at hydrogen production costs, detailed studies involving capital and operating cost estimates for the GE-SPE system were carried out. These economic data were then used with cost and availability estimates of low cost off-peak electricity to calculate the quantity and cost of electrolytic hydrogen that could be produced with the available off-peak electricity.

The capital and operating costs for the GE-SPE system are defined in Table 3. The installed cost of the electrolysis plant has been assumed to be \$150/kW of hydrogen product (1975 \$). GE has suggested that this figure might ultimately be as low as \$100/kW after a substantial amount of capacity has been built and the learning curve experience is well advanced. The efficiency of the process has been assumed to be 90% (hydrogen product/AC power in); this figure is at the high end of the GE suggested target range of 85-90%.

The production cost of the hydrogen product derived in the tabulations is plotted as a function of the cost of electricity in Figure III.

Assumptions used in developing these costs are explained in Table 3. The more important assumptions are as follows:

- * The annual recovery of capital is 17% corresponding to that for the electric utility industry in the U.S.
- * Labor and supervision costs included in this calculation assume essentially unattended operation of the electrolysis equipment. The costs employed correspond to 0.1 man/shift in Column 1 and 0.08 man/shift in Columns 2, 3, and 4. The basic assumption is that this electrolysis equipment will run essentially unattended in small units of 5.0 MW output (51,500 SCF/hr hydrogen product) at dispersed locations such as utility substations. If constant operator attention is required, production costs for small dispersed units will be

very high. If operator attention to the electrolysis facility is required, it will probably be desirable to use large units of 50-100 MW and to locate these plants at the electric generating stations where operator attention can be provided at reasonable (incremental) cost.

- * Capital costs for the power conversion equipment are proportional to the plant's hydrogen production rather than a constant annual dollar value, assuming that the power conversion equipment is providing a useful service on the utility grid in reactive power control when the electrolysis plant is not used for hydrogen production. This might not apply if it were necessary to employ large electrolysis plants at central stations rather than the smaller electrolysis units at substations. If this reactive power control credit were not realized, the electrolytic hydrogen production costs would be increased by \$0.10/MBtu for the capacity factor cases.
- * Maintenance and general overhead annual charges are assumed to be 6.6% of investment. This corresponds to rather low overall annual maintenance costs.

It will be noticed that hydrogen storage has not been factored into any of the prior considerations. The Committee came to the firm conclusion that costs associated with any technically feasible hydrogen storage techniques would be prohibitive in the mid-term. This is especially true with the relatively small (5 MW) facility. The concept for handling pure hydrogen and injecting it into a flowing natural gas pipeline is conceived as essentially a flow-through operation with only "surge" or "buffer" storage involved.

Third Criteria - The electric power industry must be motivated to devote their low cost off-peak power generating potential to hydrogen production.

Off-peak electric capacity is a commodity under continuous and intensive study. Utilities seek to minimize its availability by power pooling and the optimum design of their generating facility "mix". It is subject to change in availability as a new plant goes on line and then load grows to utilize this capacity. Changes in operating practices, such as "time-of-day" billing, which could change the historic peak vs. off-peak relationship to reduce the availability of off-peak power, are contemplated. Techniques for energy storage including pumped hydro, compressed air, battery, and sensible heat thermal storage are in use or under study. Finally, alternate end uses of electricity such as battery charging for transportation could change the off-peak picture. All of these reduce the attractiveness and probability for hydrogen generation as a supplement to natural gas on a national scale although it could be viable in more localized regions.

Given the limited reduction in natural gas requirements which could be derived from hydrogen blending and the unfavorable production cost picture versus other alternative fuels, the Committee judged that a low probability factor must be applied for commercialization. These factors taken together prompted the decision against recommending a major research, development and demonstration project at

this time.

Fourth Criteria - No overriding environmental, safety, legal, code or regulatory considerations would preclude the hydrogen - natural gas supplementation concept.

Throughout the study, this criteria was constantly reviewed by the various groups investigating major aspects of the concept such as supply, injection, transmission, distribution and utilization. Similar concerns were developed in each group relative to these considerations but the general consensus was that no insurmountable obstacles exist. Put another way, if the first three criteria were met, the fourth could be handled.

Sufficient experience and expertise exists for the design and construction of hydrogen handling facilities. The space program and various chemical plant operations including synthetic natural gas development have provided much knowledge. Likewise, numerous parallels exist between the hydrogen blending requirement and long standing gas utility peak-shaving operations which utilize propane-air mixtures blended with natural gas.

However, hydrogen does have different characteristics from more conventional gaseous fuels which must be compensated for. These properties include:

- * Low density (0.07 specific gravity) which makes containment more difficult.
- * Wide flammable limits (4-75% by volume in air), as well as lack of odor and ability to burn without visible flames which create greater hazards.
- * The potential for hydrogen embrittlement of materials under certain operating conditions which requires special attention.

In spite of the above difficulties, hydrogen is handled successfully in refinery operations and chemical plants.

A full range of clearances would be needed for the construction of hydrogen facilities including environmental impact statements, hearings, appeals and decisions. Operating demonstrations would serve a real purpose in establishing precedents if hydrogen supplementation were to be pursued for mid-term commercialization.

Facilities would be required to meet the Minimum Federal Safety Standards, Part 192 - Transportation of Natural and Other Gases by Pipeline - administered by the Office of Pipeline Safety Operations (OPSO). Also, State Public Service Commissions operating as agents for OPSO or on their own authority could impose safety requirements. At present there is no specific coverage for hydrogen facilities in the regulations governing gas transmission and distribution. Useful developmental work could be done by compiling existing standards and codes through governmental agencies, various industry agencies, and recognized standards organizations such as ASME and ANSI. Such a compilation would be valuable in orienting the safety codes, such as Part 192, toward hydrogen coverage.

Hydrogen was distributed in manufactured gas, at concentrations in excess of 30% by volume, for over 125 years. There is no record of it being a problem

constituent during that entire era. Even today, some companies use appreciable percentages of hydrogen in their send-out gases. High pressure (500 psig) transmission mains are used to transport some of this gas to the distribution network. Based on this experience, it would appear that no insurmountable obstacles or significant hazardous conditions would preclude the transmission and distribution of 10-15% by volume mixtures of hydrogen in natural gas. However, the degree of relative uncertainty combined with the risk of widespread exposure warrants a closer look at potential concerns.

Regulatory involvement could also be incurred by the intermittent but routine injection of hydrogen and its effect on the Btu content of gases reaching end-use customers. The heating value would vary for those customers served by the supplemented gas and, in addition, be different from the unmixed natural gas served to other areas of the system. These influences could cause complications in billing practices and might require more detailed monitoring of heating value by geographical area within a service territory than is currently practiced.

Utilities are subject to State and local codes governing the installation of piping and equipment in buildings. Most reference the National Fuel Gas Code which is American National Standard (ANSI) Z 223.1. Little, if any, change in this code is contemplated as a result of the low hydrogen concentration being considered. However, an interface with ANSI would be prudent if a demonstration program was instituted.

The same comment applies to the ANSI Z 21 series of standards covering gas appliance construction and performance. Almost all such equipment is certified under these standards for use with natural gas and certain other commonly used gaseous fuels through the American Gas Association Laboratories.

SUMMARY

The Ad Hoc Committee examined one possible mid-term application of hydrogen. In light of rapidly changing circumstances it may be appropriate to re-examine hydrogen's prospective role in alternative mid-term applications on a regular basis. The Committee recommended that the proposed hydrogen-

for-natural-gas-supplementation scheme be re-examined in a time period beyond three years. As a result of technology advances some of the hydrogen production options eliminated by this study, such as wind, solar, ocean, thermal, biomass, and thermochemical production, may be reconsidered. Furthermore, the entire issue of availability and cost of off-peak power is not only relevant to hydrogen production but also bears directly on electric energy storage and electric automotive programs and should be periodically examined. Such continuous studies are valuable to several on-going ERDA-EPRI and industry R&D programs in addition to being relevant to the issue of hydrogen production from electric sources. ERDA, in association with the utility industry, should remain alert to identify possible new mid-term hydrogen applications. Escalating fossil fuel prices must be considered; the expectation that synthetic gas from coal will be available at competitive prices should be questioned. Also, changes in the projected rate of addition to nuclear or other low cost base load capacity must be considered. Major changes in the above circumstances would require a reassessment of the present decision not to recommend a demonstration project at this time.

The Committee believes that its report presents a fair appraisal of the potential for mid-term supplementation of natural gas with hydrogen. General agreement on the contents was reached through many meetings and discussions. This brief presentation cannot do justice to the full report which is now available. Much effort was given to the final Conclusions and Recommendations which are reproduced in full as Appendices A and B.

REFERENCES

1. "An Evaluation of the Use of Hydrogen as a Supplement to Natural Gas" Report of the Ad Hoc Committee, ERDA 1977
2. "Graphic Approach to the Problem of Interchangeability" A.G.A. Procedures 1953: 938-47

TABLE 1
Representative Natural Gas Composition
and Properties

<u>Constituent</u>	<u>Symbol</u>	<u>% Volume</u>
Methane	CH ₄	96.53
Ethane	C ₂ H ₆	2.38
Propane	C ₃ H ₈	0.18
Iso-Butane	C ₄ H ₁₀	-
N. Butane	C ₄ H ₁₀	.02
Carbon Dioxide	CO ₂	0.77
Nitrogen	N ₂	0.12
		<u>100.00</u>
Gross Heating Value	Btu/Ft ³ (dry)	1026
Specific Gravity	S.G. (air = 1.0)	0.576
<hr/>		
Hydrogen	H ₂	100.0
Gross Heating Value	Btu/Ft ³ (dry)	325.0
Specific Gravity	S.G.	0.07

Change in Heating Value and Specific Gravity
With Various % Hydrogen Mixtures

<u>% Hydrogen in Mixture</u>	<u>Mixture with N.G.</u>	
	<u>Btu/CF</u>	<u>Sp.Gr.</u>
0	1026.0	0.576
5	990.95	0.551
10	955.9	0.525
15	920.85	0.500
20	885.80	0.475
25	850.75	0.450

TABLE 2

**Goals of Advanced Electrolyzer Technology
Compared to Present State-of-the-Art**

	<u>Present</u>	<u>Advanced</u>
Installed Capital Costs \$/KW	300.00	150.00
Operating Efficiency %	65.0	90.0
Space Requirements Amps/sq.ft.	250.0	1000.0
Output H ₂ pressure PSIG	14.7	450.0
Time to come on line	Minutes	Seconds
Time to drop off line	Minutes	Seconds
Operation Mode	Manned	Unmanned
Maintenance Costs	Medium	Low
Minimum Life	10-15 Years	20 Years

TABLE 3

Electrolytic Hydrogen Cost by GE-SPE Process

Operation by a utility using off-peak electricity
1985 operation, 1975 \$

Plant - SPE electrolysis with forced commutated converter interface
Location - Northeast U.S.
Utilization factor for converter = 0.90
Utilization factor for electrolyzer = 0.45
Electrolyzer capacity = 5.0 MW hydrogen product = 17.075 MBtu/hr hydrogen product
= 52,538 SCF/hr of hydrogen or 26,269 SCF/hr of oxygen
Thermal efficiency = 90.0%
Electrical input for capacity operation = 5.556 MW
Hydrogen product pressure - 450 psig

<u>Investment</u>	<u>\$/KW out</u>	<u>\$ thousands</u>
Power conversion and switchgear	45	225
Electrolysis modules	20	100
Other process equipment	23	115
Installation costs	22	110
Offsites	15	75
Contingency	25	125
Total	150	750

Column No.	1	2	3	4
Converter capacity factor	0.90	0.90	0.90	0.90
Electrolyzer capacity factor	0.90	0.45	0.45	0.45
Electrolyzer operating hours per year	7884	3842	3942	3942
Hydrogen production MBtu/yr X 10 ³	134.6	67.3	67.3	67.3
Electricity input kWhr/yr X 10 ⁶	43.8	21.9	21.9	21.9
Electricity cost, ¢/kWhr	1.0	0.6	0.8	1.1
Working capital, \$ X 10 ³ (Note 1)	78	26	33	44

Annual Costs, \$ Thousands

Electricity		438	131	175	240
Water and chemicals (Note 2)		7	4	4	4
Labor and supervision (Note 3)		25	18	18	18
Maintenance and general overhead (Note 4)					
o Power conversion (Note 5)		15	8	8	8
o All other		35	35	35	35
Capital charges (Note 6)					
o Power conversion (Note 5)		38	19	19	19
o All other		89	89	89	89
Working capital charges (Note 7)		16	5	7	9
Total		663	309	355	422

TABLE 3 (cont'd)

Column No.	1	2	3	4
Electrolyzer capacity factor	0.90	0.45	0.45	0.45
Electricity cost, c/kWhr	1.0	0.6	0.8	1.1
<u>Costs, \$/MBtu of hydrogen product</u>				
Electricity	3.25	1.95	2.60	3.57
Water and chemicals	0.05	0.05	0.05	0.05
Labor and supervision	0.19	0.27	0.27	0.27
Maintenance and general overhead	0.37	0.64	0.64	0.64
Capital charges	0.95	1.61	1.61	1.61
Working capital charges	0.12	0.07	0.10	0.13
Total	4.93	4.59	5.27	6.27

Oxygen credit (Note 8)

-
- Note 1 - Working capital = 2 months costs of electricity, water + chemicals, and labor and supervision.
 Note 2 - Charges for water and chemicals are \$0.054/MBtu hydrogen product.
 Note 3 - Labor and supervision for 1.0 man/shift would be \$236,000/yr.
 Note 4 - Maintenance and general overhead are 6.6% of investment each year.
 Note 5 - Maintenance and general overhead and capital charges for the power conversion and switchgear equipment is charged in proportion to its use for electrolysis since when not used for electrolysis it provides credits to the utility for power factor correction.
 Note 6 - Capital charges are 17.0% of investment per year.
 Note 7 - Working capital charges are 21.0% of working capital per year.
 Note 8 - If oxygen production could be marketed at \$24/ton, the credit would correspond to \$1.53/MBtu of hydrogen.

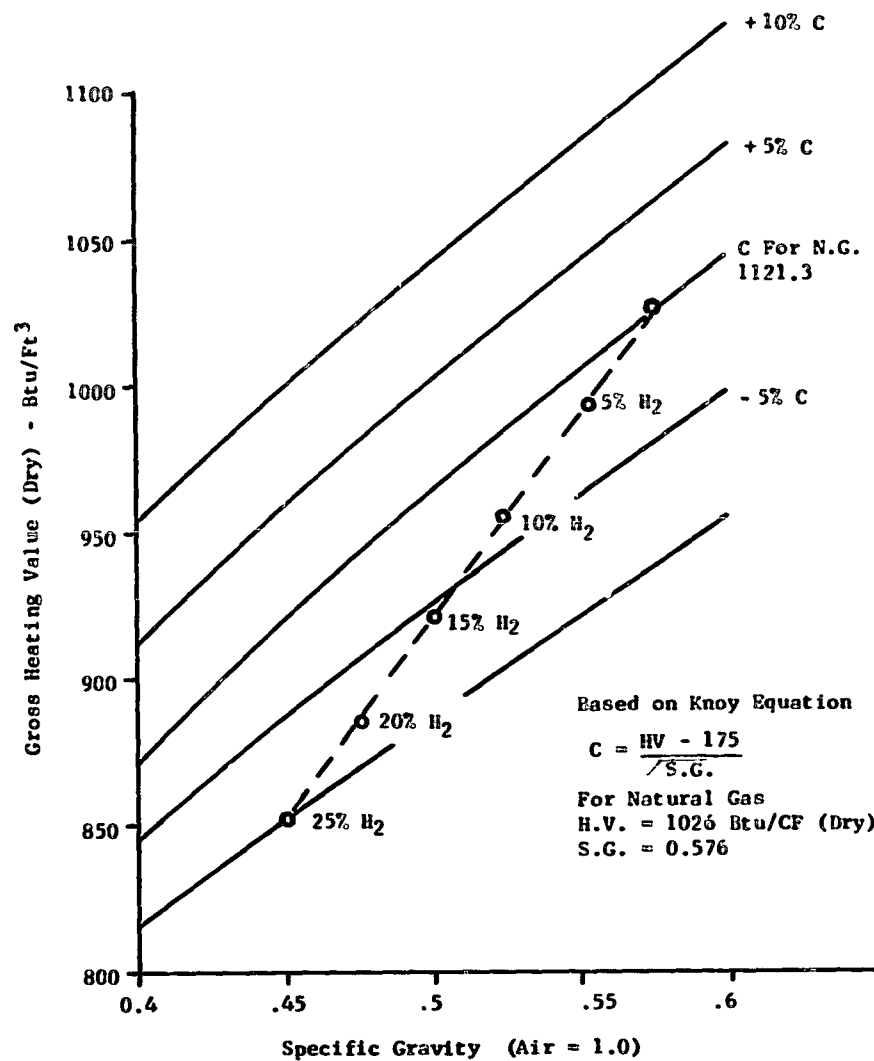


Figure I. Interchangeability Relationship Of Hydrogen Blending With Typical Natural Gas

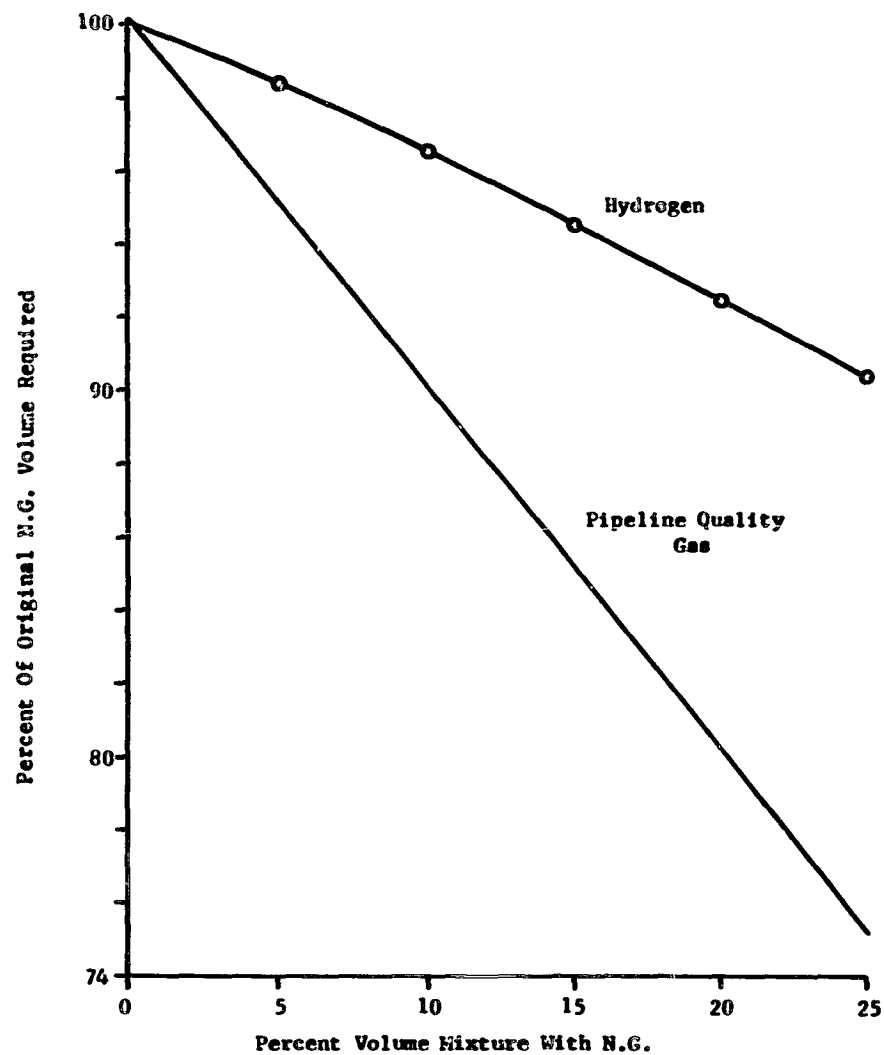


Figure II. Effect Of Blending On N.G. Requirements

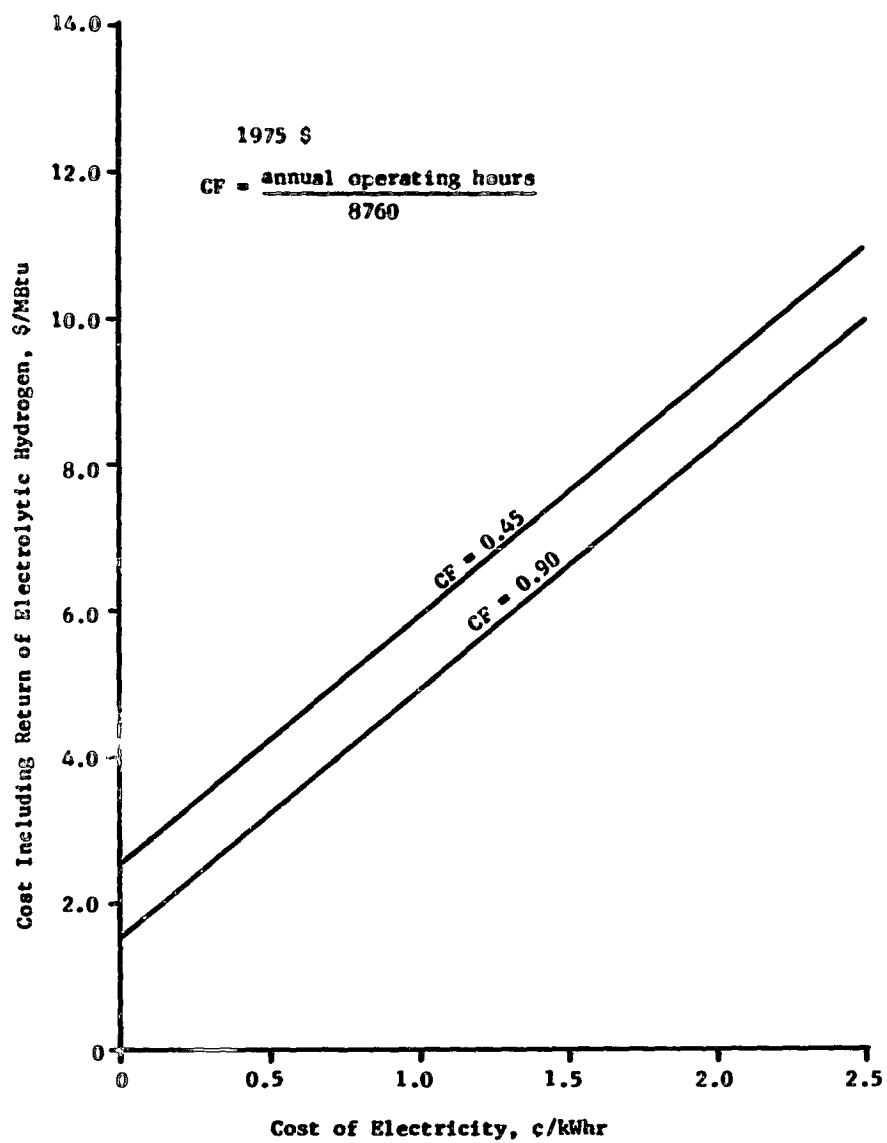


Figure III. Cost of Electrolytic Hydrogen Including Utility Rate of Return vs. Electricity Cost

APPENDIX A

Conclusions

- A. Electrolytic hydrogen is presently too expensive relative to other supplemental gas supplies but such hydrogen may become a limited quantity supplemental fuel in the future, especially in cases where low-cost "off-peak" capacity is available.
- B. There are no insurmountable problems in the safety, environmental, or regulatory areas which would prevent or preclude commercialization of hydrogen supplementation of natural gas. Excluding the production of hydrogen, the incremental system costs (such as transmission, distribution and injection) would not be significant.
- C. Laboratory tests and calculations indicate that the composition of blends would be limited to 10% hydrogen by volume without changes in system or end-use devices. With changes in end-use devices, levels could go to 20-25% hydrogen by volume blended with natural gas for satisfactory operation.
- D. Opportunities for supplementing natural gas using refinery and chemical plant by-product gases may exist today at economically feasible costs.
- E. Hydrogen may be more valuable as a chemical commodity rather than as a supplement to natural gas provided that storage would be available to deal with the intermittent nature of the source.
- F. If coal is the primary energy source being considered for natural gas supplementation, it may be more appropriate to produce synthetic natural gas (SNG) rather than hydrogen.
- G. For some utility companies, electrolytic hydrogen integrated with the gas grid and dispersed generation devices (fuel cells or high temperature turbines) may offer a unique electric/gas peak-shaving system that can be used for weekly or seasonal duty cycles not covered by batteries or other load management schemes. This approach may result in significant overall system benefits.
- H. The Committee recognizes that beyond the year 2000 there may be alternate energy sources providing for existing natural gas end uses such as increased electrification. A significant role for hydrogen is anticipated but competition with alternate energy supply mediums for end-use applications must continue to be examined. Particular consideration should be given to production from renewable resources which can interface with the gas grid.
- I. The conclusions drawn by the Ad Hoc Committee with respect to natural gas supplementation cannot be generalized. Since there are other applications of significant potential, the ERDA electrolyzer and other hydrogen RD&D programs should be continued.

APPENDIX B

Recommendations

- A. The Committee found no justification to initiate implementing a demonstration of hydrogen production and natural gas supplementation within the next five years. If significant interest is shown by a utility or utility consortium, the government should evaluate these proposals on their own merits.
- B. The federal government should continue to support these research activities aimed at solving natural gas supplementation related problems.
- C. The federal government should continue to support advanced electrolyzer development.
- D. The natural gas industry should investigate the availability and cost of by-product gases from industries such as refinery and chemical plants as a supplement to natural gas.
- E. ERDA should foster research related to longer range use of hydrogen as a possible and gradual replacement for natural and/or synthetic gases.
- F. The gas and electric utility industries should continue to be involved in establishing the technology base in anticipation of the time when hydrogen could play a more significant role. To the extent that ERDA assistance is warranted, that assistance should be on a cost-sharing basis (as distinct from sole ERDA funding) wherever practical.

Caveat

- A. The availability and cost of "off-peak" and "spinning reserve" capacity in the electric power industry along with an assessment of market penetration for electrolytic hydrogen is being developed separately by the Public Service Electric and Gas Company through an ERDA funded study.
- B. All costs in this report are shown in 1975 dollars. Cost data was derived from different sources, and, although the best presently available, may not have equal reliability. For example, production costs for synthetic natural gas from coal were developed by the ERDA Fossil Fuels Division while advanced electrolyzer hydrogen production costs were provided by General Electric, developers of the GE-SPE process.
- C. The limit of 10% by volume mixture of hydrogen in natural gas for interchangeability was taken from ERDA funded research work currently in progress at PSE&G. This limit is subject to verification by further research and ultimate field demonstration.

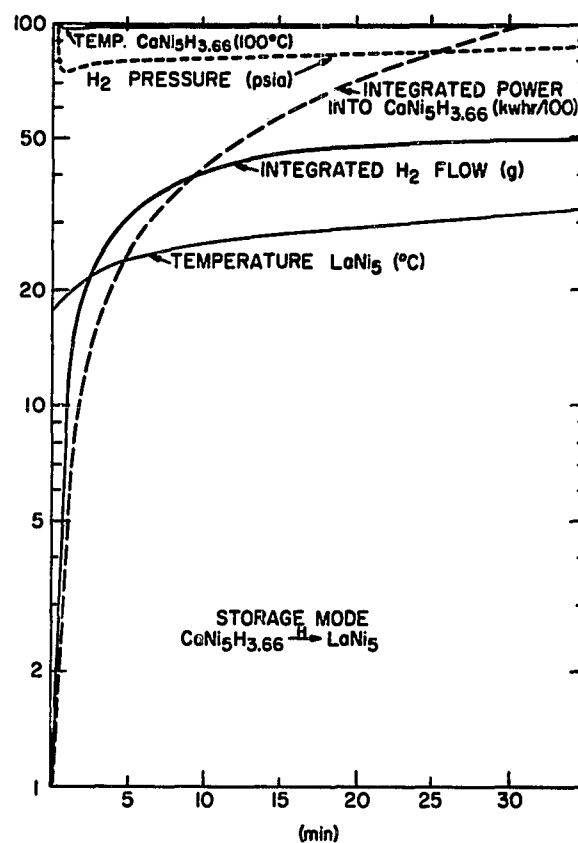


Fig. 7. Storage Mode: $\text{CaNi}_5\text{H}_{3.66} \xrightarrow{\text{H}} \text{LaNi}_5$

DRI RESEARCH PROGRAM ON IMPROVED HYDRIDES

C.E. Lundin, F.E. Lynch, and C.B. Magee
Denver Research Institute
University of Denver
Denver, Colorado 80208

ABSTRACT

The emphasis in this research program is to develop new and improved hydride storage materials. The approach will be to employ DRI developed predictive techniques to select candidate systems. Those systems with potential will be fully characterized and ultimately optimized by alloy addition. The goal is to develop hydrides with more than 3 weight percent hydrogen.

The studies during this review period were devoted principally to five subject areas. These were: (1) studies of AB₂ Laves phases and their hydriding characteristics, (2) the analysis of hysteresis effects in hydride storage materials and the development of a rationale for hysteresis effects, (3) hydriding studies of ANi₅ systems in which Ni was partially replaced with two neighboring elements, (4) hydriding studies of titanium-base, beta solid solution alloys, and (5) design, procurement, and construction of a new Sievert's apparatus and an activation apparatus.

I. Introduction

A research program was initiated approximately four months ago between the Brookhaven National Laboratory and the Denver Research Institute, University of Denver to develop hydrogen storage materials for application to energy needs. The principal program objectives are to develop hydrides with hydrogen capacities of at least three weight percent. The general approach to selection of materials will rely heavily on a predictive criterion developed in our laboratories⁽¹⁾. The criterion to be employed is a correlation of the free energy of formation of the hydride with the interstitial hole sizes in the metallic lattice. Attention will also be given to establishing the following properties: 1) decreased materials cost, 2) contamination resistance, 3) minimized hysteresis, 4) maximized kinetics, 5) good thermal conductivity, 6) safe handling properties, and 7) long-term recyclability. Ultimately, a series of fully characterized, hydrogen storage materials should be made available for various applications.

II. Research Progress

During the period covered by this project review, five separate subject areas of study have been initiated. These were:

A. Experimental study of the hydriding characteristics of selected AB₂ compounds of the Laves phase type including an analysis of the general structural and geometric characteristics of the C14 and C15 Laves phases and the type and number of interstitial sites for hydrogen occlusion.

B. Literature review of hysteresis effects in hydrides, development of a rationale from an analysis of prior theories that would be applicable to current lesser stable hydrides of interest, and preparation of a paper summarizing the significant findings to promote a better understanding of hysteresis effects for presentation at the International Symposium on Hydrides for Energy Storage in Gjeilo, Norway during August 14-19, 1977.

C. Initiation of hydriding studies on ANi₅ compounds where Ni is partially replaced by two neighboring elements.

D. Initiation of hydriding studies on titanium-base, beta solid solution alloys.

E. Design, procurement, and construction of a new Sievert's apparatus and design, procurement, and construction of an activation apparatus.

As stated in the Introduction, the selection of candidate materials is not to be left to intuitive or statistical sampling as has been the case in many previous studies. Several selection rules have evolved which are generally known and accepted. These will be employed as required. For instance, compounds which hydride are those in which one of the elements is a former hydride itself. Earlier studies⁽¹⁾ at DRI have also provided a better understanding of the hydrogen occlusive process. These studies resulted in the development of a useful predictive criterion⁽²⁾. The criterion entails a linear correlation between the standard free energy of formation of the hydride (or logarithm of the plateau pressure) and

the interstitial hole size of the metallic compound lattice. The correlation teaches that the larger the interstitial hole size, the more stable the hydride, basing the comparison at a constant temperature (usually 25°C). The correlation for each structure type is different and must be established first with experimental hydriding and lattice parameter data for several representative compounds. The stabilities of unknown compounds with the same structure type can then be determined by converting lattice parameter data into the interstitial hole size and obtaining the stability from the correlation plot. With more complex structure types, where the hole size is difficult to locate or calculate, atomic volumes can be used. The atomic volume is roughly proportional to the volume of the interstitial holes.

The stability-size correlation has been verified by data from many investigators as well as by our own. Also, it has been demonstrated with many different structure types. Only a few exceptions have been observed. This predictive tool is not only useful for locating new storage compounds, but also for adjusting or tailoring the stability of known materials to higher or lower pressure levels by the properly selected alloy addition.

The experimental study of AB₂ Laves phase intermetallic compounds, was initiated first with the pseudo-binary system, Fe₂Y-Fe₂Ti. These two binary systems were selected first for several reasons. The 66.7 atomic percent Fe in the AFe₂ compound is an inexpensive component with a relatively large fraction of the metallic content. The Ti at 33.3 atomic percent is somewhat more expensive, but is the lightest weight transition metal (other than Sc). Yttrium is more expensive, but hopefully a small amount would be required. Yttrium is also light-weight. Hypothetically, if the Fe₂Ti_{0.75}Y_{0.25} alloy forms an AB₂H₄ hydride, the hydrogen content would be about 2.4 weight percent, which is considerably better than FeTi and LaNi₅ hydrides. The Fe₂Y compound is the C15 (cubic) Laves phase, whereas the Fe₂Ti compound is the C14 (hexagonal) Laves phase. The Fe₂Ti compound melts congruently, while the Fe₂Y compound is formed peritectically. In the studies of Sandroock, Reilly, and Johnson⁽³⁾ it was found that, under the experimental conditions employed, the Fe₂Ti phase did not hydride. The Fe₂Y phase has been found to hydride to Fe₂YH₄ by Van Mal, et al.⁽⁴⁾. It is postulated by DRI investigators that Fe₂Ti does hydride under the proper experimental conditions. Ultra-high pressures at low temperatures would be expected to cause hydriding to an AB₂-hydride. On the other hand, the Fe₂Y is very stable and readily forms a hydride with extremely low equilibrium pressures at ambient temperatures. These factors can be readily predicted from the stability-size correlation. The atomic volume of Fe₂Ti was calculated to be 38.4 Å³ (per formula weight), and the atomic volume of Fe₂Y was calculated to be 49.8 Å³ (per formula weight). According to the correlation the smaller volume should be very unstable, whereas the larger volume should be very stable, as is the case. The experimental AB₂ data of Shaltiel, et al.⁽⁵⁾ were plotted in conformance with the size-stability correlation. It was found that the stability range of 1 to 10 atm plateau pressure corresponded to about 45 Å³ atomic volume. Thus, the Fe₂Ti-Fe₂Y pseudo-binary system should bracket the right pressure range, namely 1 to 10 atmospheres. The

obvious next step was to prepare alloys in the $\text{Fe}_2\text{Ti}-\text{Fe}_2\text{Y}$ pseudo-binary intermediate range in an attempt to form an appropriate atomic volume in between 38.4\AA^3 and 49.8\AA^3 . First, the Fe_2Ti and Fe_2Y alloys were prepared and subjected to hydriding to verify the previous studies. Hydriding attempts with Fe_2Ti up to about 120 atm were unsuccessful in the formation of a hydride phase, whereas the Fe_2Y reacted immediately at room temperature to form a hydrided alloy. The composition was not readily determined, because the as-cast sample was not single-phase due to the peritectic solidification. Next, a series of alloys were arc melted in the $\text{Fe}_2\text{Ti}-\text{Fe}_2\text{Y}$ pseudo-binary system. These have been examined metallographically, since a two-phase region was expected in which the C14 and C15 phases co-existed. It was hoped that considerable solubility existed at either end of the pseudo-binary system to allow adjustment of the size factor and, in turn, stability. However, the two-phase region was found to be extensive, covering between about $\text{Fe}_2\text{Ti}_{.85}\text{Y}_{.15}$ and $\text{Fe}_2\text{Ti}_{.15}\text{Y}_{.85}$. One alloy in the two-phase region was hydrided to determine what the hydriding characteristics of the dual phase combination were. The alloy was the $\text{Fe}_2\text{Ti}_{.75}\text{Y}_{.25}$ composition. The Fe_2Ti phase with Y in solution did not hydride appreciably, while the Fe_2Y phase with Ti in solution was still very stable. The composition of the Fe-Y base hydride was estimated to be about 4.5 H/ AB_2 . This system had to be abandoned due to the extensive two-phase region and the gross stability and instability of the two phases in equilibrium in the two-phase region.

The next related pseudo-binary system which was felt to allow more possibilities for adjustment to the proper hydriding properties was the $\text{Fe}_2\text{Zr}-\text{Fe}_2\text{Y}$ system. Should an $\text{Fe}_2\text{Zr}_{.75}\text{Y}_{.25}$ alloy form an AB_2H_4 hydride, the hydrogen content would be about 2 weight percent. This may then be used as a starting phase to modify in the direction of increased hydrogen capacity. In this case, the two Laves-phase structures are of the C15 (cubic) type. Complete solid solubility is expected. The atomic volumes are 44.2\AA^3 for Fe_2Zr and 49.8\AA^3 for Fe_2Y , which are closer together compared to the $\text{Fe}_2\text{Ti}-\text{Fe}_2\text{Y}$ systems. Also, the atomic volumes still bracket the estimated 45\AA^3 atomic volume for AB_2 structures which is projected to give the correct stability range. The Fe_2Zr compound was subjected to hydriding first. Pressures up to about 120 atm did not cause hydriding. Obviously, the size of the lattice or interstices is still too small to allow a sufficiently high degree of stability. Alloys have been made, and hydriding characteristics are being determined in the pseudo-binary system. So far, alloys in the compositional range from $\text{Fe}_2\text{Zr}_{.9}\text{Y}_{.1}$ to $\text{Fe}_2\text{Zr}_{.5}\text{Y}_{.5}$ appear to be single-phase alloys. An alloy at $\text{Fe}_2\text{Zr}_{.7}\text{Y}_{.3}$ was found to hydride at room temperature. Alloys in this compositional region are currently being studied to establish the total saturation and the pressure-temperature-composition relationships.

An associated topic of study with the AB_2 Laves phases was concurrently initiated. An analysis is being made of the general structural and geometrical characteristics of the C14 (hexagonal) and C15 (cubic) type Laves phases in conjunction with the pseudo-binary system hydriding investigation.

In the AB_2 compounds there are three types of tetrahedral holes encompassed by metallic atoms as follows: B_4 , A_2B_2 , and AB_3 . Current analyses are directed toward characterization of these holes as follows: 1) Determination of the radii of these holes in the AB_2 compounds as a function of the lattice parameters; and 2) Determination of the number of each of these types of holes, and the relative geometric positions of these holes in the crystal lattices of these compounds. The following correlations are being made: 1) Experimentally determined hydrogen concentration with number of available holes; 2) Experimentally determined hydride stabilities with hole type and size; and 3) Occupancy and stability with the electronic structures of the A and B elements involved.

The unit cell of the cubic AB_2 (C15) compound contains 8 A atoms and 16 B atoms. The relative positions are best understood by looking at a three dimensional model. Close packing within this structure requires that the atomic distances (closest approach) satisfy the following criteria:

$$\text{A-A: } \frac{2\sqrt{3}}{8} a,$$

$$\text{B-B: } \frac{2\sqrt{2}}{8} a,$$

$$\text{A-B: } \frac{\sqrt{11}}{8} a,$$

where a is the lattice parameter of the crystal.

The relative positions of the atoms and the specifications of interatomic distances presented above have been used to calculate the "hard sphere" radii of the three types of tetrahedral holes that are found in this structure. The radii of the spheres that touch the four encompassing atoms are given below:

B_4 tetrahedron (4 touching B atoms):

$$R_s = \frac{a}{8} (\sqrt{3} - \sqrt{2}) = \frac{a}{8} (0.31784)$$

AB_3 tetrahedron (three touching B atoms, A-B distance $(\sqrt{11}/8)a$):

$$R_s = \frac{a}{8} \left(\frac{\sqrt{3}}{\sqrt{6}+2} \right)$$

$$R_s = \frac{a}{8} (0.38927)$$

A_2B_2 tetrahedron (B atoms touching, A atoms touching, and A-B distance $(\sqrt{11}/8)a$):

$$R_s = \frac{a}{8} \left(\frac{3}{1+2\sqrt{6}} \right) \{ -(\sqrt{3}+\sqrt{2}) + \sqrt{2}(3+2\sqrt{6})^{\frac{1}{2}} \}$$

$$R_s = \frac{a}{8} (0.42129)$$

The coordinates of the three different types of holes closest to the origin of the cell are given below:

$$\text{B}_4: x=2\left(\frac{a}{8}\right), y=2\left(\frac{a}{8}\right), z=-2\left(\frac{a}{8}\right)$$

$$\text{AB}_3: x = \left(\frac{\sqrt{3}}{2}\right)\left(\frac{a}{8}\right), y = \left(\frac{\sqrt{3}}{2}\right)\left(\frac{a}{8}\right),$$

$$z = -\left(\frac{\sqrt{3}}{2}\right)\left(\frac{a}{8}\right)$$

$$x = -\frac{a}{8} (1.2247) = y$$

$$z = -\frac{a}{8} (1.2247)$$

$$A_2B_2: x = y = \frac{a}{8} (1.5223)$$

$$z = -\frac{a}{8} (0.044634)$$

Along certain planes the holes are arranged in clusters, each with one B_4 and $2AB_3$ and 2 A_2B_2 holes. Counting the holes in these clusters gives 5 B_4 , 20 AB_3 , and 16 A_2B_2 holes. This number of holes is reported by Febler and Gulbransen⁽⁶⁾. However, there are many A_2B_2 holes in the cell which are not contained in these planar clusters. Three-dimensional clusters about each of the B_4 holes accounts for a total of 5 B_4 , 20 AB_3 , and 48 A_2B_2 holes. This counting of A_2B_2 holes does not take into account those holes originating from clusters outside the unit cell but shared by the cell. Depending on how these holes are considered to be shared by adjoint unit cells, there can be as many as 40 additional A_2B_2 holes per unit cell.

The second area of study involved the hysteresis effects observed almost universally in these hydrogen storage materials. A large hysteresis results in a reduced thermodynamic efficiency when employed cyclically in various applications and dilutes the argument that hydrides are safer than high pressure hydrogen systems. Thus, it is important both scientifically and technologically to understand the phenomenon of hysteresis. Considerable effort was expended to conduct a literature survey of hysteresis effects in hydrides, develop a rationale from an analysis of prior theories that would be applicable to current hydrogen storage materials, and prepare a paper⁽⁷⁾ summarizing the significant findings, all to promote a better understanding of hysteresis effects. The paper was then presented during August 14-19, 1977 at the International Symposium on Hydrides for Energy Storage in Norway.

The salient features of the rationale are presented in this review paper. Briefly, the rationale proposes that strain effects are the fundamental cause of the hysteresis. The hysteresis effects are thought to be manifested at the atomic level, thus powder particle size would have little effect on hysteresis. The hysteresis appears to be an irreversible property in these materials. Thus, no single path in absorption-desorption should be possible. The desorption plateau is regarded as the closest approach to "equilibrium" conditions since the strain is irreversible plastic deformation. Localized compressive strain is imposed on the unfilled interstitial sites during hydrogen absorption in the metal solid-solution region, and during the large expansion on absorption in the two-phase region. The α and β phases are thus subject to plastic deformation at the micro level. On desorption from the β phase, the elastic portion of the strain is relieved on approaching the two-phase region and through the two-phase region which causes the desorption plateau pressure to fall below that of the absorption plateau pressure. The pressure difference is attributed to the effect observed in the size stability correlation wherein

the stability of the hydride decreases (higher pressure plateau) due to the compressive strain reducing the size of the unfilled sites. On relief of strain during desorption, the size of the sites is increased which increases the hydride stability (lower pressure plateau). The strain sensitivity of stability for these hydrides is extremely large, so only a small amount of strain is necessary to cause hysteresis.

A relationship was found which describes the hysteresis pressure difference in any one system as a function of temperature. This was expressed as $\ln(P_2/P_1) = \text{constant}$. A survey of the experimental data from the SmCo_5 , LaNi_5 , and FeTi hydride systems supports this relationship rather well.

The case of hysteresis in CeCo_5 and CeNi_5 hydrides was given special attention. Although the Co and Ni atoms are similar in all respects, their AB_5 compound hydrides react very differently. The CeNi_5 shows an enormous hysteresis; 240 atm in absorption and 50 atm in desorption at 25°C, whereas the CeCo_5 has only a fraction of one atmosphere difference in the absorption/desorption plateau pressure at 25°C. Also, the hydriding characteristics are quite different. CeCo_5 forms a CeCo_5H_3 hydride, whereas CeNi_5 forms a CeNi_5H_6 hydride. The small hysteresis of CeCo_5 hydride and the large hysteresis of CeNi_5 hydride are attributed to their different capacities to promote 4f electrons into the conduction band. The large hysteresis observed in MischmetalNi_5 hydride is attributed to the Ce content as a result of this analysis and a former investigation⁽¹⁾ conducted for the Advanced Research Projects Agency. Removal of the cerium can be accomplished easily during the extraction process from the mineral concentrate. The cerium-free, Mischmetal pentanickel compound hydrides readily and is much more stable. The hysteresis has been almost entirely removed by eliminating the Ce.

The third area of study conducted during this period was with LaNi_5 as a base for alloy additions. The objectives were to substitute for the nickel component with less expensive elements such as Mn, Fe, Cu or Zn and, in doing so, to gain insight into the factors determining the extent of hydrogen capacity in metal hydrides. The substitution must be done with pairs of elements. The effect is somewhat analogous to forming ferromagnetic alloys, known as Heusler alloys, from Cu and Mn (which in themselves are non-ferromagnetic). They bracket Fe in atomic number and are alloyed to replace Fe, employing a size effect relationship of the CuMn solid solution that averages out to that of Fe. Since Mn, Fe, or Co and Cu or Zn bracket Ni in atomic number, respectively without much change in size, they could be substituted appropriately in pairs. Hopefully, one could prepare a hydride of less expensive materials and still not decrease hydride capacity, or maybe increase capacity. Thus, an alloy with the composition $\text{LaCo}_{1.25}\text{Ni}_{2.5}\text{Cu}_{1.25}$ was selected as the first candidate to test feasibility. The phase equilibria are such that an essentially single-phase alloy would be expected. Metallography was employed to verify that this was the case. The alloy hydrided readily at room temperature to the H/alloy ratio of 5.5, which is excellent considering the cobalt content. The plateau has considerable slope in the as-cast specimen. Heat treatment has, as yet, been

unsuccessful in developing a single plateau. It appears instead that two or three distinct hydrogen occlusion modes will develop in this system as they have in others, e.g., $\text{LaCo}_5\text{-H}$ and FeTi-H .

The fourth area of study is currently being initiated. This is the hydriding characteristics of Ti-base, beta solid solutions. Selection of alloys is to be made in terms of the predictive correlation. Once the binary, Ti-base alloy hydride has been optimized, ternary alloy additions will be made for further optimization. The first binary system to be investigated is the Ti-Mo, binary system. Alloys are currently being prepared to initiate hydriding studies.

The fifth area of project activity was as follows: Design, procurement, and construction of a new Sievert's apparatus, and design, procurement, and construction of an activation apparatus.

Although a Sievert's apparatus with provision for three reaction chambers already exists and has been used on prior projects, it was felt necessary to expand the capabilities for increased screening and characterization studies for the ERDA program. Improvements in design and pressure capability have been incorporated in the new system which is provided with three reaction chambers each of which can be operated concurrently. The apparatus is essentially completed and will be operative in about a month.

In conjunction with the Sievert's apparatus, another activation unit is being assembled. It will allow pre-activation and sample break-in prior to conducting the absorption and desorption isotherms on candidate samples. The system has three stations to activate three samples simultaneously. It is fitted with a hydriding bed which will provide activation and cycling for several cycles automatically. The samples can then be removed easily without disturbing the reaction chamber atmosphere and moved to the Sievert's apparatus where quantitative characterization of absorption and desorption isotherms can be conducted.

ACKNOWLEDGEMENTS

The authors are grateful for the support of the Brookhaven National Laboratory under Contract No. 414771-S. Also, recognition must be given for the assistance of Dr. J. Liu, and the laboratory technicians, R. Nye and Y. Shinton.

REFERENCES

- (1) Lundin, C. E. and Lynch, F.E., "Solid State Hydrogen Storage Materials for Application to Energy Needs", Denver Research Institute University of Denver, Final Report No. AFOSR-TR-76-1124, August 1976, Under Contract to ARPA, Order 2552.
- (2) Lundin, C.E., Lynch, F.E., and Magee, C.B., To be published in November 1977, Journal of Less Common Metals.
- (3) Sandrock, G.D., Reilly, J.J., Johnson, J.R., Technical Paper 936T-OP, 11th IECEC, Proceedings September 1976, Nevada.
- (4) Van Mal, H.H., Buschow, K.H.J., Miedema, A.R., Journal of Less Common Metals, 49(1976) 473-475.
- (5) Shaltiel, D., Jacob I., and Davidov, D., Journal of Less Common Metals, 53 (1977) 117-131.
- (6) Pebler, A., and Gulbranson, E.A., Trans AIME, 239 (1967) 1593.
- (7) Lundin, C.E. and Lynch, F.E., Proceedings of International Symposium on Hydrides for Energy Storage, Geilo, Norway, Institutt for Atomenergi, August 1977.

A THERMODYNAMIC AND ECONOMIC STUDY OF VARIOUS TECHNIQUES FOR THE
LARGE SCALE PRODUCTION OF HYDRIDING GRADE FeTi

C.J. Trozzi and G.D. Sandrock
The International Nickel Company, Inc.
Paul D. Merica Research Laboratory
Sterling Forest, Suffern, NY 10901

Abstract

The intermetallic compound FeTi has considerable potential as a hydrogen storage medium. This paper represents a survey of possible large scale production methods for FeTi and related compounds. Direct and indirect reduction of ilmenite ore is considered in thermodynamic and economic detail. Results show that thermodynamics, economics and impurity effects make the direct production of FeTi from ilmenite unlikely. For the foreseeable future FeTi will be made by the melting of primary sponge Ti and scrap steel at final selling prices slightly above \$2.00/pound.

INTRODUCTION

Work at Brookhaven National Labs has shown that the intermetallic compound FeTi, along with related alloys, has considerable potential for use as a rechargeable hydride. This is the result of two factors: (a) it has attractive hydrogen storage properties in the vicinity of room temperature(1) and (b) it has the lowest raw materials cost of any presently known rechargeable hydride. As large scale engineering applications for FeTi-base alloys develop, it becomes important to establish the basic information on the metallurgy and production of the system to optimize the properties on a practical, multiton basis. This paper provides a survey of the thermodynamic and economic feasibility of producing FeTi by employing direct or indirect reduction of ilmenite ore and the direct melting of Ti and Fe metal. The factors considered were raw materials, process thermodynamics, effect of residual elements on hydriding capacity, and economics.

It has been established that FeTi is quite complex metallurgically and that a number of compositional factors must be considered in its production(2). The basic roles of Fe/Ti ratio, effect of O, N, C and Si contamination and the role of a number of ternary transition element substitutions have been established. A survey of the technical aspects of conventional induction melting was conducted and two new quasi-conventional melting techniques for large scale FeTi production were developed(2,3).

The thermodynamic and rough economic analyses of techniques which might conceivably be used to produce FeTi directly or indirectly from an ore have been investigated, discussed in detail(4) and will be summarized here. The study also involved the examination of the technical and economic feasibility of directly melting elemental titanium and iron.

The study was directed toward the achievement of a good quality hydriding grade FeTi. By this we mean a homogeneous alloy of about 54 wt. % Fe and 46 wt. % Ti with oxygen content less than 0.1 wt. %. Such an alloy should be capable of hydriding to a capacity on the order of $H/M = 0.85$ or more. The effect of other impurities (e.g., Al or Si) will be considered in context where appropriate.

SURVEY APPROACH

The basic information for the thermodynamic and economic calculations made below were derived predominantly from the following:

1. Open literature.
2. Personal contacts within the primary titanium and ferrotitanium industries.
3. Internal Inco information for comparable metallurgical processes or procedures.

Various sources of information have been utilized in this study. In some cases a given piece of information can be referenced. Often it represents internal information or a composite from several sources that cannot be readily referenced. The numbers used in this study are felt to represent valid estimates for 1977. Of course, in a study of this sort, there are always technical unknowns which could affect the end result. These unknowns have been identified wherever possible.

The technical processes surveyed were the following:

- A. Direct Reduction of Ilmenite
 1. Gaseous Reduction
 - a. Hydrogen
 - b. Carbon Monoxide
 - c. Methane
 2. Carbon Reduction
 3. Metallothermic Reduction
 - a. Silicon
 - b. Magnesium
 - c. Calcium
 - d. Aluminum
- B. Indirect Reduction Processes
 1. Chloride (Kroll) Process
 2. Electrolytic
- C. Conventional Melting of Primary or Scrap Ti
 1. Air Induction Melting
 2. Vacuum Induction Melting
 3. Consumable Electrode Arc Melting

It should be recognized that FeTi is not necessarily the optimum alloy for a given application. Because of this, along with the fact that the composition of the ore will vary over wide limits,

remelting and composition adjustment is mandatory for any of the direct or indirect reduction processes considered.

Any reduction method employed would require a final remelting, composition adjustment, and mischmetal (rare earth) deoxidation of the alloy product(2,3). Oxygen (greater than 0.1 wt. %) has a deleterious effect on the hydrogen storage capacity of FeTi, so its removal is desirable. Similarly, FeTi directly melted from elemental Fe and Ti should also be mischmetal treated. The small additional cost assures a high hydrogen capacity for vehicular applications and minimum decrepitation for stationary applications, as well as aiding activation(2).

The final number presented for each analysis is the FeTi selling price in \$/pound. This involves a mark-up from the overall production costs. The mark-up used throughout this study is 42%, based on the assumption of a 50% tax on income and a 15% after-tax return on sales. This mark-up can vary slightly with a number of factors, but we feel it is representative of the metallurgical industry that would be called upon to produce multimillion pound quantities of FeTi for energy storage applications.

ORE SOURCES - RUTILE VS. ILMENITE

In order to survey various processes for producing FeTi, a survey of raw material resources was necessary.

Titanium originates from two ores: rutile (nominally TiO_2) and ilmenite (nominally $FeTiO_3$). Rutile (generally ~96-98% TiO_2) is a higher grade ore than ilmenite, having a higher titanium content. Neither of these ores are totally free of other oxides. Ilmenite, however, contains more additional oxides than rutile. The U.S. has an abundance of ilmenite, but is dependent on Australia for rutile which is presently used in manufacturing, pigment, welding rod coatings and titanium metal. The increased rutile consumption has placed increased demands on rutile reserves and is subsequently driving prices up(5).

Rutile is 59% titanium, while ilmenite is only 31.6% titanium. Although the purity of rutile may seem attractive, it lacks the iron necessary for the production of FeTi. Since ilmenite contains a considerable amount of iron (both in the ilmenite phase and in the form of various iron oxides), it would be beneficial to find a method of reduction which would yield both titanium and iron metal simultaneously.

In view of our future energy situation, future raw material availability is a critical factor. The limited quantity of rutile leaves ilmenite as the only long range alternative. There are a wide variety of grades of ilmenite but that of the highest purity is desired for FeTi production.

Some typical ilmenite compositions are shown in Table I and Reference 4. The ilmenite concentrate, used as a basis for the calculations, is only one of the many concentrates available. The mineral analysis can vary widely from grade to grade. Therefore, the material and heat balance for each ore will be different. The ore price varies depending on the ore grade and lot size.

DIRECT REDUCTION OF ILMENITE

The primary reduction reactions ($FeTiO_3 \rightarrow Fe + TiO_2 + 1/2O_2$) and secondary reduction reactions ($TiO_2 \rightarrow Ti + O_2$) with reducing agents such as C, H, CO, Si, Al, Mg and Ca have been examined using basic thermodynamics. When examining the feasibility of applying each reducing agent, the following questions need to be asked: Is the reaction thermodynamically possible? How effectively does it reduce ilmenite? And in doing so, how much of the reducing agent residual is left in the alloy? Does this residual have a deleterious effect on its hydriding properties? How pure is the product?

The equation $\Delta G^\circ = -4.574 T \log K$ illustrates that at a given temperature ($^\circ K$) the equilibrium constant (K) and hence, the equilibrium state is determined entirely by the standard free energy change, ΔG° . Quantitative information on the chemical equilibrium state is given by either K or ΔG° . A value of K greater than 1 corresponds to a negative value of ΔG° , which means that when reactants and products are present in their standard states the reaction will proceed spontaneously toward equilibrium, as written. Consequently, the larger the negative free energy change is for a given reaction, the more likely it is that that reaction will take place. The values and equilibrium constants for the primary and secondary reactions involving each reducing agent have been calculated (for details see Reference 4). The primary reduction reaction involving each reducing agent is thermodynamically possible; but the degree to which the reduction will take place will depend on which reducing agent is employed. Complications arise during the secondary reduction reactions due to the large affinity Ti has for oxygen. Figure 1(6) illustrates the $Ti + O_2 \rightarrow TiO_2$ oxidation reaction (reverse for the reduction reaction) and its relationship with the oxidation curves of the reducing agents considered. A basic thermodynamic rule can be applied while referring to Figure 1. All of those elements which have " ΔG° vs. T " curves lying below the curve of the oxide being reduced are eligible as reducing agents for that oxide (corresponding to a negative free energy change), and it follows that the larger the free energy gap, the more effective the reducing agent will be. Elements associated with " ΔG° vs. T " curves lying above the curve of the oxide being reduced are not potential reducing agents (corresponding to a positive free energy change). In other words, for those reducing agents under consideration, that which has the largest equilibrium constant for the reduction reaction is the most desirable.

Titanium's great affinity for oxygen is a major drawback of all of the reduction processes considered. The partial free energy change per mole of oxygen has been plotted by Kubashewski et al(7) as a function of oxygen content in the Ti-O system. This curve illustrates the affinity Ti has for oxygen. Upon careful examination of the O-Ti phase diagram one can observe that there is no significant change in phases occurring between 1000°C and 1500°C. Therefore, even though Figure 2 has been calculated at 1000°C, it is reasonable to assume that it would have a very similar shape at temperatures up to at least 1500°C.

The graph illustrates that a reducing agent that

can overcome the affinity of oxygen to TiO_2 , Ti_2O_3 , Ti_2O_5 and TiO may not produce pure titanium owing to the affinity of oxygen dissolved in the metallic titanium. Therefore, thermochemical calculations which do not account for the solution phase may fail, reduction being less complete than would be expected from the calculations(7).

The heat of oxide formation is another factor which will affect the manner in which the reduction is carried out. If the reaction is endothermic (positive heat of oxide formation), then an outside heat source will be required to carry out the reaction. If the reaction is exothermic (negative heat of oxide formation), an outside heat source is not required in order to carry out the reaction. Any reserve heat left after the ore oxides are dissociated can contribute to heating the charge.

The elements which thermodynamics predicted could not be effective reducing agents for TiO_2 were not considered further. Those elements which looked promising were examined more closely (for details of the material, equilibrium calculations, balance, economics and heat balance, see Reference 4). Once the technical feasibility was established, the most important factor was economic feasibility. Calculations made for the reduction reactions which proved to be economically unfeasible (due to the high cost of reducing agent) were not carried out in great detail.

The arrival and growth of the steel industry brought a need for ferroalloys (i.e., Fe-Ti, Fe-Si, etc.). The three production methods employed were carbon reduction, silicon reduction and aluminum reduction.

Gaseous Reduction

Hydrogen Reduction. Hydrogen is utilized as a reducing agent in only a few limited cases. Ferrotitanium cannot be produced by ferroalloy producers in this manner because its stable oxides are not reducible by hydrogen. The equilibrium constant for the critical reduction reaction is one of the lowest of all reduction reactions considered. At temperatures in the vicinity of the melting point of FeTi (1623°K), the free energy change remains positive. It has also been shown that the equilibrium constant for the secondary reaction $TiO_2 + 2 H_2 \rightarrow Ti + 2 H_2O$ is $K = 7.18 \times 10^{-11}$ at 1623°K(4). Under equilibrium conditions only iron is reduced by hydrogen, leaving rutile (TiO_2) unreduced(8). Therefore, if this method were employed, subsequent reduction of TiO_2 by some other method (i.e., metallothermic) would be required. Thus, direct hydrogen reduction of ilmenite is thermodynamically unfeasible. Partial reduction with H_2 followed by subsequent reduction of TiO_2 with a more powerful reductant, though unexplored technically, may be of interest. However, this procedure does not offer any hope of a major production cost breakthrough.

Carbon Monoxide Reduction. Carbon monoxide is the least likely candidate for ilmenite reduction from a thermodynamic standpoint. The free energy to drive the reaction is positive throughout the entire temperature range under consideration. The secondary reaction $TiO_2 + 2 CO \rightarrow Ti + 2 CO_2$ near the melting point of the alloy has a very unfavor-

able equilibrium constant $K = 7.14 \times 10^{-12}$ (4).

Examination of the possibility of ilmenite reduction by CO illustrates that even if the reaction were achieved under special conditions, the formation of carbide would be favored. As mentioned below, carbon ties up titanium as TiC, thus hindering FeTi's H-storage capacity.

Methane Reduction. Recently some success in reducing titaniferous magnetite (i.e., a magnetite-ilmenite mixture) with CH_4 has been reported(9) although the thermodynamics tend to favor the ultimate formation of TiC; there appears to be a critical time-temperature realm where some of the TiFe phase can form. This represents a possibility for the production of FeTi from ilmenite, but information at this time is not adequate to judge either economics or technical feasibility on a commercial scale.

Carbon Reduction

Carbon reduction of TiO_2 is possible at high temperatures (Figure 1 - at temperatures above 1600°C where the $2 C + O_2 \rightarrow 2 CO$ curve lies below the $Ti + O_2 \rightarrow TiO_2$ curve). Carbon is a poor reducing agent for ilmenite at low temperatures, requiring a large amount of heat and therefore must be carried out in an electric arc furnace. Equilibrium constants for the primary and secondary reactions are shown in Reference 4. As illustrated by the equilibrium values and Figure 3, the titanium carbide reaction will tend to predominate. This is indicative of the fact that ferrotitanium alloys produced carbothermally (by the ferroalloy industry) have a high carbon content (~3-8%)(10).

Though reduction of ilmenite with carbon is thermodynamically possible, its employment in FeTi production is undesirable due to the residual carbon which takes the form of TiC and would very seriously inhibit its hydrogen storage capacity. Each weight percent carbon would tie up about 4%Ti as TiC. Thus an 8%C alloy would have only about 46-48% = 14% free titanium left for the formation of the FeTi phase. The capacity would be further lowered by substantial amounts of residual oxygen. Carbon reduced ilmenite would probably have less than 20% of the H-storage capacity of high purity FeTi.

Metallurgical Reduction

The principle by which metallothermic reduction takes place is very basic. A metal oxide can be reduced to metal by a particular metal reducing agent if that chosen reducing agent has a greater affinity for oxygen than that of the metal to be reduced. A complex equilibrium occurs in which those metals with higher affinity for oxygen will be found in the slag phase and those that do not will be found in the metallic phase.

The following basic considerations(11) must be made in order to determine the feasibility of producing titanium and iron from ilmenite, in a metallothermic process according to the general chemical equation:



*The chemical equation will require balancing, depending on the oxide and reducing agent employed.

M is the metal to be reduced.

X is another metal used as a reducing agent.

Y is some non-metallic element or radical.

- (1) Is the driving force of the reaction sufficient?
- (2) Will the reaction proceed to within a reasonable approach of completion?
- (3) Will sufficient heat be evolved to melt the products of reaction?
- (4) Will the reaction products separate?

Metallothermic reduction processes are batch processes which guarantee a carbon-free product. When employing this kind of process, there are two kinds of approaches, both of which are self-propagating reactions(12): (a) top igniting a mixture of powdered charge (reducing agent, ore, flux and boosters) and allowing the reaction to complete by itself (in-furnace or out-of-furnace) and (b) preheat the reducing agent (i.e., ingot form) and add the powdered charge to the top of the heat, thus allowing the preheated reductant to ignite the reaction (in-furnace). In the former approach, the process begins from the top and the products of reaction travel by gravity through the mixture to the entire mass. In the latter approach*, the fresh mixture travels by gravity through the hot reaction products.

Once the reaction is complete for an out-of-furnace application, the vessel is allowed to cool and the ingot is knocked out. The resultant slag layer, which has protected the ingot from the atmosphere, can be knocked off.

After a complete reaction in-furnace, the alloy and slag must be removed from the furnace and allowed to solidify. Application of an in-furnace method would only require furnace power to initially heat the reductant. Once the reaction is ignited, it will proceed without assistance.

Thermodynamically, there is free energy sufficient to drive the reduction reaction of ilmenite using Al, Mg or Ca as reducing agents. Each of these has an oxide with a large exothermic heat of formation, but which is not totally sufficient to carry out reduction of ilmenite metallothermically out-of-furnace(4). Each reduction reaction would require a thermal booster plus excess reducing agent to react with the booster to produce extra heat. The reaction efficiency will improve with the reduction of slag/alloy volume ratio. If the reduction were carried out in an electric arc furnace, a thermal booster and excess reductant would not be necessary and therefore the slag volume would be considerably reduced. Though furnace production insures greater efficiency, there is a risk of refractory contaminants.

There is associated with each of these reduction reactions, a high equilibrium constant(4) in the temperature range in which the reaction will take place (1600-1800°C). But Ti has a high affinity for oxygen, which is responsible for equilibrium inevitably occurring with a high concentration of

Ti in the slag phase, rather than in the metallic phase. Two factors which will help decide the technical feasibility of a reducing agent are its boiling point and its melting point. A good reaction is one which occurs above the reductant's melting point and below its boiling point. This maximizes the activity of the reducing agent and minimizes its loss to vaporization.

The calculations (heat and charge balance) made for metallothermic reduction of ilmenite are somewhat crude. It is not practical to burden the analysis with details which are subject to variations. Furthermore, for aluminothermic reduction of complex ores, calculations sometimes become unrealistic. In commercial practice the right proportions of the mixture are established by trial reductions on small batches.

In order to obtain a reasonable idea of production cost/lb FeTi, all calculations(4) have been based upon 100 kgs ilmenite concentrate (Chemalloy Co., Inc. ilmenite composition analysis as basis - Table I) the stoichiometric quantity of reducing agent, and 50% Ti recovery from the concentrate. The 50% Ti recovery assumption was based upon the thermodynamics extracted from the literature and industrial contacts. Economics has been considered only for those methods which have been proven thermodynamically feasible. In such cases the costs have been normalized to cost per pound of FeTi produced.

If a metallothermic process is employed, optimization will involve many variables(4).

Silicothermic Reduction. Silicon is an inefficient reductant for ilmenite and requires an electric arc furnace. There is enough free energy to drive the reaction to produce Fe and TiO_2 (4); however, reduction of TiO_2 by Si (Figures 1 and 3) involves a positive free energy change. Si is apparently a very weak reducing agent for Ti oxides over the entire temperature range of interest. Even though the presence of iron facilitates reduction, the final product is a low Ti-high Si alloy (i.e., ~30%Ti, ~30%Si)(10). The hydriding capacity of FeTi will be hindered by Si residuals(4). Thus from an overall point of view, silicon reduction of ilmenite is thermodynamically unfeasible.

Magnesiothermic Reduction. Magnesium, from a heat of reaction standpoint is a more efficient reducing agent than aluminum(13). One of its most unattractive characteristics in this application is its low boiling point (1103°C), since the smelting temperatures will be in the vicinity of 1800°C (some Mg will be lost as vapor). The melting point of pure MgO oxide is 2800°C. The iron oxide and titanium oxide products are good fluxes for MgO. Therefore, it is not likely that any additional flux would be needed to lower the slag melt point and increase slag fluidity. The heat generated by Mg oxidation is greater than that generated by Al(4). The slag which is composed of predominantly MgO and TiO is not as massive as that produced by aluminothermic reduction. A very important factor to consider when dealing with Mg powder is safe transport and handling.

Although the technical aspects of the process make utilizing Mg as a reducing agent undesirable, the factor that makes it impossible is the economics.

*This procedure may prove to be more explosive.

Good quality Mg powder presently costs \$2.20/lb. The material cost of Mg/lb FeTi has been listed in Table II as \$1.70. In calculating this value(4) excess Mg, which is necessary to react with a thermal booster and possible material loss due to vaporization, has not been accounted for. After calculating all possible costs involved using the out-of-furnace approach, including a mark-up for profit and taxes, magnesiothermic reduction will produce a FeTi alloy at approximately \$4.59/lb (out-of-furnace method).

In an effort to reduce the cost, one might be inclined to alter the process, to avoid using costly fine Mg powder in a mixture of powdered charge materials. Alternatively, magnesium (ingot) could be melted (in furnace) and the flux-core mixture top charged into the molten Mg and subsequently allowing the reduction reaction to take place. Though it may not greatly improve the technical feasibility, it can improve the economic feasibility because the current price per pound of Mg ingot (\$.98/lb) is half that of Mg powder. The approximate cost per pound FeTi produced would then be approximately \$2.26. The actual cost will undoubtedly be higher because of excessive Mg volatilization.

Calciothermic Reduction. The most desirable feature of calciothermic reduction is calcium's large heat of oxide formation, its high equilibrium constant associated with its reduction of ilmenite, and its low solubility in Ti metal. Although these factors meet the criteria for deciding a material's effectiveness as a reducing agent, there is much else to be considered. The boiling point of Ca (1482°C) is below the temperature at which the process will be carried out (some Ca will be lost as vapor), and its oxide melting point is 2580°C. The efficiency of a metallothermic reduction process depends on these factors. When reducing with calcium, similar problems will arise, as did when reducing with Mg. Calcium produces more of a problem because it rapidly forms an oxide layer in air at room temperature which would interfere with its effectiveness in reducing ilmenite. Handling and transporting calcium powder would be hazardous and expensive, requiring an argon atmosphere.

An estimated calculation was made in order to obtain approximate material cost(4). The producer price/lb calcium powder* (6 mesh) is currently \$2.13. The cost of calcium per pound of FeTi produced would be \$2.67 without accounting for excess Ca to react with booster, loss due to vaporization and dust loss. The thermicity of this reaction is greater than that obtained by reducing with either Al or Mg, but is insufficient to run the reaction. Therefore, the reaction will require some thermal booster for extraneous heat and a flux (if necessary) to lower the slag melting point and increase slag fluidity. The estimated alloy cost/lb FeTi produced employing calciothermic reduction out-of-furnace will be \$6.59 (Tables II and III). An alternate approach which would reduce the cost of the reducing agent is to melt Ca (crowns or ingot) and top charge the flux and ore into the molten Ca. In this case, the Ca charge could be composed of the cheapest form of Ca (crowns - 99.5% pure) at \$1.49/lb*.

The cost of Ca/lb FeTi produced would then be \$1.87 (NOTE: this does not account for excess Ca additions), and consequently (in-furnace) the approximate cost/lb FeTi would be \$3.91. This modification would be slightly more technically feasible and less hazardous than using Ca powder. But the high cost of Ca still makes it economically unfeasible. Consequently, calciothermic reduction of ilmenite is neither technically or economically desirable.

Aluminothermic Reduction. The most efficient aluminothermic reactions which produce a high metal recovery occur when a pure oxide is reduced (subsequently producing alumina slag and metal). The reactions are very short and therefore a minimum amount of heat is lost(12). The more complex the ore is the more it is burdened with secondary reactions. The slag will contain reaction products which will absorb a considerable amount of heat from the reaction and thus decrease its efficiency. Even though the equilibrium constant for Al reduction of ilmenite is high, a low Ti recovery (~50%) is expected, due to titanium's high affinity for oxygen. The 50% Ti recovery assumed was in agreement with a ferroalloy producer(14) who due to past experience with ferroalloy production informed us that a 40-50% Ti ferrotitanium alloy could be expected by this method (this implies a ~50% Ti recovery from the ore). Al will reduce FeTiO₃ to TiO₂(4). Analysis of the secondary reactions shows some TiO₂ reducing to TiO. The thermodynamics illustrates that the major reactions which take place insure Ti loss in the slag as oxide and Al residual in the alloy. The titanium recovery may be somewhat improved by reducing with Al in the presence of some nascent Fe (a good Ti solvent) which will help shift the equilibrium to the right(15).

An approximate slag and heat balance was calculated(4). The exothermic heat generated by the reaction is barely sufficient to dissociate the oxides in the concentrate. Therefore, a large amount of extra heat will be required to help reduce the ilmenite and melt the charge and slag. Assuming approximately a 30% heat loss in an out-of-furnace application, the final quantity of extra heat which is needed to carry out the reduction process must be supplied by an external heat source (booster or furnace).

A flux addition is necessary to reduce the Al₂O₃-TiO slag melting point and to increase the fluidity. Lime was considered as the most appropriate flux. CaO is a more basic oxide than TiO and weakens its bond with Al₂O₃, facilitating a more efficient reduction(10).

The aluminothermic reduction of ilmenite will take place above the melting point of Al (659°C) and below its boiling point (1800°C), where Al has a higher activity, making Al more technically attractive than any other reducing agent.

A stoichiometric Al addition will generally produce a 5-10% Al alloy (as produced by various ferrotitanium producers). As illustrated in Figure 4, Al greatly reduces the H-capacity of FeTi. Since the steel industry has little concern for the residual Al in ferrotitanium, the ferroalloy industry optimization requires maximizing Ti recovery. However, since our interests lie in producing a pure FeTi intermetallic compound with

*Chas. Pfizer, Inc.

good hydriding properties, the most critical factor involved in its production is the residual elements, especially Al. Therefore, optimization would involve minimization of the Al content, regardless of Ti recovery. Even if Al residuals as low as 1-2 wt. % were achieved by optimizing, the hydrogen storage capacity would be hindered. Any Ti deficiency could be corrected by adding Ti sponge during remelting.

Purity of the alloy product is questionable. Only experimental trials will indicate applicability of this process. It is doubtful that aluminothermic reduction will produce a pure enough product for hydriding purposes, even after remelting and deoxidation.

From an economic standpoint Al reduction of ilmenite is the least costly, and creates the fewest technical difficulties(4). The total price/lb FeTi has been estimated (Table II) to be \$1.93/lb FeTi (out-of-furnace method). Alternatively, in an effort to reduce the cost of Al/lb FeTi (\$.34), utilizing Al ingot in place of powder had been considered. This approach would involve melting Al ingot in a furnace, and top charging the ore, flux and thermal booster (mixture). The high temperature of the Al should ignite the mass. Al ingot is \$.51/lb, and therefore cost of Al/lb FeTi is reduced to \$.29/lb FeTi. The total estimated price/lb FeTi would then be \$1.62.

INDIRECT REDUCTION PROCESSES

Chloride (Kroll) Process

All primary sponge is made by the Kroll (or closely related Hunter) process. Usually rutile is chlorinated and the resultant chlorides purified to produce high purity $TiCl_4$. The $TiCl_4$ is then reduced with Mg to form Ti metal and $MgCl_2$ (Na is used as the reductant in the Hunter process). After leaching or inert gas purging out the $MgCl_2$ the result is Ti sponge which forms the basis of the metallurgical Ti industry.

It has been well established that ilmenite can be directly chlorinated and the resultant chlorides purified to produce a $TiCl_4$ that can be Mg reduced in a Kroll vessel to produce Ti sponge(16). Ilmenite will no doubt be the future feedstock for the Kroll process when rutile runs out.

For the purpose of producing FeTi directly, let us consider taking the unpurified mixed chloride product of ilmenite chlorination ($TiCl_4$, $FeCl_3$, plus various impurity chlorides) and Kroll reduce that with Mg to form a Fe-Ti alloy sponge. From a technical point of view it is not completely clear that this can be done because $FeCl_3$ first condenses as a solid and $TiCl_4$ condenses as a liquid so that the condensed mixed chlorides will be in a pasty form that may be hard to feed into a Kroll reaction vessel. It is felt that the resultant FeTi alloy will be very inhomogeneous and will certainly require remelting. A final technical unknown is the fact that impurity chlorides (e.g., those of Si, Mn, Mg, V and Al) will be produced along with $TiCl_4$ and $FeCl_3$ during the ilmenite chlorination process and will be incorporated into the final product.

Even if the above technical problems can be

overcome with the chloride process, there remain serious economic problems. A cost estimate based on this procedure is outlined in Table II. The final estimated FeTi price is high, about \$3.00/lb FeTi. The key problem, of course, is that a relatively expensive process and relatively expensive Mg is used to reduce the relatively cheap Fe component in addition to Ti. Thus, the mixed chloride process seems to be unfeasible from an economic point of view, if not a technical point of view. As will be shown later it offers no advantages over the direct production of Ti sponge and the remelting of that sponge with scrap Fe.

Molten Salt Electrolysis

It is possible to produce quality Ti by electrolyzing. The process involves the electrolytic decomposition of $TiCl_4$ in a molten alkaline or alkaline earth electrolyte(17). No commercial size cells are yet in operation, although substantial pilot scale experience has been obtained by the Timet Division of The Titanium Metals Corporation of America(18). Electrolytic Ti production has an advantage over the Kroll process in that its operating costs are lower. However, capital equipment costs are significantly higher, the process requiring carefully constructed, gas-tight, high temperature cells. When both operating and capital cost considerations are taken into account, it is felt that the final selling price of electrolytic Ti could be about 10% lower than present sponge made by the Kroll process.

The question at hand is "Could FeTi be made directly by simultaneous electrolytic co-deposition of Fe and Ti using mixed $TiCl_4$ + $FeCl_3$ feedstock from chlorinated ilmenite?" Although it is impossible to completely answer this without extensive experimental study, the answer is probably "no" both from technical and economic points of view. First, from a technical point of view, it has been observed that as $FeCl_3$ is added to the $TiCl_4$ feedstock, the resultant electrodeposit becomes extremely fluffy with a high surface area(18). Such a structure is subject to corrosion and oxygen pickup during handling and can even be pyrophoric! The homogeneity of such a product is doubtful and would certainly require remelting. Finally, with respect to economics, we are saddled with an analogous problem to the production of FeTi. In this case we are using expensive equipment and expensive electric power to produce the Fe component of FeTi. It is impossible to make an accurate cost estimate at this time. However, it seems reasonable to assume that electrolytic FeTi, if technically feasible, would cost at least 90% of the price of Kroll reduced FeTi, i.e., at least \$2.70/lb.

DIRECT MELTING OF ELEMENTAL Fe AND Ti

All of the FeTi production schemes discussed so far have components of doubt for technical and economic reasons. If a large market for hydriding grade FeTi developed tomorrow, the only certain way of producing it would be by direct melting of the elements. In this section we discuss the economics of melting. In all cases it will be assumed that the source of the iron would be scrap steel at \$0.05/lb (\$100/ton). We will consider both scrap and primary sponge for the Ti source.

Melting with Scrap Ti

The melting of FeTi from scrap Ti provides interesting problems in terms of scrap availability and price. At first glance it would seem that substantial quantities of scrap are available. The U.S. titanium industry produces more than 30 million pounds of scrap annually(19). However, virtually all of this is either recycled in the Ti industry or used in the steel or aluminum industry as an alloying element. Furthermore, most of the scrap is of an aerospace grade and contains a substantial amount of Al (e.g., the most common aerospace alloy is Ti-6Al-4V). Because of the extremely deleterious effect of Al on hydriding behavior (Figure 4), it appears that the Al-containing scrap, which probably constitutes more than 90% of the scrap, will be unusable for hydriding grade FeTi.

The remaining commercial purity (CP) grade scrap is in high demand and it commands a price premium over the rest of the scrap. The price of Ti scrap is rather volatile(4). CP grade scrap must be used in the melting of hydriding grade FeTi and its limited availability would support only a small level of FeTi production (at most only a few hundred thousand pounds) before driving the scrap price to near that of primary sponge Ti.

Cost estimates have been developed, bearing the above difficulties in mind, for the air induction melting of scrap Ti and scrap Fe using the 4% rare earth deoxidation procedure developed earlier in this contract(2,3). The basic calculations are shown in Reference 4 and the results outlined in Table II. The results of these calculations are shown as a function of scrap price (Ti) and recovery (R)(4). Based on an early 1977 CP scrap Ti price of \$1.55/lb and an anticipated recovery of 80%, a FeTi price of \$2.00/lb is calculated. Again bear in mind this price is artificial and would rapidly escalate if much additional demand were put on scrap CP titanium.

Melting with Sponge Ti

In the end it appears that the only guaranteed method of producing multimillion pound quantities of hydriding grade FeTi is the direct melting of primary Ti sponge and scrap Fe. The present U.S. sponge capacity is on the order of 50 million pounds per year with substantial additional quantities available as imports from Japan and the U.S.S.R.(19). At present most plants are operating below capacity so that a new market of several million annual pounds of FeTi could be tolerated without difficulty. If a substantially larger FeTi hydride market should develop, then new installed capacity would be required. It would probably be electrolytic and result in a slightly lower Ti price (perhaps 10%, as cited earlier).

Price estimates for the production of FeTi from sponge Ti and scrap Fe are outlined in Table II for: (a) air melting with mischmetal deoxidation(2, 3), (b) vacuum induction melting in a graphite crucible(2,3), and (c) consumable electrode, vacuum arc melting. Calculations are based on 10,000 pound melt sizes. The price we used for Ti sponge was \$2.50/lb [the present published price ranges from \$2.50/lb for imported sponge to \$2.75/lb for domestic sponge(20)]. For the vacuum melting no mischmetal is required for deoxidation

purpose; however, 1% was added to aid in activation(2).

Of the three techniques considered, air melting is more expensive, primarily because of the relatively low recovery associated with the rare earth deoxidation technique (see Ref. 2). Vacuum induction and vacuum arc melting are lower in cost and are almost the same, within the accuracy of the calculations (on the order of \$2.20/lb). These calculations assume the purchase of Ti sponge at the \$2.50 from a Ti producer by a melter who is not a Ti producer. If the melting were done by one of the major sponge producers (i.e., Timet, RMI, or Oremet), some of the profit may be absorbed in the primary sponge operation resulting in a somewhat lower effective markup than the 42% we used. However, it still seems unlikely to us that a price much lower than about \$2.00 for good hydriding grade FeTi can be expected.

SUMMARY AND GENERAL COMMENTS

All of the obvious methods of producing FeTi have been briefly examined from technical and economic points of view. To put things into perspective, the main results(4) for each method are summarized and compared in Tables II and III). The overall picture is pessimistic. The lowest FeTi price (\$1.64/lb) was obtained with aluminothermic reduction, although this result is rather clouded by the fact that the Al residual lowers hydrogen storage capacity greatly(4). The only sure procedures are vacuum induction and arc melting of primary Ti and scrap Fe which narrow down to a FeTi price slightly above \$2.00/lb.

Although ilmenite ore is very abundant and fairly cheap, we are dealing with a fundamental chemical problem of nature - the intensely strong bond between Ti and oxygen atoms. The energy required to break that bond is large and therefore the extractive metallurgy of Ti is expensive, just as it is with all other "energy intensive" metals. The problem is further complicated by the apparent fact that good hydriding grade FeTi is not tolerant of impurities, especially Al and O.

The solution to this dilemma is not obvious. There is always hope of a new breakthrough that will substantially lower the cost of Ti or FeTi extraction from ilmenite. Within the present state of the art there is little hope for an immediate or even long term cost reduction of any significant size. There are a number of things that can be examined further: CH_4 reduction, perhaps more thorough studies of electrolytic processes, a metallothermic reduction using a combination of reductants, quaternary additions to FeTi to counteract the negative Al effect, etc. In the end, however, what is needed is a radical new approach to the extractive metallurgy of Ti. Nature seems to have made this a very formidable task.

ACKNOWLEDGEMENTS

We are grateful to a number of individuals at Inco, Brookhaven, and numerous outside industrial organizations.

REFERENCES

1. Reilly, J.J. and Wiowall, Jr., R.H., *Inorganic Chem.*, 13 (1974), p. 218.
2. Sandrock, G.D., *Interrelations Among Composition, Microstructure, and Hydriding Behavior for Alloys Based on the Intermetallic Compound FeTi*, The International Nickel Company, Inc., Final Report, BNL Contract 352410S, June 30, 1976.
3. Sandrock, G.D., *New Melting Techniques for the Production of Hydriding Grade FeTi*, Proceedings of the ERDA Contractors Review Meeting on Chemical Energy Storage and Hydrogen Energy Systems, Airlie, VA, Nov. 8-9, 1976, ERDA Report CONF-761134, p. 143.
4. Sandrock, G.D. and Trozzi, C.J., "Thermodynamic, Economic, and Metallurgical Studies of Various Techniques for the Large Scale Production of Hydriding Grade FeTi and Related Compounds", Final Report, Contract BNL 352410S (Second Year), in preparation.
5. Elger, G.W., Kirby, D.E., Rhoads, S.C., and Stickney, W.A., *Synthesis of Rutile from Domestic Ilmenites*, Bureau of Mines, RI-7985, U.S. Department of Interior, 1974.
6. Richardson, F.D. and Jeffes, J.H.E., *J. Iron Steel Inst.*, 160, 261, 1948.
7. Kubaschewski, O., Evans, E. LL. and Alcock, C.B., *Metallurgical Thermochemistry*, Pergamon Press, 1967.
8. Shomate, C.H., Naylor, B.F. and Boericke, F.S., *Thermodynamic Properties of Ilmenite and Selective Reduction of Iron in Ilmenite*, Report of Investigations, Bureau of Mines, U.S. Department of Interior, May 1946.
9. Ajersch, F., *Ecole Polytechnique de Montreal*, private communication.
10. Elyutin, V.P., Paulov, Yu A., Leuint, B.E., Alekseev, E.M., *Ferrotitanium, Production of Ferroalloys*, The State Scientific and Technical Publishing House, Moscow, 1957, p. 318.
11. Pargeter, J.K., *The Production of Ferroalloys by Exothermic Reduction of Metallic Oxides*, unpublished report.
12. Saklatwalia, B.D., *Thermal Reactions in Ferroalloy Metallurgy, the Basis of Alloy Steel Development*, Transactions of the Electrochemical Society, Vol. 84, 1944, p. 13.
13. Belitskus, D., *Aluminothermic Production of Metals and Alloys*, *Journal of Metals*, January 1972, p. 30.
14. Deeley, P., Spindelow, H. and Jennings, J., *Shieldalloy Corporation*, private communication.
15. Volsky, A., Sergievskays, E., *Theory of Metallurgical Processes*, (Russian) Translated by Ivan Saviu, MIR Publishers, Moscow 1971.
16. Dooley, III, G.J., *Titanium Production: Ilmenite vs. Rutile*, *Journal of Metals*, March 1975, p. 8.
17. Tukumoto, S., Tanaka, E. and Ogisu, K., *The Deposition of Titanium Metal by Fusion Electrolysis*, *Journal of Metals*, Nov. 1975.
18. Palmer, H.R., *Timet Research Labs*, Henderson, NV, private communication.
19. Wood, R.A., *The Titanium Industry in the Mid-1970's*, MCIC Report 75-26, Metals and Ceramics Information Center, Battelle, Columbus, OH, June 1975.
20. *American Metal Market*, Vol. 85, No. 108, Monday, June 6, 1977.

Table I

Chemical and Mineral Composition Analysis of Various Ilmenite Ores

Typical Analysis

Chemical Composition* (Wt. %)		Chemical Composition** (Wt. %)		Mineral Composition**	
TiO ₂	59.8	% TiO ₂	59.54	Ilmenite & Altered	
Fe ₂ O ₃	23.0	% Fe ₂ O ₃	25.11	Ilmenite	96.6
FeO	12.0	% FeO	9.19	Rutile	0.5
Al ₂ O ₃	2.0	Fe (Total)	24.63	Zircon	1.3
SiO ₂	1.2	Al ₂ O ₃	1.18	Sillimanite	0.4
Alkaline Earths	0.05	CaO	0.08	Garnet	0.3
S	0.03	MgO	0.88	Quartz	0.5
P	0.05	SiO ₂	1.19	Monazite	0.4
		MnO	0.42		100.0
		V ₂ O ₅	0.22		
		Cr ₂ O ₃	0.13		
		P ₂ O ₅	0.18		
		Nb ₂ O ₅	0.17		
		ZrO ₂	0.48		
		S	0.002		
		C	0.019		
		Loss on Ing. (900°C)	1.70		

*Chemalloy, Inc., Bryn Mawr, PA.

**N.L. Industries, Inc. [ore source - Quilon (India)].

Table II

Production Cost Estimates for FeTi(4) (in \$/lb FeTi)Cost Estimate for Reduction of FeTi by Metallothermic Reduction

Process	Total Material		Processing		Remelt & Deoxidation		Total Alloy		42% Markup/lb		Final Alloy	
	Cost/lb		Cost/lb		Cost/lb		Cost/lb		Cost/lb		Price/lb	
	Out*	In**	Out*	In**	Out*	In**	Out*	In**	Out*	In**	Out*	In**
Magnesiothermic	2.69	.98	.13	.20	.41	.41	3.23	1.59	1.36	.67	4.59	2.26
Calciothermic	4.05	2.09	.18	.25	.41	.41	4.64	2.75	1.95	1.16	6.59	3.91
Aluminothermic	.81	.59	.13	.20	.41	.41	1.35	1.14	.57	.48	1.92	1.62

Cost Estimate for Production of FeTi by the Chloride (Kroll) Process

Total Material	Processing	Vacuum Induction Melting & Deoxidation	Final Alloy
Cost/lb	Cost/lb	Cost/lb	Price/lb
1.00	.80	.31	3.00

Cost Estimates for Production of FeTi by Directly Melting Fe and Ti

Materials	Total Material Cost/lb	Processing and Melting Cost/lb	Total Cost/lb	Final Alloy Price/lb
Scrap Ti & Fe	.03 + .462 Ti***	0.38(Air Melt & 5%MM Deoxidize)	0.41 + 0.462Ti R***	1.42 (.41 + 0.462Ti) R
Sponge Ti & Scrap Fe	1.19	0.42(Air Melt & 5%MM Deoxidize)	1.62	2.87
Sponge Ti & Scrap Fe	1.19	0.31(Vac. Ind. Melt & 1%MM Deoxidize)	1.52	2.20
Sponge Ti & Scrap Fe	1.19	0.37(Consumable Elec. Vac. Melt & 1%MM Deoxid.)	1.56	2.26

TABLE III

SUMMARY OF FeTi PRODUCTION PROCESSES STUDIED

Technique	Estimated FeTi Price, \$/lb.	Technical Problems Anticipated
H ₂ Reduction of Ilmenite	--	Thermodynamically unfeasible.
CO Reduction of Ilmenite	--	Thermodynamically unfeasible.
CH ₄ Reduction of Ilmenite	?	Probably difficult to control on commercial basis to prevent TiC formation.
C Reduction of Ilmenite	--	Thermodynamically impractical. Strong tendency toward TiC formation.
Silicothermic Reduction of Ilmenite	--	Thermodynamically unfeasible.
Magnesiothermic Reduction of Ilmenite	2.26*/4.59**	High vapor pressure of Mg may make process impractical or result in very low recoveries.
Calciothermic Reduction of Ilmenite	3.91*/6.59**	High vapor pressure of Ca may make process impractical or result in very low recoveries.
Aluminothermic Reduction of Ilmenite	1.62*/1.92**	High Al and O residuals will probably lower hydrogen capacity.
Molten Salt Electrolysis	2.70?	Deposition problems when Ti and Fe chlorides mixed. Impurities may reduce capacity. May be difficult to handle mixed chlorides.
Chloride (Kroll) Process	3.00	
Air Induction Melting of Scrap Ti and Scrap Fe	2.00+	Requires CP Ti scrap of limited availability
Air Induction Melting of Scrap Fe and Sponge Ti (MM Deoxidation)	2.87	Recovery, slag handling, and crucible cleanup.
Vacuum Induction Melting of Scrap Fe and Sponge Ti (Graphite Crucible)	2.20	None.
Consumable Electrode Vacuum Arc Melting of Scrap Fe and Sponge Ti	2.26	None.

*Required for an out-of-furnace process (booster substitutes for furnace power).

**Required for an in-furnace process, without booster.

***Variable price of Ti and recovery R.

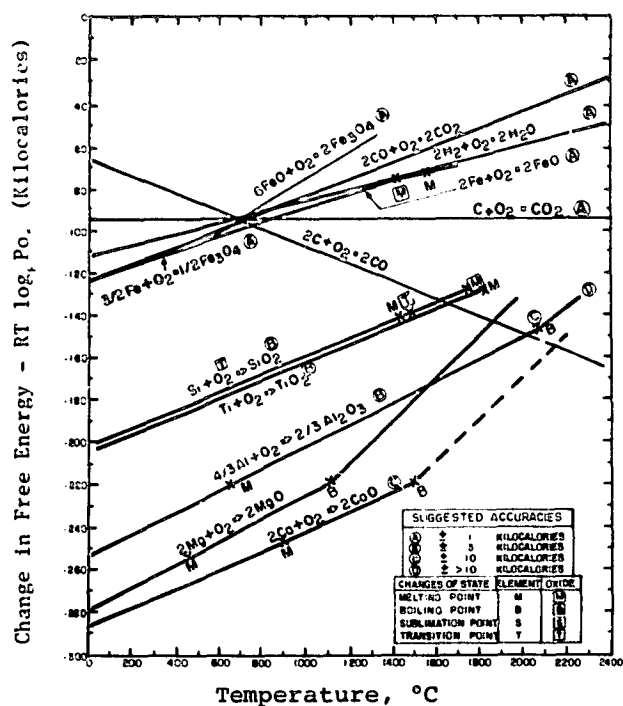


Fig.1. Standard free energy of formation of oxides(5,6)

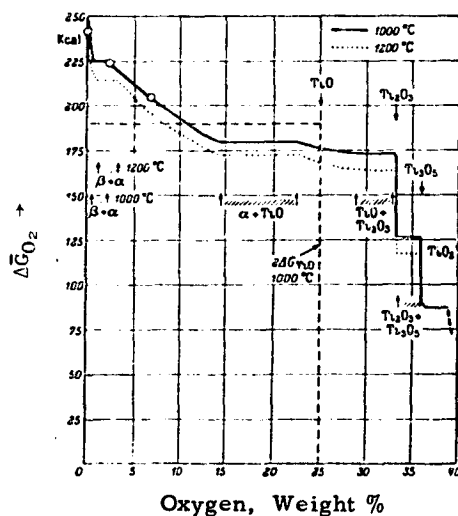


Fig.2. Partial free energies of dissociation of 1 mole oxygen in the titanium-oxygen system(7, p. 54)

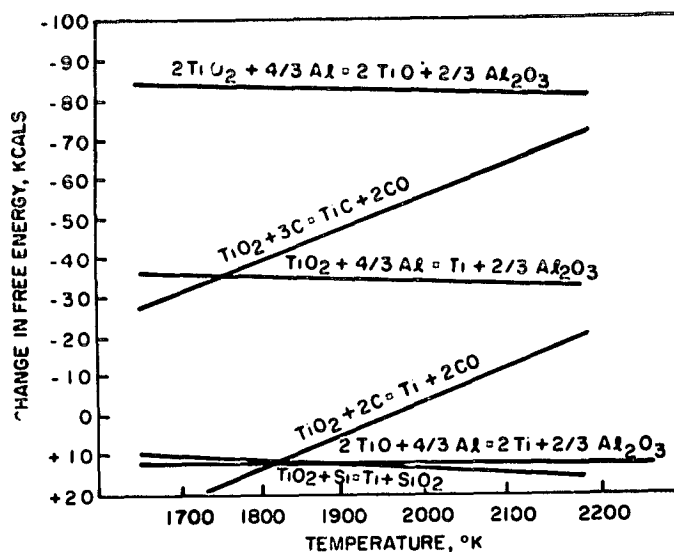


Fig.3. Dependence of the free energy of reduction of titanium oxides on the temperature(10)

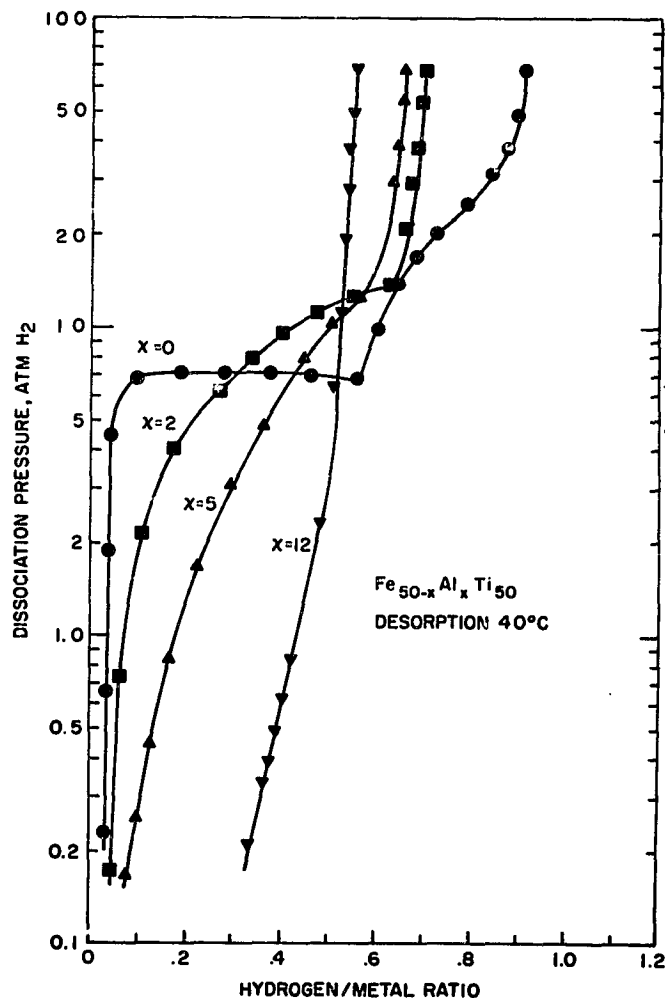


Fig.4. Effect of Al-content x on the 40°C desorption isotherm of Fe_{50-x}Al_xTi₅₀ alloys(4)

STATIONARY HYDRIDE VESSEL OF LARGE DIAMETER-
PROGRAM PLAN

Roger E. Fillings, Ronald L. Woolley and Jack H. Ruckman
Billings Energy Corporation
Provo, Utah 84601

Abstract

A metal hydride vessel of engineering scale has recently been installed as a peak shaving component of the BEC "Hydrogen Homestead." Operational performance and vessel behavior are to be computer monitored for a one-year period. Of particular interest are heat transfer characteristics and the consequence of hydride packing in a large hydride vessel with a hemispherical end cap. This paper discusses planned experiments and operation of the vessel. Instrumentation debugging is now proceeding preparatory to the start of data collection.

I. INTRODUCTION

Hydrogen provides a common energy carrier that unites all energy resources with all energy users. The purpose of the "Hydrogen Homestead" is to demonstrate this fact with working hardware. A key component is a metal hydride storage vessel. Energy demand in a home fluctuates. Hydrogen production from many energy resources such as wind or solar energy is also nonuniform and may cease for several days. Storage of hydrogen is thus an essential part of a successful system.

II. SYSTEM DESCRIPTION

In the first phase of the homestead, hydrogen will be produced by electrolysis using electricity generated by hydroelectric, wind, coal, or solar energy (Fig. 1).

Hydrogen will pass through a water trap and then flow either directly to the homestead or into the hydride vessel, passing first through an oxygen catalyst and a molecular sieve dryer before entering. Homestead uses of hydrogen are as follows: 1) a Cadillac Seville that may be switched from hydrogen to gasoline while driving, 2) a Jacobsen lawn and garden tractor, 3) oven, 4) range, 5) barbeque, 6) fireplace log, 7) hot water supplementary heat when solar energy is inadequate, and 8) a hydrogen boiler to aid the heat pumps in the winter.

Low grade heat for dissociation of the hydrogen from the hydride will come from two sources: solar energy and reaction heat when the alloy is hydrided. Both energies will be stored in a 275 gallon (1041 l) water tank for later use. Water will be circulated continuously between the holding tank and a belt water jacket around the hydride vessel midriff in an attempt to maintain temperature uniformity at a level consistent with the solar collectors (approximately 131° F or 55° C). Temperature nonuniformity, pressure, tank expansion, and other data will be monitored and reduced by a BCC microcomputer.

A specially designed electrolyzer will produce 3 pounds/day (1.4 Kg/day) of hydrogen at a pressure of 500 psig (3450 KPa) continuously. At this supply pressure, the hydride will approach maximum loading even though the temperature is elevated. Starting from these nominal operating conditions of elevated temperature and pressure, the vessel should be capable of discharging three or more days of production without additional heat transfer because of the thermal capacity of the hydride. Discharge of the remainder of the contents will be limited by the heat exchange rate and by heat conduction within the hydride bed.

In order to monitor the temperature

nonuniformity, thermistor probes have been inserted into the hydride bed and placed around the vessel periphery. Pressure taps have been placed at four locations to monitor pressure drop through the bed. The pressure sensors will also reveal possible filter clogging.

The pressure vessel (Figure 2) consists of two hemispherical end caps joined by a cylindrical section (internal diameter=36.5 inches=92.7 cm, internal max height of bed=46.4 inches=118.4 cm). This low carbon steel vessel is fitted with pressure taps, a hydrogen flow port with a 5 micron filter, a hydride sample port, a sight glass (Figure 3), and a loosening jet arrangement at the base. Approximately 4,000 pounds (1814 Kg) of titanium-iron manganese-alloy is contained within the vessel (Ti₅₁ Fe₄₄ Mn₅). It was activated externally and then poured into the vessel at an overall vessel density of 190 lb/ft³ (3040 Kg/m³).

III. EXPERIMENTS

A number of experiments are planned to define the operating characteristics of the system and the behavior of the vessel. These are as follows:

1. Total hydrogen capacity at equilibrium.
2. Discharge capacity at constant flow rate (set by flow controller and mass flowmeter).
3. Change of hydride particle (Fig. 4) size and activity with time (sample removed periodically).
4. Pressure drop through the bed.
5. Pressure drop across the filter.
6. Temperature profile within hydride bed.
7. Temperature gradient on vessel surface.
8. Heat transfer to circulation water.
9. Filter clogging.
10. Alloy mobilization in the outlet gas stream.
11. Change in tank girth with pressure, temperature, and hydride packing.
12. Visual observation of hydride motion and size change.
13. Effectiveness of loosening jets in breakup of hydride packing and lock-up.
14. Effectiveness of circulation of heat-

od hydrogen in discharging the vessel.

IV. CONCLUSIONS

Tests of the metal hydride storage vessel, a component in the BEC Hydrogen Homestead, will provide engineering scale information relative to the use of hydriding alloy in a pressure vessel. Data on heat transfer, pressure drop, working capacity, and changes in vessel dimensions

will be gathered in the program. The storage vessel represents practical application of new technology as an important part of an independent energy system.

V. ACKNOWLEDGEMENT

This program is sponsored by the U.S. Department of Energy under a subcontract with the Brookhaven National Laboratory.

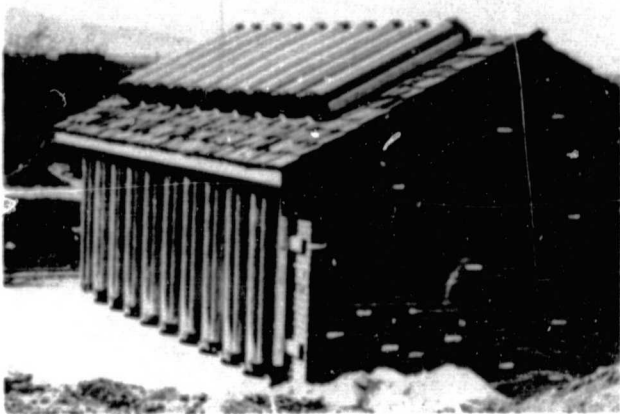


Fig. 1. Solar collectors on roof and side of energy shed

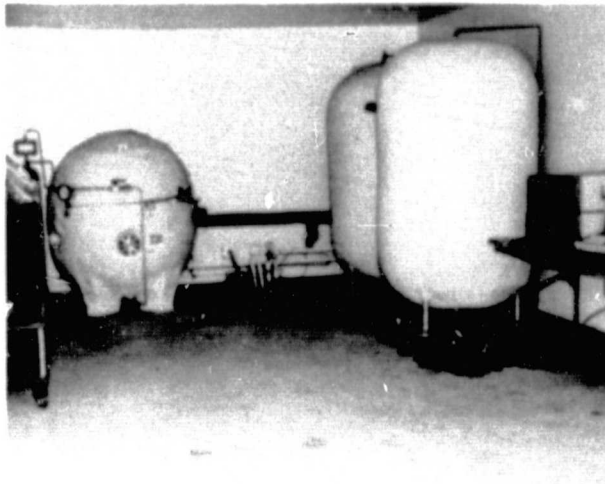


Fig. 2. Inside energy shed from L to R: electrolyser, metal hydride vessel, hot water storage tanks, and computer monitoring system

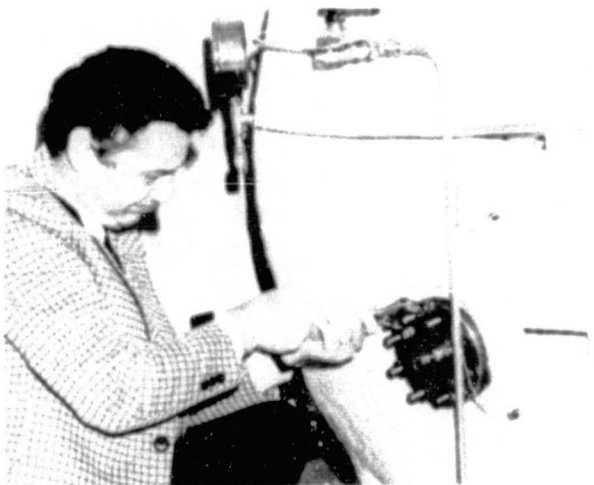


Fig. 3. Removing protective cover to expose sight glass

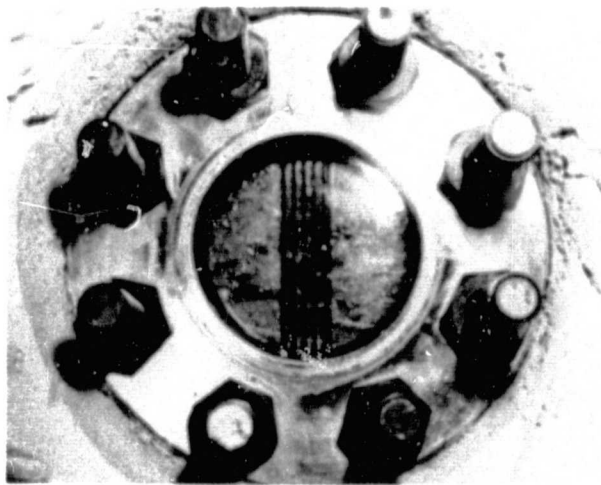


Fig. 4. Metal hydride particles within vessel

SESSION V
SYSTEM STUDIES

HYDROGEN AS A CHEMICAL FEEDSTOCK (STUDY AND WORKSHOP)

C. J. Huang
University of Houston
K. K. Tang
Jet Propulsion Laboratory

USE OF HYDROGEN ENERGY SYSTEMS TO IMPLEMENT SOLAR ENERGY

T. Fujita, C. Miller, K. H. Chen, G. Voecks, and W. Mueller
Jet Propulsion Laboratory

**SOLAR-CHEMICAL ENERGY CONVERSION AND STORAGE:
CYCLOHEXANE DEHYDROGENATION**

A. B. Ritter, G. B. DeLancey, J. Schneider, and H. Silla
Stevens Institute of Technology

**SYSTEM EVALUATION OF SUPPLEMENTING NATURAL GAS SUPPLY
WITH HYDROGEN**

W. S. Ku
Public Service Electric and Gas Company

**HYDROGEN FROM FALLING WATER: ASSESSMENT OF THE RESOURCE
AND CONCEPTUAL DESIGN PHASE**

W. J. D. Escher
Institute of Gas Technology
J. P. Palumbo
Pennsylvania Gas & Water Company

HYDROGEN ENGINE/STORAGE SYSTEM -- APPLICATION STUDIES

A. M. Karaba and T. J. Pearsall
Teledyne Continental Motors

**HYDROGEN AS A CHEMICAL FEEDSTOCK
(STUDY AND WORKSHOP)**

**C. J. Huang
University of Houston
Houston, Texas 77004**

**K. K. Tang
Jet Propulsion Laboratory
California Institute of Technology
Pasadena, California 91103**

Abstract

The objective of this study and workshop is to determine steps which can, and should, be taken to enable and encourage a shift in the chemical industries from natural gas and naphtha as hydrogen sources to other energy forms.

Preliminary findings of informal interviews conducted prior to the workshop are summarized for key segments of the hydrogen market. Plans for the workshop to be held in December, 1977 are discussed.

HYDROGEN AS A CHEMICAL FEEDSTOCK (STUDY & WORKSHOP)

1. INTRODUCTION

Current hydrogen use in the U.S. is dominated by applications in the chemical and petroleum industries, with a projected annual growth during the next 25 years of between 6 and 12 percent. The supply of the traditional hydrogen feedstocks, principally natural gas, is becoming a problem. This will tend to increase the market penetration of hydrogen produced from feedstocks and techniques less affected by increasing scarcity and rising cost. New government energy policies may accelerate this trend toward non-traditional sources, particularly from coal in the near future.

The HEST study quantified the supply and use of hydrogen in the U.S., developed projections for the balance of the century, and identified alternatives to the present practices. The alternative High vs Low Merchant to Captive ratios for Hydrogen Supply scenarios were developed and documented in Hydrogen Tomorrow (Ch. III and IV). For each industry, the fractions of hydrogen which could be supplied as merchant were calculated. This was done based on extensive contacts with the industries involved in addition to, and as a basis for, our own analyses.

The present study is intended to determine steps which can, and should, be taken (particularly by the government) to enable and encourage a shift in the chemical industries from natural gas and naphtha as hydrogen sources to other energy forms. This may come about through merchant supplies of hydrogen, or through shifts in captive production to the other energy forms. The steps may include technology enhancement, further analyses or assessments, or recommended regulatory modifications. The technologies may be in the areas of hydrogen production, delivery or storage.

The study will interface closely with the University of Houston Workshop (see Sect. 3), using the workshop as a data source. It will concentrate on the chemical and petro-chemical industries but will consider other users of hydrogen as appropriate. Alternative hydrogen production from coal gasification, electrolysis, and heavy oil will be considered. For each industry, the needed mixtures of gases with hydrogen, and the value of hydrogen purity will be determined, as will the prospects of biproduct utilization.

It is anticipated that the workshop and study will identify and lead to approaches for significant conservation of natural gas and petroleum distillates. Based on the findings and recommendations of the Houston Workshop, a study contract will be issued to conduct the in-depth analysis in phase two during FY'78.

2. PRE-WORKSHOP FINDINGS

A series of informal interviews was conducted prior to the Houston workshop with various chemical industry representatives, to gain some insight into the issues of concern to the industry. The preliminary findings of these interviews are summarized below for several key segments of the hydrogen market.

A. AMMONIA AND METHANOL

Essentially all ammonia and methanol production in the U.S. uses natural gas as both feedstock and fuel. Together, these two markets account for about one-third of the natural gas consumed by the chemical and allied products sector in the U.S., or 3.3% of the total natural gas consumption in the nation.

The heavy dependence of these markets on natural gas as feedstock and fuel would lead one to believe that ammonia and methanol producers must be busily investigating alternative sources of feedstock and fuels. A survey of major ammonia producers by the IGT in 1975 revealed that "of the 30 plants responding, half have some concerns about meeting their natural gas requirements through 1985, 23 have experienced some form of service curtailment or interruption, and 16 have had to alter or cancel expansion plans because of a lack of natural gas. Almost half of these plants are developing background information on other kinds of processes not using natural gas, but only two are switching some of their fuel uses to oil."

A survey of major methanol producers by the IGT revealed a similar response regarding their natural gas supply situation. The consensus appears to be that our natural gas production will not increase significantly in the next decade. Demand projections for ammonia and methanol, on the other hand, range from 3% annual growth or higher. Translated to hydrogen demand, these two markets may well require twice the present 0.5 Quad of Hydrogen by 1990, at a 6% growth rate.

Our recent interviews with chemical industry representatives revealed that many economic studies are underway, particularly in the coal conversion area. One recently published report (Brookhaven-Exxon) concluded, on the basis of production economics studies, that coal gasification technology (improved K-T process) could become competitive with natural gas reforming for methanol production by 1982 and ammonia production by 1989. (A key assumption made in this report is that the cost of natural gas and petroleum products will escalate at 1.5% per year over the general inflation rate of 5%.) All of the new ammonia plants announced for construction by 1985 are based on the use of natural gas.

In an effort to survey the synthetic fuels industry, the Koppers Company sent questionnaires in 1976 to presidents or chief executive officers of 161 U.S. and 6 Canadian companies or research organizations, with an interest in coal gasification.

The survey was designed to provide meaningful answers in the following areas:

- the impact of the energy crisis to date on each organization
- the interest in alternate energy supply from coal
- the attitude toward energy allocation by the federal government
- the interest in government incentives for establishment of synthetic fuel plants

The response to Item No. 10 of the questionnaire is of particular interest, as it reflects the views of industry on the issue of government incentives. Of the six types of incentives listed, the survey revealed the following order of preference by the respondents:

- (1) Accelerated depreciation of facilities (3-5 years)
- (2) Increase of present investment tax credit
- (3) Ability to issue tax-free bonds
- (4) Loan guarantees by the federal government
- (5) Government equalizing prices of substitute fuels with that of imported oil
- (6) Government project financing with provision for lease to industry

The following comments from chemical companies may be noted:

"The most important government incentive, in our opinion, is price protection so that the synthetic gas from coal gasification plants does not incur the grave risk of being undermined by sudden reduction in OPEC oil prices. In conjunction with this type of price protection from the government, we feel that issuance of tax-free bonds and increasing the investment tax credit from say 10 to 20 percent would be the most effective incentives involving minimum subsequent government interference."

B. COAL LIQUEFACTION

Hydrogenation is a key conversion reaction of coal liquefaction processes. A coal liquefaction process, such as the H-Coal process, requires 18,600 SCFT of hydrogen for each ton of coal to be liquefied. Since one ton of coal is converted to 4.44 Bbls of Syncrude, a liquefaction plant with a daily capacity of 100,000 Bbls Syncrude demands 419 millions SCFT of hydrogen for hydrogenation, in addition to 50 million SCFT for desulfurization. In terms of mass, the hydrogen requirement of a 100,000 Bbl/day Syncrude plant is 2.64 million pounds per day. If this hydrogen requirements is to be met by a coal gasification plant affiliated with the liquefaction facilities, and if the hydrogen yield from coal is 4.9% by weight, the amount of coal required for the hydrogen production is 24,490 tons per day. Since the liquefaction facilities convert 22,520 tons of coal to Syncrude, it means that for each ton of coal converted to Syncrude, an additional ton of coal would be expanded to generate the necessary hydrogen. If and when the nation's capacity for coal liquefaction reaches one million Bbls per day, the annual requirement of hydrogen will be equal to 4 million tons. This is equivalent to 34.4% of the hydrogen required for methanol and ammonia syntheses in the year 2000. (4.5×10^{12} SCF/YR.)

The above figures also indicate that if the hydrogen requirement of 4 million tons can be met from other sources, then the coal required for this purpose can be converted to another million Bbls/day of Syncrude.

Technologically, coal liquefaction to produce syncrude has been proven. Its full industrialization is dependent on factors such as:

- (1) The nation's industrial capacity of fabricating the necessary process equipment
- (2) Code modification for the process equipment
- (3) Guarantee for raw material supply and its price
- (4) Guarantee for products sales and prices
- (5) Investment finance

C. DIRECT IRON REDUCTION

At the present time (November 1977), there are six direct reduction plants in operation in this country, with an annual production capacity of 1,260,000 metric tons. By 1980 the national capacity will be increased by 900,000 metric tons with the expected completion of an additional plant in Texas. Thus in 1980, the direct reduction capacity in this country will reach 2,160,000 metric tons per year. In four of the above seven plants, totaling the annual capacity of 2 million tons the reducing agents are manufactured by reforming natural gas or oil. The reductant gas mixture contains 74% hydrogen and it is estimated that approximately 100 pounds of hydrogen is required for each ton of the reduced product. By 1980, the hydrogen requirement for direct iron reduction will be 91,000 tons per year. This amount is relatively small compared with the other hydrogen requirements such as ammonia or methanol production. It is noted that a direct iron reduction plant becomes economically not competitive if its capacity goes beyond 1,000,000 tons per year. Furthermore, the national capacity of direct reduction is not expected to grow substantially in this country. For these reasons, the hydrogen consumption in this industrial sector is not significant. In contrast with the slow development in the U.S., Venezuela will expand its capacity for direct reduction from the present 1 million tons to 5 million tons a year in 1980.

D. PETROLEUM REFINING

Petroleum refining consumes approximately 47% of the total industrial hydrogen consumed in this country. Even though it is the largest sector in the hydrogen supply/demand picture, there seems to be a lack of fairly accurate quantitative data available. A petroleum refinery is a producer as well as a consumer of hydrogen and therefore it does not, in general, report its demand/supply data to the outside. This is a major reason for the lack of quantitative data. Furthermore, the hydrogen consumption in a refinery is determined by complicated and inter-related factors such as:

- (1) Quantity of crude oil processed
- (2) Quality and source of crude oil processed
- (3) Refining processes
- (4) Product-mix
- (5) Environmental constraints

Each petroleum refinery seems to have its own unique set of the above factors influencing its refining operation, and consequently its hydrogen requirements. However, as a good approximation to determine the national demand in this sector, it may be assumed that the catalytic reforming in refineries supplies enough hydrogen to meet the demands for desulfurization of light distillate and other minor hydro-treating operations. And that the hydrogen consumed by gas oil desulfurization, residue desulfurization and residue hydrocracking will be supplied with merchant hydrogen or specifically installed hydrogen production units such as steam reformer of natural gas or oil. There is another reason for the special hydrogen production units to supply hydrogen to these three operations. The processes require a hydrogen stream of high concentration (up to 95% purity) whereas the hydrogen stream from a conventional catalytic reforming unit is only 70 or 80% purity. The hydrogen requirement for these three refining processes, as reported in the Brookhaven-Exxon report, is approximately 2.75 million tons of hydrogen a year in 1990. The estimate is also based on another assumption that the residue treatment processes are characterized by "carbon removal" rather than "hydrogen addition". A definitive study of hydrogen requirements for petroleum refining operation is not available in the literature.

E. FUEL CELL ELECTRICITY GENERATION

Conversion of fuels to electricity by means of fuel cells can be accomplished in a highly efficient and environmentally acceptable manner. Two major areas of application are envisioned for fuel cells. Large multi-megawatt fuel cell power plants may be constructed within electric utility networks to complement large-scale systems. The generation needs of small private and public utilities may be provided by these power plants. Smaller size fuel cells may be installed at building locations to provide integrated electric and thermal service for commercial and industrial complexes. There are varying estimates of the market for liquid and gaseous fueled electric generation equipment. Its market growth is estimated to be in a range of 5% to 6.7%.

The penetration of fuel cell power plants into the market is clouded by uncertainties associated with the growth rate. Nevertheless, a specific market, i.e., replacement of retired generation plants in areas of fuel shortage and critical environment, appears extremely attractive. It is estimated that the market for fuel cell power plants will be largest in private utilities, followed by the on-site integrated energy system for commercial and industrial complexes. An estimate for the total fuel cell market for the five year period of 1980-1985

is between 26,800 and 82,300 MW. The annual demand of hydrogen required for these fuel cell plants is estimated to be between 2.4×10^{12} SCF to 6.9×10^{12} SCF. This is indeed a tremendous market for hydrogen, comparable to that needed for manufacturing ammonia and methanol.

Several other attractive benefits are associated with fuel cell application for power plants but its technological and economic feasibility should be demonstrated for commercial-scale facilities.

F. FOOD INDUSTRY

In the food industry, hydrogen is mainly used to hydrogenate fats and oils. The hydrogen requirement is rather small, approximately 27,000 tons per year. This hydrogen market has the following unique features:

- (1) Demand per plant is small, from 50 to 1,000 MSCF/day/plant
- (2) High purity hydrogen is required with pressure range of 60-200 psig
- (3) Hydrogen cost is insignificant in determining the final price of the products. (Thus, the industry is more concerned with its steady and easy access to hydrogen than with the hydrogen cost itself.)
- (4) Since hydrogen is not produced within its manufacturing processes, it is supplied by small-scale hydrogen production units on-site or by purchasing merchant hydrogen
- (5) Hydrogenating plants are located across the country, currently there are 50 plants in 20 states

3. WORKSHOP PLANS

The University of Houston has received a grant from ERDA to conduct a workshop on the "Supply and Demand of Hydrogen as Chemical Feedstock" on December 12-14, 1977, at the University. The workshop is being organized by Dr. C. J. Huang, Professor of Chemical Engineering.

The objectives of this workshop are:

- (1) to assess and predict the present and future demand and supply of hydrogen as a chemical feedstock,
- (2) to discuss and evaluate the available technology and economic feasibility of manufacturing hydrogen from sources other than oil or natural gas
- (3) to develop implementation scenarios and to formulate recommendations for obtaining chemical raw material hydrogen from sources other than oil or natural gas

Approximately sixty participants, including some from outside the U.S., have been invited. They include executives, plant managers, economic planners and process engineers from the:

- Oil refining industry
- Petrochemical industry
- Agricultural chemicals and other industry
- Potential hydrogen supplier industries
- Independent engineering consultants
- Chemical plant engineers and constructors

- Academic and non-profit research organizations
- Government agencies

A preliminary conference was held in September 1977 to work out the details of the workshop program. There will be a total of six sessions, with short papers on various key issues to be presented for discussion by all participants. The final session will conclude with recommendations on the future supply of hydrogen as chemical feedstock, following detailed discussion of alternative scenarios and their technical and economic feasibility. A report on the workshop will be submitted to ERDA by April 1978.

USE OF HYDROGEN ENERGY SYSTEMS
TO
IMPLEMENT SOLAR ENERGY

T. Fujita, C. Miller, K. H. Chen
G. Voeks and W. Mueller
Jet Propulsion Laboratory
Pasadena, CA

Abstract

As the first phase of a study to explore the use of hydrogen energy systems to implement solar energy, potential roles are broadly identified in terms of future markets and the formulation of implementation scenarios. By converting solar energy to hydrogen, an energy pathway is created whereby solar energy can supply major new markets comprising (1) production of chemicals such as ammonia and methanol, (2) total energy/cogeneration, (3) synfuel/chemical feedstock production, (4) direct fuel uses, and (5) other small but important uses such as ore reduction. These new market opportunities for implementing solar energy are predicated primarily on the unique role of hydrogen as a key element in the chemical/industry sector.

Implementation of solar-hydrogen systems to fulfill these new markets is analyzed in terms of key issues. By considering the renewable fuel era (estimated to start in ≈ 2030), where fossil sources are sharply declining, a critical and major role for hydrogen systems is identified. In the absence of fossil fuels, the survival of our entire hydrocarbon-based chemical industry requires use of solar (or other non-fossil sources) to generate hydrogen from water. The key issues then revolve about developing and implementing solar-hydrogen systems to effect a smooth transition directed toward fulfilling this ultimate role. Issues governing implementation include conservation policies, possible environmental impacts from carbon dioxide generated from continuing accelerated usage of fossil fuels, and emergence of large markets for byproduct oxygen. These issues are addressed in terms of their potential for accelerating implementation of solar-hydrogen systems.

I. Introduction

A major thrust in the Department of Energy's (DOE) overall program is to develop and support implementation of solar energy systems to conserve rapidly depleting natural gas and petroleum reserves. By combining solar energy with hydrogen systems, new possibilities may be uncovered which could enhance the implementation of solar energy. In such solar-hydrogen energy systems, solar energy is used to generate hydrogen from water. This hydrogen is then transmitted, stored, and used in myriad ways, e.g., it can be used as a fuel to generate electrical energy or as a chemical feedstock to produce ammonia and methanol.

The overall objective of the present effort is to examine roles for solar-hydrogen systems as a basis for projecting which roles are likely to be fulfilled and in what sequence. Emphasis is placed on roles which utilize unique characteristics of hydrogen systems since these roles are considered to have a greater likelihood of being implemented. That is, unique roles are capable of creating new opportunities for enhancing the implementation of solar energy.

A. Approach

As shown in Fig. 1, the effort is divided into two phases and the present paper covers only the first phase which was completed in FY77. This Phase 1 activity identifies potential roles for solar-hydrogen systems. The follow-on Phase 2 effort will examine solar hydrogen systems in terms of practicability and required technology development to fulfill the roles identified in Phase 1.

The approach to identifying roles/options involved the delineation of future markets in terms of potential size as a function of time. Then, implementation scenarios were formulated in terms of timeframe, key issues, and alternatives.

A basic premise for the Phase 1 effort is that technology for both solar and hydrogen systems will be successfully developed and that goals in terms of performance and cost will be achieved per present development program schedules. The identified roles and implementation scenarios from Phase 1 only show potential for solar-hydrogen systems and do not address the likelihood of achieving this potential or consider ultimate efficiencies.

The Phase 2 effort (Fig. 1) will examine system options primarily in terms of technology status and associated uncertainties in projected costs and performance. The effect of these uncertainties on expected implementation will be evaluated in terms of estimated R&D requirements (both time and funds) and relative technical risks. Basic steps involved in the Phase 2 activity and their interaction are depicted on Fig. 1. The technical development activities which will potentially provide the greatest contribution toward implementation of solar-hydrogen systems will be delineated to serve as an input for DOE's Hydrogen Storage Systems program.

B. Scope

Solar energy systems are in a very early stage of development and are not commercially competitive with fossil and nuclear systems for large

scale power generation. The rate of implementation of solar energy systems will be governed by depletion rates (and associated price escalations) for fossil fuels, the viability of solar systems vis-à-vis other renewable or large energy source alternatives such as nuclear fusion, ocean thermal gradient geothermal, etc., and the degree of success in developing solar energy systems tailored to meet application system/end-use requirements.

The implementation of solar energy systems and in particular solar-hydrogen systems is therefore dependent on the complex interrelations of overall energy usage and the evolving policies which will govern this usage. Projections of energy usage range from simple extrapolation of current use pattern and growth rates to reduced consumption based on conservation and development of more energy-efficient systems and processes.

Within the scope of the present study, the many different energy futures and their complex ramifications on implementation of solar-hydrogen systems cannot be assessed in detail. The effort is thus limited to the well-established energy futures which were previously used as the basis for projecting hydrogen demand (Ref. 1). The rationale inherent in these futures provides a framework within which specific issues relating to implementation of solar-hydrogen systems can be analyzed.

The energy futures employed in Ref. 1 stressed conservation of fossil resources by use of technically improved and more efficient devices and the shifting of energy sources from natural gas and petroleum to coal and nuclear energy. The futures covered a period up to the year 2000 during which depletable resources of natural gas, petroleum, and coal play major roles. Renewable sources such as solar energy will of necessity assume the dominant role when these depletable sources become scarce. Baseline projections of solar energy implementation to the year 2020 for the present study are derived from ERDA-49 (Ref. 2).

Thus, when identifying roles for solar-hydrogen systems, it is necessary to extend the energy futures of Ref. 1 and look beyond the depletable fossil fuel era. Within the scope of the present study, major roles that were identified for solar-hydrogen systems in the post fossil or renewable fuel era could only be explored in terms of basic first order considerations; however, the existence of potentially major roles in the post fossil era provides a perspective regarding technology development activities. The development effort during the fossil era should be regarded as a transitional phase where specific activities will be ordered to provide a smooth transition in meeting the requirements of the post fossil era.

II. Solar-Hydrogen Systems

A solar-hydrogen system is herein defined as a system where solar energy is collected and used to generate hydrogen which is then transmitted, stored, and supplied to end-use markets.

A. Utility Hydrogen Energy Storage

Hydrogen energy systems were initially directed primarily towards being an energy

transmission and storage medium for electric utilities (Ref. 3). The basic system is shown in Fig. 2 (Ref. 4). Off-peak utility power in the form of electricity and/or heat is used to decompose water into hydrogen and oxygen. The hydrogen can then be stored and used in fuel cells or turbines to generate electrical energy during peak power demand periods. As indicated on Fig. 2, the byproduct oxygen can be either sold to oxygen users or used as the oxidant for the fuel cells and turbines.

A major feature of this storage system is flexibility with regard to the location of components. For the usually considered case of electrolytic decomposition of water, the electrolyzer can be located near available water since electrical energy can be supplied from the central power plant via electric transmission lines. The hydrogen can then be transported in pipelines to another site such as an underground storage reservoir. From the storage reservoir, the hydrogen can again be piped to a conversion plant located, e.g., within the load center.

B. Solar Energy Systems

Solar energy systems encompass a wide spectrum which is broken down into the following two basic categories (Ref. 5):

- Natural Collection - Indirect Use
 - Photosynthetic processes in plants
 - Generation of winds and waves
 - Creation of ocean thermal gradients
- Engineered Collection - Direct Use
 - Conversion of photons to electricity
 - Conversion of insolation to thermal energy
 - Use for heating needs
 - Convert to electricity via heat engines
 - Thermionic

All of the above methods of collecting solar energy are being pursued (Ref. 6). Biomass systems are based on photosynthetic processes. Programs to use wind power and ocean thermal gradients to generate power (OTEC - Ocean Thermal Energy Conversion) are underway (Ref. 2). Engineered collection systems are focused on photovoltaic systems (photons to electricity) and solar thermal power systems. A 10 MW solar thermal power plant is presently being developed for installation at Barstow, CA. The concept involves a central receiver mounted on a tower. A field of two-axis tracking mirrors (or heliostats) reflects energy on the receiver in which steam is generated. The steam is then used to power a steam power plant as shown on Fig. 3.

C. Solar-Hydrogen Production Pathways

The solar-hydrogen production pathways corresponding to natural and engineered solar collection systems are presented on Figs. 4 and 5, respectively. For natural collection systems of Fig. 4, the photosynthesis process embodies several options. First, the green plants, produced from photosynthesis can be either burned directly to produce heat or they can be processed (chemical conversion) to form products such as methanol which can be used as a fuel for combustion or a chemical feedstock. The thermal energy of combustion can be used to drive either a thermochemical plant which uses heat to split water via a series of

closed loop chemical reactions or a power conversion (heat engine) system to produce electrical power which is fed to an electrolysis plant.

The pathway for wind power involves only electrolysis since the energy is initially in mechanical form. The OTEC plant uses small differential temperatures of ~20°F to drive a heat engine cycle which is coupled to an electrolysis plant. The wind power plant can employ storage such as batteries or flywheels to smooth out wind speed variations and thereby allow the electrolysis plant to be sized for operating loads that are lower than peak wind energy loads. The OTEC plant is expected to generate a steady load so that storage ahead of the electrolysis plant is not needed.

For engineered collection systems (Fig. 5), the photovoltaic plant directly converts solar energy to electricity and is therefore coupled to an electrolysis plant for hydrogen production. Solar-thermal plants have two optional pathways involving power conversion - electrolysis or thermochemical plants. Photolytic plants capture photons and directly split water via electrochemical processes. Compared to the photovoltaic approach, the intermediate step of generating electricity is avoided, but the photolytic approach is in the early research stage, whereas photovoltaic and solar-thermal systems are in the development and design phase. The thermochemical plant is also considered to be in the early research stage.

D. Basic Roles for Hydrogen Systems

After hydrogen is produced from solar energy via any of the spectrum of pathways shown on Figs. 4 and 5, the major role of hydrogen systems involves energy storage and transmission of energy to users as illustrated on Fig. 6. For the system on the upper portion of Fig. 6, electricity is generated on the outskirts of the load center and the electrical distribution network is used to transmit energy within the load center. A portion of the hydrogen is also supplied to large industrial users. For the system on the lower portion of Fig. 6, hydrogen is distributed via pipelines within the load center and electricity is generated by small substations within the load center where waste heat from electrical production can be used to meet heat loads.

In the context of large scale implementation of solar energy, two features of hydrogen systems are particularly attractive. Pipeline transmission coupled with underground gas storage has potential for achieving low-cost, long distance delivery of energy (Ref. 4). As shown on Fig. 7, the region of highest insolation is in the Southwest and this energy could be transported to major load centers via hydrogen pipelines with storage accomplished in underground reservoirs which generally exist near major load centers. Present underground natural gas reservoirs as shown on Fig. 7 will become available for hydrogen storage as natural gas is depleted and additional new reservoirs could be found and/or developed.

III. Future Markets

The primary thrust of present engineered solar collection system programs is to supply heat and electrical energy markets. Hydrogen energy systems

permit solar energy to supply major new markets as shown on Fig. 8.

A. Chemical Markets

Hydrogen is a basic feedstock for producing essential chemicals such as ammonia for fertilizers and methanol for the plastic industry. It also has a major role in petroleum refining. As indicated in Ref. 1, this market accounts for ~90% of present hydrogen usage which is of the order of $\sim 3 \times 10^{12}$ SCF/year.

Over ~70% of present hydrogen requirements are supplied by natural gas via steam reforming. As natural gas reserves become depleted, shifts to other sources such as coal are anticipated. As governed by conservation policies, environmental impacts, and related issues, solar may initially make some penetration into this market.

For both coal and solar, the possibility of supplying this chemical market via externally-generated merchant hydrogen exists. That is, hydrogen can be generated in large coal or solar plants and then be shipped via pipelines to industrial users. A factor which could stimulate a move toward merchant hydrogen is the possibility of capital cost savings for chemical plants via removal of equipment associated with the captive (on-site) hydrogen generation. As shown on Fig. 9, a major portion of present ammonia plants is associated with the generation of hydrogen and nitrogen. If external hydrogen is supplied, this equipment (inside the dashed box) can be removed and this will reduce capital costs by ~50%. A nitrogen plant will have to be added, but a substantial net cost savings will result.

B. Total Energy/Cogeneration

The use of total energy and cogeneration systems, where electrical and heat needs are provided by an on-site conversion plant, is being pursued by DOE since high overall energy efficiencies are possible. Basically, the reject heat from electrical generation is used for heat needs and detailed matching of heat and electrical loads is required. Cogeneration and total energy both involve the concept of reject heat utilization, but cogeneration has the added flexibility that part of the electrical power generated on-site can be supplied to the utility grid.

The near term emphasis for total energy/cogeneration systems involves the use of fossil fuel energy. The use of on-site solar-thermal total energy systems is also being investigated (Ref. 7). The solar-hydrogen pathway can provide several major advantages. The on-site location of a solar-thermal total energy system requires substantial land area for solar collection and this could rule out some potential applications, particularly in crowded industrial centers. With solar-hydrogen systems, the solar collection plant can be located at an off-site location while the more compact energy conversion components can be located on-site. Hydrogen can be supplied via pipelines from the solar collection plant to the industrial or commercial use site. Hydrogen can also be stored, e.g., in underground reservoirs, and when fossil fuel reserves become depleted, total energy/cogeneration plants using fossil fuels can be converted to use solar-hydrogen.

Markets for total energy/cogeneration systems are shown in Table 1 (Ref. 8). The process heat requirements listed in Table 1 could be supplied by reject heat from electrical generation, where the reject heat must be supplied in the application temperature range shown. As shown in Table 2, hydrogen/oxygen and hydrogen/air fuel cells and gas turbines can furnish reject heat temperatures suitable for a large portion of the process heat needs of Table 1.

C. Synfuel/Chemical Feedstock Production

As natural gas and petroleum reserves are depleted, fossil sources such as coal, oil shale, tar sands, and also biomass can be processed to produce synfuels. Processes for synthetic natural gas (SNG) and liquid fuels require hydrogenation since the source feedstocks are hydrogen deficient in relation to the output product. A sizable fraction of the synfuel process is therefore devoted to the production of the required hydrogen using the source feedstock as an energy source.

If the required hydrogen were supplied from an external solar-hydrogen source, the capital costs of the synfuel plants could be reduced. Additionally, the product yield per unit feedstock source would increase and carbon dioxide emissions would be reduced. These benefits are presented on Table 3 for coal-based processes. For the same product yield, coal savings of the order of 50% to 60% are indicated for SNG and synthetic gasoline production. The reduction in carbon dioxide emissions is approximately the same as the coal savings. Substantial capital cost savings of at least 35% are indicated for these two processes. Lesser but significant savings of the order of ~8% accrue to the process for producing solvent refined coal (SRC).

Process diagrams for the SNG and liquid fuel (I. G. Farben) processes are shown on Figs. 10 and 11, respectively. It is indicated that substantial portions of the process plant can be removed when external hydrogen is supplied. The economic viability of using external hydrogen is of course governed by the cost of this hydrogen. However, the prospects of substantial savings in both capital and feedstocks tend to push for earlier entry of external hydrogen.

D. Direct Fuel Uses

Hydrogen from solar can also be supplied for direct fuel uses such as industrial process heat, transportation, and commercial/residential needs. When fossil fuels are in relatively plentiful supply, solar-hydrogen can only make a small penetration since it is more costly. Use of some hydrogen as a fuel is a possibility for uses requiring clean burning/low air pollution.

As fossil sources such as natural gas become scarce, hydrogen can potentially serve as a replacement where competitors will be other synfuels. The penetration of solar-hydrogen into the direct fuel market could initially be accomplished in a gradual manner by using hydrogen to supplement natural gas as shortfalls develop.

E. Other Small Uses

Hydrogen is needed for numerous small but important markets such as ore reduction, reducing

agent, heat transfer fluid, etc. When fossil sources for hydrogen production are no longer available, solar-hydrogen systems can supply the needed hydrogen to sustain these markets.

F. Potential Market for Solar-Hydrogen

The potential new markets for solar energy via hydrogen systems are dominated by chemical industry requirements. In the Hydrogen Energy Systems Technology (HEST) study of Ref. 1, projections of hydrogen demand were made for a Reference projection based on the Ford FTFB scenario (Ref. 9). For this Reference projection a high merchant supply option was formulated where energy policies based on conservation would tend to stimulate earlier introduction of solar (renewable) sources.

Results of projections for solar-hydrogen based on this HEST projection are shown on Fig. 12 as additions to solar projections for other markets per ERDA-49 (Ref. 2). It is seen that the potential solar-hydrogen markets (dashed lines) represent a substantial increase in the solar market. It is noted that the energy shown on Fig. 12 is in terms of source energy or the solar energy that has to be supplied. The actual energy delivered to the end use is a fraction of this energy as determined by the system efficiency.

In projecting solar-hydrogen to the year 2020, it was assumed that solar would displace all of the natural gas while assuming half of the percentage burden carried by petroleum in the year 2000. These trends follow from the expected depletion of natural gas and petroleum. It is noted that solar comprises ~1%, ~10%, and ~30% of the total source energy in the years 1985, 2000, and 2020, respectively. This provides a measure of the anticipated development timeframe for solar and the logical increase in implementation rate as fossil reserves decline.

IV. Implementation Issues

The rate at which solar-hydrogen systems will be implemented to fulfill the identified markets depends on three key issues which are:

(1) the timeframe, since availability of fossil fuels is declining, (2) existence of markets for byproduct oxygen, and (3) environmental impacts associated with an increase in atmospheric carbon dioxide.

A. Fossil Fuel Era

During the fossil fuel era, where fossil sources are dominant, the primary candidate energy sources are fossil, nuclear, and renewable/nonfossil. Energy carriers include electricity, hydrogen, and fossil fuels. Major end use categories are electric utilities, chemical industry, and fuel requirements.

The primary and secondary pathways for hydrogen during this fossil fuel era are shown on Fig. 13. The primary pathway involves the use of fossil fuels to generate hydrogen for use in the chemical industry. This pathway employs well-developed technology and is the most economical as long as fossil sources are available.

The secondary pathway involves nuclear and renewable sources with the possibility of some supplementation of natural gas in the latter portion of the fossil fuel era. This coincides with the projections of Fig. 12, where solar (renewable) sources begin to penetrate the market after 1985 and grow rapidly only after the year 2000.

B. Renewable Fuel Era

In the renewable fuel era (estimated to start in ~2030) where fossil sources are no longer dominant, a critical pathway involving hydrogen energy systems is identified on Fig. 14. In the absence of fossil fuels, the survival of our hydrocarbon-based chemical industry requires hydrogen from water and carbon from sources such as biomass/waste recycling. Thus, hydrogen systems provide a vital energy pathway between solar and other renewable energy sources and the chemical industry.

The identification of a critical future need for hydrogen systems using solar and other non-fossil sources provides a basic framework for a coherent development program and implementation plan. The development and implementation sequence can be structured to provide a smooth transition directed toward ultimately fulfilling the essential role of hydrogen systems in maintaining our chemical-based industrial complex.

As shown in Fig. 14, fuel requirements can be met by either hydrogen or other synfuels. However, hydrogen is required for production of synfuel. Hence, hydrogen systems also play a critical role with regard to satisfying fuel requirements.

C. Markets for Byproduct Oxygen

When hydrogen is produced via the decomposition of water, oxygen is formed as a byproduct. If this byproduct oxygen could be sold as a merchant gas, the costs of the solar-hydrogen system can be spread over both hydrogen and oxygen. The net effect will be a lower cost for hydrogen production and an associated greater market penetration.

As shown in Table 4, the potential market for merchant oxygen is projected to grow rapidly. Large new markets for waste water treatment and synfuel/feedstock production are identified. The byproduct oxygen associated with projected solar-hydrogen (Fig. 12) can satisfy a substantial portion of the oxygen demand as shown on Fig. 15. Thus, it appears that byproduct oxygen from solar-hydrogen systems can be sold at prices competitive with alternative sources of oxygen production such as air separation plants.

D. Increase in Atmospheric Carbon Dioxide

Potentially large and catastrophic environmental impacts are possible as a result of continued growth in atmospheric carbon dioxide concentration associated with fossil fuel usage (Refs. 10, 11, and 12). Based on detailed measurements of atmospheric carbon dioxide since 1958, a 13% increase has been observed.

For over 100 years, carbon dioxide emissions have increased at the rate of ~4.3% per year. The consequence of continued carbon dioxide emission is an increase in climatic temperatures which can cause impacts such as relocation of agricultural regions and melting of polar ice caps. When polar ice caps melt, there will be a rise in sea level and a modification of the shoreline.

Regarding this problem, society is faced with two choices. Fossil fuel rates can be allowed to

grow until impacts force a change. This involves a risk since the adverse effects will probably persist for long periods of time. The other course of action is to modify fossil fuel usage to control the severity of the impacts. This would require earlier usage of more costly renewable source energy systems for which solar-hydrogen systems could play a major role. This substitution would enable fossil sources to be used under conditions which would greatly reduce carbon dioxide emissions (e.g., Table 3).

REFERENCES

1. Kelley, J. H., "Hydrogen Tomorrow, Demands and Technology Requirements," JPL Report 5040-1, NASA/Jet Propulsion Laboratory, Pasadena CA., December 1975.
2. ERDA, "A National Plan for Energy Research, Development, and Demonstration," Washington, D.C., 1975.
3. Gregory, D. P., "The Hydrogen Economy," Scientific American, Jan. 1973, Vol. 228, No. 1.
4. Fujita, T., "Underground Energy Storage for Electric Utilities Employing Hydrogen Energy Systems," JPL Report 900-744, EM 342-339, Jet Propulsion Laboratory, Pasadena, CA., June 1976.
5. Reuyl, J. S., et. al., "Solar Energy in America's Future," Second Edition, ERDA Contract E(04-3)-115, SRI Project URU-4996, Stanford Research Institute, Menlo Park, CA., March 1977.
6. Bockris, J. O'M., Energy, The Solar-Hydrogen Alternative, John Wiley & Sons, New York, 1975.
7. Bush, L. R., "Solar Thermal Dispersed Power Program, Total Energy System Project," Technical Progress Report ATR-77(7692-01)-1, Aerospace Corp., El Segundo, CA., 1 August 1977.
8. Intertechnology, "Analysis of the Economic Potential of Solar Thermal Energy to Provide Industrial Process Heat," Intertechnology Report No. 00028-1, ERDA 000/2829-1, Dist. Category VC-596, Final Report, Vol. I, 7 Feb 1977
9. Ford Foundation, Energy Policy Project, "A Time to Choose," Ballinger Publishing Co., Cambridge, Mass., 1974.
10. Baes, C. F., et. al., "The Global Carbon Dioxide Problem," Report ORNL-5194, Oak Ridge National Laboratory, Oak Ridge, TN, August 1976.
11. Bolin, B., "The Impact of Production and Use of Energy on the Global Climate," Annual Review of Energy, Vol. 2, Annual Reviews Inc., Palo Alto, CA, 1977.
12. "Energy and Climate," pp. 110 ff, National Academy of Sciences Report, November 1977.

Table 1. Markets for total energy/cogeneration

SUMMARY OF PROCESS HEAT DATA BASE BY INDUSTRY* AND PROCESS TEMPERATURE REQUIREMENTS

<u>INDUSTRY</u>	<u>PROCESS HEAT 10¹²Btu/YR</u>	<u>APPLICATION TEMPERATURE REQUIREMENTS, °F</u>
MINING	129.00	250-2500
FOOD & KINDRED PRODUCTS	319.00	100-550
TOBACCO PRODUCTS	1.40	~ 220
TEXTILE MILLS	116.00	200-275
LUMBER & WOOD PRODUCTS	172.00	212-300
FURNITURE	12.00	70-150
PAPER & ALLIED PRODUCTS	1,093.00	150-1900
CHEMICALS	534.00	80-2200
PETROLEUM PRODUCTS	2,640.00	250-1600
RUBBER	9.70	250-425
LEATHER	2.50	85-140
STONE, CLAY & GLASS	991.00	120-3300
PRIMARY METALS	3,770.00	100-2700
FABRICATED METAL PRODUCTS	.03	130-850
ELECTRICAL EQUIPMENT	1.60	150-1700
TRANSPORTATION	24.00	250-2650
TOTAL	9,815.00	

*REF: INTERTECHNOLOGY CORP, 1974 SURVEY

Table 2. Potential for total energy/cogeneration

WASTE HEAT AMOUNT AND LEVEL FOR H₂ FUEL CELLS AND TURBINES

	<u>WASTE HEAT % HHV OF H₂</u>		<u>WASTE HEAT TEMPERATURE °F</u>
	H ₂ /O ₂	H ₂ /AIR	
● FUEL CELLS			
● ACID ELECTROLYTE			
• STATE OF ART	56	58	325 ~ 375
• FUTURE	49	53	250 (1)
● BASIC ELECTROLYTE			
• FUTURE	40	48	ROOM TEMPERATURE (1)
● MOLTEN CARBONATE- SOLID OXIDE			
• FUTURE	53	55	1100 (2)
● TURBINES	40 ~ 47	~ 55	110 ~ 770 (3)

(1) JPL ESTIMATES

(2) FROM ATOMICS INTERNATIONAL

(3) BASED ON OPERATING CONDITIONS FROM NASA LeRC

Table 3. Synfuels production
POTENTIAL SAVINGS VIA EXTERNAL SOLAR-HYDROGEN
(COAL-BASED PROCESSES)

<u>PROCESS</u>	<u>COAL SAVINGS, %</u> (ALSO CO ₂ REDUCTION)	<u>CAPITAL COST SAVINGS, %</u>
● KOPPERS-TOTZEK (SNG)	~ 60	~ 35 ⁽¹⁾
● SOLVENT REFINING (SRC)	~ 8	~ 9
● I. G. FARBEN (GASOLINE)	~ 50	40-68 ⁽²⁾

(1) INCLUDES EXTERNAL OXYGEN SAVINGS OF ~ 31%

(2) RANGE BASED ON TECHNOLOGY STATUS

Table 4. Potential merchant oxygen market

PROJECTED CONSUMPTION, 10⁹ SCF

<u>PRESENT MARKETS</u>	<u>1972</u>	<u>1978</u>	<u>1985</u>	<u>2000</u>
● STEEL MAKING	251	289	342	488
● METAL FABRICATION	42	51	64	105
● CHEMICAL INDUSTRY	61	80	115	238
● OTHER/MISCELLANEOUS	4	25	54	108
SUBTOTAL	358	445	575	939
<hr/>				
<u>NEW MARKETS</u>				
● WASTE WATER TREATMENT	--	--	41	2,190
● SYNFUEL/FEEDSTOCK PRODUCTION				
LIQUID FUELS (SLF)	--	--	165	1,237
GASEOUS FUELS (SNG)	--	--	260	2,184
● DRINKING WATER PURIFICATION	--	--	--	61
SUBTOTAL	--	--	466	5,672
<hr/>				
TOTAL	358	445	1,041	6,611

FY77
IDENTIFY ROLES/OPTIONS

FY78 AND 1st QUARTER FY79
ANALYZE ROLES/OPTIONS AND DETERMINE TECHNOLOGY REQUIREMENTS

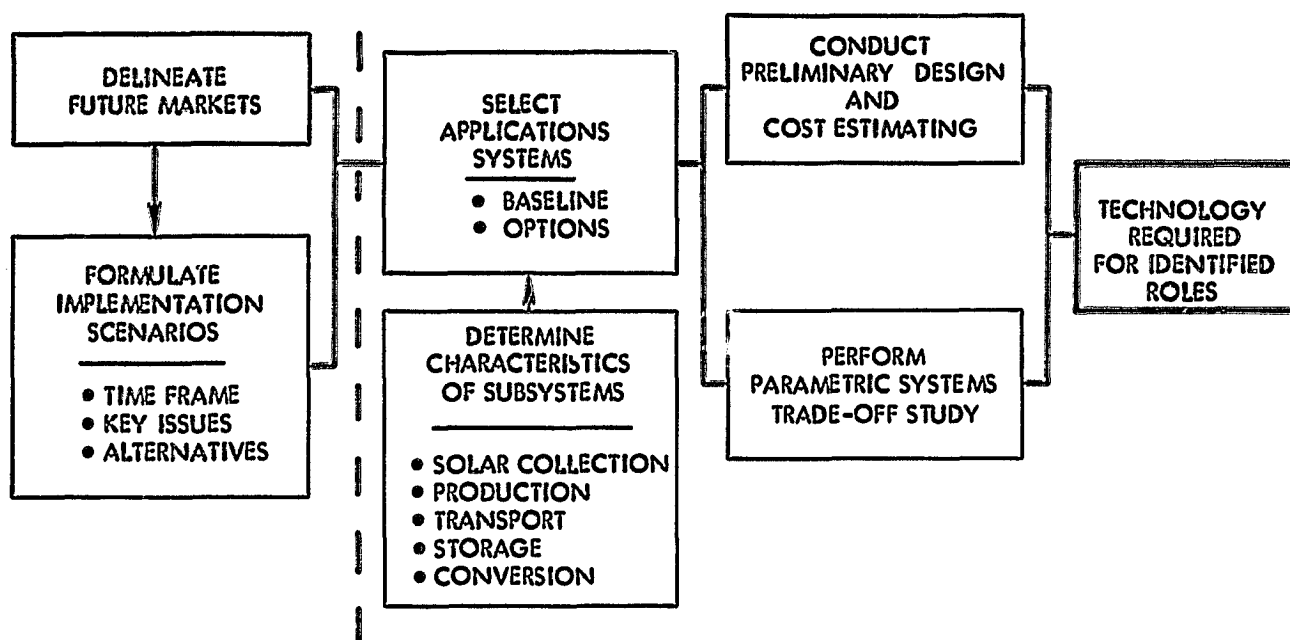


Fig. 1. Organization of Study Effort

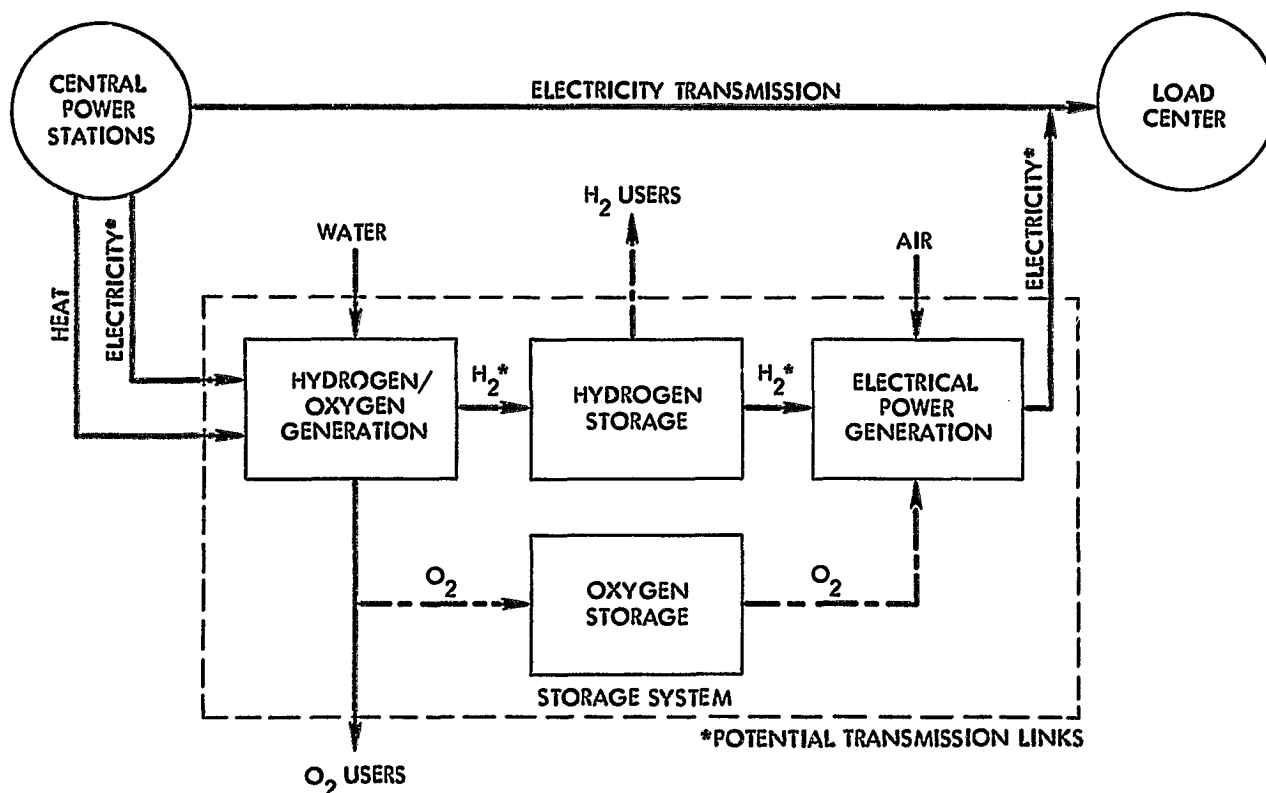


Fig. 2. Hydrogen Energy Systems for Electric Utility Energy Storage

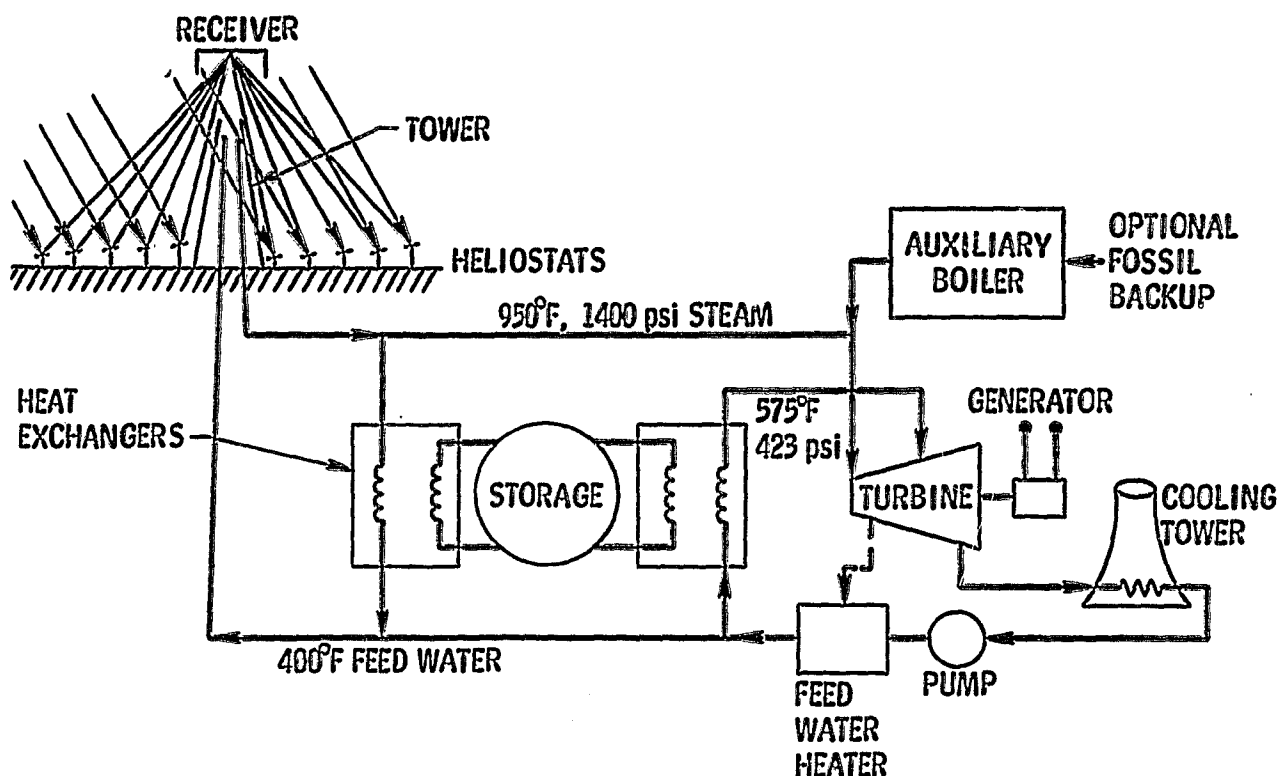


Fig. 3. Central receiver solar thermal-electric power plant

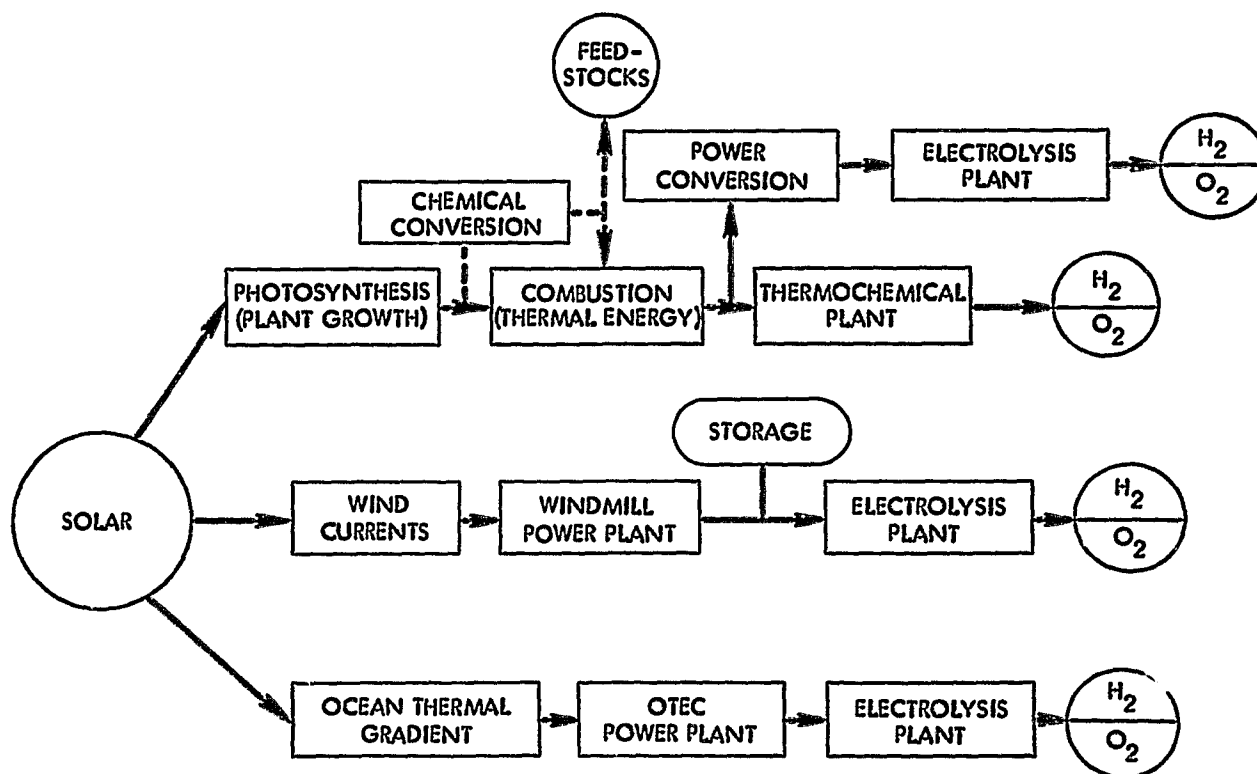


Fig. 4. Solar-hydrogen production pathways
natural solar collection systems

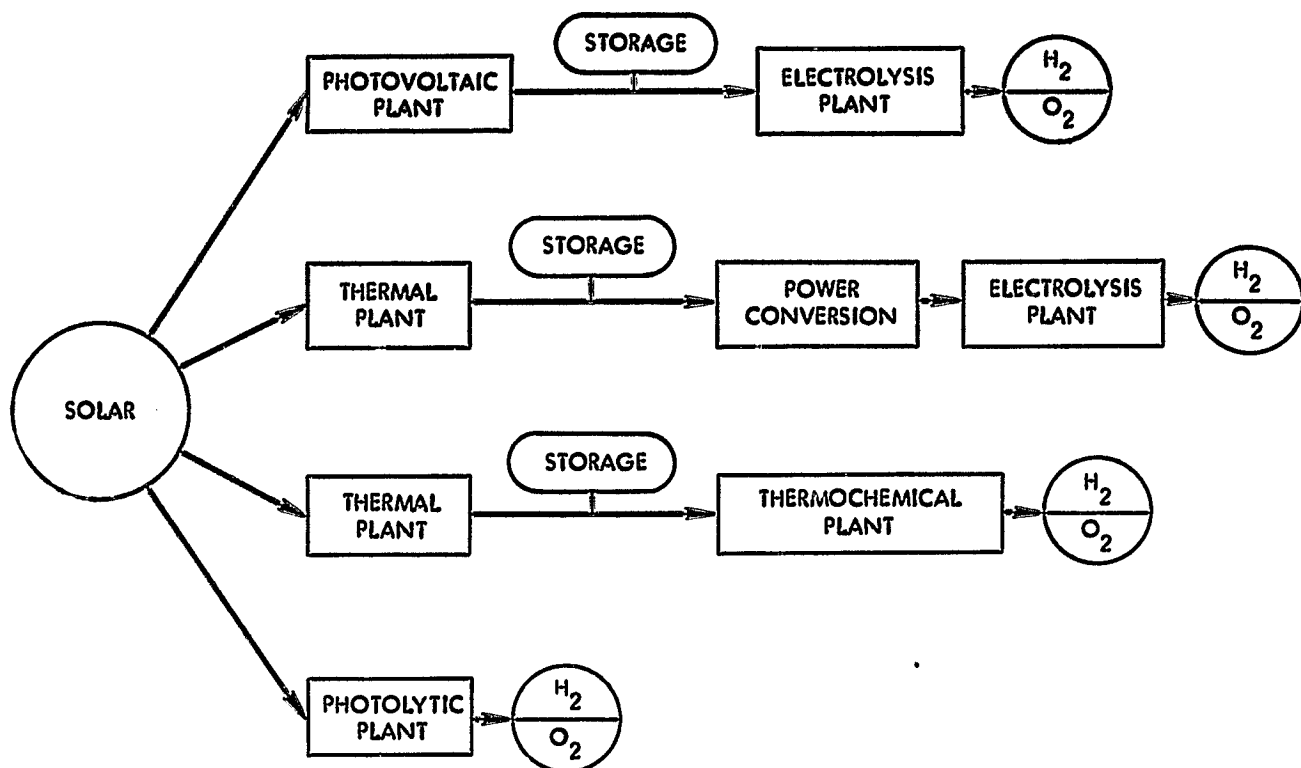


Fig. 5. Solar-hydrogen production pathways engineered solar collection systems

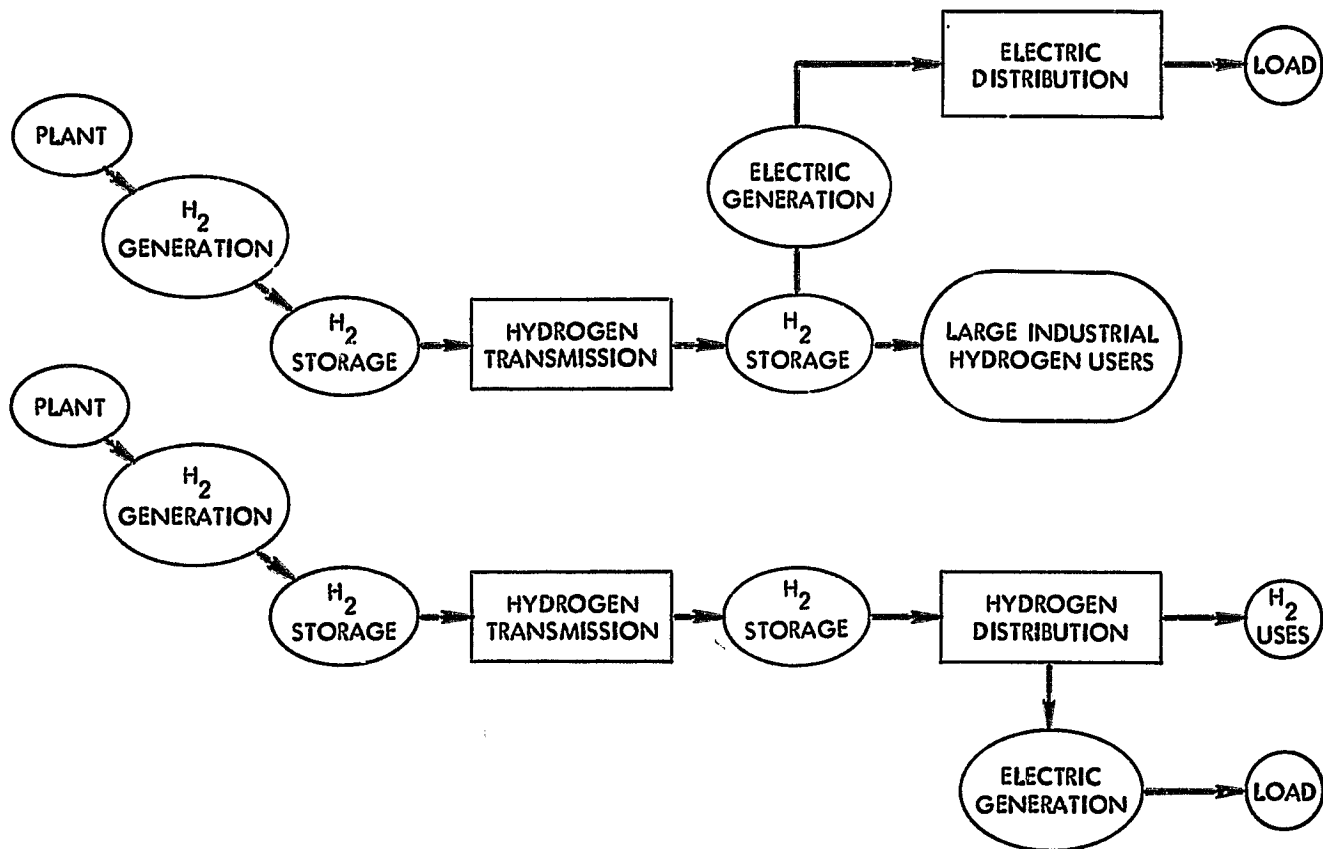


Fig. 6. Hydrogen transmission systems



Fig. 7. Potential for low cost bulk storage and transmission of solar-hydrogen

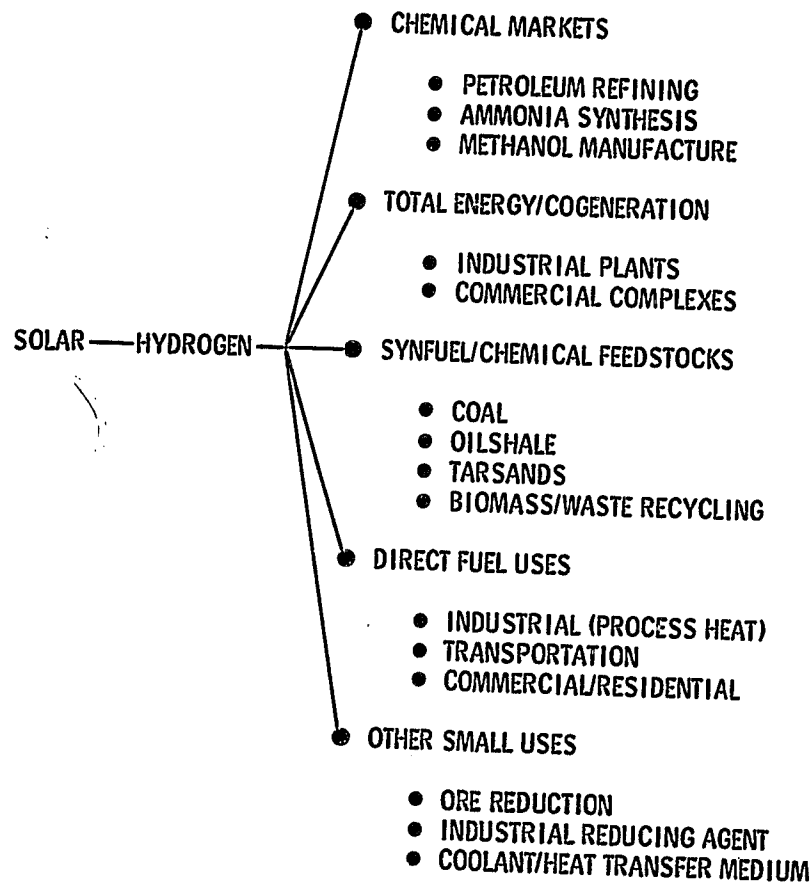


Fig. 8. Solar markets via hydrogen systems

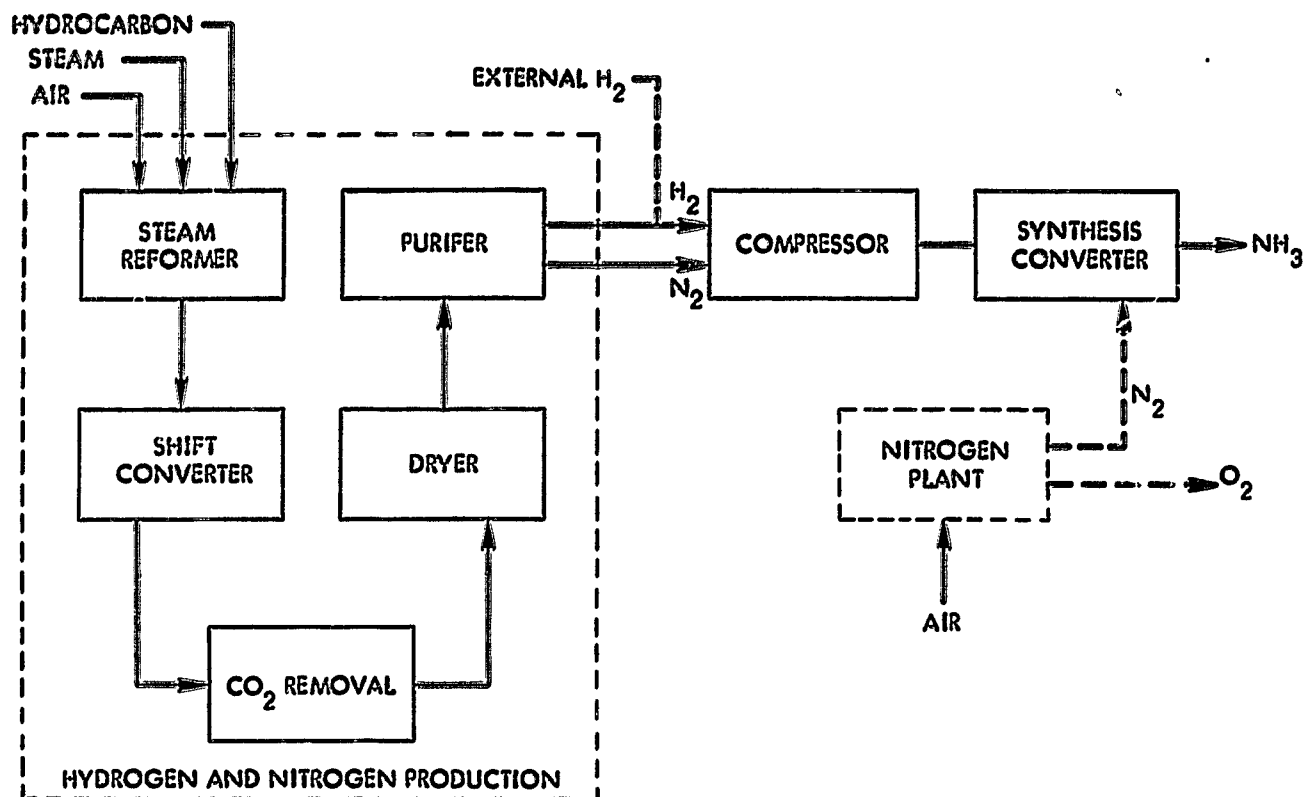


Fig. 9. Effect of external hydrogen on ammonia plant design

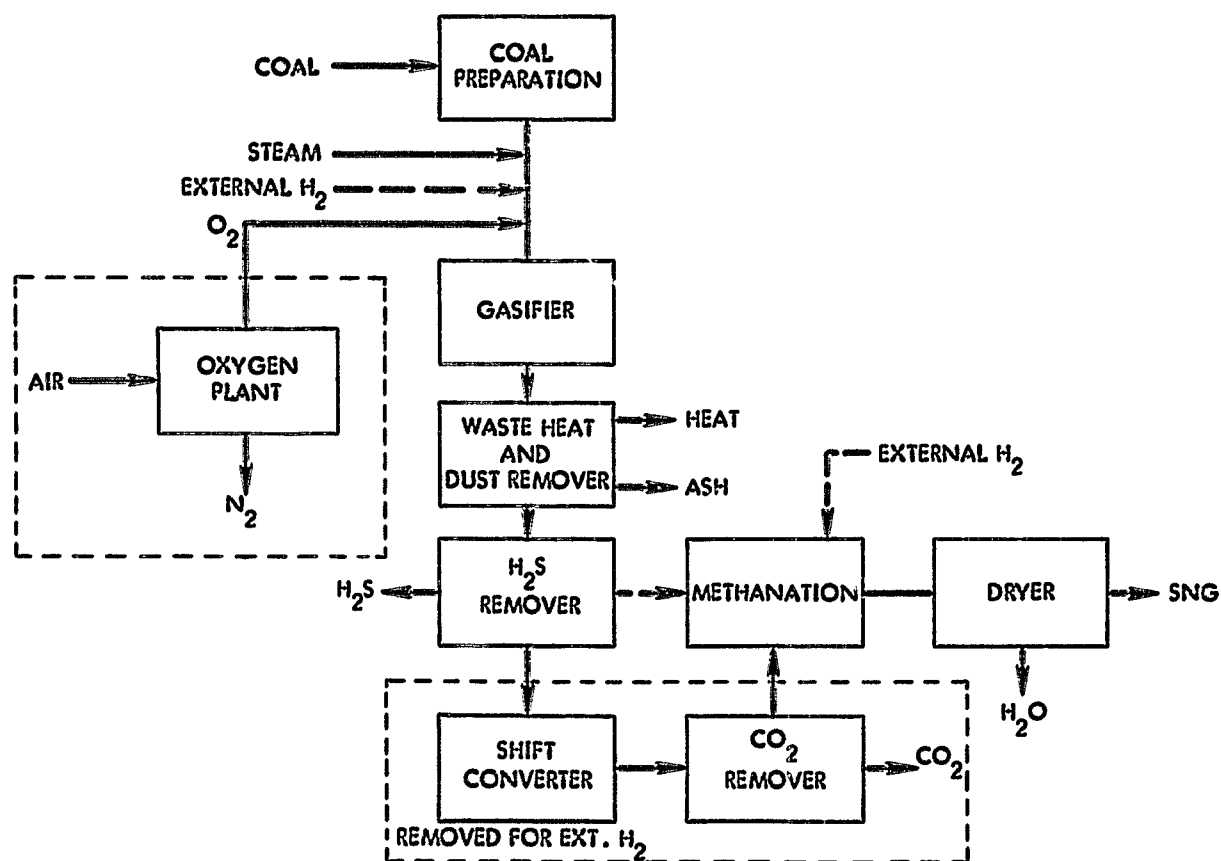


Fig. 10. Effect of external hydrogen on coal gasification (SNG) plant design

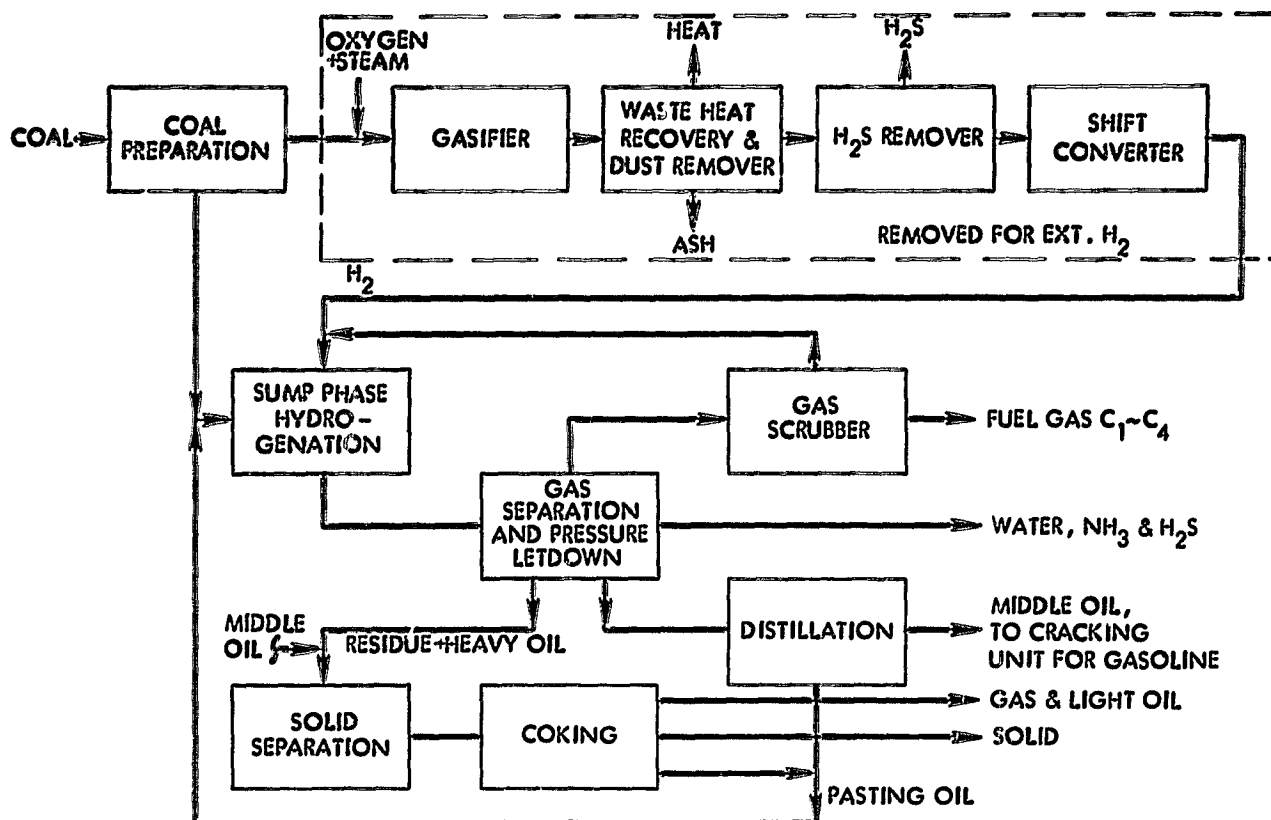


Fig. 11. Effect of external hydrogen on coal catalytic hydrogenation plant design (I. G. Farben)

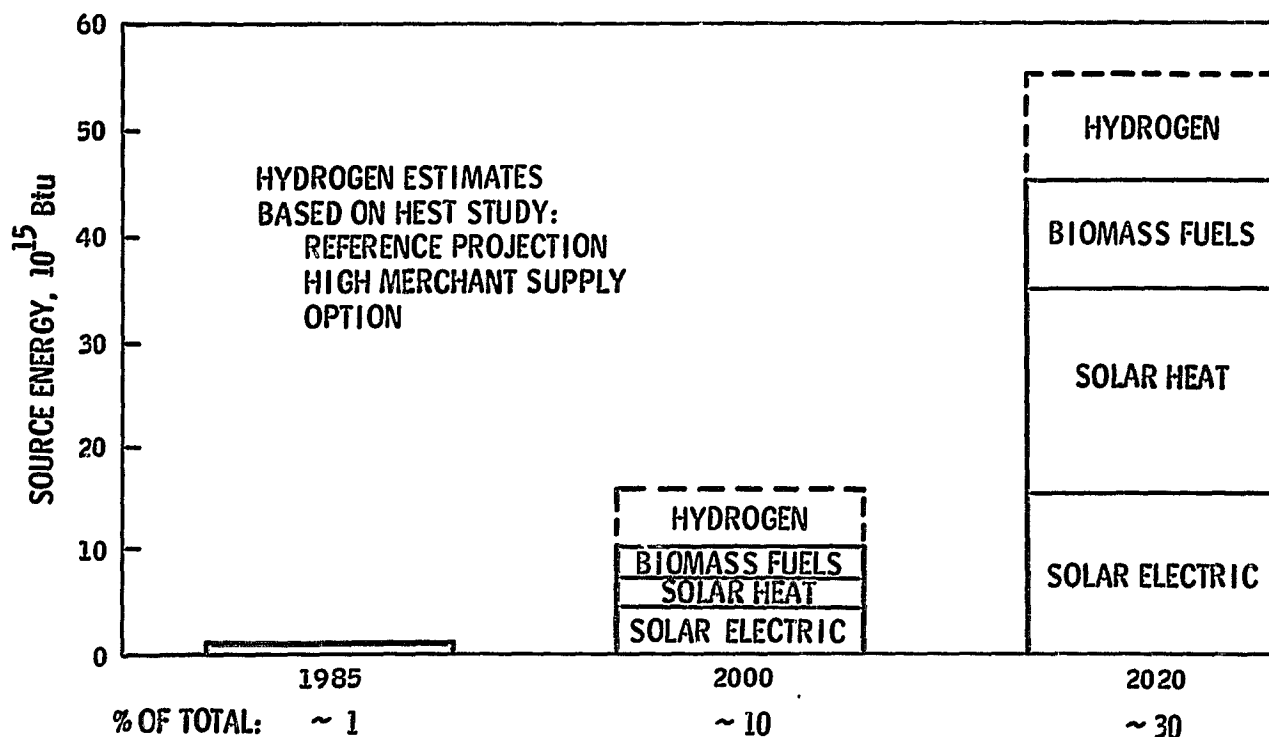


Fig. 12. United States solar energy projections (Baseline from ERDA-49)

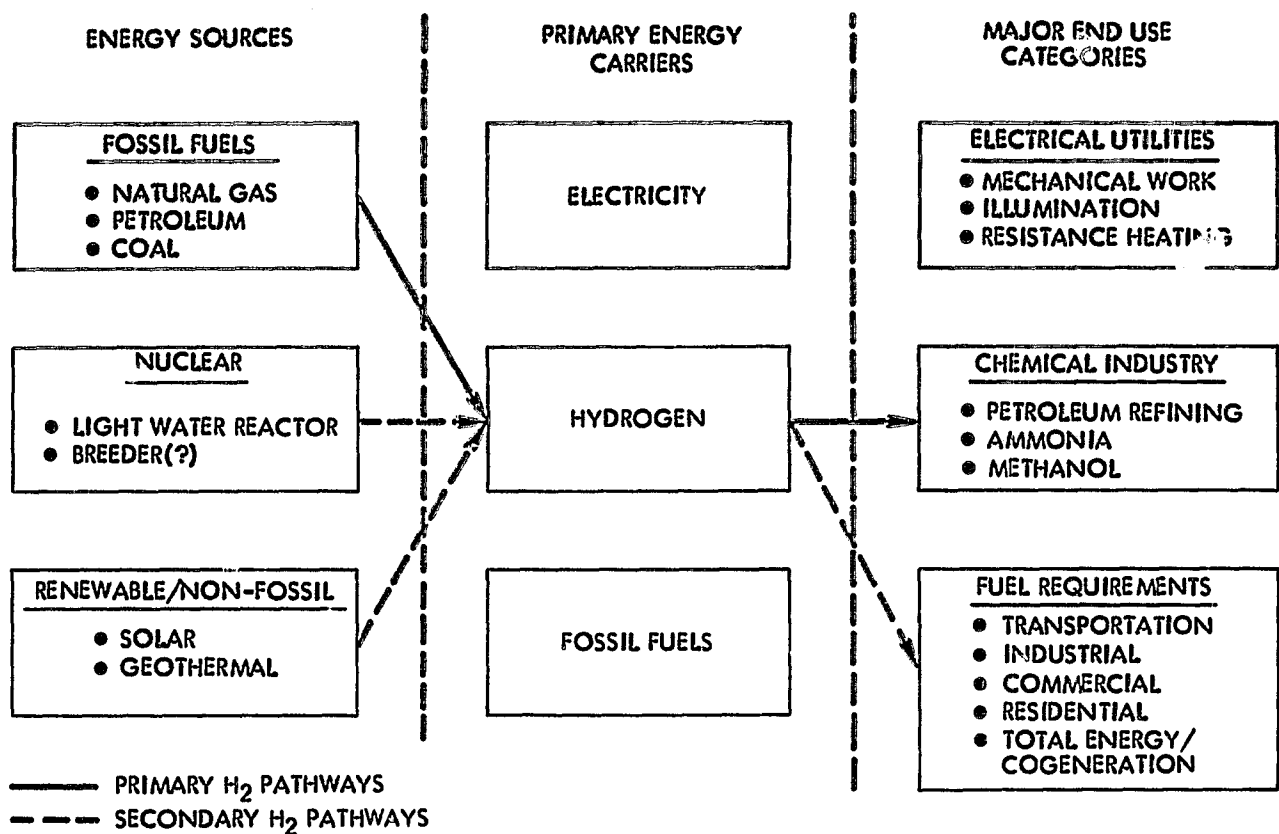


Fig. 13. Primary and secondary hydrogen pathways, fossil fuel era

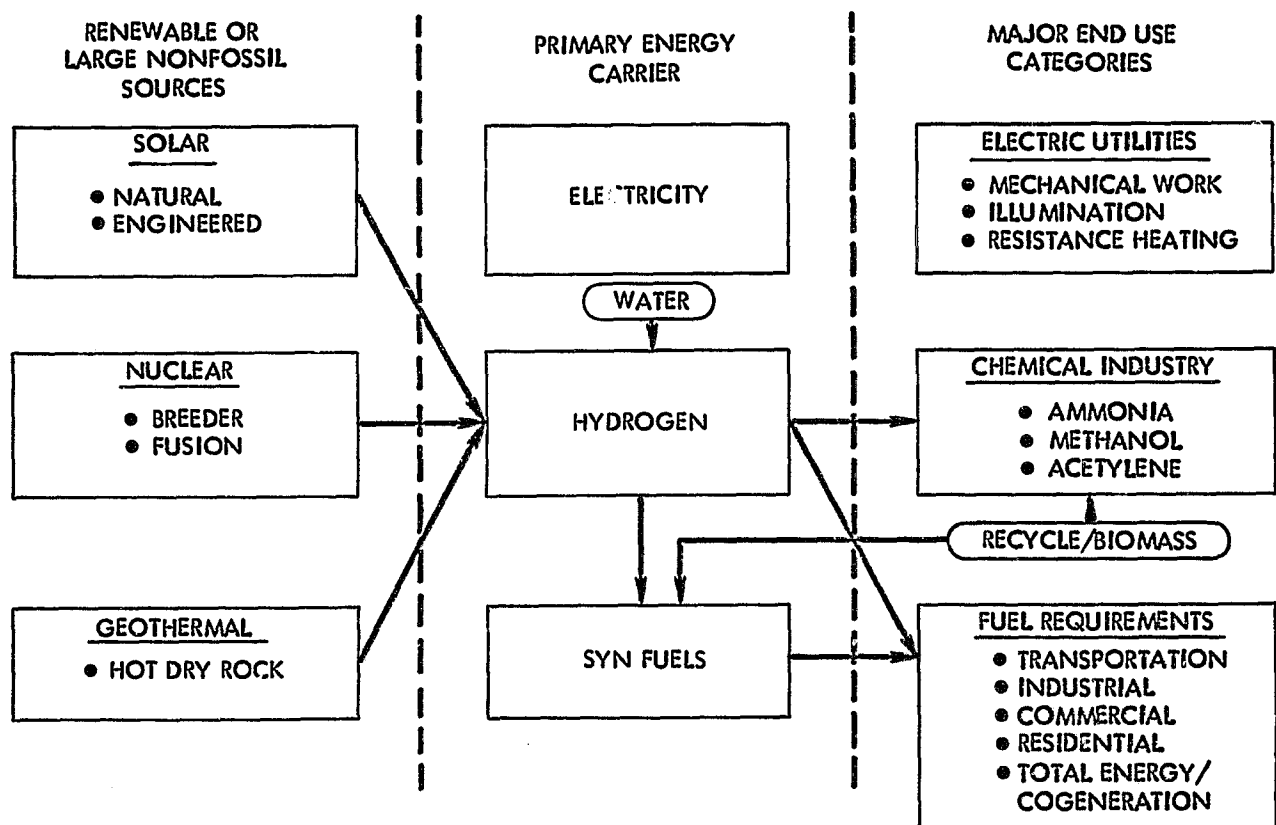


Fig. 14. Critical hydrogen pathways, renewable fuel era

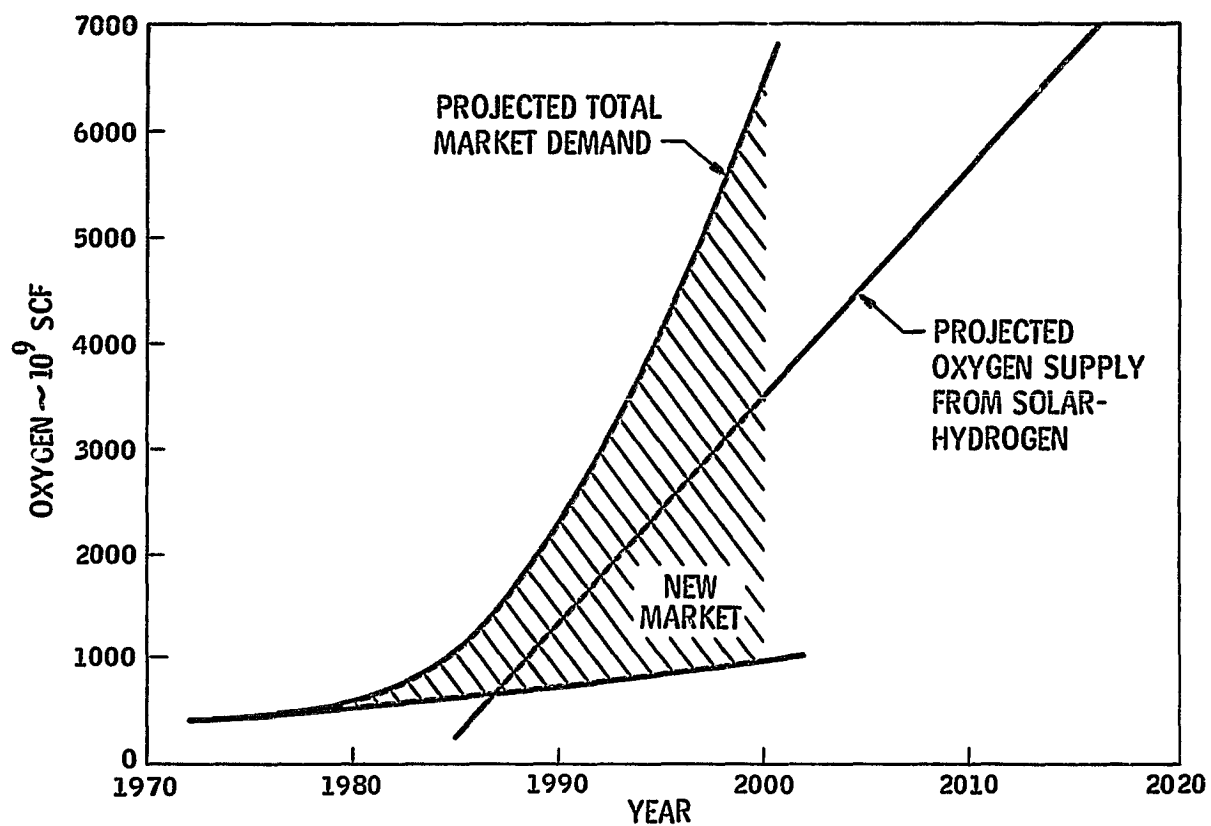


Fig. 15. Byproduct oxygen from solar-hydrogen, supply and demand

SOLAR-CHEMICAL ENERGY CONVERSION AND STORAGE:

CYCLOHEXANE DEHYDROGENATION

Arthur B. Ritter, George B. DeLancey,
James Schneider and Harry Silla

Department of Chemistry and Chemical Engineering
Stevens Institute of Technology
Hoboken, New Jersey 07030

Abstract

The concept of storing excess Thermal Energy as chemical bond energy and the subsequent recovery of this energy on demand by utilizing reversible catalytic chemical reactions shows great promise from an energy density point of view. In the intermediate temperature range (400-800°F) the cyclohexane-benzene reaction appears to be the most appropriate. While this reaction has been extensively studied in the exothermic direction, little useful design data exists for the endothermic reaction. We have studied the apparent kinetics of the gas-phase catalytic decomposition of cyclohexane to benzene in an internally recirculated (gradientless) reactor over the temperature range 400-600°F. At low space velocities (high conversions) a maximum of 0.2% of the product formed in a single pass over a commercially available naptha reforming catalyst is side products which may or may not be reversible. At high space velocities, there are significant mass transfer limitations on conversion. A test loop has been designed to enable us to study the buildup of side products and catalyst activity behavior during long term continuous cycling of the reversible reaction.

INTRODUCTION

The collection and storage of thermal energy through the destruction and reformation of chemical bonds is an attractive competitor to the utilization of sensible and latent heat effects as the energetics of chemical reactions are considerably more intense than the energetics of the latter two processes. In addition, and equally important, chemical energy storage offers the potential of low storage volumes and thermally efficient storage conditions at ambient temperatures. The basic principles on which chemical energy storage and transmission is based are broadly outlined in (7). Essentially, the chemical energy storage-recovery scheme we have developed involves a reversible gas-phase catalytic reaction which is endothermic in one direction and exothermic in the reverse direction. The endothermic step is driven by a source of excess thermal energy (e.g. solar) and the products of the reaction are stored until such time as the thermal energy is needed. Often it will be economically justifiable to store the reaction products at ambient temperatures since the sensible heat required to raise the temperature of the reactants up to the reaction temperature will only constitute a small fraction of the enthalpy of reaction. The presence of a catalyst is necessary for the reverse reaction to proceed so that the reaction products (and therefore the chemical bond energy they contain) can be stored indefinitely. Recovery of the thermal energy takes place on demand by running the reverse (exothermic) reaction over an appropriate catalyst. In a reversible reaction the products of the endothermic reaction are just the reactants for the exothermic reaction and vice-versa. The net result of this cyclic process is the storage of thermal energy during times when supply exceeds demand and recovery of the energy during times when demand exceeds supply. No net consumption of any of the reacting species occurs over the cycle. Furthermore, it is not necessary that the collection and utilization of energy take place at the same location. For example, the endothermic reaction (energy collection step) can be carried out at one location (e.g. where sunshine is plentiful and regular) and the reaction products shipped via the existing natural gas and/or petroleum pipeline distribution system to one or more users. At the utilization site, the exothermic reaction (energy recovery step) can then be carried out and the products of this reaction returned to the collection site, again, via the pipeline distribution systems. This is the so-called "Chemical Heat Pipe" concept (16).

Reaction Selection

A brief review of some of the reactions which have been suggested and at least partially evaluated is given in table 1. Chemical systems which have been proposed with the primary objective of hydrogen production have not been included. The emphasis here is on chemical storage cycles from a more general point of view. Reactions suitable for thermal storage applications fall into two basic categories: catalytic and thermal decomposition reactions (where the reactants and products exist in different phases). Reactions in both of these categories are susceptible to precise control which is required for efficient storage and/or transmission operations. The proposed thermal sources for all of these reactions are solar or

nuclear either via direct contact between the thermal source and the reactive system or via an intermediate heat transfer fluid. The primary focus of attention has been on reactions whose endothermic steps are operative in the temperature range 600-900°F as higher temperature sources such as gas cooled nuclear reactors (~1600°F) of the Pebble Bed Reactor (~2000°F) will not be readily available in the United States in the near future (4). The object here is to address the question of a suitable reaction which can absorb thermal energy at approximately 600°F and release this energy at a temperature of 400°F which is suitable for saturated process steam and electrical energy generation.

In searching for a suitable reaction, attention was focused primarily on catalytic reactions since such reactions very often exhibit high reaction rates which are important for the applications considered here and because this class of reactions is very extensive and includes many of the most energetic and thoroughly studied systems. In addition, the survey was not limited to the 400-600°F range of interest since little additional effort was required to include the high temperature regime. An abbreviated version of the results of a review of catalytic systems whose kinetics have been studied is given in table 1. The full table contains over 20 catalytic reaction systems which show some measure of potential for application to solar-chemical conversion systems and which have been studied to a sufficient degree that past experience has shown them technically worthy of consideration.

Once the desired temperature range has been selected, the choice from among the wide variety of catalytic reactions will be governed by the following general criteria:

1. The chemical capacity for energy storage should be large, i.e. the enthalpy change for the reaction should be large.
2. The system should exhibit significant conversions at the temperature extremes to effectively exploit the energy storage potential, although in some cases it may be more economically feasible to operate at lower conversions and recycle the unreacted product. If a gas phase reaction involves mole changes, as most do, the pressure at the energy absorption and desorption stages may be adjusted to enhance the equilibrium conversions.
3. The catalyst, which may be different for the reverse reaction, should be stable and inexpensive.
4. The rate of reaction should be large to minimize reactor volumes and heat transfer areas. The reaction should not proceed to any significant extent in the absence of the catalyst.
5. The selectivity of the catalyst in both endothermic and exothermic directions should be near 100%. However, side reactions which are reversible and do not cause deactivation of the catalyst can be tolerated.
6. The reactants and products should be economically stored at high energy densities.

7. Inexpensive materials of construction must be available that will not be attacked by the chemical species or act as unfavorable catalysts for the reaction(s) involved.

These characteristics are not independent and must be weighed together in the final selection of a catalytic reaction. Similar criteria have been proposed by others (5) (11).

One of the selection criteria requires the calculation of an energy density for the reaction. Since the reactions are reversible, the energy density can be based on the reactants, entirely on the products or some average of the two. Consequently in table 1, we present three different forms of the energy density. The first, e_r , is based entirely on the reactants. The second, e_p , is based on the products; while the third, e_t , is based on the average and is given by:

$$\frac{1}{e_t} = \frac{1}{e_r} + \frac{1}{e_p}$$

The value of e_p (for example) was calculated as:

$$e_p = \frac{(-\Delta H_R)}{\sum \frac{v_i}{\text{products } M_i \rho_i}}$$

$(-\Delta H_R)$ - enthalpy change for the reaction

v_i - stoichiometric coefficient of species i

ρ_i - density of species i

The summation was taken over the reactants for the calculation of e_r . The energy densities are calculated for the storage conditions listed beneath the products and reactants. All species are assumed to be stored, stoichiometrically, at 300°K. Gases are supposed to be compressed to 100 atm.

Based on this and other information concerning the availability of catalysts and kinetic data, we can conclude that the following reactions show the most promise for successful application to chemical energy storage and conversion systems.

In the high temperature range (1000°F-1500°F), the oxidation of sulphur dioxide is the most appropriate. The kinetics of this reaction have been thoroughly studied (17) in the exothermic direction. Also, considerable process technology has been accumulated (3). The high energy densities are both due to the condensation temperatures of the sulphur oxides and low stoichiometric coefficient for oxygen. This reaction has been considered for energy storage by several investigators (1) (9) (14). A recent study in this laboratory (6) has indicated a pronounced hysteresis phenomenon in the temperature - conversion history of this system which must be studied further. However, it appears that, for this case, the hysteresis phenomenon is beneficial rather than detrimental from an energy storage point of view.

In the intermediate temperature range (400°F-

600°F), the hydrogenation of benzene appears to be the most appropriate. The most popular catalyst for the exothermic direction appears to be the Ni catalysts, although others are available (2). The reverse reaction can be catalyzed effectively with industrial reforming catalysts as well as carbides, silicates and sulphides of carbon (8). It should be noted that although the density for energy storage is large, the density would be appreciably increased if the hydrogen were stored in the hydride form (10) (15).

We have chosen to concentrate our efforts in the intermediate temperature range (400-600°F). In particular we believe that the benzene hydrogenation-cyclohexane dehydrogenation reversible catalytic reaction is the vehicle by which the chemical energy storage concept can be most readily demonstrated on a commercial scale. Some of the reasons for this position are given in (12). The primary technical questions that are associated with the current proposal lie in the reactor technology associated with the cyclohexane dehydrogenation reactor (energy collection step) and the possibility of detrimental side reactions concomitant to the dehydrogenation step. On the other hand, the technology for the benzene hydrogenation step (energy recovery) is well known and readily available on a commercial scale (18).

With respect to the dehydrogenation reactor, one must investigate the nature of the procedures required to effectively provide transient operation as opposed to the steady state technology that is available in the chemical industry. Start up and shut down algorithms must be developed. Such an investigation is most appropriately done computationally in the preliminary stages with engineering models of the reactor.

The chemical aspects of the dehydrogenation step must be investigated experimentally. The results of a preliminary investigation in this laboratory are presented below.

KINETIC STUDY OF C_6H_{12} DEHYDROGENATION

Flow System

We have measured the kinetics of the cyclohexane dehydrogenation reaction in the temperature range 400°F-750°F over a commercially available naphtha reforming catalyst (RD 150) manufactured by Englehard Industries in a fully instrumented internally recirculated (gradientless) stirred tank reactor built by Autoclave engineers. A schematic diagram of the experimental system is shown in figure 1.

Cyclohexane feed is introduced into the reactor by means of a Harvard constant infusion syringe pump. This is a positive displacement pump that provides very precise control of flow-rate over the range 0.025-38.2 ml/min depending on the size of the syringe used and the speed selected. A double syringe model is used along with a 3-way ball valve arrangement to insure virtually continuous precise flow of the cyclohexane feed to the reactor. The calibration of the pump has been checked at all speeds using a graduated cylinder and stopwatch. The reactor has a one gallon working capacity. The catalyst is supported in a cylindrically shaped bed approximately

5.8 cm in diameter by 13.0 cm long located on the axis of the fan. The catalyst bed is an integral part of the fan system which is designed to circulate the gas phase through the catalyst bed to insure intimate contact between the gas and catalyst. A rheostat allows the fan speed to be adjusted over the range 1000-2100 rpm. The speed is measured by means of a strobe tachometer. Two thermocouples located 2.0 from the top and 2.0 cm from the bottom of the catalyst bed allow us to monitor the temperature change across the bed. The location of these thermocouples can be adjusted to monitor the temperature at any two points along the catalyst bed. Temperature control is provided by means of three 650 watt resistance heaters located around the reactor. The three heaters provide 3 independently regulated zones of heat at the top, middle and bottom of the reactor. All 3 heaters are used for startup, while only the bottom heater is generally required for temperature control during operation. The reactor is well insulated and the temperature variation is usually less than $\pm 0.5^{\circ}\text{F}$ during a run. The pressure in the reactor is controlled manually by means of a needle valve and pressure gauge on the outlet line. The data in these studies were taken at a constant reactor pressure of 2.0 psig. The outlet from the reactor is split into two streams. The major part is passed through a total condenser. The cooling water for the condenser is provided by a refrigeration unit operating near 0°C (although capable of going to -10°C with the use of a heat transfer fluid such as Dowtherm). The condensed product (benzene and cyclohexane) is collected in glass containers and disposed of in a safe manner. Non-condensibles (mostly hydrogen saturated with benzene and cyclohexane vapors at 0°C) are vented through the laboratory hood system. A small portion of the outlet stream is piped directly to a Hewlett-Packard 5830A computer controlled gas chromatograph equipped with a heated, automatic, programmable gas sampling valve. The detector is a hydrogen flame ionization unit and excellent separation of benzene and cyclohexane is achieved by a $1/4" \times 6 \text{ ft.}$ column packed with carbowax. The chromatograph is calibrated both for concentration of cyclohexane and benzene and total sample size by injecting known amounts of carefully prepared mixtures of benzene and cyclohexane. A correction for sample size is required since at high conversions, large volumes of hydrogen are present in the product stream along with the cyclohexane and benzene. The hydrogen essentially acts as a diluent when the sample passes through the hydrogen flame ionization detector. The computer on the chromatograph automatically computes the total areas under all the curves (related to sample size) as well as the fraction of the areas under each curve. It should be emphasized that the experimental apparatus are flexible enough so that the kinetics of many gas phase catalytic reactions can be readily studied with only minor modifications to the system.

Experimental Procedure and Data

At the end of each days operation the flow system is thoroughly flushed with nitrogen and left overnight under a slight nitrogen positive pressure for safety. To start operation, the system is first brought up to the desired operating temperature, the nitrogen is shut off and cyclohexane feed is introduced at a liquid flowrate of about 2.75 ml/min to flush the reactor. After

approximately 5 residence times of flushing ($\sim 25 \text{ min.}$), the cyclohexane flowrate is adjusted to the desired experimental value. Conditions of temperature, pressure and flowrate in the reactor are maintained constant until the concentration of benzene leaving the reactor (as indicated on the gas chromatograph) reaches a constant value. The rule of thumb is to wait at least 5 residence times after any system changes have been made to insure that a steady-state condition has been reached.

The feed to the reactor is reagent grade cyclohexane. As each new bottle of cyclohexane is opened, its purity is checked by running several samples through the chromatograph. Occasionally trace quantities of toluene and other impurities are detected in the cyclohexane. The naptha reforming catalyst is in the form of pellets approximately $1/16" \text{ D} \times 3/16" \text{ L.}$ The catalyst is weighed and loosely packed into the cylindrically shaped bed support. Layers of glass beads of several different sizes are randomly interspersed with the catalyst pellets to fill the unused portion of the bed with inert material and provide a matrix to insure adequate flow in and around each catalyst pellet and through the bed. Before each new set of runs the catalyst is activated by a nitrogen flush (to eliminate any oxygen present) followed by a hydrogen purge at 900°F for 2 hours. The catalyst activity is checked at the beginning and end of each set of runs by duplicating a high conversion ($>90\%$) data point at 600°F and comparing the conversion with the conversion obtained when the catalyst was fresh. We have used the same batch of catalyst over the past year and a half, including over 2 dozen reactivations and many start ups and shut downs (temperature cycling). As far as we can tell the catalyst activity has remained constant.

At each temperature and feedrate (space velocity), the reactor is run at several different agitator speeds to determine the effects of external mass transfer on the conversions. Figure 2 shows the results for several flowrates at 600°F . One can see that at low space velocities, where conversions close to equilibrium are obtained, the external mass transfer can keep pace with the (relatively low) reaction rate. However, as the space velocities are increased and the reaction gets farther from equilibrium, the external mass transfer can't keep pace with the (relatively rapid) reaction rate and so the mass transfer effects limit the observed conversion. Under these conditions the conversion becomes a function of the agitator speed and the "true" conversion must be obtained from the data by extrapolation to infinite agitator speed (elimination of external mass transfer effects). Figure 3 is a plot of the conversion of cyclohexane obtained over a range of space velocities, with temperature in the range $500\text{--}750^{\circ}\text{F}$ as a parameter. Figure 4 is even more descriptive in that it shows the reaction rate times the space velocity - vs - conversion at each temperature. The data in figure 4 clearly point out the effects of mass transfer limitation. The dashed line is data taken at 600°F at low agitator speeds. The data at each temperature approach the calculated equilibrium values at low space velocities.

By Products

At high conversions (low space velocities) and at temperatures above 540°F at 2 psig, several side products are produced along with the benzene and hydrogen over this catalyst. The total amount of these products is never more than 0.2% in a single pass through the reactor and is generally <0.1% except at the most severe conditions. Using a chemical ionization mass spectrometer (CIMS) we analyzed the components in the vapor phase leaving the condensor for one run at 600°F and a space velocity of 0.029 moles cyclohexane/g-catalyst-hr. The major side product has clearly been identified as toluene. Based on the gas-chromatograph data, when side products are produced, toluene constitutes somewhere between 60-100% of the side product formation. We have not, as yet, identified the remaining side products, although there is some evidence that methylcyclopentane may be present. However, this molecular weight is masked on the CIMS by the presence of cyclohexane. A peak at molecular weight 54 corresponds to 1 or 2 butene or might correspond to one of the fragmentation products produced in the spectrometer. Similarly, the presence or absence of C₁ to C₄ hydrocarbons in the product stream is masked by the fragmentation products of the spectrometer. Accordingly, we have ordered some pure methylcyclopentane and 1 and 2 butene. We will introduce these into the gas chromatograph and compare their retention time on the chromatograph column with our unknown peak. Similarly we have ordered a chromatograph column which will allow us to separate the C₁ to C₄ hydrocarbons to see if any are present in our product stream. It should be noted that toluene is reversible and methylcyclopentane is not reversible to cyclohexane over a suitable catalyst (13).

Table 2 summarizes the chemistry of the cyclohexane decomposition reaction as we have been able to determine it to date.

FUTURE PLANS

The questions we plan to answer in the next phase of our study center around the behavior of the system under long term cycling. In particular we must ascertain whether or not the side products produced are reversible and if not whether or not they reach an acceptably low equilibrium value under long term cycling. We must also study the behavior of the catalyst(s) under long term cycling to see what effects there are on such parameters as catalyst activity and attrition.

Accordingly, we have designed a test loop to study these and related questions. A schematic diagram of the test loop is shown in figure 5. The major pieces of equipment in the loop have been sized and will be purchased in the near future. This loop will allow us to continuously cycle the cyclohexane, benzene and hydrogen over both the reforming catalyst and a hydrogenation catalyst. Periodic sampling of the product streams in each loop and the catalyst beds should allow us to answer some of the questions posed above. The loop was designed on the basis of a hydrogen flow of 1 SCFM with a hydrogen surge-storage capacity of 10 minutes (1 ft³, 34 atm). The cyclohexane and benzene liquid flowrates were sized at a nominal value of 60 ml/min. with 10 gal. feed tanks. Except for the hydrogen compressor, the test loop will fit in one corner of our research laboratory (10 x

12 ft).

A second set of questions we expect to answer over the next year concerns the behavior of cyclohexane decomposition reaction at high pressure (up to 500 psig). Because hydrogen is produced in the decomposition reaction, higher pressures will tend to shift the equilibrium to lower conversions (hence lower energy storage capacities). However, for chemical heat pipe applications, it is desirable to operate the collector at higher pressures. This means increasing the operating temperature to compensate for the higher pressure. We also know that at higher temperatures greater quantities of the side products are produced and there is also the possibility of thermally cracking the benzene molecule. The answers to these and other questions related to the catalyst stability at the higher temperature and pressures will be pursued over the next year.

Finally, we have developed a mathematical model which describes the transient behavior of a gas phase catalytic reactor dedicated to the collection of thermal energy. The results have been reported previously (12). The model will prove useful in simulating startup, shutdown and in developing control algorithms for chemical energy storage systems. The model is being modified to take into account the mass transfer limitations we have observed in the cyclohexane decomposition reaction. Over the next several months we expect to develop the model to the point where we are able to simulate the transient behavior of the collector reactor in the test loop under varying conditions of startup, shutdown and changes in the thermal energy flux reaching the reactor.

ACKNOWLEDGEMENTS

We wish to thank Robert Yarrington of Englehard Industries who supplied us with the RD 150 naphtha reforming catalyst used in this study and the Union Carbide Corp. for their donation of the reactor. We also gratefully acknowledge the many long days and nights spent by Stevens undergraduates Mike Kosusko, Rochelle Chernikoff and Richard Jarosz in collecting and analyzing the data. Their enthusiasm, energy and good humor went far beyond the requirements of their work-study jobs. Also to Dominick Quagliato for his help with the Chemistry, and to Marianna Buzzerio and Abram Addonizo for their help in the lab. Finally, we would like to acknowledge the financial support given to Jim Schneider through the R.C. Stanley Fellowship fund at Stevens Institute of Technology and the Energy Research and Development Administration through ERDA grant no. E(11-1) 4031, which partially supported this research.

REFERENCES

1. Chubb, T.A., Solar Energy, **17**, 129 (1975).
2. Dini, P., et al., "A Study of Platinum - Polyamide Catalysts. Catalytic Behavior in the Benzene Hydrogenation Reaction", J. Catalysis, **30**, 1 (1973).
3. Duecker, W., West, J., The Manufacture of Sulfuric Acid, Reinhold Publishing Corp., New York, 1959.

4. Golibersirch, D., F.P. Bundy, P.G. Kosby and H.B. Vakil, "Thermal Energy Storage for Utility Applications," Thermal Energy Storage Conference, NATO, Turberry, Scotland, March, 1976.
5. Hanneman, R.E., Vakil, H.B. and Wentorf, R.H., "Closed Loop Chemical Systems for Energy Transmission, Conversion and Storage", 9th IECEC, San Francisco, 435 (1974).
6. Kovenklioglu, S. and DeLancey, G.B. "A Study of the Apparent Kinetic of the Reversible Catalytic Oxidation of Sulphur Dioxide," Submitted to AIChE J (1977).
7. Kovich, E.G. (Ed.) "Thermal Energy Storage", report of a NATO Science Committee Conference held at Turberry, Scotland, March, 1976.
8. Krylov, O.V., in Catalysis by Nonmetals, translated by Happel, J., et al., Academic Press, New York, 1970.
9. Lynn, S., and Foss, A., "The Sulphur Dioxide System for Energy Storage", Proceedings of the ERDA Contractors review meeting, Brookhaven National Laboratory, April, 1976.
10. "On the Shelf: Scientists seek ways of Storing Electricity to Prevent Brownouts", Wall Street Journal, Vol. CLXXXIV, No. 4, July 5, 1974.
11. Prengle, H.W. and Sun, C.H., Solar Energy 18, 561 (1976).
12. Ritter, A.B. and DeLancey, G.B., "Thermo-Chemical Energy Conversion and Storage", Proc. ERDA Contractors Review Meeting on Chemical Energy Storage and Hydrogen Energy Systems, ERDA CONF-761134, Airlie, Va., Nov. 8-9, 1976.
13. Personal Communication from Matthew Rosso, Jr. Brookhaven National Laboratory, Sept. 20, 1977.
14. Spewock, S., Brecher, L.E. and Talks, F., "The Thermal Decomposition of Sulphur Trioxide to Sulphur Dioxide and Oxygen", 1st World Hydrogen Energy Conference, Miami Beach, Fla., March 1-3, 1976.
15. "Solar Energy work Advancing Rapidly," Chem. and Eng. News, Sept. 16, 1974.
16. Vakil, H.B., "Energy Transmission by Chemical Heat Pipe," General Electric Technical Report No. 76CRD281, Schenectady, N.Y., 1976.
17. Weychert, S. and Urbanek, A., "Kinetic Equations for the Catalytic Oxidation of Sulphur Dioxide", Int. Chem. Eng., 9, 396 (1969).
18. Thomas, C.L. Catalytic Processes and Proven Catalysts, Academic Press, New York (1970), p. 138-139.

Table 1

Review of Some Candidate Reactions Currently Proposed For Thermal Energy Storage Applications

Reaction (Exothermic)	(-ΔH _R) (Kcal/g-mole)	Energy Density (BTU/ft ³) x 10 ⁻³			Energy Absorption			Energy Desorption		
		e _r	e _p	e _t	T (°F)	P (ATM)	CAT.	T (°F)	P (ATM)	CAT
(Storage Conditions) for Energy Density Calculations										
SO ₂ + ½ O ₂ = SO ₃ liq. gas liq. at 4.1 atm 0.44atm	23.5	15.8	63.5	12.6	1500- 1800	3	Pt	900- 1100	3	V ₂ O ₅
*CO + 3H ₂ = CH ₄ + H ₂ O CO ₂ + H ₂ = H ₂ O + CO H ₂ O = liq at .03atm, rest = gases	53.0 -10.0	5.8 4.2	21.0 3.9	4.6 2.0	1500	40	N ₂ + EXCESS H ₂ O	950	40	Ru, N _i
C ₆ H ₆ + 3H ₂ = C ₆ H ₁₂ liq gas liq at 0.13atm 0.13atm	49.25	6.7	51.7	5.93	400- 600	1.0-1.5	N ₂ , Pt	300- 500	40	N _i , Pt
CaO(s) + H ₂ O = Ca(OH) ₂ (s)	12.2	-	-	-	950	1.0	NONE	950	1.0	NONE
MgO(s) + H ₂ O = Mg(OH) ₂ (s) H ₂ O = liq. at 0.03 atm.	18.5	-	-	-	500	1.0	NONE	500	1.0	NONE
NH ₃ + H ₂ O + SO ₃ = liq. liq. liq. NH ₄ HSO ₄ (s) at 10 at 0.03 0.44 and 1.0 atm	80.4	-	-	-	1800 950	1.0 142.0	NONE NONE	900 790	1.0 1.46	NONE NONE

* The ADAM-EVA Chemical Energy Storage Process, seriously considered in Europe, involves only the first reaction. The combined set of reactions have been proposed for use in a chemical heat pipe system (5) (16).

Table 2

Summary of Cyclohexane Dehydrogenation Chemistry



Space Velocity = 0.03 g cyclohexane/g cat. hr.

Temperature ($^{\circ}\text{F}$)	Conversion (% Benzene)	% Side Products
500	42.0	0.11 - Toluene < 0.01 - Other(s)
540	68.0	0.10 - Toluene < 0.01 - Other(s)
575	76.5	0.09 - Toluene 0.03 - Other(s)
600	84.0	0.09 - Toluene 0.09 - Other(s)

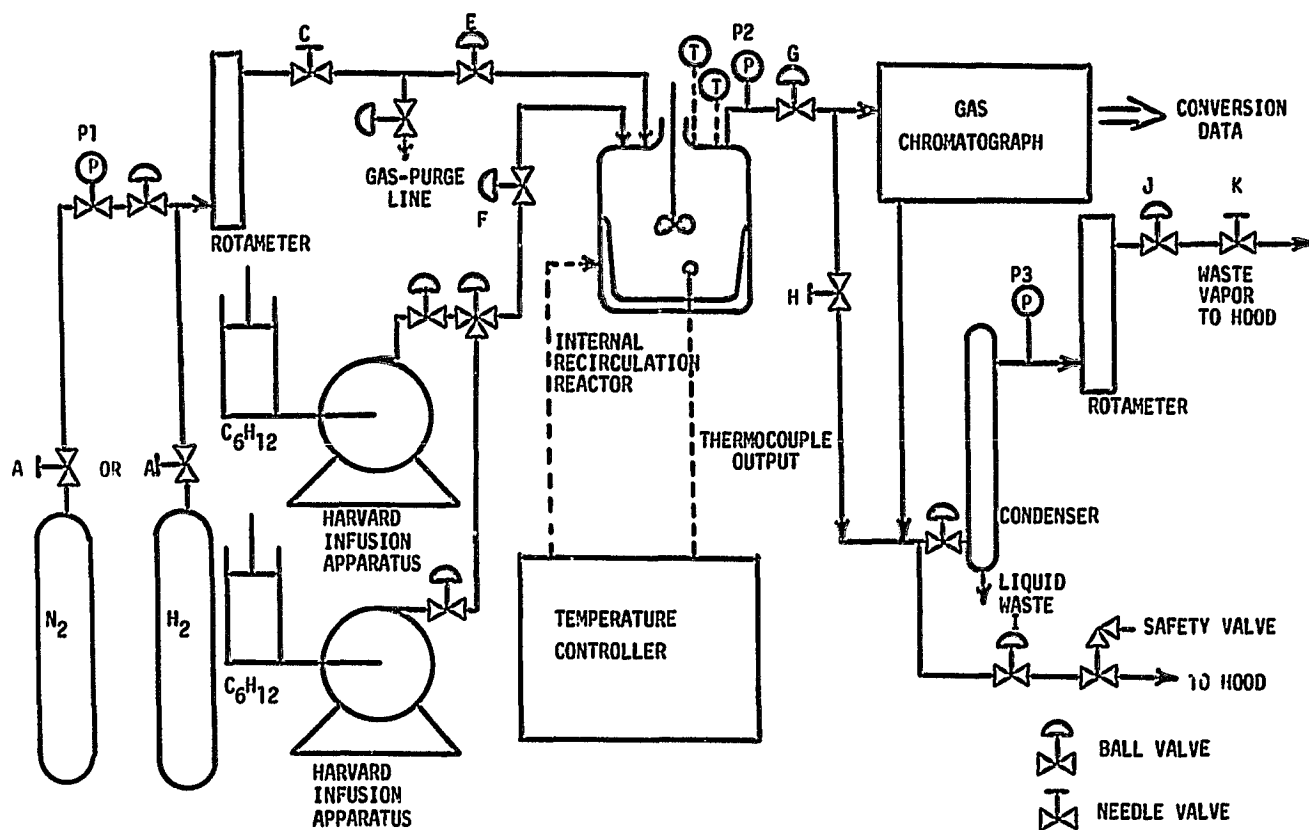


Fig. 1. The experimental flow system for studying the kinetics of gas phase catalytic reactions

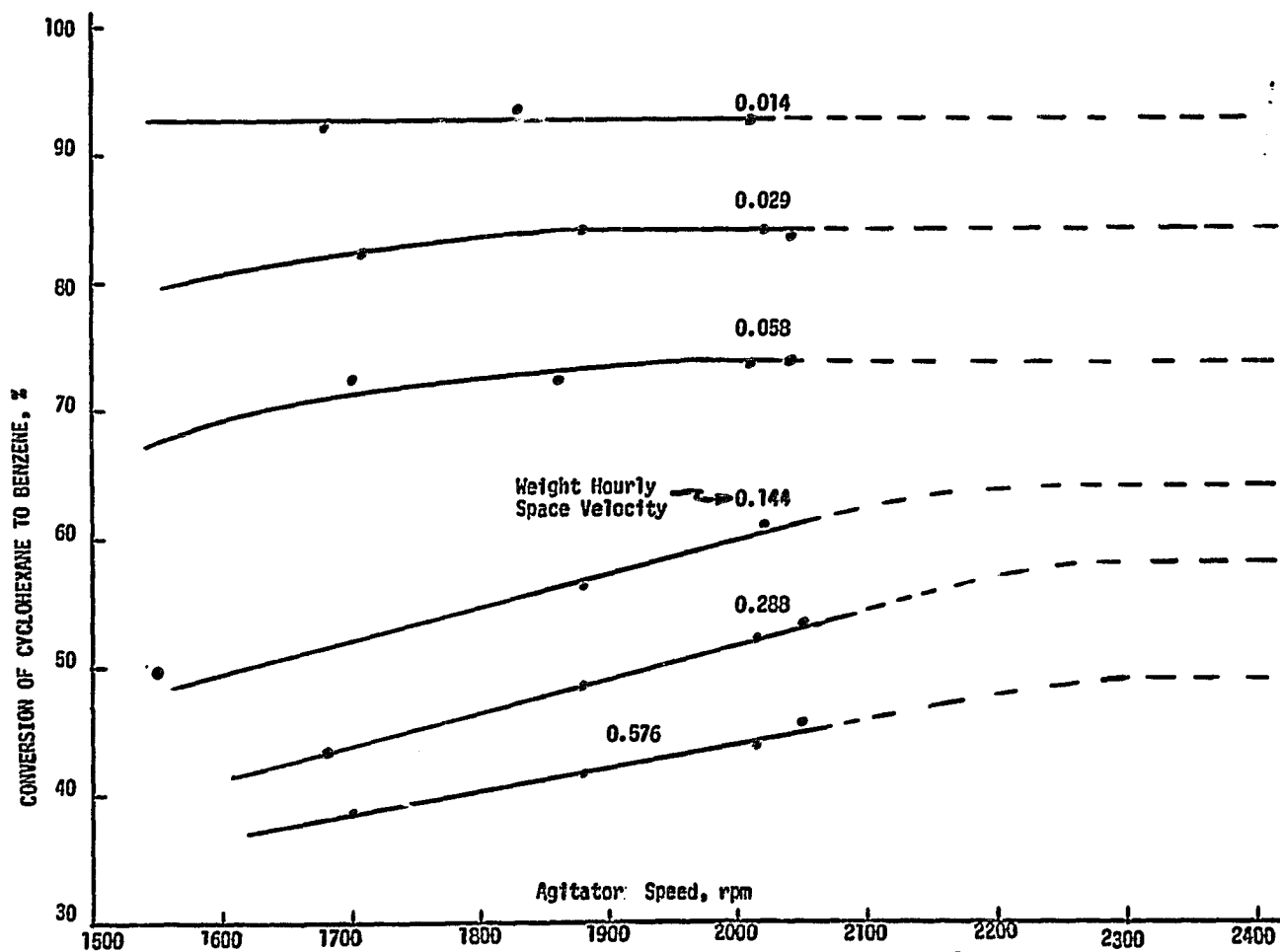


Fig. 2. The effects of external mass transfer on conversion at 600°F

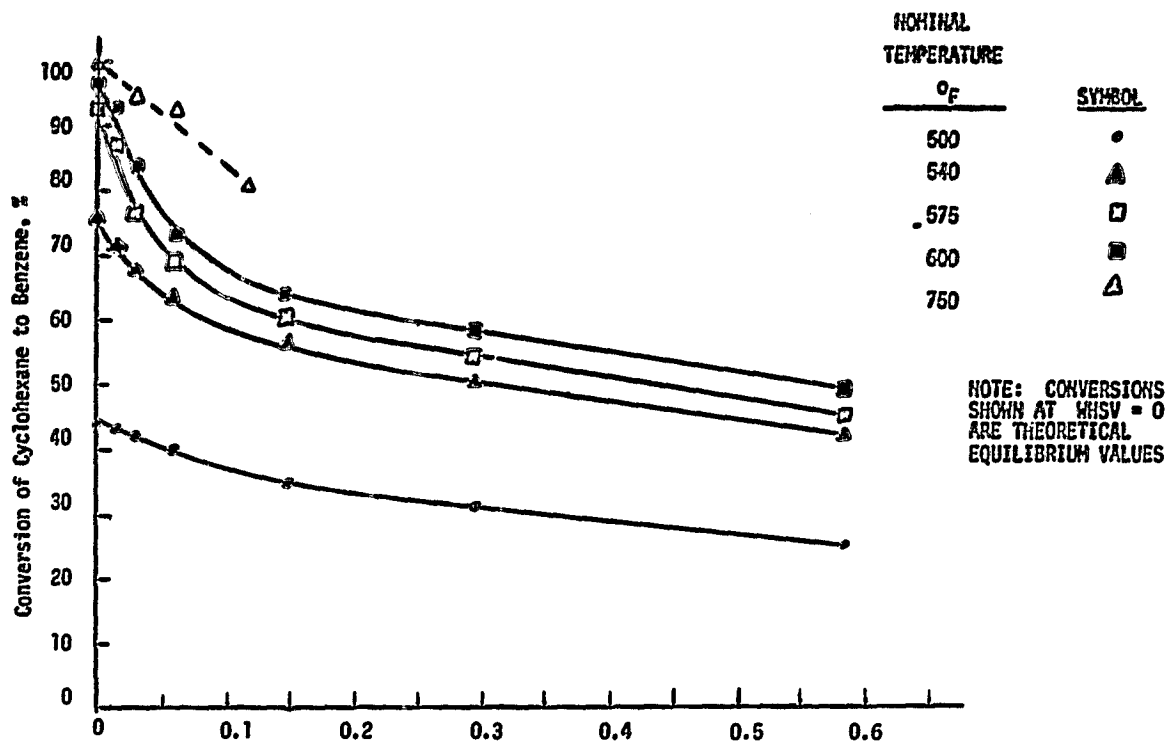


Fig. 3. Cyclohexane conversion vs weight hourly space velocity over the temperature range 500-750°F at 0.2 psig

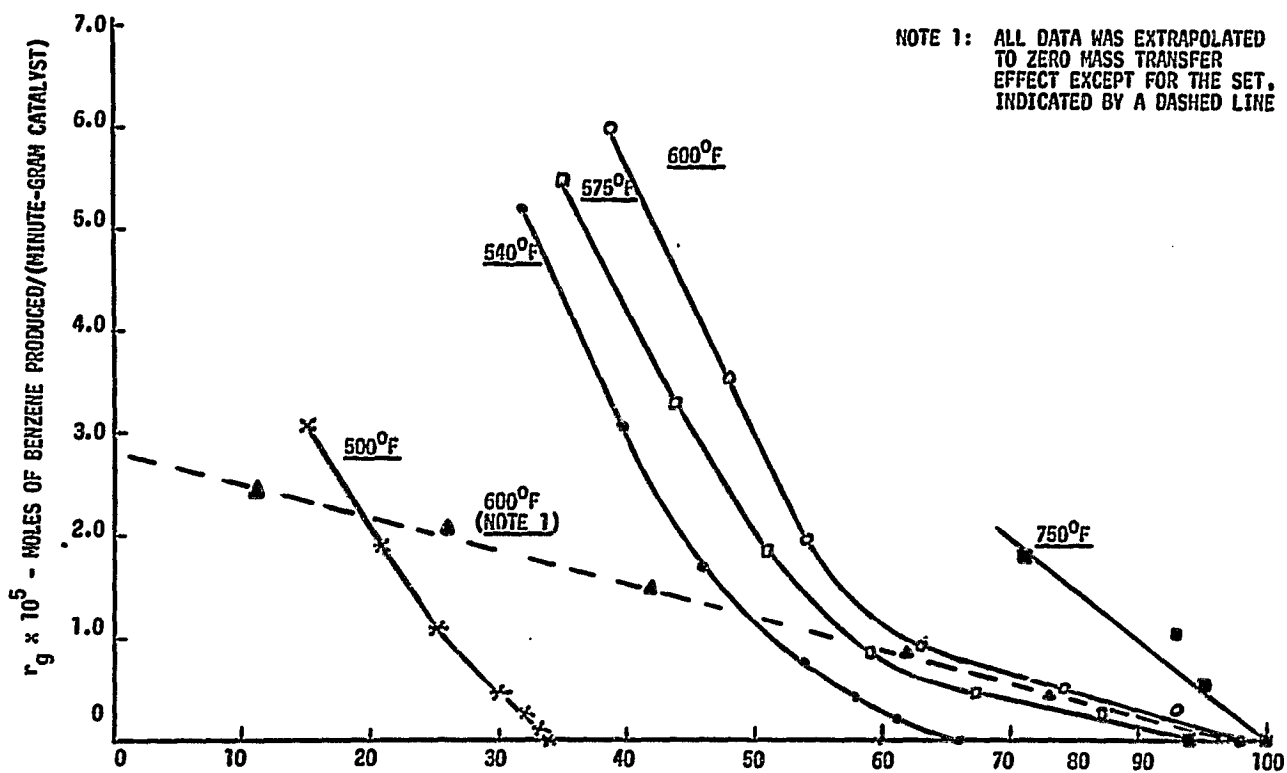


Fig. 4. Reaction rate times space velocity vs fractional conversion of cyclohexane over the temperature range 500-750°F

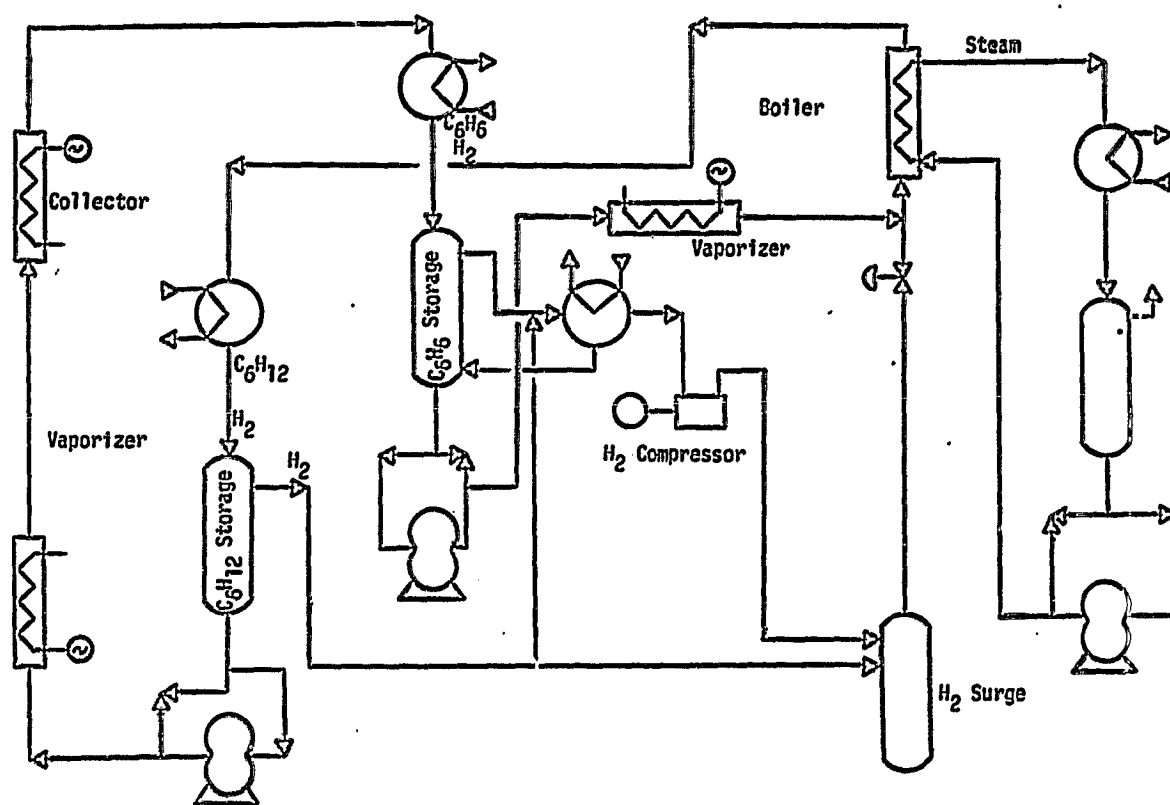


Fig. 5. The experimental flow system for studying long term cycling of the cyclohexane-benzene system

**SYSTEM EVALUATION OF SUPPLEMENTING
NATURAL GAS SUPPLY WITH HYDROGEN**

**W. S. Ku
Public Service Electric and Gas Company
Newark, New Jersey**

Abstract

The production of hydrogen by electrolysis using excess energy available from base-load electric generating units provides one potential means of supplemental future dwindling natural gas supply. Advanced electrolyzer technology now in the research stage was applied for the evaluation. A maximum of 15% volume blending of hydrogen was assumed. No hydrogen storage was applied. The results indicate that electrolytic hydrogen could become economically competitive in the 1990-2000 period with high-cost supplemental natural gas supply.

Introduction

With the natural gas supply picture becoming increasingly critical for future years, alternative technologies are being explored to provide supplemental gas supplies. One such potential means would be to blend hydrogen with natural gas if hydrogen could be economically produced.

Public Service Electric and Gas Company (PSE&G) under a contract with Associated Universities, Inc. and U. S. Energy Research and Development Administration, has completed a system evaluation study to investigate the economic potential of supplementing natural gas with hydrogen produced by electrolysis. The major objectives of the study are:

1. To determine the amounts and associated costs of off-peak electric energy available in typical electric utility systems that could be utilized for producing hydrogen.
2. To determine the economic competitiveness and feasible extent of utilizing electrolytic hydrogen in a "companion" gas utility system.

Study Scope and Guidelines

1. Selected Test Utility Systems - Four electric-gas utility system pairs were selected for the study. These systems are either of a combination company or of two different utilities serving a common territory and represent different geographical regions: A. Mid-Atlantic, B. Midwest, C. Northeast, D. Pacific Coast.
2. Basic Concept of Producing Electrolytic Hydrogen - The principle concept of making hydrogen from electrolysis is to utilize excess energy available from base-load electric generating units during off-peak periods. The base-load units are those with lower fuel costs and are expected to be operating around the clock delivering full-capacity energy output during most of these hours. In future years nuclear and coal-fired steam units are generally classified as base-load generation. The off-peak periods cover those weekday hours from late evening to early morning and most of the hours during weekends when average electric demands are substantially lower.
3. Electrolyzer Technology - Advanced electrolyzer technology, such as the General Electric's solid polymer electrolyzer concept, was considered as the basis for this evaluation. Based on the ERDA guideline, such electrolyzer was assumed to require a capital cost of \$150/kw (1975 dollars), including power conversion

and substation equipment, supervisory control, electric, gas and water connections, and installation. It has an efficiency of 90% and an average life of 20 years.

4. Hydrogen Blending - The companion investigation undertaken by PSE&G for ERDA revealed that with a 10% volume blending no problems are apparent. With a 15 to 20% blending, some modifications of gas burners appear required. For the purpose of this system evaluation study, a more conservative maximum permissible blending level of 15% was used.
5. Hydrogen Storage - One of the ERDA guidelines was not to consider the use of hydrogen storage in this study. Without storage, hydrogen produced electrolytically must be injected directly into the gas distribution system for immediate utilization.
6. Study Period - The period chosen for the study was 1985 through the year 2000.

Electric and Gas System Evaluation

1. Electric Phase

The electric load demand of a utility system varies from hour to hour, day to day, and season to season. Most utility systems now experience its annual peak demands during the summer season. Figures 1 and 2 show respectively the average summer and winter week load curves of a representative electric utility system.

The amount of base-load generating capacity installed will determine the extent of excess energy available from the base-load capacity during off-peak periods. Figures 3 and 4 illustrate this relation. For simplicity the available base-load generation is shown as a common straight line in both figures. The actual available amount of base-load generation in each week is determined by probabilistic analysis taking into account forced and maintenance outages of various units. The excess amounts of base-load energy available each hour can then be determined.

Table 1 shows the amounts of installed base-load capacity, in percent, of the four test systems. Table 2 shows the calculated total excess base-load energy expressed as a percent of total energy produced in that system.

2. Gas Phase

Similarly the gas demand of a utility system also varies continuously. The annual peak demands generally occur in winter. Figures 5 and 6 show respectively the average winter and summer week load curves of a representative gas utility system.

Based on the designated maximum volume blending of 15% hydrogen, the amount of hydrogen that can be absorbed hourly into each test system can be determined. If the selection of the overall electrolyzer capacity is based on the amount of hydrogen that can be absorbed during the minimum gas demand period of the year because of lack of storage, then the actual amounts of blending during other time periods will be substantially less. Tables 3 and 4 show respectively the average percents of hydrogen blending and associated electric energy utilized for the testing systems A and B.

The reason that only the results of two of the four test systems are shown is because the evaluation results of Systems A and B appear to be more meaningful. The other two systems did not provide sufficient future-system data and essentially all their excess base-load energy would be from non-nuclear units as indicated in Table 2.

3. Economic Evaluation

In determining the economic competitiveness of hydrogen supplementation against other forms of supplemental gas supply, the hydrogen cost based on the lowest fuel cost of available excess energy, namely nuclear, should be compared first with the highest-cost supplemental natural gas supply, such as naphtha-derived synthetic natural gas (SNG). Coal-fueled electric energy should be considered next and will increase the volume of hydrogen produced but also the average electric energy cost for producing such hydrogen.

Tables 5 and 6 show respectively the cost comparison between electrolytic hydrogen and supplemental natural gas supply for the test systems A and B. For the Mid-Atlantic system (System A), an annual escalation rate of 4% was applied for both electric system fuel and SNG costs. For the Mid-western system (System B), an escalation rate of 4% was used for electric fuel costs and 7% for natural gas cost.

Summary

1. Adequate amounts of excess electric energy are expected to be available

from base-load generating units of electric utility systems during off-peak periods for producing hydrogen by electrolysis which can be effectively utilized by their companion gas systems. However, the actual availability must take into account such energy uses by other forms of energy storage. Also, economics may justify only the utilization of that portion of available off-peak energy from the lowest fuel-cost units, such as nuclear.

2. The amount of excess energy available from base-load generation is a function of the relative amount of this installed base-load capacity as a percentage of total installed capacity of a system. Generally, this base-load level is in the order of 50 to 60%. With such a level, the excess base-load energy is available during off-peak periods only. On the other hand, if the base-load capacity level is raised to 80% or higher, then certain excess base-load energy would also be available during certain heavy-load time periods, resulting in more electric energy available for making hydrogen during more hours of each day.
3. About 35 to 50% of all excess base-load energy is available on weekends. Therefore without the application of hydrogen storage, a major portion of this electric energy could not be utilized for producing hydrogen.
4. Electrolytic hydrogen may become economically competitive in the 1990-2000 period with SNG on other forms of high-cost supplemental gas supply. Much will depend on:
 - (a) A breakthrough in electrolyzer technology particularly with regard to cost and efficiency,
 - (b) the extent of base-load electric generation in nuclear capacity, and
 - (c) the future cost escalation of SNG or other forms of supplemental gas supply, with respect to the cost escalation of electric generation fuels.

Acknowledgments

The author would like to acknowledge the valuable contributions provided by the following PSE&G personnel who participated in this study: D. C. Nielsen, J. Zemkoski, D. L. Leich, P. Yatchko, J. M. Torres and G. P. Gaebe (formerly with PSE&G).

TABLE 1
BASELOAD CAPACITY MIX
IN PERCENT OF TOTAL INSTALLED CAPACITY

<u>SYSTEM</u>	<u>YEAR</u>	<u>NUCLEAR (%)</u>	<u>COAL (%)</u>	<u>OIL (%)</u>	<u>TOTAL (%)</u>
A	1985	32	16	15	63
	1990	39	13	4	56
	1995	45	11	3	59
	2000	48	9	1	58
B	1985	45	36	0	81
	1990	47	38	0	85
	1995	50	39	0	89
	2000	50	40	0	90
C	1985	34	52	0	86
	1990	49	40	0	89
	1995	*	*	*	*
	2000	*	*	*	*
D	1985	23	6	17	46
	1990	31	11	14	56
	1995	*	*	*	*
	2000	*	*	*	*

*System data unavailable for study

TABLE 2
TOTAL ANNUAL BASE-LOAD OFF-PEAK
SPINNING RESERVE ENERGY

<u>SYSTEM</u>	<u>YEAR</u>	<u>PERCENT OF TOTAL SYSTEM ENERGY REQUIREMENTS</u>	<u>AMOUNT (Gwh)</u>	<u>PERCENT BY TYPE</u>		
				<u>NUCLEAR</u>	<u>COAL</u>	<u>OIL</u>
A	1985	11.4	4,918	0	25	75
	1990	9.5	4,942	13	58	29
	1995	11.4	7,278	28	52	20
	2000	10.1	7,872	40	50	10
B	1985	31.4	34,700	6	94	0
	1990	37.0	54,938	7	93	0
	1995	40.7	81,229	8	92	0
	2000	43.3	116,099	6	94	0
C	1985	31.1	5,285	0	100	0
	1990	41.2	8,530	5	95	0
	1995	*	*	*	*	*
	2000	*	*	*	*	*
D	1985	0.4	461	0	0	100
	1990	2.4	3,405	0	3	97
	1995	*	*	*	*	*
	2000	*	*	*	*	*

*System data unavailable for study

TABLE 3
STATUS OF ELECTROLYTIC HYDROGEN PRODUCED
(MID-ATLANTIC SYSTEM)

<u>YEAR</u>	<u>% BLENDING</u>	<u>ELECTROLYZER LOAD FACTOR %</u>	<u>% OF TOTAL AVAILABLE OFF-PEAK BASE- LOAD ELECTRIC ENERGY USED</u>
1985	1.6	42	7.3
1990	2.0	55	9.7
1995	3.0	60	10.7
2000	2.9	60	10.0

TABLE 4
STATUS OF ELECTROLYTIC HYDROGEN PRODUCED
(MIDWESTERN SYSTEM)

<u>Year</u>	<u>% Blending</u>		<u>Electrolyzer Load Factor %</u>		<u>% of Total Available Off-Peak Base-Load Electric Energy Used</u>	
			*	**		
1985	1.7		37		1.8	
		4.6		100		5.0
1990	2.1		45		1.4	
		4.6		100		3.2
1995	2.3		50		1.1	
		4.6		100		2.2
2000	2.2		48		0.7	
		4.6		100		1.5

* Utilizes nuclear only
** Utilizes nuclear and coal

TABLE 5

**COST COMPARISON BETWEEN ELECTROLYTIC
HYDROGEN AND SYNTHETIC NATURAL GAS
(MID-ATLANTIC SYSTEM)**

<u>PRODUCTION FACILITY</u>	<u>HYDROGEN AND SNG COSTS (\$/DEKATHERM)</u>			
	<u>1985</u>	<u>1990</u>	<u>1995</u>	<u>2000</u>
Electrolyzer (35% to 65% Load Factor)	13.25	12.75	13.50	14.75
SNG Plant (50% Load Factor)	7.30	9.30	12.00	15.50

1 Dekatherm = 1 million Btu

TABLE 6

**COST COMPARISON BETWEEN ELECTROLYTIC HYDROGEN AND SUPPLEMENTAL
NATURAL GAS SUPPLY
(MID-WESTERN SYSTEM)**

<u>Production Facility</u>	<u>Hydrogen and Natural Gas Costs (\$/Dekatherm)</u>			
	<u>1985</u>	<u>1990</u>	<u>1995</u>	<u>2000</u>
Electrolyzer (35 to 50%* Load Factor)	8.80	8.60	9.40	10.90
(100 Load Factor**)	7.20	8.20	9.90	12.50
Supplemental Natural Gas Supply	7.40	11.00	16.90	22.50

1 Dekatherm - 1 million Btu

*Utilizes nuclear only. The load factor increases from about 35% in 1985 to about 50% by 1995-2000.

**Utilizes nuclear and coal

FIGURE 1. SUMMER TYPICAL ELECTRIC LOAD CURVE

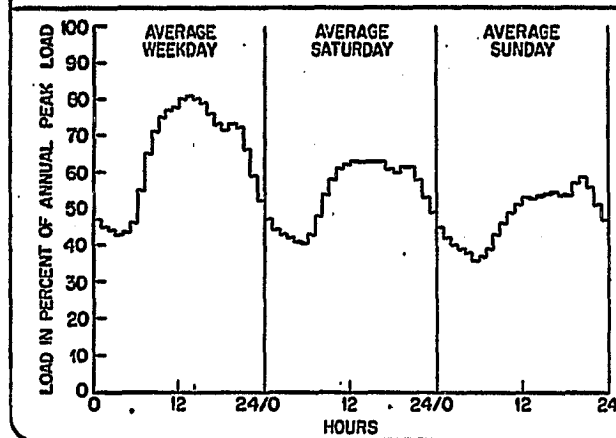


FIGURE 2. WINTER TYPICAL ELECTRIC LOAD CURVE

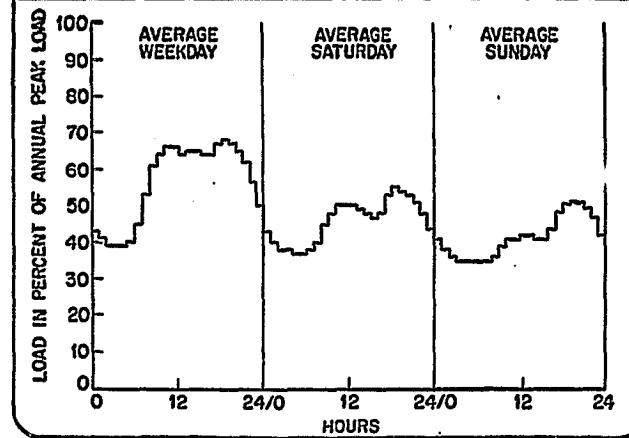


FIGURE 3. SUMMER TYPICAL ELECTRIC LOAD CURVE
(WITH EXCESS OFF-PEAK ENERGY SHOWN)

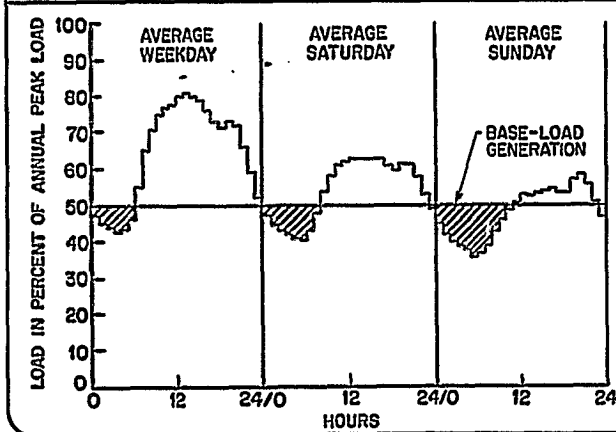


FIGURE 4. WINTER TYPICAL ELECTRIC LOAD CURVE
(WITH EXCESS OFF-PEAK ENERGY SHOWN)

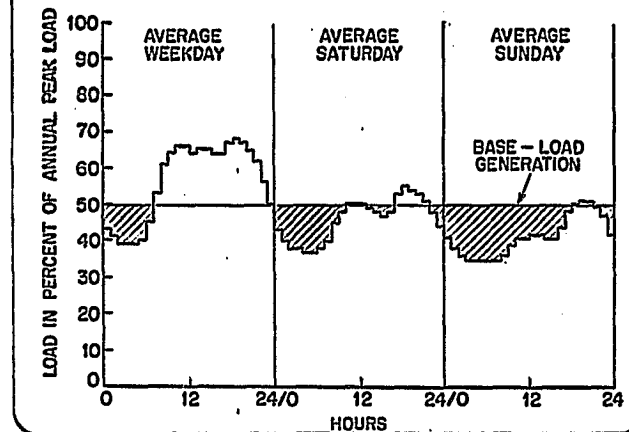


FIGURE 5. WINTER TYPICAL GAS SENDOUT

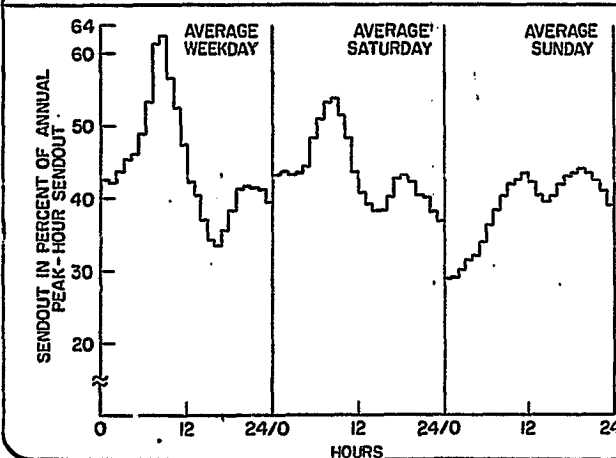
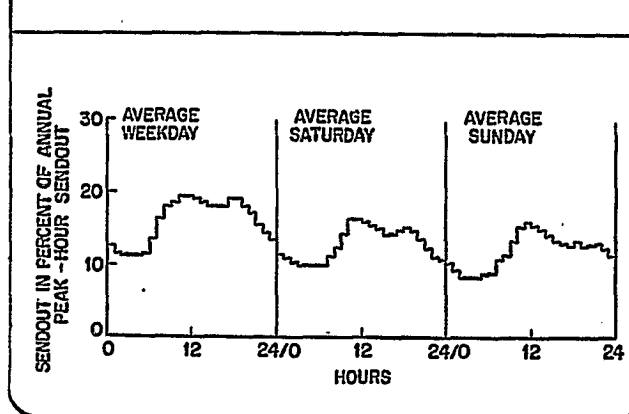


FIGURE 6. SUMMER TYPICAL GAS SENDOUT



**HYDROGEN FROM FALLING WATER:
ASSESSMENT OF THE RESOURCE
AND CONCEPTUAL DESIGN PHASE**

**William J. D. Escher
Institute of Gas Technology
Chicago, IL
and**

**James P. Palumbo
Pennsylvania Gas & Water Company
Wilkes-Barre, PA**

Abstract

A unique opportunity to develop a supplemental solar-hydrogen gas energy system presents itself in the many small, presently unused hydropower facilities in the United States. As opposed to generating conventional electricity, turbine-generators would be directly coupled to water electrolyzers for the production of hydrogen and oxygen. There appear to be significant advantages to this approach from the standpoint of delivering energy via a distribution system to the end user.

At present, an assessment of the falling water resource in terms of hydrogen energy potential is being conducted for the U. S. Northeastern states. Conceptual design efforts on the energy conversion station are also being carried out. If these initial results are favorable, the construction of an operating falling water to hydrogen energy conversion facility would be in order. Such a station might serve as a flexible R&D facility for further development of this approach at achieving new energy supplies from inexhaustible resources.

Introduction

In recent months, there has been expressed a great deal of interest in the potential of harnessing presently undeveloped or unused hydropower as a clean, domestically-available source of energy (1,2).

A special 3-month study was carried out at the request of the Administration by the Corps of Engineers which estimated that 159,3 kWh of hydropower annually is potentially available from such sites (3). Additionally, assessments have been, and are being made, at the state level.

Emphasis so far has been on generating conventional electricity, i.e. synchronized 60 Hz alternating current compatible with the electric utility grid.

Another approach, under investigation by the Institute of Gas Technology and Pennsylvania Gas & Water Company, sponsored by the U.S. Department of Energy, provides for the conversion of the work of falling water to hydrogen using water electrolysis. Because hydrogen is storable and, as a chemical energy form, flexibly applied to many use sectors, this concept may prove advantageous in capitalizing on the availability of such hydropower resources as a complement to conventional electricity generation.

Objective of the IGT/PG&W Study

Presently IGT and PG&W are carrying out a 4-month "Phase 0" step which is proposed to be followed up with further efforts, potentially leading to the development of a pilot facility useful for research and development of hydrogen from falling water.

The purposes of the present effort are primarily two-fold:

- (1) To assess the total undeveloped resource in terms of hydrogen energy production in the 9 Northeastern states of the U.S.
- (2) To a "concept-level", characterize in technical and economic terms the hardware systems which will be required for the production of hydrogen from small falling water resources.

The results of the effort are scheduled to be reported early in Calendar Year 1978.

Technical Concept

The essence of the technical concept being pursued is shown in the functional block diagram of Figure 1.

As shown in the figure, the energy of falling water (which is a function of water mass flow rate and differential pressure or head) is extracted in a water turbine. The resulting shaftpower operates an electrical generator, which, however, may be rather different from that used in conventional hydropower systems since it is used to power an electrolyzer as opposed to being fed into the utility grid. For example, it could be advantageous to use a dc generator which might be directly interfaced with the electrolyzer. Such might significantly reduce the equipment cost as well as avoid efficiency losses in rectification and power conditioning of ac power.

Feedwater provided to the electrolyzer, and the power input, produce hydrogen and oxygen gas. The hydrogen is shown to be delivered to the energy using sectors, and the oxygen as a coproduct.

In the particular example shown, in which the falling water derives from an upper reservoir and is to be used for municipal water supplies, such ultimate usage of the water is indicated. In such systems, which are illustrated by a number of reservoirs in the PG&W service area, the pressure "energy" is lost, sometimes intentionally in pressure regulator stations.

As to end-use of the hydrogen, a number of possibilities present themselves. Generally, there has been emphasis on "local use" of the energy product:

Natural Gas Supplement

Straight Hydrogen

Industrial gas use (non-fuel)
Direct fuel gas for residences
" " " " industries
Transportation fuel

Project Status of 1 November 1977

Work to date has focused mainly on the assessment of the falling water resource in the Northeast, with PG&W taking the lead. Telephone contacts and meetings have been held with representatives in all the states being canvassed. Documentation, not in hand at the beginning of the project (when it was first proposed), is being gathered from both federal and state organizations. Generally, more information than first supposed is proving to be available. Consequently, emphasis is now being applied to the cataloging step. IGT is providing its electronic data processing facilities to this task.

IGT, assisted by PG&W who carried out initial contacts, is surveying the applicable equipment manufacturers in support of the conceptual design.

Preliminary Summary of Findings

Following are some of the Project's initial findings:

- (1) The data-base on the falling water resource is fairly expansive, but definitely of uneven quality and quantity from region to region.
- (2) Electronic data processing appears to be an appropriate way to catalog the data so that it will be readily available for specific use.
- (3) As anticipated, we have found no manufacturers of equipment oriented to this application; this suggests the need for a special systems integration effort in which component suppliers are consulted in an iterative manner.
- (4) There do appear to be significant advantages for hydrogen (vis-a-vis electricity) in

tying the small hydro-energy resources into the distribution system, primarily a consequence of hydrogen's storability.

These preliminary findings are being followed up at present with results to be presented in the Project report early in Calendar Year 1978.

Reference

1. Lilienthal, D. E., "Energy from Waters," New York Times, December 1976
2. Christiansen, D., "Water Over the Dam," IEEE Spectrum 14, No. 2, February 1977
3. Anon., "Estimate of National Hydroelectric Power Potential at Existing Dams," U.S. Army Corps of Engineers, July 20, 1977

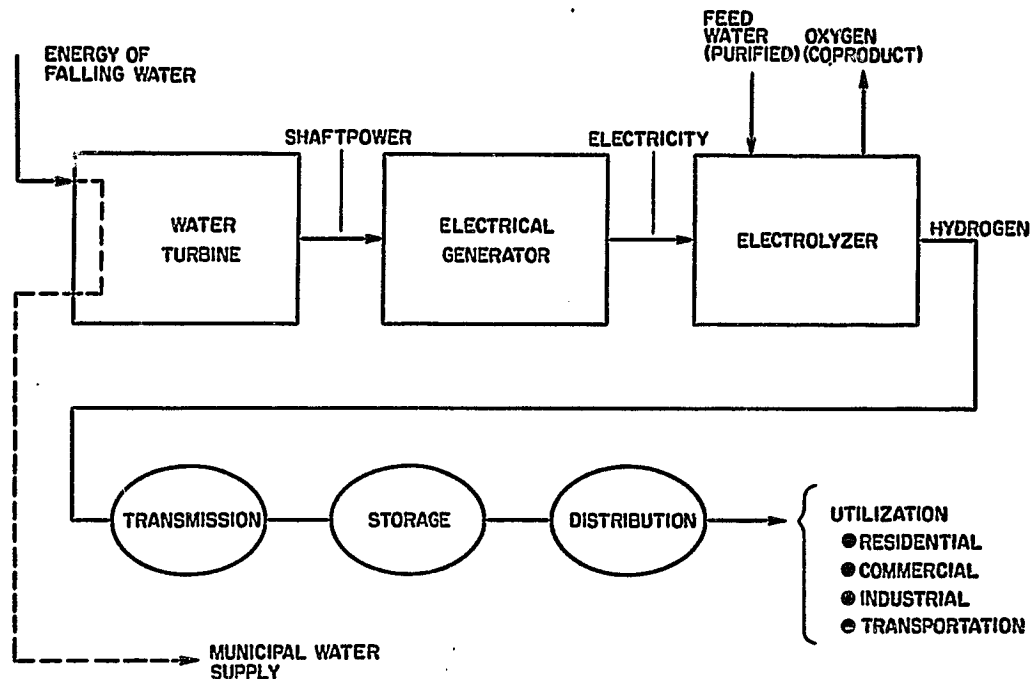


Figure 1. SYSTEM TECHNICAL CONCEPT

A. M. Karaba and T. J. Pearsall

ABSTRACT

The costs to own and operate a hydrogen fueled engine were analyzed, and it was concluded that early applications will require incentives other than economic. Several practical problems need to be addressed now. An expansion of the present effort, including development of both components and integrated systems, was recommended.

PROGRAM OBJECTIVE

IDENTIFY AND DEFINE

AN ATTRACTIVE EARLY VEHICLE APPLICATION FOR A METAL-HYDRIDE STORAGE SYSTEM COUPLED TO A HYDROGEN FUELED PISTON ENGINE.

Contract No. 412123-S

Duration: July 1977 to November 1977

Contracting Organization: Brookhaven National Laboratories

Contractor: Teledyne Continental Motors General Products Division

Project Officer: Mr. Matt Rosso, Jr.

Principal Investigators: Messrs. A.M. Karaba and T.J. Pearsall

PROGRAM ELEMENTS

1. REVIEW BACKGROUND INFORMATION

- A. ENGINE TYPES**
- B. HYDRIDE TYPES**
- C. SAFETY ASPECTS**

2. ESTABLISH FUELING REQUIREMENTS

3. IDENTIFY AN EARLIEST APPLICATION

The study addressed practical methods of dealing with the unique problems of the storage, engine, and safety aspects of a near term installation.

STUDY RESULTS (GENERAL)

1. NEAR TERM APPLICATIONS MUST RELY ON LOCALLY GENERATED HYDROGEN
2. ELECTROLYTICALLY GENERATED HYDROGEN IS CONSIDERED THE ONLY PRACTICAL NEAR TERM SYSTEM
3. APPLICATIONS THAT CAN BENEFIT FROM THE LOWER INDUSTRIAL ELECTRICAL RATES APPEAR MOST ATTRACTIVE
4. INCENTIVES OTHER THAN ECONOMIC ONES WILL ESTABLISH THE FIRST SERIOUS APPLICATIONS

Teledyne Continental Motors General Products Division concludes that no near term application can rely on a low cost hydrogen source. Local generation electrolytically would favor industrial plants where electrical rates are typically 60 to 80 percent of residential rates. The higher fuel costs of H₂ mean that motivations, such as low emissions must provide the incentive for conversion.

EVALUATION OF CANDIDATES

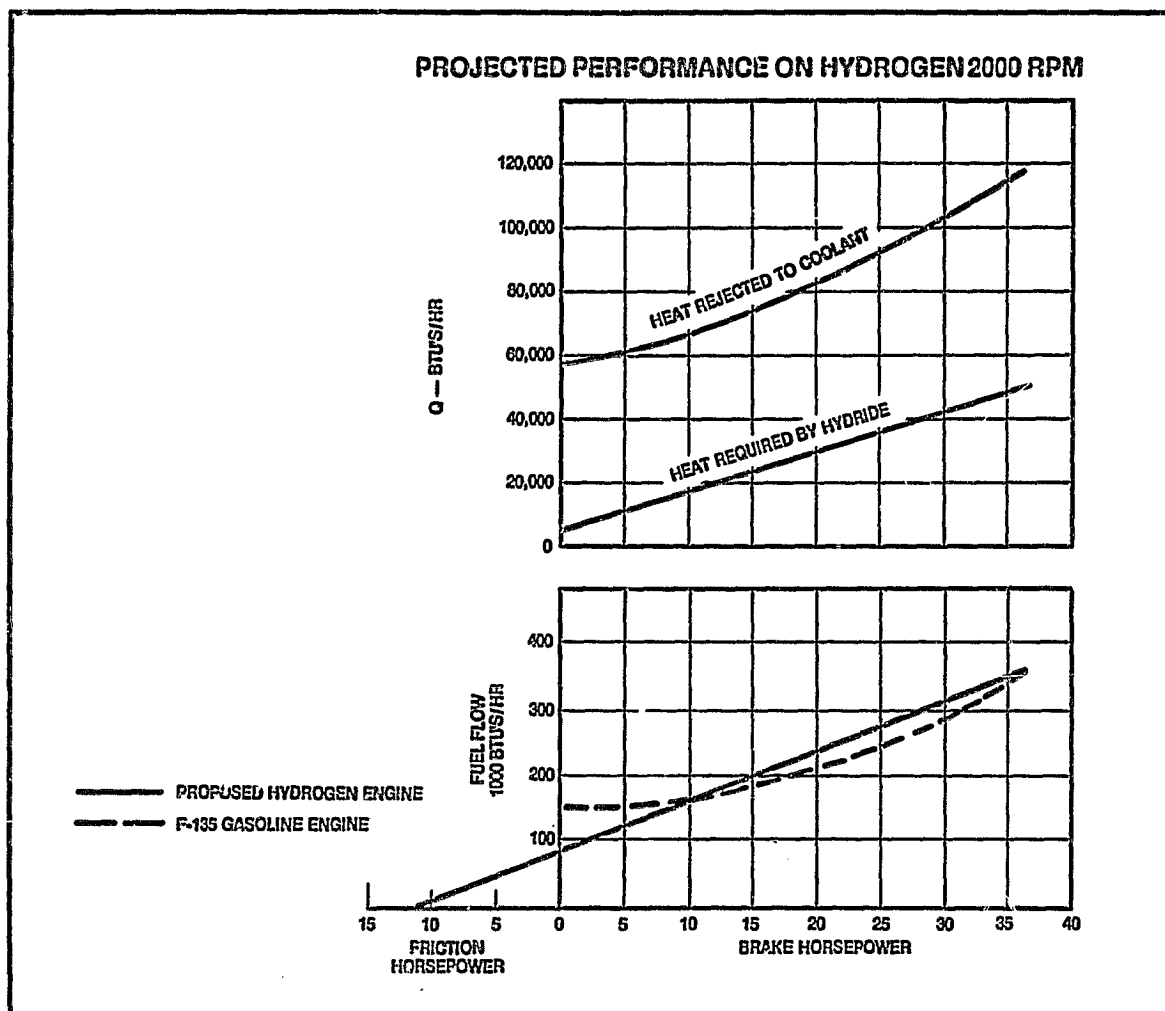
1.	2.	3.	4.	5.
WEIGHT IS AN ADVANTAGE	ECONOMIC OR ENVIRONMENTAL BENEFIT DERIVED	GOOD FLEET SIZE	CONSISTENT WITH CENTRAL FUEL STATION	DIFFUSION SPACE AVAILABLE
SWEEPERS LOADERS AGRICULTURAL TRACTORS BACK HOES ROLLERS SCRAPERS	SWEEPERS (IN-PLANT)		SWEEPERS (IN-PLANT)	AGRICULTURAL TRACTORS BACK HOES ROLLERS SCRAPERS
LIFT TRUCKS CRANES SHOVELS	LIFT TRUCKS	LIFT TRUCKS	LIFT TRUCKS	CRANES SHOVELS
OFF-HIGHWAY EQUIPMENT	DELIVERY VANS MAIL TRUCKS	DELIVERY VANS MAIL TRUCKS	DELIVERY VANS MAIL TRUCKS	OFF-HIGHWAY EQUIPMENT DELIVERY VANS MAIL TRUCKS
BULLDOZERS	TAXI CABS GOLF CARTS URBAN CAR URBAN BUS	TAXI CABS URBAN BUS	TAXI CABS GOLF CARTS URBAN BUS	BULLDOZERS TAXI CABS GOLF CARTS URBAN CAR URBAN BUS

Teledyne Continental Motors General Products Division established five criteria for evaluating potential applications. No candidate met all five criteria. The diffusion space criteria was weighted low because of the "enclosed" storage and control system to be employed. On that basis, the industrial lift truck appeared the most attractive.

INDUSTRIAL TRUCK SELECTION

- A. OPERATIONAL HOURS CAN BE ACCUMULATED RAPIDLY**
- B. OPERATION CAN BE CONTROLLED**
- C. CHANGES OR MODIFICATIONS CAN BE EASILY AND QUICKLY APPLIED**
- D. SKILLED MAINTENANCE PERSONNEL ARE ALWAYS CLOSE AT HAND**

In addition to the practical aspects identified as necessary to justify any application, considerations that relate to the technical and information gathering aspects of the program recommend an industrial application.



A 2000 rpm fuel hook comparing a 135 in 3 conventionally carbureted gasoline engine is shown compared to a hydrogen fueled engine of 20 percent more displacement to provide comparable horsepower.

The unthrottled hydrogen fueled engine can be expected to exhibit fuel flow versus horsepower similar to an unthrottled diesel engine. The obvious point to note is the significant reduction in required fuel energy at light load.

The figure also illustrates the heat rejection to the coolant as a function of load as compared to the heat required by the hydride bed for release of the fuel.

INDUSTRIAL TRUCK OPERATING MODES

MODE	RPM	PERCENT POWER	PERCENT TIME	BTU'S/HOUR	
				GASOLINE	H ₂
IDLE	600	0	40%	19,000	9,500
FULL POWER	2800	100%	5%	20,900	20,900
DECELERATION	2000/600	0	5%	2,400	1,200
LIGHT LOAD	2000	10%	25%	39,000	29,250
LIGHT LOAD	2000	40%	25%	45,000	48,750
				126,300	109,600

In quantifying fuel required for the hydrogen fueled vehicle we made use of the fuel hooks described in the previous chart.

Overall thermal efficiency of the gasoline truck is 14 percent with the hydrogen truck at 16 percent.

Vehicles employed in more rigorous service could be less attractive from a thermal efficiency point while light load applications with a high percentage of standby idle and light load could be more attractive.

HYDROGEN STORAGE

1. BED IS IMMERSED IN ENGINE COOLANT AND RELEASE IS CONTROLLED BY COOLANT FLOW MODULATION
2. TUBE DIAMETER IS SMALL — APPROXIMATELY 3 INCHES I.D. FOR IMPROVED TRANSIENT PERFORMANCE
3. "START UP" BED IS EXHAUST HEAT ACTIVATED
4. EXTRUDED ALUMINUM HYDRIDE STORAGE VESSELS APPEAR MOST ATTRACTIVE
5. FeTiMn MATERIAL APPEARS MOST ATTRACTIVE BECAUSE OF INCREASED USABLE CAPACITY

The totally immersed bed proposed offers a practical system for insuring good heat transfer. Usable hydrogen in the bed was projected to be 1.4 percent by weight.

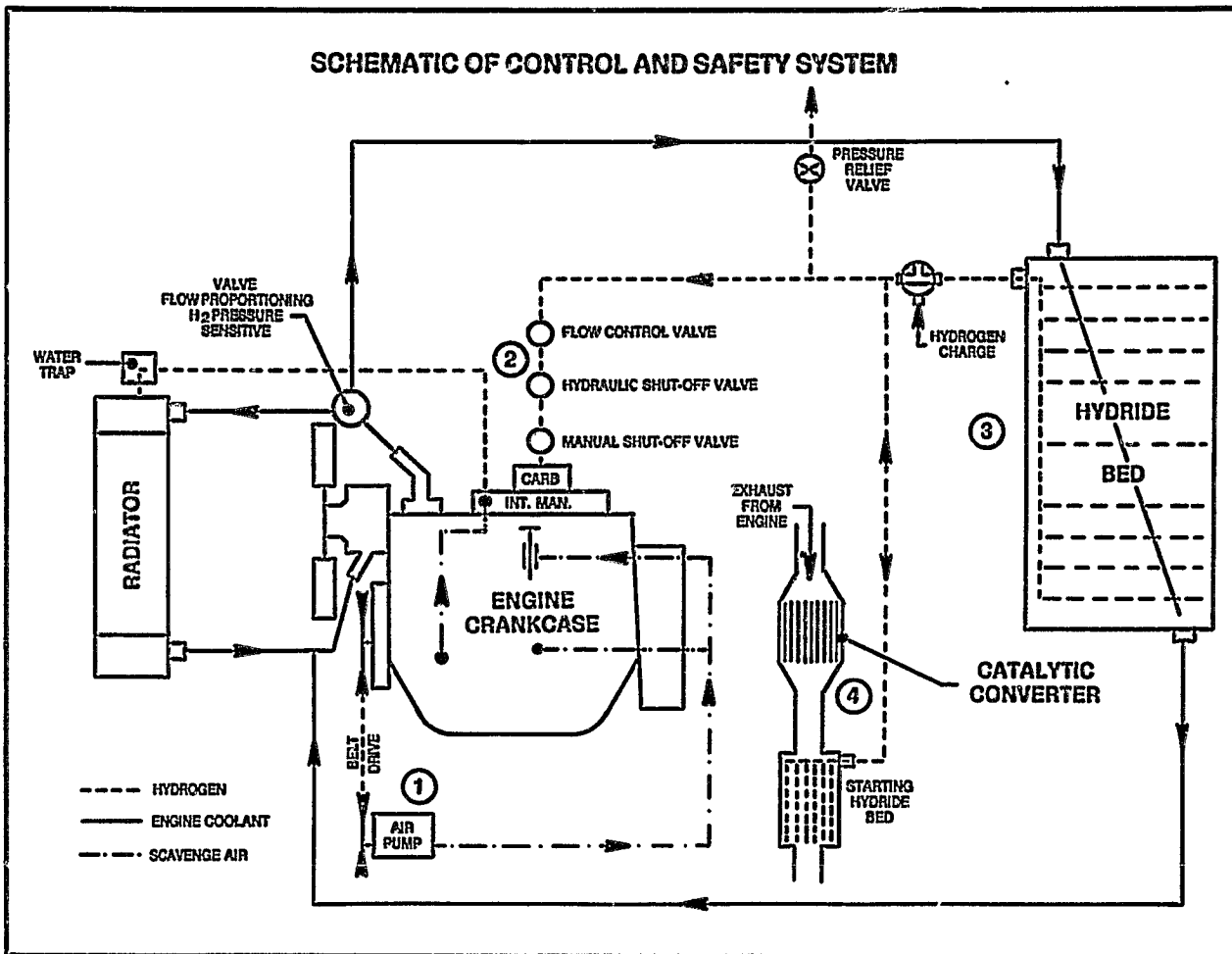
Cold start-up problems are addressed with an exhaust heated bed estimated to be 5 percent of the total. Cold start-ups will require a warm up period to bring the entire engine and hydride bed system up to temperature.

ENGINE CHANGES

- 1. ALUMINUM HEAD AND PISTON**
- 2. IMPROVED OIL CONTROL**
- 3. COOLED EXHAUST VALVE**
- 4. POSITIVE CRANKCASE VENTILATION**
- 5. EXHAUST DILUTION WITH CATALYST**

Engine changes are proposed to address these problems:

- 1. Both intake and exhaust backfire.*
- 2. Worn engines developing ignitable mixtures in the crankcase.*
- 3. Elimination of free hydrogen in exhaust.*



Significant features of the control system include:

1. An air pump employed to:

- (a) Cool the exhaust valves
- (b) Provide positive crankcase ventilation
- (c) Exhaust dilution

2. Fuel to the engine — limited by:

- (a) Ignition switch for positive shut-off
- (b) Oil pressure switch limits fuel delivery until cranking speed is achieved
- (c) Fuel flow modulation without throttling

3. Hydride bed controls include:

- (a) Flow control modulated by hydrogen pressure
- (b) Venting of the cooling system into the intake manifold insuring a hydrogen leak from the bed is routed thru the engine
- (c) Fuel shut-off does not stop ignition system which continues should a bed leak exist

4. Exhaust system incorporating:

A conventional catalytic converter with over temperature warning to indicate a defective ignition system.

COST SUMMARY (\$/YEAR)*

	<u>GASOLINE</u>	<u>ELECTRIC TRUCK</u>	<u>LPG TRUCK</u>	<u>H₂ POWER [ELEC]</u>	<u>H₂ POWER [PIPELINE]</u>
COST TO OWN	1,669	3,417	1,739	2,247	2,247
COST TO OPERATE	1,822	759	3,220	5,534	1,922 **
COST TO MAINTAIN	2,529	1,877	2,529	2,529	2,529
TOTAL DOLLARS/YEAR	6,020	6,053	7,488	10,310	6,698

* BASED ON A 7.5 YEAR LIFE

** BASED ON H₂ COST OF \$5.00/10⁶ BTU'S

The economics of an industrial truck operating in a normal environment are strongly related to fuel cost.

Early applications that will not have the low fuel cost advantages ultimately projected and will require incentives other than economic.

CONCLUSIONS

1. SEVERAL APPLICATIONS FOR HYDRIDE STORAGE COUPLED TO A HYDROGEN FUELED PISTON ENGINE ARE ATTRACTIVE
2. THE ECONOMICS OF FUEL PRODUCTION COST RECOMMEND FIRST APPLICATIONS IN THE INDUSTRIAL FIELD WHERE LOWER ELECTRICAL COSTS AND ENVIRONMENTAL CONSIDERATIONS ARE BOTH ATTRACTIVE
3. A PRACTICAL AND SAFE SYSTEM CAN BE PUT INTO SERVICE TODAY

Engine/hydride systems have several practical problems that need to be addressed now. The evolution of practical systems capable of long term, trouble free and safe operation, requires performance of systems in real environments. An expansion of the present effort is recommended. That expansion should include both component and integrated system applications.

BLANK PAGE

SESSION VI
NATURAL GAS SUPPLEMENTATION

NATURAL GAS SUPPLEMENTATION WITH HYDROGEN
C. R. Guerra, J. E. Griffith, K. Kelton, and D. C. Nielsen
Public Service Electric and Gas Company

HYDROGEN AS A MID-TERM GASEOUS FUEL SUPPLEMENT BY
BLENDING WITH NATURAL GAS
G. F. Steinmetz
Baltimore Gas and Electric Company

NATURAL GAS SUPPLEMENTATION
WITH HYDROGEN

C. R. Guerra, J. E. Griffith, K. Kelton and D. C. Nielsen
Public Service Electric and Gas Company
80 Park Place
Newark, New Jersey 07101

Abstract

The potential supplementation of natural gas with hydrogen is being evaluated. The studies include: (1) combustion tests of gas blends in burners and appliances, (2) computation of capacity of a distribution network and system adjustments to deliver gas blends and (3) measurement of gas leakage from prototype joints of mains removed from a gas distribution grid.

The results show that main burners can burn blends with up to 20-25% hydrogen in natural gas, but target pilots limit the hydrogen concentration to 6-11%. After modification of pilot orifice or increase in gas supply pressure, blends with up to 20% hydrogen were found satisfactory for use in most burners and appliances. The flow studies indicate that natural gas with up to 20% hydrogen could be readily adapted to utility operations at the gas pressure and flows used in the distribution, utilization and service subsystems of the grid. The metering station appears to be the most suitable site for introducing hydrogen into the distribution system. Measurements of gas leakage from joints containing blends of hydrogen with natural gas are currently under way.

Introduction

The supplementation of natural gas with hydrogen is an attractive concept because, as a gas, hydrogen is readily adaptable to existing utility distribution systems and to the utilization equipment owned by gas users. Gas T&D pipeline networks and customer appliances and equipment represent, as an aggregate, a large investment with a productive life and usefulness highly dependent on the availability of natural gas and certain gas substitutes and supplements.

Hydrogen is pre-eminent as a natural gas supplement because it can be derived from various primary energy sources ranging from fossil to nonfossil sources, including fusion and solar energy. Gradual supplementation of natural gas with hydrogen is expected to be a key element in the smooth transition from fossil fuel dependence to the nonfossil economy of the future.

Under contract with ERDA and with funding support from Public Service Electric and Gas Company (PSE&G), various aspects concerning the delivery of blends of hydrogen with natural gas, via existing utility systems, are being studied. The program focuses on the following:

(1) the limitations which the use of hydrogen blends may bring about in customer appliances and equipment, (2) the operation of a utility grid distributing hydrogen blends, (3) the selection of suitable points for injecting hydrogen into the distribution system, (4) the effectiveness in hydrogen containment by typical components of a utility grid and (5) certain nontechnical aspects related to safety and regulatory requirements.

Combustion Tests of Blends in Burners and Appliances

The objective of this investigation was to determine the maximum amount of hydrogen that could be blended in natural gas, maintaining the reliability and efficiency of typical utilization devices with minimal or no adjustment or conversion.

Although interchangeability criteria, which may be calculated from the gas analysis, are available, these methods are not mutually consistent and were developed over 20 years ago. Since that time, new varieties of burners have been developed, and others have been modified, and burners which were critical are no longer used. In addition, use of these criteria to predict ignition or extinction noise; flashback on rapid turn-down or short-cycling; faulty ignition performance, with either thermal elements or flash tubes; and unfamiliar gas odors have not been successful. The preferred method of assessing interchangeability is to (1) determine the possible interchangeable

mixtures using established criteria, (2) set up in a laboratory selected burners/appliances representative of the most critical types served and (3) operate the proposed mixtures on the critical burners/appliances.

A preliminary study, using Weaver Indexes of interchangeability, indicated that mixtures containing up to approximately 20% hydrogen should be interchangeable with natural gas. Of the five conditions which must be met for satisfactory interchangeability: (1) little change in burner input, (2) no lifting of flames, (3) no flashback of flames, (4) no excessive yellow tipping of flames, (5) no incomplete combustion, it appeared that these mixtures would be critical with respect to flashback. Laboratory tests were undertaken to substantiate the preliminary finding.

Test Methods and Equipment

Test gases were prepared by mixing natural gas and hydrogen in cylinders and the gas blends analyzed. Each test burner was adjusted on natural gas to obtain proper input and the best possible flame characteristics. The following parameters, where applicable, were then evaluated with natural gas and the substitute mixtures of natural gas and hydrogen:

1. Gas rate (input)
2. Inner cone height
3. Primary aeration
4. Occurrence of yellow-tipping
5. Thermocouple output
6. Occurrence of flashback
 - a. under steady state conditions
 - b. under modulating conditions
 - c. on ignition
 - d. on turndown
 - e. on extinction
 - f. on short cycling
7. Occurrence of lifting
8. Noise of extinction
9. Incomplete combustion

Where adjustment of the primary air was provided on burners, the above observations were also made with hard and soft flame adjustments.

The test equipment used in this investigation consisted of 11 pilot burners, 13 main burners, and 10 appliances. Tables 1, 2 and 3 summarize the type of gas utilization equipment tested.

Table 1
Pilot Burners Tested

<u>No.</u>	<u>Burner Type</u>	<u>Use</u>	<u>Safety Type</u>	<u>Input - Btu/Hr</u>
P 1	Primary Aerated	Boiler, Furnace	Thermocouple	1,505
P 2	Incinerating	Boiler, Furnace	Differential Expansion	742
P 3	Primary Aerated	Boiler, Furnace	Differential Expansion	1,705
P 4	Non-Aerated	Range Oven	Liquid Expansion	632
P 5	Non-Aerated	Range Oven	Liquid Expansion	351
P 6	Non-Aerated	Range Top	---	110
P 7	Target	Boiler, Furnace	Thermopile	1,753
P 8	Target	Boiler, Furnace	Thermocouple	912
P 9	Target	Boiler, Furnace	Thermocouple	852
P 10	Target	Boiler, Furnace	Thermocouple	740
P 11	Target	Water Heater	Thermocouple	833

Table 2
Main Burners Tested

<u>No.</u>	<u>Burner Type</u>	<u>Material</u>	<u>Use</u>	<u>Test Input - Btu/Hr</u>	<u>Rated Input - Btu/Hr</u>
B 1	Ribbon	Cast Iron	Boiler	18,878	20,000
B 2	Ribbon	Pressed Steel	Furnace	25,256	25,000
B 3	Drilled Port	Cast Iron	Boiler	76,339	75,000
B 4	Drilled Port	Pressed Steel	Water Heater	40,120	40,000
B 5	Drilled Port	Cast Iron	Water Heater	18,765	18,000
B 6	Slotted Port	Pressed Steel	Water Heater	40,120	40,000
B 7	Slotted Port	Pressed Steel	Furnace	24,332	25,000
B 8	Luminous Flame	Aluminum Alloy	Room Heater	32,413	30,000
B 9	Luminous Flame	Aluminum Alloy	Room Heater	45,711	45,000
B 10	Drilled Port	Cast Iron	Range Top	14,262	12,000
B 11	Slotted	Pressed Steel	Air Conditioner	18,697	18,000
B 12	Single Port	Pressed Steel	Clothes Dryer	28,074	25,000
B 13	Target	Pressed Steel	Clothes Dryer	25,109	25,000

Table 3
Appliances Tested

<u>No.</u>	<u>Appliance</u>	<u>Burner Type</u>	<u>Burner Material</u>	<u>Test Input - Btu/Hr</u>	<u>Rated Input - Btu/Hr</u>
A 1	Boiler	Single Port	Cast Iron	131,293	130,000
A 2	Furnace	Slotted Port	Pressed Steel	79,976	80,000
A 3	Water Heater	Drilled Port	Cast Iron	37,913	36,000
A 4	Furnace	Single Port	Cast Iron	70,712	75,000
A 5	Range Oven	Drilled Port	Cast Iron	18,599	16,000
A 6	Range Top	Slotted Port	Pressed Steel	10,152	12,000
A 7	Room Heater	Slotted Port	Cast Iron	20,839	20,000
A 8	Range Oven	Slotted Port	Pressed Steel	18,599	19,000
A 9	Range Top	Slotted Port	Pressed Steel	10,152	10,000
A 10	Clothes Dryer	Single Port	Pressed Steel	28,269	30,000

Conclusions

1. Gas blends containing more than 6-11% hydrogen (by volume) are the limiting mixtures for target type pilot burners.
2. Gas blends containing more than 20-22% hydrogen are the limiting mixtures for main burners operating in the open.
3. Gas blends containing more than 22-25% hydrogen are the limiting mixtures for main burners tested in appliances.
4. Modification of the orifice in target pilots or increasing the supply pressure to a minimum of seven inches water column will permit the use of gas blends with 20% hydrogen.
5. The limiting conditions result from the tendency of target type pilot burner flames to burn back at the orifice and not above it as designed, resulting in reduced thermocouple output.
6. Main burner performance was limited by flashback under turn down conditions with a tendency to noise when the flame was turned off.
7. Minor changes in burner adjustment such as adjustment of primary air has little effect on the amount of hydrogen which can be satisfactorily utilized.
8. Although no tests were performed on industrial equipment, the limiting percentages of hydrogen found for residential equipment should operate satisfactorily on industrial equipment because it is readily capable of adjustment to meet variations in gas composition. Some industries, such as glass, would probably welcome the addition of hydrogen to natural gas since a more clearly defined sharp flame results.
9. The Weaver Indexes of interchangeability do not accurately predict the interchangeability of hydrogen and natural gas mixtures. Additional work needs to be undertaken to modify these indexes to arrive at a method which is universally applicable.
10. A statistical analysis of the number of types of burners in use needs to be undertaken so that accurate predictions can be made as to the costs of conversion, and the extent of the problems which may occur with various substitute gases.

Determination of Gas Distribution System Flows

This study examines the ability of a typical utility distribution system to deliver hydrogen while conforming to the pressure limitations of a system designed for natural gas. Natural gas is distributed in the U.S. today by means of a well integrated network of transmission lines operated by pipeline companies and by the distribution systems of hundreds of utilities which carry the gas to the ultimate user. The moving force which causes the gas to flow from wellhead to customer is the difference in the pressure of the gas from one point in the system to another. Different gases, since they have different characteristics such as heating value and specific gravity, require different pressure differentials for the delivery of an equivalent amount of energy.

Methodology

The flow of gas in a pipe segment can be computed by well known flow formulae which give rate of gas flow (Q) as a function of gas pressure differential (P or h), specific gravity of the gas (S), length of pipe segment (L), and a factor (C) which takes into account pipe diameter and friction. Operating personnel rely on different formulae according to the gas pressure in the mains.

For intermediate pressures (1 psig to 60 psig)

$$Q = C \sqrt{\frac{P_1^2 - P_2^2}{SL}}$$

For utilization pressures (below 1 psig)

$$Q = C \sqrt{\frac{h_1 - h_2}{SL}}$$

Computing the flow in a given pipe for different types of gases is relatively simple; however, flow computations for complicated networks of mains such as those common in gas distribution systems can be quite tedious and time consuming. For this reason, PSE&G commonly conducts network studies on a Univac 1106 Digital Computer.

Table 4 lists the principal elements of the natural gas T&D system from the wellhead to the customer's appliance. In the network studies, two subsystems of primary concern with regard to the flow of gas blends were examined in detail:

(1) a distribution pressure subsystem involving a large PSE&G feeder main network and (2) a utilization pressure subsystem involving a medium sized PSE&G grid. Network analyses were carried out for 100% natural gas at peak load conditions and for blends containing 10% and 20% hydrogen at peak load conditions. Comparisons of the results were made to determine the system modifications needed to carry the different gas blends. The service pressure subsystem was only briefly examined because it is expected that excess capacity is available to accommodate the flow of gas blends.

b. Install additional supply points to the system.

c. Uprate the system to operate at higher pressures. Uprating consists of raising the pressure in stages and conducting extensive leakage tests at each stage. In some cases, some system components must be replaced with higher rated components before uprating begins. Uprating costs can vary widely from system to system, but generally uprating is the most economic method of correcting pressure problems.

Utilization Pressure Subsystem

The network chosen for computer analysis consists of about 18,000 feet of 3", 4", 6", and 8" cast-iron and plastic mains. There are 383 customers served by this system and most of them use gas for space heating. Gas is fed into this system from two distribution regulators. The estimated consumption of this system during the maximum hour of a zero degree day (winter of 1976/77) was about 29.4×10^3 cubic feet per hour of natural gas. The design criteria which must be met for this system is that the pressure at the lowest point cannot be below 4.2" water column, and the outlet pressure at the distribution regulator cannot exceed 7.5 inches water column under normal circumstances.

If the flow studies show that the load on a zero degree day maximum hour with maximum input pressures results in pressures at any point lower than the minimum allowable, then modifications of some type must be made to the system. These could consist of one or more of the following:

a. Increasing main sizes at key points in the system to increase load carrying capacity.

b. Installing additional distribution regulators to supply the system.

Conclusions

1. A maximum-design-hour load of about 9×10^6 cubic feet per hour of 100% natural gas could be handled by the distribution pressure system studied without violating any design criteria or requiring reinforcements. The lowest system pressures were estimated to be 3.5 psig on the basis of sendout pressures of 35 psig (7.9×10^6 CFH supply source A) and 31 psig (693×10^3 CFH supply sources B&C).

2. To distribute a blend of natural gas with 10% hydrogen in the system described in (1) above, it is required that the sendout pressure at all three supply sources (A, B, and C) be kept at 35 psig to maintain a minimum acceptable pressure of 3 psig at any point in the system.

Table 4

Principal Elements of the Natural Gas T&D Network

Gas Well
Pumping Station
Underground Storage
Transmission Line
Metering Station
High or Medium Pressure Feeder Main
Distribution Regulator
Utilization Pressure Main
Service Main
Service Regulator
Customer Meter
Customer Line
Customer Appliance or Equipment

Distribution Pressure Subsystem

The network studied is made up of 300 miles of feeder mains ranging in size from 2" to 36". Approximately 142,000 customers in an area of 421 square miles are served by this system which receives gas from two meter stations and a regulating station. The estimated consumption of these 142,000 customers during the maximum hour of a zero degree day (winter of 1976/77) is about 9×10^6 cubic feet per hour of natural gas. The System is designed for 60 psig with a previous maximum operating pressure of 35 psig. It must operate at a maximum of 35 psig, unless it is uprated according to DOT (Department of Transportation) Operating Procedures. In accordance with PSE&G design criteria concerning minimum pressures, it can have no pressure below 3 psig.

If the flow studies show that the load on a zero degree day maximum hour results in pressures lower than the minimum allowable, then modifications of some type must be made to the system. These modifications could consist of one or more of the following:

a. Installing additional feeder mains at key points of the system to increase load carrying capacity.

3. To distribute a gas blend with 20% hydrogen in the system described in (1) on the preceding page, it is required that the sendout pressure at the supply points be 35 psig (7.88×10^5 CFH supply source, A) and 38.4 psig (900×10^3 and 667×10^3 CFH supply sources B&C) to maintain a minimum pressure of 3 psig throughout the system.

4. A maximum-design-hour load of 29.4×10^3 CFH of 100% natural gas could be handled by the utilization pressure system studied without violating any design criteria or requiring reinforcements. The lowest system pressure was estimated to be 5.38 inches water column with the two regulators feeding gas at 6" pressure.

5. The system described in (4) above could distribute blends of hydrogen with natural gas and maintain the minimum allowable pressure of 4.2" throughout the system. Blends with 10% and 20% hydrogen resulted in minimum pressures of 5.35" and 5.32", respectively.

Points of Potential Hydrogen Admission

The selection of the points at which hydrogen should be admitted to a distribution system to supplement natural gas is closely related to the requirements of the State Utility Commission. Aside from safety considerations, the utility commission's chief concern will most likely be that customers receiving the lower heating value blend are billed accordingly. To this end, the commission will probably require that the limits of the area receiving the blend are clearly defined so that these customers can be easily identified. From the utility's standpoint, the simplest way to define these limits would be to supply the blend to an entire distribution system, or if this cannot be done, at least to some easily defined sub-section of the distribution system. This can be done most easily if the utility blends hydrogen into natural gas at the meter stations supplying a particular distribution system.

Impact of Regulatory Standards

An analysis of the Regulatory Commission rules in one state (New Jersey) reveals few problem areas with regard to distributing hydrogen blends, but certain topics need further study.

1. Possible conflicts with a variety of existing codes, including piping and plumbing codes, welding codes, electrical codes, and compressor station codes.

2. Gas detector calibration could be difficult when the percentage of hydrogen in the blend is constantly varying.

3. Odorizing hydrogen-natural gas blends could present problems.

4. Purging mains for hydrogen-natural gas blends may need development of special procedures.

5. Heating value calculations for billing purposes will be more complicated.

Regulatory standards regarding gas distribution and hydrogen handling may vary significantly among states and localities and further studies should be made in this regard.

Performance of Gas Distribution Equipment

The rate of gas leakage or hydrogen permeation through prototype utility pipes and joints will be measured using a special test facility. The facility circulates natural gas or blends at a rate of 3,000 cubic feet per day and pressures in the utilization and distribution ranges. Cast iron, plastic pipe and steel joints removed from the PSE&G system, after various service lives, are being tested for leakage. The facility has been used for baseline tests with dry natural gas and, presently, a dry gas blend with 10% hydrogen is being tried.

HYDROGEN AS A MID-TERM GASEOUS FUEL SUPPLEMENT
BY BLENDING WITH NATURAL GAS

G. F. Steinmetz
Baltimore Gas and Electric Company
Baltimore, Maryland

Abstract

The Ad Hoc Committee studied the potential for mid-term (1985-2000) commercial application of the use of hydrogen for blending into the present natural gas delivery system as an energy supplement. Successful development of advanced electrolyzer technology and the availability of low cost "off-peak" electric generating capacity are basic to this concept.

The Committee determined that a major, federally funded research, development, and demonstration program aimed at proving the technical feasibility is not justified within the next five years. Basic reasons are that even a completely successful RD&D program would not spur mid-term commercialization to:

- * Produce sufficient hydrogen to significantly alleviate the natural gas shortage on a national basis.
- * Produce hydrogen at a cost competitive with other supplemental gaseous fuels if present price projections hold true.
- * Provide the electric power industry with incentives to devote available generating capacity to this end in competition with various storage concepts, operating alternatives, and end uses under development.

The Committee found no overriding environmental, safety, legal, code, or regulatory considerations which would preclude the hydrogen-natural gas supplementation concept.

INTRODUCTION

Several divisions of the United States Energy Research and Development Administration (ERDA) support research efforts relating to the use of hydrogen as a medium for energy transmission and distribution. While the general consensus of technical experts projects hydrogen as an energy carrier in the long-term (beyond the year 2000), its prospective role as an energy delivery medium in the mid-term (1985-2000) must also be examined. Such analyses should be within the framework of U.S. Energy systems and emphasize comparison between hydrogen and competitive alternatives available and/or under development.

At the invitation of ERDA's Chemical and Thermal Storage Branch, Division of Energy Storage Systems, Office of Conservation, an Ad Hoc Committee was established to conduct this analysis and comparison. The Committee was charged with determining the potential of hydrogen supplementation for mid-term commercial development and the appropriateness of a major government supported research, development, and demonstration (RD&D) project. If the results were positive, the Committee was asked to present a plan for implementing such a program within five years. Production of electrolytic hydrogen from off-peak electric generating capacity was emphasized as the likely hydrogen sources.

Participation was solicited from a broad base of electric, electric and gas, gas transmission and distribution utilities, related trade associations, industry, government agencies, and national laboratories. Thus, a balance of diverse perspectives and views on the value of the proposed project was included.

This activity was formally instituted at an organizational meeting held at ERDA Headquarters on April 21, 1976. Work was essentially completed in January, 1977 and a report entitled "An Evaluation of the Use of Hydrogen as a Supplement to Natural Gas" (1) was finally edited for publication during the summer of 1977. This paper is a presentation of the significant findings of the Ad Hoc Committee.

EVALUATION OF CRITERIA

Four criteria were used by the Ad Hoc Committee to evaluate the potential for mid-term commercialization of the hydrogen - natural gas blending concept. These are discussed in turn below to explain the Committee's reasoning and judgement.

First Criteria - Volumes of hydrogen produced and utilized would make a significant contribution to alleviating the natural gas shortage on a national basis.

Inherent in this criteria are the dual questions of interchangeability and production potential. Interchangeability is defined as the ability to interchange one gas with another without incurring unacceptable performance of equipment. The prime aspects of performance are:

- * No incomplete combustion, i.e., the generation of carbon monoxide beyond acceptable limits.
- * No lifting of flames from burner ports.
- * No flash-back of flames into the burner.

- * No excessive yellow tipping of flames.
- * Little change in burner input (less than $\pm 10\%$).

The interchangeability of one gas with another on all the appliances and equipment connected to distribution pipelines is not subject to exact determination. Much work has been done over the past twenty-five years to develop approaches which are indicative of satisfactory performance but not conclusive. A brief treatment is given using the Knoy "C" Equation (2) approach to gain some perspective on the effect of hydrogen blending. Table 1 shows a typical natural gas analysis and the resultant change in heating value and specific gravity as hydrogen is introduced in various percentages by volume. The Knoy "C" Equation is a simplified approach to interchangeability which permits a rapid assessment based on relationship of heating value and specific gravity. Its basic premise states that if "C" developed by the following formula for an adjustment gas remains constant within limits for substitute gases they will be interchangeable.

$$C = \frac{\text{Heating Value} - 175}{\sqrt{\text{Specific Gravity}}}$$

Interchangeability results from the maintenance of a primary air-gas mixture of approximately 175 BTU/ft.³ within the burner head. On a plot of heating value versus specific gravity, a constant "C" or interchangeability line can be developed for the adjustment gas. A variation in "C" of $\pm 5\%$ is considered to be a tolerance band within which satisfactory appliance performance can be expected. A second tolerance band to $\pm 10\%$ variation in "C" indicates an area within which some degree of difficulty with appliance performance will be experienced and burner adjustments needed. Beyond this band, substitute gases cannot be considered for satisfactory performance. Figure 1 shows the Knoy "C" plot for the typical natural gas as the adjustment gas and the various hydrogen percentage mixtures as substitute gases.

Laboratory research done on a variety of gas appliances by actually imposing hydrogen mixtures has shown approximately 10% to be the limit for interchangeability which is in good correlation with the Knoy result. Higher mixtures result in flashback problems with certain burners. The indications are that with modification of equipment to some degree and at a commensurate cost a maximum of 25% hydrogen by volume might be distributed. None of the interchangeability techniques, even laboratory testing, are capable of giving broad consideration to the "in situ" condition of equipment regarding field adjustment, deterioration, accumulation of dirt and debris and venting conditions. Neither do they fathom the nuances of customers exposed to changes in the appearance or operation of appliances. Performance on an operating distribution system is the only conclusive index of interchangeability.

With an apparent 10% assured minimum to 25% doubtful maximum, it is important to consider the effects of hydrogen mixing on natural gas requirements. Since hydrogen has a heating value of only about one-third that of natural gas, any mixing of hydrogen will lower the heating value of the gas distributed. However, the system will require the

same total heat usage regardless of the gas distributed. Thus more cubic feet of the lower heating value gas will be required during a given time period. When the relative volumes of natural gas required to satisfy a given heat load are calculated for various percentage mixtures of hydrogen, the results produce Figure II. A 10% mixture of hydrogen will decrease natural gas requirements by only 3.40% and a 25% mixture by 9.55%. Hydrogen blending then has a limited potential for alleviating natural gas shortages due to the interchangeability factor. In contrast, alternative gaseous fuels such as synthetic natural gas from either coal or naphtha and imported liquified natural gas are directly interchangeable on a cubic foot for cubic foot basis.

Although limited, the use of hydrogen would be worth pursuing if sufficient quantities were available at a competitive price. Production potential was explored by the Committee through a detailed review of possible sources. Possibilities considered and conclusions reached are summarized below:

a) Coal Gasification

SNG production from coal is more attractive than hydrogen production for natural gas blending from efficiency, cost, and compatibility viewpoints. Hydrogen production by coal gasification may be attractive for natural gas substitution in industries such as oil refining, ammonia manufacture, or production of methanol and other chemicals.

b) Renewable Resources

Of the nine possibilities examined, none appears to be feasible for large-scale application in the mid-term. There is little probability that a solar photovoltaic electrolyzer will be economically feasible in the mid-term unless breakthroughs in improved photovoltaic cell efficiency and at least a fifty-fold reduction in manufacturing costs occur. Because of high costs for electricity generation in a capital-intensive facility operating at a low annual capacity factor, there is also little hope for solar thermal electrolysis due to high cost of electricity generation and remote siting requirements. None of the photochemical concepts under development are realistically close to commercial operation by 2000, and more fundamental research is required before this concept can be adequately assessed. Bio-gasification favors methane production and anaerobic digestion of organic waste materials produces much more methane than hydrogen; reforming methane to hydrogen would be uneconomical. No prospects are seen for either solar or nuclear-based thermochemical hydrogen for commercial application before 2000. Also, considerable work remains to be done on the earth's magma as a potential hydrogen source before economic feasibility can even be assessed. Once technology is proven, wind electrolysis could be attractive under the right conditions and there is a slight chance for mid-term commercialization; however, because of regional applicability requirements, it could only be employed on a minor and very select basis.

c) Electrolytic Hydrogen from Installed Generating Capacity

Because there is presently no large-scale

electrolytic equipment industry in the United States, production on a megawatt scale requires acquisition of equipment from European manufacturers. Thus, the Committee firmly concluded that advanced electrolyzer technology is required to make mid-term commercialization feasible because burdens imposed by present technology in compression requirements and manned operations preclude any hope of competitive pricing. Table 2 presents an evaluation of present state-of-the-art electrolysis technology compared to postulated goals for advanced technology.

The General Electric Solid Polymer Electrolyte (GE-SPE) approach, now under development by the Electric Direct Energy Conversion Laboratory at Wilmington, Massachusetts with partial funding from ERDA and the Niagara Mohawk Power Company, is an advanced concept. This process employs a solid perfluorinated polymer as the electrolyte rather than aqueous KOH which is used in current systems. The GE-SPE electrolysis process is an outgrowth of the solid polymer electrolyte fuel cells supplied by General Electric for use on several aerospace vehicles.

Thus electrolytic hydrogen from "off-peak" electric generating capacity was found to be the only source capable of mid-term commercialization. Production potential then centers around the availability of "off-peak" power. Estimates by the Committee, using the advanced electrolyzer capability for hydrogen generation, were developed as follows:

Nuclear generating capacity in some geographical areas may be about equal to or slightly in excess of the base load by about 1985, and in the 1985-2000 period this excess nuclear capacity above the base load will probably gradually increase. The availability of off-peak nuclear generating capacity in the year 1995 for the contiguous 48 states has been estimated using future generating plant capacity and load data from 1976 reports filed with the Federal Power Commission by each of the nine electric utility regional reliability councils. This estimate indicates that by the year 2000 there may be as much as 72 billion kwhr of off-peak nuclear electricity that would be available about 12 hours per day at an incremental cost (fuel + O&M) of 0.6-0.8 ¢/kwhr (1975 \$). This off-peak nuclear electricity is likely to be available along the East Coast north of Virginia, in the Northern Mid-West, and on the Pacific Coast. This 72 billion kwhr/year would provide 0.2 Quad/year of electrolytic hydrogen at a cost of \$4.60-5.25/MBtu (1975 \$) including the utility rate of return on the electrolysis plant investment. This 0.2 Quad/year would be about 1% of the U.S. requirement for gaseous fuel.

The conversion of coal to electricity and then to hydrogen by electrolysis involves an overall thermal efficiency (coal to hydrogen) of about 34% compared to 60-65% for converting coal to SNG by the Lurgi process or by the newer coal gasification processes now being developed. However, in spite of this serious efficiency debit, electrolytic hydrogen production from off-peak coal fired generating

capacity may be attractive at some locations. For example, the use of electrolysis would allow electric utilities to replace cycling type coal fired generators with high efficiency (low heat rate) plants that are not readily cycled.

Estimates have been made of the availability of off-peak electricity in the years 1985 and 1990 from hydro, nuclear, and low cost coal fired plants at a maximum incremental cost (fuel + O&M) of 1.1 ¢/kwhr (1975 \$). These estimates are based on data provided by two of the larger utility systems that represent 8.5% of the total U.S. generating capacity. These data indicate that this category of U.S. off-peak electricity may be 256 billion kwhr/year in 1985, 314 billion in 1990, and may reach 465 billion in the year 2000. This larger quantity of off-peak electricity includes the off-peak nuclear electricity, discussed above; it also is available about 12 hours/day and would vary somewhat from season to season. It was assumed that 260 billion kwhr/year of this 465 billion total could be used for electrolysis in the year 2000. This would provide 0.8 Quad/year of electrolytic hydrogen or about 4% of the U.S. gaseous fuel requirements in the year 2000. This electrolytic hydrogen would cost about \$6.20/MBtu (1975 \$) including return on the electrolysis plant.

While the estimates of future available electrolytic hydrogen are significant, up to 4.0% of U.S. gaseous fuel requirements in year 2000, the probability of actually achieving this output must be considered. This probability factor is rather low because low cost off-peak electricity may not be available due to greater than anticipated electrical demand or delays in the construction of nuclear power plants. It may not be attractive to use electrolysis if SNG from coal gasification develops more rapidly than is now anticipated. There is also the distinct possibility that, if available, the low cost off-peak electricity may be utilized in an energy storage system such as pumped hydro or underground compressed air or by the use of time-of-day electricity pricing or for the night-time recharging of electric vehicles. Obviously, the competition for this energy is real. Utility managements will determine the end use which is most apt to be directed toward optimum profitability and benefit for the electric system operation. There is no apparent strong incentive for the use of this energy as a natural gas supplement by producing hydrogen. Accordingly, the Committee judged that a factor of no more than 0.10 would be applicable. Such probability scales down the anticipated hydrogen production to an order of about 0.4% of U.S. gaseous fuel requirements in year 2000 and increases the expectation that it would be on a limited regional basis rather than having national effect. On this basis, using 20 quads of energy requirement annually, electrolytic hydrogen production for supplementation would approach 0.08 quads or 0.25 trillion cubic feet. This is less than 0.1 trillion cubic feet of natural gas equivalent but worth approximately 0.5 billion dollars at the calculated production cost of \$6.20 per million BTU.

Second Criteria - Hydrogen will be cost competitive with other supplemental fuels (all costs based on 1975 dollars).

Present electrolyzer technology and industry in the U.S. is not adequate for hydrogen generation on the required scale because MW capacity units are not available and hydrogen production costs are prohibitive.

Commercialization requires successful development of advanced electrolyzers such as the General Electric Solid Polymer Electrolyte (SPE) process. Granting such development, at an approximate cost of 20 million dollars, hydrogen production costs (1975 \$) range from \$4.60-\$5.25 per million Btu (from nuclear off-peak generation only) to \$6.20 per million Btu (from all off-peak generation up to 1.1 ¢/kWh in 1975 \$). The lowest hydrogen production costs are comparable to the highest supplemental gaseous fuel costs of past years, namely substitute natural gas from naphtha, at \$4.50 per million Btu. The major competitive gaseous fuel under development, substitute natural gas from coal (SNG) at a projected cost of \$3.50 per million Btu, shows hydrogen to be 77.1% higher, although these projections might be revised upward along the course of development to commercialization.

In order to arrive at hydrogen production costs, detailed studies involving capital and operating cost estimates for the GE-SPE system were carried out. These economic data were then used with cost and availability estimates of low cost off-peak electricity to calculate the quantity and cost of electrolytic hydrogen that could be produced with the available off-peak electricity.

The capital and operating costs for the GE-SPE system are defined in Table 3. The installed cost of the electrolysis plant has been assumed to be \$150/kW of hydrogen product (1975 \$1). GE has suggested that this figure might ultimately be as low as \$100/kW after a substantial amount of capacity has been built and the learning curve experience is well advanced. The efficiency of the process has been assumed to be 90% (hydrogen product/AC power in); this figure is at the high end of the GE suggested target range of 85-90%.

The production cost of the hydrogen product derived in the tabulations is plotted as a function of the cost of electricity in Figure III.

Assumptions used in developing these costs are explained in Table 3. The more important assumptions are as follows:

- * The annual recovery of capital is 17% corresponding to that for the electric utility industry in the U.S.
- * Labor and supervision costs included in this calculation assume essentially unattended operation of the electrolysis equipment. The costs employed correspond to 0.1 man/shift in Column 1 and 0.08 man/shift in Columns 2, 3, and 4. The basic assumption is that this electrolysis equipment will run essentially unattended in small units of 5.0 MW output (51,500 SCF/hr hydrogen product) at dispersed locations such as utility substations. If constant operator attention is required, production costs for small dispersed units will be

very high. If operator attention to the electrolysis facility is required, it will probably be desirable to use large units of 50-100 MW and to locate these plants at the electric generating stations where operator attention can be provided at reasonable (incremental) cost.

- * Capital costs for the power conversion equipment are proportional to the plant's hydrogen production rather than a constant annual dollar value, assuming that the power conversion equipment is providing a useful service on the utility grid in reactive power control when the electrolysis plant is not used for hydrogen production. This might not apply if it were necessary to employ large electrolysis plants at central stations rather than the smaller electrolysis units at substations. If this reactive power control credit were not realized, the electrolytic hydrogen production costs would be increased by \$0.10/MBtu for the capacity factor cases.
- * Maintenance and general overhead annual charges are assumed to be 6.6% of investment. This corresponds to rather low overall annual maintenance costs.

It will be noticed that hydrogen storage has not been factored into any of the prior considerations. The Committee came to the firm conclusion that costs associated with any technically feasible hydrogen storage techniques would be prohibitive in the mid-term. This is especially true with the relatively small (5 MW) facility. The concept for handling pure hydrogen and injecting it into a flowing natural gas pipeline is conceived as essentially a flow-through operation with only "surge" or "buffer" storage involved.

Third Criteria - The electric power industry must be motivated to devote their low cost off-peak power generating potential to hydrogen production.

Off-peak electric capacity is a commodity under continuous and intensive study. Utilities seek to minimize its availability by power pooling and the optimum design of their generating facility "mix". It is subject to change in availability as a new plant goes on line and then load grows to utilize this capacity. Changes in operating practices, such as "time-of-day" billing, which could change the historic peak vs. off-peak relationship to reduce the availability of off-peak power, are contemplated. Techniques for energy storage including pumped hydro, compressed air, battery, and sensible heat thermal storage are in use or under study. Finally, alternate end uses of electricity such as battery charging for transportation could change the off-peak picture. All of these reduce the attractiveness and probability for hydrogen generation as a supplement to natural gas on a national scale although it could be viable in more localized regions.

Given the limited reduction in natural gas requirements which could be derived from hydrogen blending and the unfavorable production cost picture versus other alternative fuels, the Committee judged that a low probability factor must be applied for commercialization. These factors taken together prompted the decision against recommending a major research, development and demonstration project at

this time.

Fourth Criteria - No overriding environmental safety, legal, code or regulatory considerations would preclude the hydrogen - natural gas supplementation concept.

Throughout the study, this criteria was constantly reviewed by the various groups investigating major aspects of the concept such as supply, injection, transmission, distribution and utilization. Similar concerns were developed in each group relative to these considerations but the general consensus was that no insurmountable obstacles exist. Put another way, if the first three criteria were met, the fourth could be handled.

Sufficient experience and expertise exists for the design and construction of hydrogen handling facilities. The space program and various chemical plant operations including synthetic natural gas development have provided much knowledge. Likewise, numerous parallels exist between the hydrogen blending requirement and long standing gas utility peak-shaving operations which utilize propane-air mixtures blended with natural gas.

However, hydrogen does have different characteristics from more conventional gaseous fuels which must be compensated for. These properties include:

- * Low density (0.07 specific gravity) which makes containment more difficult.
- * Wide flammable limits (4-75% by volume in air), as well as lack of odor and ability to burn without visible flames which create greater hazards.
- * The potential for hydrogen embrittlement of materials under certain operating conditions which requires special attention.

In spite of the above difficulties, hydrogen is handled successfully in refinery operations and chemical plants.

A full range of clearances would be needed for the construction of hydrogen facilities including environmental impact statements, hearings, appeals and decisions. Operating demonstrations would serve a real purpose in establishing precedents if hydrogen supplementation were to be pursued for mid-term commercialization.

Facilities would be required to meet the Minimum Federal Safety Standards, Part 192 - Transportation of Natural and Other Gases by Pipeline - administered by the Office of Pipeline Safety Operations (OPSO). Also, State Public Service Commissions operating as agents for OPSO or on their own authority could impose safety requirements. At present there is no specific coverage for hydrogen facilities in the regulations governing gas transmission and distribution. Useful developmental work could be done by compiling existing standards and codes through governmental agencies, various industry agencies, and recognized standards organizations such as ASME and ANSI. Such a compilation would be valuable in orienting the safety codes, such as Part 192, toward hydrogen coverage.

Hydrogen was distributed in manufactured gas, at concentrations in excess of 30% by volume, for over 125 years. There is no record of it being a problem

constituent during that entire era. Even today, some companies use appreciable percentages of hydrogen in their send-out gases. High pressure (500 psig) transmission mains are used to transport some of this gas to the distribution network. Based on this experience, it would appear that no insurmountable obstacles or significant hazardous conditions would preclude the transmission and distribution of 10-15% by volume mixtures of hydrogen in natural gas. However, the degree of relative uncertainty combined with the risk of widespread exposure warrants a closer look at potential concerns.

Regulatory involvement could also be incurred by the intermittent but routine injection of hydrogen and its effect on the Btu content of gases reaching end-use customers. The heating value would vary for those customers served by the supplemented gas and, in addition, be different from the unmixed natural gas served to other areas of the system. These influences could cause complications in billing practices and might require more detailed monitoring of heating value by geographical area within a service territory than is currently practiced.

Utilities are subject to State and local codes governing the installation of piping and equipment in buildings. Most reference the National Fuel Gas Code which is American National Standard (ANSI) Z 223.1. Little, if any, change in this code is contemplated as a result of the low hydrogen concentration being considered. However, an interface with ANSI would be prudent if a demonstration program was instituted.

The same comment applies to the ANSI Z 21 series of standards covering gas appliance construction and performance. Almost all such equipment is certified under these standards for use with natural gas and certain other commonly used gaseous fuels through the American Gas Association Laboratories.

SUMMARY

The Ad Hoc Committee examined one possible mid-term application of hydrogen. In light of rapidly changing circumstances it may be appropriate to re-examine hydrogen's prospective role in alternative mid-term applications on a regular basis. The Committee recommended that the proposed hydrogen-

for-natural-gas-supplementation scheme be re-examined in a time period beyond three years. As a result of technology advances some of the hydrogen production options eliminated by this study, such as wind, solar, ocean, thermal, biomass, and thermochemical production, may be reconsidered. Furthermore, the entire issue of availability and cost of off-peak power is not only relevant to hydrogen production but also bears directly on electric energy storage and electric automotive programs and should be periodically examined. Such continuous studies are valuable to several on-going ERDA-EPRI and industry R&D programs in addition to being relevant to the issue of hydrogen production from electric sources. ERDA, in association with the utility industry, should remain alert to identify possible new mid-term hydrogen applications. Escalating fossil fuel prices must be considered; the expectation that synthetic gas from coal will be available at competitive prices should be questioned. Also, changes in the projected rate of addition to nuclear or other low cost base load capacity must be considered. Major changes in the above circumstances would require a reassessment of the present decision not to recommend a demonstration project at this time.

The Committee believes that its report presents a fair appraisal of the potential for mid-term supplementation of natural gas with hydrogen. General agreement on the contents was reached through many meetings and discussions. This brief presentation cannot do justice to the full report which is now available. Much effort was given to the final Conclusions and Recommendations which are reproduced in full as Appendices A and B.

REFERENCES

1. "An Evaluation of the Use of Hydrogen as a Supplement to Natural Gas" Report of the Ad Hoc Committee, ERDA 1977
2. "Graphic Approach to the Problem of Interchangeability" A.G.A. Procedures 1953: 938-47

TABLE 1
Representative Natural Gas Composition
and Properties

<u>Constituent</u>	<u>Symbol</u>	<u>% Volume</u>
Methane	CH ₄	96.53
Ethane	C ₂ H ₆	2.38
Propane	C ₃ H ₈	0.18
Iso-Butane	C ₄ H ₁₀	-
N. Butane	C ₄ H ₁₀	.02
Carbon Dioxide	CO ₂	0.77
Nitrogen	N ₂	0.12
		<u>100.00</u>
Gross Heating Value	Btu/Ft ³ (dry)	1026
Specific Gravity	S.G. (air = 1.0)	0.576
<hr/>		
Hydrogen	H ₂	100.0
Gross Heating Value	Btu/Ft ³ (dry)	325.0
Specific Gravity	S.G.	0.07

Change in Heating Value and Specific Gravity
With Various % Hydrogen Mixtures

<u>% Hydrogen in Mixture</u>	<u>Mixture with N.G.</u>	
	<u>Btu/CF</u>	<u>Sp.Gr.</u>
0	1026.0	0.576
5	990.95	0.551
10	955.9	0.525
15	920.85	0.500
20	885.80	0.475
25	850.75	0.450

TABLE 2

**Goals of Advanced Electrolyzer Technology
Compared to Present State-of-the-Art**

	<u>Present</u>	<u>Advanced</u>
Installed Capital Costs \$/KW	300.00	150.00
Operating Efficiency %	65.0	90.0
Space Requirements Amps/sq.ft.	250.0	1000.0
Output H ₂ pressure PSIG	14.7	450.0
Time to come on line	Minutes	Seconds
Time to drop off line	Minutes	Seconds
Operation Mode	Manned	Unmanned
Maintenance Costs	Medium	Low
Minimum Life	10-15 Years	20 Years

TABLE 3

Electrolytic Hydrogen Cost by GE-SPE Process

Operation by a utility using off-peak electricity
1985 operation, 1975 \$

Plant - SPE electrolysis with forced commutated converter interface
Location - Northeast U.S.
Utilization factor for converter = 0.90
Utilization factor for electrolyzer = 0.45
Electrolyzer capacity = 5.0 MW hydrogen product = 17.075 MBtu/hr hydrogen product
= 52,538 SCF/hr of hydrogen or 26,269 SCF/hr of oxygen
Thermal efficiency = 90.0%
Electrical input for capacity operation = 5.556 MW
Hydrogen product pressure - 450 psig

<u>Investment</u>	<u>\$/KW out</u>	<u>\$ thousands</u>
Power conversion and switchgear	45	225
Electrolysis modules	20	100
Other process equipment	23	115
Installation costs	22	110
Offsites	15	75
Contingency	<u>25</u>	<u>125</u>
Total	150	750

<u>Column No.</u>	<u>1</u>	<u>2</u>	<u>3</u>	<u>4</u>
Converter capacity factor	0.90	0.90	0.90	0.90
Electrolyzer capacity factor	0.90	0.45	0.45	0.45
Electrolyzer operating hours per year	7884	3942	3942	3942
Hydrogen production MBtu/yr X 10 ³	134.6	67.3	67.3	67.3
Electricity input kWhr/yr X 10 ⁶	43.8	21.9	21.9	21.9
Electricity cost, c/kWhr	1.0	0.6	0.8	1.1
Working capital, \$ X 10 ³ (Note 1)	78	26	33	44

Annual Costs, \$ Thousands

Electricity		438	131	175	240
Water and chemicals (Note 2)		7	4	4	4
Labor and supervision (Note 3)		25	18	18	18
Maintenance and general overhead (Note 4)					
o Power conversion (Note 5)		15	8	8	8
o All other		35	35	35	35
Capital charges (Note 6)					
o Power conversion (Note 5)		38	19	19	19
o All other		89	89	89	89
Working capital charges (Note 7)		<u>16</u>	<u>5</u>	<u>7</u>	<u>9</u>
Total		663	309	355	422

TABLE 3 (cont'd)

Column No.	1	2	3	4
Electrolyzer capacity factor	0.90	0.45	0.45	0.45
Electricity cost, ¢/kWhr	1.0	0.6	0.8	1.1
<u>Costs, \$/MBtu of hydrogen product</u>				
Electricity	3.25	1.95	2.60	3.57
Water and chemicals	0.05	0.05	0.05	0.05
Labor and supervision	0.19	0.27	0.27	0.27
Maintenance and general overhead	0.37	0.64	0.64	0.64
Capital charges	0.95	1.61	1.61	1.61
Working capital charges	<u>0.12</u>	<u>0.07</u>	<u>0.10</u>	<u>0.13</u>
Total	4.93	4.59	5.27	6.27

Oxygen credit (Note 8)

Note 1 - Working capital = 2 months costs of electricity, water + chemicals, and labor and supervision.

Note 2 - Charges for water and chemicals are \$0.054/MBtu hydrogen product.

Note 3 - Labor and supervision for 1.0 man/shift would be \$236,000/yr.

Note 4 - Maintenance and general overhead are 6.6% of investment each year.

Note 5 - Maintenance and general overhead and capital charges for the power conversion and switchgear equipment is charged in proportion to its use for electrolysis since when not used for electrolysis it provides credits to the utility for power factor correction.

Note 6 - Capital charges are 17.0% of investment per year.

Note 7 - Working capital charges are 21.0% of working capital per year.

Note 8 - If oxygen production could be marketed at \$24/ton, the credit would correspond to \$1.53/MBtu of hydrogen.

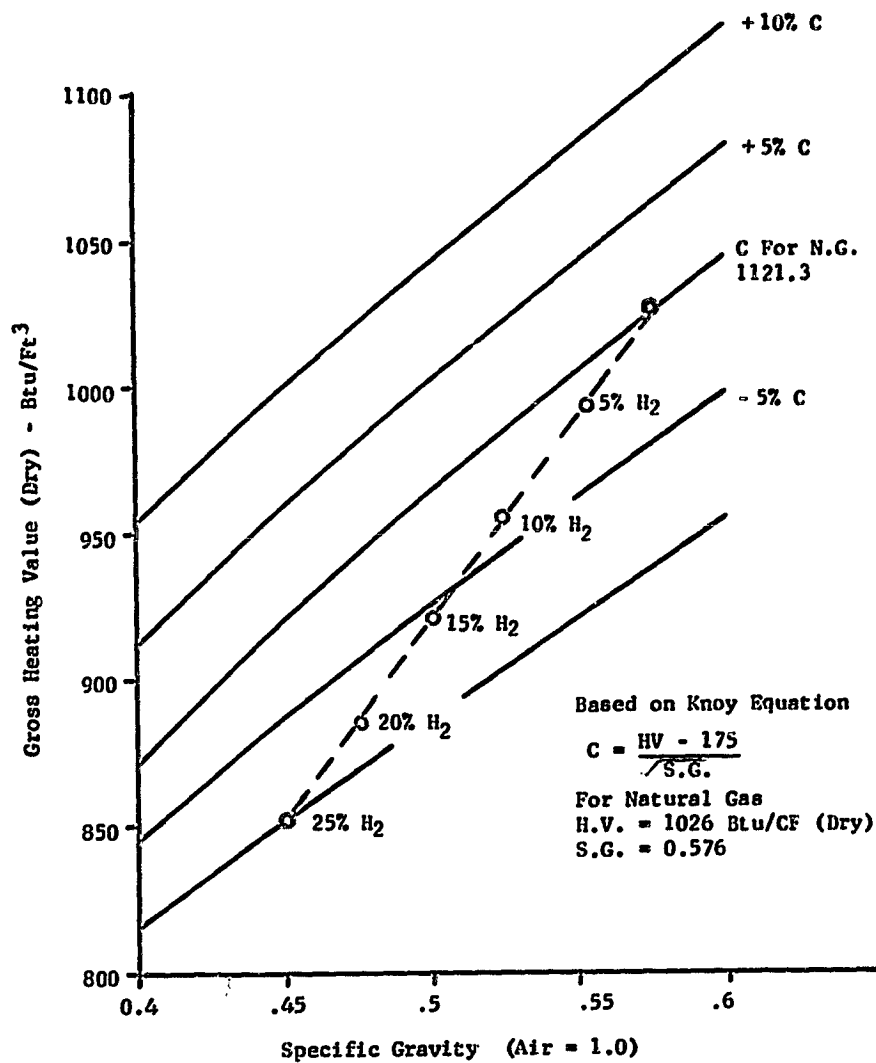


Figure I. Interchangeability Relationship Of Hydrogen Blending With Typical Natural Gas

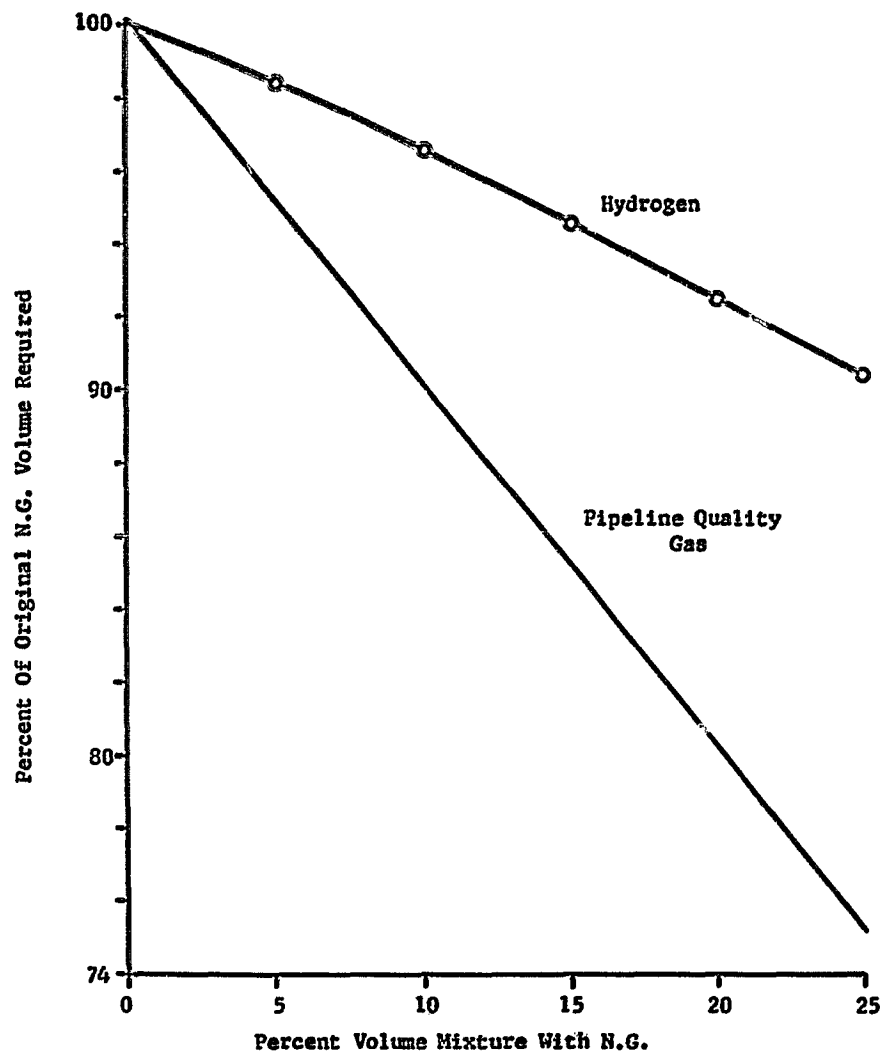


Figure II. Effect Of Blending On N.G. Requirements

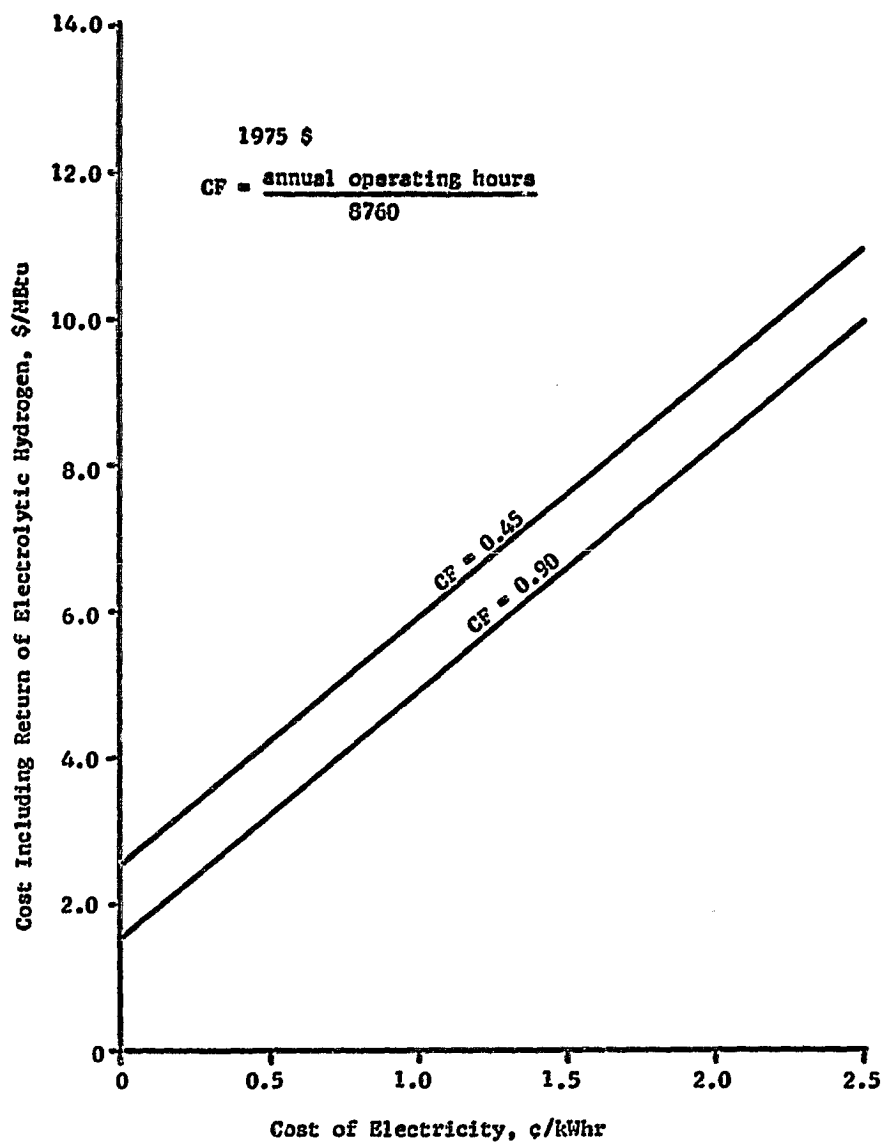


Figure III. Cost of Electrolytic Hydrogen Including Utility Rate of Return vs. Electricity Cost

APPENDIX A

Conclusions

- A. Electrolytic hydrogen is presently too expensive relative to other supplemental gas supplies but such hydrogen may become a limited quantity supplemental fuel in the future, especially in cases where low-cost "off-peak" capacity is available.
- B. There are no insurmountable problems in the safety, environmental, or regulatory areas which would prevent or preclude commercialization of hydrogen supplementation of natural gas. Excluding the production of hydrogen, the incremental system costs (such as transmission, distribution and injection) would not be significant.
- C. Laboratory tests and calculations indicate that the composition of blends would be limited to 10% hydrogen by volume without changes in system or end-use devices. With changes in end-use devices, levels could go to 20-25% hydrogen by volume blended with natural gas for satisfactory operation.
- D. Opportunities for supplementing natural gas using refinery and chemical plant by-product gases may exist today at economically feasible costs.
- E. Hydrogen may be more valuable as a chemical commodity rather than as a supplement to natural gas provided that storage would be available to deal with the intermittent nature of the source.
- F. If coal is the primary energy source being considered for natural gas supplementation, it may be more appropriate to produce synthetic natural gas (SNG) rather than hydrogen.
- G. For some utility companies, electrolytic hydrogen integrated with the gas grid and dispersed generation devices (fuel cells or high temperature turbines) may offer a unique electric/gas peak-shaving system that can be used for weekly or seasonal duty cycles not covered by batteries or other load management schemes. This approach may result in significant overall system benefits.
- H. The Committee recognizes that beyond the year 2000 there may be alternate energy sources providing for existing natural gas end uses such as increased electrification. A significant role for hydrogen is anticipated but competition with alternate energy supply mediums for end-use applications must continue to be examined. Particular consideration should be given to production from renewable resources which can interface with the gas grid.
- I. The conclusions drawn by the Ad Hoc Committee with respect to natural gas supplementation cannot be generalized. Since there are other applications of significant potential, the ERDA electrolyzer and other hydrogen RD&D programs should be continued.

APPENDIX B

Recommendations

- A. The Committee found no justification to initiate implementing a demonstration of hydrogen production and natural gas supplementation within the next five years. If significant interest is shown by a utility or utility consortium, the government should evaluate these proposals on their own merits.
- B. The federal government should continue to support those research activities aimed at solving natural gas supplementation related problems.
- C. The federal government should continue to support advanced electrolyzer development.
- D. The natural gas industry should investigate the availability and cost of by-product gases from industries such as refinery and chemical plants as a supplement to natural gas.
- E. ERDA should foster research related to longer range use of hydrogen as a possible and gradual replacement for natural and/or synthetic gases.
- F. The gas and electric utility industries should continue to be involved in establishing the technology base in anticipation of the time when hydrogen could play a more significant role. To the extent that ERDA assistance is warranted, that assistance should be on a cost-sharing basis (as distinct from sole ERDA funding) wherever practical.

Caveat

- A. The availability and cost of "off-peak" and "spinning reserve" capacity in the electric power industry along with an assessment of market penetration for electrolytic hydrogen is being developed separately by the Public Service Electric and Gas Company through an ERDA funded study.
- B. All costs in this report are shown in 1975 dollars. Cost data was derived from different sources, and, although the best presently available, may not have equal reliability. For example, production costs for synthetic natural gas from coal were developed by the ERDA Fossil Fuels Division while advanced electrolyzer hydrogen production costs were provided by General Electric, developers of the GE-SPE process.
- C. The limit of 10% by volume mixture of hydrogen in natural gas for interchangeability was taken from ERDA funded research work currently in progress at PSE&G. This limit is subject to verification by further research and ultimate field demonstration.